AD_____

Award Number: DAMD17-99-1-9565

TITLE: Proteolytic Mechanisms of Cell Death Following Traumatic
         Brain Injury

PRINCIPAL INVESTIGATOR: Ronald L. Hayes, Ph.D.

CONTRACTING ORGANIZATION: University of Florida
                            Gainesville, Florida   32611-5500

REPORT DATE: October 2004

TYPE OF REPORT: Final

PREPARED FOR: U.S. Army Medical Research and Materiel Command
                Fort Detrick, Maryland   21702-5012

DISTRIBUTION STATEMENT: Approved for Public Release;
                        Distribution Unlimited

The views, opinions and/or findings contained in this report are
those of the author(s) and should not be construed as an official
Department of the Army position, policy or decision unless so
designated by other documentation.

20050407 121

REPORT DOCUMENTATION PAGE

Public reporting burden for this collection of information is estimated to average 1 hour per response, including the time for reviewing instructions, searching existing data sources, gathering and maintaining the data needed, and completing and reviewing this collection of information. Send comments regarding this burden estimate or any other aspect of this collection of information, including suggestions for reducing this burden to Washington Headquarters Services, Directorate for Information Operations and Reports, 1215 Jefferson Davis Highway, Suite 1204, Arlington, VA 22202-4302, and to the Office of Management and Budget, Paperwork Reduction Project (0704-0188), Washington, DC 20503

1. AGENCY USE ONLY (Leave blank)	2. REPORT DATE October 2004	3. REPORT TYPE AND DATES COVERED Final (1 Oct 99 – 30 Sep 04)	

4. TITLE AND SUBTITLE
Proteolytic Mechanisms of Cell Death Following Traumatic Brain Injury

5. FUNDING NUMBERS
DAMD17-99-1-9565

6. AUTHOR(S)
Ronald L. Hayes, Ph.D.

7. PERFORMING ORGANIZATION NAME(S) AND ADDRESS(ES)
University of Florida
Gainesville, Florida 32611-5500

E-Mail: hayes@mbi.ufl.edu

8. PERFORMING ORGANIZATION REPORT NUMBER

9. SPONSORING / MONITORING AGENCY NAME(S) AND ADDRESS(ES)
U.S. Army Medical Research and Materiel Command
Fort Detrick, Maryland 21702-5012

10. SPONSORING / MONITORING AGENCY REPORT NUMBER

11. SUPPLEMENTARY NOTES
Original contains color plates. All DTIC reproductions will be in black and white.

12a. DISTRIBUTION / AVAILABILITY STATEMENT
Approved for Public Release; Distribution Unlimited

12b. DISTRIBUTION CODE

13. ABSTRACT (Maximum 200 Words)

We have examined the pathological significance of calcium accumulation in the central nervous system (CNS) following a variety of insults including cerebral ischemia, spinal cord and traumatic brain injury (TBI). This research has been motivated by recognition that disturbances in neuronal calcium homeostasis can result in activation of several calcium sensitive enzymes including lipases, kinases, phosphatases and, importantly, proteases. Recent studies have provided strong evidence that activation of the calpains, calcium activated intracellular proteases, is a major pathological event in a number of acute CNS injuries including TBI. In addition to calpains, other data have implicated another important family of cysteine proteases, caspases. Caspase-3 is an effector caspase especially important to caspase mediated pathology. Western blot immunoassays of calpain and caspase-3 specific breakdown products proposed in SOW 1 provided an efficient means of determining which brain regions and time points were most usefully incorporated into studies of SOW 2 which provided more detailed information on mechanisms of calpain activation. SOW 3 focused on endogenous modulation of proteolytic activity, including the enzyme calpastatin. SOW 4 addressed the task of providing more direct evidence of the pathological significance of activation of calpains and caspases.

14. SUBJECT TERMS
No subject terms provided.

15. NUMBER OF PAGES
241

16. PRICE CODE

17. SECURITY CLASSIFICATION OF REPORT	18. SECURITY CLASSIFICATION OF THIS PAGE	19. SECURITY CLASSIFICATION OF ABSTRACT	20. LIMITATION OF ABSTRACT
Unclassified	Unclassified	Unclassified	Unlimited

Table of Contents

INTRODUCTION

A vast body of research has examined the pathological significant of calcium accumulation in the central nervous system (CNS) following a variety of insults including cerebral ischemia, spinal cord and traumatic brain injury (TBI). This research has been motivated by recognition that disturbances in neuronal calcium homeostasis can result in activation of several calcium sensitive enzymes including lipases, kinases, phosphatases and, importantly, proteases. Recent studies have provided strong evidence that activation of the calpains, calcium activated intracellular proteases, is a major pathological event in a number of acute CNS injuries including TBI. In addition to calpains, other data have implicated another important family of cysteine proteases, caspases. Caspase-3 is an effector caspase especially important to caspase mediated pathology. Much of the evidence on calpain and caspase activation following TBI and other acute injuries has been indirect. This project incorporated an integrated approach to study protease activity in a clinically relevant rodent model of cortical impact injury using complementary techniques. Western blot immunoassays of calpain and caspase-3 specific breakdown products proposed in SOW 1 provided an efficient means of determining which brain regions and time points were most usefully incorporated into studies of SOW 2 which provided more detailed information on mechanisms of calpain activation. SOW 3 focused on endogenous modulation of proteolytic activity, including the enzyme calpastatin. SOW 4 addressed the task of providing more direct evidence of the pathological significance of activation of calpains and caspases. This SOW focused on investigating predictive relationships between proteolytic activity and indices of injury such as morphopathology.

As this final report documents, we have made dramatic progress towards these SOWs and have provided compelling evidence that both calpains and caspases are important pathological mediators of TBI under specific conditions. We believe these studies have significantly advanced our understanding of proteolytic destruction of neural tissue following acute injury and laid a firm foundation for progress and development of therapies that could have relevance to treatment of soldiers even in combat environments.

BODY

The findings of this research have been communicated in 17 peer reviewed manuscripts, 37 abstracts and 65 oral presentations during the funding period. Copies of peer reviewed manuscripts are included with this report. Below are summarized some of the major findings of our research.

SOW 1 and SOW 2 focused on systematic examination of calpain and caspase-3 activation following TBI. We have conducted the first systematic study of the effects of injury severity on regional and temporal mRNA expression levels of calpains and caspases after TBI in rats (**Ringger et al., J Neurotrauma, 2004**). These data provided important insights into the interrelationship between these two protease families and the distinct, but overlapping cascades of cell death after TBI. With regard to caspase-3 activation, these data implicated a prominent role of caspase-8 activation in regulating caspase-3 activity. We further examined the temporal and spatial profile of caspase-8 expression and proteolysis after experimental TBI in rats (**Beer et al., J Neurochem., 2001**). These findings further confirm the contributory role of caspase-8 activation to caspase-3 mediated apoptotic cell death following experimental TBI *in vivo*. To further understand the regulatory mechanisms underlying caspase-3 activation, we studied the temporal and spatial profile of Bid cleavage after experimental TBI (**Beer et al., JCBFM, 2002**). These data support the hypothesis that Bid cleavage, may be associated with activation of caspase-8 and caspase-9 and subsequently contribute to apoptotic degeneration in different CNS cells in the injured cortex. Finally, we have provided exciting and novel evidence that the unfolded protein response and associated activation of caspase-12 could be a previously unrecognized mechanism of apoptotic cell death following TBI.

Work related to SOW 1 and 2 have significantly enhanced our understanding of proteolytic mechanisms mediating cell damage and death following acute CNS insults such as TBI. We feel it

is important to develop biochemical markers of injury. The goal of these studies is to devise non-invasive diagnostics that will be useful in assessing brain injury in a combat environment. Our recent experience in Iraq has indicated that more than half of combat casualties suffer from attendant brain injuries, highlighting the need for the development of this diagnostic. Thus, we have confirmed that accumulation of calpain-cleaved breakdown products in cerebrospinal fluid after TBI in rats **(Pike et al., J Neurochem., 2001)**. We have further confirmed that this calpain-cleavage biomarker is reliably associated with injury magnitude and outcome. Thus confirming its diagnostic potential **(Ringger et al., J Neurotrauma, 2004)**. We have expanded these observations to detect both calpain and caspase-3 proteolytic biomarkers in cerebrospinal fluid after middle cerebral artery occlusion in rats **(Pike et al., JCBFM, 2004)**. We have also reviewed the status of literature on biomarkers of proteolytic damage following TBI **(Pineda et al., Brain Path., 2004)**.

SOW 3 addressed modulation of proteolytic activity by endogenous inhibitors of proteolysis. Following up on our earlier work on calpastatin, we demonstrated the cell-specific up-regulation of survivin after experimental TBI in rats. Survivin is an endogenous, anti-apoptotic protein that may also affect cell proliferation. This research has opened novel opportunities to look at endogenous modulation of proteolytic activity as well as potential increases in the natural regenerative capacity of the brain **(Johnson et al., J Neurotrauma, 2004)**.

SOW 4 attempted to develop more direct evidence of the pathological significance of caspase and calpain activation after acute CNS injury. In an elegant series of *in vitro* studies, we examined concurrent assessment of calpain and caspase activation after oxygen-glucose deprivation in primary septo-hippocampal cultures **(Newcomb et al., JCBFM, 2001)**. These data demonstrated that calpain and caspase-3 activation is associated with expression of apoptotic cell phenotypes after oxygen-glucose deprivation and that calpain activation, in combination with caspase-activation, could contribute to the expression of apoptotic cell death by assisting in the degradation of important cellular proteins. Additional studies of the relationship between protease activation and morphological changes were examined rigorously in studies by Beer et al. and Larner et al. cited above. In addition, we have provided even more direct evidence of the role of calpain in acute CNS injury. Subarachnoid hemorrhage is a prominent component of TBI. Thus, we examined the effects of systemic administration of a calpain inhibitor on behavioral deficits in blood-brain barrier permeability after experimental subarachnoid hemorrhage in the rat **(Germano et al., J Neurotrauma, 2002)**. These data suggested that pharmacological inhibition of a relative selective, membrane-permeant calpain inhibitor can significantly reduce certain pathophysiological consequences of subarachnoid hemorrhage and support the hypothesis that calpain inhibition may be a beneficial therapeutic approach in acute CNS injuries.

The overall goal of the proposed research was to look at the effects of a calcium dependent protease on acute CNS injury. Our research has lead to an interest in understanding changes in another calcium dependent enzyme, tissue-type transglutaminase (TG-2). TG-2 has been implicated in neurodegenerative diseases, and TBI is a major risk factor for all Alzheimer's disease. We confirmed the up-regulation of TG-2 after TBI in rats **(Tolentino et al., J Neurochem., 2002)**.

We confirmed similar changes following middle cerebral artery occlusion in rats **(Tolentino et al., J Neurochem., 2004)**. These data provide novel insights into mechanisms that may predispose sufferers of TBI to subsequent neurodegenerative diseases. In addition, we have expanded our interest in proteolytic damage by looking at the role of cathepsin B in contusion following spinal cord injury in rats **(Ellis et al., J Neurochem., 2004)**. We have also developed a new model to facilitate studies of proteolytic damage following TBI. This model involves use of a hippocampal slice to study acute brain injury **(Shepherd et al., JCBFM, 2003)**. Finally, our studies have highlighted the complexity of biochemical mechanisms regulating cell injury and death following acute insults to the CNS. We are convinced that further progress in this area will require more refined technologies than have been applied historically. Thus, we have pioneered the

application of high throughput proteomics to the study of TBI **(Wang et al., Internat'l Rev Neurobiol., 2004; Denslow et al., J Neurotrauma, 2003).**

KEY RESEARCH ACCOMPLISHMENTS

- Provided the first systematic examination of the effects of injury severity on regional and temporal transcriptional changes of calpains and caspases after TBI in rats.
- Provided the first examination of the effects of TBI on important regulators of caspase-3 activation. Studies showed that caspase-8 activation was a more prominent regulator of caspase-3 activity than caspase-9. Related studies provided the first information on the protein, Bid, which regulates caspase-8 and caspase-9 interactions.
- Provided the first evidence of increased expression and processing of caspase-12 after TBI, an important component of the unfolded protein response. This pathway could be one mediator of increased risks of TBI patients to develop neurodegenerative diseases.
- Developed the first systematic program to identify biochemical markers of proteolytic damage to the central nervous system. These markers will be important diagnostic tools in combat environments where rapid diagnosis of brain injury is critical.
- Provided the first evidence that TBI up-regulates an anti-apoptotic protein, survivin. This protein can inhibit casapase-3 activation.
- Provided the first evidence that concurrent activation of both calpains and caspases may be important mediators of apoptotic cell death, in contrast to previous hypotheses that these pathways operated entirely independently.
- Provided additional evidence that systemic administration of calpain inhibitors could be a useful therapy for acute CNS injury.
- Provided the first evidence that TBI can up-regulate tissue-type transglutaminase. This up-regulation may be an important factor in predisposing patients suffering TBI to subsequent neurodegenerative disorders.
- Pioneered the application of proteomics to the study of acute CNS injury, laying the ground work for even more significant future advances in this field.

REPORTABLE OUTCOMES

Manuscripts

Brian R Pike, Jeremy Flint, Satavisha Dutta, Erik Johnson, Kevin K W Wang, and **Ronald L Hayes**. Accumulation of non-erythroid αII-spectrin and calpain-cleaved αII-spectrin breakdown products in cerebrospinal fluid after traumatic brain injury in rats. J Neurochemistry, 78, 1-11, 2001.

Ronny Beer, Gerhard Franz, Stanislaw Krajewski, Brian R Pike, **Ronald L Hayes**, John C Reed, Kevin K Wang, Christian Klimmer, Erich Schmutzhard, Werner Poewe and Andreas Kampfl. Temporal and spatial profile of caspase 8 expression and proteolysis after experimental traumatic brain injury. J of Neurochemistry, 78, 862-873, 2001.

Jennifer K. Newcomb-Fernandez, Xiurong Zhao, Brian R. Pike, Kevin K.W. Wang, Andreas Kampfl, Ronald Beer, S. Michelle DeFord and **Ronald L. Hayes**. Concurrent assessment of calpain and caspase-3 activation after oxygen-glucose deprivation in primary septo-hippocampal cultures. JCBFM 21:1281-1294, 2001.

Paul J. Tolentino, S. Michelle DeFord, Lucia Notterpek, Christopher C. Glenn, Brian R. Pike, Kevin K.W. Wang and **Ronald L. Hayes**. Up-regulation of tissue-type transglutaminase after traumatic brain injury. J. Neurochem., 80: 579-588, 2002.

Germano A., Imperatore C., d'Avella D., Pupo C., Costa C., Pike B.R., Newcomb J.K., Zhao X., **Hayes R.L.**, Tomasello F. Systemic administration of a calpain inhibitor reduces behavioral deficits and blood-brain barrier permeability changes after experimental subarachnoid hemorrhage in the rat. J. Neurotrauma. 19 (7): 887-896, 2002.

Gerhard Franz, Ronny Beer, Denis Intemann, Stanislaw Krajewski, John C. Reed, Klaus Engelhardt, Brian R. Pike, **Ronald L. Hayes,** Kevin K.W. Wang, Erich Schmutzhard and Andreas Kampfl. Temporal and spatial profile of bid cleavage after experimental traumatic brain injury. JCBFM, 22(8): 951-958, 2002.

Brian R. Pike, Jeremy Flint, Jitendra R. Dave, X.-C. May. Lu, Kevin K.W. Wang, Frank C. Tortella and **Ronald L. Hayes**. Accumulation of calpain and caspase-3 proteolytic fragments of brain-derived αII-spectrin in CSF after middle cerebral artery occlusion in rats. JCBFM, 24(1): 98-106, 2003.

Timothy M. Shepherd, Peter E. Thelwall, Stephen J. Blackband, Brian R. Pike, **Ronald L. Hayes** and Edward D. Wirth, III. Diffusion MRI study of a rat hippocampal slice model for acute brain injury. JCBFM, 23: 1461-1470, 2003.

N. Denslow, M.E. Michel, M.D. Temple, C.Y. Hsu, K. Saatman and **R.L. Hayes**. Application of proteomics technology to the field of neurotrauma: Report from the human proteome project meeting. J. Neurotrauma 20(5): 401-407, 2003.

Stephen F. Larner, **Ronald L. Hayes**, Deborah M. McKinsey, Brian R. Pike, Michael Kalai, Peter Vandenabeele and Kevin K.W. Wang. Increased expression and processing of caspase-12 after traumatic brain injury in rats. J Neurochem., 88: 78-90, 2004.

Paul J. Tolentino, Anuradha Waghray, Kevin K.W. Wang and **Ronald L. Hayes**. Increased expression of tissue-type transglutaminase following middle cerebral artery occlusion in rats. J Neurochem, 89(5): 1301-1307, 2004.

Rebecca C. Ellis, J. Nicole Earnhardt, **Ronald L. Hayes**, Kevin K.W. Wang and Douglas K. Anderson. Cathepsin B mRNA and protein expression following contusion spinal cord injury. J. Neurochem., 88: 689-697, 2004.

Jose A. Pineda, Kevin K.W. Wang, **Ronald L. Hayes**. Biomarkers of proteolytic damage following traumatic brain injury. Brain Pathology, 14(2): 202-209, 2004.

NC Ringger, PJ Tolentino, DM McKinsey, BR Pike, KKW Wang, **RL Hayes**. Effects of injury severity on regional and temporal mRNA expression levels of calpains and caspase after traumatic brain injury in rats. J Neurotrauma 21(7), 829-841, 2004.

Erik A Johnson, Stanislav I Svetlov, Brian R Pike, Paul J Tolentino, Gerald Shaw, Kevin KW Wang, **Ronald L. Hayes** and Jose A Pineda. Cell-specific upregulation of survivin after experimental traumatic brain injury in rats. J Neurotrauma 21(9), 1183-1195, 2004.

Wang KKW, Ottens AK, Haskins WE, Liu MC, Kobeissy F, Denslow ND, Chen S, **Hayes RL**. Proteomics studies of traumatic brain injury in International Review of Neurobiology, Vol. 62, Human Brain Proteome. Neubold EL, Ed. Elsevier, New York, 2004, pp 215-340.

4

NC Ringger, BE O'Steen, JG Brabham, X Siler, J Pineda, KKW Wang, **RL Hayes**. A novel marker for traumatic brain injury: CSF αII-spectrin breakdown product levels. J. Neurotrauma, 21(10) 1443-1456, 2004.

Abstracts
R.L. Hayes, J.K. Newcomb, B.R. Pike, X.Zhao, K.K.W.Wang, D.K. Anderson. Oxygen-glucose deprivation produces concurrent calpain and caspase-3 activation. 18th Annual National Neurotrauma Society Symposium, November, 2000.

Beer, R., Franz, G., Hayes, R.L., Pike, B.R., Srinivasan, A., and Kampfl, A. Temporal profile and cell subtype distribution of activated caspase-3 following experimental traumatic brain injury. Society for Neuroscience Abstracts 26(2): 2300, 2000.

RL Hayes, JK Newcomb-Fernandez, BR Pike, X Zhao, KKW Wang, DK Anderson. Concurrent calpain and caspase-3 activation following oxygen-glucose deprivation. Purdue University, 2001.

RL Hayes, CC Glenn, DM McKinsey, JN Earnhardt, BR Pike, HS Nick and DK Anderson. Proteolytic mechanisms of cell death following TBI: Novel molecular and biochemical strategies. Spring Brain Conference, Sedona, AZ, 2001.

BR Pike, J Flint, S Dutta, EA Johnson, SM DeFord, CC Glenn, KKW Wang, **RL Hayes**. Accumulation of calpain-cleaved α-II spectrin breakdown products in CSF after TBI in rats. FASEB Summer Research Conference, June, 2001.

SM DeFord, BR Pike, **RL Hayes**. Temporal profile of alpha-spectrin breakdown products after repeated vs. single mild heal injury in mice. FASEB Summer Research Conference, June, 2001.

BR Pike, J Flint, S Dutta, EA Johnson, SM DeFord, CC Glenn, KKW Wang, **RL Hayes**. Accumulation of calpain-cleaved α-II spectrin breakdown products in CSF after TBI in rats. Society for Neuroscience (SFN), November, 2001.

SM DeFord, BR Pike, **RL Hayes**. Temporal profile of alpha-spectrin breakdown products after repeated vs. single mild heal injury in mice. SFN, November, 2001.

NC Ringger, TM Shepherd, EA Johnson, SF Larner, MF Est, **RL Hayes**, BR Pike. Comparison of calpain and caspase-3 activation during necrosis, apoptosis and endoplasmic reticulum stress. SFN, November, 2001.

P.J. Tolentino, S.M. DeFord, L. Notterpek, C.C. Glenn, B.R. Pike, K.K.W. Wang, and **R.L. Hayes**. Upregulation of tissue-type transglutaminase after TBI. SFN, November, 2001.

E.A. Johnson, K.K.W. Wang, B.R. Pike, **R.L. Hayes**. Evidence of calpain activation in brain macrophages after TBI. SFN, November, 2001.

R.C. Ellis, J.N. Earnhardt, H.S. Nick, **R.L. Hayes**, P.J. Tolentino, W.A. O'Steen, G.P. Shaw, D.K. Anderson. Changes in cathepsin B gene and protein expression following acute spinal acute injury. SFN, November 2001.

T.M. Shepherd, B.R. Pike, **R.L. Hayes,** E.W. Wirth III. Cell death in the hippocampus following calpain activation. SFN, November, 2001.

P.J. Tolentino, S.M. DeFord, L. Notterpek, C.C. Glenn, B.R. Pike, K.K.W. Wang and **R.L. Hayes.** Upregulation of tissue-type transglutaminase after traumatic brain injury. 19th Annual National Neurotrauma Society Symposium, November, 2001.

J. Flint, S. Dutta, K.K.W., Wang, S.M. DeFord, **R.L. Hayes,** and B.R. Pike. Accumulation of α-II spectrin and calpain-cleaved α-II spectrin breakdown products in CSF after TBI in rats. 19th Annual National Neurotrauma Society Symposium, November, 2001.

SM DeFord, BR Pike, **RL Hayes.** Temporal profile of alpha-spectrin breakdown products after repeated vs. single mild head injury in mice. 19th Annual National Neurotrauma Society Symposium, November, 2001.

EA Johnson, KKW Wang, BR Pike, **RL Hayes.** Evidence of calpain activation in brain macrophages after traumatic brain injury. 19th Annual National Neurotrauma Society Symposium, November, 2001.

NC Ringger, TM Shepherd, EA Johnson, SF Larner, MF West, **RL Hayes,** BR Pike. Comparison of calpain and caspase-3 activation during necrosis, apoptosis, and endoplasmic reticulum stress. 19th Annual National Neurotrauma Society Symposium, November, 2001.

T.M. Shepherd, B.R. Pike, P.E. Thelwall, **R.L. Hayes,** E.D. Wirth III. Diffusion-weighted magnetic resonance imaging of cell death in rat hippocampal slices. 19th Annual National Neurotrauma Society Symposium, November, 2001.

Pike, BR, Flint, J, Dutta, S, Wang, DS, Wang, KKW, Hayes, RL. Accumulation of spectrin and calpain-cleaved spectrin breakdown products in CSF after TBI in rats.ASN, June 2002.

Wang, D.S., Tolentino, P.J., Fan, T., Pike, B.R., Wang, K.K.W., Day, A.L., **Hayes, R.L.** Induction of tissue transglutaminase in response to ischemic brain injury. ASN, June 2002.

Ellis, R.C., Earnhardt, J.N., Nick, H.S., **Hayes, R.L.,** Anderson, D.K. Characterization of cathepsin B expression following contusion spinal., cord injury (SCI). ASN, June 2002.

D. d'Avella, M. Aguennouz, F.F. Angilieri, O. deDivitis, A. Germano, A. Toscano, F. Tomasello, G. Vita, B.R. Pike, K.K.W. Wang & **R.L. Hayes.** Accumulation of calpain and caspase-3 cleaved αII-spectrin breakdown products in CSF of patients with severe traumatic brain injury. NINTS, Oct. 2002.

SM DeFord, JE Slemmer, JT Weber, CI DeZeeuw, BR Pike & **RL Hayes.** *In vivo* and *in vitro* evidence of cytoskeletal and synaptic protein alterations following repeated mild TBI. NINTS, Oct. 2002.

J Flint, BR Pike, **RL Hayes,** JR Moffett, JR Dave, X-CM Lu, FC Tortella. Accumulation of calpain and caspase03 cleaved αII-spectrin breakdown products in CSF after middle cerebral artery occlusion in rats. NINTS, 2002.

E.A. Johnson, B.R. Pike, P. Tolentino, **R.L. Hayes** & J. Pineda. Up-regulation of the cell cycle/inhibitor of apoptosis protein, survivin, is co-localized with other cell cycle proteins in astrocytes and neurons after TBI in rats. NINTS, Oct. 2002.

S.F. Larner, B.R. Pike, **R.L. Hayes**. Effects of injury severity on regional and temporal caspase-12 mRNA and protein expression levels after TBI in rats. NINTS, Oct. 2002

B.R. Pike, N.C. Ringger, D.M. McKinsey, P.J. Tolentino, S.M. DeFord, J.G. Brabham & **R.L. Hayes**. Effects of injury severity on regional and temporal mRNA expression levels of calpains and caspases after TBI in rats. NINTS, Oct. 2002.

Jose A Pineda, Jada M Aikman, Erik A Johnson, Barbara E. O'Steen, Tao Fan & **Ronald L Hayes**. Temporal profile of αII-spectrin breakdown products after TBI in immature rats. NINTS, Oct. 2002.

N.C. Ringger, X. Silver, B. O'Steen, J.G. Brabham, S.M. DeFord, B.R. Pike, J. Pineda & **R.L. Hayes**. CSF Accumulation of calpain-specific αII-spectrin breakdown products are associated with injury magnitude and lesion volume after TBI in rats. NINTS, Oct., 2002.

PJ Tolentino, A Waghray, BR Pike, CC Glenn, L Notterpek, KKW Wang & **RL Hayes**. Tissue-type transglutaminase expression following middle cerebral artery occlusion. NINTS, Oct., 2002.

A Waghray, SM DeFord, PJ Tolentino, BR Pike, CC Glenn, L Notterpek, KKW Wang & **RL Hayes**. Tissue-type transglutaminase distribution and expression after TBI. NINTS, Oct., 2002.

R.L. Hayes, N.C. Ringger, X. Silver, B. O'Steen, J.G. Brabham, S.M. DeFord, B.R.Pike, J. Pineda. CSF accumulation of calpain-specific αII-spectrin breakdown products correlate with injury magnitude and lesion volume after traumatic brain injury in rats. Winter Conference on Brain Research, Jan., 2003.

Stephen F. Larner, Deborah M. McKinsey, Miguel Torres, Brian R. Pike, Kevin K.W. Wang and **Ronald L. Hayes**. Increased expression and activation of caspase-12 after traumatic brain injury in rats. Graduate and Professional Student Medical Guild, March, 2003.

Kevin K.W. Wang, Ming Cheng Liu, Clair Ringger and **Ronald L. Hayes**. Biomarkers for traumatic brain injury. CNS Injury 2nd Pannonian Symosium, Hungary, May 2003.

William E. Haskins, Kevin K.W. Wang, Ming Chen Liu, Scott H. McClung, Alexi G. Lundberg, Barbara E. O'Steen, Marjorie M. Chow, Jose A. Pineda, Nancy D. Denslow and **Ronald L. Hayes**. Discovering novel protein biomarkers of traumatic brain injury in hippocampus and CSF by 1D-DIGE/CLC/MS. American Society for Mass Spectrometry, June, 2003.

Ronald L. Hayes. Comparison of biomarkers alpha-II spectrin breakdown products, S100B, and tau after traumatic brain injury. Advanced Technology Application for Combat Casualty Care (ATACCC) meeting in St. Petersburg, FL, Aug. 2003.

Oral Presentations
Invited Speaker, Brain Injury Association-Florida Benefit, Boca Raton, FL, 1999
Invited Lecture, Department of Neuroscience, Univ of Florida, Gainesville, FL, 2000

Invited Lecture, Department of Neurosurgery Trauma Group, Virginia Commonwealth, 2000, Richmond, VA

Invited Lecture, Department of Clinical & Health Psychology, Shands Rehab, 2000, Gainesville, FL

Invited Lecture, Department of Clinical & Health Psychology, Univ of Florida, 2000, Gainesville, FL

Invited Speaker and Colloquium Chair, American Society for Neurochemistry, 2000, 31st Annual Meeting, Chicago, IL

Invited Speaker, James A. Haley Veterans Hospital/Defense and Veterans Head Injury, 2000, Tampa, FL

Invited Lecture, Junior Honors Seminar 2000, Neuroscience Section, Univ of Florida Brain Institute, 2000, Gainesville, FL

Invited Lecture, The Miami Project to Cure Paralysis, Univ of Miami, Miami, FL, 2000

Invited Speaker, Malcolm Randall VA Medical Center "Research Day", Gainesville, 2000

Invited Speaker, Neurotrauma Symposium Coordinated by The Center for Applied Research in Head Injuries and the Department of Neurosurgery at the Rambam Medical Center, Haifa, Israel [2 talks], 2000

Invited Lecture, Department of Neurology Weekly CNS Seminar, Univ of Florida, 2000,Gainesville, FL

Invited Panel Member & Speaker, Mathematics Curriculum for Health & Life Science Students, Virginia Commonwealth University, Richmond, VA, 2000

Keynote Speaker, 2nd Annual TBI/SCI Symposium, Co-sponsored by HealthSouth Tallahassee and the Florida Brain & Spinal Cord Injury Program, Tallahassee, FL, 2000

Invited Speaker, Shands Rehabilitation Hospital Brain Injury Support Group, Gainesville, FL, 2000

Invited Speaker, Department of Psychology, Univ of Florida, Gainesville, FL, 2000

Invited Speaker, Brain Injury Association 14th Annual Conference for Attorneys, Palm Beach, FL, 2000

Chairman and Invited Speaker, 5th International Neurotrauma Symposium, Garmisch-Partenkirchen, Germany, 2000

Invited Speaker, Brain Injury Assoc. of Florida Board of Directors Meeting Pompano Beach, FL, 2000

Participant, National Neurotrauma Society meeting, New Orleans, LA, 2000

Invited Lecturer, Department of Neurology Residents, University of Florida, Gainesville, FL, 2000

Invited Lecturer, 26th Annual Course in Behavioral Neurology and Neuropsychology, Lake Buena Vista, FL, 2000

Invited Speaker, National Association of Retired Federal Employees, Gainesville, FL 2001

Invited Speaker, University of Florida Foundation, Gainesville, FL, 2001

Invited Speaker, Dedication/Naming Ceremonies, Evelyn F. and William L. McKnight, 2001

Invited Reviewer, Scientific Advisory Board of the National Brain Injury Research, Treatment, and Training Foundation, Charlottesville, VA, 2001

Invited Lecturer, Purdue University, West Lafayette, IN, 2001

Invited Plenary Session Speaker, Spring Brain Conference, Sedona, AZ, 2001

Invited Participant, Workshop on DoD Sponsored Parkinson's Related Research, Potomac, MD, 2001

Speaker, Evelyn F. & William L. McKnight Brain Institute of the University of Florida (MBI-UF), Brain Trauma Foundation, Gainesville, FL, 2001

Speaker, MBI-UF presentation to Cogent Neuroscience, Gainesville, FL, 2001

Invited Speaker, Roskamp Institute, Tampa, FL, 2001

Invited Speaker, FASEB Summer Research Conference, Whitefish, MT, 2001

Invited Speaker, Building Research Capacity in Rehabilitation Science Conference co-organized by the Amer Academy of Physical Med & Rehab & the NIH, Bethesda, MD, 2001

8

Invited Speaker, Brian Injury Association's Annual Symposium, Atlanta, GA 2001

Invited Speaker, Signal Transduction and Apoptosis Working Group Mini-Retreat, Gainesville, FL, 2001

Invited Speaker, Advanced Technology Applications for Combat Casualty Care, sponsored by the DoD, Fort Walton Beach, FL, 2001

Chair of Session, National Neurotrauma Society Symposium, San Diego, CA, 2001

Invited Lecturer (2 lectures), UCLA Division of Neurosurgery, Los Angeles, CA, 2002

Invited Speaker, "Family Day" for UF College of Medicine, 2002

Speaker, Weekly Neuroscience Seminar, University of Florida, Gainesville, FL, 2002

Invited Discussant, 1st NINDS/NIH "Proteomics in the Neurosciences" Workshop,Washington, DC, 2002

Poster Presentation, Winter Conference on Brain Research, Snowbird, Utah, 2003

Invited Speaker, Santa Lucia Hospital, Rome, Italy, 2003

Invited Speaker, Integra Neurosciences, Plainsboro, NJ, 2003

Invited Lecturer, Quantitative Neuroscience/Neural Engineering Seminar, Gainesville, FL, 2003

Invited Speaker, NIH/NINDS, 2003

Invited Lecturer, Center for Neuropsychological Studies, Gainesville, FL, 2003

Invited Speaker, Gainesville Area Innovation Network, Gainesville, Fl, 2003

Invited Speaker, Uniformed Services University of the Health Sciences And NBIRTT sponsored conference, Bethesda, MD, 2003

Poster Presentation, Advanced Technology Applications for Combat Casualty Care (ATACCC), St. Petersburg, FL, 2003

Invited Speaker, Post Traumatic Brain Contusions and Lacerations International meeting Rimini, Italy, 2003

Invited Speaker, 3rd International Conference on Biochemical Markers for Brain Damage Lund, Sweden, 2003

Invited Speaker, National Neurotrauma Society annual meeting, Biloxi, MS, 2003

Invited Participant, NIH Bullock DSMB, Richmond, VA, 2003

Award Recipient and Invited Speaker, Lance Award Ceremony, Charlotte, NC, 2004

Invited Attendee, CHI's Utilizing Biomarkers in Diagnostic Research conference, San Francisco, CA, 2004

Invited Speaker, Applied Math Seminar, Dept. of Mathematics, UF-Gainesville, 2004

Invited Speaker, Grand Rounds, Univ of Mississippi Dept Neurosurgery, Jackson MS, 2004

Invited Speaker & Poster Presentation, DoD Peer Review Medical Research Program Meeting, San Juan, Puerto Rico, 2004

Invited Speaker, Brain Injuries Conference, Tampa, FL, 2004

Invited Speaker, Kentucky Spinal Cord & Head Injury Research Symposium, Lexington, KY, 2004

Invited Speaker, ROSE 20th Annual Seminar, Minneapolis, MN, 2004

Invited Speaker, Combine ATACCC & NATO Meetings, St. Petersburg, FL, 2004

Invited Speaker, ACRM-ASNR Joint Conference, Ponte Vedra, FL, 2004

CONCLUSIONS

Research funded by this proposal has produced dramatic increases in our understanding of proteolytic mechanisms of cell death. We have gained novel insights into the temporal and regional profile of protease activation as well as mechanisms regulating activity of two distinct families of cysteine proteases, calpains and caspases. Our data suggests that these proteases may interact in important and unanticipated ways. These studies have established a firm foundation for development of therapies that could block protease activation, and our preclinical studies have further confirmed the potential utility of calpain inhibitors. We have applied these insights to the development of practical and novel techniques to diagnose TBI even in combat environments. Thus,

we have initiated the first systematic study to develop non-invasive biochemical markers of TBI. We believe these markers will importantly facilitate the ability of combat medics to diagnose acute CNS insults even in austere medical environments associated with combat.

In addition, our studies of cell death mechanisms have revealed at least 2 pathways that could contribute to the increased risks for neurodegenerative diseases associated with TBI. Both tissue-type transglutaminase and caspase-12 could be important mediators of aberrant protein processing, forming pathological aggregates that are the hallmark of neurodegenerative disorders.

PERSONNEL

The following personnel received salary support during the project. Not all personnel were paid the whole project; some were only used for a portion of the project.

Ronald L. Hayes
Ming C. Liu
Guangling Huang
Dena Howland
Anuradha Waghray
Jeremy Flint
Jose Pineda
Stan Svetlov
Andrew Ottens
Kevin Wang
Barbara O'Steen
Jennifer Frank
Regina Last
Erik Johnson
Jason Kitlen
Nancy Ringger
Nancy Kupma
Douglas Anderson
Justin Bickford
Stephen Larner
Gitte Kitlen
Jada Aikman
Erin Golden
Veronica Akle
Ming Qian

Effects of Injury Severity on Regional and Temporal mRNA Expression Levels of Calpains and Caspases after Traumatic Brain Injury in Rats

N.C. RINGGER,[1,4] P.J. TOLENTINO,[2] D.M. McKINSEY,[4] B.R. PIKE,[5] K.K.W. WANG,[1,3,4] and R.L. HAYES[1,3,4]

ABSTRACT

Despite a preponderance of studies demonstrating gene expression and/or enzymatic activation of calpain and caspase proteases after traumatic brain injury (TBI), no studies have examined the effects of injury magnitude on expression levels of these cell death effectors after TBI. Determination of the degree to which injury severity affects specific expression profiles is critical to understanding the relevant pathways contributing to post-trauma pathology and for developing targeted therapeutics. This investigation tested the hypothesis that different injury magnitudes (1.0, 1.2, and 1.6 mm) cause alterations in the regional and temporal patterns of mRNA expression of calpain-related (calpain-1 and -2, calpastatin) and caspase-related (caspases -3, -8, -9, BID) gene products after cortical impact in rats. Quantitative RT-PCR was used to compare effects of injury severity on mRNA levels in ipsilateral (injured) cortex and hippocampus, 6 h to 5 days post-injury. TBI caused increases in mRNA expression of all proteins examined, with the highest expression detected in the cortex. Generally, injury magnitude and levels of gene expression were positively correlated. High levels of gene induction were observed with BID, caspase-3, and -8, while caspase-9 mRNA had the lowest level of induction. Interestingly, although calpains are activated within minutes of TBI, calpain mRNA expression was highest 72 h to 5 days post-TBI. This study is the first analysis of the regional and temporal expression of calpains and caspases after TBI. These data provide insight into the inter-relationship of these two protease families and on the distinct but overlapping cascades of cell death after TBI.

Key words: apoptosis; injury magnitude; neuronal death; proteases; RT-PCR

INTRODUCTION

UNMITIGATED PRIMARY AND SECONDARY neuronal damage and cell death following TBI play a significant role in poor clinical outcome, and emerging evidence suggests that both necrotic and apoptotic cell death contribute to TBI-induced neuropathology (Yakovlev et al., 1997; Conti et al., 1998; Newcomb et al., 1999a). Caspase-3 is a calcium-independent cysteine protease and a critical effector of apoptotic cell death that can be activated through an

[1]Department of Neuroscience, [2]Department of Neurosurgery, [3]Department of Psychiatry, [4]Center for Traumatic Brain Injuries, Evelyn F. and William L. McKnight Brain Institute of the University of Florida, Gainesville, Florida.
[5]National Institutes of Health–NIGMS, Bethesda, Maryland.

extrinsic receptor-mediated caspase-8 pathway or through an intrinsic mitochondrial caspase-9 pathway (Budihardjo et al., 1999). Calpains are calcium-dependent cysteine proteases that contribute to apoptotic and necrotic cell death (Pike et al., 1998b; Zhao et al., 1999; Newcomb-Fernandez et al., 2001). Importantly, calpain and caspase-3 have been shown to be independently and concurrently activated after TBI in different brain regions and at various times post-injury (Pike et al., 1998a). In addition, recent evidence indicates that calpains and caspases can negatively or positively modulate each other's activity depending on the model system employed (Shi et al., 2000; Rami et al., 2000; Blomgren et al., 2001; Chen et al., 2001, Witkowski et al., 2002, McGinnis et al., 1999, Wang et al., 2000). Thus, therapeutic strategies targeting both calpain and caspase proteases may prove more efficacious than selective inhibition of a single family of cysteine proteases. For instance, our laboratory has demonstrated that combined administration of calpain and caspase inhibitors in an *in vitro* model of mixed primary neuronal and glial cells provides significantly greater protection than when given separately (Pike et al., 1998b). Moreover, Rami et al., (2000) showed synergistic protection with both inhibitors in an *in vivo* model of ischemia. Importantly, while inhibition of caspase-3 and calpain protein synthesis prevents apoptotic cell death in primary neuronal cultures (Pike et al., 1998b), systematic concurrent comparison of regional and temporal assessment of *de novo* mRNA synthesis of caspase-3 and calpain related gene products after TBI has never been examined.

Increased severity of injury is associated with worse outcome and greater levels of tissue pathology and cell death (Goodman et al., 1994; Cherian et al., 1994; Raghupathi et al., 2000). For instance, in *in vivo* models of TBI, severe injury correlates with larger lesion volume, increased intracranial pressure, and decreased cortical perfusion of the contralateral cortex (Goodman et al., 1994; Cherian et al., 1994). Moderate levels of experimental TBI result in a predominately necrotic morphology (Conti et al., 1998; Newcomb et al., 1999a), while equal levels of necrotic and apoptotic morphology are observed following mild lateral fluid percussion TBI (Raghupathi et al., 2000). Factors such as the presence and duration of ischemia and increased levels of calcium, nitric oxide, and glutamate may contribute to the influence of injury magnitude on the extent and type of cell death. *In vitro*, high concentrations of A23187 (a calcium ionophore), NMDA agonists, or nitric oxide cause necrosis while lower doses are associated with apoptosis (Gwag et al., 1999; Bonfoco et al., 1995). Similarly, different injury magnitudes of mechanical stretch injury (tensile strain) to septohippocampal cell cultures result in disparate patterns of calpain and caspase-3 activation and only a moderate level of injury causes concurrent activation of cal-

pain and caspase-3 (Pike et al., 2000). In addition, magnitude of injury is correlated with temporal increases and regional distribution of intracellular calcium after controlled cortical impact TBI in rats (Fineman et al., 1993). Thus, different magnitudes of injury may trigger divergent signaling pathways that ultimately lead to calpain and/or caspase-3 mediated cell death (Wang et al., 2000). Although both calpain and caspase-3 protease activation and mRNA expression are increased in response to TBI, no study has examined the effects of different injury magnitudes on mRNA expression levels of these two major effectors of cell death. Thus, this investigation tested the hypothesis that injury magnitude would differentially affect the temporal and regional distribution of mRNA expression levels of a variety of specific genes known to be involved in cell death after TBI.

Advances in the technology of quantitative reverse transcription polymerase chain (RT-PCR) reaction in the last 5 years allow the quantitation of PCR products in real time (Gibson et al., 1996; Heid et al., 1996). Furthermore, this technology allows the simultaneous evaluation of changes in multiple transcripts. This study examined temporal and quantitative changes in caspase-3, -8, -9, BID, calpain-1, calpain-2, and calpastatin message after three magnitudes of controlled cortical impact TBI in rats. This is the first study of concurrent changes in these seven transcripts after TBI and the first study to document the dynamic relationship of injury severity with expression levels post-injury. We demonstrate that TBI increases cortical and hippocampal expression of caspase-3, caspase-8, BID, calpain-1 (mu-calpain large subunit), calpain-2 (milli-calpain large subunit), and calpastatin, and cortical caspase-9 mRNA products. Minimal induction of caspase-9 was observed in the hippocampus. Importantly, we also demonstrate that the level of injury magnitude and time are important factors affecting regional and quantitative expression of the gene products. Examining concurrent changes in message level may shed light on the inter-relationship of these two important cysteine protease families and on the distinct but overlapping cascades to cell death after TBI. The quantitative and temporal differences between mild and severe injury magnitudes may lead to a more specific, and hence, more effective therapeutic intervention.

MATERIALS AND METHODS

Rat Traumatic Brain Injury Model

As previously described (Dixon et al., 1991), a controlled cortical impact device (CCI) was used to produce traumatic brain injury (TBI) in rodents. Cortical impact TBI results in cortical deformation within the vicinity of

the impactor tip associated with contusion and neuronal and axonal damage (Gennarelli, 1994; Meaney et al., 1994). Adult male (280–300 g) Sprague-Dawley rats (Harlan, Indianapolis, IN) were initially anesthetized with 4% isoflurane in a carrier gas of 1:1 O_2/N_2O (4 min) followed by maintenance anesthesia of 2.5% isoflurane in the same carrier gas. Core body temperature was monitored continuously by a rectal thermistor probe and maintained at $37 \pm 1°C$ by placing an adjustable temperature-controlled heating pad beneath the rats. Animals were mounted in a stereotactic frame in a prone position and secured by ear and incisor bars. A midline cranial incision was made, the soft tissues were reflected, and a unilateral (ipsilateral to site of impact) craniotomy (7 mm diameter) was performed adjacent to the central suture, midway between bregma and lambda. The dura mater was kept intact over the cortex. Brain trauma in rats was produced by impacting the right cortex (ipsilateral cortex) with a 5-mm-diameter aluminum impactor tip (housed in a pneumatic cylinder) at a velocity of 3.5 m/sec with a 150-msec dwell time (compression duration). Compression depth was adjusted to produce different injury magnitudes: 1.0 mm for mild injury, 1.2 mm for moderate injury, or 1.6 mm for severe injury. Velocity was controlled by adjusting the pressure (compressed N_2) supplied to the pneumatic cylinder. Velocity and dwell time were measured by a linear velocity displacement transducer (Lucas Shaevitz™ model 500 HR; Detroit, MI) that produces an analogue signal by a storage-trace oscilloscope (BK Precision, model 2522B; Placentia, CA). Three naive animals did not undergo any procedures prior to euthanasia. Sham-injured animals underwent the identical surgical procedure of a craniotomy but did not receive an injury. Sham-injured animals were euthanized at 6, 24, 72, and 120 h after craniotomy. Two rats per sham group were used at four time points (eight rats). Three rats per injury group at three injury levels were used at four time points (36 rats) of 6, 24, 72, and 120 h after TBI. Appropriate pre- and post-injury management were maintained, and these measures complied with all guidelines set forth by the University of Florida Institutional Animal Care and Use Committee and the National Institutes of Health guidelines detailed in the *Guide for the Care and Use of Laboratory Animals*.

Quantitative-PCR

Quantitative PCR analysis was performed as previously described in our laboratory (Tolentino et al., 2002). The ipsilateral cortex and hippocampus were dissected from each rat, and snap frozen in liquid nitrogen and stored at $-80°C$. Tissue was homogenized in 50 mg/mL TRIzol (Invitrogen, Carlsbad, CA), and total RNA was extracted according to the manufacturer's directions. After suspension in DEPC water, concentration was calculated by A_{260} measurement for individual rat cortex and hippocampus.

For synthesis of first strand cDNA, 3 μg RNA of each sample was incubated with 0.01 M DTT, 0.5 mM dNTP mix (each dNTP), 0.5 μg oligo (dT) primer, and 200 U Superscript II reverse transcriptase at 37°C for 1 h. The resulting cDNA products were diluted fivefold with DEPC water. cDNA product (1 μL) was used per PCR reaction. Primer and probe sets for quantitative RT-PCR were designed using Primer3 interface available online from Whitehead Institute for Biomedical Research. The primer sequences and GeneBank accession number of relevant templates are shown in Table 1.

TABLE 1. PRIMER SEQUENCES FOR ALL GENES IN THIS STUDY

Target genes	Accession no.	Primer set	Primer sequences
Caspase-3	NM012922	Forward primer	5′-ggccctgaaatacgaagtca
	Rat	Reverse primer	5′-ggcagtagtcgcctctgaag
Caspase-9	AF286006	Forward primer	5′-ctcaggccagaggttctcac
	Rat	Reverse primer	5′-caggaaccgctcttcttgtc
Caspase-8	AF279308	Forward primer	5′-gcgacaggttacagctctcc
	Rat	Reverse primer	5′-atcaagcaggctcgagttgt
BID	AF259503	Forward primer	5′-accgtgatttccaccaagag
	Rat	Reverse primer	5′-gcaccctcagtccatctcat
Calpain-1	U53858	Forward primer	5′-cagtttggggagtgggtaga
	Rat	Reverse primer	5′-gtcctccatcttgaccctca
Calpain-2	L09120	Forward primer	5′-cttccaggatccttccttcc
	Rat	Reverse primer	5′-gggcagttgtcattccactt
Calpastatin	X56729	Forward primer	5′-aatgctgctttggatgacctg
	Rat	Reverse primer	5′-acctgtactcagcaggtactg
GAPDH	AF106860	Forward primer	5′-ggctgccttctcttgtgac
	Rat	Reverse primer	5′-ggccgcctgcttcaccac

Quantitative PCR was carried out using a Roche Light-Cycler (Roche Diagnostics, Indianapolis, IN) on the cDNA products: 1 × LightCycler FastStart DNA Master SYBR Green I (Roche Diagnostics, Indianapolis, IN), 1.5 mM $MgCl_2$ (Roche Diagnostics, Indianapolis, IN), 6% DMSO (FisherBrand), 0.5 μM each primer (Integrated DNA Technologies). Caspase 3, 8, 9, BID, calpastatin, and calpain-1 were run at 95°C for 5 min, 1 cycle of 95°C for 5 sec, 65°C for 10 sec, 72°C for 35 sec; 1 cycle of 95°C for 5 sec, 63°C for 10 sec, 72°C for 35 sec; and 38 cycles of 95°C for 5 sec, 60°C for 10 sec, 72°C for 35 sec. Calpain-2 was run at 95°C for 5 min, followed by 40 cycles of 95°C for 5 sec, 55°C for 10 sec, and 72°C for 35 sec. Additional reactions on known dilutions of cDNA template were performed during each LightCycler run to allow construction of a standard curve. The housekeeping gene glyceraldehydes-3-phosphate dehydrogenase (GAPDH) was used as the quality control for the RNA purification and reverse transcription.

Statistical Analysis

For each type of mRNA studied, the average expression from three naive rats was set to 100%. The mean level (± SE) of each transcript at each timepoint from rats after craniotomies and after three injury magnitudes of TBI was calculated as a percent of the average of naive expression. Two-way ANOVA was used to examine main effects and interaction effects of time and injury magnitude. One-way ANOVA with contrast to do pairwise comparisons was used to determine significance between mean levels of mRNA at individual timepoints.

RESULTS

RT-PCR was employed to examine changes in mRNA levels for caspase-3, caspase-9, caspase-8, BID, calpain-1, calpain-2, and calpastatin in rats subjected to CCI at three different levels of injury magnitude (1.0, 1.2, 1.6 mm) or to craniotomy. Statistically significant differences were found between the injured and sham-injured animals for the majority of mRNA transcripts examined.

Caspase-3

Injury and time interacted to significantly affect levels of caspase-3 mRNA in the ipsilateral cortex ($p < 0.0001$). Across time, severe (1.6 mm) and moderate (1.2 mm) injury increased levels of cortical caspase-3 mRNA compared to levels after sham injury ($p \leq 0.001$ and $p \leq 0.01$, respectively) and levels were higher after severe (1.6 mm) injury than after mild (1.0 mm) injury ($p < 0.05$).

Differences in levels of cortical caspase-3 mRNA at individual timepoints compared to sham-injury are shown in Figure 1. After severe (1.6 mm) injury, caspase-3 mRNA levels peaked at 24 h (529%, $p < 0.05$) and remained significantly high at 72 h (460%, $p < 0.05$), decreasing at 120 h (405%, $p < 0.05$). After moderate injury (1.2 mm), caspase-3 mRNA levels were significantly increased 24 h (455%, $p < 0.05$) and 72 h (475%, $p < 0.05$) after injury. Caspase-3 mRNA levels following mild injury (1.0 mm) were not significantly different at any timepoint from sham-injury levels.

In the ipsilateral hippocampus, injury and time interacted to significantly affect levels of caspase-3 ($p < 0.0001$). Across time, severe (1.6 mm) injury increased levels of hippocampal caspase-3 mRNA compared to levels after sham injury ($p < 0.001$) and levels were higher after severe (1.6 mm) injury than after mild (1.0 mm) injury ($p < 0.001$).

Differences in levels of hippocampal caspase-3 mRNA at individual timepoints compared to sham-injury are shown in Figure 2. Caspase-3 mRNA levels were significantly increased 24 h (207%, $p < 0.01$) and 72 h (198%, $p < 0.01$) after severe (1.6 mm) injury compared to sham-injury. Following moderate injury, caspase-3 mRNA levels were significantly increased at 72 h (198%, $p < 0.01$) in the hippocampus. After mild injury, hippocampal caspase-3 mRNA did not increase compared to sham injury. Hippocampal caspase-3 mRNA levels were higher after severe (1.6 mm) injury than after moderate (1.2 mm) injury at 24 h ($p < 0.01$) and than after mild (1.0 mm) injury at 24 h ($p < 0.001$) and at 72 h ($p < 0.01$). At 72 h, levels of caspase-3 mRNA were different between moderate (1.2 mm) and mild (1.0 mm) injury ($p < 0.01$).

Caspase-9

Injury and time interacted to significantly affect levels of caspase-9 mRNA in the ipsilateral cortex ($p < 0.0001$). Across time, severe (1.6 mm) injury increased levels of cortical caspase-9 mRNA compared to levels after sham-injury ($p \leq 0.05$) and levels were higher after severe (1.6 mm) injury than after mild (1.0 mm) injury ($p < 0.01$).

Differences in levels of cortical caspase-9 mRNA at individual timepoints compared to sham-injury are shown in Figure 1. Caspase-9 mRNA levels in the ipsilateral cortex increased significantly at 6 h (235%, $p < 0.01$) and 72 h (246%, $p < 0.05$) after severe injury (1.6 mm). After moderate (1.2 mm) and mild (1.0) injury, no significant change was noted compared to sham-injury. Cortical caspase-9 mRNA levels were significantly higher after severe (1.6 mm) injury than after mild (1.0 mm) injury ($p < 0.05$) at 6 h and 72 h ($p < 0.001$). At 120 h,
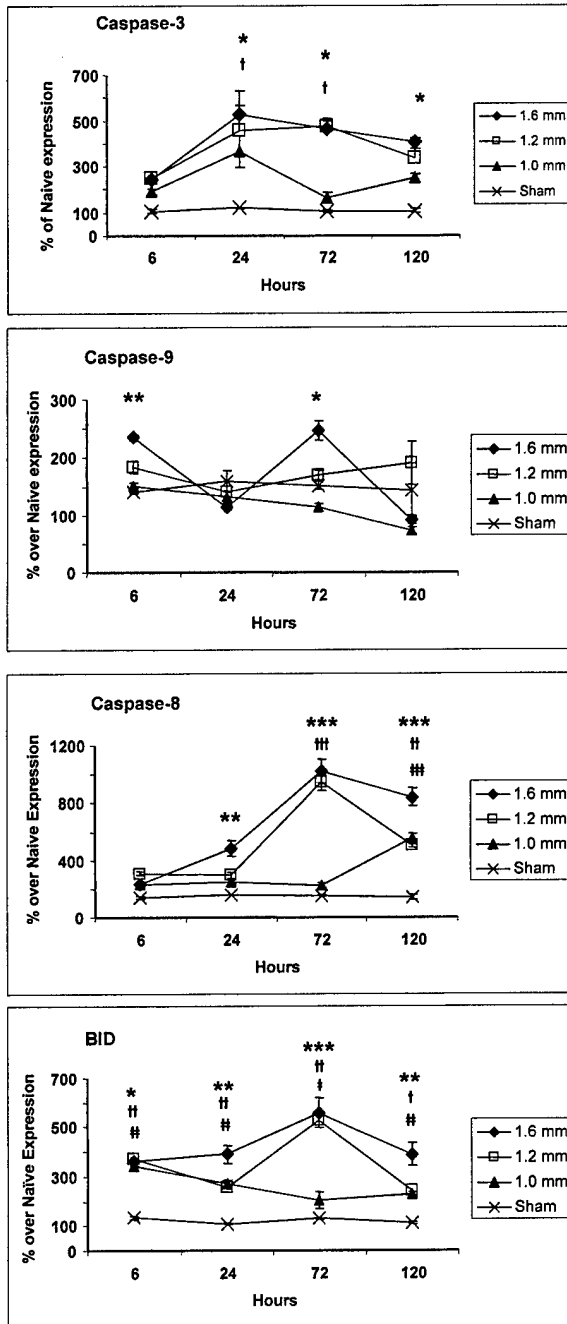
Ipsilateral Cortex

FIG. 1. Temporal expressions of caspase-3, caspase-9, caspase-8, and BID mRNA levels are affected by the severity of injury magnitude in the ipsilateral cortex. Mean levels of mRNA ($\pm$ SEM) of caspase-3, caspase-9, caspase-8, and BID were analyzed 6, 24, 72, and 120 h following mild (1.0 mm), moderate (1.2 mm), and severe (1.6 mm) CCI injury by semi-quantitative PCR analysis. Mean levels of mRNA from rats after ($\blacklozenge$) 1.6 mm injury; after ($\square$) 1.2 mm injury; after ($\blacktriangle$) 1.0 mm injury, or after ($\times$) sham-craniotomy are expressed as a percentage of the average of mRNA from three naive rats set to 100%. One-way ANOVA with contrast to do pair-wise comparisons was used to determine significance between mean mRNA levels after sham injury compared to mean levels after injury at individual timepoints. In general, greater injury severity was associated with higher relative increased expression of gene products over control levels. *$p < 0.05$, **$p < 0.01$, and ***$p < 0.0001$ for 1.6 mm injury compared to sham-injured controls. $^\dagger p < 0.05$, $^{\dagger\dagger} p < 0.01$, and $^{\dagger\dagger\dagger} p < 0.0001$ for 1.2-mm injury compared to sham-injured controls. $^\ddagger p < 0.05$, $^{\ddagger\ddagger} p < 0.01$, and $^{\ddagger\ddagger\ddagger} p < 0.0001$ for 1.0 mm injury compared to sham-injured controls.

caspase-9 mRNA levels were higher after moderate (1.2 mm) injury than mild (1.0 mm) injury ($p < 0.05$).

In the ipsilateral hippocampus, injury and time interacted to significantly affect levels of caspase-9 ($p < 0.0001$). At individual timepoints, caspase-9 mRNA levels were significantly less at 6 h after severe (1.6 mm) and mild (1.0 mm) injury compared to sham-injury ($p < 0.05$) (Fig. 2). At 72 h, caspase-9 mRNA was higher af-

ter mild (1.0 mm) injury than after moderate (1.2 mm) or severe (1.6 mm) injury ($p < 0.05$).

Caspase-8

Injury and time interacted to significantly affect levels of caspase-8 mRNA in the ipsilateral cortex ($p < 0.0001$) and across time, all treatment groups were significantly
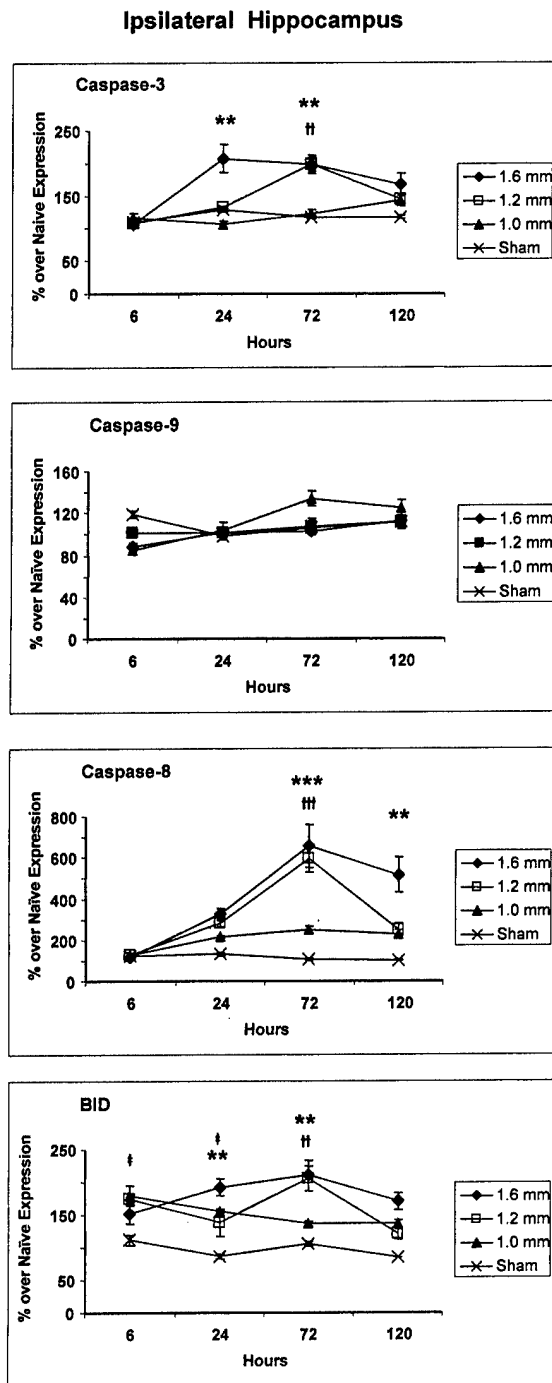
Ipsilateral Hippocampus

FIG. 2. Temporal expressions of caspase-3, caspase-9, caspase-8, and BID mRNA levels are affected by the severity of injury magnitude in the ipsilateral hippocampus. Mean levels of mRNA ($\pm$ SEM) of caspase-3, caspase-9, caspase-8, and BID were analyzed 6, 24, 72, and 120 h following mild (1.0 mm), moderate (1.2 mm), and severe (1.6 mm) CCI injury by semi-quantitative PCR analysis. Mean levels of mRNA from rats after ($\blacklozenge$) 1.6 mm injury; after ($\square$) 1.2 mm injury; after ($\blacktriangle$) 1.0 mm injury, or after ($\times$) sham-craniotomy are expressed as a percentage of the average of mRNA from three naive rats set to 100%. One-way ANOVA with contrast to do pair-wise comparisons was used to determine significance between mean mRNA levels after sham injury compared to mean levels after injury at individual timepoints. $*p < 0.05$, $**p < 0.01$, and $***p < 0.0001$ for 1.6 mm injury compared to sham-injured controls. $^{\dagger}p < 0.05$, $^{\dagger\dagger}p < 0.01$, and $^{\dagger\dagger\dagger}p < 0.0001$ for 1.2 mm injury compared to sham-injured controls. $^{\ddagger}p < 0.05$, $^{\ddagger\ddagger}p < 0.01$, and $^{\ddagger\ddagger\ddagger}p < 0.0001$ for 1.0 mm injury compared to sham-injured controls.

different from each other. Across time, levels of cortical caspase-8 mRNA were higher after severe (1.6 mm) injury than after moderate (1.2 mm) injury ($p < 0.01$), after mild (1.0 mm) injury ($p < 0.0001$) and after sham-injury ($p < 0.0001$). Caspase-8 mRNA levels were higher after moderate (1.2 mm) injury than after mild (1.0 mm) injury ($p < 0.001$) or after sham-injury ($p < 0.0001$) and

levels were higher after mild (1.0 mm) injury than after sham-injury ($p < 0.01$).

Differences in levels of cortical caspase-8 m RNA at individual timepoints compared to sham-injury are shown in Figure 1. Levels of caspase-8 mRNA were significantly increased 24, 72, and 120 h after severe injury and 72 and 120 h after moderate in the ipsilateral cortex com-

834

pared to after sham-injury. Following severe (1.6 mm) injury, caspase-8 mRNA levels increased at 24 h (484%, $p < 0.01$), 72 h (1016%, $p < 0.0001$), and 120 h (840%, $p < 0.0001$). After moderate (1.2 mm) injury, caspase-8 mRNA levels were increased by 72 h (941%, $p < 0.0001$), and 120 h (504%, $p < 0.01$) after injury. Caspase-8 mRNA levels were significantly increased 120 h (553%, $p < 0.0001$) following mild (1.0 mm) injury. Levels of caspase-8 mRNA were elevated after severe (1.6 mm) injury compared to moderate (1.2 mm) injury at 24 h ($p < 0.05$) and 120 h ($p < 0.05$) and compared to mild (1.0 mm) injury at 24 h ($p < 0.05$), 72 h ($p < 0.0001$), and 120 h ($p < 0.01$). Cortical caspase-8 levels significantly differed between moderate (1.2 mm) and mild (1.0 mm) injury at 72 h ($p < 0.0001$).

In the ipsilateral hippocampus, injury and time interacted to significantly affect levels of caspase-8 mRNA ($p < 0.0001$). Across time, levels of hippocampal caspase-8 mRNA were higher after severe (1.6 mm) injury than after mild (1.0 mm) injury ($p < 0.001$) and after sham-injury ($p < 0.0001$). Caspase-8 mRNA levels were higher after moderate (1.2 mm) injury than after mild (1.0 mm) injury ($p < 0.05$) or after sham-injury ($p = 0.001$).

At individual timepoints, hippocampal caspase-8 mRNA levels significantly increased 72 h following both moderate (594%) and severe (657%) injury ($p < 0.0001$) compared to sham-injury (Fig. 2). Levels of hippocampal caspase-8 did not differ after mild (1.0 mm) injury compared to sham-injury. At 72 h, caspase-8 mRNA was less after mild (1.0 mm) injury than after moderate (1.2 mm) ($p < 0.01$) or severe (1.6 mm) injury ($p < 0.001$). Hippocampal caspase-8 mRNA was higher after severe (1.6 mm) injury at 120 h than after sham injury ($p < 0.001$) or after moderate (1.2 mm) injury ($p < 0.05$).

BID

Injury and time interacted to significantly affect levels of BID mRNA in the ipsilateral cortex ($p < 0.0001$) and across time, all treatment groups were significantly different from each other. Across time, levels of cortical BID mRNA were higher after severe (1.6 mm) injury than after moderate (1.2 mm) injury ($p < 0.05$), after mild (1.0 mm) injury ($p < 0.0001$) and after sham-injury ($p < 0.05$). BID mRNA levels were higher after moderate (1.2 mm) injury than after mild (1.0 mm) injury ($p < 0.05$) or after sham-injury ($p < 0.0001$) and levels were higher after mild (1.0 mm) injury than after sham-injury ($p < 0.001$).

Differences in levels of cortical BID mRNA at the individual timepoints compared to sham-injury are shown in Figure 1. BID mRNA levels significantly increased at all three injury levels at all time points in the ipsilateral cortex. After 1.6 mm injury, BID mRNA levels significantly increased at 6 h, (360%, $p < 0.05$) (at 24 h, 390%,

$p < 0.001$), at 72 h, (557%, $p < 0.001$), and at 120 h (388%, $p < 0.001$). After moderate (1.2 mm) injury, BID mRNA levels significantly increased at 6 h (372%, $p < 0.001$), at 24 h (254% $p < 0.001$), at 72 h (526%, $p < 0.001$) and at 24 h (240%, $p < 0.05$). After mild (1.0) mm injury, BID mRNA levels increased at 6 h (341%, $p < 0.001$), at 24 h (268%, $p < 0.001$), at 72 h (203%, $p < 0.05$), and at 120 h (227%, $p < 0.001$) after injury. Cortical BID mRNA levels were significantly less after mild (1.0 mm) injury than after severe (1.6 mm) injury at 72 h ($p < 0.0001$) and at 120 h ($p < 0.05$) and less than after moderate (1.2 mm) injury at 72 h ($p < 0.0001$).

In the ipsilateral hippocampus, injury and time interacted to significantly affect levels of BID mRNA ($p < 0.0001$). Across time, hippocampal BID mRNA levels were increased after severe (1.6 mm) injury ($p < 0.0001$), moderate (1.2 mm) injury ($p < 0.001$), and mild (1.0 mm) injury ($p < 0.01$) compared to after sham injury.

At individual timepoints, BID mRNA levels in the ipsilateral hippocampus after severe (1.6 mm) injury increased significantly at 24 h (192%, $p < 0.01$) and at 72 h (210%, $p < 0.01$) (Fig. 2) compared to levels after sham injury. After moderate (1.2 mm) injury, BID mRNA levels increased significantly at 72 h after TBI (205%, $p < 0.01$). After mild (1.0 mm) injury, BID mRNA levels increased significantly (180%, $p < 0.05$) at 6 h and (155%, $p < 0.05$) at 24 h. At 72 h, hippocampal BID mRNA was less after mild (1.0 mm) injury than after moderate (1.2 mm) or severe (1.6 mm) injury ($p < 0.05$).

Calpain-1

Injury and time interacted to significantly affect levels of calpain-1 (mu-calpain large subunit) mRNA in the ipsilateral cortex ($p < 0.0001$) and across time, all treatment groups were significantly different from each other. Across time, calpain-1 mRNA levels were higher after severe (1.6 mm) injury than after moderate (1.2 mm) injury ($p < 0.05$), after mild (1.0 mm) injury ($p < 0.0001$) and after sham-injury ($p < 0.0001$). Calpain-1 mRNA levels were higher after moderate (1.2 mm) injury than after mild (1.0 mm) injury ($p < 0.05$) or after sham injury ($p < 0.001$), and levels were higher after mild (1.0 mm) injury than after sham-injury ($p < 0.05$).

Differences in levels of cortical calpain-1 mRNA at individual timepoints compared to sham-injury are shown in Figure 3. Calpain-1 mRNA levels in the ipsilateral cortex significantly increased at 72 h (511%, $p < 0.001$) and at 120 h (330%, $p < 0.001$) after severe (1.6 mm) injury. Calpain-1 mRNA levels increased at 72 h (434%, $p < 0.0001$) after moderate (1.2 mm) injury. There was no significant change after mild (1.0 mm) injury in calpain-1 mRNA levels compared to after sham-injury. Calpain-1 mRNA levels were higher after severe (1.6 mm) injury
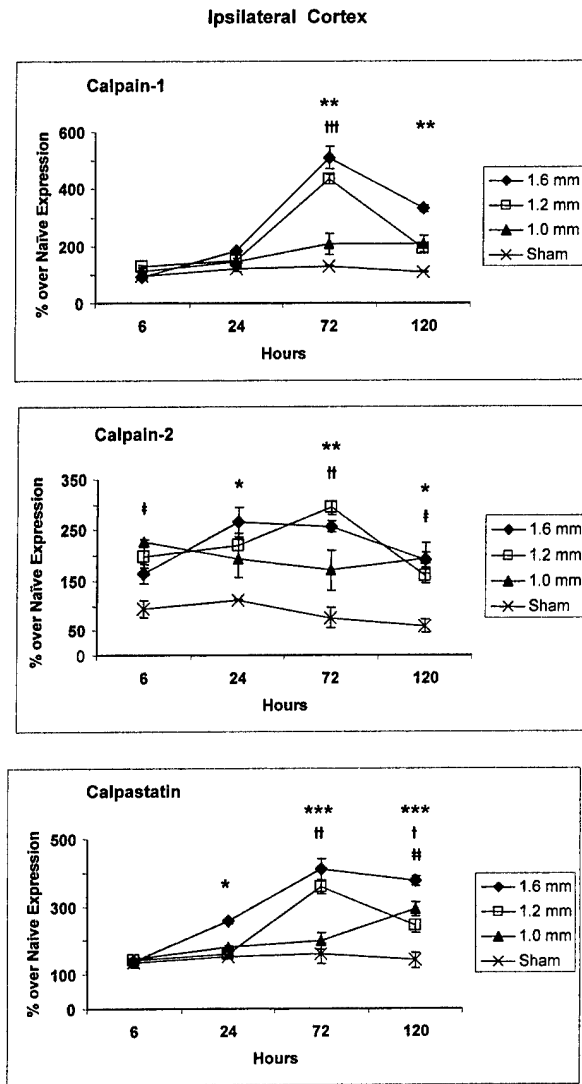
835

Ipsilateral Cortex

FIG. 3. Temporal expression of calpain-1, calpain-2, and calpastatin mRNA levels are affected by the severity of injury magnitude in the ipsilateral cortex. Mean levels of mRNA (± SEM) of calpain-1, calpain-2, and calpastatin were analyzed 6, 24, 72, and 120 h following mild (1.0 mm), moderate (1.2 mm), and severe (1.6 mm) CCI injury by semi-quantitative PCR analysis. Mean levels of mRNA from rats after (◆) 1.6 mm injury; after (□) 1.2 mm injury; after (▲) 1.0 mm injury, or after (✕) sham-craniotomy are expressed as a percentage of the average of mRNA from three naive rats set to 100%. One-way ANOVA with contrast to do pair-wise comparisons was used to determine significance between mean mRNA levels after sham-injury compared to mean levels after injury at individual timepoints. As with the caspases, greater injury severity was associated with higher relative increased expression of gene products over control levels. $*p < 0.05$, $**p < 0.01$, and $***p < 0.0001$ for 1.6 mm injury compared to sham-injured controls. $^{\dagger}p < 0.05$, $^{\dagger\dagger}p < 0.01$, and $^{\dagger\dagger\dagger}p < 0.0001$ for 1.2 mm injury compared to sham-injured controls. $^{\ddagger}p < 0.05$, $^{\ddagger\ddagger}p < 0.01$, and $^{\ddagger\ddagger\ddagger}p < 0.0001$ for 1.0 mm injury compared to sham-injured controls.

than after mild (1.0 mm) injury at 72 h ($p < 0.0001$) and 120 h ($p < 0.05$).

In the ipsilateral hippocampus, injury and time interacted to significantly affect levels of calpain-1 mRNA ($p < 0.0001$). Across time, hippocampal calpain-1 mRNA was significantly increased after severe (1.6 mm) and moderate (1.2 mm) injury ($p < 0.01$) compared to after sham injury.

At individual timepoints, calpain-1 mRNA levels significantly increased after severe (1.6 mm) injury at 72 h (207%, $p < 0.05$) in the ipsilateral hippocampus (Fig. 4). After moderate (1.2 mm) injury, calpain-1 mRNA levels significantly increased at 24 h (198%, $p < 0.05$) and 72 h (190%, $p < 0.05$). There was no significant change in calpain-1 mRNA levels after the mildest (1.0 mm) injury.

Calpain-2

Injury and time interacted to significantly affect levels of calpain-2 mRNA in the ipsilateral cortex ($p < 0.0001$). Across time, calpain-2 mRNA levels were increased after severe (1.6 mm) injury ($p < 0.001$), moderate (1.2 mm) injury ($p < 0.001$), and mild (1.0 mm) injury ($p < 0.01$) compared to after sham injury.

At individual time points, cortical calpain-2 mRNA levels after severe (1.6 mm) injury increased significantly at 24 h (266%, $p < 0.05$), 72 h (256%, $p < 0.01$), and 120 h (190%, $p < 0.05$) (Fig. 3). After moderate (1.2 mm) injury, calpain-2 levels increased significantly (294%, $p < 0.01$) at 72 h. Calpain-2 mRNA levels after the mildest (1.0 mm) injury were significantly higher than after sham injury at (229.2%, $p < 0.05$) 6 h and (195.2, $p < 0.05$) 120 h. Calpain-2 mRNA levels differed between moderate (1.2 mm) and mild (1.0 mm) injury at 72 h ($p < 0.05$).

In the ipsilateral hippocampus, injury and time interacted to significantly affect levels of calpain-2 ($p < 0.0001$). Across time, hippocampal calpain-2 mRNA was significantly less after sham-injury than after mild (1.0 mm) injury ($p < 0.05$) or after severe (1.6 mm) injury ($p < 0.01$).

At individual timepoints, hippocampal calpain-2 mRNA levels at 24 h after TBI were significantly greater after severe (1.6 mm) injury (302%, $p < 0.001$), moderate (1.2 mm) injury (230%, $p < 0.05$), and after mild (1.0 mm) injury (287%, $p < 0.01$) compared to sham injury (Fig. 4).

Calpastatin

Injury and time interacted to significantly effect levels of calpastatin mRNA in the ipsilateral cortex ($p < 0.0001$). Across time, calpastatin mRNA levels were increased after severe (1.6 mm) injury ($p < 0.0001$), mod-
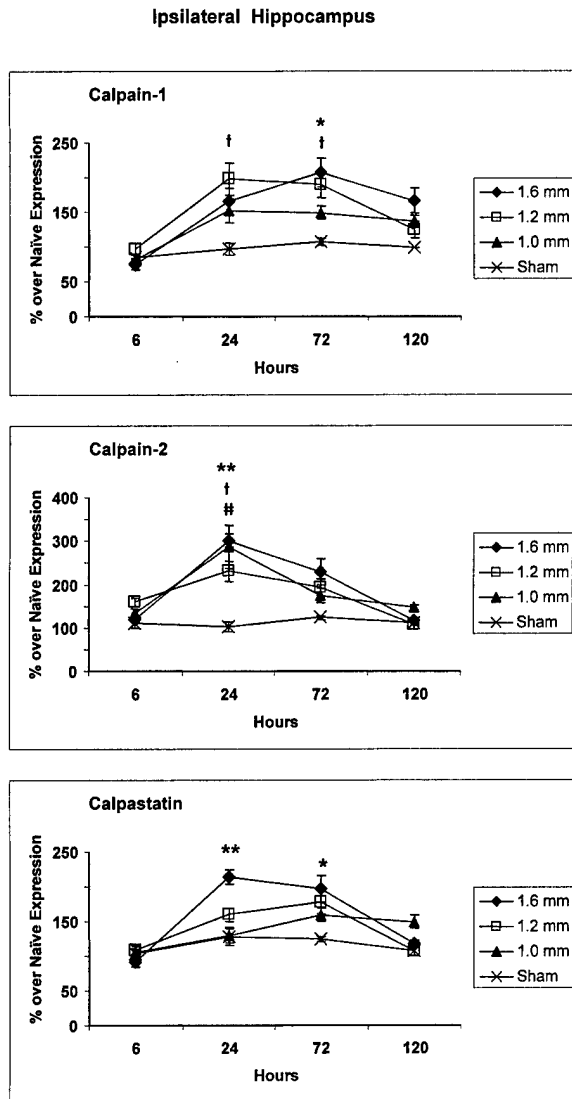
Ipsilateral Hippocampus

FIG. 4. Temporal expression of calpain-1, calpain-2, and calpastatin mRNA levels are affected by the severity of injury magnitude in the ipsilateral hippocampus. Mean levels of mRNA ($\pm$ SEM) of calpain-2, calpain-1 and calpastatin were analyzed 6, 24, 72, and 120 h following mild (1.0 mm), moderate (1.2 mm), and severe (1.6 mm) CCI injury by semi-quantitative PCR analysis. Mean levels of mRNA from rats after ($\blacklozenge$) 1.6 mm injury; after ($\square$) 1.2 mm injury; after ($\blacktriangle$) 1.0 mm injury, or after ($\times$) sham-craniotomy are expressed as a percentage of the average of mRNA from three naive rats set to 100%. One-way ANOVA with contrast to do pair-wise comparisons was used to determine significance between mean mRNA levels after sham-injury compared to mean levels after injury at individual timepoints. As with the caspases, greater injury severity was associated with higher relative increased expression of gene products over control levels. Relative increased expression of calpastatin, the endogenous inhibitor of calpains, generally paralleled relative increased expression of calpain-1 and -2. $*p < 0.05$, $**p < 0.01$, and $***p < 0.0001$ for 1.6 mm injury compared to sham-injured controls. $^{\dagger}p < 0.05$, $^{\dagger\dagger}p < 0.01$, and $^{\dagger\dagger\dagger}p < 0.0001$ for 1.2 mm injury compared to sham-injured controls. $^{\ddagger}p < 0.05$, $^{\ddagger\ddagger}p < 0.01$, and $^{\ddagger\ddagger\ddagger}p < 0.0001$ for 1.0 mm injury compared to sham-injured controls.

erate (1.2 mm) injury ($p < 0.01$), and mild (1.0 mm) injury ($p < 0.05$) compared to after sham injury. Calpastatin mRNA levels were significantly higher after severe (1.6 mm) injury than after moderate (1.2 mm) injury ($p < 0.01$) and after mild (1.0 mm) injury ($p < 0.0001$).

At individual timepoints, calpastatin mRNA levels significantly increased at 24 h (258%, $p < 0.05$), at 72 h (411%, $p < 0.0001$), and at 120 h (375%, $p < 0.0001$) in the ipsilateral cortex after severe (1.6 mm) injury compared to after sham-injury (Fig. 3). After moderate (1.2 mm) injury, calpastatin mRNA levels significantly increased (357%, $p < 0.001$) at 72 h and (243%, $p < 0.05$) at 120 h. After mild (1.0 mm) injury, calpastatin mRNA levels increased (292%, $p < 0.01$) at 120 h. Higher levels of calpastatin mRNA were found after severe (1.6

mm) injury than after moderate (1.2 mm) injury at 24 h ($p < 0.05$) and 120 h ($p < 0.01$). At 72 h, calpastatin mRNA levels were lower after mild (1.0 mm) injury than after moderate (1.2 mm) injury ($p < 0.001$) or after severe (1.6 mm) injury ($p < 0.0001$).

In the ipsilateral hippocampus, injury and time interacted to significantly effect levels of calpastatin mRNA ($p < 0.0001$). Across time, hippocampal calpastatin mRNA levels were only elevated after severe (1.6 mm) injury ($p < 0.01$).

At individual timepoints, hippocampal calpastatin mRNA levels significantly increased (214%, $p < 0.01$) at 24 h and (197%, $p < 0.05$) at 72 h after severe (1.6 mm) injury (Fig. 4). Calpastatin mRNA levels did not increase after moderate (1.2 mm) or mild (1.0 mm) injury. At 24 h, hippocampal calpastatin mRNA was higher af-

RINGGER ET AL.

ter severe (1.6 mm) injury than after mild (1.0 mm) injury ($p < 0.01$).

DISCUSSION

This is the first study to concurrently examine the relative changes in gene expression of the calpain and caspase cysteine protease families after TBI. While numerous studies have shown activation of these proteins following TBI, no study has concurrently examined these proteins at a molecular level following this type of injury. We report the relative response of each gene to injury magnitude across time in the injured cortex and hippocampus after TBI. Importantly, the level of injury magnitude significantly affected the temporal and regional expression of genes that were examined. The temporal pattern of increased mRNA expression suggests that the delayed and sustained increases in mRNA expression of calpains and cysteine proteases may have an integral role in delayed neuronal cell death after TBI.

Caspase-3

Caspase-3 is activated upstream by caspase-8 and caspase-9 and is considered a key executioner of apoptosis (Eldadah and Faden, 2000). Similar to the current study, caspase-3 mRNA peaked 24 h after injury in the ipsilateral cortex and hippocampus (Yakovlev et al., 1997). Activation of constitutively expressed caspase-3 may be involved in the acute period, while *de novo* synthesis of caspase-3 may be required for delayed apoptotic cell death.

Caspase-9

Activation of the intrinsic caspase-9–mediated pathway following TBI (Nathaniel et al., 2000; Knoblach et al., 2002; Yakovlev et al., 2001) has been suggested to be due to loss of mitochondrial integrity (Verweij et al., 1997; Xiong et al., 1997; Sullivan et al., 1998; Verweij et al., 2000) and release of cytochrome-c (Buki et al., 2000; Thompson et al., 2000). A small but significant increase in caspase-9 mRNA was seen in the ipsilateral cortex across time after 1.6 mm (severe) injury magnitude, while no increases were detected in the ipsilateral hippocampus, a finding similar to that observed in a focal model of ischemia (Harrison et al., 2001). The increased caspase-9 protein activity observed after lateral fluid percussion injury (Knoblach et al., 2002; Yakovlev et al., 2001) and CCI (Nathaniel et al., 2000) may be the result of differences in constitutive versus *de novo* expression of caspase-9 protein.

Caspase-8

FAS (Beer et al., 2000; Lenzlinger et al., 2002; Matsushita et al., 2000) and TNF (Shohami et al., 1994; Fan et al., 1996) both increase after TBI and likely activate the extrinsic pathway employing caspase-8 and BID. Caspase-8 mRNA upregulation supports recent work by Beer et al. (2001), who reported an increase in caspase-8 mRNA from 1 to 72 h in the ipsilateral cortex after CCI. In the present study, increased injury magnitude plays a key role in the temporal peak of caspase-8 mRNA.

BID

This is the first paper to report an increase in both cortical and hippocampal BID message after TBI. Increased levels of caspase-8 and BID message after TBI further suggest that the extrinsic pathway may be a vital part of cell death after TBI. Caspase-8 may directly activate caspase-3 or indirectly through BID release mitochondrial factors that activate caspase-9 and caspase-3 (Budihardjo et al., 1999). Recent work has shown that BID protein was increased from 6 h to 7 days after controlled cortical impact (Franz et al., 2002). BID appears to have a significant contribution to ischemic neuronal cell death (Benchoua et al., 2001; Plesnila et al., 2001), and the continued increase in BID mRNA likely has an equally significant role in delayed or secondary neuronal cell death after TBI.

Calpain-1 and -2

Calpain, a cysteine protease, is activated in necrotic and apoptotic models of cell death (Wang et al., 2000; Chan and Mattson, 1999).

The relative gene expression of calpain-2 markedly increased in the hippocampus and peaked 24 h after all three injury magnitudes studied. A role for calpain-2 in the activation of caspase-3 has been suggested *in vitro* and *in vivo* in a neonatal hypoxia-ischemia model (Blomgren et al., 2001). Importantly, caspase-3 and calpain-2 had similar temporal peaks in response to injury magnitude in the ipsilateral cortex and their relationship warrants further attention.

Rapid activation of calpain after TBI most likely stems from activation of constitutively expressed calpains. However, *de novo* synthesis of calpains may be required for delayed apoptotic cell death. In addition, calpains may play a role in membrane repair and resealing as well as in dendritic remodeling after injury (Faddis et al., 1997). Thus, increased mRNA levels of calpain may be indicative of both a pathological as well as a normal physiological role. Additional studies are required to clarify calpain's complex role in TBI pathology.

Calpastatin

Calpastatin is an endogenous inhibitor of calpain. Previous studies by our group showed that calpastatin protein increased as calpain activity decreased in a CCI model of TBI (Newcomb et al., 1999b); however, a reciprocal relationship was not detected at the message level between calpastatin and calpain-1 and -2. Rather, calpastatin mRNA had a similar pattern of increase to calpain-1 mRNA across all three injury magnitudes in the ipsilateral cortex and hippocampus. Increases in mRNA levels for both calpains and calpastatins likely reflect the tight regulatory control of calpastatin and calpains at the cellular level.

CONCLUSION

In conclusion, we have presented the first studies to examine concurrent temporal and regional changes in mRNA levels of calpains and caspases after three levels of injury magnitude. Importantly, the magnitude of injury affected the regional distribution and temporal pattern of mRNA expression. The significant and concurrent increases in caspase-8, caspase-3, and BID implicate the extrinsic pathway for a promising target of therapeutic intervention. It is hoped that this information will further our ability to understand the pathophysiological response to different magnitudes of injury and optimize the therapeutic window. Future studies are required to address the important implications raised by this study—that injury severity causes differential expression of numerous effectors of cellular pathology and that a targeted therapeutic approach must take issues of injury severity and time post injury into account.

REFERENCES

BEER, R., FRANZ, G., SRINIVASAN, A., et al. (2000). Temporal profile and cell subtype distribution of activated caspase-3 following experimental traumatic brain injury. J. Neurochem. **75**, 1264–1273.

BEER, R., FRANZ, G., KRAJEWSKI, S., et al. (2001). Temporal and spatial profile of caspase 8 expression and proteolysis after experimental traumatic brain injury. J. Neurochem. **78**, 862–873.

BENCHOUA, A., GUEGAN, C., COURIAUD, C., et al. (2001). Specific caspase pathways are activated in the two stages of cerebral infarction. J. Neurosci. **21**, 7127–7134.

BLOMGREN, K., ZHU, C., WANG, X., et al. (2001). Synergistic activation of caspase-3 by m-calpain after neonatal hypoxia–ischemia: a mechanism of "pathological apoptosis"? J. Biol. Chem. **276**, 10191–10198.

BONFOCO, E., KRAINC, D., ANKARCRONA, M., et al. (1995). Apoptosis and necrosis: two distinct events induced, respectively, by mild and intense insults with N-methyl-D-aspartate or nitric oxide/superoxide in cortical cell cultures. Proc. Natl. Acad. Sci. USA **92**, 7162–7166.

BUDIHARDJO, I., OLIVER, H., LUTTER, M., et al. (1999). Biochemical pathways of caspase activation during apoptosis. Annu. Rev. Cell. Dev. Biol. **15**, 269–290.

BUKI, A., OKONKWO, D.O., WANG, K. K., et al. (2000). Cytochrome c release and caspase activation in traumatic axonal injury. J. Neurosci. **20**, 2825–2834.

CHAN, S.L., and MATTSON, M.P. (1999). Caspase and calpain substrates: roles in synaptic plasticity and cell death. J. Neurosci. Res. **58**, 167–190.

CHEN, M., HE, H., ZHAN, S., et al. (2001). Bid is cleaved by calpain to an active fragment *in vitro* and during myocardial ischemia/reperfusion. J. Biol. Chem. **276**, 30724–30728.

CHERIAN, L., ROBERTSON, C.S., CONTANT, C. F., JR., et al. (1994). Lateral cortical impact injury in rats: cerebrovascular effects of varying depth of cortical deformation and impact velocity. J. Neurotrauma **11**, 573–585.

CONTI, A.C., RAGHUPATHI, R., TROJANOWSKI, J.Q., et al. (1998). Experimental brain injury induces regionally distinct apoptosis during the acute and delayed post-traumatic period. J. Neurosci. **18**, 5663–5672.

DIXON, C.E., CLIFTON, G.L., LIGHTHALL, J.W., et al. (1991). A controlled cortical impact model of traumatic brain injury in the rat. J. Neurosci. Methods **39**, 253–262.

ELDADAH, B.A., and FADEN, A.I. (2000) Caspase pathways, neuronal apoptosis, and CNS injury. J. Neurotrauma **17**, 811–829.

FADDIS, B.T., HASBANI, M.J., and GOLDBERG, M.P. (1997). Calpain activation contributes to dendritic remodeling after brief excitotoxic injury *in vitro*. J. Neurosci. **17**, 951–959.

FAN, L., YOUNG, P.R., BARONE, F.C., et al. (1996). Experimental brain injury induces differential expression of tumor necrosis factor-alpha mRNA in the CNS. Brain Res. Mol. Brain Res. **36**, 287–291.

FINEMAN, I., HOVDA, D.A., SMITH, M., et al. (1993). Concussive brain injury is associated with a prolonged accumulation of calcium: a ^{45}Ca autoradiographic study. Brain Res. **624**, 94–102.

FRANZ, G., BEER, R., INTEMANN, D., et al. (2002). Temporal and spatial profile of Bid cleavage after experimental traumatic brain injury. J. Cereb. Blood Flow Metab. **22**, 951–958.

GENNARELLI, T.A. (1994). Animate models of human head injury. J. Neurotrauma **11**, 357–368.

GIBSON, U.E., HEID, C.A., and WILLIAMS, P.M. (1996). A novel method for real time quantitative RT-PCR. Genome Res. **6**, 995–1001.

GOODMAN, J.C., CHERIAN, L., BRYAN, R.M., Jr., et al. (1994). Lateral cortical impact injury in rats: pathologic effects of varying cortical compression and impact velocity. J. Neurotrauma **11**, 587–597.

GWAG, B.J., CANZONIERO, L.M., SENSI, et al. (1999). Calcium ionophores can induce either apoptosis or necrosis in cultured cortical neurons. Neuroscience **90**, 1339–1348.

HARRISON, D.C., DAVIS, R.P., BOND, B.C., et al. (2001). Caspase mRNA expression in a rat model of focal cerebral ischemia. Brain Res. Mol. Brain Res. **89**, 133–146.

HEID, C.A., STEVENS, J., LIVAK, K.J., et al. (1996). Real-time quantitative PCR. Genome Res. **6**, 986–994.

KNOBLACH, S.M., NIKOLAEVA, M., HUANG, X., et al. (2002). Multiple caspases are activated after traumatic brain injury: evidence for involvement in functional outcome. J. Neurotrauma **19**, 1155–1170.

LENZLINGER, P.M., MARX, A., TRENTZ, O., et al. (2002). Prolonged intrathecal release of soluble Fas following severe traumatic brain injury in humans. J. Neuroimmunol. **122**, 167–174.

MATSUSHITA, K., WU, Y., QIU, J., et al. (2000). Fas receptor and neuronal cell death after spinal cord ischemia. J. Neurosci. **20**, 6879–6887.

McGINNIS, K.M., GNEGY, M.E., PARK, Y.H., et al. (1999). Procaspase-3 and poly(ADP)ribose polymerase (PARP) are calpain substrates. Biochem. Biophys. Res. Commun. **263**, 94–99.

MEANEY, D.F., ROSS, D.T., WINKELSTEIN, B.A., et al. (1994). Modification of the cortical impact model to produce axonal injury in the rat cerebral cortex. J. Neurotrauma **11**, 599–612.

NATHANIEL, P.D., ZHANG, X., GRAHAM, S.H., et al. (2000). Cellular redistribution and cleavage of caspase-9 after traumatic brain injury in rats. Presented at the 18th Annual National Neurotrauma Society Symposium, New Orleans.

NEWCOMB, J.K., ZHAO, X., PIKE, B.R., et al. (1999a). Temporal profile of apoptotic-like changes in neurons and astrocytes following controlled cortical impact injury in the rat. Exp. Neurol. **158**, 76–88.

NEWCOMB, J.K., PIKE, B.R., ZHAO, X., et al. (1999b). Altered calpastatin protein levels following traumatic brain injury in rat. J. Neurotrauma **16**, 1–11.

NEWCOMB-FERNANDEZ, J.K., ZHAO, X., PIKE, B.R., et al. (2001). Concurrent assessment of calpain and caspase-3 activation after oxygen-glucose deprivation in primary septo-hippocampal cultures. J. Cereb. Blood Flow Metab. **21**, 1281–1294.

PIKE, B.R., ZHAO, X., NEWCOMB, J.K., et al. (1998a). Regional calpain and caspase-3 proteolysis of alpha-spectrin after traumatic brain injury. Neuroreport **9**, 2437–2442.

PIKE, B.R., ZHAO, X., NEWCOMB, J.K., et al. (1998b). Temporal relationships between de novo protein synthesis, calpain and caspase 3–like protease activation, and DNA fragmentation during apoptosis in septo-hippocampal cultures. J. Neurosci. Res. **52**, 505–520.

PIKE, B.R., ZHAO, X., NEWCOMB, J.K., et al. (2000). Stretch injury causes calpain and caspase-3 activation and necrotic and apoptotic cell death in septo-hippocampal cell cultures. J. Neurotrauma **17**, 283–298.

PLESNILA, N., ZINKEL, S., LE, D.A., et al. (2001). BID mediates neuronal cell death after oxygen/ glucose deprivation and focal cerebral ischemia. Proc. Natl. Acad. Sci. USA **98**, 15318–15323.

RAGHUPATHI, R., GRAHAM, D.I., and McINTOSH, T.K. (2000). Apoptosis after traumatic brain injury. J. Neurotrauma **17**, 927–938.

RAMI, A., AGARWAL, R., BOTEZ, G., et al. (2000). mu-Calpain activation, DNA fragmentation, and synergistic effects of caspase and calpain inhibitors in protecting hippocampal neurons from ischemic damage. Brain Res. **866**, 299–312.

SHI, Y., MELNIKOV, V.Y., SCHRIER, R.W., et al. (2000). Downregulation of the calpain inhibitor protein calpastatin by caspases during renal ischemia-reperfusion. Am. J. Physiol. Renal Physiol. **279**, F509–F517.

SHOHAMI, E., NOVIKOV, M., BASS, R., et al. (1994). Closed head injury triggers early production of TNF-alpha and IL-6 by brain tissue. J. Cereb. Blood Flow Metab. **14**, 615–619.

SULLIVAN, P.G., KELLER, J.N., MATTSON, M.P., et al. (1998). Traumatic brain injury alters synaptic homeostasis: implications for impaired mitochondrial and transport function. J. Neurotrauma **15**, 789–798.

TOLENTINO, P.J., DEFORD, S.M., NOTTERPEK, L., et al. (2002). Up-regulation of tissue-type transglutaminase after traumatic brain injury. J. Neurochem. **80**, 579–588.

THOMPSON, M.B., SULLIVAN, P.G., KELLER, J.N., et al. (2000). Cytochrome-C release and caspase activation after traumatic brain injury. J. Neurotrauma **17**, 953.

VERWEIJ, B.H., MUIZELAAR, J.P., VINAS, F.C., et al. (1997). Mitochondrial dysfunction after experimental and human brain injury and its possible reversal with a selective N-type calcium channel antagonist (SNX-111). Neurol. Res. **19**, 334–339.

VERWEIJ, B.H., MUIZELAAR, J.P., VINAS, F.C., et al. (2000). Improvement in mitochondrial dysfunction as a new surrogate efficiency measure for preclinical trials: dose-response and time-window profiles for administration of the calcium channel blocker Ziconotide in experimental brain injury. J. Neurosurg. **93**, 829–834.

WANG, K.K. (2000). Calpain and caspase: can you tell the difference? Trends Neurosci. **23,** 20–26.

WITKOSKI, J.M., ZMUDA-TRZEBIATOWSKA, E., SWIERCZ, J.M., et al. (2002). Modulation of the activity of calcium-activated neutral proteases (calpains) in chronic lymphocytic leukemia (B-CLL) cells. Blood **100,** 1802–1809.

XIONG, Y., PETERSON, P.L., MUIZELAAR, J.P., et al. (1997). Amelioration of mitochondrial function by a novel antioxidant U-101033E following traumatic brain injury in rats. J. Neurotrauma **14,** 907–917.

YAKOVLEV, A.G., KNOBLACH, S.M., FAN, L., et al. (1997). Activation of CPP32–like caspases contributes to neuronal apoptosis and neurological dysfunction after traumatic brain injury. J. Neurosci. **17,** 7415–7424.

YAKOVLEV, A.G., OTA, K., WANG, G., et al. (2001). Differential expression of apoptotic protease-activating factor–1 and caspase-3 genes and susceptibility to apoptosis during brain development and after traumatic brain injury. J. Neurosci. **21,** 7439–7446.

ZHAO, X., PIKE, B.R., NEWCOMB, J.K., et al. (1999). Maitotoxin induces calpain but not caspase-3 activation and necrotic cell death in primary septo-hippocampal cultures. Neurochem. Res. **24,** 371–382.

Address reprint requests to:
N.C. Ringger, D.V.M., DACVIM
100 S. Newell Drive
L1–100 (P.O. Box)
Gainesville, FL 32610

E-mail: ringger@ufbi.ufl.edu

Temporal and spatial profile of caspase 8 expression and proteolysis after experimental traumatic brain injury

Ronny Beer,* Gerhard Franz,* Stanislaw Krajewski,† Brian R. Pike,‡ Ronald L. Hayes,‡ John C. Reed,† Kevin K. Wang,§ Christian Klimmer,* Erich Schmutzhard,* Werner Poewe* and Andreas Kampfl*

*Department of Neurology, University Hospital Innsbruck, Austria

†The Burnham Institute, La Jolla, California, USA

‡Center for Traumatic Brain Injury Studies, Department of Neuroscience, Evelyn F. and William L. McKnight Brain Institute of the University of Florida, Gainesville, Florida, USA

§Department of Neuroscience Therapeutics, Pfizer Inc., Ann Arbor, Michigan, USA

Abstract

Recent studies have demonstrated that the downstream caspases, such as caspase 3, act as executors of the apoptotic cascade after traumatic brain injury (TBI) *in vivo*. However, little is known about the involvement of caspases in the initiation phase of apoptosis, and the interaction between these initiator caspases (e.g. caspase 8) and executor caspases after experimental brain injuries *in vitro* and *in vivo*. This study investigated the temporal expression and cell subtype distribution of procaspase 8 and cleaved caspase 8 p20 from 1 h to 14 days after cortical impact-induced TBI in rats. Caspase 8 messenger RNA levels, estimated by semi-quantitaive RT-PCR, were elevated from 1 h to 72 h in the traumatized cortex. Western blotting revealed increased immunoreactivity for procaspase 8 and the proteolytically active subunit of caspase 8, p20, in the ipsilateral cortex from 6 to 72 h after injury, with a peak at 24 h after TBI. Similar to our previous studies, immunoreactivity for the p18 fragment of activated caspase 3 also increased in the current study from 6 to 72 h after TBI, but peaked at a later timepoint (48 h) as compared with proteolyzed caspase 8 p20. Immuno-histologic examinations revealed increased expression of caspase 8 in neurons, astrocytes and oligodendrocytes. Assessment of DNA damage using TUNEL identified caspase 8- and caspase 3-immunopositive cells with apoptotic-like morphology in the cortex ipsilateral to the injury site, and immunohistochemical investigations of caspase 8 and activated caspase 3 revealed expression of both proteases in cortical layers 2–5 after TBI. Quantitative analysis revealed that the number of caspase 8 positive cells exceeds the number of caspase 3 expressing cells up to 24 h after impact injury. In contrast, no evidence of caspase 8 and caspase 3 activation was seen in the ipsilateral hippocampus, contralateral cortex and hippocampus up to 14 days after the impact. Our results provide the first evidence of caspase 8 activation after experimental TBI and suggest that this may occur in neurons, astrocytes and oligodendrocytes. Our findings also suggest a contributory role of caspase 8 activation to caspase 3 mediated apoptotic cell death after experimental TBI *in vivo*.

Keywords: apoptosis, astrocyte, caspase 8, neuron, oligodendrocyte, traumatic brain injury.

J. Neurochem. (2001) **78**, 862–873.

Traumatically evoked brain injury is a major cause of morbidity and mortality (Thurman *et al.* 1999). Studies over the last two decades have demonstrated that a significant amount of CNS damage after traumatic brain injury (TBI) occurs as a result of secondary autodestructive insults (Hayes *et al.* 1992; Faden 1996; McIntosh *et al.* 1998). Secondary injury involves a complex cascade of biochemical events that contributes to delayed tissue damage and cell death (Kermer *et al.* 1999; Graham *et al.* 2000). Importantly, recent research reported on a potential role for apoptosis in

cell degeneration after cerebral and spinal cord ischemia (Nitatori *et al.* 1995; Kato *et al.* 1997; Charriaut-Marlangue *et al.* 1998), traumatic spinal cord injury (Crowe *et al.* 1997; Liu *et al.* 1997), and TBI *in vitro* (Shah *et al.* 1997; Pike *et al.* 2000) and *in vivo* (Rink *et al.* 1995; Conti *et al.* 1998; Newcomb *et al.* 1999; Beer *et al.* 2000b).

Although a potential role for apoptosis in neuronal and glial cell damage after TBI has been suggested, little is known about the molecular mechanisms involved. However, recent evidence implicates a distinct class of proteases, referred to as caspases. So far, 14 mammalian caspases have been described (Nicholson 1999). Based on their proteolytic specifities, caspases further divide into three groups: the inflammatory caspases (e.g. caspase 1), which mediate cytokine maturation (Cerretti *et al.* 1992); the caspases involved in apoptotic cell death, which segregate into initiator enzymes, such as caspase 8 and caspase 9; executioner caspases, such as caspase 3 (Cohen 1997; Cryns and Yuan 1998). Caspases are synthesized as inactive pro-enzymes that contain three domains (Nicholson 1999), an N-terminal prodomain (approximately 3–24 kDa), a large subunit (approximately 17–21 kDa) and a small subunit (approximately 10–13 kDa). Depending on the cell type, procaspases have been shown to reside in various subcellular localizations (Qin *et al.* 2001; Shikama 2001) and are activated through proteolytic processing and association of the large and small subunits to form a catalytic heterotetramer (Walker *et al.* 1994).

Activation of the executioner caspase 3 has been shown in numerous chronic and acute disorders of the nervous system. For example, caspase 3 processing has been demonstrated in Alzheimer's (Stadelmann *et al.* 1999; Khan *et al.* 2000) and Parkinson's disease (Mogi *et al.* 2000). Further, caspase 3 mediated neuronal and glial cell degeneration has been found in experimental models of cerebral and spinal cord ischemia (Hayashi *et al.* 1998; Namura *et al.* 1998) and spinal cord injury (Springer *et al.* 1999). Importantly, recent data have also suggested a contributory role for activated caspase 3 in apoptotic degeneration of neurons, astrocytes and oligodendrocytes after TBI *in vivo* (Yakovlev *et al.* 1997; Beer *et al.* 2000b; Clark *et al.* 2000).

Current evidence also indicates that in receptor-triggered apoptosis the main pathway for caspase 3 activation is direct activation by caspase 8 (Scaffidi *et al.* 1998; Stennicke *et al.* 1998). Importantly, recent data suggest that receptor-mediated apoptosis indeed occurs in acute CNS injuries (Ertel *et al.* 1997; Felderhoff-Mueser *et al.* 2000). For example, increased expression of Fas and caspase 8 has been shown after experimental spinal cord ischemia (Matsushita *et al.* 2000). In addition, increased Fas and Fas ligand immunoreactivity (Beer *et al.* 2000a) and caspase 3 activation have been reported following TBI in the rat (Beer *et al.* 2000b; Clark *et al.* 2000), suggesting a putative link between the activation of caspase 8 and

caspase 3 after TBI *in vivo*. However, to our knowledge no study to date has concurrently investigated changes in the expression and activity of both caspase 8 and caspase 3 in trauma-induced CNS degeneration.

To further investigate potential changes of caspase 8 and caspase 3 expression after experimental TBI, rodents were subjected to a widely used model of experimental brain injury: lateral cortical impact injury (Dixon *et al.* 1991; Franz *et al.* 1999; Beer *et al.* 2000a,b). The present study employed semiquantitative RT-PCR and western blot analyses of procaspase 8, cleaved caspase 8 p20, and processed caspase 3 to determine the relative temporal profile of caspase 8 to caspase 3 expression and activation from 1 h to 14 days after experimental TBI. Immunohistochemical examinations were performed to investigate the cell subtype distribution of caspase 8 after impact injury *in vivo*. Further, TUNEL was used to assess whether caspase 8 and caspase 3 immunopositive cells exhibit morphological features of DNA damage consistent with apoptotic phenotype after TBI in the rat.

Materials and methods

Rat model of traumatic brain injury

A controlled cortical impact device was used to induce a moderate level of TBI, as previously described (Dixon *et al.* 1991; Franz *et al.* 1999). In brief, adult male Sprague–Dawley rats (250–350 g) were intubated and anesthetized with 2% halothane in a 2 : 1 mixture of N_2O/O_2. Core body temperature was monitored continuously using a rectal thermistor probe and maintained at 36.5–37.5°C by a heating pad. Animals were mounted in a stereotaxic frame on the injury device in a prone position secured by ear and incisor bars. A midline incision was made, the soft tissues were reflected, and two 7-mm craniotomies were made adjacent to the central suture, midway between lambda and bregma. The dura was kept intact over the cortex. Injury was induced by impacting the right (ipsilateral) cortex with a 6-mm diameter aluminum tip at a rate of 4 m/s. The injury device was set to produce a tissue deformation of 2 mm. Impact velocity was measured directly by a linear variable differential transformer (Shaevitz Model 500 HR; Shaevitz, Detroit, MI, USA), which produces an analog signal that was recorded by a PC-based data acquisition system for analysis of time/displacement parameters of the impactor. This magnitude of injury has previously been associated with significant cell degeneration restricted to the contusion site (Franz *et al.* 1999; Beer *et al.* 2000a,b). After trauma, animals were extubated and immediately assessed for recovery of reflexes (Dixon *et al.* 1991). Sham-injured animals underwent identical surgical procedures but did not receive impact injury. Naive animals were not exposed to any injury-related surgical procedures. Ninety animals were used in this study (naive rats, $n = 10$; sham-injured rats, $n = 12$; injured rats, $n = 68$). Animal care and experimental protocols complied with the guidelines outlined in the *Guide for the Care and Use of Laboratory Animals*, Austrian Department of Health and Science, and were approved by the University of Innsbruck Medical School Animal

Table 1 Systemic parameters

	Prior to craniotomy ($n = 20$)	Post surgery	
		sham ($n = 4$)	injured ($n = 16$)
MABP (mmHg)	101 ± 5	97 ± 8	103 ± 6
pH	7.46 ± 0.01	7.43 ± 0.02	7.44 ± 0.02
PaO$_2$ (mmHg)	142 ± 4	79 ± 12	85 ± 9
PaCO$_2$ (mmHg)	43 ± 6	41 ± 3	42 ± 5
Rectal temperature (°C)	37.1 ± 0.2	37.3 ± 0.2	36.9 ± 0.1

Values are mean ± SD; MABP, mean arterial blood pressure.

Welfare Committee. Importantly, all efforts were made to minimize animal suffering and to reduce the number of animals used.

Assessment of physiologic parameters
In a subgroup of animals (sham-injured rats, $n = 4$; injured rats, $n = 16$) systemic parameters were monitored as described by Dixon *et al.* (1991). Briefly, a 22-gauge Teflon catheter was advanced into the abdominal aorta through a left femoral arteriotomy for arterial blood pressure measurement and arterial blood sampling. Blood samples (100 μL) were analyzed for pH, arterial oxygen pressure (PaO$_2$), and arterial pressure of carbon dioxide (PaCO$_2$), (Table 1) using an AVL Omni 4 (Diamond Diagnostics, Holliston, MA, USA) blood gas analyzer before craniotomy and 5 min after surgery. All parameters were within the normal physiological range (Table 1) (Krinke 2000).

Sample preparation
All animals were given a lethal dose of phenobarbital intraperitoneally (20 mg/kg; Tyrol Pharma, Kundl, Austria) and subsequently killed by decapitation 6 h, 24 h, 48 h, 72 h, 7 days and 14 days after TBI ($n = 4$ for each time after injury, $n = 4$ for naive and sham-injured animals). Both cortices and hippocampi (ipsilateral and contralateral to the injury site) were removed. Excision of both cortices beneath the craniotomies extended ~4-mm laterally, ~7-mm rostrocaudally, and to a depth extending to the white matter. All samples were immediately frozen in liquid nitrogen. The microdissected tissue was homogenized at 4°C in ice-cold homogenization buffer containing 20 mM piperazine-N,N'-bis(2-ethanesulfonic acid) (pH 7.1), 2 mM EGTA, 1 mM EDTA, 1 mM dithiothreitol, 0.3 mM phenylmethylsulfonylfluoride (PMSF), and 0.1 mM leupeptin. Chelators and protease inhibitors (Sigma, St Louis, MO, USA) were added to prevent endogenous *in vitro* activation of proteases and subsequent artifactual degradation of caspase 8 and caspase 3 during tissue processing.

Sodium dodecyl sulfate–polyacrylamide gel electrophoresis, immunoblotting and quantification
Protein concentrations were determined by bicinchoninic acid microprotein assay (Sigma) with albumin standards. Protein-balanced samples were prepared for polyacrylamide gel electrophoresis in two-fold loading buffer containing 0.25 M Tris (pH 6.8), 0.2 M dithiothreitol, 2% sodium dodecyl sulfate, 0.005% bromophenol blue and 5% glycerol in distilled water. Samples were heated for 5 min at 95°C. Sixty micrograms of protein per lane was

routinely resolved on 16% Tris/glycine gels (Invitrogen, Groningen, the Netherlands). After separation, proteins were transferred to nitrocellulose membranes using western blotting with transfer buffer made up of 0.192 M glycine and 0.025 M Tris (pH 8.3). Coomassie blue (Bio-Rad, Hercules, CA, USA) and Ponceau red (Sigma) stainings were performed to confirm that equal amounts of protein were loaded in each lane. Five percent non-fat milk in phosphate buffered saline (PBS) with 0.05% Tween 20 was used to reduce non-specific binding. Immunoblots were probed with either a mouse monoclonal antibody (Santa Cruz Biotechnology, Santa Cruz, CA, USA), reacting with the p20 subunit and precursor of caspase 8, diluted 1 : 1000, or a rabbit polyclonal antiserum (CM1; IDUN Pharmaceuticals, La Jolla, CA, USA; dilution 1 : 5000), directed against the p18 subunit of activated caspase 3. Specifity and sensitivity of CM1 has been described in detail in previous investigations (Namura *et al.* 1998; Srinivasan *et al.* 1998; Beer *et al.* 2000b). After incubation with primary antibodies overnight at 4°C, nitrocellulose membranes (Amersham Pharmacia Biotech, Uppsala, Sweden) were incubated with secondary antibodies linked to horseradish peroxidase (Amersham Pharmacia Biotech) for 1 h at 20°C (automated climate control). Enhanced chemiluminescence reagents (Amersham Pharmacia Biotech) were used to visualize the immunolabeling on X-ray film. In each blot, the constitutively expressed protein α-tubulin (Sigma) was used as an internal standard to further indicate that sample processing was carried out correctly.

Semiquantitative RT-PCR
Total RNA was isolated from frozen ipsilateral and contralateral cortex and hippocampus of naive ($n = 2$), sham-injured ($n = 4$), and injured animals (1 h, 6 h, 24 h, 48 h and 72 h; $n = 4$ for each time point after injury) with Trizol reagent (Life Technologies, Rockville, MD, USA). Ten micrograms of total RNA was treated with 1 U of amplification grade DNase I (Life Technologies) to eliminate residual genomic DNA and was reverse transcribed into first-strand cDNA using Superscript II reverse transcriptase (Life Technologies) with oligo(dT) as primer. The resulting cDNAs were diluted to 100 μL and subjected to PCR analysis. Each PCR mixture contained equal amounts of diluted cDNA corresponding to 200 ng of total RNA, 100 pM of each primer, 10 pM dNTPs, onefold Ampli-Taq reaction buffer and 2.5 U Ampli-Taq-Gold DNA polymerase (PE Biosystems, Foster City, CA, USA). All cDNAs were amplified with primers specific for the housekeeping

gene glyceraldehyde-3-phosphate dehydrogenase (GAPDH; Gen-Bank Acc. No. X02231; 5'-CCCACGGCAAGTTCAACGG-3' and 5'-CTTTCCAGAGGGGCCATCCA), and caspase 8 (GenBank Acc. No. AF279308; 5'-ACTGGCTGCCCTCAAGTTCCTGTGC-3' and 5'-TCCCTCACCATTTCCTCTGGGCTGC-3'). PCR amplification was carried out for 34 cycles of 45 s at 94°C, 45 s at 60°C, and 45 s at 72°C, followed by a final step of 10 min at 72°C in the UNO II Thermocycler (Biometra, Göttingen, Germany). The number of cycles and reaction temperature conditions were optimized to provide a linear relationship between the quantity of input template and the quantity of PCR product. PCR products were analyzed by agarose gel electrophoresis in 2% NuSieve agarose gels (FMC BioProducts, Rockland, ME, USA) and visualized by ethidium-bromide staining. The identity of the PCR products obtained was confirmed by Southern blot analysis using an internal oligonucleotide as hybridization probe.

Immunohistochemistry

Prior to perfusion, animals from all treatment groups were given a lethal injection of phenobarbital (20 mg/kg intraperitoneally). Rats were transcardially perfused through the left ventricle (120 mL of 0.9% saline and 200 mL of 4% paraformaldehyde) at 6 h, 24 h, 48 h, 72 h, 7 days and 14 days after TBI ($n = 4$ for each time point after injury; $n = 4$ for sham-injured and naive animals). The brains were removed, grossly sectioned coronally at 2-mm intervals, processed through graded alcohols and xylene substitute (Histoclear; National Diagnostics, Atlanta, GA, USA), and routinely embedded in paraffin. Sections were cut at 3–4 µm on a rotary microtome, mounted on aminoalkylsilated glass slides, and processed for immunohistochemistry as follows: deparaffinized and rehydrated sections were microwaved in 10 mM sodium citrate buffer, pH 6.0, and allowed to cool to room temperature. Endogenous peroxidase was blocked by treatment with 0.3% H_2O_2 in methanol followed by incubation with 10% fetal calf serum (FCS) in Tris-buffered saline (TBS) for 60 min. Rabbit polyclonal antibodies against caspase 8 (The Burnham Institute, La Jolla, CA, USA) and caspase 3 p18 (IDUN Pharmaceuticals) were diluted 1 : 5000 in 10% FCS and permitted to bind overnight at 4°C.

Rabbit antiserum against caspase 8 was generated as previously described (Krajewska et al. 1997) using recombinant catalytic C-terminal fragment of human caspase 8 protein using construct pET15b MGS H_6-Ser216-TAA. This protein was expressed in BL 21 (DE3) cells by induction with 1 mM IPTG. After cell growth and lysis, the clarified cell lysate was applied to an Ni-NTA column and eluted with an imidazole gradient. The pooled caspase 8 fractions were dialyzed against 50 mM Tris at pH 8.8 and applied to a FPLC Mono Q HR 10/10 column (Amersham Pharmacia Biotech) and eluted with an NaCl gradient. New Zealand white female rabbits were injected subcutaneously with a mixture of recombinant protein (0.1–0.15 mg protein per immunization) and 0.5 mL Freund's complete adjuvant with the dose divided over 10 injection sites, and then boosted three times at weekly intervals followed by another 3–20 boostings at monthly intervals with 0.15 mg each of recombinant protein immunogen in Freund's incomplete adjuvant. Antiserum specificity was confirmed by pre-absorption with full-length or fully cleaved caspase 8 protein, respectively. This polyclonal antibody reacts with the unprocessed zymogen form of caspase 8 and detects the processed large subunit

(p20) of active caspase 8. In addition, specificity of the caspase 8 antiserum has been described recently (Stoka et al. 2001).

Biotinylated goat anti-rabbit (Vector Laboratories, Burlingame, CA, USA) was then applied at a dilution of 1 : 200 in 3% rat serum in TBS for 1 h at room temperature followed by avidin-peroxidase (Sigma), diluted 1 : 100 in TBS, also for 1 h at room temperature. The reaction was visualized by treatment with 0.05% 3,3'-diamino-benzidine tetrahydrochloride solution in TBS containing 0.05% H_2O_2. The color reaction was stopped with several washes of TBS. Immunostaining results were confirmed by the use of pre-immune serum from the same animals and by pre-absorption of the polyclonal antibodies with the relevant protein.

For double immunostaining using brightfield chromagens, sections were pretreated with the rabbit polyclonal antiserum against caspase 8 as described above. Sections were then incubated with a mouse anti-neuron-specific nuclear protein (NeuN) antibody (Wolf et al. 1996) (Chemicon, Temecula, CA, USA) for neuronal staining. For staining of astrocytes, oligodendrocytes and microglia, a mouse anti-GFAP (Debus et al. 1983) (Roche Molecular Biochemicals, Mannheim, Germany), a mouse anti-CNPase (Sprinkle 1989) (Sternberger Monoclonals Inc., Lutherville, MD, USA) and an anti-ED1 monoclonal antibody (Graeber et al. 1990) (Serotec, Kidlington, Oxford, UK) were used. All antibodies were diluted 1 : 500 in 10% FCS in TBS and allowed to bind overnight at 4°C. After being rinsed, sections were incubated with a biotinylated horse anti-mouse antibody (Vector Laboratories) at a dilution of 1 : 200 for 1 h at room temperature followed by incubation with an alkaline phosphatase avidin-biotin substrate and then reaction with blue chromagen (Vector Blue; Vector Laboratories). Sections were dehydrated through graded ethanol, cleared in a xylene substitute (Histoclear; National Diagnostics, Atlanta, GA, USA), mounted in Permount (Fisher Scientific, Nepean, Ontario, Canada) and coverslipped. Sections without primary antibodies were similarly processed to control for binding of the secondary antibodies. On control sections no specific immunoreactivity was detected.

Histochemical detection of DNA fragmentation (terminal deoxynucleotidyl transferase-mediated deoxyuridine-biotin nick end labeling)

To confirm the presence of cell degeneration by an apoptotic mechanism, terminal deoxynucleotidyl transferase-mediated deoxyuridine-biotin nick end labeling (TUNEL) was performed as described by Gavrieli et al. (1992) with minor modifications. Briefly, for double-label experiments, dewaxed and rehydrated sections of all animal groups from regions between − 1.5 and − 3.4 mm bregma were stained with primary and secondary antisera as described earlier. Immunohistochemical staining was visualized by exposure to 3-amino-9-ethylcarbazole in N,N'-dimethylformamide (Sigma). Sections were then rinsed thoroughly and incubated with labeling mix (TdT buffer containing 100 U/mL TdT and 20 nM/mL biotin-conjugated 16 deoxyuridine) in a humidified chamber for 60 min at 37°C. After three washes in TBS, slides were incubated in Converter alkaline phosphatase for 15 min in a humidified chamber at 37°C. All reagents were purchased from Roche Molecular Biochemicals. The reaction was visualized by treatment for 3 min with 5-bromo-4-chloro-3-indolyl phosphate/nitro blue tetrazolium substrate system (Dako Corporation, Carpinteria, CA, USA). Primary antibody, labeling mix or

secondary antibody were omitted in control sections. Sections were mounted using an aqueous mounting fluid (Dako Corporation) and examined under the light microscope.

Statistical analysis

Semiquantitative evaluation of RT-PCR band density and of immunoreactivity detected by western blotting was performed using computer-assisted two-dimensional densitometric scanning with a MacIntosh computer using the public domain NIH IMAGE program (developed at the US National Institutes of Health and available on the internet at http://rsb.info.nih.gov/nih-image/). Relative band densities on RT-PCR and western blots ($n = 1$/ blot) were expressed as arbitrary densitometric units for each time point. This procedure was performed for the data of four independent experiments for a total of four different animals per time point. Data acquired in arbitrary densitometric units were transformed to percentages of the densitometric levels observed for scans from sham animals on the same agarose gel (for RT-PCR analysis) and same blot. Group differences were determined by ANOVA and Tukey's *post hoc* honestly significant difference (HSD) test. Values given are means ± SD of four independent experiments. Differences were considered significant when $p \leq 0.05$. For quantitative analysis of immunohistochemistry, the numbers of caspase 8 and caspase 3 positive cells of three non-consecutive sections (each separated by at least 50 μm) of four different animals for each time point were counted by an independent observer in the entire anatomic regions of the cortex from the primary injury zone at bregma -3.4 mm ± 0.2 mm (Paxinos and Watson 1997) using light microscopy at a magnification of 100×. The total number of caspase 8- and caspase 3-immunopositive cells was obtained for each section. Further, the numbers of cells labeled with anti-caspase 8 antibody and NeuN, GFAP and CNPase were counted on sections (three sections per animal) processed for double-label immunohistochemistry. Values for each animal (four animals per time point) were averaged to calculate the mean number of immunopositive cells per time point (6–72 h after TBI). Cell counts (caspase 8 vs. caspase 3 and double-labeled neurons vs. double-labeled glia) were analyzed with ANOVA and Bonferroni's *post hoc* analysis for selected pairs of columns. Values given are means ± SD of four different animals. Differences were considered significant when $p \leq 0.05$.

Results

Caspase 8 messenger RNA levels increase after TBI

Caspase 8 messenger RNA was detected by semiquantitative RT-PCR analysis in cortical and hippocampal samples (not shown) of sham and injured animals, respectively (Fig. 1). Cortical impact injury resulted in an increase of caspase 8 messenger RNA levels in the ipsilateral cortex (Fig. 1). Starting at 1 h after injury, a significant increase in caspase 8 messenger RNA levels was observed. Rising rapidly, band intensity reached a maximum level by 6 h after the trauma (386% increase relative to sham animals) and remained thereafter at a steady-state level (332% increase relative to sham animals) at 24 h after TBI. Caspase 8 messenger RNA levels then declined thereafter to a level of approximately
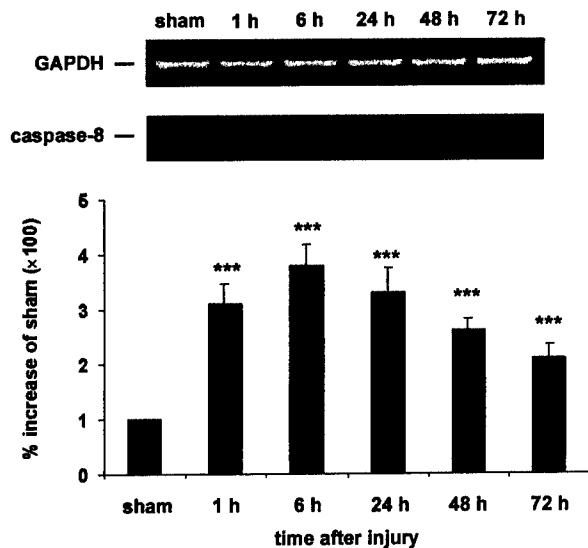

Fig. 1 RT-PCR analysis of caspase 8 mRNA in the ipsilateral cortex following TBI. Cortical samples of single control animals (sham) and single injured animals were prepared for RT-PCR at the indicated times after TBI *in vivo*. Values are presented as percentages of the densitometric levels observed on scans from sham animals visualized on the same agarose gel. Data are mean ± SD values of four independent experiments. Levels of caspase 8 mRNA increased within 1 h after TBI as compared with controls. Levels of caspase 8 mRNA peaked at 6 h after TBI and remained elevated as late as 72 h after the injury. ***$p < 0.001$.

two-fold (220% increase relative to sham animals) above controls at 72 h after the impact. No statistically significant increases in caspase 8 messenger RNA levels were observed in cortical samples contralateral to the injury site and hippocampal samples ipsi- and contralateral to the injury site from 1 h to 72 h after the impact (data not shown).

Proteolytic processing of caspase 8 and caspase 3 occurs after TBI

To determine whether caspase 8 and caspase 3 are activated after TBI, brain extracts from cortex and hippocampus ipsi- and contralateral to the injury site were examined for the expression of the p55 subunit (procaspase 8), the p20 subunit (processed caspase 8) and of the p18 subunit (cleaved caspase 3) by western blotting. Cortical impact injury resulted in an increase of p55 and p20 caspase 8 immunoreactivity in the ipsilateral cortex (Fig. 2a). The p55 and p20 caspase 8 immunoreactivity increased within 6 h after TBI and peaked at 24 h after the impact (376% increase relative to sham animals for p55, and 653% increase as compared with sham animals for p20, respectively), declining thereafter. After 7 and 14 days, no significant increases were evident in the p55 and p20 fragments when compared with levels in sham-injured control animals. Similar to a previous study (Beer *et al.*
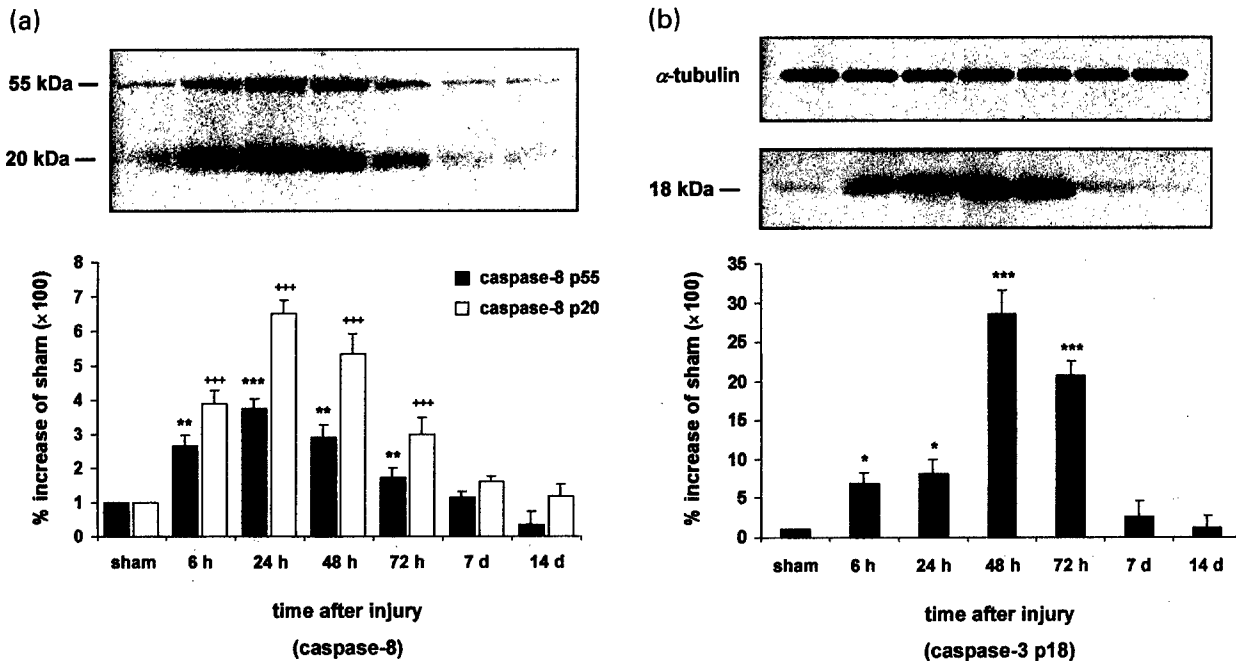
Fig. 2 Time-course of caspase 8 (a) and caspase 3 p18 (b) protein expression after TBI. Samples from single control (sham) and single injured animals were prepared for western blotting between 6 h and 14 days after TBI. Levels of protein are expressed as arbitrary densitometric units. Data were transformed to percentages of the densitometric levels observed on scans from sham animals visualized on the same blot. Values given are mean ± SD of four independent experiments. (a) Ipsilateral cortex: immunoblots demonstrated that procaspase 8 (p55) is constitutively expressed in sham-injured brains. Following TBI, immunoreactivity of p55 (filled bars) (**$p < 0.01$) and p20 (processed caspase 8; open bars) ($^{+++}p < 0.001$) increased significantly at 6 h after TBI and peaked at 24 h post injury. Immunoreactivity of p55 (*$p < 0.05$) and p20 ($^{+++}p < 0.001$) was still significantly increased up to 72 h post trauma. (b) Ipsilateral cortex: the proteolytically active p18 fragment of caspase 3 increased significantly within 6 h after TBI (*$p < 0.05$). p18 immunoreactivity peaked at 48 h after TBI (***$p < 0.001$) and was still significantly elevated at 72 h after impact injury (***$p < 0.001$). α-tubulin was used as an internal standard.

2000b), immunoreactivity for activated caspase 3 (p18) increased within 6 h after TBI in the traumatized cortex (Fig. 2b). However, the maximal increase of p18 immunoreactivity was seen at later times (48 h after TBI; 2850% increase relative to sham animals), when compared with caspase 8 p20. Caspase 3 p18 immunoreactivity then declined to a 2060% increase relative to sham at 72 h after TBI. Similar to proteolyzed caspase 8, no statistically significant differences in caspase 3 p18 immunoreactivity were observed between cortical samples ipsilateral to the injury site at 7 and 14 days after TBI and in cortical samples from sham-injured animals. In addition, no significant increases in p55, p20 and p18 immunoreactivity were seen between sham and injured animals in cortical samples contralateral to the injury site and hippocampal samples ipsi- and contralateral to the injury site between 6 h and 14 days after TBI (data not shown).

Caspase 8 is expressed in traumatized cortical neurons, astrocytes and oligodendrocytes

Ipsilateral and contralateral cortical and hippocampal tissues were examined rostrocaudally from + 0.2 to − 3.8 mm

bregma. No caspase 8 immunoreactivity was present in the tissue from sham-injured (Fig. 3a) or naive (data not shown) control rats. Positive immunoreactivity for caspase 8 was found throughout the ipsilateral cortex at the primary injury zone (from − 1.5 to − 3.4 mm bregma) from 6 h to 72 h after the trauma (Figs 3b and c; time point = 24 h after TBI; − 3.4 mm bregma). To further investigate if caspase 8 is expressed in glial and/or neuronal cells, we performed double-labeling experiments for caspase 8 using the neuronal cell specific marker NeuN, the astrocytic marker GFAP, the microglial marker ED-1, and the oligodendroglial marker CNPase. These immunohistochemical analyses of caspase 8-positive cells from 6 to 72 h after TBI (Figs 3i–k; time point = 24 h after trauma; − 3.4 mm bregma) identified labeling with NeuN, GFAP and CNPase, and demonstrated the expression of caspase 8 in cortical neurons (Fig. 3i), astrocytes (Fig. 3j) and oligodendrocytes (Fig. 3k), respectively. Interestingly, immunoreactivity for caspase 8 was observed to be mainly cytosolic in neurons (Figs 3g and i), but appeared rather nuclear in astrocytes (Fig. 3j) and oligodendrocytes (Fig. 3k). No caspase 8 immunoreactivity was detected in microglial cells.
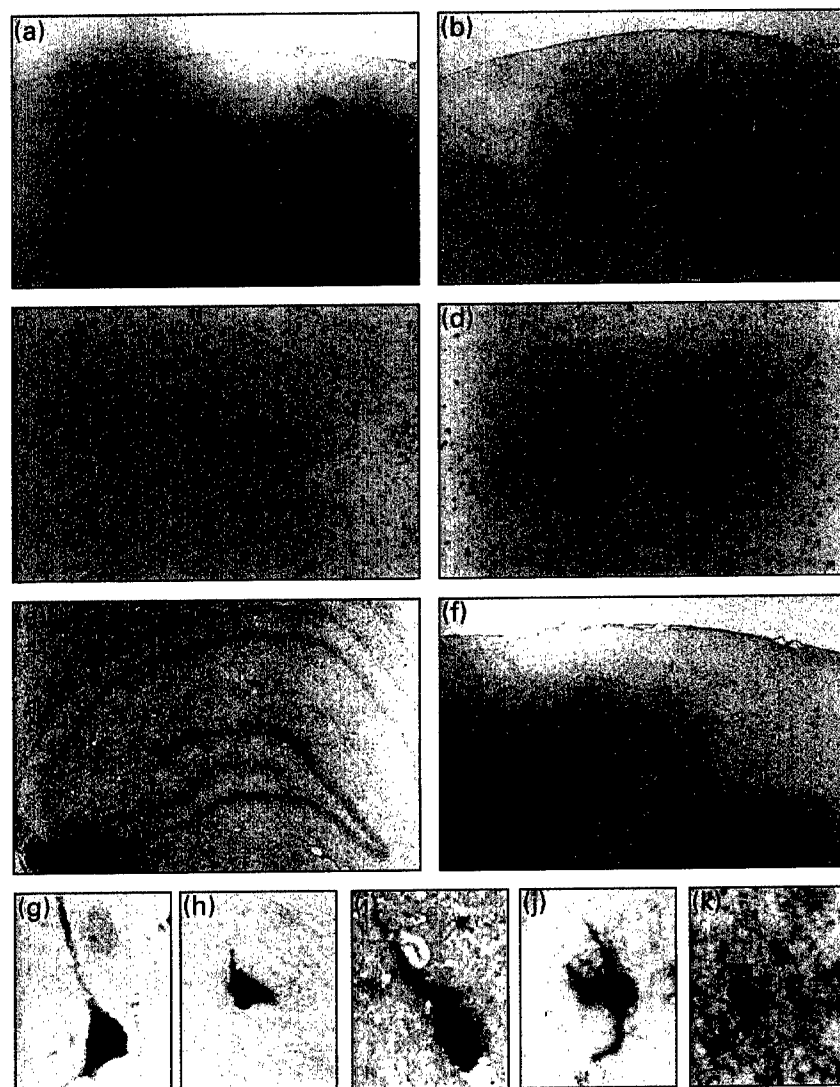
Fig. 3 Cell subtype distribution of caspase 8 in the traumatized cortex (− 3.4 mm bregma) at 24 h after TBI. Sham injured brains showed no specific caspase 8 immunolabeling (a). Low (b), intermediate (c) and high magnification (g) photomicrographs revealed specific caspase 8 expression in the ipsilateral cortex following cortical impact injury. Cells immunopositive for activated caspase 3 are found within similar brain regions (d and h). Double immunostaining experiments with caspase 8 (brown color; i, j and k) and NeuN (blue color; i), GFAP (blue color; j), and CNPase (blue color; k) provided evidence that caspase 8 is expressed in cortical neurons (i), astrocytes (j), and oligodendrocytes (k) after TBI. Magnifications: (a) and (b), 40×; (c) and (d), 100×; (e), 20×; (f), 40×; (g–k), 1000×.
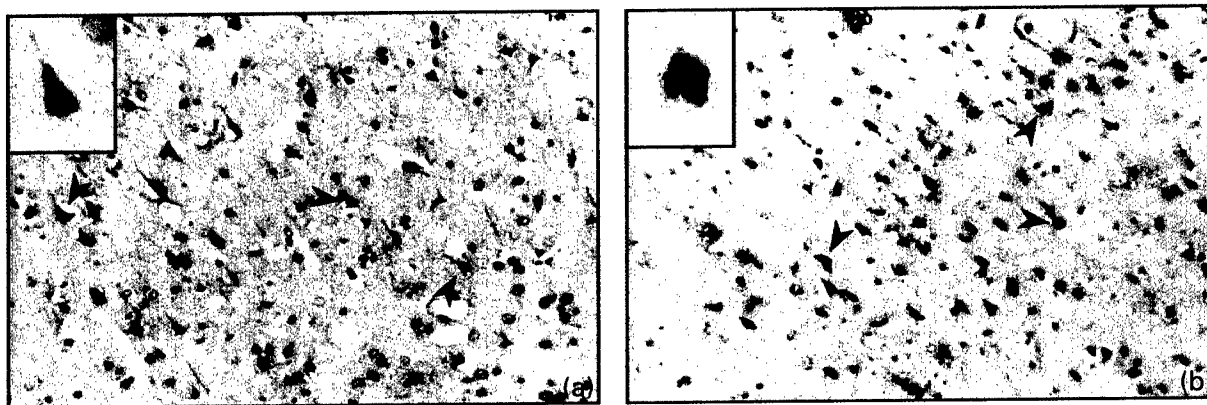
Fig. 4 Appearance of caspase 8 and processed caspase 3 p18 in TUNEL-positive cells. Combined immunohistochemistry for caspase 8 (red color; a) and TUNEL (dark blue color; a) (24 h after TBI) and caspase 3 p18 (red color; b) and TUNEL (dark blue; b) (48 h after TBI) demonstrated caspase 8 (a) and activated caspase 3 (b) in cells with gross nuclear apoptotic-like morphology. TUNEL-positive cells exhibited chromatin condensation and nuclear fragmentation (arrows). Magnifications: (a) and (b), 200×; inserts, 1000×.
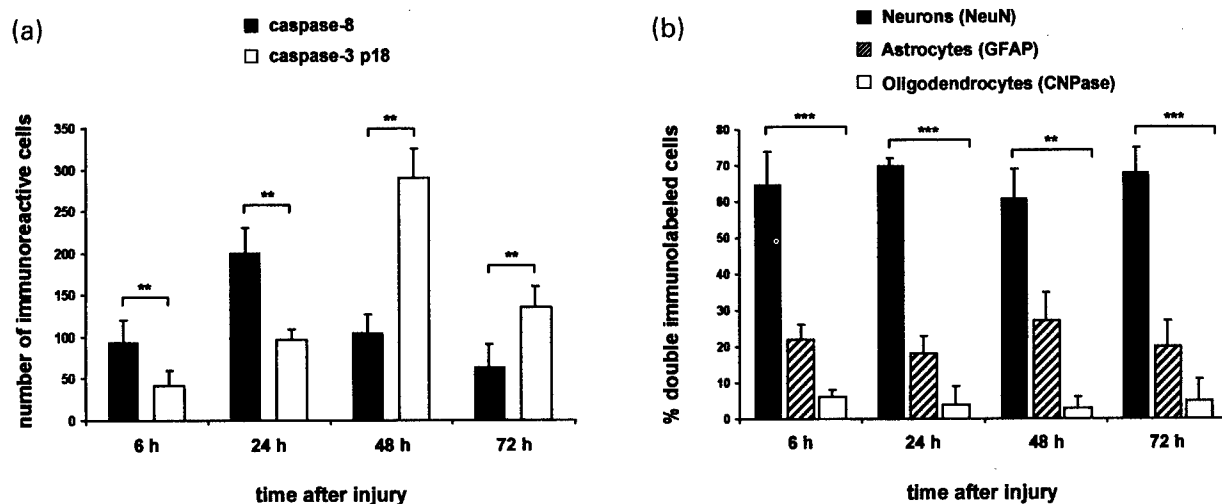
Fig. 5 Quantification of caspase 8 and caspase 3 p18 positive cells in the ipsilateral cortex after TBI (a) and quantification of caspase 8 cell subtype staining (b). Cells were counted in the entire anatomic regions of the cortex at the primary injury zone (bregma − 3.4 mm). (a) The number of caspase 8 positive cells (filled bars) was significantly greater than that of caspase 3 p18 positive cells (open bars) before 48 h after TBI. (b) Quantitative analysis was conducted of caspase 8 and NeuN (filled bars), caspase 8 and GFAP (hatched bars), and caspase 8 and CNPase (open bars) immunopositive cells. Columns indicate double-labeled neurons (filled bars), double-labeled astrocytes (hatched bars), and double-labeled oligodendrocytes (open bars) as percentages of caspase 8-positive cells from 6 to 72 h after TBI. Cell counts of caspase 8-positive neurons were significantly higher as compared with caspase 8-positive glia (i.e. astrocytes and oligodendrocytes at 6, 24, 48 and 72 h after TBI, respectively). Cell counts were evaluated by ANOVA with Bonferroni's *post hoc* analysis (**$p < 0.01$, ***$p < 0.001$). Values given are mean $\pm$ SD of four different animals per time point.

Caspase 8 immunoreactivity was absent in ipsilateral hippocampal samples (Fig. 3e) and contralateral samples of cortex (Fig. 3f) and hippocampus (data not shown) at all times investigated.

Caspase 8- and caspase 3-immunopositive cells exhibit nuclear apoptotic-like morphology

To verify further an apoptotic component of post-traumatic cell death and to support the possibility that caspase 8 and caspase 3 are associated with trauma-induced apoptosis, sections immunopositive for caspase 8 and caspase 3 p18 were stained with TUNEL to assess DNA damage. Double-labeling experiments demonstrated that a substantial proportion of TUNEL positive cells with shrunken morphology, condensed nuclei and chromatin margination also expressed caspase 8 (Fig. 4a) and activated caspase 3 (Fig. 4b) in layers 2–5 of the injured parietal cortex after TBI. However, cells with either caspase 8 or activated caspase 3 reactivity or gross apoptotic-like morphology alone were also detected.

Quantification of caspase 8- and caspase 3-positive cells and caspase 8 cell subtype staining after TBI

Activated caspase 3 was detected in the ipsilateral traumatized cortex from 6 to 72 h after impact injury. Similar to our findings for caspase 8, p18 positive cells were seen within cortical layers 2–5 at the primary impact zone (Fig. 3d) (Beer *et al.* 2000b). In contrast to caspase 8, the intracellular localization of activated caspase 3 was

predominantly nuclear (Fig. 3h). Quantitative analysis of caspase 8- and p18-positive cells revealed that the number of caspase 8- and p18-labeled cells increased up to 24 and 48 h after trauma, respectively, with the number of caspase 8-positive cells being significantly higher until 24 h after TBI (Fig. 5a).

Quantification of caspase 8 and NeuN, GFAP and CNPase revealed that the number of caspase 8-positive neurons is significantly higher as compared with glia (i.e. astrocytes and mature oligodendrocytes) from 6 to 72 h after injury, respectively (Fig. 5b).

Discussion

Our results provide the first evidence for caspase 8 expression and processing after experimental TBI. Proteolyzed caspase 8 appeared in samples of the traumatized cortex from 6 to 72 h after impact injury. Furthermore, double labeling experiments revealed expression of caspase 8 in neurons, astrocytes and oligodendrocytes after experimental brain injury. Moreover, our data indicate that expression of caspase 8 and cleaved caspase 3 p18 is associated with apoptotic-like cell death phenotypes detected in TUNEL-positive cells. Finally, our results suggest that caspase 8 may at least in part contribute to caspase 3-mediated cell death after experimental TBI in the rat.

Reverse transcription PCR and western blotting data revealed increased expression of caspase 8 messenger RNA and increased immunoreactivity for procaspase 8 and caspase 8 p20 in the ipsilateral cortex from 1 h to 72 h after the impact. Similar to our results, current data also suggest that caspase 8 messenger RNA, procaspase 8 and activated caspase 8 are over-expressed at early time points after experimental spinal cord ischemia (Matsushita *et al.* 2000) and focal cerebral ischemia (Harrison *et al.* 2001) in the mouse. Moreover, increased expression of proteolyzed caspase 8 has also been described after experimental focal ischemia in the rat up to 48 h after the insult (Velier *et al.* 1999). In this regard, it is noteworthy that cortical impact injury may produce focal ischemia in the cortex ipsilateral to the injury site (Bryan *et al.* 1995). Thus, reduced cerebral blood flow may have also contributed to activation of caspase 8 in our experiments. Taken together, these data demonstrate that caspase 8 is up-regulated and activated as an early event after various acute CNS injuries *in vivo*.

Previous reports on the cell subtype distribution have found increased immunoreactivity for caspase 8 in neurons after focal ischemia in the rat (Velier *et al.* 1999). In addition, recent data provided evidence that caspase 8 is also over-expressed in neurons following experimental spinal cord ischemia in the mouse (Matsushita *et al.* 2000) and in oligodendrocytes undergoing staurosporine-induced apoptosis *in vitro* (Gu *et al.* 1999). These findings indicate that whereas caspase 8 has been reported only to be weakly expressed in normal brain parenchyma (Velier *et al.* 1999), the brain readily over-expresses caspase 8 after a variety of pathological stimuli. Our immunohistochemical results, however, are the first to show that caspase 8 is over-expressed in neurons, astrocytes and oligodendrocytes after experimental brain injury *in vivo*. Moreover, our findings suggest that caspase 8 expression is mainly cytosolic in neurons, but has a rather nuclear distribution in astrocytes and oligodendrocytes after TBI *in vivo*. In this regard it is noteworthy that caspase 8 can be expressed in both the nuclear and cytosolic compartment (Xerri *et al.* 2000). Therefore, future studies are needed to further investigate the significance of caspase 8 expression in different subcellular compartments of CNS cells after experimental brain injuries *in vivo*.

The exact mechanisms leading to the activation of caspase 8 after CNS injuries have yet not been determined. Recent data suggest that caspase 8 may be activated by receptor-mediated mechanisms including the tumor necrosis factor receptor type-1 (TNF-R1) (Schulze-Osthoff *et al.* 1998) and Fas signaling pathways (Muzio *et al.* 1996; Medema *et al.* 1997). For example, it has been reported that over-expression of α-TNF and Fas ligand may induce apoptosis after experimental cerebral ischemia and brain trauma *in vivo* (Kokaia *et al.* 1998; Shohami *et al.* 1996; Martin-Villalba *et al.* 1999). Moreover, increased Fas expression has been implicated in glutamate-induced apoptotic cell death of CNS neurons *in vitro* (Li *et al.* 1998). Importantly, excessive excitatory amino acid release with subsequent neurotoxicity also has been described after TBI *in vivo* (for review see Globus *et al.* 1995). Finally, recent data by Beer *et al.* (2000a) indicate that the Fas/Fas ligand system is also up-regulated in similar brain regions and at similar times after TBI as caspase 8 expression seen in our study (cortical layers 2–5, and 15 min to 72 h after impact injury, respectively). Taken together, these results suggest that excitatory amino acids and the Fas/Fas ligand system may indeed participate in activation of caspase 8 after TBI. In this regard, it is noteworthy that coexpression of Fas and caspase 8 has been observed in spinal cord neurons after experimental spinal cord ischemia *in vivo* (Matsushita *et al.* 2000).

Recent data suggest that cell loss induced by traumatic spinal cord injury and TBI may be attributed in part to apoptotic mechanisms (for a review see Beattie *et al.* 2000; Raghupathi *et al.* 2000). Moreover, several *in vivo* and *in vitro* studies have documented the significance of caspases in apoptotic cell degeneration following acute CNS injuries (for reviews see Eldadah and Faden 2000; Mattson *et al.* 2000). In addition, it has also been reported that caspase 3 is activated after experimental cerebral ischemia (Namura *et al.* 1998; Velier *et al.* 1999), fluid percussion (Yakovlev *et al.* 1997), and cortical impact models of TBI (Beer *et al.* 2000b; Clark *et al.* 2000). Our western blotting data also indicate that caspase 3 is activated after TBI, and our double-labeling immunohistochemical studies using TUNEL and p18 antiserum demonstrated caspase 3-positive cells with gross DNA damage in the traumatized cortex, suggesting a mechanistic link between caspase 3 activation and apoptosis.

Recent evidence from *in vitro* studies suggests that caspase 3 can be activated directly by caspase 8 (Stennicke *et al.* 1998). However, coexpression of caspase 8 and activated caspase 3 after various CNS injuries *in vivo* has not been studied extensively. One recent report indicated that caspase 8 and activated caspase 3 are coexpressed within CNS cells after experimental spinal cord ischemia up to 24 h after the insult (Matsushita *et al.* 2000). Our present findings provide further evidence of expression of both, caspase 8 and activated caspase 3 in multiple cortical CNS cell populations after TBI *in vivo*. Importantly, the expression of caspase 8 and activated caspase 3 in similar cortical brain regions suggests that caspase 8 may participate in caspase 3 activation in cortical CNS cells after TBI. Moreover, the greater number of caspase 8 positive cells (compared with caspase 3 immunoreactive cells) at early time points (6 and 24 h post trauma) followed by a greater number of caspase 3 positive cells (compared with caspase 8 positive cells) at later time points (48 h and 72 h post trauma) supports the hypothesis that caspase 8 may indeed be upstream of caspase 3. However, it was of interest that

caspase 8 immunoreactivity is found also in cells with evidence of DNA damage as indicated by TUNEL. In this regard it is noteworthy that caspase 8 may also function as an amplifying executioner caspase in drug-induced apoptosis *in vitro* (Engels *et al.* 2000). Therefore, future studies have to investigate the exact role of caspase 8 in the activation and/or execution phase of the apoptotic cascade after acute CNS injuries *in vivo*. This also implicates the need for further investigations on the significance of caspase 8 independent activation of caspase 3, including the mitochondrial pathway (Eldadah and Faden 2000).

Our study failed to detect increased expression of caspase 8, activated caspase 3 and apoptotic CNS morphology in the hippocampus ipsilateral to the injury site from 6 h to 14 days after the trauma. This is in contrast to previous reports, which clearly describe features of apoptotic neuronal degeneration in the hippocampus following fluid percussion injury (Yakovlev *et al.* 1997; Conti *et al.* 1998) and cortical impact injury (Clark *et al.* 2000; Colicos and Dash 1996). However, previous studies from our laboratory (Franz *et al.* 1999; Beer *et al.* 2000a,b) have shown that cortical impact injury may not necessarily be associated with hippocampal neuronal degeneration. Probable reasons for discrepancies in the appearance of hippocampal damage may be subtle methodological differences in animal models of TBI. For example, differences in angulation and velocity of the impact devices could account for the presence or absence of hippocampal cell degeneration.

In conclusion, our results provide evidence for induction of caspase 8 expression in cortical neurons and glial cells after TBI *in vivo*. Moreover, our data raise the possibility that caspase 8 may contribute to caspase 3 activation after impact injury in the rat. In addition to these *in vivo* findings, we also provided evidence that caspase 8 and activated caspase 3 may participate in mechanisms of apoptotic CNS cell degeneration in the traumatized cortex. However, future studies are needed to further elucidate the precise role of caspase 8 and activated caspase 3 for cellular CNS degeneration after TBI, including the significance of apoptotic cell death on functional outcome after acute brain injuries *in vivo*.

Acknowledgements

References

Beattie M. S., Farooqui A. A. and Bresnahan J. C. (2000) Review of current evidence for apoptosis after spinal cord injury. *J. Neurotrauma* **17**, 915–925.

Beer R., Franz G., Schöpf M., Reindl M., Zelger B., Schmutzhard E., Poewe W. and Kampfl A. (2000a) Expression of Fas and Fas ligand after experimental traumatic brain injury in the rat. *J. Cereb. Blood Flow Metab.* **20**, 669–677.

Beer R., Franz G., Srinivasan A., Hayes R. L., Pike B. R., Newcomb J. K., Zhao X., Schmutzhard E., Poewe W. and Kampfl A. (2000b) Temporal profile and cell subtype distribution of activated caspase-3 following experimental traumatic brain injury. *J. Neurochem.* **75**, 1264–1273.

Bryan R. M., Cherian L. and Robertson C. (1995) Regional cerebral blood flow after controlled cortical impact injury in rats. *Anesth. Analg.* **80**, 687–695.

Cerretti D. P., Kozlosky C. J., Mosley B., Nelson N., Van Ness K., Greenstreet T. A., March C. J., Kronheim S. R., Druck T. and Cannizzaro L. A. (1992) Molecular cloning of the interleukin-1 beta converting enzyme. *Science* **256**, 97–100.

Charriaut-Marlangue C., Remolleau S., Aggoun-Zouaoui D. and Ben-Ari Y. (1998) Apoptosis and programmed cell death: a role in cerebral ischemia. *Biomed. Pharmacother.* **52**, 264–269.

Clark R. S., Kochanek P. M., Watkins S. C., Chen M., Dixon C. E., Seidberg N. A., Melick J., Loeffert J. E., Nathaniel P. D., Jin K. L. and Graham S. H. (2000) Caspase-3 mediated neuronal death after traumatic brain injury in rats. *J. Neurochem.* **74**, 740–753.

Cohen G. M. (1997) Caspases: the executioners of apoptosis. *Biochem. J.* **326**, 1–16.

Colicos M. A. and Dash P. K. (1996) Apoptotic morphology of dentate gyrus granule cells following experimental cortical impact injury in rats: possible role in spatial memory deficits. *Brain Res.* **739**, 120–131.

Conti A. C., Raghupathi R., Trojanowski J. Q. and McIntosh T. K. (1998) Experimental brain injury induces regionally distinct apoptosis during the acute and delayed post-traumatic period. *J. Neurosci.* **18**, 5663–5672.

Crowe M. J., Bresnahan J. C., Shuman S. L., Masters J. N. and Beattie M. S. (1997) Apoptosis and delayed degeneration after spinal cord injury in rats and monkeys. *Nat. Med.* **3**, 73–76.

Cryns V. and Yuan J. (1998) Proteases to die for. *Genes Dev.* **12**, 1551–1570.

Debus E., Weber K. and Osborn M. (1983) Monoclonal antibodies specific for glial fibrillary acidic (GFA) protein and for each of the neurofilament triplet polypeptides. *Differentiation* **25**, 193–203.

Dixon C. E., Clifton G. L., Lighthall J. W., Yaghmai A. A. and Hayes R. L. (1991) A controlled cortical impact model of traumatic brain injury in the rat. *J. Neurosci. Meth.* **39**, 253–262.

Eldadah B. A. and Faden A. I. (2000) Caspase pathways, neuronal apoptosis, and CNS injury. *J. Neurotrauma* **17**, 811–829.

Engels I. H., Stepczynska A., Stroh C., Lauber K., Berg C., Schwenzer R., Wajant H., Jänicke R. U., Porter A. G., Belka C., Gregor M., Schulze-Osthoff K. and Wesselborg S. (2000) Caspase-8/FLICE functions as an executioner caspase in anticancer drug-induced apoptosis. *Oncogene* **19**, 4563–4573.

Ertel W., Keel M., Stocker R., Imhof H. G., Leist M., Steckholzer U., Tanaka M., Trentz O. and Nagata S. (1997) Detectable concentrations of Fas ligand in cerebrospinal fluid after severe head injury. *J. Neuroimmunol.* **80**, 93–96.

Faden A. I. (1996) Pharmacologic treatment of acute traumatic brain injury. *J. Am. Med. Assoc.* **276**, 569–570.

Felderhoff-Mueser U., Taylor D. L., Greenwood K., Kozma M., Stibenz D., Joashi U. C., Edwards A. D. and Mehmet H. (2000) Fas/CD95/APO-1 can function as a death receptor for neuronal cells in vitro

and in vivo and is upregulated following cerebral hypoxic-ischemic injury to the developing rat brain. *Brain Pathol.* **10**, 17–29.

Franz G., Reindl M., Patel S. C., Beer R., Unterrichter I., Berger T., Schmutzhard E., Poewe W. and Kampfl A. (1999) Increased expression of apolipoprotein D following experimental traumatic brain injury. *J. Neurochem.* **73**, 1615–1625.

Gavrieli Y., Sherman Y. and Ben-Sasson S. A. (1992) Identification of programmed cell death in situ via specific labeling of nuclear DNA fragmentation. *J. Cell Biol.* **119**, 493–501.

Globus M. Y., Alonso O., Dietrich W. D., Busto R. and Ginsberg M. D. (1995) Glutamate release and free radical production following brain injury: effects of posttraumatic hypothermia. *J. Neurochem.* **65**, 1704–1711.

Graeber M. B., Streit W. J., Kiefer R., Schoen S. W. and Kreutzberg G. W. (1990) New expression of myelomonocytic antigens by microglia and perivascular cells following lethal motor neuron injury. *J. Neuroimmunol.* **27**, 121–132.

Graham D. I., McIntosh T. K., Maxwell W. L. and Nicoll J. A. (2000) Recent advances in neurotrauma. *J. Neuropathol. Exp. Neurol.* **59**, 641–651.

Gu C., Casaccia-Bonnefil P., Srinivasan A. and Chao M. V. (1999) Oligodendrocyte apoptosis mediated by caspase activation. *J. Neurosci.* **19**, 3043–3049.

Harrison D. C., Davis R. P., Bond B. C., Campbell C. A., James M. F., Parsons A. A. and Philpott K. L. (2001) Caspase mRNA expression in a rat model of focal cerebral ischemia. *Brain Res. Mol. Brain Res.* **89**, 133–146.

Hayashi T., Sakurai M., Abe K., Sadahiro M., Tabayashi K. and Itoyama Y. (1998) Apoptosis of motor neurons with induction of caspases in the spinal cord after ischemia. *Stroke* **29**, 1007–1012.

Hayes R. L., Jenkins L. W. and Lyeth B. G. (1992) Neurotransmitter-mediated mechanisms of traumatic brain injury: acetylcholine and excitatory amino acids. *J. Neurotrauma* **9**, S173–S187.

Kato H., Kanellopoulos G. K., Matsuo S., Wu Y. J., Jacquin M. F., Hsu C. Y., Kouchoukos N. T. and Choi D. W. (1997) Neuronal apoptosis and necrosis following spinal cord ischemia in the rat. *Exp. Neurol.* **148**, 464–474.

Kermer P., Klocker N. and Bähr M. (1999) Neuronal death after brain injury. Models, mechanisms, and therapeutic strategies in vivo. *Cell Tissue Res.* **298**, 383–395.

Khan S. M., Cassarino D. S., Abramova N. N., Keeney P. M., Borland M. K., Trimmer P. A., Krebs C. T., Bennett J. C., Parks J. K., Swerdlow R. H., Parker W. D. and Bennett J. P. (2000) Alzheimer's disease cybrids replicate beta-amyloid abnormalities through cell death pathways. *Ann. Neurol.* **48**, 148–155.

Kokaia Z., Andsberg G., Martinez-Serrano A. and Lindvall O. (1998) Focal cerebral ischemia in rats induces expression of P75 neurotrophin receptor in resistant striatal cholinergic neurons. *Neuroscience* **84**, 1113–1125.

Krajewska M., Wang H. G., Krajewski S., Zapata J. M., Shabaik A., Gascoyne R. and Reed J. C. (1997) Immunohistochemical analysis of in vivo patterns of expression of CPP32 (Caspase-3), a cell death protease. *Cancer Res.* **57**, 1605–1613.

Krinke G. J. (2000) Part 6: Physiology in, *The Laboratory Rat* (Bullock, G., Bunton, T., eds). San Diego, Academic Press.

Li Y., Maher P. and Schubert D. (1998) Phosphatidylcholine-specific phospholipase C regulates glutamate-induced nerve cell death. *Proc. Natl Acad. Sci. USA* **95**, 7748–7753.

Liu X. Z., Xu X. M., Du Hu R. C., Zhang S. X., McDonald J. W., Dong H. X., Wu Y. J., Fan G. S., Jacquin M. F., Hsu C. Y. and Choi D. W. (1997) Neuronal and glial apoptosis after traumatic spinal cord injury. *J. Neurosci.* **17**, 5395–5406.

McIntosh T. K., Saatman K. E., Raghupathi R., Graham D. I., Smith

D. H., Lee V. M. and Trojanowski J. Q. (1998) The Dorothy Russell Memorial Lecture. The molecular and cellular sequelae of experimental traumatic brain injury: pathogenetic mechanisms. *Neuropathol. Appl. Neurobiol.* **24**, 251–267.

Martin-Villalba A., Herr I., Jeremias I., Hahne M., Brandt R., Vogel J., Schenkel J., Herdegen T. and Debatin K. M. (1999) CD95 ligand (Fas-L/APO-1L) and tumor necrosis factor-related apoptosis-inducing ligand mediate ischemia-induced apoptosis in neurons. *J. Neurosci.* **19**, 3809–3817.

Matsushita K., Wu Y., Qiu J., Lang-Lazdunski L., Hirt L., Waeber C., Hyman B. T., Yuan J. and Moskowitz M. A. (2000) Fas receptor and neuronal cell death after spinal cord ischemia. *J. Neurosci.* **20**, 6879–6887.

Mattson M. P., Culmsee C. and Yu Z. F. (2000) Apoptotic and anti-apoptotic mechanisms in stroke. *Cell Tissue Res.* **301**, 173–187.

Medema J. P., Scaffidi C., Kischkel F. C., Shevchenko A., Mann M., Krammer P. H. and Peter M. E. (1997) FLICE is activated by association with the CD95 death-inducing signaling complex (DISC). *EMBO J.* **16**, 2794–2804.

Mogi M., Togari A., Kondo T., Mizuno Y., Komure O., Kuno S., Ichinose H. and Nagatsu T. (2000) Caspase activities and tumor necrosis factor receptor R1 (p55) level are elevated in the substantia nigra from parkinsonian brain. *J. Neural. Transm.* **107**, 335–341.

Muzio M., Chinnaiyan A. M., Kischkel F. C., O'Rourke K., Shevchenko A., Ni J., Scaffidi C., Bretz J. D., Zhang M., Gentz R., Mann M., Krammer P. H., Peter M. E. and Dixit V. M. (1996) FLICE, a novel FADD-homologous ICE/CED-3-like protease, is recruited to the CD95 (Fas/APO-1) death-inducing signaling complex. *Cell* **85**, 817–827.

Namura S., Zhu J., Fink K., Endres M., Srinivasan A., Tomaselli K. J., Yuan J. and Moskowitz M. A. (1998) Activation and cleavage of caspase-3 in apoptosis induced by experimental cerebral ischemia. *J. Neurosci.* **18**, 3659–3668.

Newcomb J. K., Zhao X., Pike B. R. and Hayes R. L. (1999) Temporal profile of apoptotic-like changes in neurons and astrocytes following controlled cortical impact injury in the rat. *Exp. Neurol.* **158**, 76–88.

Nicholson D. W. (1999) Caspase structure, proteolytic substrates, and function during apoptotic cell death. *Cell Death Differ.* **6**, 1028–1042.

Nitatori T., Sato N., Waguri S., Karasawa Y., Araki H., Shibanai K., Kominami E. and Uchiyama Y. (1995) Delayed neuronal death in the CA1 pyramidal cell layer of the gerbil hippocampus following transient ischemia is apoptosis. *J. Neurosci.* **15**, 1001–1011.

Paxinos G. and Watson C. (1997). *The Rat Brain in Stereotaxic Coordinates*, 4th edn. San Diego, CA: Academic Press.

Pike B. R., Zhao X., Newcomb J. K., Glenn C. C., Anderson D. K. and Hayes R. L. (2000) Stretch injury causes calpain and caspase-3 activation and necrotic and apoptotic cell death in septo-hippocampal cell cultures. *J. Neurotrauma* **17**, 283–298.

Qin Z. H., Wang Y., Kikly K. K., Sapp E., Kegel K. B., Aronin N. and DiFiglia M. (2001) Pro-caspase-8 is predominatly localized in mitochondria and released into cytoplasm upon apoptotic stimulation. *J. Biol. Chem.* **276**, 8079–8086.

Raghupathi R., Graham D. I. and McIntosh T. K. (2000) Apoptosis after traumatic brain injury. *J. Neurotrauma* **17**, 927–938.

Rink A., Fung K. M., Trojanowski J. Q., Lee V. M., Neugebauer E. and McIntosh T. K. (1995) Evidence of apoptotic cell death after experimental traumatic brain injury in the rat. *Am. J. Pathol.* **147**, 1575–1583.

Scaffidi C., Fulda S., Srinivasan A., Friesen C., Li F., Tomaselli K. J.,

Debatin K. M., Krammer P. H. and Peter M. E. (1998) Two CD95 (APO-1/Fas) signaling pathways. *EMBO J.* **17**, 1675–1687.

Schulze-Osthoff K., Ferrari D., Los M., Wesselborg S. and Peter M. E. (1998) Apoptosis signaling by death receptors. *Eur. J. Biochem.* **254**, 439–459.

Shah P. T., Yoon K. W., Xu X. M. and Broder L. D. (1997) Apoptosis mediates cell death following traumatic injury in rat hippocampal neurons. *Neuroscience* **79**, 999–1004.

Shikama Y. (2001) Comprehensive studies on subcellular localizations and cell death-inducing activities of eight gfp-tagged apoptosis-related caspases. *Exp. Cell Res.* **264**, 315–325.

Shohami E., Bass R., Wallach D., Yamin A. and Gallily R. (1996) Inhibition of tumor necrosis factor alpha (TNF alpha) activity in rat brain is associated with cerebroprotection after closed head injury. *J. Cereb. Blood Flow Metab.* **16**, 378–384.

Springer J. E., Azbill R. D. and Knapp P. E. (1999) Activation of the caspase-3 apoptotic cascade in traumatic spinal cord injury. *Nat. Med.* **8**, 943–946.

Sprinkle T. J. (1989) 2′,3′-cyclic nucleotide 3′-phosphodiesterase, an oligodendrocyte-Schwann cell and myelin-associated enzyme of the nervous system. *Crit. Rev. Neurobiol.* **4**, 235–301.

Srinivasan A., Roth K. A., Sayers R. O., Shindler K. S., Wong A. M., Fritz L. C. and Tomaselli K. J. (1998) In situ immunodetection of activated caspase-3 in apoptotic neurons in the developing nervous system. *Cell Death Differ.* **5**, 1004–1016.

Stadelmann C., Deckwerth T. L., Srinivasan A., Bancher C., Bruck W., Jellinger K. and Lassmann H. (1999) Activation of caspase-3 in single neurons and autophagic granules of granulovacuolar degeneration in Alzheimer's disease. Evidence for apoptotic cell death. *Am. J. Pathol.* **155**, 1459–1466.

Stennicke H. R., Jurgensmeier J. M., Shin H., Deveraux Q., Wolf B. B., Yang X., Zhou Q., Ellerby H. M., Ellerby L. M., Bredesen D., Green D. R., Reed J. C., Froelich C. J. and Salvesen G. S. (1998) Pro-caspase-3 is a major physiologic target of caspase-8. *J. Biol. Chem.* **273**, 27084–27090.

Stoka V. V., Turk B., Schendel S. L., Kim T. H., Cirman T., Snipas S. J., Ellerby L. M., Bredesen D., Freeze H., Abrahamson M., Bromme D., Krajewski S., Reed J. C., Yin X. M., Turk V. V. and Salvesen G. S. (2001) Lysosomal protease pathways to apoptosis: cleavage of bid, not pro-caspases, is the most likely route. *J. Biol. Chem.* **276**, 3149–3157.

Thurman D. J., Alverson C., Dunn K. A., Guerrero J. and Sniezek J. E. (1999) Traumatic brain injury in the United States: a public health perspective. *J. Head Trauma Rehabil.* **14**, 602–615.

Velier J. J., Ellison J. A., Kikly K. K., Spera P. A., Barone F. C. and Feuerstein G. Z. (1999) Caspase-8 and caspase-3 are expressed by different populations of cortical neurons undergoing delayed cell death after focal stroke in the rat. *J. Neurosci.* **19**, 5932–5941.

Walker N. P., Talanian R. V., Brady K. D., Dang L. C., Bump N. J., Ferenz C. R., Franklin S., Ghayur T., Hackett M. C. and Hammill L. D. (1994) Crystal structure of the cysteine protease interleukin-1 beta-converting enzyme: a (p20/p10), 2 homodimer. *Cell* **78**, 343–352.

Wolf H. K., Buslei R., Schmidt-Kastner R., Schmidt-Kastner P. K., Pietsch T., Wiestler O. D. and Bluhmke I. (1996) NeuN: a useful neuronal marker for diagnostic histopathology. *J. Histochem. Cytochem.* **44**, 1167–1171.

Xerri L., Palmerini F., Devilard E., Defrance T., Bouabdallah R., Hassoun J. and Birg F. (2000) Frequent nuclear localization of ICAD and cytoplasmic co-expression of caspase-8 and caspase-3 in human lymphomas. *J. Pathol.* **192**, 194–202.

Yakovlev A. G., Knoblach S. M., Fan L., Fox G. B., Goodnight R. and Faden A. I. (1997) Activation of CPP32-like caspases contributes to neuronal apoptosis and neurological dysfunction after traumatic brain injury. *J. Neurosci.* **17**, 7415–7424.

NCBI   **Pub Med**   National Library of Medicine **NLM**

Entrez   PubMed   Nucleotide   Protein   Genome   Structure   OMIM   PMC   Journals   Boo

Search PubMed   for   Go   Clear

Limits   Preview/Index   History   Clipboard   Details

Display   Abstract   Show: 20   Sort   Send to   Text

LWWonline
LIPPINCOTT WILLIAMS & WILKINS

Temporal and spatial profile of Bid cleavage after experimental traumatic brain injury.

**Franz G, Beer R, Intemann D, Krajewski S, Reed JC, Engelhardt K, Pik
BR, Hayes RL, Wang KK, Schmutzhard E, Kampfl A.**

Department of Neurology, University Hospital Innsbruck, Austria.

Apoptosis plays an essential role in the cascade of CNS cell degeneration afte
traumatic brain injury. However, the underlying mechanisms are poorly
understood. The authors examined the temporal profile and cell subtype
distribution of the proapoptotic protein Bid from 6 hours to 7 days after corti
impact injury in the rat. Increased protein levels of tBid were seen in the cort
ipsilateral to the injury site from 6 hours to 3 days after trauma.
Immunohistologic examinations revealed expression of tBid in neurons,
astrocytes, and oligodendrocytes from 6 hours to 3 days after impact injury, a
concurrent assessment of DNA damage using TUNEL identified tBid-
immunopositive cells with apoptoticlike morphology in the traumatized corte
Moreover, Bid cleavage and activation of caspase-8 and caspase-9 occurred a
similar time points and in similar brain regions (i.e., cortical layers 2 to 5) aft
impact injury. In contrast, there was no evidence of caspase-8 or caspase-9
processing or Bid cleavage in the ipsilateral hippocampus, contralateral corte
and hippocampus up to 7 days after the injury. The results provide the first
evidence of Bid cleavage in the traumatized cortex after experimental trauma
brain injury in vivo, and demonstrate that tBid is expressed in neurons and gl
cells. Further, findings indicate that cleavage of Bid may be associated with t
activation of the initiator caspase-8 and caspase-9. Finally, these data suppor
the hypothesis that cleavage of Bid contributes to the apoptotic degeneration
different CNS cells in the injured cortex.

PMID: 12172380 [PubMed - indexed for MEDLINE]

Display   Abstract   Show: 20   Sort   Send to   Text

Temporal and spatial profile of Bid cleavage after experimental traumatic brain injury

Gerhard Franz, Ronny Beer, Denis Intemann, *Stanislaw Krajewski, *John C. Reed,

Klaus Engelhardt, [†]Brian R. Pike, [†]Ronald L. Hayes, [‡]Kevin K. Wang,

Erich Schmutzhard, and Andreas Kampfl

Department of Neurology, University Hospital Innsbruck, Austria, *The Burnham Institute,
La Jolla, California, [†]Evelyn F. and William L. McKnight Brain institute of the University of
Florida, Department of Neuroscience, Gainesville, Florida, [‡]Department of Neuroscience
Therapeutics, Pfizer Inc., Ann Arbor, Michigan, U.S.A.

Correspondence:

Prof. Andreas Kampfl, MD

Department of Neurology, University Hospital Innsbruck

6020 Innsbruck, Anichstrasse 35

Austria

Tel: +43 (512) 504-4273, Fax: +43 (512) 504-3987

E-mail: andreas.kampfl@uibk.ac.at

ABSTRACT

Apoptosis plays an essential role in the cascade of CNS cell degeneration after traumatic brain injury. However, the underlying mechanisms are poorly understood. In the present study we examined the temporal profile and cell subtype distribution of the proapoptotic protein Bid from 6 hours to 7 days following cortical impact injury in the rat. Increased protein levels of the truncated active form of Bid (tBid) were seen in the cortex ipsilateral to the injury site from 6 hours to 3 days after trauma. Immunohistological examinations revealed expression of tBid in neurons, astrocytes and oligodendrocytes from 6 hours to 3 days after impact injury and concurrent assessment of DNA damage using TUNEL identified tBid immunopositive cells with apoptotic-like morphology in the traumatized cortex. Moreover, Bid cleavage and activation of caspase-8 and caspase-9 occurred at similar time points and in similar brain regions (i.e., cortical layers 2 to 5) after impact injury. In contrast, there was no evidence of processing of caspase-8, caspase-9 and Bid cleavage in the ipsilateral hippocampus, contralateral cortex and hippocampus up to 7 days after the injury.

Our results provide the first evidence of Bid cleavage in the traumatized cortex after experimental TBI *in vivo* and demonstrate that tBid is expressed in neurons and glial cells. Further, our findings indicate that cleavage of Bid may be associated with the activation of the initiator caspase-8 and caspase-9. Last, our data support the hypothesis that cleavage of Bid contributes to the apoptotic degeneration of different CNS cells in the injured cortex.

KEY WORDS

Apoptosis---Bid---Caspases---Neurons---Glia---Traumatic brain injury

ABBREVIATIONS

CNPase, 2',3'-cyclic-nucleotide-3'-phosphodiesterase; GFAP, glial fibrillary acid protein;

NeuN, neuron-specific nuclear protein (neuronal nuclei); PBS, phosphate buffered saline;

tBid, truncated form of Bid; TBI, traumatic brain injury; TUNEL, terminal deoxynucleotidyl

transferase (TdT)---mediated deoxyuridine-biotin nick end labeling.

RUNNING TITLE

Bid cleavage after experimental brain trauma

INTRODUCTION

Apoptosis is a feature of acute neurodegenerative diseases including cerebral ischemia and traumatic brain injury (TBI) (Faden, 1996; McIntosh et al., 1998; Conti et al., 1998; Rink et al., 1995). Moreover, members of the caspase family of cysteine proteases have been implicated as important regulators of apoptosis following TBI. For example, caspase-3 has been shown to be the major executioner caspase involved in neuronal and glial apoptosis after TBI *in vivo* (Clark et al., 2000; Beer et al., 2000b; Yakovlev et al., 1997) and *in vitro* (Pike et al., 2000).

At present two major caspase-3 activating pathways have been identified. The extrinsic pathway involves cell surface receptors such as Fas. Binding of Fas ligand to Fas allows the recruitment and activation of the initiator caspase-8 (Li et al., 1998). Active caspase-8, in turn activates executioner caspase-3 and caspase-7 (Stennicke et al., 1998; van de Craen et al., 1999). Importantly, recent data have emphasized a contributory role for the extrinsic pathway in TBI induced CNS apoptosis (Beer et al., 2000a; 2001; Keane et al., 2001).

The intrinsic apoptotic pathway is initiated by the release of cytochrome c to the cytosol. Cytochrome c then binds to the adaptor protein Apaf-1, which allows the recruitment and activation of the initiator caspase-9 in the presence dATP (Green and Reed, 1998; Crompton, 2000). Activated caspase-9 then results in processing of caspase-3 (Slee et al., 1999). A role for caspase-9 activation for CNS apoptosis in TBI *in vivo* has been established recently (Yakovlev et al., 2001).

One pro-apoptotic member of the Bcl-2 family, referred to as Bid, has been suggested to play an important role in the sequence of events leading to caspase activation (Crompton, 2000). For example, recent *in vitro* studies have shown that Bid is a specific substrate of caspase-8 in the Fas apoptotic signaling pathway (Li et al., 1998). While inactive full length (p22) Bid is present in the cytosol, truncated Bid (tBid; p15) translocates to mitochondria and

induces conformational changes in Bax and Bak and triggers cytochrome c release into the cytosol with subsequent activation of caspase-9 (McDonnell et al., 1999; Grinberg et al., 2002, Krajewska et al., 2002). Thus, Bid represents an important mediator of cross-talk between the death receptor and the mitochondria pathways.

Although previous findings on the processing of caspase-8, caspase-9 and caspase-3 would suggest a contributory role of Bid induced apoptosis of CNS cells after brain trauma, no studies to date have examined the temporal and spatial profile of Bid cleavage after TBI *in vivo*. To further investigate the processing of Bid after experimental TBI, rodents were subjected to a widely used model of experimental mechanical brain injury --- lateral cortical impact injury (Dixon et al., 1991; Franz et al., 1999). Western blot analyses of cortical and hippocampal samples were used to determine the expression and cleavage of Bid after TBI. Further, immunohistochemical examinations were performed to investigate the cell subtype distribution of tBid and TUNEL was used to assess whether tBid immunopositive cells exhibit morphological features of apoptosis related DNA damage. Last, Western blotting and immunolabeling for tBid, caspase-8 and activated caspase-9 was performed to address whether these proteins are expressed at similar time points and in similar brain regions after experimental TBI *in vivo*.

MATERIALS AND METHODS

Rat model of traumatic brain injury

A controlled cortical impact device was used to induce a moderate level of TBI as described previously (Dixon et al., 1991; Franz et al., 1999; Beer et al., 2001). Briefly, adult male Sprague-Dawley rats (250 to 350 g) were intubated and anesthetized with 2% halothane in a 2:1 mixture of N_2O/O_2. Core body temperature was monitored continuously by a rectal thermistor probe and maintained at 36.5° to 37.5°C. Animals were mounted in a stereotaxic frame on the injury device in a prone position secured by ear and incisor bars. The head was held in a horizontal plane with respect to the interaural lines. A midline incision was made, the soft tissues reflected, and two 7-mm craniotomies were made between lambda and bregma and centered 5 mm laterally on either side of the central suture. The dura was kept intact over the cortex. Injury was induced by impacting the right cortex (ipsilateral cortex) with a 6-mm diameter tip at a rate of 4 m/s. The injury device was set to produce a tissue deformation of 2 mm. Velocity was measured directly by the linear velocity displacement transducer (Shaevitz Model 500 HR, Detroit, MI, U.S.A.), which produces an analog signal that was recorded by a PC-based data acquisition system for analysis of time/displacement parameters of the impactor. After cortical impact, animals were extubated and immediately assessed for recovery of reflexes (Dixon et al., 1991). Sham-injured animals underwent identical surgical procedures but did not receive impact injury. Naive animals were not exposed to any injury-related surgical procedures. A total of fifty-six animals were used in this study (naive, n = 8; sham injured rats, n = 8; injured rats, n = 40). All animal studies carefully conformed to the guidelines outlined in the *Guide for the Care and Use of Laboratory Animals* from the Austrian Department of Health and Science and were approved by the University of Innsbruck Medical School Animal Welfare Committee. Importantly, all efforts were made to minimize animal suffering and to reduce the number of animals used.

Sample preparation, sodium dodecyl sulfate-polyacrylamide gel electrophoresis (SDS-PAGE), immunoblotting, and quantification

Before killing, all animals (n = 28) were given a lethal dose of phenobarbital intraperitoneally (20 mg/kg; Tyrol Pharma, Austria). The animals were killed by decapitation 6 hours, 1 day, 2 days, 3 days, and 7 days after TBI (n = 4 for each time point after injury; n = 2 for sham and naive animals). Sham animals were killed at 6 hours and 2 days after sham surgery, respectively. Both cortices and hippocampi (ipsilateral and contralateral to the injury site) were removed. Excision of both cortices beneath the craniotomies extended approximately 4 mm laterally, approximately 7 mm rostrocaudally, and to a depth extending to the white matter. All samples were immediately frozen in liquid N_2. The microdissected tissue was homogenized at 4°C in ice-cold homogenization buffer containing 20 mmol/L piperazine-N,N'-bis (2-ethanesulfonic acid) (pH 7.1), 2 mmol/L ethylene glycol-bis (β-aminoethyl ether)-N,N,N′,N′-tetraacetic acid, 1 mmol/L ethylenediamine tetraacetic acid, 1mmol/L dithiothreitol, 0.3 mmol/L phenylmethylsulfonylfluoride, and 0.1 mmol/L leupeptin. Chelators and protease inhibitors (Sigma, St. Louis, MO, U.S.A) were added to prevent endogenous *in vitro* activation of proteases and subsequent artifactual degradation of Bid and caspases during tissue processing.

Protein concentrations were determined by bicinchoninic acid microprotein assays (Sigma) with albumin standards. Protein balanced samples were prepared for polyacrylamide gel electrophoresis. Sixty micrograms of protein per lane was routinely resolved on 16% Tris/glycine gels (Invitrogen, Groningen, the Netherlands). After separation, proteins were immediately transferred to nitrocellulose membranes using Western blotting as described previously (Beer et al., 2001). Coomassie Blue (Bio-Rad, Hercules, CA, U.S.A) and Ponceau Red (Sigma) staining were routinely performed to confirm successful transfer of protein and to insure that equal amounts of protein was loaded in each lane. Five percent nonfat milk in phosphate-buffered saline (PBS) with 0.05% Tween 20 was used to reduce non-specific

7

binding. Immunoblots were probed with a mouse monoclonal antibody (Santa Cruz Biotechnology, Santa Cruz, CA, U.S.A.), diluted 1 : 1000 reacting with the p20 subunit and precursor of caspase-8 (Beer et al., 2001), a rabbit polyclonal antiserum against the large subunit (p35) of caspase-9 (The Burnham Institute), diluted 1 : 2500 (Krajewski et al., 1999), a rabbit polyclonal antibody (Pharmingen, San Diego, CA, U.S.A.) directed against full length Bid, diluted 1 : 2500, or a polyclonal anti-Bid antiserum (The Burnham Institute, La Jolla, CA, U.S.A.) recognizing preferably cleaved tBid (Krajewska et al., 2002), diluted 1 : 2500. Specificity of the anti-Bid antisera was confirmed by pre-absorption with recombinant full-length or truncated Bid (obtained by incubation of recombinant Bid with recombinant active caspase-8), respectively. After incubation with primary antibodies overnight at 4°C, nitrocellulose membranes (Amersham Pharmacia Biotech, Uppsala, Sweden) were incubated with secondary antibodies linked to horseradish peroxidase (Amersham Pharmacia Biotech) for 1 hour at ambient temperature. Enhanced chemiluminescence reagents (Amersham Pharmacia Biotech) were used to visualize the immunolabeling on X-ray film. In each blot, the constitutively expressed protein alpha-tubulin (Sigma) was used as an internal standard to further indicate that sample processing was carried out correctly.

Immunohistochemistry

Animals from all treatment groups (n = 28) were given a lethal injection of phenobarbital (20 mg/kg) intraperitoneally before perfusion. Rats were transcardially perfused through the left ventricle (120 mL of 0.9% saline and 200 ml of 4% paraformaldehyde) at 6 hours, 1 day, 2 days, 3 days, and 7 days after TBI (n = 4 for each time point after injury; n = 4 for sham and naive animals). The brains were then removed, grossly sectioned coronally at 2 mm intervals and routinely embedded in paraffin. Sections were then cut at 3 to 4 microns on a rotary microtome, mounted on aminoalkylsilated glass slides and processed for immunohistochemical staining as described previously (Beer et al., 2000a;b; 2001).

Consecutive sections from the primary injury zone were probed with anti-caspase-8 (rabbit polyclonal; The Burnham Institute) (Beer et al., 2001), anti-caspase-9 p35 (rabbit polyclonal; The Burnham Institute) (Krajewski et al., 1999) and anti-Bid (rabbit polyclonal; The Burnham Institute) (Krajewska et al., 2002). Antibodies were diluted 1 : 5000 in 10% fetal calf serum in PBS and permitted to bind overnight at 4°C. Biotinylated goat anti-rabbit (Vector Laboratories, Burlingame, CA, U.S.A.) was then applied at a dilution of 1 : 200 in 3% rat serum in PBS for 1 hour at ambient temperature followed by avidin-peroxidase (Sigma), diluted 1 : 100 in PBS, also for 1 hour at ambient temperature. The reaction was visualized by treatment with 0.05% 3,3-diaminobenzidine tetrahydrochloride solution in PBS containing 0.05% H_2O_2. The color reaction was stopped with several washes of PBS. Immunostaining results were confirmed by the use of pre-immune serum from the same animals and by pre-absorption of the polyclonal antibodies with the relevant recombinant protein. In addition, sections without primary antibodies were similarly processed to control for binding of the secondary antibody. On control sections, no specific immunoreactivity was detected.

For double immunostaining using brightfield chromagens, sections were pretreated with the rabbit polyclonal antiserum against Bid as described above. Sections were then incubated with a mouse monoclonal anti-NeuN antibody (Wolf et al., 1996) (Chemicon, Temecula, CA, U.S.A.) for neuronal staining. For staining of astrocytes and oligodendrocytes, a mouse monoclonal anti-GFAP antibody (Debus et al., 1983) (Roche Molecular Biochemicals, Mannheim, Germany) or an anti-CNPase monoclonal antibody (Sprinkle, 1989) (Sternberger Monoclonals Inc., Lutherville, MD, U.S.A.) were used. All antibodies were diluted 1 : 500 in 10% fetal calf serum in PBS and allowed to bind overnight at 4°C. After being rinsed, sections were incubated with a biotinylated horse anti-mouse antibody (Vector Laboratories) at a dilution of 1 : 200 for 1 h at ambient temperature followed by incubation with an alkaline phosphatase avidin-biotin substrate and then reaction with blue chromagen (Vector Blue; Vector Laboratories). The color reaction was stopped with several

9

washes of PBS. Sections were dehydrated through graded ethanol, cleared in a xylene substitute (Histoclear, National Diagnostics, Atlanta, GA, U.S.A.), mounted in Permount (Fisher Scientific, Nepean, Ontario, Canada) and coverslipped. Control experiments were performed in which the primary antibodies were omitted. No staining was observed under these conditions.

For histochemical detection of DNA fragmentation on selected representative sections, terminal deoxynucleotidyl transferase-mediated dUTP-biotin nick end labeling (TUNEL) was performed as described by Gavrieli et al. (1992) with minor modifications (Beer et al., 2000a; 2001). TUNEL reaction was visualized by treatment for 5 minutes with 5-bromo-4-chloro-3-indolyl phosphate/nitro blue tetrazolium substrate system (Dako Corporation, Carpinteria, CA, U.S.A.). For double-label experiments, sections were then processed for Bid immunohistochemistry as described earlier. Immunohistochemical staining was visualized by exposure to 3-amino-9-ethylcarbazole in N,N'-dimethylformamide (Sigma). Primary antibody, labeling mix, or secondary antibody were omitted in control sections. Sections were mounted using an aqueous mounting fluid (Dako Corporation) and examined under the light microscope.

Statistical analysis

Semiquantitative evaluation of immunoreactivity detected by Western blotting was performed using computer-assisted two dimensional densitometric scanning on a Macintosh computer using the public domain NIH Image program (developed at the U.S. National Institutes of Health and available on the Internet at http://rsb.info.nih.gov/nih-image/). Relative band densities on Western blots (n = 1 per blot) were expressed as arbitrary densitometric units for each time point. This procedure was performed for the data of four independent experiments for a total of four different animals per time point. Data acquired in arbitrary densitometric units were transformed to percentages of the densitometric levels

observed for scans from sham animals on the same blot. Group differences were determined by analysis of variance and Tukey's *post hoc* honestly significant difference test. Values given are mean ± SD of four independent experiments. Differences were considered significant when $P < 0.05$.

RESULTS

Western blotting

Cortical impact injury leads to cleavage of Bid in the ipsilateral cortex

To determine whether Bid is cleaved after TBI, brain extracts from cortex and hippocampus ipsi- and contralateral to the injury site were examined by Western blotting for the expression of full length Bid (22 kDa) and the truncated form of Bid (tBID; 15 kDa). In the ipsilateral cortex, cortical impact resulted in decreased protein levels of full length Bid from 6 hours to 3 days after trauma (Fig. 1A) with lowest immunoreactivity seen at 1 day after injury (64% decrease relative to sham animals). Concomitantly, tBid immunoreactivity increased within 6 hours after TBI, peaked at 1 day after the impact (793% increase relative to sham animals), and was still significantly increased at 2 days and 3 days after impact injury (Fig. 1B). After 7 days, no statistically significant increase in tBid immunoreactivity was evident when compared with levels of sham-injured control animals. In the ipsilateral hippocampus, contralateral cortex and hippocampus, TBI resulted in no apparent alteration in immunoreactivity of full length and cleaved Bid (data not shown).

Proteolytic processing of caspase-8 and caspase-9 occurs in the injured cortex

Because Bid cleavage infers with the activation of caspase-8 and caspase-9, processing of these two caspases was examined by Western blot analysis. Using a monoclonal anti-caspase-8 antibody that recognizes both procaspase-8 (p55) and its large subunit (p20), an increase of p55 and p20 caspase-8 immunoreactivity was observed in the ipsilateral cortex from 6 hours to 3 days after TBI (Fig. 2A). Immunoreactivity for caspase-8 p20 increased significantly within 6 hours, peaked at 1 day after the impact (860% increase as compared with sham animals), and was still significantly increased at 2 days and 3 days after impact injury. After 7 days, no significant increase was evident in the p55 and p20 fragments when

12

compared with levels in sham-injured control animals. These results are consistent with a previous report on caspase-8 expression and proteolysis after experimental TBI (Beer et al., 2001). Further, immunoblots of cortical samples ipsilateral to the injury site showed an increase in the immunoreactivity for the large subunit (p35) of activated caspase-9 from 6 hours to 3 days after TBI. Densitometric measures of caspase-9 p35 protein levels from injured animals revealed an increase by 325% relative to sham levels at 6 hours after TBI (Fig. 2B). The increase of caspase-9 p35 immunoreactivity reached a maximum level at 2 days after impact injury (840% increase relative to sham animals) and declined to 520% increase relative to sham at 3 days after TBI. At 7 days post trauma, no statistically significant difference in caspase-9 p35 immunoreactivity was observed between cortical samples ipsilateral to the injury ite and cortical samples from sham-injured animals.

No significant increases in caspase-8 and caspase-9 p35 immunoreactivity were seen between sham and injured animals in cortical samples contralateral to the injury site and hippocampal samples ipsi- and contralateral to the injury site at 6 hours to 7 days after TBI (data not shown).

Immunohistochemistry

Immunohistochemical staining for tBid, caspase-8, caspase-9 and cell subtype distribution of tBid after traumatic brain injury

Ipsilateral and contralateral cortical and hippocampal tissues were examined rostrocaudally from +0.2 to −3.8 mm bregma. No immunoreactivity for tBid (Fig. 3A), caspase-8 and activated caspase-9 was present in the tissue from sham-injured or naive (data not shown) control rats. Positive immunoreactivity for tBid (Fig. 3B,E), caspase-8 (Fig. 3C) and processed caspase-9 (Fig. 3D) was found throughout the ipsilateral cortex at the primary injury zone (from −1.5 to −3.4 mm bregma, cortical layers 2 to 5) from 6 hours to 3 days after the trauma (time point = 1 day after trauma, −3.4 mm bregma). Immunoreactivity for tBid,

13

caspase-8, and activated caspase-9 was absent in contralateral cortical samples and hippocampal samples ipsi- and contralateral to the injury site at all time points investigated (data not shown).

To further investigate if tBid is expressed in neurons and/or glial cells, we performed double-labeling experiments for tBid and the neuronal cell specific marker NeuN, the astrocytic marker GFAP, and the oligodendroglial marker CNPase, respectively. These immunohistochemical analyses of tBid-positive cells from 6 hours to 3 days after TBI (Fig. 3F---H; time point = 1 day after trauma, −3.4 mm bregma) identified labeling with NeuN, GFAP, and CNPase, and demonstrated the expression of tBid in neurons (Fig. 3F), astrocytes (Fig. 3G), and oligodendrocytes (Fig. 3H).

tBid immunopositive cells exhibit nuclear apoptotic-like morphology

To verify further an apoptotic component of post-traumatic cell death and to determine the role of tBid in trauma-induced apoptosis, sections immunopositive for tBid were processed for TUNEL to assess DNA damage. Double-labeling experiments (Fig. 4) demonstrated that a substantial proportion of TUNEL positive cells with shrunken morphology, condensed nuclei and chromatin margination (Fig. 4, arrows) also expressed tBid in layers 2 to 5 at the primary injury zone (time point = 1 day after trauma, bregma −3.4 mm). However, cells with either tBid immunoreactivity or gross apoptotic-like morphology alone were also detected (Fig. 4).

14

DISCUSSION

Our results provide the first evidence for Bid expression and activation after experimental TBI. In the cortex ipsilateral to the injury site, increased immunoreactivity for activated (truncated) Bid (tBid) was detected from 6 hours to 3 days after TBI, and immunohistochemistry demonstrated expression of tBid in neurons, astrocytes and oligodendrocytes at similar time points. In addition, our data revealed expression of tBid in CNS cells with apoptotic like morphology in the traumatized cortex. Last, our data suggest that caspase-8, caspase-9, and Bid are activated in similar brain regions of the injured cortex from 6 hours to 3 days after experimental brain trauma.

Only limited data exist on the putative role of Bid for apoptotic degeneration in chronic and acute neurologic disorders. For example, cleaved Bid has been implicated in apoptosis of neurons in Parkinson's disease (Viswanath et al., 2001) and experimental epilepsy (Henshall et al., 2001). Further, tBid may also mediate apoptotic neuronal cell death after focal cerebral ischemia (Plesnila et al., 2001). In this regard, it is noteworthy that cortical impact injury may produce focal ischemia in the cortex ipsilateral to the injury site (Bryan et al., 1995). Thus, reduced cerebral blood flow may have also contributed to activation of Bid in our experiments.

Bid has been shown to be a specific substrate of the initiator caspase-8 in the Fas apoptotic signaling pathway (Li et al., 1998). Importantly, we and others documented increased expression of Fas and activation of caspase-8 following experimental brain trauma (Beer et al., 2000a; 2001; Keane et al., 2001). Our data now indicate that activated caspase-8 and tBid are expressed at similar time points and in similar cortical regions after cortical impact injury, which may suggest a contributory role for activated caspase-8 in cleavage and activation of Bid. However, a current report also provided evidence that other proteases such as calpain may cleave Bid to an active fragment capable in mediating cytochrome c release in experimental myocardial ischemia (Chen et al., 2001). Therefore, future studies are needed to

further investigate the potential role of other proteases in Bid processing following experimental brain injury, as in particular calpain has been shown to play an important role in degeneration of CNS cells after brain trauma (Kampfl et al., 1997; Saatman et al., 2000) and cerebral ischemia (Neumar et al., 1996) *in vivo*.

Our double labeling experiments revealed expression of tBid in neurons, astrocytes and oligodendrocytes. Interestingly, expression of tBid has been also shown recently in neurons and astrocytes following oxygen/glucose depravation *in vitro* (Plesnila et al., 2001). Importantly, our results are the first to indicate that tBid is expressed in neurons and glial cells after up to 3 days following experimental brain injury *in vivo* and that tBid is seen in CNS cells with apoptotic like morphology. These results may suggest that even delayed treatment paradigms targeting Bid cleavage may prevent apoptotic cell death following acute brain injuries *in vivo*. In this regard, it is noteworthy that a recent report revealed that Bid deficient neurons are more resistant to death after oxygen/glucose depravation *in vitro* (Plesnila et al., 2001).

Current data suggest that tBid casues cytochrome c release from mitochondria, which results in the activation of caspase-9 and subsequently caspase-3 (Budihardjo et al., 1999). However, only limited data exist on the release of cytochrome c and activation of caspase-9 following TBI *in vivo* (Buki et al 2000; Yakovlev et al., 2001; Keane et al 2001). Interestingly, in our present study we found that tBid and activated caspase-9 are expressed in similar brain regions at similar time points after cortical impact injury in the rat. These data may support the hypothesis that tBid may contribute to activation of caspase-9 in the traumatized cortex from 6 hours to 3 days after TBI. However, future studies are needed to further elucidate the exact role of tBid for caspase-9 activation following different acute CNS injuries *in vitro* and *in vivo*.

Our study failed to detect tBid, caspase-8, caspase-9 and apoptotic CNS morphology in the hippocampus ipsilateral to the injury site at the investigated time points. This is in

contrast to previous reports, which clearly describe features of apoptotic neuronal degeneration in the hippocapus (Yakovlev et al., 1997, Clark et al., 2000). However, previous studies of our laboratory (Franz et al., 1999; Beer et al., 2000a;b; 2001) have shown that cortical impact injury may not necessarily be associated with hippocampal neuronal degeneration. Probable reasons for discrepancies in the appearance of hippocampal damage my be subtle methodological differences in animals models of TBI. For example, differences in angulation and velocity of the impact devices could account for the presence of absence of hippocampal degeneration.

In summary, our data suggest that activation of Bid occurs in the traumatized cortex following cortical impact injury in the rat. Further, our findings indicate that Bid cleavage is associated with caspase-8 and caspase-9 activation. As Bid is strategically located upstream of mitochondria and caspase-3 processing, it may represent an attractive therapeutic target for CNS diseases in which apoptotic cell death is prominent. However, this implicates the need for further investigations on the significance of inhibition of Bid cleavage on functional outcome after TBI.

ACKNOWLEDGMENT

REFERENCES

Austrian Department of Health and Science. Guide for the Care and Use of Laboratory Animals. *Federal Law Gazette* 501/1989.

Beer R, Franz G, Krajewski S, Pike BR, Hayes RL, Reed JC, Wang KK, Klimmer C, Schmutzhard E, Poewe W, Kampfl A (2001) Temporal and spatial profile of caspase 8 expression and proteolysis after experimental traumatic brain injury. *J Neurochem* 78:862---873

Beer R, Franz G, Schöpf M, Reindl M, Zelger B, Schmutzhard E, Poewe W, Kampfl A (2000a) Expression of Fas and Fas ligand after experimental traumatic brain injury in the rat. *J Cereb Blood Flow Metab* 20:669---677

Beer R, Franz G, Srinivasan A, Hayes RL, Pike BR, Newcomb JK, Zhao X, Schmutzhard E, Poewe W, Kampfl A (2000b) Temporal profile and cell subtype distribution of activated caspase-3 following experimental traumatic brain injury. *J Neurochem* 75:1264---1273

Budihardjo I, Oliver H, Lutter M, Luo X, Wang X (1999) Biochemical pathways of caspase activation during apoptosis. *Annu Rev Cell Dev Biol* 15:269---290

Bryan RM, Cherian L, Robertson C (1995) Regional cerebral blood flow after controlled cortical impact injury in rats. *Anesth Analg* 80:687---695

Buki A, Okonkwo DO, Wang KK, Povlishock JT (2000) Cytochrome c release and caspase activation in traumatic axonal injury. *J Neurosci* 20:2825---2834

Chen M., He H., Zhan S., Krajewski S., Reed J. C., Gottlieb R. A. (2001) Bid is cleaved by calpain to an active fragment in vitro and during myocardial ischemia/reperfusion. *J Biol Chem* 276:30724---30728

Clark RS, Kochanek PM, Watkins SC, Chen M, Dixon CE, Seidberg NA, Melick J, Loeffert JE, Nathaniel PD, Jin KL, Graham SH (2000) Caspase-3 mediated neuronal death after traumatic brain injury in rats. *J Neurochem* 74:740---753

Conti AC, Raghupathi R, Trojanowski JQ, McIntosh TK (1998) Experimental brain injury induces regionally distinct apoptosis during the acute and delayed post-traumatic period. *J Neurosci* 18:5663---5672

Crompton M (2000) Bax, Bid and the permeabilization of the mitochondrial outer membrane in apoptosis. *Current Opinion in Cell Biology* 12:414---419

Debus E, Weber K, Osborn M (1983) Monoclonal antibodies specific for glial fibrillary acidic (GFA) protein and for each of the neurofilament triplet polypeptides. *Differentiation* 25:193---203

Dixon CE, Clifton GL, Lighthall JW, Yaghmai AA, Hayes RL (1991) A controlled cortical impact model of traumatic brain injury in the rat. *J Neurosci Methods* 39:253---262

Faden AI (1996) Pharmacologic treatment of acute traumatic brain injury. *J Am Med Assoc* 276:569---570

Franz G, Reindl M, Patel SC, Beer R, Unterrichter I, Berger T, Schmutzhard E, Poewe W, Kampfl A (1999) Increased expression of apolipoprotein D following experimental traumatic brain injury. *J Neurochem* 73:1615---1625

Green DR, Reed JC (1998) Mitochondria and apoptosis. *Science* 281:1309---1312

Grinberg M, Sarig R, Zaltsman Y, Frumkin D, Grammatikakis N, Reuveny E, Gross A (2002) tBID homooligomerizes in the mitochondrial membrane to induce apoptosis. *J Biol Chem*, in press (published online ahead of print on January 22nd, 2002)

Henshall DC, Bonislawski DP, Skradski SL, Lan JQ, Meller R, Simon RP (2001) Cleavage of bid may amplify caspase-8-induced neuronal death following focally evoked limbic seizures. *Neurobiol Dis* 8:568---580

Kampfl A, Posmantur RM, Zhao X, Schmutzhard E, Clifton GL, Hayes RL (1997) Mechanisms of calpain proteolysis following traumatic brain injury: implications for pathology and therapy: implications for pathology and therapy: a review and update. *J Neurotrauma* 14:121---134

Keane RW, Kraydieh S, Lotocki G, Alonso OF, Aldana P, Dietrich WD (2001) Apopotic and antiapoptotic mechanisms after traumatic brain injury. *J Cereb Blood Flow Metab* 21:1189---1198

Krajewska M, Mai JK, Zapata JM, Ashwell KW, Schendel SL, Reed JC, Krajewski S (2002) Dynamics of expression of apoptosis-regulatory proteins Bid, Bcl-2, Bcl-X, Bax and Bak during development of murine nervous system. *Cell Death Differ* 9:145---157

Krajewski S, Krajewska M, Ellerby LM, Welsh K, Xie Z, Deveraux QL, Salvesen GS, Bredesen DE, Rosenthal RE, Fiskum G, Reed JC (1999) Release of caspase-9 from mitochondria during neuronal apoptosis and cerebral ischemia. *Proc Natl Acad Sci USA* 96:5752---5757

Li H, Zhu H, Xu CJ, Yuan J (1998) Cleavage of BID by caspase 8 mediates the mitochondrial damage in the Fas pathway of apoptosis. *Cell* 94:491---501

McDonnell JM, Fushmann D, Milliman CL, Korsmeyer SJ, Cowburn D (1999) Solution structure of the proapoptotic molecule Bid: a structural basis for apoptotic agonists and antagonists. *Cell* 96:625---634

McIntosh TK, Saatman KE, Raghupathi R, Graham DI, Smith DH, Lee VM, Trojanowski JQ (1998) The Dorothy Russell Memorial Lecture. The molecular and cellular sequelae of experimental traumatic brain injury: pathogenetic mechanisms. *Neuropathol Appl Neurobiol* 24:251---267

Neumar RW, Hagle SM, DeGracia DJ, Krause GS, White BC (1996) Brain mu-calpain autolysis during global cerebral ischemia. *J Neurochem* 66:421---424

Pike BR, Zhao X, Newcomb JK, Glenn CC, Anderson DK, Hayes RL (2000) Stretch injury causes calpain and caspase-3 activation and necrotic and apoptotic cell death in septo-hippocampal cell cultures. *J Neurotrauma* 17:283---298

Plesnila N, Zinkel S, Le DA, Amin-Hanjani S, Wu Y, Qiu J, Chiarugi A, Thomas SS, Kohane DS, Korsmeyer SJ, Moskowitz MA (2001) BID mediates neuronal cell death after oxygen/glucose deprivation and focal cerebral ischemia. *Proc Natl Acad Sci USA* 98:15318---23

Rink A, Fung KM, Trojanowski JQ, Lee VM, Neugebauer E, McIntosh TK (1995) Evidence of apoptotic cell death after experimental traumatic brain injury in the rat. *Am J Pathol* 147:1575---1583

Saatman KE, Zhang C, Bartus RT, McIntosh TK (2000) Behavioral efficacy of posttraumatic calpain inhibition is not accompanied by reduced spectrin proteolysis, cortical lesion, or apoptosis. *J Cereb Blood Flow Metab* 20:66---73

Slee EA, Harte MT, Kluck RM, Wolf BB, Casiano CA, Newmeyer DD, Wang HG, Reed JC, Nicholson DW, Alnemri ES, Green DR, Martin SJ (1999) Ordering the cytochrome c-initiated caspase cascade: hierarchical activation of caspases-2, -3, -6, -7, -8, and -10 in a caspase-9-dependent manner. *J Cell Biol* 144:281---292.

Sprinkle TJ (1989) 2',3'-cyclic nucleotide 3' phosphodiesterase, an oligodendrocyte-Schwann cell and myelin-associated enzyme of the nervous system. *Crit Rev Neurobiol* 4:235---301

Stennicke HR, Jurgensmeier JM, Shin H, Deveraux Q, Wolf BB, Yang X, Zhou Q, Ellerby HM, Ellerby LM, Bredesen D, Green DR, Reed JC, Froelich CJ, Salvesen GS (1998) Pro-caspase-3 is a major physiologic target of caspase-8. *J Biol Chem* 273:27084---27090

Van de Craen M, Declercq W, Van den Brande I, Fiers W, Vandenabeele P (1999) The proteolytic procaspase activation network: an in vitro analysis. *Cell Death Differ* 6:1117---1124

Viswanath V, Wu Y, Boonplueang R, Chen S, Stevenson FF, Yantiri F, Yang L, Beal MF, Andersen JK (2001) Caspase-9 activation results in downstream caspase-8 activation and bid

cleavage in 1-methyl-4-phenyl-1,2,3,6-tetrahydropyridine-induced Parkinson's disease. *J Neurosci* 21:9519---9528

Wolf HK, Buslei R, Schmidt-Kastner R, Schmidt-Kastner PK, Pietsch T, Wiestler OD, Bluhmke I (1996) NeuN: a useful neuronal marker for diagnostic histopathology. J Histochem Cytochem 44:1167---1171

Yakovlev AG, Knoblach SM, Fan L, Fox GB, Goodnight R, Faden AI (1997) Activation of CPP32-like caspases contributes to neuronal apoptosis and neurological dysfunction after traumatic brain injury. *J Neurosci* 17:7415---7424

Yakovlev AG, Ota K, Wang G, Movsesyan V, Bao WL, Yoshihara K, Faden AI (2001) Differential expression of apoptotic protease-activating factor-1 and caspase-3 genes and susceptibility to apoptosis during brain development and after traumatic brain injury. *J Neurosci* 21:7439---7446

FIGURES

FIG. 1. Time-course of Bid protein expression (A) and cleavage (B) after TBI. Samples from single control (sham) and single injured animals were prepared for Western blotting between 6 hours and 7 days after TBI. Immunoreactivity is expressed as arbitrary densitometric units. Data were transformed to percentages of the densitometric levels observed on scans from sham animals visualized on the same blot. Values given are mean $\pm$ SD of four independent experiments. (A) Ipsilateral cortex: immunoblots demonstrated processing of full length Bid (22 kDa) at 6 hours (++$P < 0.01$), 1 day (+++$P < 0.001$), 2 days (++$P < 0.01$), and 3 days (+$P < 0.05$) after TBI. (B) Immunoreactivity of cleaved Bid (tBid; 15 kDa) increased significantly at 6 hours after TBI (+++$P < 0.001$), peaked at 1 day post injury (+++$P < 0.001$), and was still significantly increased up to 3 days post trauma (++$P < 0.01$).

FIG. 2. Time course of caspase-8 p20 (A) and caspase-9 p35 (B) protein expression after TBI. Samples from single control (sham) and single injured animals were prepared for Western blotting between 6 hours and 7 days after TBI. Immunoreactivity is expressed as arbitrary densitometric units. Data were transformed to percentages of the densitometric levels observed on scans from sham animals visualized on the same blot. Values given are mean $\pm$ SD of four independent experiments. Ipsilateral cortex: the proteolytically active fragments of caspase-8 p20 (Fig. 2A) and caspase-9 p35 (Fig. 2B) increased significantly within 6 hours after TBI (++$P < 0.01$). (A) Caspase-8 p20 immunoreactivity peaked at 1 day post injury (+++$P < 0.001$) and remained increased until 3 days post trauma (++$P < 0.01$). (B) Caspase-9 p35 immunoreactivity showed its maximum at 2 days after TBI (+++$P < 0.001$) and was still significantly elevated at 3 days after impact injury (++$P < 0.01$).

FIG. 3. Immunohistochemical analysis of tBid, caspase-8 p20, caspase-9 p35 and cell subtype distribution of tBid in the traumatized cortex (–3.4 mm bregma) at 1 day after TBI. Sham

controls showed no specific immunolabeling for tBid (A). Intermediate (B) and high

magnification (E) photomicrographs demonstrated specific tBid expression in the ipsilateral

cortex after impact injury. Cells immunopositive for caspase-8 p20 and caspase-9 p35 were

found within similar brain region on consecutive sections (± 10 µm; C and D). Double

immunostaining experiments with tBid (brown color; F---H) and NeuN (blue color; F), GFAP

(blue color; G), and CNPase (blue color; H) provided evidence that tBid is expressed in

cortical neurons (F), astrocytes (G), and oligodendrocytes (H) after TBI. Magnifications: A,

40X; B---D, 100X; E---H, 1000X.

FIG. 4. Appearance of tBid in TUNEL-positive cells in the traumatized cortex (–3.4 mm

bregma) at 1 day after TBI. Combined immunohistochemistry for tBid (red color) and

TUNEL (dark blue color) demonstrated processing of Bid in cells with gross nuclear

apoptotic-like morphology. TUNEL-positive cells exhibited chromatin condensation and

nuclear fragmentation (arrows). Magnification: 200X; insert, 1000X.

Accumulation of non-erythroid αII-spectrin and calpain-cleaved αII-spectrin breakdown products in cerebrospinal fluid after traumatic brain injury in rats

Brian R. Pike,* Jeremy Flint,* Satavisha Dutta,† Erik Johnson*, Kevin K. W. Wang† and Ronald L. Hayes*

*Department of Neuroscience, Evelyn F. and William L. McKnight Brain Institute of the University of Florida, Gainesville, Florida, USA

†Department of Neuroscience Therapeutics, Pfizer Inc, Ann Arbor, Michigan, USA

Abstract

Although a number of increased CSF proteins have been correlated with brain damage and outcome after traumatic brain injury (TBI), a major limitation of currently tested biomarkers is a lack of specificity for defining neuropathological cascades. Identification of surrogate biomarkers that are elevated in CSF in response to brain injury and that offer insight into one or more pathological neurochemical events will provide critical information for appropriate administration of therapeutic compounds for treatment of TBI patients. Non-erythroid αII-spectrin is a cytoskeletal protein that is a substrate of both calpain and caspase-3 cysteine proteases. As we have previously demonstrated, cleavage of αII-spectrin by calpain and caspase-3 results in accumulation of protease-specific spectrin breakdown products (SBDPs) that can be used to monitor the magnitude and temporal duration of protease activation. However, accumulation of αII-spectrin and αII-SBDPs in CSF after TBI has never been examined. Following a moderate level (2.0 mm) of controlled cortical impact TBI in rodents, native αII-spectrin protein was decreased in brain tissue and increased in CSF from 24 h to 72 h after injury. In addition, calpain-specific SBDPs were observed to increase in both brain and CSF after injury. Increases in the calpain-specific 145 kDa SBDP in CSF were 244%, 530% and 665% of sham-injured control animals at 24 h, 48 h and 72 h after TBI, respectively. The caspase-3-specific SBDP was observed to increase in CSF in some animals but to a lesser degree. Importantly, levels of these proteins were undetectable in CSF of uninjured control rats. These results indicate that detection of αII-spectrin and αII-SBDPs is a powerful discriminator of outcome and protease activation after TBI. In accord with our previous studies, results also indicate that calpain may be a more important effector of cell death after moderate TBI than caspase-3.

Keywords: calpain, caspase-3, cell death, cerebrospinal fluid, spectrin, traumatic brain injury.

J. Neurochem. (2001) 78, 1297–1306.

The incidence of traumatic brain injury (TBI) in the United States of America is conservatively estimated to be more than 2 million persons annually with approximately 500 000 hospitalizations (Goldstein 1990). Of these, about 70 000–90 000 head injury survivors are permanently disabled. The annual economic cost to society for care of head-injured patients is estimated at $25 billion (Goldstein 1990). Thus, accurate and reliable measurement of outcome following head injury is of great interest to both head injury survivors and clinicians. Assessment of pathology and neurological impairment immediately after TBI is crucial for determination of appropriate clinical management and for predicting long-term outcome. The outcome measures most often used in head-injured patients are the Glasgow coma scale (GCS), the Glasgow outcome scale (GOS), and computed tomography (CT) scans to detect intracranial pathology.

However, despite dramatically improved emergency triage systems based on these outcome measures, most TBI survivors suffer long-term (for a number of years) impairment, and a large number of TBI survivors are severely affected by TBI despite predictions of 'good recovery' on the GOS (Marion 1996). Because of the limitations of current clinical assessments of TBI severity, there has been an increased interest in the development of neurochemical markers for determining injury severity and for clinical evaluation of pathophysiological mechanisms operative in traumatized brain.

For example, TBI results in neuronal tissue death that can cause a variety of neurochemicals such as amino acids, ions and lactate, as well as a number of cellular proteins and enzymes, to be released into the blood and CSF (Goodman and Simpson 1996). Although assessment of cardiac and liver protein levels in the blood has routinely been used in medical practice for years (e.g. creatine kinase MB or troponin-T), assessment of CNS proteins in blood or CSF is far less developed. Thus, recent studies have measured a variety of neurochemical substances in the CSF or blood in attempt to identify specific surrogate markers of cellular damage and outcome after TBI and other CNS disorders (Haber and Grossman 1980; Inao *et al.* 1988; Robinson *et al.* 1990; Lyeth *et al.* 1993; Raabe and Seifert 1999; Raabe *et al.* 1999; Zemlan *et al.* 1999; Clark *et al.* 2000a; Tapiola *et al.* 2000). For example, creatine kinase BB, lactate dehydrogenase, myelin basic protein, and neuron-specific enolase have been measured in blood or CSF in various CNS disorders including TBI. However, these proteins are non-specific to the brain, offer no insight as to mechanism of injury, and/or prediction of outcome utilizing these proteins has not proven reliable (Goodman and Simpson 1996). Other proteins detected in CSF after brain injury such as S-100B are highly specific to the CNS and have been more robustly correlated with outcome (Raabe and Seifert 1999; Raabe *et al.* 1999). Although brain-specific surrogate biomarkers like S-100B may be useful indicators of outcome after brain injury, detection of these proteins in blood or CSF offers no insight into neurochemical alterations that mediate brain damage after TBI. Thus, identification of neurochemical markers that are specific to the CNS and that provide information about specific ongoing neurochemical events would prove immensely beneficial for both prediction of outcome and for guidance of targeted therapeutic delivery.

Non-erythroid αII-spectrin is the major structural component of the cortical membrane cytoskeleton, is particularly abundant in axons and presynaptic terminals (Riederer *et al.* 1986; Goodman *et al.* 1995), and is a major substrate for both calpain and caspase-3 cysteine proteases (Wang *et al.* 1998). The calpain-mediated cleavage of αII-spectrin occurs between Tyr^{1176} and Gly^{1177} resulting in the formation of calpain-signature spectrin breakdown products (SBDPs) of

150 and 145 kDa (Harris *et al.* 1988). The caspase-3-mediated cleavages of αII-spectrin occur at Asp^{1185}, Ser^{1186}, Asp^{1478} and Ser^{1479} resulting in the formation of caspase-3-signature SBDPs of 150 and 120 kDa, respectively (Wang *et al.* 1998). Importantly, numerous investigations have documented increased pathological activation of calpain and/or caspase-3 proteases after TBI (Saatman *et al.* 1996a, 2000; Kampfl *et al.* 1997; Newcomb *et al.* 1997; Posmantur *et al.* 1997; Yakovlev *et al.* 1997; Pike *et al.* 1998a; Clark *et al.* 1999, 2000b; LaPlaca *et al.* 1999; Okonkwo *et al.* 1999; Zhang *et al.* 1999; Beer *et al.* 2000; Buki *et al.* 2000). In addition, our laboratory and others have provided extensive evidence that αII-spectrin is processed by calpains and/or caspase-3 to signature cleavage products *in vivo* after TBI (Beer *et al.* 2000; Newcomb *et al.* 1997; Pike *et al.* 1998a; Buki *et al.* 2000) and in *in vitro* models of mechanical stretch injury (Pike *et al.* 2000b), necrosis (Zhao *et al.* 1999), apoptosis (Nath *et al.* 1996a, 1996b; Pike *et al.* 1998b), glutamate or NMDA excitotoxicity (Nath *et al.* 2000; Zhao *et al.* 2000), and oxygen-glucose deprivation (Nath *et al.* 1998; Newcomb *et al.* 1998). Moreover, use of selective αII-SBDP antibodies has been used to demonstrate that brain regions with the highest accumulation of SBDPs also have the highest levels of neuronal cell death (Roberts-Lewis *et al.* 1994; Newcomb *et al.* 1997). Thus, the ubiquitous distribution of αII-spectrin in the brain coupled with the ability to utilize signature αII-spectrin proteolytic fragments generated by pathological activation of calpain and/or caspase-3 after TBI makes αII-spectrin a potentially important biomarker of brain damage. To test this hypothesis, the present investigation examined alterations in brain levels of αII-spectrin and αII-SBDPs after controlled cortical impact TBI in rodents, and compared these changes to accumulation of αII-spectrin and αII-SBDPs in CSF in the same animals.

Materials and methods

Surgical Preparation and controlled cortical impact traumatic brain injury

As previously described (Dixon *et al.* 1991; Pike *et al.* 1998a), a cortical impact injury device was used to produce TBI in rodents. Cortical impact TBI results in cortical deformation within the vicinity of the impactor tip associated with contusion, and neuronal and axonal damage that is constrained in the hemisphere ipsilateral to the site of injury (Gennarelli 1994; Meaney *et al.* 1994). Adult male (280–300 g) Sprague–Dawley rats (Harlan; Indianapolis, IN, USA) were initially anesthetized with 4% isoflurane in a carrier gas of 1 : 1 O_2/N_2O (4 min) followed by maintenance anesthesia of 2.5% isoflurane in the same carrier gas. Core body temperature was monitored continuously by a rectal thermistor probe and maintained at 37 ± 1°C by placing an adjustable temperature controlled heating pad beneath the rats. Animals were mounted in a stereotactic frame in a prone position and secured by ear and

incisor bars. A midline cranial incision was made, the soft tissues were reflected, and a unilateral (ipsilateral to site of impact) craniotomy (7 mm diameter) was performed adjacent to the central suture, midway between bregma and lambda. The dura mater was kept intact over the cortex. Brain trauma in rats ($n = 9$) was produced by impacting the right cortex (ipsilateral cortex) with a 5-mm diameter aluminum impactor tip (housed in a pneumatic cylinder) at a velocity of 3.5 m/s with a 2.0-mm compression and 150 ms dwell time (compression duration). Velocity was controlled by adjusting the pressure (compressed N_2) supplied to the pneumatic cylinder. Velocity and dwell time were measured by a linear velocity displacment transducer (Lucas Shaevitz™ model 500 HR; Detroit, MI, USA) that produces an analogue signal that was recorded by a storage-trace oscilloscope (BK Precision, model 2522B; Placentia, CA, USA). Sham-injured animals ($n = 4$) underwent identical surgical procedures but did not receive an impact injury. Appropriate pre- and post-injury management was maintained to insure that all guidelines set forth by the University of Florida Institutional Animal Care and Use Committee and the National Institutes of Health guidelines detailed in the Guide for the Care and use of Laboratory Animals were complied with.

CSF and cortical tissue preparation

The CSF and brain cortices were collected from animals at various intervals after sham-injury or TBI. At the appropriate time-points, TBI or sham-injured animals were anesthetized as described above and secured in a stereotactic frame with the head allowed to move freely along the longitudinal axis. The head was flexed so that the external occipital protuberance in the neck was prominent and a dorsal midline incision was made over the cervical vertebrae and occiput. The atlanto-occipital membrane was exposed by blunt dissection and a 25G needle attached to polyethylene tubing was carefully lowered into the cisterna magna. Approximately 0.1–0.15 mL of CSF was collected from each rat. Following CSF collection, animals were removed from the stereotactic frame and immediately killed by decapitation. Ipsilateral and contralateral (to the impact site) cortices were then rapidly dissected, rinsed in ice cold PBS, and snap frozen in liquid nitrogen. Cortices beneath the craniotomies were excised to the level of the white matter and extended ~4 mm laterally and ~7 mm rostrocaudally. The CSF samples were centrifuged at 4000 g for 4 min at 4°C to clear any contaminating erythrocytes. Cleared CSF and frozen tissue samples were stored at $-80°C$ until ready for use. Cortices were homogenized in a glass tube with a Teflon dounce pestle in 15 volumes of an ice-cold triple detergent lysis buffer (20 mM HEPES, 1 mM EDTA, 2 mM EGTA, 150 mM NaCl, 0.1% SDS, 1.0% IGEPAL 40, 0.5% deoxycholic acid, pH 7.5) containing a broad range protease inhibitor cocktail (cat. #1-836-145Roche Molecular Biochemicals, Indianapolis, IN, USA).

Immunoblot analyses of CSF and cortical tissues

Protein concentrations of tissue homogenates and CSF were determined by bicinchoninic acid microprotein assays (Pierce Inc., Rockford, IL, USA) with albumin standards. Protein balanced samples were prepared for sodium dodecyl sulfate–polyacrylamide gel electrophoresis (SDS–PAGE) in twofold loading buffer containing 0.25 M Tris (pH 6.8), 0.2 M DTT, 8% SDS, 0.02%

bromophenol blue, and 20% glycerol in distilled H_2O. Samples were heated for 10 min at 100°C and centrifuged for 1 min at 8160 g in a microcentrifuge at ambient temperature. Forty micrograms of protein per lane was routinely resolved by SDS–PAGE on 6.5% Tris/glycine gels for 1 h at 200 V. Following electrophoresis, separated proteins were laterally transferred to polyvinylidene fluoride (PVDF) membranes in a transfer buffer containing 0.192 M glycine and 0.025 M Tris (pH 8.3) with 10% methanol at a constant voltage of 100 V for 1 h at 4°C. Blots were blocked for 1 h at ambient temperature in 5% non-fat milk in TBS and 0.05% Tween-20. Panceau Red (Sigma, St Louis, MO, USA) was used to stain membranes to confirm successful transfer of protein and to insure that an equal amount of protein was loaded in each lane.

Antibodies and immunolabeling of PVDF membranes

Immunoblots containing brain or CSF protein were probed with an anti-α-spectrin (fodrin) monoclonal antibody (FG 6090 Ab; clone AA6; cat. # FG 6090; Affiniti Research Products Limited; Mamhead Castle, Mamhead, Exeter, UK) that detects intact non-erythroid αII-spectrin (280 kDa) and 150, 145 and 120 kDa cleavage fragments to αII-spectrin. A cleavage product of 150 kDa is initially produced by calpains or caspase-3 proteases (each proteolytic cleavage yields a unique amino-terminal region; Nath *et al.* 1996b; Wang *et al.* 1998). The calpain-generated 150 kDa product is further cleaved by calpain to yield a specific calpain signature product of 145 kDa (Harris *et al.* 1988; Nath *et al.* 1996a,b) whereas the caspase-3 generated 150 kDa product is further cleaved by caspase-3 to yield a specific caspase-3 signature product of 120 kDa (Nath *et al.* 1998; Wang *et al.* 1998). To further confirm the specificity of calpain-cleaved spectrin in CSF after TBI, a second antibody (anti-SBDP150; rabbit polyclonal) that recognizes only the calpain-cleaved N-terminal region (GMMPR) of the 150 kDa αII-spectrin breakdown product (SBDP) was also used (Saido *et al.* 1993; Nath *et al.* 1996b). Some immunoblots were immunolabeled with an antibody that recognizes erythroid αI-spectrin (Cat.# BYA10881; Accurate Chemical & Scientific Corp, Westbury, NY, USA). Following an overnight incubation at 4°C with the primary antibodies (FG 6090 Ab, 1 : 4000 for brain tissue and 1 : 2000 for CSF; SBDP150 Ab, 1 : 1000; BYA10881, 1 : 400), blots were incubated for 1 h at ambient temperature in 3% non-fat milk that contained a horseradish peroxidase-conjugated goat anti-mouse IgG (1 : 10 000 dilution) or goat-anti-rabbit IgG (1 : 3000). Enhanced chemiluminescence (ECL; Amersham) reagents were used to visualize immunolabeling on Kodak Biomax ML chemiluminescent film.

Statisitical analyses

Semi-quantitative evaluation of protein levels detected by immunblotting was performed by computer-assisted densitometric scanning (AlphaImager 2000; Digital Imaging System, San Leandro, CA, USA). Data were acquired as integrated densitometric values and transformed to percentages of the densitometric levels obtained on scans from sham-injured animals visualized on the same blot. Data was evaluated by least squares linear regression followed by ANOVA. All values are given as mean ± SEM. Differences were considered significant if $p < 0.05$.

Results

Proteolysis of αII-spectrin in the cortex by calpain, but not caspase-3 after TBI

In the ipsilateral cortex, TBI resulted in decreased protein levels of αII-spectrin (280 kDa) that were associated with concomitant accumulation of calpain-generated 150 and 145 kDa αII-SBDPs (Fig. 1). However, there was little to no detectable increase in the caspase-3-genearated 120 kDa αII-SBDP. These results replicate our previous investigation that reported calpain but not caspase-3 processing of αII-spectrin following a moderate level of lateral controlled cortical impact TBI (Pike *et al.* 1998a). Decreased αII-spectrin (280 kDa) protein levels were 65%, 48% and 39% of sham-injured protein levels at 24 h, 48 h, and 72 h after TBI, respectively (Fig. 2). Increased 150 kDa αII-SBDP levels were 189%, 157%, and 153% of sham-injured levels at 24 h, 48 h and 72 h after TBI, respectively, while increased 145 kDa αII-SBDP levels were 237%, 203% and 198% of sham-injured levels at 24 h, 48 h and 72 h after TBI, respectively (Fig. 2).

In the contralateral cortex, traumatic brain injury resulted in no apparent alteration in protein levels of αII-spectrin (280 kDa) or in any apparent accumulation of calpain-generated 150 or 145 kDa αII-SBDPs, or in caspase-3 generated 120 kDa αII-SBDP as compared to sham-injured control animals (Fig. 1). These results are also in accord with our previous report that calpain-mediated processing of αII-spectrin is predominately confined to ipsilateral brain regions after moderate lateral controlled cortical impact TBI (Newcomb *et al.* 1997; Pike *et al.* 1998a).
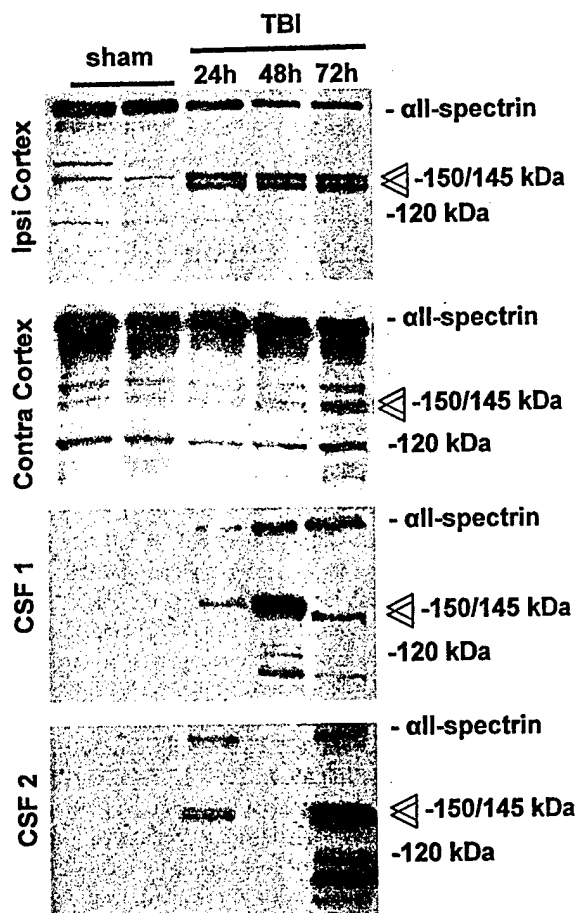
Fig. 1 Traumatic brain injury (TBI) results in prominent accumulation of αII-spectrin (280 kDa) and calpain-cleaved 150 kDa and 145 kDa αII-SBDPs in CSF (FG 6090 Ab). The caspase-3 generated 120 kDa fragment was also apparent in CSF of some animals. TBI caused proteolysis of constitutively expressed brain αII-spectrin (280 kDa) in ipsilateral but not contralateral cortex. Increases in the caspase-3-mediated 120 kDa αII-SBDP were not as apparent in ipsilateral or contralateral cortex after TBI. Immunolabeling of additional unknown bands at ~110 kDa and 95 kDa were also detected in CSF at 48 h and 72 h after injury. CSF1 and CSF2 are from two separate series of animals shown to illustrate that there was more variability in CSF levels of SBDPs than in brain levels, which may reflect individual differences in injury severity.
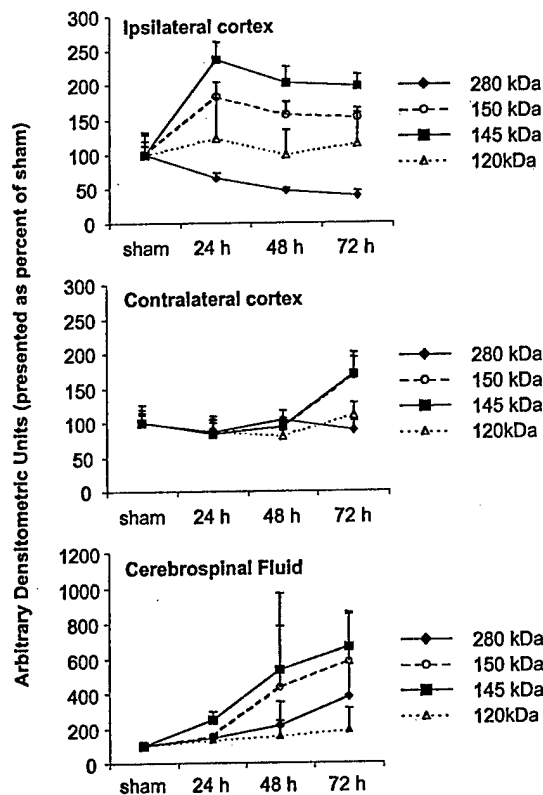

Fig. 2 Mean arbitrary densitometric units obtained from 280 kDa αII-spectrin and the 150 kDa and 145 kDa αII-SBDPs were converted to percent of sham-injured values. Decreases in 280 kDa αII-spectrin and increases in 150 kDa and 145 kDa αII-SBDPs (ipsilateral cortex) were associated with concomitant increases of these proteins in the CSF. Mean accumulation of the caspase-3 generated 120 kDa fragment in these tissues was relatively flat.
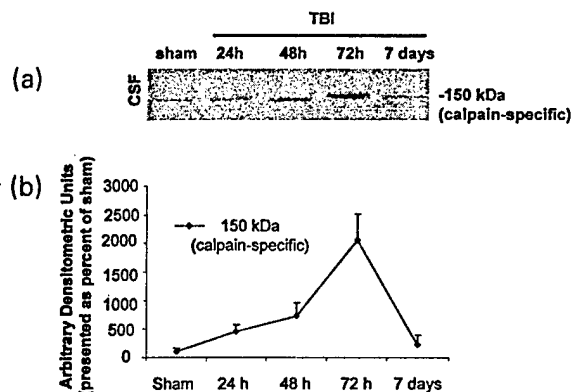
Fig. 3 N-terminal fragment-specific detection of calpain-generated SBDP150 in CSF after traumatic brain injury (SBDP150 Ab). (a) As with the FG 6090 Ab, the SBDP150 Ab detected a progressive increase in the calpain-cleaved 150 kDaA SBDP from 24 h to 72 h after TBI. Levels of 150 kDa SBDP had resolved to sham-injured control levels by seven days after TBI. (b) Mean arbitrary densitometric units of SBDP150 levels detected with anti-SBDP150 Ab.

Accumulation of calpain-mediated αII-SBDPs in CSF after TBI

Immunoblot analyses of CSF levels of non-erythroid αII-spectrin and αII-SBDPs (FG 6090 Ab) showed no detectable levels of these proteins in CSF of sham-injured control animals (Fig. 1). However, after TBI, accumulation of αII-spectrin (280 kDa) and calpain-generated 150 and 145 kDa SBDPs were markedly increased at 24 h, 48 h and 72 h, after injury (Fig. 1). In addition, there was an increase in the caspase-3-generated 120 kDa fragment in one animal at 48 h after TBI, and in another animal at 72 h after TBI (Fig. 1). Accumulation of αII-spectrin (280 kDa) protein levels was 143%, 212%, and 379% of sham-injured animals at 24 h, 48 h, and 72 h after TBI, respectively (Fig. 2). Similarly, accumulation of 150 kDa αII-SBDP after TBI was 155%, 434%, and 583% of sham-injured levels at 24 h, 48 h, and 72 h, respectively, while accumulation of 145 kDa αII-SBDP after TBI was 244%, 530%, and 665% of sham-injured levels at 24 h, 48 h and 72 h, respectively (Fig. 2). In contrast, although accumulation of the caspase-3 cleaved 120 kDa fragment was detected in two animals, the average response was relatively flat. In addition, several lower molecular weight species of αII-spectrin were detected. The protease(s) responsible for these lower molecular weight fragments are currently unknown. However, future identification of these bands may provide important new information regarding other neurochemical events in the brain after TBI.

To provide further confirmation of calpain-generated αII-SBDP accumulation in CSF after TBI, an additional group of animals ($n = 5$ per time-point) was injured as described above and immunoblots of CSF samples were probed with anti-SBDP150 Ab. In this experiment, an additional time-point (7 days post-TBI) was also examined. The SBDP150 Ab specifically recognizes only the calpain-cleaved 150 kDa αII-spectrin fragment and does not recognize the intact 280 kDa protein or other proteolytic fragments (Saido et al. 1993; Nath et al. 1996b). Results with the SBDP150 Ab were nearly identical to those obtained with the FG-6090 Ab (Fig. 3). The calpain-cleaved 150 kDa SBDP was nearly undetectable in CSF of sham-injured animals, and a progressive increase in immunoreactivity was observed from 24 h to 72 h after TBI. Importantly, this experiment also demonstrated that levels of calpain-cleaved 150 kDa SBDP were decreased back to sham-injured control levels by seven days after TBI (Fig. 3).

Linear regression analyses of Cortical versus CSF levels of αII-spectrin and αII-SBDPs

Least squares linear regression was calculated to determine the relationship between brain and CSF levels of αII-spectrin and αII-SBDPs over days post-injury. The slope of the regression lines for αII-spectrin and αII-SBDPs in brain and CSF were analyzed by ANOVA.

For cortical levels of 280 kDa αII-spectrin protein, the slope of the regression line was relatively steep and negative indicating large decreases over days in cortical levels of native αII-spectrin protein (Fig. 4). In contrast, the slope of the regression line for CSF levels of 280 kDa αII-spectrin was relatively steep and positive indicating large increases over days in CSF levels of αII-spectrin protein after TBI. In addition, ANOVA indicated that there was a significant difference ($F = 19.95$, $p < 0.001$) between cortical and CSF slopes for 280 kDa αII-spectrin protein level. This significance indicates that as brain levels of αII-spectrin decrease over days, CSF levels of αII-spectrin increase over days.

For cortical and CSF levels of 150 kDa αII-SBDP, both slopes of the regressions lines were positive indicating large increases in the calpain-cleaved 150 kDa αII-SBDP in brain and CSF over days (Fig. 4). ANOVA indicated no significant difference ($F = 1.86$, $p = 0.1873$) between slopes indicating that the relative accumulation of 150 kDa αII-SBDP in cortex and CSF were similar. However, the slope for CSF 150 kDa αII-SBDP was relatively steeper than the slope for cortical 150 kDa αII-SBDP. This result reflects the densitometric data (Fig. 2) indicating that, in the cortex, peak levels of the 150 kDa αII-SBDP accumulated rapidly (24 h) and were maintained at 48 h and 72 h post-injury. This result also reflects densitometric data (Fig. 2) indicating that CSF levels of the 150 kDa αII-SBDP accumulated more slowly early after injury (24 h) with a greater rate of further accumulation at 48 h and 72 h post-injury. Observed statistical differences in accumulation rates can be appreciated visually in the immunoblot data (Fig. 1). The stability of αII-spectrin and αII-SBDPs in CSF may be increased due to lack of endogenous proteases. For example,
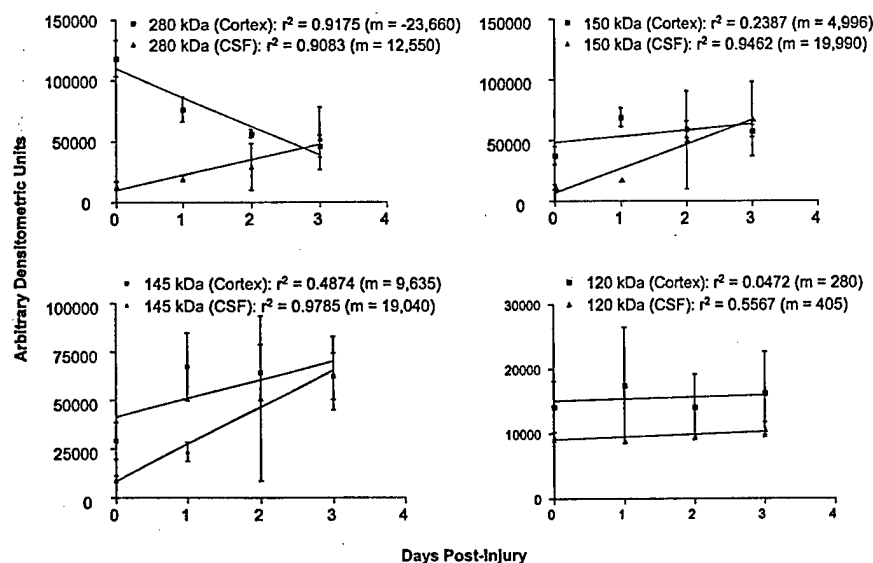
Fig. 4 Cortical versus CSF levels of αII-spectrin (280 kDa) and αII-SBDPs (150, 145, and 120 kDa) over days post-injury. Least squares regression lines of brain and CSF spectrin and SBDP levels were plotted on the same graph. Pearson correlation coefficients for each regression line are indicated. Results indicate that parenchymal decreases in levels of native αII-spectrin (280 kDa) are associated with increases in CSF accumulation while increased parenchymal levels of calpain-mediated αII-SBDPs (150 and 145 kDa) are associated with increased CSF accumulation. On average, there were no changes in parenchymal or CSF levels of the caspase-3-mediated 120 kDa αII-SBDP, although individual rats at different time points showed some increase in CSF levels of the 120 kDa product.

when CSF from TBI animals was stored in individual aliquots at either − 85°C or at ambient laboratory temperature (~26°C) without protease inhibitors for 48 h, αII-SBDP levels from ambient temperature aliquots were only decreased by 28% compared to aliquots stored at − 85°C (Fig. 5). Importantly, the relative stability of αII-SBDP protein in CSF at ambient temperature further indicates this protein as a useful biomarker after TBI.

For cortical and CSF levels of calpain-cleaved 145 kDa αII-SBDP, both slopes of the regression lines were steep and positive indicating large increases in the 145 kDa αII-SBDP in brain and CSF over days (Fig. 4). ANOVA indicated no

48 h storage temperature

− 85°C   ambient

150 kDa-

Fig. 5 Stability of αII-SBDP in CSF after prolonged storage in the absence of protease inhibitors at ambient laboratory temperature. The αII-SBDP protein levels only decreased by 28% when stored at ambient temperature (~26°C) for 48 h compared to identical samples stored at − 85°C for 48 h. These results indicate that αII-SBDPs in CSF are relatively stable at room temperature. This is an important practical consideration for clinical utility.

significant difference ($F = 0.69$, $p = 0.4153$) between slopes indicating that the relative accumulation of 145 kDa αII-SBDP in cortex and CSF were similar as compared to the respective controls. Comparison of slopes for 150 kDa and 145 kDa αII-SBDPs in the brain revealed that the slope of the brain 145 kDa αII-SBDP over days was considerably steeper than the slope of the brain 150 kDa αII-SBDP. This result indicates that brain 145 kDa αII-SBDP protein levels accumulate at a greater rate over days than brain 150 kDa αII-SBDP protein levels. This observation is most likely the result of lower basal levels of brain 145 kDa αII-SBDP than brain 150 kDa αII-SBDP in sham-injured animals and of continued calpain digestion of the larger 150 kDa αII-SBDP to the smaller 145 kDa αII-SBDP over time.

For cortical and CSF levels of caspase-3-cleaved 120 kDa αII-SBDP, both slopes were nearly horizontal, indicating no increased accumulation of caspase-3-generated 120 kDa αII-SBDP over days after TBI (Fig. 4). In addition, ANOVA indicated no significant difference between slopes ($F = 0.002$, $p = 0.9621$).
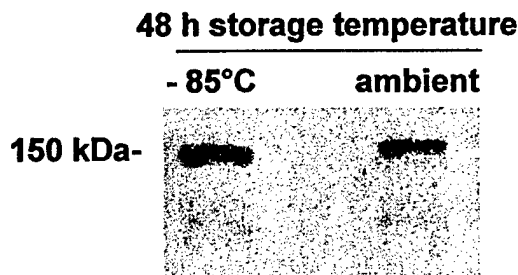
Erythroid αI-spectrin versus non-erythroid αII-spectrin

After head injury, the most likely source of CSF contamination will be from blood. Both neurons and blood contain the erythroid form αI-spectrin protein. However, erythrocytes do not contain non-erythroid αII-spectrin protein. To demonstrate that the source of αII-spectrin immuno-reactivity in the CSF is not blood borne, we probed
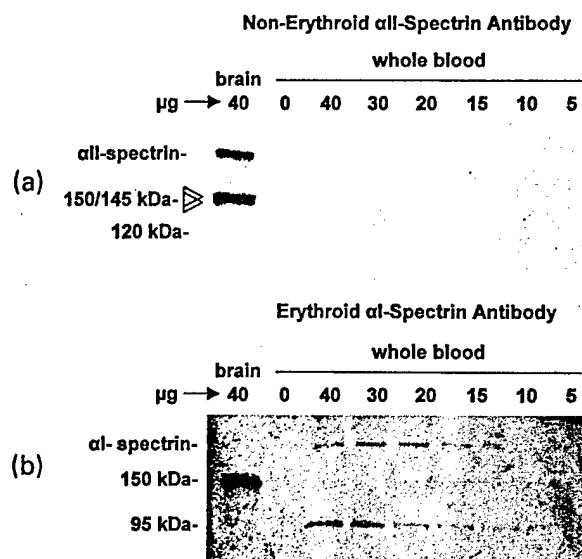
Non-Erythroid αII-Spectrin Antibody

whole blood

brain

| μg → 40 | 0 | 40 | 30 | 20 | 15 | 10 | 5 |

αII-spectrin-

(a) 150/145 kDa- ▷

120 kDa-

Erythroid αI-Spectrin Antibody

whole blood

brain

| μg → 40 | 0 | 40 | 30 | 20 | 15 | 10 | 5 |

αI- spectrin-

(b) 150 kDa-

95 kDa-

Fig. 6 (a) Non-erythroid αII-spectrin protein is not detected in whole blood. After TBI, the most probable source of non-CNS accumulation of proteins in the CSF is from blood. This immunoblot demonstrates that non-erythroid αII-spectrin is detectable in brain protein homogenates but not in blood protein homogenates. (b) In contrast, use of an erythroid αI-spectrin antibody on the same blot that has been stripped and re-probed reveals immunoreactivity for both blood and brain spectrin. These results demonstrate that potential blood contamination of CSF samples does not affect detection of brain-derived αII-spectrin.

immunoblots containing various concentrations of whole blood proteins and brain protein with either an erythroid anti-αI-spectrin antibody or with an anti-αII-spectrin antibody (Fig. 6a,b). As predicted, no immunoreactivity was observed at any concentration of whole blood protein (0–40 μg) while brain spectrin was highly reactive to the non-erythroid anti-αII-spectrin antibody. In contrast, both the brain and blood protein samples were immunoreactive to the erythroid anti-αI-spectrin antibody. This result clearly indicates that use of the non-erythroid, but not the erythroid, anti-spectrin antibody can be used to discriminate non-blood borne spectrin protein in CSF samples.

Discussion

This paper provides the first evidence for accumulation of non-erythroid αII-spectrin protein and calpain-mediated αII-SBDPs in CSF after TBI. Detection of calpain-specific proteolytic fragments to αII-spectrin were confirmed with two antibodies, one that recognizes both intact αII-spectrin and calpain-specific SBDPs (FG 6090 Ab), and one that recognizes only the N-terminal region of calpain-cleaved 150 kDa SBDP (SBDP150 Ab). Results of this investigation indicate that CSF detection of αII-spectrin and αII-SBDPs can provide both a sensitive surrogate biochemical measure

of TBI pathology and provide important information about specific neurochemical events that have occurred in the brain after TBI. To our knowledge, this is the first investigation of any CNS pathology to indicate that identification of accumulated CSF proteins or protein metabolic products can be used to infer specific neurochemical events (i.e. calpain activation) in the brain. Thus, use of αII-SBDPs as surrogate biochemical markers of TBI has important clinical ramifications for assessment of outcome after injury and for determination of specific pathological proteolytic cascades known to occur after TBI. Although other CNS proteins have been detected in CSF after brain injury (e.g. S-100B) and have been correlated with outcome, these proteins offer no insight into pathological mechanisms that have occurred in the brain after TBI. Obviously, identification of metabolic products with known neurochemical etiology will be beneficial for appropriate application of targeted therapeutics (such as calpain inhibitors) after TBI.

Calpain and caspase-3 cysteine proteases are important mediators of cell death and dysfunction in numerous CNS diseases and injuries including TBI. The calpains have historically been associated with necrotic (oncotic) cell death although recent evidence indicates a role in apoptotic cell death as well (Linnik et al. 1996; Nath et al. 1996a,b; Newcomb et al. 1998; Pike et al. 1998b). Numerous investigations have reported calpain activation after TBI (Saatman et al. 1996a, 2000; Kampfl et al. 1997; Newcomb et al. 1997; Posmantur et al. 1997; Pike et al. 1998a) and inhibitors of calpains have been shown to confer neuroprotection after TBI (Posmantur et al. 1997; Saatman et al. 1996b, 2000). Caspase-3 is a critical executioner of apoptosis and caspase-3 activation has been reported in in vitro (Shah et al. 1997; Allen et al. 1999; Pike et al. 2000b) and in vivo (Beer et al. 2000; Yakovlev et al. 1997; Pike et al. 1998a; Clark et al. 2000b) models of TBI. However, it should be noted that at least in our hands, the magnitude of calpain activation after TBI is much greater than that of caspase-3, and that at the moderate level of brain injury employed in the current study, caspase-3 is only transiently elevated in deep, non-cortical brain regions (Pike et al. 1998a). This result most likely accounts for the detection of relatively minimal amounts of the 120 kDa caspase-3-mediated αII-SBDP in CSF after TBI. In contrast to our injury model, Beer et al. (2000) have observed prominent levels of caspase-3 activation in the cortex after cortical impact TBI. However, while our cortical impact model is typically characterized by prominent tissue necrosis and progressive cortical cavitation to the gray-white interface (Kampfl et al. 1996; Newcomb et al. 1997; Dixon et al. 1998; Newcomb et al. 1999; Pike et al. 2000a), the model employed by Beer et al. (2000) was not. Thus, differences in injury magnitude may be important factors affecting calpain and/or caspase-3 activation after TBI, and

this hypothesis warrants further investigation. However, it should be pointed out that although caspase-3 activation has not been a prominent feature in our model of cortical impact TBI, we have detected substantial levels of apoptotic cell death in the cortex after TBI (Newcomb *et al.* 1999). This apparent discrepancy between apoptotic cell death and caspase-3 activation raises the intriguing possibility that apoptosis may occur via a caspase-3-independent pathway after TBI. This observation also warrants further examination.

That different injury magnitudes may result in differential activation of calpain or caspase-3 proteases has important implications for targeted therapeutic intervention after TBI, and importantly, further validates the utility of using surrogate markers of TBI that have known neurochemical etiologies. For example, the current investigation detected CSF accumulation of the calpain-mediated αII-SBDP and not the caspase-3-mediated αII-SBDP. Based on this evidence, administration of calpain but not caspase-3 inhibitors would be predicted to have the most beneficial effect on outcome. However, other injury magnitudes may result in more caspase-3 activation indicating use of caspase-3 inhibitors or a combination of calpain/caspase-3 protease inhibitors. Thus, surrogate measures of TBI will result in selective pharmaceutical therapies based on clinical assessment of neuropathology, and this approach is a superior strategy to promiscuous prophylactic administration of unnecessary and potentially harmful compounds.

The most probable source of peripheral contamination of the CSF after TBI will be blood born. Indeed, we did detect visible red blood cell contamination of CSF after experimental TBI (which was removed by centrifugation). However, our control experiments with brain and whole blood immnuoblots (Fig. 6a,b) clearly demonstrated that the non-erythroid anti-αII-spectrin antibody did not detect any αII-spectrin protein in whole blood samples. Conversly, the erythroid αI-spectrin antibody labeled both brain and blood samples. These results indicate that the major source of potential peripheral CSF contamination after TBI, blood, is not detected by the non-erythroid anti-αII-spectrin antibody. This finding supports the utility of αII-spectrin and αII-SBDPs as surrogate biomarkers of injury after TBI, and importantly, as biomarkers of calpain and/or caspase-3 activation after TBI.

One caveat to the current investigation is the finding that there was more variability in levels of CSF SBDPs than there were in brain levels of SBDPs. This variability is indicated by the larger error bars in Fig. 2 and 4 and can be observed in individual animals in Fig. 1. The reason for the larger variability in CSF protein accumulation is unknown, but may reflect differences in individual animal's CSF circulation after TBI. For example, differences in increased intracranial pressure after TBI may restrict passage of CSF through various foramina that may preclude detection of

secreted proteins into the cisterna magna (source of CSF in the present study). Additional studies should examine differences in intraventricular versus intracisternal levels of accumulated SBDPs.

Nonetheless, future studies focused on development of neuron-specific antibodies targeted against calpain-specific and caspase-3-specific αII-SBDPs (such as the SBDP150 Ab) will further strengthen the utility and specificity of αII-SBDPs as surrogate markers of brain injury. In addition, development of enzyme-linked immunosorbent assays (ELISA) will allow greater quantification of calpain and caspase-3 SBDPs and provide a more rapid and practical approach to CSF detection of these proteins.

References

Allen J. W., Knoblach S. M. and Faden A. I. (1999) Combined mechanical trauma and metabolic impairment in vitro induces NMDA receptor-dependent neuronal cell death and caspase-3-dependent apoptosis. *FASEB J.* 13, 1875–1882.

Beer R., Franz G., Srinivasan A., Hayes R. L., Pike B. R., Newcomb J. K., Zhao X., Schmutzhard E., Poewe W. and Kampfl A. (2000) Temporal profile and cell subtype distribution of activated caspase-3 following experimental traumatic brain injury. *J. Neurochem.* 75, 1264–1273.

Buki A., Okonkwo D. O., Wang K. K. and Povlishock J. T. (2000) Cytochrome C release and caspase activation in traumatic axonal injury. *J. Neurosci.* 20, 2825–2834.

Clark R. S., Kochanek P. M., Chen M., Watkins S. C., Marion D. W., Chen J., Hamilton R. L., Loeffert J. E. and Graham S. H. (1999) Increases in Bcl-2 and cleavage of caspase-1 and caspase-3 in human brain after head injury. *FASEB J.* 13, 813–821.

Clark R. S., Kochanek P. M., Adelson P. D., Bell M. J., Carcillo J. A., Chen M., Wisniewski S. R., Janesko K., Whalen M. J. and Graham S. H. (2000a) Increases in Bcl-2 protein in cerebrospinal fluid and evidence for programmed cell death in infants and children after severe traumatic brain injury. *J. Pediatr.* 137, 197–204.

Clark R. S., Kochanek P. M., Watkins S. C., Chen M., Dixon C. E., Seidberg N. A., Melick J., Loeffert J. E., Nathaniel P. D., Jin K. L. and Graham S. H. (2000b) Caspase-3 mediated neuronal death after traumatic brain injury in rats. *J. Neurochem.* 74, 740–753.

Dixon C. E., Clifton G. L., Lighthall J. W., Yaghmai A. A. and Hayes R. L. (1991) A controlled cortical impact model of traumatic brain injury in the rat. *J. Neurosci. Meth.* 39, 253–262.

Dixon C. E., Markgraf C. G., Angileri F., Pike B. R., Wolfson B., Newcomb J. K., Bismar M. M., Blanco A. J., Clifton G. L. and Hayes R. L. (1998) Protective effects of moderate hypothermia on behavioral deficits but not necrotic cavitation following cortical impact injury in the rat. *J. Neurotrauma* 15, 95–103.

Gennarelli T. A. (1994) Animate models of human head injury. *J. Neurotrauma* 11, 357–368.

Goldstein M. (1990) Traumatic brain injury: a silent epidemic. *Ann. Neurol.* **27**, 327.

Goodman S. R., Zimmer W. E., Clark M. B., Zagon I. S., Barker J. E. and Bloom M. L. (1995) Brain spectrin: of mice and men. *Brain Res. Bull.* **36**, 593–606.

Goodman J. C. and Simpson R. K. Jr (1996) Biochemical monitoring in head injury. In: R. K. Narayan, J. E. Wilberger and J. T. Povlishock, eds. *Neurotrauma*, pp. 577–591. McGraw-Hill, New York.

Haber B. and Grossman R. G. (1980) Acetylcholine metabolism in intracranial and lumbar spinal cerebrospinal fluid and in blood. In: J. H. Wood, ed. *Neurobiology and Cerebrospinal Fluid*, pp. 345–350. Plenum, New York.

Harris A. S., Croall D. E. and Morrow J. S. (1988) The calmodulin-binding site in alpha-fodrin is near the calcium-dependent protease-I cleavage site. *J. Biol. Chem.* **263**, 15754–15761.

Inao S., Marmarou A., Clarke G. D., Anderson B. J., Fatouros P. P. and Young H. F. (1988) Production and clearance of lactate from brain tissue, cerebrospinal fluid, and serum following experimental brain injury. *J. Neurosurg.* **69**, 736–744.

Kampfl A., Posmantur R., Nixon R., Grynspan F., Zhao X., Liu S. J., Newcomb J. K., Clifton G. L. and Hayes R. L. (1996) Mu-calpain activation and calpain-mediated cytoskeletal proteolysis following traumatic brain injury. *J. Neurochem.* **67**, 1575–1583.

Kampfl A., Posmantur R. M., Zhao X., Schmutzhard E., Clifton G. L. and Hayes R. L. (1997) Mechanisms of calpain proteolysis following traumatic brain injury: implications for pathology and therapy: implications for pathology and therapy: a review and update. *J. Neurotrauma.* **14**, 121–134.

LaPlaca M. C., Raghupathi R., Verma A., Pieper A. A., Saatman K. E., Snyder S. H. and McIntosh T. K. (1999) Temporal patterns of poly (ADP-ribose) polymerase activation in the cortex following experimental brain injury in the rat. *J. Neurochem.* **73**, 205–213.

Linnik M. D., Markgraf C. G., Mason P. J., Velayo N. and Racke M. M. (1996) Calpain inhibition attenuates apoptosis in vitro and decreases infarct size in vivo. In: *Pharmacology of Cerebral Ischemia.* J. Krieglstein, ed. CRC Press, Boca Raton:pp. 33.–40.

Lyeth B. G., Jiang J. Y., Robinson S. E., Guo H. and Jenkins L. W. (1993) Hypothermia blunts acetylcholine increase in CSF of traumatically brain injured rats. *Mol. Chem. Neuropath.* **18**, 247–256.

Marion D. W. (1996) Outcome from severe head injury. In: R. K. Narayan, J. E. Wilberger and J. T. Povlishock, eds. *Neurotrauma*, pp. 767–777. McGraw-Hill, New York.

Meaney D. F., Ross D. T., Winkelstein B. A., Brasko J., Goldstein D., Bilston L. B., Thibault L. E. and Gennarelli T. A. (1994) Modification of the cortical impact model to produce axonal injury in the rat cerebral cortex. *J. Neurotrauma* **11**, 599–612.

Nath R., McGinnis K. J., Nadimpalli R., Stafford D. and Wang K. K. W. (1996a) Effects of ICE-like proteases and calpain inhibitors on neuronal apoptosis. *Neuroreport* **8**, 249–255.

Nath R., Raser K. J., Stafford D., Hajimohammadreza I., Posner A., Allen H., Talanian R. V., Yuen P., Gilbertson R. B. and Wang K. K. (1996b) Non-erythroid α-spectrin breakdown by calpain andinterleukin 1β-converting-enzyme-like protease (s) in apoptotic cells: contributory roles of both protease families in neuronal apoptosis. *Biochem. J.* **319**, 683–690.

Nath R., Probert A., McGinnis K. M. and Wang K. K. W. (1998) Evidence for activation of caspase-3-like protease in excitotoxin- and hypoxia/hypoglycemia-injured neurons. *J. Neurochem.* **71**, 186–195.

Nath R., Scott M., Nadimpalli R., Gupta R. and Wang K. K. (2000) Activation of apoptosis-linked caspase(s) in NMDA-injured brains in neonatal rats. *Neurochem. Int.* **36**, 119–126.

Newcomb J. K., Kampfl A., Posmantur R. M., Zhao X., Pike B. R., Liu S. J., Clifton G. L. and Hayes R. L. (1997) Immunohistochemical study of calpain-mediated breakdown products to alpha-spectrin following controlled cortical impact injury in the rat. *J. Neurotrauma.* **14**, 369–383.

Newcomb J. K., Zhao X., Pike B. R., Wang K. K. W. and Hayes R. L. (1998) Proteolytic mechanisms of cell injury following glucose-oxygen deprivation in primary septo-hippocampal cell cultures. *J. Neurotrauma.* **15**, 887.

Newcomb J. K., Zhao X., Pike B. R. and Hayes R. L. (1999) Temporal profile of apoptotic-like changes in neurons and astrocytes following controlled cortical impact injury in the rat. *Exp. Neurol.* **158**, 76–88.

Okonkwo D. O., Buki A., Siman R. and Povlishock J. T. (1999) Cyclosporin A limits calcium-induced axonal damage following traumatic brain injury. *Neuroreport.* **10**, 353–358.

Pike B. R., Zhao X., Newcomb J. K., Posmantur R. M., Wang K. K. W. and Hayes R. L. (1998a) Regional calpain and caspase-3 proteolysis of α-spectrin after traumatic brain injury. *Neuroreport.* **9**, 2437–2442.

Pike B. R., Zhao X., Newcomb J. K., Wang K. K. W., Posmantur R. M. and Hayes R. L. (1998b) Temporal relationships between de novo protein synthesis, calpain and caspase 3-like protease activation, and DNA fragmentation during apoptosis in septo-hippocampal cultures. *J. Neurosci. Res.* **52**, 505–520.

Pike B. R., Johnson E., Flint J., Glenn C. C. and Hayes R. L. (2000a) Prolonged calpain activation in regions of tissue atrophy after traumatic brain injury. *Restor. Neurol. Neurosci.* **16** (3, 4), 166.[abstract].

Pike B. R., Zhao X., Newcomb J. K., Glenn C. C., Anderson D. K. and Hayes R. L. (2000b) Stretch injury causes calpain and caspase-3 activation and necrotic and apoptotic cell death in septo-hippocampal cell cultures. *J. Neurotrauma.* **17**, 283–298.

Posmantur R., Kampfl A., Siman R., Liu J., Zhao X., Clifton G. L. and Hayes R. L. (1997) A calpain inhibitor attenuates cortical cytoskeletal protein loss after experimental traumatic brain injury in the rat. *Neuroscience.* **77**, 875–888.

Raabe A. and Seifert V. (1999) Fatal secondary increase in serum S-100B protein after severe head injury. *J. Neurosurgery.* **91**, 875–877.

Raabe A., Grolms C., Sorge O., Zimmermann M. and Seifert V. (1999) Serum S-100B protein in severe head injury. *Neurosurgery.* **45**, 477–483.

Riederer B. M., Zagon I. S. and Goodman S. R. (1986) Brain spectrin (240/235) and brain spectrin (240/235E): two distinct spectrin subtypes with different locations within mammalian neural cells. *J. Cell Biol.* **102**, 2088–2097.

Roberts-Lewis J. M., Savage M. J., Marcy V. R., Pinsker L. R. and Siman R. (1994) Immunolocalization of μ-calpain mediated spectrin degradation to vulnerable neurons in ischemic gerbil brain. *J. Neurosci.* **14**, 3934–3944.

Robinson S. E., Martin R. M., Davis T. R., Gyenes C. A., Ryland J. E. and Enters E. K. (1990) The effect of acetylcholine depletion on behavior following traumatic brain injury. *Brain Res.* **509**, 41–46.

Saatman K. E., Bozyczko-Coyne D., Marcy V., Siman R. and McIntosh T. K. (1996a) Prolonged calpain-mediated spectrin breakdown occurs regionally following experimental brain injury in the rat. *J. Neuropathol. Exp. Neurol.* **55**, 850–860.

Saatman K. E., Murai H., Bartus R. T., Smith D. H., Hayward N. J., Perri B. R. and McIntosh T. K. (1996b) Calpain inhibitor AK295 attenuates motor and cognitive deficits following experimental brain injury in the rat. *Proc. Natl Acad. Sci. USA* **93**, 3428–3433.

Saatman K. E., Zhang C., Bartus R. T. and McIntosh T. K. (2000)

Behavioral efficacy of posttraumatic calpain inhibition is not accompanied by reduced spectrin proteolysis, cortical lesion, or apoptosis. *J. Cereb. Blood Flow Metab.* **20**, 66–73.

Saido T. C., Yokota M., Nagao S., Yamaura I., Tani E., Tsuchiya T., Suzuki K. and Kawashima S. (1993) Spatial resolution of fodrin proteolysis in postischemic brain. *J. Biol. Chem.* **268**, 25239–25243.

Shah P. T., Yoon K. W., Xu X. M. and Broder L. D. (1997) Apoptosis mediates cell death following traumatic injury in rat hippocampal neurons. *Neuroscience.* **79**, 999–1004.

Tapiola T., Pirttila T., Mikkonen M., Mehta P. D., Alafuzoff I., Koivisto K. and Soininen H. (2000) Three-year follow-up of cerebrospinal fluid tau, β-amyloid 42 and 40 concentrations in Alzheimer's disease. *Neurosci. Lett.* **280**, 119–122.

Wang K. K. W., Posmantur R. M., Nath R., McGinnis K. M., Whitton M., Talanian R. V., Glantz S. B. and Morrow J. S. (1998) Simultaneous degredation of αII and βII spectrin by caspase-3 (CPP32) in apoptotic cells. *J. Biol. Chem.* **273**, 22490–22497.

Yakovlev A. G., Knoblach S. M., Fan L., Fox G. B., Goodnight R. and Faden A. I. (1997) Activation of CPP32-like caspases contributes to neuronal apoptosis and neurological dysfunction after traumatic brain injury. *J. Neurosci.* **17**, 7415–7424.

Zemlan F. P., Rosenberg W. S., Luebbe P. A., Cambell T. A., Dean G. E., Weiner N. E., Cohen J. A., Rudick R. A. and Woo D. (1999) Quantification of axonal damage in traumatic brain injury: affinity purification and characterization of cerebrospinal fluid tau proteins. *J. Neurochem.* **72**, 741–750.

Zhang C., Raghupathi R., Saatman K. E., LaPlaca M. C. and McIntosh T. K. (1999) Regional and temporal alterations in DNA fragmentation factor (DFF)-like proteins following experimental brain trauma in the rat. *J. Neurochem.* **73**, 1650–1659.

Zhao X., Pike B. R., Newcomb J. K., Wang K. K., Posmantur R. M. and Hayes R. L. (1999) Maitotoxin induces calpain but not caspase-3 activation and necrotic cell death in primary septo-hippocampal cultures. *Neurochem. Res.* **24**, 371–382.

Zhao X., Newcomb J. K., Pike B. R., Wang K. K., d'Avella D. and Hayes R. L. (2000) Novel characteristics of glutamate-induced cell death in primary septohippocampal cultures: relationship to calpain and caspase-3 protease activation. *J. Cereb. Blood Flow Metab.* **20**, 550–562.

A Novel Marker for Traumatic Brain Injury: CSF αII-Spectrin Breakdown Product Levels

N.C. RINGGER,[1,4] B.E. O'STEEN,[1,4] J.G. BRABHAM,[1] X. SILVER,[5] J. PINEDA,[3,4]
K.K.W. WANG,[1,2,4] and R.L. HAYES[1,2,4]

ABSTRACT

Currently, there is no definitive diagnostic test for traumatic brain injury (TBI) to help physicians determine the seriousness of injury or the extent of cellular pathology. Calpain cleaves αII-spectrin into breakdown products (SBDP) after TBI and ischemia. Mean levels of both ipsilateral cortex (IC) and cerebral spinal fluid (CSF) SBDP at 2, 6, and 24 h after two levels of controlled cortical impact (1.0 mm and 1.6 mm of cortical deformation) in rats were significantly elevated by injury. CSF and IC SBDP levels were significantly higher after severe (1.6 mm) injury than mild (1.0 mm) injury over time. The correlation between CSF SBDP levels and lesion size from T2-weighted magnetic resonance images 24 hours after TBI as well as correlation of tau and S100β was assessed. Mean levels of CSF SBDP ($r = 0.833$) and tau ($r = 0.693$) significantly correlated with lesion size while levels of CSF S100β did not ($r = 0.188$). Although levels of CSF and IC SBDP and lesion size are all significantly higher after 1.6 mm than 1.0 mm injury, the correlation between CSF SBDP and lesion size was not significant following the removal of controls from the analysis. This indicates CSF SBDP is a reliable marker of the presence or absence of injury. Furthermore, larger lesion sizes 24 h after TBI were negatively correlated with motor performance on days 1–5 after TBI ($r = -0.708$). Based on these data, evaluation of CSF SBDP levels as a biomarker of TBI is warranted in clinical studies.

Key words: biomarker; CSF; injury magnitude; lesion size; spectrin; S100β; tau

◄(AU1)

INTRODUCTION

THE DIFFICULTY of diagnosis and prediction of outcome after acute traumatic brain injury (TBI) is associated with the limitations of clinical assessment and neuroimaging (Zink, 2001). Sedatives may be used to treat patients with TBI that exhibit confusion, agitation, or non-compliance with accompanying increased brain metabolism (Mirski et al., 1995). Treatment with anticonvulsant or sedative drugs may confound information obtained from a clinical neuropsychological examination (Mirski et al., 1995). Many mild head trauma patients with a Glasgow Coma Scale (GCS) between 13 and 15 may have coincidental intoxication with drugs and alcohol that may also confound clinical neuropsychological examinations (Kelly, 1995). Head injuries may also be overlooked

---

[1]Department of Neuroscience, [2]Department of Psychiatry, [3]Department of Pediatrics, [4]Center for Traumatic Brain Injuries, and [5]Advanced Magnetic Resonance Imaging and Spectroscopy (AMRIS) Facility, Evelyn F. and William L. McKnight Brain Institute, University of Florida, Gainesville, Florida.

in multi-trauma patients (Buduhan and McRitchie, 2000). Clinical indicators may not predict significant intracranial trauma (Harad and Kerstein, 1992). Neurologic damage from TBI, stroke or perinatal asphyxia may precede changes seen by modern neuroimagining techniques. Although mild traumatic injury may cause long term disabilities, mild trauma may not be seen acutely with radiologic or magnetic resonance imaging (MRI). Computed tomography (CT) scanning is the quickest and most available neuroimaging, yet has low sensitivity for diffuse brain damage. In a critical care patient, cost, availability, and the time to acquire images limits use of the more sensitive measures of MRI and single photon emission CT scans. Single photon emission CT scans detect regional changes of blood flow but not necessarily structural damage. Furthermore, MRI and CT often do not predict outcome (Kido et al., 1992; Kurth et al., 1994; Wilson et al., 1995; Hanlon et al., 1999). Thus there is a need for a biochemical marker of neuronal injury to improve diagnosis and prediction of outcome after TBI.

An ideal biomarker would incorporate several properties. A good biomarker would diagnose neurologic damage before neuro-radiographic signs are evident. A biomarker of acute neuronal injury would provide a measure of injury magnitude and predict neuropsychological outcome. The biomarker would also serve as an indicator of the pathogenesis of cell death including secondary cell death and indicate a target for treatment. With earlier recognition, the window for therapeutic intervention could be extended. Furthermore, a good biomarker would allow for longitudinal monitoring of the effectiveness of therapy. A biomarker with these characteristics could be used as a surrogate marker and lower the cost of clinical trials. An ideal biomarker should also be specific to the central nervous system and provide a sensitive and specific test of neuronal injury.

Earlier biomarkers such as neuron-specific enolase, lactate dehydrogenase, or creatine kinase are not been specific to the CNS and failed to reflect pathophysiology, lesion size and outcome of the injury further reinforcing the need for research into better CNS trauma indicators (Ingebrigtsen and Romner, 2002). S100β, a low molecular weight calcium-binding protein released from astrocytes, has been examined in numerous TBI studies. Serum levels of S100β have been correlated with contusion volume (Raabe et al., 1998; Herrmann et al., 2000); injury severity (Herrmann et al., 2000); neuropsychological dysfunction (Herrmann et al., 2001); GCS on admission (Elting et al., 2000); and outcome measures such as the Glasgow Outcome Score (GOS) (McKeating et al., 1998; Elting et al., 2000; Jackson et al., 2000; Raabe and Seifert, 2000; Rothoerl et al., 2000). S100β appears to be a valuable indicator of brain lesion but it is not specific to the CNS. Importantly in multitrauma patients without head injuries, S100β reached high serum levels after bone fractures and thoracic contusion (Anderson et al., 2001). Another biomarker that is being examined as an indicator of brain injury is tau (Zemlan et al., 1999). Tau is a microtubule associated protein that is expressed predominantly in axon of neurons and implicated in microtubule stability, axon elongation and axon transport (Garcia and Cleveland, 2001). In severe TBI patients, increased CSF levels of cleaved tau were found to be significant predictors of intracranial pressure and GOS at discharge (Zemlan et al., 2002), but in recent studies, CSF total tau levels did not correlate with GOS in patients with severe TBI (Franz et al., 2003) nor did serum cleaved tau levels correlate with outcome measures (Chatfield et al., 2002).

αII-spectin in the CNS is primarily localized to axons and to the presynaptic terminal of neurons (Riederer et al., 1986). In acute neuronal injury, αII-spectin, a cytoskeletal protein, is a substrate for the calcium activated cysteine proteases, calpain (calpain-1 and -2) and caspase-3. After acute neuronal injury, calcium influx initiates a cytotoxic cascade of proteases, phospholipases, kinases and phosphatases including activation of calpain and caspases which results in necrotic and apoptotic cell death respectively. Calpain and caspase-3 both cleave the 280-kDa parent band of αII-spectrin into a 150-kDa breakdown product (SBDP150). Calpain and caspase-3 cleave signature breakdown products of 145 (SBDP145) and 120 kDa (SBDP120), respectively, *in vivo* and *in vitro* (Nath et al., 1996; Wang et al., 1998; Wang, 2000). Both the calpain-mediated SBDP 145 and SBDP 150 increased acutely in the injured cortex whereas the caspase-3 mediated SBDP 120 was absent in an unilateral controlled cortical impact (CCI) model of TBI (Pike et al., 1998). This may reflect a more prominent role of oncosis than apoptosis in the cortex in our CCI model.

αII-spectrin breakdown products (SBDP) have been used as an indicator of calpain activity in models of TBI (Newcomb et al., 1997) and ischemia (Saido et al., 1993; Roberts-Lewis et al., 1994; Bartus et al., 1998) In our laboratory, levels of SBDP have recently been found to increase in rat CSF after experimental controlled cortical impact TBI (Pike et al., 2001) and middle cerebral artery occlusion (Pike et al., 2004). In this study we extend this work by systematically comparing CSF SBDP to their counterpart in injured cortex, to injury magnitude, to CSF tau and S100â and to lesion volume (accessed by MRI). This study subjects a marker of CNS injury to rigorous preclinical examination. Based on the data we have obtained, we propose that CSF SBDP levels are a promising biomarker of injury and further study is warranted in clinical TBI.

MATERIALS AND METHODS

Animals

Three groups of adult male (280–300 g) Sprague-Dawley rats (Harlan; Indianapolis, IN) were used. For study 1, CSF was withdrawn from one group of 90 rats that were sacrificed 2, 6, and 24 h after TBI. At each time point of 2, 6, and 24 h, 9 rats received mild (1.0 mm of cortical deformation) injury, 9 rats received severe (1.6 mm of cortical deformation) injury, 8 rats received a craniotomy but no cortical deformation and 4 rats remained naive (no craniotomy or cortical deformation). For study 2, a second group of rats were sequentially scanned by MRI, subjected to CSF withdrawal, and were sacrificed at 24 h following TBI. Of the second group, 9 rats each received severe (1.6 mm) injury, mild (1.0 mm) injury or craniotomy surgery and 8 rats remained naive. One rat with severe injury was removed from the study because the CSF sample contained blood that could potentially dilute out the concentration of the marker in the CSF and introduce blood-born markers. For study 3, 35 rats were administered a rotarod test on days 1–5 after TBI and scanned by MRI at 24 h and 28 days after TBI. Of the third group of rats, 10 rats each received severe (1.6 mm) injury, mild (1.0 mm) injury or a craniotomy, and 5 rats remained naive.

Surgical Preparation and Controlled Cortical Impact Traumatic Brain Injury

As previously described (Dixon et al., 1991; Pike et al., 2001), a cortical impact injury device was used to produce TBI. Adult male rats were initially anesthetized with 4% isoflurane in a carrier gas of 1:1 O_2/N_2 (4 min) followed by maintenance anesthesia of 2.5% isoflurane in the same carrier gas. Core body temperature was maintained at $37 \pm 1°C$ by placing an adjustable temperature controlled heating pad beneath the rats. Animals were mounted in a stereotactic frame in a prone position and secured by ear and incisor bars. A midline cranial incision was made, the soft tissues were reflected and a unilateral (ipsilateral to site of impact) craniotomy (7 mm diameter) was performed adjacent to the central suture, midway between bregma and lambda. The dura mater was kept intact over the cortex. Brain trauma in rats was produced by impacting the right cortex (ipsilateral cortex) with a 5 mm diameter aluminum impactor tip (housed in a pneumatic cylinder) at a velocity of 3.5 m/sec with a 150-msec dwell time (compression duration). Compression depth was set at 1.0 mm (mild), or 1.6 mm (severe). Velocity was controlled by adjusting the pressure (compressed N_2) supplied to the pneumatic cylinder. Velocity and dwell time were measured by a linear velocity displacement transducer (Lucas Shaevitz™ model 500 HR; Detroit, MI) that produces an analogue signal by a storage-trace oscilloscope (BK Precision, model 2522B; Placentia, CA). Animals underwent identical craniotomy procedures but did not receive cortical compression. Naive rats did not undergo surgery or injury. Appropriate pre- and post-injury management was maintained to insure that all guidelines set forth by the University of Florida Institutional Animal Care and Use Committee and the National Institutes of Health guidelines detailed in the *Guide for the Care and Use of Laboratory Animals* were complied with.

CSF Withdrawal

Under anesthesia, the rat was secured in the same stereotactic frame as used in surgery. The neck was flexed to optimize exposure of the atlanto-occipital space. A mid-line incision was made over the superficial cervical muscles. A 25-gauge needle attached to polyethylene tubing was inserted into the atlanto-occipital space and CSF was gently withdrawn. CSF was immediately spun at $9,000g$ for 5 min at 4°C to remove any red blood cells from the cortical impact or from the tap. CSF was frozen at −80°C until examined.

Tissue Lysis

Cortical tissues were collected from naive animals or at 2, 6, and 24 h after craniotomy or TBI. At the appropriate post-injury time-points, the animals were anesthetized with 4% isoflurane in a carrier gas of 1:1 O_2/N_2 (4 min) and subsequently sacrificed by decapitation. Ipsilateral (to the impact site) cortex samples were rapidly dissected and snap-frozen in liquid nitrogen. Tissue samples were stored at −80°C until further processing. Frozen samples were thawed and homogenized in a glass tube with a Teflon dounce pestle in 15 volumes of ice-cold detergent-free buffer (50 mM Tris-HCl, pH 7.4, 1 mM EDTA, 2 mM EGTA, 0.33 M sucrose, 1 mM DTT) containing a broad-range protease inhibitor cocktail (Roche Molecular Biochemicals, no. 1-836-145) and sonicated. Homogenized samples were then centrifuged at $9000g$ for 5 min at 4°C. The supernatant was stored at −80°C until immunoblot analysis.

Immunoblotting

Prior to sodium dodecyl sulfate–polyacrylamide gel electrophoresis (SDS-PAGE), protein content was assayed by the Micro BCA method (Pierce, Rockford, IL) using albumin standards. For each sample, 40 μg of protein from cortical tissue or 40 μg of protein from CSF samples were added to 2 × loading buffer containing 0.2 M Tris (pH 6.8), 400 mM 2-mercapto-ethanol, 8% SDS,

0.04% Bromophenol Blue, and 40% glycerol. The amount of protein for CSF samples was optimized to identify SBDP after both mild (1.0 mm) and severe (1.6 mm) injury. The optimal amount of protein to see the 145/150 band after mild injury resulted in an amount of protein after severe (1.6 mm) injury that sometimes would make the 145 and 150 bands indistinguishable. Semi-quantitation by densitometry was used to evaluate the 145–150-kDa band together thus the blurring of the 145/150 band was not a problem. The 145–150-kDa spectrin breakdown product represents primarily calpain initiated cleavage of spectrin in our model. Consistent with a previous report that CCI in our laboratory does not produce prominent caspase-3 levels (Pike et al., 1998), caspase-3–mediated SBDP 120 was inconsistent after severe (1.6 mm) injury and absent after mild (1.0 mm) injury and was not analyzed in this set of experiments. Semi-quantitation by densitometry evaluated both the 145–150-kDa band together thus the blurring was not a problem. Samples were heated at 96°C for 10 min and then centrifuged for 1 min at 10,000g. Samples were resolved in a vertical electrophoresis chamber for 70 min at 150 V. A 6.5% percent stacking acrylamide gel or a 4–20% Tris-Glycine gel (Invitrogen Life Technologies, Carlsbad, CA) were used. Separated proteins were either laterally transferred as a wet transfer to a nitrocellulose membrane (0.45 μM) using a transfer buffer consisting of glycine (192 mM) and tris (25 mM), (pH 8.3) with 10% methanol at a constant voltage of 100V for 70 min at 4°C or were horizontally transferred as a semi-dry transfer to an Immobilon-P polyvinylidene fluoride (PVDF) membrane (Millipore, Bedford, MA) using 39 mM glycine, 48 mM Tris, and 5% methanol at 20 V for 2 h at room temperature. All gels were stained with coomassie blue to confirm equal loading of protein on the gel. Selected blots were also stained with Panceau red (Sigma, St. Louis, MO) to confirm transfer and that equal amounts of protein were loaded in each lane. Blots were blocked for one hour in 5% non-fat milk in TBST (20 mM Tris, 0.15 M NaCl, and 0.005% Tween-20). Following overnight incubation with the primary antibody, anti-α-spectrin monoclonal antibody (1:10,000 dilution for cortex and 1:5,000 dilution for CSF; Affiniti Research Products, UK) and 1% non-fat milk/TBST at 4°C temperature, the blots were incubated with goat anti-mouse secondary antibody (1:1000 for cortex and 1:5000 for CSF; Biorad) and 3% non-fat milk/TBST for 1 h. Blots were then washed for 1 h in TBST. Enhanced chemiluminescence reagents (ECL and ECL-Plus, Amersham) were used to visualize immunolabeling of cortical tissue and CSF, respectively, and developed on Kodak BioMax Light Film (Kodak). Semi-quantitative evaluation of protein levels was conducting using computer-assisted one-dimensional densitometric scanning (ImageJ, version 1.29, NIH). Data were acquired as integrated densitometric values from similarly exposed films.

ELISA

CSF S100β levels were measured using a rat specific ELISA kit, Nexus D$_x$™ Rat S100 Test Kit from SynX (Toronto, Ontario, Canada) and CSF tau was measured using a kit,Innotest™ hTau Antigen from Innogenetics, Inc. (Alpharetta, GA). The sensitivities of the S100β and tau ELISA kits were 0.02 ng/mL and 75 pg/mL, respectively.

T2-Weighted Magnetic Resonance Imaging

Animals were scanned in the Advanced Magnetic Resonance Imaging and Spectroscopy (AMRIS) facility located in the McKnight Brain Institute of the University of Florida. Animals undergoing these imaging sessions were anesthetized using isoflurane (maintenance anesthesia of 1.5–2.5% isoflurane in 1 L/min 100% O$_2$ continuously delivered via a nose cone). Ophthalmic lubricant was used to prevent drying of the eyes during anesthesia. Anesthetized rats were placed on a custom Plexiglas cradle constructed to support the rat comfortably in the supine position. Oxygen saturation was monitored using a pulse oxymeter positioned on the left hind limb. Body temperature was monitored using a rectal flouroptic probe and maintained using warm air. A 4.7-Tesla magnet (Oxford Instruments) and Bruker Avance Console (Bruker, Germany) and a custom built 3.3-cm (inner diameter) quadrature birdcage coil were used for all image acquisitions. T2-weighted images were acquired at 24 h and 28 days after TBI. Twelve contiguous 1.25-mm coronal slices were acquired with the following parameters: a field of view = 3.6 × 3.6 cm^2, repetition time (TR) = 2.1 seconds, echo time (TE) = 81 msec, matrix = 256 × 256 points per dimension (140 μm in plane). Areas of hypo-intensity on MRI were associated with hemorrhage or mechanical disruption and areas of hyper-intensity were associated with edema (Albensi et al., 2000). Lesion size was drawn using ParaVision Image Analysis tools (Bruker, Germany) similar to the methodology in (Neumann-Haefelin et al., 2000). The area of each lesion in each coronal slice was multiplied by the slice thickness and then added to calculate the total lesion size.

Neurological Functional Evaluation

Motor behavior was assessed in the sub-acute period after TBI by a blinded observer using a Rota-rod (Ugo Basile, Comerio, Italy; Hamm et al., 1994). Rats were placed on a Rota-rod, a rotating rod, which was set to

slowly accelerate from 4 to 40 rpm within 5 min. The Rota-rod requires the rat to walk as the revolving rod accelerates and maintain balance. The trial lasted until the rat fell off and tripped a plate that recorded the time or until the rat had stayed on the rod for 300 sec was reached. Rats underwent conditioning of two trials a day for three days prior to TBI. After TBI, the rats were tested for two trials a day on days 1–5. The average of the latency in seconds of the two trials was recorded.

Statistical Analysis

Means and standard errors of the means were calculated from individual rat densitometric values of the 145–150-kDa SBDP combined as one value. Two-way ANOVA was used to examine main effects and interaction effects of time and injury magnitude. One-way ANOVA with contrast to do pair-wise comparisons was used to determine significance between levels of SBDP and between lesion sizes of the corresponding experimental groups. Regression analysis was performed with lesion size as the outcome variable and CSF markers (SBDP, tau, S100â) as the predictor variable. Pearson correlations were calculated and tested using the asymptotic Z-test. Correlations were calculated in the individual animal between CSF SBDP levels and lesion size. The analysis of the correlations included animals in all groups (naive, craniotomy, 1.0 mm and 1.6 mm injury) unless stated otherwise. Repeated measures ANOVA (4 groups $\times$ 5 time points) were performed to determine individual group differences over the five time points on the Rota-rod test.

RESULTS

Injury Magnitude Is Associated with Increased Levels of SBDP in the Cortex and CSF after TBI

SBDP were measured by Western blot from the CSF and ipsilateral cortex (IC) at 2, 6, and 24 h after two magnitudes of TBI. Naive rats and rats that had undergone a craniotomy served as controls for this study. The two response variables, SBDP in the CSF and SBDP in the IC were analyzed via ANOVA with terms for injury magnitude, time, and the interaction of time and injury magnitude.

The results indicated there was no interaction effect ($p = 0.88$) or time effect ($p = 0.12$) on IC SBDP levels. The analysis also indicated that injury magnitude significantly increased the level of cortical SBDP ($p \leq 0.0001$). Mean levels of IC SBDP after severe (1.6 mm) injury were significantly higher than the mean levels of

IC SBDP after mild (1.0 mm) injury ($p < 0.05$). Mean levels of IC SBDP after both severe (1.6 mm) and mild (1.0 mm) injury were significantly greater than mean levels of SBDP after craniotomy or in naive controls ($p < 0.0001$). Mean levels of IC SBDP did not differ between naive and after craniotomy. Representative gels show that levels of SBDP increased with injury magnitude in the ipsilateral cortex and the CSF (Fig. 1A). Levels of SBDP (both 145 and 150 kDa are densitometrically quantified together) were highest after 1.6-mm injury in the IC and CSF at all time points (Fig. 1B).

After severe (1.6 mm) injury, the mean levels of IC SBDP were 116.4 ± 8.9, 135.9 ± 14.1, and 135.6 ± 17.7 and after mild (1.0 mm) injury, the mean levels of IC SBDP reached 78.1 ± 9.9, 110.1 ± 19.4, and 102.8 ± 17.2 at 2, 6, and 24 h, respectively. After craniotomy, the mean levels of IC SBDP reached 22.6 ± 9.1, 40.9 ± 18.2, and 11.8 ± 4.6 at 2, 6, and 24 h, respectively. In naive rats, the mean levels of IC SBDP were 4.4 ± 1.6, 15.4 7.0, and 4.4 ± 6.5 at 2, 6, and 24 h, respectively.

There was no interaction effect ($p = 0.39$) or time effect ($p = 0.13$) on CSF SBDP levels. The analysis also indicated that injury magnitude significantly increased the levels of CSF SBDP ($p \leq 0.0001$). Mean levels of CSF SBDP after severe (1.6 mm) injury were significantly higher than the mean levels of CSF SBDP after mild (1.0 mm) injury ($p = 0.0001$). Mean levels of CSF SBDP after both severe (1.6 mm) and mild (1.0 mm) injury were significantly greater than mean levels of CSF SBDP after craniotomy or in naive controls ($p < 0.0001$). Mean levels of CSF SBDP did not differ between naive and after craniotomy.

After 1.6 mm injury, the mean levels of CSF SBDP were 153.4 ± 11.3, 114.4 ± 19.1, and 91.2 ± 23.8 and after 1.0 mm injury, the mean CSF SBDP were 82.2 ± 17.3, 71.4 ± 17.3, and 64.3 ± 17.2 at 2, 6, and 24 h, respectively. After craniotomy, the mean levels of CSF SBDP reached 7.8 ± 2.7, 19.1 ± 6.0, and 10.3 ± 5.3 at 2, 6, and 24 h, respectively. In naive rats, the mean levels of CSF SBDP were 1.0 ± 0.7, 5.7 ± 3.4, and 3.0 ± 1.4 at 2, 6, and 24 h, respectively.
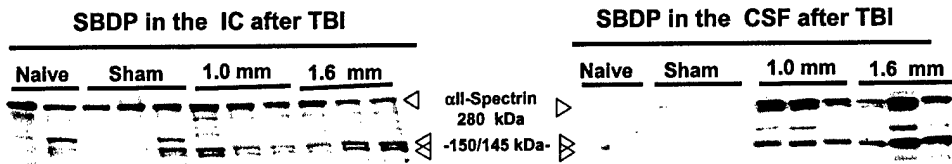
The Relationship of CSF SBDP Levels with Lesion Size at 24 h Post-Injury

CSF extraction to measure SBDP and T2-weighted imaging to measure lesion size was performed in the same groups of rats at 24 h after TBI. Representative T2-weighted images of a naive rat and a rat 24 h after craniotomy, mild (1.0 mm) injury and severe (1.6 mm) injury are shown in Figure 2A. Severe (1.6 mm) injury resulted in disruption of normal architecture and swelling of the ipsilateral cortex (arrow in Fig. 2A). Less disrup-
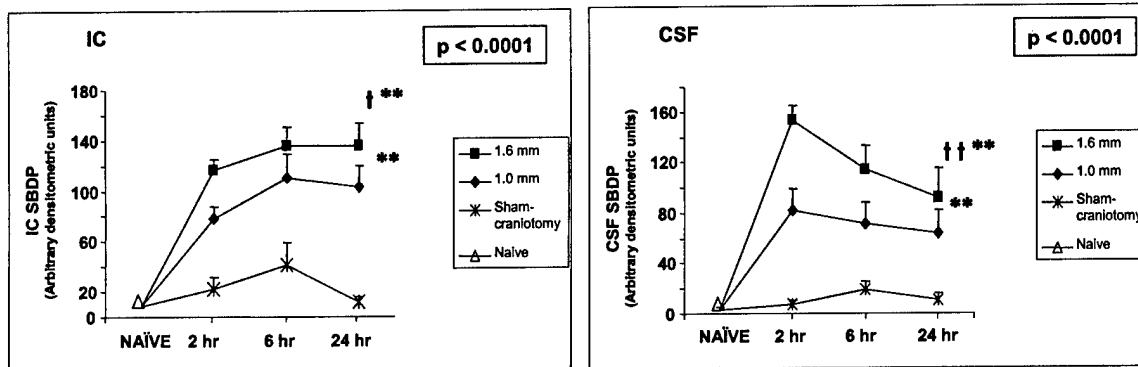
A

SBDP in the IC after TBI

Naive Sham 1.0 mm 1.6 mm

⊲ αII-Spectrin ▷
280 kDa

⊴ -150/145 kDa- ⬙

SBDP in the CSF after TBI

Naive Sham 1.0 mm 1.6 mm

B

IC

p < 0.0001

180
140
100
60
20
0

IC SBDP (Arbitrary densitometric units)

NAÏVE 2 hr 6 hr 24 hr

†**
**

■ 1.6 mm
♦ 1.0 mm
✳ Sham-craniotomy
△ Naive

CSF

p < 0.0001

160
120
80
40
0

CSF SBDP (Arbitrary densitometric units)

NAÏVE 2 hr 6 hr 24 hr

††**
**

■ 1.6 mm
♦ 1.0 mm
✳ Sham-craniotomy
△ Naive

FIG. 1. Injury magnitude increases levels of SBDP in the ipsilateral cortex (IC) and CSF. (A) A representative Western blot of αII-spectrin and SBDP in the IC (left) and CSF (right) at 24 and 2 h, respectively, after TBI. Samples were collected after severe (1.6 mm) injury, mild (1.0 mm) injury, sham-craniotomy or from naive rats. Higher levels of SBDP are seen after severe (1.6 mm) injury than after mild (1.0) injury. Minimal SBDP is seen in the IC or CSF of naive rats or after sham-craniotomy in rats. (B) SBDP levels (145–150-kDa fragments) in the IC (left panel) and CSF (right panel) after sham-craniotomy, mild (1.0 mm) injury and severe (1.6 mm) injury at 2, 6, and 24 h were quantified using computer-assisted densitometric analysis (ImageJ, version 1.29X, NIH, USA). Values from naive animals were averaged as a separate time point. At each time point of 2, 6, and 24 h, 9 rats received severe (1.6 mm) injury, 9 rats received mild (1.0 mm) injury, 8 rats received a sham-cra-niotomy and 4 rats remained naive. An ANOVA was performed followed by contrast with pair-wise comparisons. Data is presented as the mean plus standard error. Standard error bars on the shams are present but not easily visable. Injury magnitude significantly increased mean levels of IC and CSF SBDP over time ($p < 0.0001$). Mean levels of SBDP after severe (1.6 mm) injury were significantly higher from the mean levels of SBDP after mild (1.0 mm) injury ($^{\dagger\dagger}p = 0.0001$ and $^{\dagger}p < 0.05$, respectively, for CSF and IC levels of SBDP). Mean levels of IC and CSF SBDP after both severe (1.6 mm) and mild (1.0 mm) injury were significantly greater than mean levels of SBDP after sham-craniotomy or in naive controls ($^{**}p < 0.0001$). Mean levels of CSF and IC SBDP did not differ between naive and sham.

FIG. 2. Lesion size on T2 weighted images increases with injury magnitude 24 h after TBI. (A) Representative serial T2-weighted magnetic resonance images of a naive rat and a rat 24 h after sham-craniotomy, mild (1.0 mm) and severe (1.6 mm) injury are shown. Twelve contiguous coronal 1.25 mm slices were acquired with the following parameters: a field of view = 3.6 × 3.6 cm², repetition time (TR) = 2100 sec, echo time (TE) = 81 msec, matrix = 256 × 256 points per dimension (140 μm in plane). Four of the 12 coronal slices for each rat are shown. Severe (1.6 mm) injury resulted in disruption of normal architecture and swelling of the ipsilateral cortex (arrow). Less disruption of normal architecture is noted after mild (1.0 mm) injury (arrowhead). Sham-craniotomy resulted in varying amounts of hyper-intensity in the ipsilateral cortex (arrowhead). (B) Lesion size was drawn using ParaVision Image Analysis tools (Bruker, Germany) similar to the methodology in (Neumann-Haefelin et al., 2000). The area of each lesion in each coronal slice was multiplied by the slice thickness and then added to calculate the total lesion size. One-way ANOVA with contrast to do pair-wise comparisons was used to determine difference between lesion sizes of the treatment groups. Nine rats each received severe (1.6 mm) injury, mild (1.0 mm) injury or sham surgery and 8 rats remained naive. The lesion after severe (1.6 mm) injury is significantly greater than the lesion size after mild (1.0 mm) injury ($^{\#\#}p \leq 0.001$) and both are significantly greater than after sham-craniotomy ($^{\dagger\dagger}p \leq 0.001$) or naive animals ($^{**}p \leq 0.001$) Sham injury is greater than the absense of a lesion in naive animals ($^{*}p < 0.05$).

1448

tion of normal architecture is noted after mild (1.0 mm) injury (arrowhead in Fig. 2A). Craniotomy resulted in varying amounts of hyper-intensity in the ipsilateral cortex (arrowhead in Fig. 2A). Average lesion size was 0.044 $cm^3 \pm 0.00058$ after craniotomy, $0.100 \ cm^3 \pm 0.010$ after 1.0 mm injury, and $0.166 \ cm^3 \pm 0.016$ after 1.6 mm injury (Fig. 2B). Mean lesion size was significantly different between 1.6 mm and 1.0 mm injury groups and

A

T2-weighted Magnetic Resonance Images

1.6 mm injury

1.0 mm injury

Sham-craniotomy

Naïve-control

B
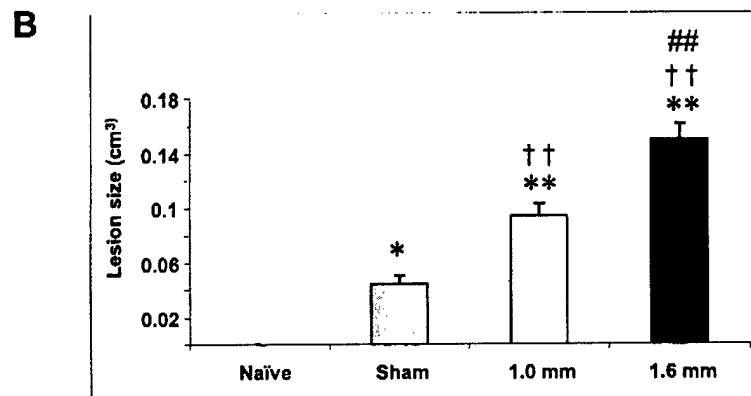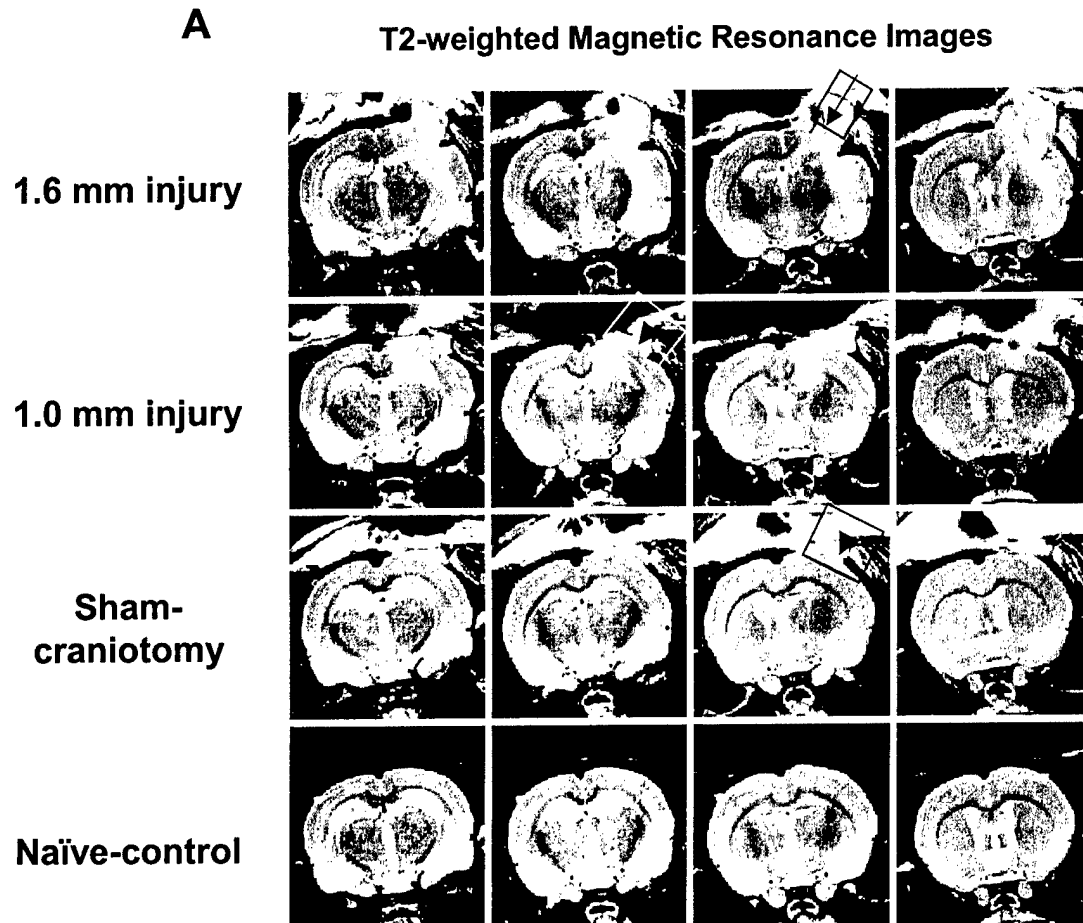
between both injury groups and after craniotomy ($p \leq$ 0.001; Fig. 2B). Mean levels of CSF SBDP significantly correlated with lesion size (r = 0.833, $p < 0.0001$) when including all 4 groups (1.6 mm and 1.0 mm injury, craniotomy, and naive rats) (Fig. 3A). This correlation was not significant if craniotomy and sham rats were not considered in the analysis. To explore the ability of SBDP to predict lesion size, a regression analysis was run with lesion size as the outcome variable and CSF SBDP as the predictor variable from individual rats from all 4 groups. The regression weight for CSF SBDP was estimated to be 1059.86, and the parameter estimate of the intercept was 10.707. The regression analysis revealed CSF SBDP contributed significantly to predicting lesion volume ($p < 0.0001$).

Levels of CSF tau significantly correlated with lesion size (r = 0.693, $p < 0.0001$) (Fig. 3B) as levels of CSF S100β did not (r = 0.188) (Fig. 3C). The regression weight for CSF tau was estimated to be 0.00001258, and the parameter estimate of the intercept was 0.03485. CSF levels of tau significantly contributed to the prediction of lesion volume ($p < 0.0001$). Neither CSF tau or CSF S100β were correlated if just the 1.6-mm and 1.0-mm injured rats were used for analysis.

A regression analysis was performed to determine which marker or combination of markers (SBDP, tau and S100β) best predicted lesion size. A full regression model indicated the only significant variable was SBDP ($p < 0.0001$). S100β was eliminated from the model and the regression re-run looking at SBDP and tau as predictors of lesion size. CSF SBDP was again the only significant predictor of lesion size ($p < 0.0001$). CSF SBDP and CSF tau are significantly correlated (r = 0.750, $p < 0.0001$) and CSF SBDP has a higher correlation with CSF tau than CSF tau's correlation with lesion size.
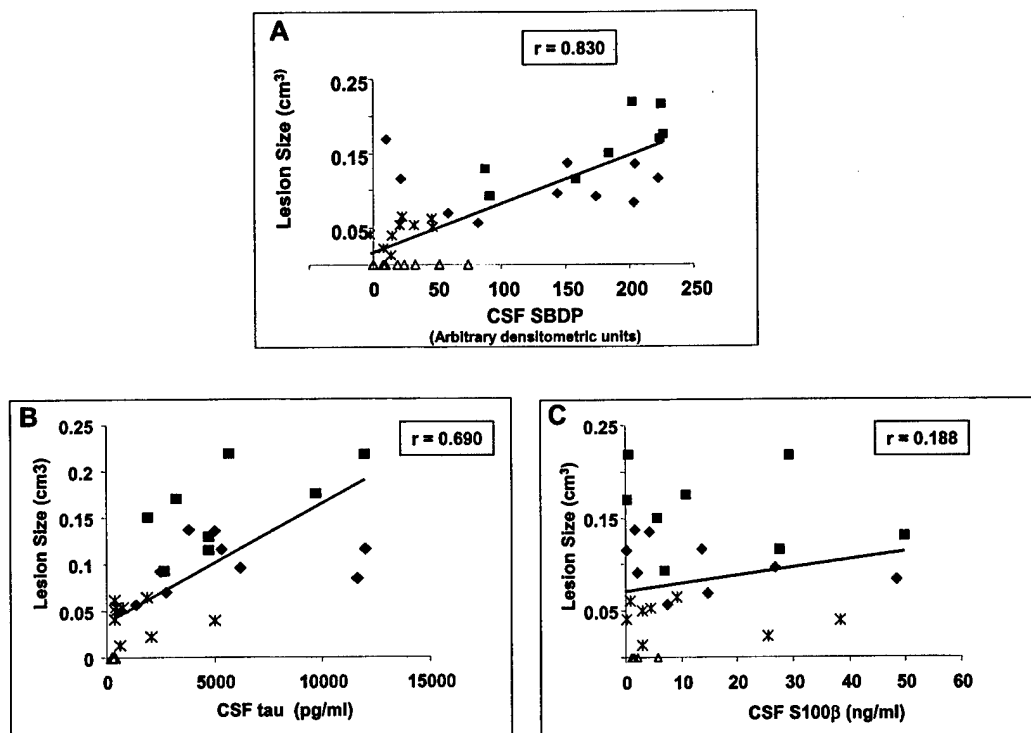
FIG. 3. The relationship of levels of CSF SBDP and tau with lesion size 24 h after TBI. Regression analysis was performed with lesion size as the out-come variable and levels of CSF markers (SBDP, tau, S100β) 24 h after TBI as the predictor variable. (A) Levels of CSF SBDP correlate with lesion size after TBI (r = 0.83, $p \leq 0.0001$). A linear regression equation showed that CSF SBDP significantly contributed to prediction of lesion size ($p \leq 0.0001$). (B) Levels of CSF tau correlate with lesion size after TBI (r = 0.690, $p < 0.001$). A linear regression equation showed that CSF tau significantly contributed to prediction of lesion size ($p \leq 0.0001$). The correlation with CSF SBDP and tau was not significant if craniotomy and sham rats were not considered in the analysis. (C) Levels of CSF S100β did not correlate with lesion size (r = 0.188). ■, rats after 1.6 mm injury; ◆, rats after 1.0 mm injury, *, rats after sham-craniotomy; △, naive rats.

1450

Injury Magnitude Is Associated with Decreased Performance on the Rota-Rod Test and Increased Lesion Size

Because CSF SBDP correlated with lesion size at 24 hours, we looked at the relationship between lesion size and motor performance. Motor performance was assessed in the same (study 3) rats that lesion size was measured at 24 h and 28 days (Fig. 4A). Similar to 24 h, at 28 days lesion size varied with injury magnitude. Lesion size at 24 h in the individual animal was significantly correlated with lesion size at 28 days ($r = 0.881$, $p < 0.0001$). Assessment of Rota-rod performance prior to treatment revealed no significant differences between groups. Injury magnitude had a significant effect on Rota-rod performance ($p < 0.0001$). Mean Rota-rod scores were significantly lower after 1.6-mm injury at all time points (1–5 days after TBI) compared to mild (1.0 mm) injury, craniotomy, or naive rats ($p \leq 0.05$). After 1.0-mm injury, mean Rota-rod scores were significantly lower than in naive rats ($p < 0.01$) and showed a trend toward being lower than after craniotomy (Fig. 4A). Naive rats averaged close to a perfect score of 300 sec at all time points. Naive rats had significantly higher scores than rats after craniotomy ($p < 0.05$). Furthermore, larger lesion sizes were associated with decreased performance on the Rota-rod (Fig. 4B). In the individual rat, the average of the 5 days of Rota-rod scores correlated negatively with lesion size at 24 h ($r = -0.708$; $p < 0.0001$).

DISCUSSION

This paper examined the relationship between IC and CSF levels of SBDP and injury magnitude and outcome measures. The results show that SBDP levels in both CSF and IC SBDP increase with injury magnitude. Although both IC and CSF levels of SBDP increased, they did not parallel each other. Levels of CSF SBDP peaked at 2 h and decreased over time, while IC levels of SBDP slowly increased over the first 6 h after TBI. The correlation between lesion size and CSF levels of SBDP supported CSF SBDP as an indicator of injury. Correlational analysis of relationships between lesion size and CSF levels of SBDP indicated that CSF SBDP is a reliable marker of the presence or absence of injury but failed to be a reliable marker of injury magnitude. Although both CSF and IC SBDP levels and lesion size were significantly higher after 1.6-mm injury than after 1.0-mm injury, the correlation between CSF SBDP and lesion size was not significant following the removal of the control groups (naive and craniotomy) from the analysis. Further study is needed to show if CSF SBDP levels are a useful predictor of outcome such as lesion size.

Factors that affect brain derived protein levels in the CSF after injury have not been extensively explored and are likely to affect the variability of CSF SBDP levels and correlations with CSF SBDP. Petzold et al. (2003) suggest the main determinants of brain tissue proteins in the CSF are the extent of the primary lesion, the total pathological severity causing imbalance of brain home-
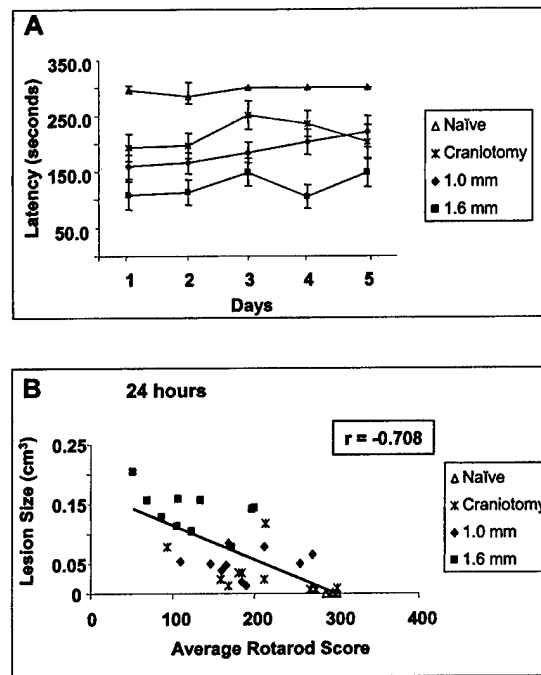

FIG. 4. Performance on the Rota-rod test decreases with increased injury magnitude and lesion size. (**A**) Rats were placed on a rotating rod, which slowly accelerated from 4 to 40 rpm within 5 min on days 1–5 after TBI. The rats were tested for two trials a day and the average of the latency in seconds of the two trials was recorded. Repeated measures ANOVA (4 groups × 5 time points) were performed to determine individual group differences over the five time points on the Rota-rod test. Of the third group of rats, 10 rats each received severe (1.6 mm) injury, mild (1.0 mm) injury or sham surgery and 5 rats remained naive. Data is presented as the mean ± SE. Injury magnitude significantly effected rotarod performance ($p < 0.0001$). Severely (1.6 mm) injured rats performed significantly worse on days 1–5 after TBI on the Rota-rod test than mildly (1.0 mm) injured rats or the sham-craniotomy group ($p < 0.05$ and $p < 0.01$, respectively). Both severe and mild injured groups performed significantly worse than the naive rats ($p < 0.01$). (**B**) Rotarod scores were averaged for the 5 days of testing for each individual rat. The average performance on the Rota-rod test was negatively correlated with lesion size at 24 h after TBI in the individual rat ($r = -0.708$; $p < 0.0001$). ■, rats after 1.6 mm injury; ◆, rats after 1.0 mm injury; ✳, rats after sham-craniotomy; △, naive rats.

ostasis, and the onset and duration of the brain injury. The CCI model that we have used in these studies has some inherent variability in impact force that affects lesion size, lesion severity and the location of pathology. Injured cells in the subarachnoid space can directly release protein into the CSF while protein from cells in the parenchyma must be transported to the CSF by flow of interstitial fluid or edema (Hans et al., 1999). The molecular flux/CSF flow theory suggests that changes in diffusion across the blood-brain and brain-CSF barriers are primarily predicated on CSF flow (Reiber and Peter, 2001; Reiber, 2003). If CSF flow rate is decreased after injury, then ventricular concentration of brain derived proteins is increased (Reiber, 2003). Variation of lesion impact might also cause variation in CSF flow rate and in the distance of brain-derived proteins from the CSF. As more is learned about factors effecting CSF levels of brain-derived proteins, the ability of CSF SBDP and other biomarkers to predict outcome may improve.

Hans et al. (1999) conducted one of the first studies to rigorously analyze a potential biomarker examining distribution and upregulation of mRNA and protein levels of IL-6 in tissue, and bioactivity of IL-6 in CSF and serum in a model of TBI. Similar to previous work in our lab examining mRNA of calpain-1 and calpain-2 (Ringger et al., 2004), IL-6 mRNA was upregulated after injury. Similar to our study, CSF levels of IL-6 peaked within 2–4 h after injury (Hans et al., 1999). IL-6 protein as seen on immunohistochemistry increased by 1 hour and persisted for 24 h, similar to the increase in IC SBDP on western blots at 2, 6, and 24 h after TBI. Hans et al. (1999) suggested that the increased tissue protein immunoreactivity reflected the increased IL-6 activity in the CSF. CSF levels of IL-6 were higher than serum levels between 2 and 8 h after injury. The CSF levels of IL-6 appear higher within 8 h of injury than in the CSF of sham animals, however the paper did not address this important question statistically.

Increased levels of calcium after TBI have been observed in several models (Fineman et al., 1993; Nadler et al., 1995; Verweij et al., 1997; Xiong et al., 1997). After TBI, calcium initiates a cytotoxic cascade of proteases including calpain which breaks down the cytoskeletal protein, spectrin. Higher levels of injury magnitude increased mRNA levels of calpain-1 and calpain-2 in the injured cortex and hippocampus (Ringger et al., 2004). Similar to our study, varying injury magnitude by depth or by velocity of impact, significantly effected lesion size (Goodman et al., 1994). Injury magnitude also significantly increased peak intracranial pressure and hippocampal neuron loss in similar models of TBI (Cherian et al., 1994; Goodman et al., 1994). Temporal increases in intracellular calcium were correlated with injury mag-

nitude after lateral fluid percussion model of TBI in rats (Fineman et al., 1993). The corresponding increase in calcium after more severe TBI in the Fineman study may explain the association between injury magnitude and SBDP levels in the IC and CSF in our study.

In the acute time period following TBI, both CSF and IC SBDP significantly increased with injury magnitude. Calpain-mediated SBDP have been extensively examined and shown to increase in *in vivo* and *in vitro* models of neuronal injury (Bartus et al., 1995; Nath et al., 1996; Saatman et al., 1996a; Newcomb et al., 1997). Recently, it has been shown that CSF SBDP increased in models of TBI (Pike et al., 2001) and ischemia (Pike et al., 2004). The increased levels of SBDP150/145 are primarily associated with calpain activation in our CCI model. Although caspase-3 may also cleave spectrin to SBPD150, similar to prior work in our laboratory (Pike et al., 1998), the caspase-3 signature SBDP120 was not significant in our CCI model, suggesting a much less relevant role of caspase-3 in the production of SBDP in this model. Calpain inhibitors have been neuroprotective in models of TBI (Saatman et al., 1996a,b; Buki et al., 2003), ischemia (Bartus et al., 1994; Hong et al., 1994; Markgraf et al., 1998), and spinal cord injury (Banik et al., 1998). The ability of CSF levels of SBDP to reflect increased IC SBDP levels after acute neuronal injury may provide a therapeutic target for treatment of TBI and an effective way to monitor treatment of TBI if CSF is available.

CSF cleaved tau levels were significant predictors of outcome measures (intracranial pressure and GOS at discharge; Zemlan et al., 2002) supporting the finding of a significant correlation between CSF tau and lesion size in our study. On the other hand, Franz et al. (2003) showed that CSF levels of total tau did not correlate with injury severity (initial GCS) nor with outcome (GOS). The wide range of tau levels in that study was thought to be due to distance of the white matter lesion from the ventricles. Lesion variability is less in a model of CCI than in a clinical study of TBI.

An advantage of a serum biomarker is that it can be measured by less invasive methods than CSF biomarkers. The disadvantage of serum markers is that measurable serum levels of brain tissue proteins must cross the blood–brain and the CSF–blood barriers. Use of serum tau as a biomarker has produced conflicting results. Initial examination of serum cleaved tau indicated that the presence of serum cleaved tau increased the odds of the presence of an intracranial injury and a greater chance of a poor out-come (Shaw et al., 2002). Later work indicated serum cleaved tau levels did not correlate with outcome measures (Chatfield et al., 2002). After acute stroke, total tau increased in the CSF (Hesse

et al., 2001) and serum (Bitsch et al., 2002), and serum tau levels correlated to lesion size and severity. Serum tau levels, however, increased in less than 50% of stroke patients during the first 5 days after stroke (Bitsch et al., 2002).

Analysis of S100β has primarily been from the serum in clinical studies. Two clinical studies of serum levels of S100β revealed a correlation with contusion volume (Raabe et al., 1998; Herrmann et al., 2000), while in a study of mild TBI, serum S100β levels did not correlate with MRI or CT scans (Herrmann et al., 1999). S100β may be released from damaged glial cells, and this variable may not change consistently with lesion volume.

Importantly in multi-trauma patients without head injuries, S100β reached high serum levels after bone fractures and thoracic contusion and also increased after burns and minor bruising (Anderson et al., 2001). Numerous studies examined the use of S100β to mark cerebral damage after cardio-pulmonary bypass surgery (Ali et al., 2000), but S100β was found to be released from the mediastinum of cardiopulmonary bypass patients (Anderson et al., 2001). After stroke, higher serum S100β levels were associated with larger infarcts and more severe neuropsychological deficits (Aurell et al., 1991; Abraha et al., 1997; Buttner et al., 1997). Yet despite these promising correlations, Hill et al. (2000) found only 32% of stroke patients had elevated serum S100β on admission similar to serum tau levels (Bitsch et al., 2002). Early identification of stroke is necessary for optimal treatment within three hours.

The utility of SBDP as a serum marker has not been examined in clinical cases or models of stroke or TBI to the author's knowledge. Our study did not examine serum SBDP levels but further work will be important to establish if SBDP crosses the blood–brain and blood–CSF barrier and reflects SBDP levels in the CSF and brain. áII-spectrin is not found in red blood cells (Pike et al., 2001) although it is found in very low levels in other organs systems (Pike, Flint, Wang, and Hayes, unpublished data). The utility of SBDP as a marker would also benefit from knowledge of serum levels of SBDP in multi-trauma patients without head injuries and acutely after stroke.

Changes in high resolution MRI have been shown to correlate well with histology in a lateral fluid percussion model (Albensi et al., 2000) and a closed head injury model (Assaf et al., 1997) of TBI. Areas of hypo-intensity on MRI were associated with hemorrhage or mechanical disruption and areas of hyper-intensity were associated with edema (Albensi et al., 2000). At 24 h after rats underwent craniotomy, varying amounts of hyper-intensity were noted, most likely due to edema associated with the changes in cranial pressures. In the closed head injury model, areas of hyper-intensity decreased between 2 and 7 days after TBI likely representing resolution of edema (Assaf et al., 1997). Similarly in our study, the overall size of the lesion decreased between 24 h and 28 days, although a significant correlation was maintained between lesion size in individual rats at the two time points.

This study examined *in vivo* lesion size and the correlation to neuromotor function. Higher levels of injury magnitude significantly increased lesion size and decreased motor performance. In a stroke model, lesion size from T2-weighted images at 2 and 7 days after ischemia was significantly correlated with an average of individual neurological score (Palmer et al., 2001). Similarly in our study, the larger the lesion size, the worse the performance on the motor function test. Because lesion size at 24 h was highly correlated with lesion size at 28 days and significantly negatively correlated with motor performance, it is suggestive that acute levels of SBDP might correlate with both acute motor performance and chronic lesion size. Because withdrawal of CSF is a terminal procedure in our laboratory at this time, the correlation is only speculative.

In conclusion, the results of this study show that levels of SBDP in the IC and CSF are significantly higher after 1.6-mm injury than after 1.0-mm injury paralleling the significant difference in lesion size. We further showed that 24 hours after TBI, increased levels of CSF SBDP indicate the presence of a lesion. These studies strongly support the further study of CSF SBDP as a marker of CNS injury, and warrant evaluation of SBDP as a serum marker. Further examination may elucidate whether CSF or serum SBDP levels are predictors of outcome such as lesion size, GOS or neurological dysfunction. The contribution of this work is a foundation for future studies assessing the utility of this marker in human brain injury.

ACKNOWLEDGMENTS

REFERENCES

ABRAHA, H.D., BUTTERWORTH, R.J., BATH, P.M., WASSIF, W.S., GARTHWAITE, J., and SHERWOOD, R.A. (1997). Serum S-100 protein, relationship to clinical outcome in acute stroke. Ann. Clin. Biochem. **34,** 546–550.

ALBENSI, B.C., KNOBLACH, S.M., CHEW, B.G., O'REILLY, M.P., FADEN, A.I., and PEKAR, J.J. (2000). Diffusion and high resolution MRI of traumatic brain injury in rats: time course and correlation with histology. Exp. Neurol. **162,** 61–72.

ALI, M.S., HARMER, M., and VAUGHAN, R. (2000). Serum S100 protein as a marker of cerebral damage during cardiac surgery. Br. J. Anaesth. **85,** 287–298.

ANDERSON, R.E., HANSSON, L.O., NILSSON, O., DIJLAI-MERZOUG, R., and SETTERGREN, G. (2001). High serum S100B levels for trauma patients without head injuries. Neurosurgery **48,** 1255–1260.

ASSAF, Y., BEIT-YANNAI, E., SHOHAMI, E., BERMAN, E., and COHEN, Y. (1997). Diffusion- and T2-weighted MRI of closed-head injury in rats: a time course study and correlation with histology. Magn. Reson. Imaging **15,** 77–85.

AURELL, A., ROSENGREN, L.E., KARLSSON, B., OLSSON, J.E., ZBORNIKOVA, V., and HAGLID, K.G. (1991). Determination of S-100 and glial fibrillary acidic protein concentrations in cerebrospinal fluid after brain infarction. Stroke **22,** 1254–1258.

BANIK, N.L., SHIELDS, D.C., RAY, S., et al. (1998). Role of calpain in spinal cord injury: effects of calpain and free radical inhibitors. Ann. NY Acad. Sci. **844,** 131–137.

BARTUS, R.T., DEAN, R.L., MENNERICK, S., EVELETH, D., and LYNCH, G. (1998). Temporal ordering of pathogenic events following transient global ischemia. Brain Res. **790,** 1–13.

BARTUS, R.T., ELLIOTT, P.J., HAYWARD, N.J., et al. (1995). Calpain as a novel target for treating acute neurodegenerative disorders. Neurol. Res. **17,** 249–258.

BARTUS, R.T., HAYWARD, N.J., ELLIOTT, P.J., et al. (1994). Calpain inhibitor AK295 protects neurons from focal brain ischemia. Effects of postocclusion intra-arterial administration. Stroke **25,** 2265–2270.

BITSCH, A., HORN, C., KEMMLING, Y., et al. (2002). Serum tau protein level as a marker of axonal damage in acute ischemic stroke. Eur. Neurol. **47,** 45–51.

BUDUHAN, G., and McRITCHIE, D.I. (2000). Missed injuries in patients with multiple trauma. J. Trauma **49,** 600–605.

BUKI, A., FARKAS, O., DOCZI, T., and POVLISHOCK, J.T. (2003). Preinjury administration of the calpain inhibitor MDL-28170 attenuates traumatically induced axonal injury. J. Neurotrauma **20,** 261–268.

BUTTNER, T., WEYERS, S., POSTERT, T., SPRENGELMEYER, R., and KUHN, W. (1997). S-100 protein: serum marker of focal brain damage after ischemic territorial MCA infarction. Stroke **28,** 1961–1965.

CHATFIELD, D.A., ZEMLAN, F.P., DAY, D.J., and MENON, D.K. (2002). Discordant temporal patterns of S100beta and cleaved tau protein elevation after head injury: a pilot study. Br. J. Neurosurg. **16,** 471–476.

CHERIAN, L., ROBERTSON, C.S., CONTANT, C.F., JR., and BRYAN, R.M., JR. (1994). Lateral cortical impact injury in rats: cerebrovascular effects of varying depth of cortical deformation and impact velocity. J. Neurotrauma **11,** 573–585.

DIXON, C.E., CLIFTON, G.L., LIGHTHALL, J.W., YAGHMAI, A.A., and HAYES, R.L. (1991). A controlled cortical impact model of traumatic brain injury in the rat. J. Neurosci. Methods **39,** 253–262.

ELTING, J.W., DE JAGER, A.E., TEELKEN, A.W., et al. (2000). Comparison of serum S-100 protein levels following stroke and traumatic brain injury. J. Neurol. Sci. **181,** 104–110.

FINEMAN, I., HOVDA, D.A., SMITH, M., YOSHINO, A., and BECKER, D.P. (1993). Concussive brain injury is associated with a prolonged accumulation of calcium: a ^{45}Ca autoradiographic study. Brain Res. **624,** 94–102.

FRANZ, G., BEER, R., KAMPFL, A., et al. (2003). Amyloid beta 1–42 and tau in cerebrospinal fluid after severe traumatic brain injury. Neurology **60,** 1457–1461.

GARCIA, M.L., and CLEVELAND, D.W. (2001). Going new places using an old MAP: tau, microtubules and human neurodegenerative disease. Curr. Opin. Cell Biol. **13,** 41–48.

GOODMAN, J.C., CHERIAN, L., BRYAN, R.M., JR., and ROBERTSON, C.S. (1994). Lateral cortical impact injury in rats: pathologic effects of varying cortical compression and impact velocity. J. Neurotrauma **11,** 587–597.

HAMM, R.J., PIKE, B.R., O'DELL, D.M., LYETH, B.G., and JENKINS, L.W. (1994). The rotarod test: an evaluation of its effectiveness in assessing motor deficits following traumatic brain injury. J. Neurotrauma **11,** 187–196.

HANLON, R.E., DEMERY, J.A., MARTINOVICH, Z., and KELLY, J.P. (1999). Effects of acute injury characteristics on neurophysical status and vocational outcome following mild traumatic brain injury. Brain Inj. **13,** 873–887.

HANS, V.H., KOSSMANN, T., LENZLINGER, P.M., et al. (1999). Experimental axonal injury triggers interleukin-6 mRNA, protein synthesis and release into cerebrospinal fluid. J. Cereb. Blood Flow Metab. **19,** 184–194.

HARAD, F.T., and KERSTEIN, M.D. (1992). Inadequacy of bedside clinical indicators in identifying significant intracranial injury in trauma patients. J. Trauma **32,** 359–363.

HERRMANN, M., CURIO, N., JOST, S., et al. (2001). Release of biochemical markers of damage to neuronal and glial brain tissue is associated with short- and long-term neuropsychological outcome after traumatic brain injury. J. Neurol. Neurosurg. Psychiatry **70,** 95–100.

HERRMANN, M., EBERT, A.D., TOBER, D., HANN, J., and HUTH, C. (1999). A contrastive analysis of release patterns of biochemical markers of brain damage after coronary artery bypass grafting and valve replacement and their association with the neurobehavioral outcome after cardiac surgery. Eur. J. Cardiothorac Surg. **16**, 513–518.

HERRMANN, M., JOST, S., KUTZ, S., et al. (2000). Temporal profile of release of neurobiochemical markers of brain damage after traumatic brain injury is associated with intracranial pathology as demonstrated in cranial computerized tomography. J. Neurotrauma **17**, 113–122.

HESSE, C., ROSENGREN, L., ANDREASEN, N., et al. (2001). Transient increase in total tau but not phospho-tau in human cerebrospinal fluid after acute stroke. Neurosci. Lett. **297**, 187–190.

HILL, M.D., JACKOWSKI, G., BAYER, N., LAWRENCE, M., and JAESCHKE, R. (2000). Biochemical markers in acute ischemic stroke. CMAJ **162**, 1139–1140.

HONG, S.C., GOTO, Y., LANZINO, G., SOLEAU, S., KASSELL, N.F., and LEE, K.S. (1994). Neuroprotection with a calpain inhibitor in a model of focal cerebral ischemia. Stroke **25**, 663–669.

INGEBRIGTSEN, T., and ROMNER, B. (2002). Biochemical serum markers of traumatic brain injury. J. Trauma **52**, 798–808.

JACKSON, R.G., SAMRA, G.S., RADCLIFFE, J., CLARK, G.H., and PRICE, C.P. (2000). The early fall in levels of S-100 beta in traumatic brain injury. Clin. Chem. Lab. Med. **38**, 1165–1167.

KELLY, D.F. (1995). Alcohol and head injury: an issue revisited. J. Neurotrauma **12**, 883–890.

KIDO, D.K., COX, C., HAMILL, R.W., ROTHENBERG, B.M., and WOOLF, P.D. (1992). Traumatic brain injuries: predictive usefulness of CT. Radiology **182**, 777–781.

KURTH, S.M., BIGLER, E.D., and BLATTER, D.D. (1994). Neuropsychological outcome and quantitative image analysis of acute haemorrhage in traumatic brain injury: preliminary findings. Brain Inj. **8**, 489–500.

MARKGRAF, C.G., VELAYO, N.L., JOHNSON, M.P., et al. (1998). Six-hour window of opportunity for calpain inhibition in focal cerebral ischemia in rats. Stroke **29**, 152–158.

MCKEATING, E.G., ANDREWS, P.J., and MASCIA, L. (1998). Relationship of neuron specific enolase and protein S-100 concentrations in systemic and jugular venous serum to injury severity and outcome after traumatic brain injury. Acta Neurochir. Suppl. (Wien) **71**, 117–119.

MIRSKI, M.A., MUFFELMAN, B., ULATOWSKI, J.A., and HANLEY, D.F. (1995). Sedation for the critically ill neurologic patient. Crit. Care Med. **23**, 2038–2053.

NADLER, V., BIEGON, A., BEIT-YANNAI, E., ADAMCHIK, J., and SHOHAMI, E. (1995). ^{45}Ca accumulation in rat brain after closed head injury; attenuation by the novel neuroprotective agent HU-211. Brain Res. **685**, 1–11.

NATH, R., RASER, K.J., STAFFORD, D., et al. (1996). Non-erythroid alpha-spectrin breakdown by calpain and inter-leukin 1 beta-converting-enzyme-like protease(s) in apoptotic cells: contributory roles of both protease families in neuronal apoptosis. Biochem J. **319**, Pt 3, 683–690.

NEUMANN-HAEFELIN, T., KASTRUP, A., DE CRESPIGNY, A., et al. (2000). Serial MRI after transient focal cerebral ischemia in rats: dynamics of tissue injury, blood–brain barrier damage, and edema formation. Stroke **31**, 1965–1973.

NEWCOMB, J.K., KAMPFL, A., POSMANTUR, R.M., et al. (1997). Immunohistochemical study of calpain-mediated breakdown products to alpha-spectrin following controlled cortical impact injury in the rat. J. Neurotrauma **14**, 369–383.

PALMER, G.C., PEELING, J., CORBETT, D., DEL BIGIO, M.R., and HUDZIK, T.J. (2001). T2-weighted MRI correlates with long-term histopathology, neurology scores, and skilled motor behavior in a rat stroke model. Ann. NY Acad. Sci. **939**, 283–296.

PETZOLD, A., KEIR, G., LIM, D., SMITH., M, and THOMPSON, E.J., (2003). Cerebrospinal fluid (CSF) and serum S100B: release and washout pattern. Brain Res. Bull. **61**, 281–285.

PIKE, B.R., FLINT, J., DAVE, J.R., et al. (2004). Accumulation of calpain and caspase-3 proteolytic fragments of brain-derived alphaII-spectrin in cerebral spinal fluid after middle cerebral artery occlusion in rats. J. Cereb. Blood Flow Metab. **24**, 98–106.

PIKE, B.R., FLINT, J., DUTTA, S., JOHNSON, E., WANG, K.K., and HAYES, R.L. (2001). Accumulation of non-erythroid alpha II–spectrin and calpain-cleaved alpha II–spectrin breakdown products in cerebrospinal fluid after traumatic brain injury in rats. J. Neurochem. **78**, 1297–1306.

PIKE, B.R., ZHAO, X., NEWCOMB, J.K., POSMANTUR, R.M., WANG, K.K., and HAYES, R.L. (1998). Regional calpain and caspase-3 proteolysis of alpha-spectrin after traumatic brain injury. Neuroreport **9**, 2437–2442.

RAABE, A., GROLMS, C., KELLER, M., DOHNERT, J., SORGE, O., and SEIFERT, V. (1998). Correlation of computed tomography findings and serum brain damage markers following severe head injury. Acta Neurochir. (Wien) **140**, 787–792.

RAABE, A., and SEIFERT, V. (2000). Protein S-100B as a serum marker of brain damage in severe head injury: preliminary results. Neurosurg. Rev. **23**, 136–138.

REIBER, H. (2003). Proteins in cerebrospinal fluid and blood: barriers, CSF flow rate and source-related dynamics. Restor. Neurol. Neurosci. **21**, 79–96.

REIBER, H., and PETER, J.B. (2001). Cerebrospinal fluid analysis: disease-related data patterns and evaluation programs. J. Neurol. Sci. **184**, 101–122.

ROBERTS-LEWIS, J.M., SAVAGE, M.J., MARCY, V.R., PINSKER, L.R., and SIMAN, R. (1994). Immunolocaliza-

tion of calpain I–mediated spectrin degradation to vulnerable neurons in the ischemic gerbil brain. J. Neurosci. **14,** 3934–3944.

RINGGER, N.C., TOLENTINO, P.J., McKINSEY, D.M., PIKE, B.R., WANG, K.K.W., and HAYES, R.L. (2004). Effects of injury severity on regional and temporal mRNA expression levels of calpains and caspases after traumatic brain injury in rats. J. Neurotrauma. (in press).

ROTHOERL, R.D., WOERTGEN, C., and BRAWANSKI, A. (2000). S-100 serum levels and outcome after severe head injury. Acta Neurochir. Suppl. **76,** 97–100.

SAATMAN, K.E., BOZYCZKO-COYNE, D., MARCY, V., SIMAN, R., and McINTOSH, T.K. (1996a). Prolonged calpain-mediated spectrin breakdown occurs regionally following experimental brain injury in the rat. J. Neuropathol. Exp. Neurol. **55,** 850–860.

SAATMAN, K.E., MURAI, H., BARTUS, R.T., et al. (1996b). Calpain inhibitor AK295 attenuates motor and cognitive deficits following experimental brain injury in the rat. Proc. Natl. Acad. Sci. USA **93,** 3428–3433.

SAIDO, T.C., YOKOTA, M., NAGAO, S., et al. (1993). Spatial resolution of fodrin proteolysis in postischemic brain. J. Biol. Chem. **268,** 25239–25243.

SHAW, G.J., JAUCH, E.C., and ZEMLAN, F.P. (2002). Serum cleaved tau protein levels and clinical outcome in adult patients with closed head injury. Ann. Emerg. Med. **39,** 254–257.

VERWEIJ, B.H., MUIZELAAR, J.P., VINAS, F.C., PETERSON, P.L., XIONG, Y., and LEE, C.P. (1997). Mitochondrial dysfunction after experimental and human brain injury and its possible reversal with a selective N-type calcium channel antagonist (SNX-111). Neurol. Res. **19,** 334–339.

WANG, K.K. (2000). Calpain and caspase: can you tell the difference? Trends Neurosci. **23,** 59.

WANG, K.K., POSMANTUR, R., NATH, R., et al. (1998). Simultaneous degradation of alpha-II– and beta-II–spectrin by caspase 3 (CPP32) in apoptotic cells. J. Biol. Chem. **273,** 22490–22497.

WILSON, J.T., HADLEY, D.M., WIEDMANN, K.D., and TEASDALE, G.M. (1995). Neuropsychological consequences of two patterns of brain damage shown by MRI in survivors of severe head injury. J. Neurol. Neurosurg. Psychiatry **59,** 328–331.

XIONG, Y., GU, Q., PETERSON, P.L., MUIZELAAR, J.P., and LEE, C.P. (1997). Mitochondrial dysfunction and calcium perturbation induced by traumatic brain injury. J. Neurotrauma **14,** 23–34.

ZEMLAN, F.P., JAUCH, E.C., MULCHAHEY, J.J., et al. (2002). C-tau biomarker of neuronal damage in severe brain injured patients: association with elevated intracranial pressure and clinical outcome. Brain Res. **947,** 131–139.

ZEMLAN, F.P., ROSENBERG, W.S., LUEBBE, P.A., et al. (1999). Quantification of axonal damage in traumatic brain injury: affinity purification and characterization of cerebrospinal fluid tau proteins. J. Neurochem. **72,** 741–750.

ZINK, B.J. (2001). Traumatic brain injury outcome: concepts for emergency care. Ann. Emerg. Med. **37,** 318–332.

Address reprint requests to:
N.C. Ringger, D.V.M.
Department of Neuroscience
McKnight Brain Institute
University of Florida
100 S. Newell Dr.
L1-100 (P.O. Box 100244)
Gainesville, FL 32610
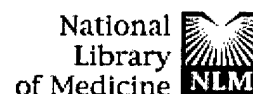
E-mail: ringger@ufbi.ufl.edu

NCBI

PubMed

National Library of Medicine NLM

Entrez   PubMed   Nucleotide   Protein   Genome   Structure   OMIM   PMC   Journals   B(

Search PubMed   for   Go   Clear

Limits   Preview/Index   History   Clipboard   Details

About Entrez

Display   Abstract   Show: 20   Sort   Send to   Text

Text Version

Entrez PubMed
Overview
Help | FAQ
Tutorial
New/Noteworthy
E-Utilities

PubMed Services
Journals Database
MeSH Database
Single Citation Matcher
Batch Citation Matcher
Clinical Queries
LinkOut
Cubby

Related Resources
Order Documents
NLM Gateway
TOXNET
Consumer Health
Clinical Alerts
ClinicalTrials.gov
PubMed Central

Privacy Policy

□ **1:** J Cereb Blood Flow Metab. 2004 Jan;24(1):98-106.   Related Articles, Lin

LWWonline
LIPPINCOTT WILLIAMS & WILKINS

Accumulation of calpain and caspase-3 proteolytic fragments of brain-derived alphaII-spectrin in cerebral spinal fluid after middle cerebral artery occlusion in rats.

Pike BR, Flint J, Dave JR, Lu XC, Wang KK, Tortella FC, Hayes RL.

Department of Neuroscience, Center for Traumatic Brain Injury Studies, E.F and W.L. McKnight Brain Institute of the University of Florida, Gainesville, Florida, USA. pikbr@mail.nih.gov

Preclinical studies have identified numerous neuroprotective drugs that attenuate brain damage and improve functional outcome after cerebral ischemia. Despite this success in animal models, neuroprotective therapies in the clinical setting have been unsuccessful. Identification of biochemical markers common to preclinical and clinical cerebral ischemia will provide a more sensitive and objective measure of injury severity and outcome to facilitate clinical management and treatment. However, there are currently n(effective biomarkers available for assessment of stroke. Nonerythroid alphaI spectrin is a cytoskeletal protein that is cleaved by calpain and caspase-3 proteases to signature alphaII-spectrin breakdown products (alphaII-SBDPs) after cerebral ischemia in rodents. This investigation examined accumulation of calpain- and caspase-3-cleaved alphaII-SBDPs in cerebrospinal fluid (CSI of rodents subjected to 2 hours of transient focal cerebral ischemia produced by middle cerebral artery occlusion (MCAO) followed by reperfusion. After MCAO injury, full-length alphaII-spectrin protein was decreased in brain tissue and increased in CSF from 24 to 72 hours after injury. Whereas alphaI SBDPs were undetectable in sham-injured control animals, calpain but not caspase-3 specific alphaII-SBDPs were significantly increased in CSF after injury. However, caspase-3 alphaII-SBDPS were observed in CSF of some injured animals. These results indicate that alphaII-SBDPs detected in CSF after injury, particularly those mediated by calpain, may be useful diagnostic indicators of cerebral infarction that can provide important information about specific neurochemical events that have occurred in the brain after acute stroke.

PMID: 14688621 [PubMed - indexed for MEDLINE]

ACCUMULATION OF CALPAIN AND CASPASE-3 PROTEOLYTIC FRAGMENTS OF BRAIN-DERIVED αII-SPECTRIN IN CSF AFTER MIDDLE CEREBRAL ARTERY OCCLUSION IN RATS

Brian R. Pike[1]*, Jeremy Flint[1], Jitendra R. Dave[3], X.-C. May Lu[3], Kevin K.K. Wang[1,2], Frank C. Tortella[3], and Ronald L. Hayes[1]

[1]Department of Neuroscience and [2]Department of Psychiatry, Center for Traumatic Brain Injury Studies, E.F. & W.L. McKnight Brain Institute of the University of Florida, Gainesville, FL, USA

[3]Department of Neuropharmacology and Molecular Biology, Division of Neurosciences, Walter Reed Army Institute of Research, Silver Spring, MD, USA

*Current Address: Office of Scientific Review, NIH/NIGMS
Bethesda, MD 20892-6200

Contact Information:
Brian R. Pike, Ph.D.
Office of Scientific Review
National Institute of General Medical Sciences
Building 45, Room 3An.18
45 Center Dr., MSC 6200
Bethesda, MD 20892-6200

Tel: 301-594-3907
Fax: 301-480-8506
Email: pikbr@mail.nih.gov

Abstract

Preclinical studies have identified numerous neuroprotective drugs that attenuate brain damage and functional outcome after cerebral ischemia. Despite this success in animal models, neuroprotective therapies in the clinical setting have been unsuccessful. Identification of biochemical markers common to preclinical and clinical cerebral ischemia will provide a more sensitive and objective measure of injury severity and outcome to facilitate clinical management and treatment. However, there are currently no effective biomarkers available for assessment of stroke. Non-erythroid αII-spectrin is a cytoskeletal protein that is cleaved by calpain and caspase-3 proteases to signature αII-spectrin breakdown products (αII-SBDPs) after cerebral ischemia in rodents. This investigation examined accumulation of calpain- and caspase-3-cleaved αII-SBDPs in CSF of rodents subjected to 2 hours of transient focal cerebral ischemia produced by middle cerebral artery occlusion (MCAO) followed by reperfusion. Following MCAO injury, full-length αII-spectrin protein was decreased in brain tissue and increased in CSF from 24 hours to 72 hours after injury. Calpain- and caspase-3-specific αII-SBDPs were also increased in brain and CSF after injury. Levels of calpain-specific αII-SBDPs were greater at each post-injury time point than levels of caspase-3-specific αII-SBDPs. Levels of these proteins were undetectable in CSF of uninjured control rats. These results indicate that calpain- and caspase-3-cleaved αII-SBDPs in CSF may be useful diagnostic indicators of cerebral infarction that can provide important information about specific neurochemical events that have occurred in the brain after acute stroke.

Keywords: calpain, caspase-3, ischemia, stroke, biomarker, fodrin, α-spectrin, cerebrospinal fluid

Running title: Biomarkers of Stroke

Introduction

Acute ischemic stroke is a significant international health concern representing a potentially catastrophic debilitating medical emergency with poor prognosis for long-term disability. With the exception of diuretics, supportive measures, and when appropriate, thrombolytic therapy with recombinant tissue plasminogen activator (tPA), there are currently no approved drug treatments for ischemic brain injury (Grotta, 2002; Lees, 2002; Broderick and Hacke, 2002). Although a number of neuroprotective drugs have proven effective in reducing infarct size or improving functional outcome in preclinical testing, none have proven successful in clinical trials (Gladstone et al., 2002; Kidwell et al., 2001). Differences between preclinical and clinical trial outcome with neuroprotective drugs in acute ischemic stroke may be due to a variety of pitfalls that arise when attempting to extrapolate from animal to human investigations. These pitfalls may include differences in drug concentration and duration, differences in the window for therapeutic efficacy, differences in preclinical vs. clinical trial design, and the lack of standardized and sensitive outcome measures (Gladstone, et al., 2002; STAIR, 1999). For example, preclinical studies (typically in rodents) have traditionally utilized reduction of acute infarct volume as the primary measure of treatment efficacy, while clinical trials typically gauge treatment efficacy based on neurological and/or functional outcome (Gladstone et al., 2002). One approach to address these discrepancies in outcome measures is for preclinical and clinical trial designs to use outcome measures that are common to both human acute ischemic stroke and to preclinical animal models of ischemia. The use of common biochemical markers may provide such an approach.

Unlike other organ-based diseases where rapid diagnosis employing biomarkers (usually involving blood tests) prove invaluable to guide treatment of the disease, no such rapid and definitive diagnostic tests exist for acute ischemic brain injury. Biomarkers would have important applications in diagnosis, prognosis, and clinical research of ischemic brain injuries.

3

Simple and rapid diagnostic tools will immensely facilitate allocation of the major medical resources required to treat acute ischemic brain injuries. Accurate diagnosis in acute care environments can significantly enhance decisions about patient management, including decisions whether to admit or discharge patients or to administer other time consuming and expensive tests, including computed tomography (CT) and magnetic resonance imaging (MRI) scans. Biomarkers could provide major opportunities for the conduct of clinical research including confirmation of injury mechanism(s) and drug target identification. The temporal profile of changes in biomarkers could guide timing of treatment. Finally, biomarkers could provide a robust and sensitive clinical trial outcome measure that is obtainable more readily and with less expense than conventional neurological assessments, thereby significantly reducing the risks and costs of human clinical trials.

Previously reported biomarkers of cerebral ischemia include neuron-specific enolase (NSE), brain specific creatine kinase enzyme (CPK-BB), S-100β, and inflammatory cytokines such as IL-6 (Laskowitz et al., 1998). Of these, NSE and S-100β have been the most studied. After cardiac arrest, NSE elevations in serum and CSF have been correlated with neurological recovery (Roine et al., 1989; Martens, 1996; Dauberschmidt et al., 1991). Serum and CSF NSE values are reported to be elevated in rodent models of focal ischemia in proportion to the eventual infarct volume (Cunningham et al., 1991, 1996; Horn et al., 1995). In clinical trials, peak serum NSE values also predicted infarct volumes as shown by CT. However, correlating serum NSE values with functional outcome was less successful (Cunningham et al., 1991, 1996; Missler et al., 1997). S-100β protein has been studied most extensively for characterization of ischemic injuries after cardiac surgery and several reports have documented post-operative serum elevations (Sellman et al., 1992; Westaby et al., 1996). However, many of these reports do not include careful studies of neurological outcome and several investigators have recently criticized the diagnostic utility of S-100β during cardiac surgery (Anderson et al.,

2001). Thus, there is clearly a need for development of better biochemical markers for use in evaluating ischemic brain injury.

Our research efforts to develop biomarkers for traumatic brain injury (TBI) and acute ischemic brain injury have focused on αII-spectrin metabolic products as prototypical biochemical markers (Pike et al., 2001; Ringger et al., 2002). αII-spectrin is the major structural component of the cortical membrane cytoskeleton and is particularly abundant in axons and presynaptic terminals (Goodman et al., 1995; Riederer et al., 1986). Importantly, αII-spectrin is a major substrate for both and calpain and caspase-3 cysteine proteases (see **Fig. 1**), and the major calpain and caspase-3 cleavage sites of αII-spectrin have been well documented (Harris et al., 1988; Wang et al., 1998). Our laboratory has provided considerable evidence that αII-spectrin is processed by calpains and/or caspase-3 to signature cleavage products *in vivo* after TBI (Beer et al., 2000; Newcomb et al., 1997; Pike et al., 1998a, 2001) and in *in vitro* models of mechanical stretch injury (Pike et al., 2000), necrotic cell death (Zhao et al., 1999), apoptotic cell death (Pike et al., 1998b), and oxygen-glucose deprivation (Newcomb-Fernandez et al., 2001). Calpain and caspase-3 proteases also cleave αII-spectrin to signature proteolytic fragments in the brain in a rodent model of transient forebrain ischemia (Zhang et al., 2002). Although we have generated considerable laboratory data on the utility of αII-spectrin degradation as a biomarker for TBI in rodents (Pike et al., 2001), and more recently with preliminary data in human TBI patients (d'Avella et al., 2002), the present investigation is the first to provide evidence that calpain- and caspase-3-mediated αII-spectrin breakdown products (αII-SBDPs) can be detected in CSF after ischemic-reperfusion brain injury, and can used as biochemical markers in a rodent model of transient focal stroke in rats.

Methods

Surgical Procedures and Middle Cerebral Artery Occlusion: A "noninvasive" filament method of MCAO occlusion used extensively by our laboratories (Berti et al., 2002; Williams et

5

al., 2003) was used to produce cerebral ischemia in rats. The method described by Longa et al. (1989) and later modified in our laboratory by Britton et al. (1997) consists of blocking blood flow into the MCA with an intraluminal 3-0 monofilament nylon sterile suture with rounded tip introduced through an incision in the external carotid artery (ECA).

Under halothane anesthesia (5% halothane via induction chamber followed by 2% halothane via nose cone), the common carotid artery (CCA) was exposed at the level of external and internal carotid artery bifurcation with a midline neck incision. The internal carotid artery (ICA) was followed rostrally to the pterygopalatine branch and the ECA was ligated and cut at its lingual and maxillary branches. To prevent bleeding during suture insertion, the CCA and ICA were temporarily clamped with micro-aneurysm clips. The nylon suture was then introduced into the ICA via an incision on the ECA stump (the path of the suture can be monitored visually through the vessel wall) and advanced through the carotid canal approximately 20 mm from the carotid bifurcation until it becomes lodged in the narrowing of the anterior cerebral artery blocking the origin of the MCA. The skin incision was then closed using sterile autoclips. The endovascular suture remained in place for 2 hr at which time the rat was briefly re-anesthetized and the suture filament was retracted to allow reperfusion. For sham MCAO surgeries, the same procedure was followed but the filament was advanced only 10 mm beyond the internal-external carotid bifurcation and was left in place until sacrifice. During all surgical procedures, animals were maintained at 37.0°C by a homeothermic heating blanket (Harvard Apparatus, Holliston, MA).

Following surgery animals were placed in recovery cages with air temperature maintained at 22°C. During the 2 hr ischemia period and the initial 4 hr post-reperfusion period, 75-watt warming lamps were positioned directly over the top of each cage in order assist in maintaining normothermic body temperature throughout the experiment. Importantly, at the conclusion of each experiment, rat brains showing pathological evidence of subarachnoid hemorrhage upon

necropsy were excluded from the study. Also, all rats exhibiting convulsant behaviors at any time post MCAO were excluded from the experiment, as well as those animals not showing maximal neurologic impairment (NS=10, see description below) immediately prior to the 2 hr reperfusion.

Brain Tissue and CSF Collection: Brain (cortex and hippocampus) and CSF was collected from animals at various intervals after sham-injury or MCAO as previously described by our laboratory (Pike et al., 2001). At the appropriate time-points, MCAO or sham-injured animals were anesthetized as described above and secured in a stereotactic frame with the head allowed to move freely along the longitudinal axis. The head was flexed so that the external occipital protuberance in the neck was prominent and a dorsal midline incision was made over the cervical vertebrae and occiput. The atlanto-occipital membrane was exposed by blunt dissection and a 25G needle attached to polyethylene tubing was carefully lowered into the cisterna magna. Approximately 0.1 to 0.15 ml of CSF was collected from each rat. Following CSF collection, animals were removed from the stereotactic frame and immediately killed by decapitation. Ipsilateral and contralateral (to the site of infarct) cortices were then rapidly dissected, rinsed in ice cold PBS, and snap frozen in liquid nitrogen. Cortices were excised to the level of the white matter and extended ~4 mm laterally and ~7 mm rostrocaudally. CSF samples were centrifuged at 4000 g for 4 min. at 4°C to clear any contaminating erythrocytes. Cleared CSF and frozen tissue samples were stored at -80°C until ready for use. Cortices were homogenized in a glass tube with a Teflon dounce pestle in 15 volumes of an ice-cold triple detergent lysis buffer (20 mM Hepes, 1 mM EDTA, 2 mM EGTA, 150 mM NaCl, 0.1% SDS, 1.0% IGEPAL 40, 0.5% deoxycholic acid, pH 7.5) containing a broad range protease inhibitor cocktail (Roche Molecular Biochemicals, cat. #1-836-145).

Immunoblot Analyses of CSF and Cortical Tissues: Protein concentrations of tissue homogenates and CSF were determined by bicinchoninic acid microprotein assays (Pierce Inc.,

7

Rockford, IL) with albumin standards. Protein balanced samples were prepared for sodium dodecyl sulfate–polyacrylamide gel electrophoresis (SDS-PAGE) in twofold loading buffer containing 0.25 M Tris (pH 6.8), 0.2 M DTT, 8% SDS, 0.02% bromophenol blue, and 20% glycerol in distilled H_2O. Samples were heated for 10 min. at 100°C and centrifuged for 1 min. at 10,000 rpm in a microcentrifuge at ambient temperature. Twenty micrograms of protein per lane was routinely resolved by SDS-PAGE on 6.5% Tris/glycine gels for 1 hour at 200 V. Following electrophoresis, separated proteins were laterally transferred to polyvinylidene fluoride (PVDF) membranes in a transfer buffer containing 0.192 M glycine and 0.025 M Tris (pH 8.3) with 10% methanol at a constant voltage of 100 V for 1 hour at 4°C. Blots were blocked for 1 hour at ambient temperature in 5% nonfat milk in TBS and 0.05% Tween-20. Panceau Red (Sigma, St. Louis, MO) was used to stain membranes to confirm successful transfer of protein and to insure that an equal amount of protein was loaded in each lane.

Antibodies and Immunolabeling of PVDF Membranes: Immunoblots containing brain or CSF protein were probed with an anti-αII-spectrin (fodrin) monoclonal antibody (FG 6090 Ab; clone AA6; cat. # FG 6090; Affiniti Research Products Limited, UK) that detects intact non erythroid αII-spectrin (280 kDa) and 150, 145, and 120 kDa cleavage fragments to αII-spectrin. A cleavage product of 150 kDa is initially produced by calpains or caspase-3 proteases (each proteolytic cleavage yields a unique amino-terminal region; Nath et al., 1996; Wang et al., 1998; **Fig. 1**). The calpain-generated 150 kDa product is further cleaved by calpain to yield a specific calpain signature product of 145 kDa (Harris et al., 1988; Nath et al., 1996) whereas the caspase-3 generated 150 kDa product is further cleaved by caspase-3 to yield an apoptotic-specific caspase-3 signature product of 120 kDa (Nath et al., 1998; Wang et al., 1998; Wang, 2000). Following an overnight incubation at 4°C with the primary antibody (FG 6090 Ab, 1:4000 for brain tissue and 1:2000 for CSF), blots were incubated for 1 hr at ambient temperature in 3% nonfat milk that contained a horseradish peroxidase-conjugated goat anti-mouse IgG (1:10,000

dilution). Enhanced chemiluminescence (ECL, Amersham) reagents were used to visualize immunolabeling on Kodak Biomax ML chemiluminescent film.

Statistical Analyses: Semi-quantitative evaluation of protein levels detected by immunoblotting was performed by computer-assisted densitometric scanning (AlphaImager 2000 Digital Imaging System, San Leandro, CA). Data were acquired as integrated densitometric values and transformed to percentages of the densitometric levels obtained on scans from sham-injured animals visualized on the same blot. Data was evaluated by least squares linear regression followed by ANOVA. All values are given as mean ± SEM. Differences were considered significant if $p < 0.05$.

Results

Proteolysis of αII-Spectrin in the Ipsilateral Cortex by Calpains and Caspase-3 After MCAO Injury. In the ipsilateral cortex, MCAO injury caused significant ($p < 0.05$) accumulation of the non-specific 150 kDa αII-SBDP (generated by calpain and/or caspase-3), and of the calpain-specific 145 kDa αII-SBDP at all post-injury time points as compared to sham-injured control rats (**Fig. 2**). Levels of the calpain-specific 145 kDa αII-SBDP were 304%, 282%, and 301% of sham-injured control values at 24, 48, and 72 hours post-injury, respectively (**Fig. 3**). Levels of the non-specific 150 kDa αII-SBDP closely matched levels of the 145 kDa fragment, and were 276%, 275%, 268% of sham-injured control valules at 24, 48, and 72 hours, respectively (**Fig. 3**). MCAO injury also resulted in more modest, but significant ($p < 0.05$ to $p < 0.001$) levels of caspase-3-specific 120 kDa αII-SBDPs at all post-injury time points (**Fig. 2**). Levels of the caspase-3-specific 120 kDa fragment were 131%, 132%, and 140% of sham-injured control values at 24, 48, and 72 hours post-injury, respectively (**Fig. 3**). Although levels of the caspase-3-specific 120 kDa αII-SBDP were smaller than those produced by calpains,

9

between animal variability was much lower for levels of caspse-3 αII-SBDPs compared to the variability for levels of calpain αII-SBDPs.

In the contralateral cortex, MCAO injury caused no significant accumulation of calpain- or caspase-3-specific αII-SBDPs at any post-injury time point as compared to sham-injured control rats (**Fig. 2**).

Accumulation of Calpain and Caspase-3 Mediated αII-SBDPs in CSF after MCAO Injury. Cerebrospinal fluid levels of αII-spectrin and αII-SBDPs were undetectable in sham-injured control animals (**Fig. 2**). However, after MCAO injury accumulation of full length αII-spectrin (280 kDa) and the 150 kDa, 145 kDa, and 120 kDa αII-SBDPs were overtly apparent on immunoblots at various post-injury time points (**Fig. 2**). Levels of the full length αII-spectrin protein were increased in CSF of MCAO injured animals and were 144%, 453%, and 395% of sham-injured control levels at 24, 48, and 72 hours post-injury. However, there was considerable between animal variability in levels of the full length protein; thus, quantitative analysis failed to reach statistical significance (**Fig. 3**). Levels of the non-specific 150 kDa αII-SBDP, and of the calpain-specific 145 kDa αII-SBDP, were apparent on immunoblot at all post-injury time points, but only levels at 48 hours and 72 hours post-injury reached statistical significance ($p < 0.001$). Levels of the non-specific 150 kDa αII-SBDP were 216%, 523%, and 467% of sham-injured control animals, and levels of the calpain-specific 145 kDa αII-SBDP were 268%, 626%, and 546% of sham-injured control values at 24, 48, and 72 hours post-injury, respectively (**Fig. 3**). Levels of the caspase-3-specific 120 kDa αII-SBDP were 84%, 439%, and 110% of sham-injured control levels at 24, 48, and 72 hours post-injury, respectively (**Fig. 3**). Although levels of caspase-3-specific 120 kDa αII-SBDPs were 439% of sham-injured control values at 48 hours post-injury, large between animal variability precluded statistical significance.

10

Linear Regression Analyses of Cortical versus CSF Levels of αII-Spectrin and αII-SBDPs. Least squares linear regression was calculated to examine the relationship between cortical and CSF levels of αII-spectrin and αII-SBDPs over days post-injury in sham-control and MCAO-injured animals. The slopes of the regression lines for brain and CSF protein levels were analyzed by ANOVA.

The slope of the regression line for protein levels of the full-length 280 kDa αII-spectrin in the cortex across days post-injury was only slightly negative (m = -4.872), indicating modest decreases in total αII-spectrin protein (**Fig. 4**). The slope of the regression line for CSF levels of the full-length αII-spectrin protein across days post-injury was positive (m = 113.5), indicating increased accumulation of αII-spectrin in CSF from 24 h to 72 h after MCAO injury.

Slopes of the regression lines for the 150 kDa αII-SBDP in cortex and CSF across days post-injury were both positive (m = 53.59 and m = 145.4, respectively; **Fig. 4**). This result is consistent with the immunoblot data demonstrating increased accumulation of the 150 kDa αII-SBDP in cortex and CSF after MCAO injury. ANOVA indicated no significant difference (F = 2.14, p = 0.2172) between cortical and CSF slopes. This result indicates that rate of accumulation of the non-specific 150 kDa αII-SBDP in brain and CSF over days post-injury was approximately equivalent.

Slopes of the regression line for the 145 kDa αII-SBDP in cortex and CSF across days post-injury were both positive (m = 60.63 and m = 170.5, respectively; **Fig. 4**). This result is also consistent with the immunoblot data demonstrating increased accumulation of the 145 kDa αII-SBDP in cortex and CSF after MCAO injury. ANOVA indicated no significant difference (F = 2.50, p = 0.1889) between cortical and CSF slopes. This result indicates that rate of

accumulation of the calpain-specific 145 kDa αII-SBDP in brain and CSF over days post-injury was approximately equivalent.

Slopes of the regression line for the 120 kDa αII-SBDP in cortex and CSF across days post-injury were both slightly positive (m = 15.12 and m = 41.28, respectively; **Fig. 4**). This result is consistent with the immunoblot data demonstrating relatively small increases in accumulation of the 120 kDa αII-SBDP in cortex and CSF after MCAO injury. Again, ANOVA indicated no significant difference (F =0.08, p = 0.7861) between cortical and CSF slopes, indicating that rate of accumulation of the caspase-3 specific 120 kDa αII-SBDP in brain and CSF over days post-injury was approximately equivalent.

Discussion

This paper provides further evidence supporting the use of calpain and caspsase-3 specific αII-SBDPs as surrogate neurochemical markers of CNS injury. Previous data from our laboratory demonstrate that TBI causes robust and detectable accumulation of calpain-mediated αII-SBDPs (and to a lesser extent, caspase-3-mediated αII-SBDPs) in CSF of brain injured rodents (Pike et al., 2001). We now demonstrate that a rodent stroke model of focal ischemic injury also results in increased levels of calpain and caspase-3 αII-SBDPs in post-injury CSF. The results of these two studies are important in that they provide the first evidence that extra-parenchymal detection of specific protein metabolic products can be used as unequivocal biochemical markers for specific neurochemical events (i.e., calpain and caspase-3 activation) that have occurred in the injured brain in at least two preclinical models of brain injury (traumatic and ischemic). Importantly, recent preliminary clinical studies in patients with severe TBI also indicate robust levels of calpain and caspase-3 mediated αII-SBDPs in CSF (d'Avella et al., 2002).

Analysis of specific biochemical markers is a mandatory component of diagnosing dysfunction in a number of organs, including the use of troponin assays in patients with acute coronary syndromes (Newby et al., 2003). Indeed, troponin testing has rapidly evolved from its initial role in aiding diagnosis of myocardial infarction to a more complex role for risk stratification and guidance of treatment strategies (Newby et al., 2003). However, there are no such biomarkers of proven clinical utility for TBI and cerebral ischemia. In the case of TBI, this may be due, in part, to the fact that TBI is difficult to assess and clinical examinations are of restricted value during the first hours and days after injury. For instance, conventional diagnoses of TBI are based on neuroimaging techniques such as CT scanning, MRI, and single-photon emission CT scanning (Jacobs et al., 1996; Kant et al., 1997; Mitchener et al., 1997). CT scanning has low sensitivity to diffuse brain damage and the availability of MRI is limited (Kesler et al., 2000; Levi et al., 1900). In addition, single-photon emission CT scanning detects regional blood-flow abnormalities not necessarily related to structural damage. In the case of stroke, investigators have also generally recognized the need for more objective assessments of outcome, including the use of biochemical markers (Dirnagl et al., 1999; Zaremba et al., 2001). The approval of tPA as a treatment for acute stroke has additionally highlighted the potential utility of biochemical markers. For example, diagnosis of stroke is relatively straightforward when patients present with typical symptoms; however, often symptoms of stroke are more subtle and can delay diagnosis by hours or days (Elkind, 2003). Additionally, other causes of neurological symptoms, such as seizure, migraine, vasospasm, syncope, and peripheral vestibulopathy, can be indistinguishable from symptoms of thromboembolic transient ischemic attacks (Johnston et al., 2003). Thus, a rapid and reliable biochemical marker of stroke will facilitate diagnosis and might give assurance to physicians considering administering thrombolytic agents for treatment of acute ischemic stroke.

Our laboratories' assessment of αII-SBDPs as biochemical markers in models of TBI and focal cerebral ischemia may result in considerable improvement over currently existing biochemical markers of CNS injury. For instance, other putative biomarkers of CNS injury (e.g., CPK-BB, NSE, S-100β, lactate dehydrogenase, etc.) are of limited value due to a lack of specificity to CNS tissues, unreliability in predicting outcome, and because they provide no specific information regarding neurochemical pathology of injured CNS tissue. Recent studies have also examined the utility of cleaved tau protein (cτP) as a predictor of outcome. However, while cτP is axonal specific, it also provides no information about specific neurochemical events that have occurred in the injured CNS. Furthermore, recent studies have presented conflicting evidence as to the utility of cτP as a predictor of outcome after TBI in humans (Chatfield et al., 2002; Zemlan et al., 1999). In contrast, αII-SBDPs offer several advantages as compared to the putative biomarkers just described. For instance, αII-SBDPs provide concurrent information on post-injury activity of two important proteolytic enzymes (calpain and caspase-3). Low basal levels of these proteases further optimizes their utility as markers of cell injury. Another important characteristic is that αII-spectrin protein is not localized in erythrocytes (Goodman et al., 1995; Riederer, et al., 1986). Blood is a major source of CSF contamination after TBI and hemorrhagic ischemia. Results from our previously published studies in TBI clearly demonstrate that αII-spectrin and αII-SBDPs are not detectable in whole blood samples. In contrast, the erythroid isoform of spectrin, αI-spectrin, is detectable in both blood and brain tissues (Pike et al., 2001).

However, one disadvantage is that while αII-spectrin is highly enriched in brain, it is not specific to brain tissue. While this is not a concern for CSF detection of αII-SBDPs, it could be problematic for detection of αII-SBDPs in serum as human head-injured patients often present with multi-organ trauma. Additional studies in preclinical models and in human patients are needed to clarify this issue.

14

An ideal biomarker for a particular neurological disease is one that is 100% specific and sensitive for that particular disease. However, with TBI or stroke, it is not critical that a biomarker be specific to one or the other disorder, rather, the biomarker need only indicate, with as much sensitivity as possible, the severity of brain damage that has occurred as a result of brain trauma or cerebral infarction (although a biomarker that can rapidly and accurately discriminate between hemorrhagic and thrombolytic stroke would certainly be useful). The use of calpain- and caspase-3-mediated αII-SBDPs could provide a powerful approach for determining the severity of brain damage caused by a TBI or stroke, and could also provide a clinical tool for monitoring the duration of the acute injury response and the effects of emergency or therapeutic interventions. For instance, calpain and caspase-3 are potent mediators of cell death that can be rapidly activated in response to traumatic (Beer et al., 2000; Pike et al., 1998a; Sullivan et al., 2002) or ischemic brain injury (Davoli et al., 2002; Zhang et al., 2002), and brain regions with the highest accumulation of αII-SBDPs have the highest level of neuronal cell death (Roberts-Lewis et al., 1994; Newcomb et al., 1997). Importantly, calpain and caspsase-3 can be concurrently or independently activated after TBI (Pike et al., 1998a) or cerebral ischemia (Zhang et al., 2002), and the temporal duration of activity can vary for each protease. Thus, the ability to monitor both calpain and caspase-3 activation during the acute period of CNS injury is a major advantage of αII-SBDPs over other biomarkers. Indeed, recent preliminary data obtained from CSF of severely injured TBI patients indicate that temporal accumulation of calpain- and caspase-3-mediated αII-SBDPs show different patterns of temporal expression that vary in each patient (d'Avella et al., 2002). This result is similar to our preclinical TBI and ischemic injury models in which accumulation of calpain and/or caspase-3 αII-SBDPs also varies between individual animals. This variability emphasizes the heterogeneous nature of TBI and ischemic pathology, and points to important implications for

15

individualized treatment of human brain injured patients that is tailored to specific neurochemical cascades operative in the injured brain.

In summary, this paper provides further evidence supporting the use of calpain- and caspase-3-mediated αII-SBDPs as neurochemical markers of CNS injury. Although numerous other proteins, peptides, amino acids, etc., have been identified in CSF after TBI and acute cerebral ischemia, no such surrogate marker of CNS injury has yet provided a window of insight into specific neurochemical events that have occurred as a result of traumatic or ischemic brain injury. The use of protease-specific αII-SBDPs as biomarkers offers several advantages over existing biomarkers of traumatic or ischemic brain injury, including the ability to provide concurrent information about the activity of two major proteolytic effectors of cell death. Additional studies to further characterize the sensitivity of αII-SBDPs (e.g., in serum and across injury magnitudes) are ongoing. In addition, it is thought that the development of other CNS-specific biomarkers used in conjunction with αII-SBDPs will provide researchers and clinicians with powerful tools for diagnosing and assessing CNS injury, for monitoring recovery, and for guiding appropriate administration of therapeutic compounds. Finally, it is thought that recent advancements in antibody-based specific identification technologies will facilitate development of rapid, sensitive, and easy-to-use kits for research and clinical environments.

References

Anderson RE, Hansson LO, Nilsson O, Dijlai-Merzoug R, Settergren G (2001) High serum S100B levels for trauma patients without head injuries. *Neurosurgery* 48(6):1255-1258

Beer R, Franz G, Srinivasan A, Hayes RL, Pike BR, Zhao X, Schmutzhard E, Poewe W, Kampfl A (2000) Temporal profile and cell subtype distribution of activated caspase-3 following experimental traumatic brain injury. *J Neurochem* 75(3):1264-1273

Berti R, Williams AJ, Moffett JR, Hale SL, Velarde LC, Elliott PJ, Yao C, Dave JR, Tortella FC (2002) Quantitative real-time RT-PCR analysis of inflammatory gene expression associated with ischemia-reperfusion brain injury. *J Cereb Blood Flow Metab* 22(9):1068-1079

Britton P, Lu XC, Laskosky M, Tortella FC (1997) Dextromethorphan protects against cerebral injury following transient, but not permanent, focal ischemia in rats. *Life Sci* 60:1729-1740

Broderick JP, Hacke W (2002) Treatment of acute ischemic stroke: Part II: neuroprotection and medical management. *Circulation* 106(13):1736-1740

Chatfield DA, Zemlan FP, Day DJ, Menon DK (2002) Discordant temporal patterns of S100beta and cleaved tau protein elevation after head injury: a pilot study. *Br J Neurosurg* 16(5):471-476

Cunningham RT, Young IS, Winder J, O'Kane MJ, McKinstry S, Johnston CF, Dolan OM, Hawkins SA, Buchanan KD (1991) Serum neurone specific enolase (NSE) levels as an indicator of neuronal damage in patients with cerebral infarction. *Eur J Clin Invest* 21(5):497-500

Cunningham RT, Watt M, Winder J, McKinstry S, Lawson JT, Johnston CF, Hawkins SA, Buchanan, KD (1996) Serum neurone-specific enolase as an indicator of stroke volume. *Eur J Clin Invest* 26(4):298-303

Dauberschmidt R, Zinsmeyer J, Mrochen H, Meyer M (1991) Changes of neuron-specific enolase concentration in plasma after cardiac arrest and resuscitation. *Mol Chem Neuropathol* 14(3):237-245

d'Avella D, Aguennouz M, Angileri FF, de Divitiis O, Germanò A, Toscano A, Tomasello F, Vita G, Pike BR, Wang KKW, Hayes RL (2002) Accumulation of calpain and caspase-3 cleaved all-spectrin breakdown products in CSF of patients with severe traumatic brain injury. [abstract] *J Neurotrauma* 19(10):1292

Davoli MA, Fourtounis J, Tam J, Xanthoudakis S, Nicholson D, Robertson GS, Ng GY, Xu D (2002) Immunohistochemical and biochemical assessment of caspase-3 activation and DNA fragmentation following transient focal ischemia in the rat. *Neuroscience* 115(1):125-136

Dirnagl U, Iadecola C, Moskowitz MA (1999) Pathobiology of ischaemic stroke: an integrated view. *Trends Neurosci* 22(9):391-397

Elkind MS (2003) Stroke in the elderly. *Mt Sinai J Med* 70(1):27-37

Gladstone DJ, Black SE, Hakim AM (2002) Toward wisdom from failure: lessons from neuroprotective stroke trials and new therapeutic directions. *Stroke* 33(8):2123-2136

Goodman SR, Zimmer WE, Clark MB, Zagon IS, Barker JE, Bloom ML (1995) Brain spectrin: of mice and men. *Brain Res Bull* 36(6):593-606

Grotta J (2002) Neuroprotection is unlikely to be effective in humans using current trial designs. *Stroke* 33(1):306-307

Harris AS, Croall DE, Morrow JS (1988) The calmodulin-binding site in alpha-fodrin is near the calcium-dependent protease-I cleavage site. *J Biol Chem* 263(30):15754-15761

Horn M, Seger F, Schlote W (1995) Neuron-specific enolase in gerbil brain and serum after transient cerebral ischemia. *Stroke* 26(2):290-296

Jacobs A, Put E, Ingels M, Put T, Bossuyt A (1996) One-year follow-up of technetium-99m-HMPAO SPECT in mild head injury. *J Nucl Med* 37(10):1605-1609

Johnston SC, Sidney S, Bernstein AL, Gress DR (2003) A comparison of risk factors for recurrent TIA and stroke in patients diagnosed with TIA. *Neurology* 60(2):280-285

Kant R, Smith-Seemiller L, Isaac G, Duffy J (1997) Tc-HMPAO SPECT in persistent post-concussion syndrome after mild head injury: comparison with MRI/CT. *Brain Inj* 11(2):115-124

Kesler SR, Adams HF, Bigler ED (2000) SPECT, MR and quantitative MR imaging: correlates with neuropsychological and psychological outcome in traumatic brain injury. *Brain Inj* 14(10):851-857

Kidwell CS, Liebeskind DS, Starkman S, Saver JL (2001) Trends in acute ischemic stroke trials through the 20th century. *Stroke* 32(6):1349-1359

Laskowitz DT, Grocott H, Hsia A, Copeland KR (1998) Serum Markers of Cerebral Ischemia. *J Stroke Cerebrovasc Dis* 7(4):234-241

Lees KR (2002) Neuroprotection is unlikely to be effective in humans using current trial designs: an opposing view. *Stroke* 33(1):308-309.

Levi L, Guilburd JN, Lemberger A, Soustiel JF, Feinsod M (1990) Diffuse axonal injury: analysis of 100 patients with radiological signs. *Neurosurgery* 27(3):429-432

Longa EL, Weinstein PR, Carlson S, Cummins R (1989) Reversible middle cerebral artery occlusion without craniectomy in rats. *Stroke* 20:84-91

Martens P (1996) Serum neuron-specific enolase as a prognostic marker for irreversible brain damage in comatose cardiac arrest surviviors. *Acad Emerg Med* 3(2):126-131

Missler U, Wiesmann M, Friedrich C, Kaps M (1997) S-100 protein and neuron-specific enolase concentrations in blood as indicators of infarction volume and prognosis in acute ischemic stroke. *Stroke* 28(10):1956-1960

Mitchener A, Wyper DJ, Patterson J, Hadley DM, Wilson JT, Scott LC, Jones M, Teasdale GM (1997) SPECT, CT, and MRI in head injury: acute abnormalities followed up at six months. *J Neurol Neurosurg Psychiatry* 62(6):633-636

Nath R, Raser KJ, Stafford D, Hajimohammadreza I, Posner A, Allen H, Talanian RV, Yuen P, Gilbertson RB, Wang KK (1996) Non-erythroid α-spectrin breakdown by calpain and interleukin 1β-converting-enzyme-like protease(s) in apoptotic cells: contributory roles of both protease families in neuronal apoptosis. *Biochem J* 319:683-690

Nath R, Probert A, McGinnis KM, Wang KKW (1998) Evidence for activation of caspase-3-like protease in excitotoxin- and hypoxia/hypoglycemia-injured neurons *J Neurochem* 71:186-195

Newby LK, Goldmann BU, Ohman EM (2003) Troponin: an important prognostic marker and risk-stratification tool in non-ST-segment elevation acute coronary syndromes. *J Am Coll Cardiol* 41(4 Suppl S):S31-S36

Newcomb-Fernandez JK, Zhao X, Pike BR, Wang KKW, Kampfl A, Beer R, DeFord SM, Hayes RL (2001) Concurrent assessment of calpain and caspase-3 activation after oxygen-glucose deprivation in primary septo-hippocampal cultures. *J Cereb Blood Flow Metab* 21(11):1281-1294

Newcomb JK, Kampfl A, Posmantur RM, Zhao X, Pike BR, Liu SJ, Clifton GL, Hayes RL (1997) Immunohistochemical study of calpain-mediated breakdown products to alpha-spectrin following controlled cortical impact injury in the rat. *J Neurotrauma* 14:369-383

Pike BR, Zhao X, Newcomb JK, Posmantur RM, Wang KKW, Hayes RL (1998a) Regional calpain and caspase-3 proteolysis of α-spectrin after traumatic brain injury. *Neuroreport* 9:2437-2442

Pike BR, Zhao X, Newcomb JK, Wang KKW, Posmantur RM, Hayes RL (1998b) Temporal relationships between *de novo* protein synthesis, calpain and caspase 3-like protease activation, and DNA fragmentation during apoptosis in septo-hippocampal cultures. *J Neurosci Res* 52: 505-520

Pike BR, Zhao X, Newcomb JK, Glenn CC, Anderson DK, Hayes RL (2000) Stretch injury causes calpain and caspase-3 activation and necrotic and apoptotic cell death in septo-hippocampal cell cultures. *J Neurotrauma* 17(4):283-298

Pike BR, Flint J, Dutta S, Johnson E, Wang KKW, Hayes RL (2001) Accumulation of calpain-cleaved non-erythroid αII-spectrin in cerebrospinal fluid after traumatic brain injury in rats. *J Neurochem* 78:297-1306

Riederer BM, Zagon IS, Goodman SR (1986) Brain spectrin(240/235) and brain spectrin(240/235E): two distinct spectrin subtypes with different locations within mammalian neural cells. *J Cell Biol* 102(6):2088-2097

Ringger NC, Silver X, O'Steen B, Brabham JG, Deford SM, Pike BR, Pineda J, Hayes RL (2002) CSF accumulation of calpain-specific αII-spectrin breakdown products are associated with injury magnitude and lesion volume after traumatic brain injury in rats. [abstract] *J Neurotrauma* 19(10):1302

Roberts-Lewis JM, Savage MJ, Marcy VR, Pinsker LR, Siman R (1994) Immunolocalization of calpain I-mediated spectrin degradation to vulnerable neurons in the ischemic gerbil brain. *J Neurosci* 14(6):3934-3944

19

Roine RO, Somer H, Kaste M, Viinikka L, Karonen SL (1989) Neurological outcome after out-of-hospital cardiac arrest. Prediction by cerebrospinal fluid enzyme analysis. *Arch Neurol* 46(7):753-756

Sellman M, Ivert T, Ronquist G, Caesarini K, Persson L, Semb BK (1992) Central nervous system damage during cardiac surgery assessed by 3 different biochemical markers in cerebrospinal fluid. *Scand J Thorac Cardiovasc Surg* 26(1):39-45

Stroke Therapy Academic Indurstry Roundtable (STAIR) (1999) Recommendations for standards regarding preclinical neuroprotective and restorative drug development. *Stroke* 30:2752-2758

Sullivan PG, Keller JN, Bussen WL, Scheff SW (2002) Cytochrome c release and caspase activation after traumatic brain injury. *Brain Res* 949(1-2):88-96

Wang KK, Posmantur R, Nath R, McGinnis K, Whitton M, Talanian RV, Glantz SB, Morrow JS (1998) Simultaneous degradation of alphaII- and betaII-spectrin by caspase 3 (CPP32) in apoptotic cells. *J Biol Chem* 273(35):22490-22497

Wang, KKW (2000) Calpain and caspase: can you tell the difference? *Trends Neurosci* 23(1):20-26

Westaby S, Johnsson P, Parry AJ, Blomqvist S, Solem JO, Alling C, Pillai R, Taggart DP, Grebenik C, Stahl E (1996) Serum S100 protein: a potential marker for cerebral events during cardiopulmonary bypass. *Ann Thorac Surg* 61(1):88-92

Williams AJ, Hale SL, Moffett JR, Dave JR, Elliott PJ, Adams J, Tortella FC (2003) Delayed treatment with MLN519 reduces infarction and associated neurologic deficit caused by focal ischemic brain injury in rats via antiinflammatory mechanisms involving nuclear factor-kappaB activation, gliosis, and leukocyte infiltration. *J Cereb Blood Flow Metab* 23(1):75-87

Zaremba J Losy J (2001) Early TNF-alpha levels correlate with ischaemic stroke severity. *Acta Neurol Scand* 104(5):288-295

Zemlan FP, Rosenberg WS, Luebbe PA, Campbell TA, Dean GE, Weiner NE, Cohen JA, Rudick RA, Woo D (1999) Quantification of axonal damage in traumatic brain injury: affinity purification and characterization of cerebrospinal fluid tau proteins. *J Neurochem* 72(2):741-750

Zhang C, Siman R, Xu YA, Mills AM, Frederick JR, Neumar RW (2002) Comparison of calpain and caspase activities in the adult rat brain after transient forebrain ischemia. *Neurobiol Dis* 10(3):289-305

Zhao X, Pike BR, Newcomb JK, Wang KKW, Posmantur RM, Hayes RL (1999) Maitotoxin induces calpain but not caspase-3 activation and necrotic cell death in primary septo-hippocampal cultures. *Neurochem Res* 24(3): 371-382

Figure Legends

Figure 1. Calpain and caspase-3 cleavage of non-erythroid αII-spectrin to protease-specific αII-spectrin breakdown products (SBDPs) . Illustrated are the calpain cleavages (left) in αII-spectrin that result in calpain-specific SBDPs (150 and 145 kDa) and the caspase-3 cleavages (right) in αII-spectrin that result in caspase-3-specific αII-SBDPS (150 and 120 kDa). Both proteases cleave αII-spectrin in repeat 11 near the calmodulin binding domain (CaM) to produce 150 kDa αII-SBDPs with unique N-terminal regions. A second cleavage by calpain in repeat 11 results in a calpain-specific 145 kDa αII-SBDP, while caspase-3 cleaves the protein in repeat 13 to produce a unique, apoptotic-specific 120 kDa fragment. For definitively identified cleavages, the flanking amino acids and initial N-terminal amino acid sequence is given.

Figure 2. MCAO injury causes accumulation of full-length αII-spectrin (280 kDa) protein, and calpain-mediated 145 kDa and caspase-3 mediated 120 kDa αII-SBDPs in CSF. MCAO resulted in proteolysis of constitutively expressed brain αII-spectrin (280 kDa) in ipsilateral but not contralateral cortex. The caspase-3-mediated, apoptotic-specific 120 kDa αII-SBDP was also increased in ipsilateral cortex after ischemia compared to sham-injured controls. Marked increases in the calpain-specific 145 kDa αII-SBDP were detected in brain and CSF of MCAO animals, but not in sham-injured animals, at all time points. Interestingly, while increased levels of the caspase-3-specific 120 kDa αII-SBDP were detected at all post-injury time points in the ipsilateral cortex, CSF levels were only detected at 48 hours post-injury.

Figure 3. Mean (± s.d.) arbitrary densitometric units obtained from full-length 280 kDa αII-spectrin protein and the 150 kDa, 145 kDa, and 120 kDa αII-SBDPs. Densitometric units were converted to percent of sham-injured values. Decreases in 280 kDa αII-spectrin and increases in 150 kDa, 145 kDa, and 120 kDa αII-SBDPs (ipsilateral cortex) were associated with concomitant increases of these proteins in the CSF. Note that while 150 kDa and 145 kDa SBDPs were visibly detectable in CSF on western blot at 24 hours post-injury, densitometric levels were not statistically significant due to greater variability at this time point. Similarly, although the full-length 280 kDa spectrin protein and the 120 kDa αII-SBDPs were visibly detectable in CSF, large variability in protein levels between animals resulted in inability to detect statistical significance. $^*p < 0.05$ and $^{***}p < 0.001$.

Figure 4. Mean (± s.d.) cortical vs. CSF levels of αII-spectrin (280 kDa) and αII-SBDPs (150, 145, and 120 kDa) over days post-injury. Least squares regression lines of brain and CSF spectrin and SBDP levels were plotted on the same graph. Pearson correlation coefficients for each regression line are indicated. Results indicate that parenchymal decreases in levels of native αII-spectrin (280 kDa) are associated with increases in CSF accumulation while increased parenchymal levels of calpain-mediated αII-SBDPs (150 & 145 kDa) are associated with increased CSF accumulation. On average, there were no changes in parenchymal or CSF levels of the caspase-3-mediated 120 kDa αII-SBDP across days. However, individual rats at different time points (particularly 48 hours post-injury) showed some increase in CSF levels of the 120 kDa product.

FIG 1

FIG2

1
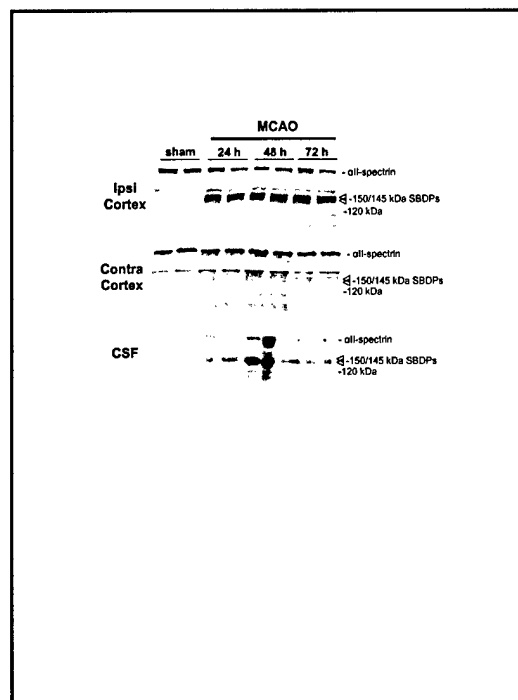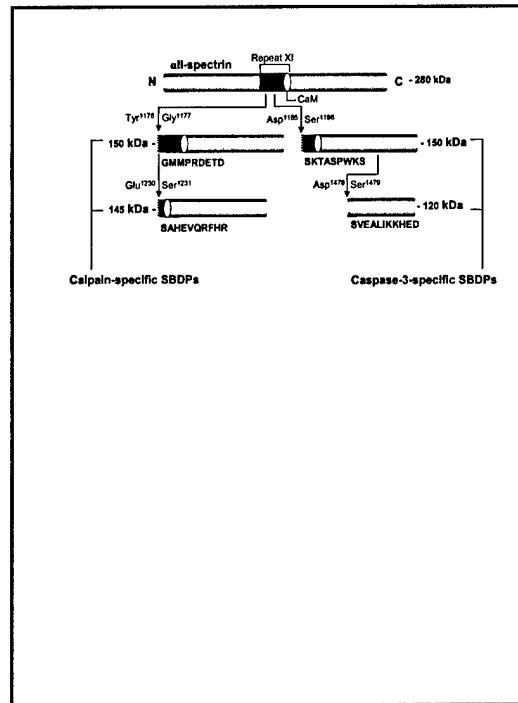
FIG 3
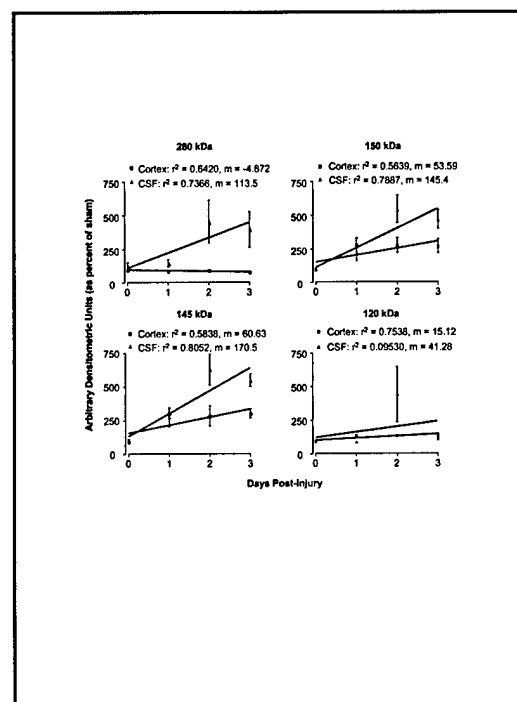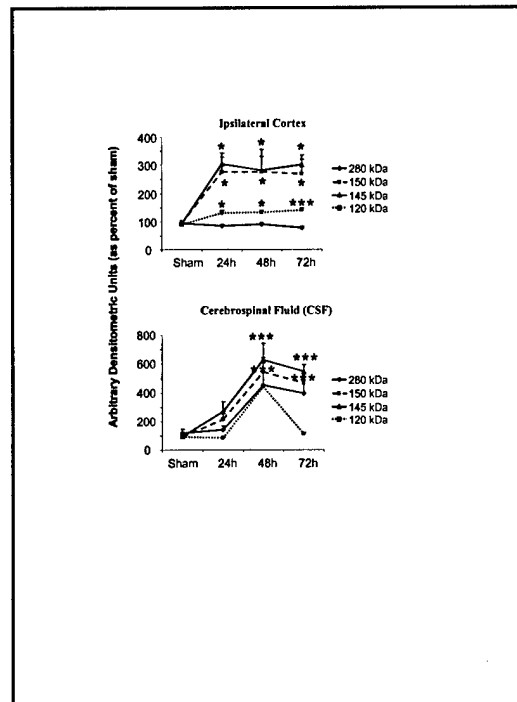
FIG 4

Biomarkers of Proteolytic Damage Following Traumatic Brain Injury

Jose A. Pineda[1,3]; Kevin K.W. Wang[1,2,4]; Ronald L. Hayes[1,2,4]

[1]Center for Traumatic Brain Injury Studies, Evelyn F. and William L. McKnight Brain Institute of The University of Florida, Gainesville.
Departments of [2]Neuroscience, [3]Pediatrics, and [4]Psychiatry, University of Florida, Gainesville.

Corresponding author:
Jose A. Pineda, MD, PICU, PO Box 100296, Gainesville, FL 32610-0296 (E-mail: pinedja@peds.ufl.edu)

The history of numerous failed clinical trials designed to identify therapeutic agents to assist in improving outcomes after traumatic brain injury points to the critical importance of understanding biochemical markers of injury. Such biomarkers should be readily accessible, provide information specific to the pathologic disruptions occurring in the central nervous system, and allow improved monitoring of the progression of secondary damage. Additionally, these biomarkers should may provide investigators a window on the individual patient's response to treatment, and should contribute to prediction of outcome. Most research on this topic to date has focused on neuron-specific enolase (NSE) and S-100 proteins but these have not proven to be satisfactory for a variety of reasons. A different approach is provided by the study of 2 important proteases, caspase-3 and calpain. This paper reports the current state of knowledge concerning caspase and calpain as specific markers of TBI, and discusses all-spectrin, a principal substrate for both caspase and calpain, as well as initial findings regarding neurofilament 68 protein (NF-68).

INTRODUCTION

Brain injury resulting from traumatic, ischemic and/or chemical etiology is a significant international health concern, representing a potentially catastrophic debilitating medical emergency with poor prognosis for long-term disability. It represents a major problem to military care, accounting for 25% of all combat casualties and is the leading cause of death (approaching 50% incidence) among wounded soldiers reaching Echelon I medical treatment (10). In civilian life, the incidence of brain injury and resultant long-term disabilities caused by traumatic insults (eg, automobile accidents, gunshots, sports) and ischemic events (eg, strokes, cerebral hemorrhage, cardiac arrest) are several orders of magnitude greater. There are more than 1 million traumatic brain injury (TBI) cases that are treated and released from an emergency department annually in the United States, resulting in more than 230 000 hospitalizations, 50 000 deaths and 80 000 disabilities. Among all age groups, the top 3 causes of TBI are motor vehicle accidents, falls and violence (1). Despite modern automobile design and injury prevention campaigns, important causes of TBI in children such as ejections from cars during traffic accidents,

have increased in recent years (111). The current estimate is that 5.3 million Americans live with a TBI-related disability. TBI is the greatest cause of death and disability in young people less than 24-years-old (2).

With the exception of supportive measures, there are currently no approved drug treatments for TBI (76). There have been a large number of clinical trials studying potential therapies for traumatic brain injury (TBI) that have resulted in negative findings with a cost of over $200 million (17, 31). Many investigators have pointed out that the absence of biochemical markers of injury could have contributed to these failures (76, 104). Unlike other organ-based diseases where rapid diagnosis employing biomarkers (usually involving blood tests) prove invaluable to guide treatment of the disease, no such rapid, definitive diagnostic tests exist for TBI to provide physicians with quantifiable neurochemical markers to help determine the seriousness of the injury, the anatomical and cellular pathology of the injury, and to guide implementation of appropriate triage and medical management.

CRITERIA FOR BIOCHEMICAL/ SURROGATE MARKERS

In the course of research on biomarkers, our laboratories have developed criteria for biomarker development. Useful biomarkers should employ readily accessible biological material such as CSF or blood (CSF is routinely accessible in severely injured TBI patients), predict the magnitude of injury and resulting functional deficits and possess high sensitivity and specificity, have a rapid appearance in blood and be released in a time-locked sequence after injury. Ideally, biomarkers should employ biological substrates unique to the CNS and provide information on injury mechanisms, a criterion often used to distinguish biochemical markers from surrogate markers of injury, which usually do not provide information on injury mechanisms. Potential gender and age related differences on biomarker profiles are also important and should be taken into account when developing useful biochemical markers (43).

USES OF BIOMARKERS

Biomarkers would have important applications in diagnosis, prognosis and clinical research of brain injuries. Simple, rapid diagnostic tools will immensely facilitate allocation of the major medical resources required to treat TBI and other brain injuries. Accurate diagnosis in acute care environments can significantly enhance decisions about patient management including decisions whether to admit or discharge, or administer other time consuming and expensive tests including computer tomography (CT) and magnetic resonance imaging (MRI) scans. Biomarkers could have important prognostic functions especially in patients suffering mild TBI, which make up an estimated 80% of the 2.5 to 6.5 million individuals who suffer from lifelong impairment as a result of TBI (3, 82). Ac-

curate identification of these patients could facilitate development of guidelines for return to duty, work or sports activities and also provide opportunities for counseling of patients suffering from these deficits. Biomarkers could provide major opportunities for the conduct of clinical research including confirmation of injury mechanism(s) and drug target identification. The temporal profile of changes in biomarkers could guide timing of treatment and assist in monitoring the response to therapy and intervention. Finally, biomarkers could provide a clinical trial outcome measure obtainable much more cheaply and readily than conventional neurological assessments, thereby significantly reducing the risks and costs of human clinical trials. Relevant, easily available biomarkers are needed in order to maximize chances of success in developing long awaited effective drugs for TBI (76).

CURRENT STATUS OF RESEARCH ON MARKERS OF TRAUMATIC BRAIN INJURY

Analysis of specific biochemical markers has provided useful information on the mechanism and diagnosis of specific organ dysfunction in humans (112). However, although analysis of cerebrospinal fluid, cerebral microdialysis samples, and brain tissue specimens has provided insight into the mechanisms of brain injury (61, 63), there are no biomarkers of proven clinical utility for TBI.

TBI is difficult to assess and clinical examinations are of restricted value during the first hours and days after injury. Conventional diagnoses of TBI are based on neuroimaging techniques such as CT scanning, MRI and single-photon emission CT scanning (46, 58, 72). CT scanning has low sensitivity to detect diffuse brain damage, and the availability of MRI is limited (60, 64). Single-photon emission CT scanning detects regional blood-flow abnormalities not necessarily related to structural damage.

A recent review of biomarkers of TBI highlighted the need for biomarker development (43). The most studied potential biochemical markers for TBI include creatine kinase (CK), glial fibrillary acidic protein (GFAP), lactate dehydrogenase (LDH), myelin basic protein (MBP), neuron-specific enolase (NSE) and S-100 proteins. The bulk of research in TBI has

focused on NSE and S-100β. The specificity of NSE for brain is high (49), sex- and age-related variability is low (30, 51, 74, 85, 97, 120, 121, 134), and NSE is rapidly detectible in serum after TBI (129). However, studies relating NSE serum levels to admission GCS in patients with severe TBI show conflicting results. Similar data have been reported concerning relationships with CT scan findings, ICP and long-term outcomes. In mild TBI, NSE failed to separate patients from controls (12, 44, 108, 132). Thus, NSE is predominantly used as a marker for tumors (24). NSE is also released in the blood by hemolysis, which could be a major source of error (24).

The S-100 protein family now consists of 19 members, of which S-100β is the one viewed as a marker of brain damage (49, 65), although it is present in other tissues such as adipocytes and chondrocytes (40). Investigators have reported that S-100β serum levels correlate to GCS scores, neuroradiologic findings at admission and long-term outcomes (98, 99, 130). However, investigators have recently raised questions about the utility of S-100β reporting that high serum levels of S-100β are detectible in trauma patients not having head injuries, a factor not adequately controlled for in earlier studies (4). In addition, serum levels of S-100β following mild TBI do not show strong correlations with neuropsychological outcome (107). Research in this area continues and recent reports have indicated the potential utility of measures of blood GFAP (71), spinal fluid interleukin-6 (115) and cleaved tau protein in serum (45, 114) and spinal fluid (136) following brain injury.

Investigators have also generally recognized the need for more objective assessments of outcome following stroke, including biochemical markers (29, 68). The approval of tPA as a treatment for acute stroke has additionally highlighted the potential utility of biochemical markers. Use of tPA may be hindered by diagnostic concerns because neurological deficits accompanying stroke can mimic those seen during transient ischemic attacks, complex migraine, space-occupying lesions and post-ictal paralysis. A reliable biochemical marker might give assurance to physicians considering administering thrombolytic agents for acute stroke (41, 50).

Previously reported biomarkers of cerebral ischemia include NSE, brain specific creatine kinase enzyme (CPK-BB), S-100β and inflammatory cytokines such as IL-6 (88). NSE and S-100β have been the most studied. After cardiac arrest, NSE elevations in serum and CSF have been correlated with neurological recovery (28, 67, 106). Serum and CSF NSE values were reported to be elevated in rodent models of focal ischemia in proportion to the eventual infarct volume (26, 27, 42). In clinical trials, peak serum NSE values also predicted infarct volumes as shown by CT. Correlating serum NSE values with functional outcome was less successful (26, 27, 70), possibly because functional neurological deficit is influenced as much by location of brain injury as by infarct size (70). S-100β protein has been studied most extensively for characterization of ischemic injuries after cardiac surgery, and several reports have documented post-operative serum elevations (5, 113, 128). However, many of these reports do not include careful studies of neurological outcome, and several investigators have recently criticized the diagnostic utility of S-100β during cardiac surgery (4).

PROTEOLYTIC DAMAGE AND THE PATHOBIOLOGY OF TRAUMATIC BRAIN INJURY

After TBI, brain cells can deteriorate by more than one pathway, and many genes and proteins may be involved. Programmed cell death is an evolutionarily conserved form of cell suicide that occurs widely throughout development (15). This type of cell death often has the morphological appearance of apoptosis (119). Apoptosis occurs following TBI in animals (22, 59, 131) and humans (18, 19). Studies of apoptosis pose special challenges since there are multiple apoptotic pathways, and apoptosis is extremely sensitive to a number of variables including injury type and magnitude (13, 16, 100), cell type (38, 57) and stimulation/antagonism of specific receptors (16, 21, 25, 38, 39, 48).

The molecular events occurring after TBI are just beginning to be understood. Elevated neuronal calcium levels activate a number of calcium-dependent enzymes such as phospholipases (83), kinases (133), phosphatases (75), and proteases (7, 80), all of which can modulate post-TBI cytoskel-

etal protein loss. Caspase-3 is a member of the caspase family of cysteine proteases. Activated caspase-3 has many cellular targets that, when interrupted and/or activated, produce the morphologic features of apoptosis (20). Calpains are calcium-activated, neutral cysteine proteases with relative selectivity for proteolysis of a subset of cellular proteins. Calpain activation has been implicated in different models of apoptosis and in different cell types, including neurons (92). Understanding of the contributions of calpains and caspases to cell injury/death following TBI may have important diagnostic and therapeutic implications.

CONTRIBUTIONS OF CASPASE-3 AND CALPAIN TO CELL DEATH FOLLOWING TRAUMATIC BRAIN INJURY

Numerous studies from our own (8, 90, 92) and other laboratories (32, 36, 73) have provided evidence that the caspase family of cysteine proteases is an important intracellular effector of apoptosis in various cell lines and apoptotic models. Caspase-3-like proteases have been shown to cleave a variety of cytoplasmic, nuclear and cytoskeletal proteins during apoptosis, including αII-spectrin (69, 77, 78, 122), poly(ADP-ribose) polymerase (PARP: 51) and others (52-57). In vitro studies in our laboratories using a model of stretch injury have demonstrated caspase-3 processing of α-spectrin to the apoptotic-linked 120-kDa fragment 24 hours after moderate, but not mild or severe injury (8). In vivo studies have provided evidence of caspase-3 activation following TBI. First, Clark et al demonstrated cleavage of capsase-3 to its p18 and p12 subunits in humans (19). Yakovlev et al reported that TBI increased caspase-3, but not caspase-1 activity (131). Caspase-3 inhibition reduced DNA fragmentation and TUNEL staining and improved behavioral outcome. We have also concurrently examined caspase-3 and calpain activation after TBI. Distinct regional and temporal patterns of calpain/caspase-3 processing of αII-spectrin in brain regions ipsilateral to the site of injury after TBI have been observed. Caspase-3-mediated breakdown products (BDP's) to αII-spectrin were absent in the cortex but showed significant increases in hippocampus and striatum early after TBI (91). Immunohistochemical examinations revealed increased expression of the proteolytically active subunit

of caspase-3, p18, in neurons, astrocytes, and oligodendrocytes from 6 to 72 hours following controlled cortical impact injury. Moreover, concurrent assessment of nuclear histopathology using hematoxylin identified p18-immunopositive cells exhibiting apoptotic-like morphological profiles in the cortex ipsilateral to the injury site (8).

Calpains are Ca^{2+} activated cysteine proteases that have been implicated in a variety of neuropathological conditions (55, 127). Intracellular substrates of activated calpain include cytoskeletal proteins, calmodulin-binding proteins, enzymes involved in signal transduction, membrane proteins and transcription factors (110, 118, 126). While calpain activation has historically been associated with necrotic cell death (81), calpain activation has also been implicated in different models of apoptosis and in different cell types, including neurons (9, 52, 77, 117, 123). Research in our own and other laboratories have documented calpain activation following TBI in vivo (55). TBI results in altered Ca^{2+} homeostasis (135) and activates several Ca^{2+}-dependent enzymes including the calpains. Overactivation of calpains occurs in many neurodegenerative diseases and injuries to the CNS (6, 55, 127). Increased calpain activity following TBI has been inferred by a variety of techniques (54, 80, 93, 96), including protection by calpain inhibitors (94, 109).

Pathological calpain activation is believed to occur when intracellular free calcium levels surpass a certain threshold. Importantly, increases in free calcium via voltage and receptor gated calcium channels have been reported in CNS trauma in vivo (21, 48, 56). Calpains are located throughout the neuron, in somatodendritic regions and in axons (57). Calpain may also be a constituent of myelin (116). Therefore, pathological calpain activity and subsequent substrate proteolysis can have profound effects on neuronal structure and function.

Cytoskeletal alterations after experimental brain injury have pointed to the likelihood of calpain mediated proteolysis. Preferred substrates for calpains include the cytoskeletal protein spectrin (47, 66), microtubule associated protein-2 (MAP-2)(34), and neurofilament proteins (22, 23, 84, 105). Increased degradation of MAP2 (33, 131), the neurofilament triplet pro-

teins (53, 86) and spectrin (79) have been reported in cerebral ischemia. In addition, loss of MAP-2 (62), neurofilament 68 (NF 68) and neurofilament 200 (NF 200)(93-95) have been reported following TBI in vivo. Additional evidence that calpain is activated in neurons following experimental brain injury has been provided by the use of antibodies which bind specifically to calpain mediated BDP's of cytoskeletal proteins in models of TBI (80).

αII-SPECTRIN DEGRADATION-A PROTOTYPE BIOMARKER

Our research program to develop biomarkers for TBI has focused on α-spectrin degradation as a prototypical biochemical marker (35, 103). αII-spectrin (280 kDa) is the major structural component of the cortical membrane cytoskeleton and is particularly abundant in axons and presynaptic terminals (37, 102). Importantly, αII-spectrin is a major substrate for both calpain and caspase-3 cysteine proteases (125). Our laboratory has provided considerable evidence that αII-spectrin is processed by calpains and/or caspase-3 to signature cleavage products in vivo after TBI (8, 14, 80, 91) and also in vitro after mechanical stretch injury (90). Calpain produces 2 major αII-spectrin breakdown products of 150 kDa and 145 kDa (SBDP150 and SBDP145) in a sequential manner. On the other hand, caspase-3 initially produces a 150 kDa SBDP that is further cleaved into a 120 kDa fragment (SBDP120)(124). Immunoblots of αII-spectrin degradation thus provide concurrent information on the activation of calpain and caspase-3, potentially important regulators of cell death following TBI. The calcium sensitivity and low basal levels of calpain optimize its utility as a marker of cell injury. Although not found in erythrocytes and thus robust to confounding by blood contamination, αII-spectrin is not specific to the CNS (89). Following injury, native αII-spectrin protein was decreased in brain tissue and increased in CSF from 24 hours to 72 hours after injury. Calpain-specific breakdown products increased in both brain and CSF after injury. Caspase-3-specific breakdown products increased in some animals, but to a lesser degree (89).

Recent efforts in our laboratory have expanded our studies of the potential clinical utility of αII-spectrin degradation as a

2 hours post-TBI

SHAM 1.0 MM 1.6 MM

— αll-spectrin
◁-150/145 kDa (Cortex)

— αll-spectrin
◁-150/145 kDa (CSF)

Cortex
**
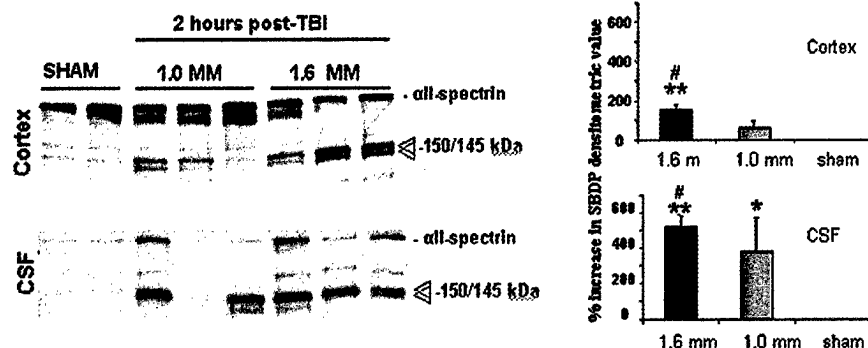1.6 m 1.0 mm sham

** *
CSF
1.6 mm 1.0 mm sham

Figure 1. *Accumulation of calpain-specific SBDPs is sensitive to injury magnitude after controlled cortical impact.* Animals were injured using a model of controlled cortical impact at two magnitudes of injury. Accumulation of brain cortex and spinal fluid levels of αll-SBDP were measured by densitometric analysis at 2 hours post-injury. The 1.6 mm injury magnitude produced the highest levels of αll-SBDP accumulation in cortex and CSF compared to 1.0 mm injury and to sham-injured controls. However, statistical significance ($p<0.05$) between 1.6 mm and 1.0 mm injuries was only achieved at 2 hours but not at 6 or 24 hours post-injury (data not shown). This finding could indicate a critical window for discriminating injury magnitude using αll-SBDP as a biomarker. CSF levels of αll-SBDP were greater in CSF than in cortex, particularly for the 1.6 mm injury. This most likely reflects a greater ratio of SBDP to total protein in CSF relative to cortex and indicates that low abundance proteins may be more easily detected in CSF after brain injury (n = 6 per group).

Control T0 T0.5 T1 T2 T3 T7 MWM

◁ 250kDa
◁ 150/145kDa
◁ 100kDa
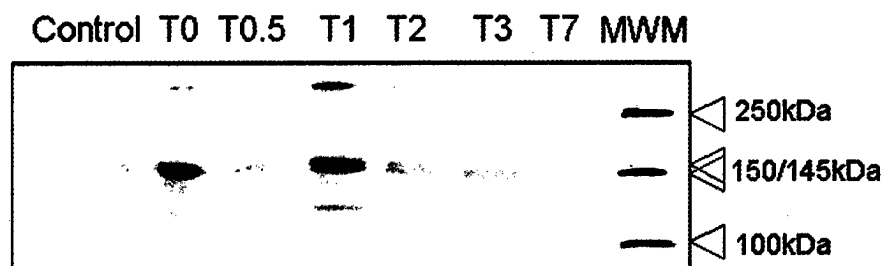
Figure 2. Western blot analysis of cerebrospinal fluid (CSF) samples from a 9-year-old patient diagnosed with severe head injury αll-spectrin breakdown products reflecting caspase-3 (150kDa and 120kDa bands) and calpain (150kDa and 145kDa bands) activity were identified as early as 12 hours after injury and persisted for at least 3 days after injury. Increased protein expression one day after injury may reflect clinical evidence of increased brain swelling and intracranial hypertension. CSF from a child with chronic hydrocephalus and no acute brain injury was used as control. T0 = admission to the intensive care unit; T0.5 = 12 hours after injury; T1 = 24 hours after injury; T2: 2 days after injury; T3: 3 days after injury; T7 = 7 days after injury; MWM = molecular weight marker.

Figure 3. *Development of biomarkers of protease activity.* Brain injury leads to activation of proteases after traumatic brain injury. Proteolytic processing of cytoskeletal proteins (i.e. αll-spectrin) leads to accumulation of both the parent protein as well as signature breakdown products (BDP's). Initial characterization will most likely require analysis of cerebrospinal fluid (CSF). Antibodies will then be developed so that an easily accessible biomarker of protease activity is available for sampling from peripheral blood.

biomarker for TBI (Figure 1). These studies focused on determining whether changes in αII-spectrin breakdown products in CSF could be useful indicators of the magnitude of brain injury. Our studies have provided the first evidence that protein degradation of a structural cytoskeletal protein can be a reliable marker of CNS injury. Equally important, our data suggests that there may be a critical period following injury during which these markers predict injury magnitude. Our laboratory has also provided the first human data on the potential utility of αII-spectrin as a biomarker (Figure 2). These preliminary studies indicate that αII-spectrin degradation is also detected in brain injury patients but not in chronic hydrocephalic controls. Equally important, our data suggests that secondary increases

in levels of breakdown products in CSF may reflect secondary deterioration in the clinical status of the patient. Thus, biomarkers such as αII-spectrin degradation may provide useful information for management of head injury patients in critical care environments. However, it is not known whether BDP's and other biomarkers that discriminate magnitudes of injury at the biochemical level (ie, magnitude differences in CSF/serum levels of a biomarker) will be useful as predictors of clinically relevant measures of outcome. That is, 2 different injury magnitudes may produce significantly different biochemical responses in the brain that are discernable in CSF or serum, but these same injury magnitudes may not result in functionally different behavioral, pathological, or other
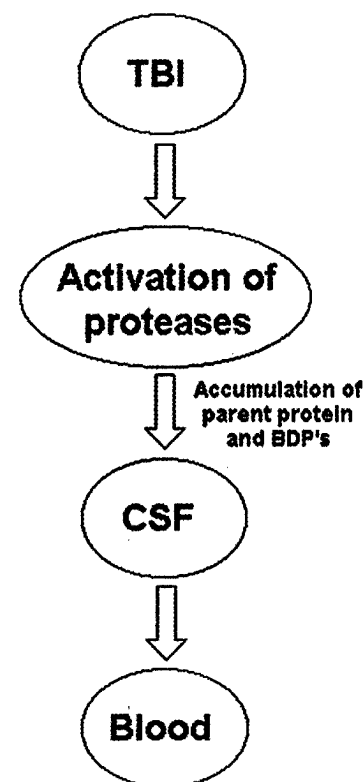
clinical outcome measures. Thus, biomarkers that do not correlate with clinically relevant outcome measures will not be useful for assessment of functional ability, functional recovery, or for gauging effects of therapy on outcome. In addition, preliminary results from our laboratories suggest that there is a spontaneous susceptibility of cytoskeletal protein degradation by calpain in aging rats (11). These findings emphasize the importance of accounting for multiple clinical variables including, but not limited to, age when evaluating the clinical utility of biomarkers of brain injury.

ADDITIONAL CYTOSKELETAL PROTEINS WITH POTENTIAL UTILITY AS BIOMARKERS

Initial research focused on proteolytic processing of cytoskeletal proteins such as lower molecular weight neurofilament 68 protein (NF-68) highlights their potential to provide useful information on activ-

ity of specific proteases such as μ-calpain and m-calpain. Importantly, 2-D gel electrophoresis studies have suggested that dephosphorylation of NF-68 may be associated with NF protein loss following TBI, a post translational modification that could have significance for biomarker development (80, 96). This important biomarker could provide important information on the pathophysiology of both dendritic and axonal damage after TBI (95). Importantly, NF-68 has been used to quantify axonal injury in closed head injury models (101). Since diffuse axonal injury (DAI) is presently considered one of the most common types of primary lesions in patients with severe closed head injury (87), a biomarker that provides information on axonal injury could potentially have clinical utility.

FUTURE DIRECTIONS

The pathology of TBI is extremely complex. As our understanding of the numerous biochemical cascades involved continues to evolve, sophisticated diagnostic tools such as biomarkers will be developed (Figure 3). Ideal biomarkers will provide information on the pathobiology of TBI and facilitate better stratification of patients by the severity of their injury, better monitoring of the progression of secondary damage, response to treatment/intervention, and prediction of outcome. Although the initial characterization of biomarkers will be mainly based on spinal fluid analysis, methods for measurement of such biomarkers in blood (plasma or serum) will be developed. The development of accessible and reliable biomarkers is likely to change the way clinical studies of head injury are conducted, resulting in more mechanism driven, optimally timed therapies.

ACKNOWLEDGMENTS

REFERENCES

1. (1999) Consensus conference. Rehabilitation of persons with traumatic brain injury. NIH Consensus Development Panel on Rehabilitation of Persons With Traumatic Brain Injury. *Jama* 282:974-983.

2. (2000) TBI State Demonstration Grants. *J Head Trauma Rehabil* 15:750-760.

3. Alexander MP (1995) Mild traumatic brain injury: pathophysiology, natural history, and clinical management. *Neurology* 45:1253-1260.

4. Anderson RE HL, Nilsson O, Dijlai-Merzoug R, Settergen G (2001) High serum S100B levels for trauma patients without head injuries. *Neurosurgery* 49:1272-1273.

5. Astudillo R, Van der Linden J, Radegran K, Hansson LO, Aberg B (1996) Elevated serum levels of S-100 after deep hypothermic arrest correlate with duration of circulatory arrest. *Eur J Cardiothorac Surg* 10:1107-1112; discussion 1113.

6. Bartus RT, Elliott PJ, Hayward NJ, Dean RL, Harbeson S, Straub JA, Li Z, Powers JC (1995) Calpain as a novel target for treating acute neurodegenerative disorders. *Neurol Res* 17:249-258.

7. Bartus RT, Hayward NJ, Elliott PJ, Sawyer SD, Baker KL, Dean RL, Akiyama A, Straub JA, Harbeson SL, Li Z (1994) Calpain inhibitor AK295 protects neurons from focal brain ischemia. Effects of postocclusion intra-arterial administration. *Stroke* 25:2265-2270.

8. Beer R, Franz G, Srinivasan A, Hayes RL, Pike BR, Newcomb JK, Zhao X, Schmutzhard E, Poewe W, Kampfl A (2000) Temporal profile and cell subtype distribution of activated caspase-3 following experimental traumatic brain injury. *J Neurochem* 75:1264-1273.

9. Behrens MM, Martinez JL, Moratilla C, Renart J (1995) Apoptosis induced by protein kinase C inhibition in a neuroblastoma cell line. *Cell Growth Differ* 6:1375-1380.

10. Bellamy R (1984) The causes of death in conventional land warfates: implications for combat casualty research. *Military Medicine* 149:55-62.

11. Bernath ED, Durham R, Duddy S, Wang KKW (In Preparation) Spontaneous cytoskeletal protein proteolysis in aged Wistar rat brains.

12. Bertrand R, Solary E, O'Connor P, Kohn KW, Pommier Y (1994) Induction of a common pathway of apoptosis by staurosporine. *Exp Cell Res* 211:314-321.

13. Bonfoco E, Krainc D, Ankarcrona M, Nicotera P, Lipton SA (1995) Apoptosis and necrosis: two distinct events induced, respectively, by mild and intense insults with N-methyl-D-aspartate or nitric oxide/superoxide in cortical cell cultures. *Proc Natl Acad Sci U S A* 92:7162-7166.

14. Buki A, Okonkwo DO, Wang KK, Povlishock JT (2000) Cytochrome c release and caspase activation in traumatic axonal injury. *J Neurosci* 20:2825-2834.

15. Chang LK, Putcha GV, Deshmukh M, Johnson EM (2002) Mitochondrial involvement in the point of no return in neuronal apoptosis. *Biochimie* 84:223-231.

16. Choi DW (1996) Ischemia-induced neuronal apoptosis. *Curr Opin Neurobiol* 6:667-672.

17. Choi SC Bullock R (2001) Design and statistical issues in multicenter trials of severe head injury. *Neurol Res* 23:190-192.

18. Clark RS, Kochanek PM, Adelson PD, Bell MJ, Carcillo JA, Chen M, Wisniewski SR, Janesko K, Whalen MJ, Graham SH (2000) Increases in bcl-2 protein in cerebrospinal fluid and evidence for programmed cell death in infants and children after severe traumatic brain injury. *J Pediatr* 137:197-204.

19. Clark RS, Kochanek PM, Chen M, Watkins SC, Marion DW, Chen J, Hamilton RL, Loeffert JE, Graham SH (1999) Increases in Bcl-2 and cleavage of caspase-1 and caspase-3 in human brain after head injury. *Faseb J* 13:813-821.

20. Clark RS, Kochanek PM, Watkins SC, Chen M, Dixon CE, Seidberg NA, Melick J, Loeffert JE, Nathaniel PD, Jin KL, Graham SH (2000) Caspase-3 mediated neuronal death after traumatic brain injury in rats. *J Neurochem* 74:740-753.

21. Cohen GM (1997) Caspases: the executioners of apoptosis. *Biochem J* 326:1-16.

22. Colicos MA, Dash PK (1996) Apoptotic morphology of dentate gyrus granule cells following experimental cortical impact injury in rats: possible role in spatial memory deficits. *Brain Res* 739:120-131.

23. Conti AC, Raghupathi R, Trojanowski JQ, McIntosh TK (1998) Experimental brain injury induces regionally distinct apoptosis during the acute and delayed post-traumatic period. *J Neurosci* 18:5663-5672.

24. Cooper E (1994) Neuron-specific enolase. *Int J Biol Markers* 4:205-210.

25. Copin JC, Li Y, Reola L, Chan PH (1998) Trolox and 6,7-dinitroquinoxaline-2,3-dione prevent necrosis but not apoptosis in cultured neurons subjected to oxygen deprivation. *Brain Res* 784:25-36.

26. Cunningham RT, Watt M, Winder J, McKinstry S, Lawson JT, Johnston CF, Hawkins SA, Buchanan KD (1996) Serum neurone-specific enolase as an indicator of stroke volume. *Eur J Clin Invest* 26:298-303.

27. Cunningham RT, Young IS, Winder J, O'Kane MJ, McKinstry S, Johnston CF, Dolan OM, Hawkins SA, Buchanan KD (1991) Serum neurone specific enolase (NSE) levels as an indicator of neuronal damage in patients with cerebral infarction. *Eur J Clin Invest* 21:497-500.

28. Dauberschmidt R, Zinsmeyer J, Mrochen H, Meyer M (1991) Changes of neuron-specific enolase concentration in plasma after cardiac arrest and resuscitation. *Mol Chem Neuropathol* 14:237-245.

29. Dirnagl U, Iadecola C, Moskowitz MA (1999) Pathobiology of ischaemic stroke: an integrated view. *Trends Neurosci* 22:391-397.

30. Donato R (1999) Functional roles of S100 proteins, calcium-binding proteins of the EF-hand type. *Biochim Biophys Acta* 1450:191-231.

31. Egon MR, Doppenberg SCC, Bullock R (1997) Clinical trials in TBI, what can we learn from previous studies. *Ann NY Acad Sci* 825:305-322.

32. Eldadah BA, Yakovlev AG, Faden AI (1997) The role of CED-3-related cysteine proteases in apoptosis of cerebellar granule cells. *J Neurosci* 17:6105-6113.

33. Ellis EF, McKinney JS, Willoughby KA, Liang S, Povlishock JT (1995) A new model for rapid stretch-induced injury of cells in culture: characterization of the model using astrocytes. *J Neurotrauma* 12:325-339.

34. Fischer I, Romano-Clarke G, Grynspan F (1991) Calpain-mediated proteolysis of microtubule associated proteins MAP1B and MAP2 in developing brain. *Neurochem Res* 16:891-898.

35. Flint JP, Pike BR , Hayes RL, Moffett JR, Dave JR, X.-CM Lu, and Tortella F (2002 In Press) Accumulation of calpain and caspase-3 cleaved alpha-II spectrin breakdown products in CSF after middle cerebral artery occulsion in rats. *J Neurotrauma* (in press).

36. Fraser A, Evan G (1996) A license to kill. *Cell* 85:781-784.

37. Goodman SR, Zimmer WE, Clark MB, Zagon IS, Barker JE, Bloom ML (1995) Brain spectrin: of mice and men. *Brain Res Bull* 36:593-606.

38. Gottron FJ, Ying HS, Choi DW (1997) Caspase inhibition selectively reduces the apoptotic component of oxygen-glucose deprivation-induced cortical neuronal cell death. *Mol Cell Neurosci* 9: 159-169.

39. Gwag BJ, Lobner D, Koh JY, Wie MB, Choi DW (1995) Blockade of glutamate receptors unmasks neuronal apoptosis after oxygen-glucose deprivation in vitro. *Neuroscience* 68:615-619.

40. Haimoto H, Hosoda S, Kato K (1987) Differential distribution of immunoreactive S100-alpha and S100-beta proteins in normal nonnervous human tissues. *Lab Invest* 57:489-498.

41. Hill MD, Jackowski G, Bayer N, Lawrence M, Jaeschke R (2000) Biochemical markers in acute ischemic stroke. *Cmaj* 162:1139-1140.

42. Horn M, Seger F, Schlote W (1995) Neuron-specific enolase in gerbil brain and serum after transient cerebral ischemia. *Stroke* 26:290-296; discussion 296-297.

43. Ingebrigtsen T, Romner B (2002) Biochemical Serum Markers of TBI. The Journal of Trauma Injury, Infection, and Critical Care, 52, 798-808.

44. Ingebrigtsen T Romner B, Trumpy JH (1997) Management of minor head injury: the value of early CT and serum protein S-100 measurements. *J Clin Neurosci* 4:29-33.

45. Irazuzta JE, de Courten-Myers G, Zemlan FP, Bekkedal MY, Rossi J, 3rd (2001) Serum cleaved Tau protein and neurobehavioral battery of tests as markers of brain injury in experimental bacterial meningitis. *Brain Res* 913:95-105.

46. Jacobs A, Put E, Ingels M, Put T, Bossuyt A (1996) One-year follow-up of technetium-99m-HMPAO SPECT in mild head injury. *J Nucl Med* 37: 1605-1609.

47. Jenkins LW, Moszynski K, Lyeth BG, Lewelt W, DeWitt DS, Allen A, Dixon CE, Povlishock JT, Majewski TJ, Clifton GL, Young HF, Becker DP, Hayes RL (1989) Increased vulnerability of the mildly traumatized rat brain to cerebral ischemia: the use of controlled secondary ischemia as a research tool to identify common or different mechanisms contributing to mechanical and ischemic brain injury. *Brain Res* 477:211-224.

48. Johnson EM, Jr., Greenlund LJ, Akins PT, Hsu CY (1995) Neuronal apoptosis: current understanding of molecular mechanisms and potential role in ischemic brain injury. *J Neurotrauma* 12:843-852.

49. Johnsson P (1996) Markers of cerebral ischemia after cardiac surgery. *J Cardiothorac Vasc Anesth* 10:120-126.

50. Jonas S, Aiyagari V, Vieira D, Figueroa M (2001) The failure of neuronal protective agents versus the success of thrombolysis in the treatment of ischemic stroke. The predictive value of animal models. *Ann N Y Acad Sci* 939:257-267.

51. Jonsson H, Johnsson P, Hoglund P, Alling C, Blomquist S (2000) Elimination of S100B and renal function after cardiac surgery. *J Cardiothorac Vasc Anesth* 14:698-701.

52. Jordan J, Galindo MF, Miller RJ (1997) Role of calpain- and interleukin-1 beta converting enzyme-like proteases in the beta-amyloid-induced death of rat hippocampal neurons in culture. *J Neurochem* 68:1612-1621.

53. Kaku Y, Yonekawa Y, Tsukahara T, Ogata N, Kimura T, Taniguchi T (1993) Alterations of a 200 kDa neurofilament in the rat hippocampus after forebrain ischemia. *J Cereb Blood Flow Metab* 13: 402-408.

54. Kampfl A, Posmantur R, Nixon R, Grynspan F, Zhao X, Liu SJ, Newcomb JK, Clifton GL, Hayes RL (1996) Mu-calpain activation and calpain-mediated cytoskeletal proteolysis following traumatic brain injury. *J Neurochem* 67:1575-1583.

55. Kampfl A, Posmantur RM, Zhao X, Schmutzhard E, Clifton GL, Hayes RL (1997) Mechanisms of calpain proteolysis following traumatic brain injury: implications for pathology and therapy: implications for pathology and therapy: a review and update. *J Neurotrauma* 14:121-134.

56. Kampfl A, Whitson JS, Zhao X, Posmantur R, Clifton GL, Hayes RL (1995) Calpain inhibitors reduce depolarization induced loss of tau protein in primary septo-hippocampal cultures. *Neurosci Lett* 194:149-152.

57. Kampfl A, Zhao X, Whitson JS, Posmantur R, Dixon CE, Yang K, Clifton GL, Hayes RL (1996) Calpain inhibitors protect against depolarization-induced neurofilament protein loss of septo-hippocampal neurons in culture. *Eur J Neurosci* 8:344-352.

58. Kant R, Smith-Seemiller L, Isaac G, Duffy J (1997) Tc-HMPAO SPECT in persistent post-concussion syndrome after mild head injury: comparison with MRI/CT. *Brain Inj* 11:115-124.

59. Kaya SS, Mahmood A, Li Y, Yavuz E, Goksel M, Chopp M (1999) Apoptosis and expression of p53 response proteins and cyclin D1 after cortical impact in rat brain. *Brain Res* 818:23-33.

60. Kesler SR, Adams HF, Bigler ED (2000) SPECT, MR and quantitative MR imaging: correlates with neuropsychological and psychological outcome in traumatic brain injury. *Brain Inj* 14:851-857.

61. Kochanek PM, Clark RS, Ruppel RA, Dixon CE (2001) Cerebral resuscitation after traumatic brain injury and cardiopulmonary arrest in infants and children in the new millennium. *Pediatr Clin North Am* 48:661-681.

62. Lammie GA, Piper IR, Thomson D, Brannan F (1999) Neuropathologic characterization of a rodent model of closed head injury--addition of clinically relevant secondary insults does not significantly potentiate brain damage. *J Neurotrauma* 16:603-615.

63. Laskowitz DT, Grocott HP, Hsia A, Copeland KR (1998) Serum Markers of Cerebral Ischemia. *J Stroke Cerebro Dis* 7:234-241.

64. Levi L, Guilburd JN, Lemberger A, Soustiel JF, Feinsod M (1990) Diffuse axonal injury: analysis of 100 patients with radiological signs. *Neurosurgery* 27:429-432.

65. Leviton A, Dammann O (2002) Brain damage markers in children. Neurobiological and clinical aspects. *Acta Paediatr* 91:9-13.

66. Lyeth BG, Jenkins LW, Hamm RJ, Dixon CE, Phillips LL, Clifton GL, Young HF, Hayes RL (1990) Prolonged memory impairment in the absence of hippocampal cell death following traumatic brain injury in the rat. *Brain Res* 526:249-258.

67. Martens P (1996) Serum neuron-specific enolase as a prognostic marker for irreversible brain damage in comatose cardiac arrest surviviors. *Acad Emerg Med* 3:126-131.

68. Martens P, Raabe A, Johnsson P (1998) Serum S-100 and neuron-specific enolase for prediction of regaining consciousness after global cerebral ischemia. *Stroke* 29:2363-2366.

69. Martin SJ, O'Brien GA, Nishioka WK, McGahon AJ, Mahboubi A, Saido TC, Green DR (1995) Proteolysis of fodrin (non-erythroid spectrin) during apoptosis. *J Biol Chem* 270:6425-6428.

70. Missler U, Wiesmann M, Friedrich C, Kaps M (1997) S-100 protein and neuron-specific enolase concentrations in blood as indicators of infarction volume and prognosis in acute ischemic stroke. *Stroke* 28:1956-1960.

71. Missler U, Wiesmann M, Wittmann G, Magerkurth O, Hagenstrom H (1999) Measurement of glial fibrillary acidic protein in human blood: analytical method and preliminary clinical results. *Clin Chem* 45:138-141.

72. Mitchener A, Wyper DJ, Patterson J, Hadley DM, Wilson JT, Scott LC, Jones M, Teasdale GM (1997) SPECT, CT, and MRI in head injury: acute abnormalities followed up at six months. *J Neurol Neurosurg Psychiatry* 62:633-636.

73. Miura M, Zhu H, Rotello R, Hartwieg EA, Yuan J (1993) Induction of apoptosis in fibroblasts by IL-1 beta-converting enzyme, a mammalian homolog of the C. elegans cell death gene ced-3. *Cell* 75:653-660.

74. Moore B (1965) A soluble protein characteristic of the nervous system. *Biochem Biophys Res Commun* 19:739-744.

75. Morioka M, Fukunaga K, Yasugawa S, Nagahiro S, Ushio Y, Miyamoto E (1992) Regional and temporal alterations in Ca2+/calmodulin-dependent protein kinase II and calcineurin in the hippocampus of rat brain after transient forebrain ischemia. *J Neurochem* 58:1798-1809.

76. Narayan RK, Michel ME, Ansell B, Baethmann A, Biegon A, Bracken MB, Bullock MR, Choi SC, Clifton GL, Contant CF, Coplin WM et al (2002) Clinical trials in head injury. *J Neurotrauma* 19:503-557.

77. Nath R, Raser KJ, McGinnis K, Nadimpalli R, Stafford D, Wang KK (1996) Effects of ICE-like protease and calpain inhibitors on neuronal apoptosis. *Neuroreport* 8:249-255.

78. Nath R, Raser KJ, Stafford D, Hajimohammadreza I, Posner A, Allen H, Talanian RV, Yuen P, Gilbertsen RB, Wang KK (1996) Non-erythroid alpha-spectrin breakdown by calpain and interleukin 1 beta-converting-enzyme-like protease(s) in apoptotic cells: contributory roles of both protease families in neuronal apoptosis. *Biochem J* 319:683-690.

79. Neumar RW, Meng FH, Mills AM, Xu YA, Zhang C, Welsh FA, Siman R (2001) Calpain activity in the rat brain after transient forebrain ischemia. *Exp Neurol* 170:27-35.

80. Newcomb JK, Kampfl A, Posmantur RM, Zhao X, Pike BR, Liu SJ, Clifton GL, Hayes RL (1997) Immunohistochemical study of calpain-mediated breakdown products to alpha-spectrin following controlled cortical impact injury in the rat. *J Neurotrauma* 14:369-83.

81. Newcomb JK, Zhao X, Pike BR, Hayes RL (1999) Temporal profile of apoptotic-like changes in neurons and astrocytes following controlled cortical impact injury in the rat. *Exp Neurol* 158:76-88.

82. NIH (1998) Rehabilitation of persons with traumatic brain injury. *NIH Consensus Statement* 16:1-41.

83. Nishida A, Emoto K, Shimizu M, Uozumi T, Yamawaki S (1994) Brain ischemia decreases phosphatidylcholine-phospholipase D but not phosphatidylinositol-phospholipase C in rats. *Stroke* 25:1247-1251.

84. Nitatori T, Sato N, Waguri S, Karasawa Y, Araki H, Shibanai K, Kominami E, Uchiyama Y (1995) Delayed neuronal death in the CA1 pyramidal cell layer of the gerbil hippocampus following transient ischemia is apoptosis. *J Neurosci* 15:1001-1011.

85. Nygaard O, Langbakk B, Romner B (1998) Neuron-specific enolase concentrations in serum and cerebrospinal fluid in patients with no previous history of neurological disorder. *Scand J Clin Lab Invest* 58:183-186.

86. Ogata N, Yonekawa Y, Taki W, Kannagi R, Murachi T, Hamakubo T, Kikuchi H (1989) Degradation of neurofilament protein in cerebral ischemia. *J Neurosurg* 70:103-107.

87. Paterakis K, Karantanas AH, Komnos A, Volikas Z (2000) Outcome of patients with diffuse axonal injury: the significance and prognostic value of MRI in the acute phase. *J Trauma* 49:1071-1075.

88. Perini F, Morra M, Alecci M, Galloni E, Marchi M, Toso V (2001) Temporal profile of serum anti-inflammatory and pro-inflammatory interleukins in acute ischemic stroke patients. *Neurol Sci* 22:289-296.

89. Pike BR, Flint J, Dutta S, Johnson E, Wang KK, Hayes RL (2001) Accumulation of non-erythroid alpha II-spectrin and calpain-cleaved alpha II-spectrin breakdown products in cerebrospinal fluid after traumatic brain injury in rats. *J Neurochem* 78:1297-1306.

90. Pike BR, Zhao X, Newcomb JK, Glenn CC, Anderson DK, Hayes RL (2000) Stretch injury causes calpain and caspase-3 activation and necrotic and apoptotic cell death in septo-hippocampal cell cultures. *J Neurotrauma* 17:283-298.

91. Pike BR, Zhao X, Newcomb JK, Posmantur RM, Wang KK, Hayes RL (1998) Regional calpain and caspase-3 proteolysis of alpha-spectrin after traumatic brain injury. *Neuroreport* 9:2437-2442.

92. Pike BR, Zhao X, Newcomb JK, Wang KK, Posmantur RM, Hayes RL (1998) Temporal relationships between de novo protein synthesis, calpain and caspase 3-like protease activation, and DNA fragmentation during apoptosis in septo-hippocampal cultures. *J Neurosci Res* 52:505-520.

93. Posmantur R, Hayes RL, Dixon CE, Taft WC (1994) Neurofilament 68 and neurofilament 200 protein levels decrease after traumatic brain injury. *J Neurotrauma* 11:533-545.

94. Posmantur R, Kampfl A, Siman R, Liu J, Zhao X, Clifton GL, Hayes RL (1997) A calpain inhibitor attenuates cortical cytoskeletal protein loss after experimental traumatic brain injury in the rat. *Neuroscience* 77:875-888.

95. Posmantur RM, Newcomb JK, Kampfl A, Hayes RL (2000) Light and confocal microscopic studies of evolutionary changes in neurofilament proteins following cortical impact injury in the rat. *Exp Neurol* 161:15-26.

96. Posmantur RM, Zhao X, Kampfl A, Clifton GL, Hayes RL (1998) Immunoblot analyses of the relative contributions of cysteine and aspartic proteases to neurofilament breakdown products following experimental brain injury in rats. *Neurochem Res* 23:1265-1276.

97. Raabe A, Grolms C, Keller M, Dohnert J, Sorge O, Seifert V (1998) Correlation of computed tomography findings and serum brain damage markers following severe head injury. *Acta Neurochir (Wien)* 140:787-791; discussion 791-792.

98. Raabe A, Grolms C, Seifert V (1999) Serum markers of brain damage and outcome prediction in patients after severe head injury. *Br J Neurosurg* 13:56-59.

99. Raabe A, Menon DK, Gupta S, Czosnyka M, Pickard JD (1998) Jugular venous and arterial concentrations of serum S-100B protein in patients with severe head injury: a pilot study. *J Neurol Neurosurg Psychiatry* 65:930-932.

100. Raghupathi R, Conti AC, Graham DI, Krajewski S, Reed JC, Grady MS, Trojanowski JQ, McIntosh TK (2002) Mild traumatic brain injury induces apoptotic cell death in the cortex that is preceded by decreases in cellular Bcl-2 immunoreactivity. *Neuroscience* 110:605-616.

101. Raghupathi R, Margulies SS (2002) Traumatic axonal injury after closed head injury in the neonatal pig. *J Neurotrauma* 19:843-853.

102. Riederer BM, Zagon IS, Goodman SR (1987) Brain spectrin(240/235) and brain spectrin(240/235E): differential expression during mouse brain development. *J Neurosci* 7:864-874.

103. Ringger NC, Silver X, O'Steen B, Brabham JG, Deford SM, Pike BR, Pineda J, Hayes RL (In Preparation) CSF Calpain-induced spectrin breakdown products predict injury magnitude and chronic lesion sized in a rat model of TBI.

104. Ringleb PA, Schellinger PD, Schranz C, Hacke W (2002) Thrombolytic therapy within 3 to 6 hours after onset of ischemic stroke: useful or harmful? *Stroke* 33:1437-1441.

105. Rink A, Fung KM, Trojanowski JQ, Lee VM, Neugebauer E, McIntosh TK (1995) Evidence of apoptotic cell death after experimental traumatic brain injury in the rat. *Am J Pathol* 147:1575-1583.

106. Roine R O, Somer H, Kaste M, Viinikka L, Karonen S L (1989) Neurological outcome after out-of-hospital cardiac arrest. Prediction by cerebrospinal fluid enzyme analysis. *Arch Neurol* 46:753-756.

107. Romner B, Ingebrigtsen T, Kongstad P, Borgesen SE (2000) Traumatic brain damage: serum S-100 protein measurements related to neuroradiological findings. *J Neurotrauma* 17:641-647.

108. Ross SA, Cunningham RT, Johnston CF, Rowlands BJ (1996) Neuron-specific enolase as an aid to outcome prediction in head injury. *Br J Neurosurg* 10:471-476.

109. Saatman KE, Bozyczko-Coyne D, Marcy V, Siman R, McIntosh TK (1996) Prolonged calpain-mediated spectrin breakdown occurs regionally following experimental brain injury in the rat. *J Neuropathol Exp Neurol* 55:850-860.

110. Saido TC, Sorimachi H, Suzuki K (1994) Calpain: new perspectives in molecular diversity and physiological-pathological involvement. *Faseb J* 8:814-822.

111. Scheidler MG, Shultz BL, Schall L, Ford HR (2000) Risk factors and predictors of mortality in children after ejection from motor vehicle crashes. *J Trauma* 49:864-868.

112. Schwartz SM, Duffy JY, Pearl JM, Nelson DP (2001) Cellular and molecular aspects of myocardial dysfunction. *Crit Care Med* 29:S214-219.

113. Sellman M, Ivert T, Ronquist G, Caesarini K, Persson L, Semb BK (1992) Central nervous system damage during cardiac surgery assessed by 3 different biochemical markers in cerebrospinal fluid. *Scand J Thorac Cardiovasc Surg* 26:39-45.

114. Shaw GJ, Jauch EC, Zemlan FP (2002) Serum cleaved tau protein levels and clinical outcome in adult patients with closed head injury. *Ann Emerg Med* 39:254-257.

115. Singhal A, Baker AJ, Hare GM, Reinders FX, Schlichter LC, Moulton RJ (2002) Association between Cerebrospinal Fluid Interleukin-6 Concentrations and Outcome after Severe Human Traumatic Brain Injury. *J Neurotrauma* 19:929-937.

116. Sloviter RS (1996) Hippocampal pathology and pathophysiology in temporal lobe epilepsy. *Neurologia* 11 Suppl 4:29-32.

117. Squier MK, Miller AC, Malkinson AM, Cohen JJ (1994) Calpain activation in apoptosis. *J Cell Physiol* 159:229-237.

118. Suzuki K, Sorimachi H, Yoshizawa T, Kinbara K, Ishiura S (1995) Calpain: novel family members, activation, and physiologic function. *Biol Chem Hoppe Seyler* 376:523-529.

119. Thomaidou D, Mione MC, Cavanagh JF, Parnavelas JG (1997) Apoptosis and its relation to the cell cycle in the developing cerebral cortex. *J Neurosci* 17:1075-1085.

120. Usui A, Kato K, Abe T, Murase M, Tanaka M, Takeuchi E (1989) S-100ao protein in blood and urine during open-heart surgery. *Clin Chem* 35:1942-1944.

121. van Engelen BG, Lamers KJ, Gabreels FJ, Wevers RA, van Geel WJ, Borm GF (1992) Age-related changes of neuron-specific enolase, S-100 protein, and myelin basic protein concentrations in cerebrospinal fluid. *Clin Chem* 38:813-816.

122. Vanags DM, Porn-Ares MI, Coppola S, Burgess DH, Orrenius S (1996) Protease involvement in fodrin cleavage and phosphatidylserine exposure in apoptosis. *J Biol Chem* 271:31075-31085.

123. Villa PG, Henzel WJ, Sensenbrenner M, Henderson CE, Pettmann B (1998) Calpain inhibitors, but not caspase inhibitors, prevent actin proteolysis and DNA fragmentation during apoptosis. *J Cell Sci* 111:713-722.

124. Wang KK (2000) Calpain and caspase: can you tell the difference? *Trends Neurosci* 23:20-26.

125. Wang KK, Posmantur R, Nath R, McGinnis K, Whitton M, Talanian RV, Glantz SB, Morrow JS (1998) Simultaneous degradation of alphaII- and betaII-spectrin by caspase 3 (CPP32) in apoptotic cells. *J Biol Chem* 273:22490-22497.

126. Wang KK, Villalobo A, Roufogalis BD (1989) Calmodulin-binding proteins as calpain substrates. *Biochem J* 262:693-706.

127. Wang KK, Yuen PW (1994) Calpain inhibition: an overview of its therapeutic potential. *Trends Pharmacol Sci* 15:412-419.

128. Westaby S, Johnsson P, Parry AJ, Blomqvist S, Solem JO, Alling C, Pillai R, Taggart DP, Grebenik C, Stahl E (1996) Serum S100 protein: a potential marker for cerebral events during cardiopulmonary bypass. *Ann Thorac Surg* 61:88-92.

129. Woertgen C, Rothoerl RD, Holzschuh M, Metz C, Brawanski A (1997) Comparison of serial S-100 and NSE serum measurements after severe head injury. *Acta Neurochir (Wien)* 139:1161-1164; discussion 1165.

130. Woertgen C, Rothoerl RD, Metz C, Brawanski A (1999) Comparison of clinical, radiologic, and serum marker as prognostic factors after severe head injury. *J Trauma* 47:1126-1130.

131. Yakovlev AG, Knoblach SM, Fan L, Fox GB, Goodnight R, Faden AI (1997) Activation of CPP32-like caspases contributes to neuronal apoptosis and neurological dysfunction after traumatic brain injury. *J Neurosci* 17:7415-7424.

132. Yamazaki Y, Yada K, Morii S, Kitahara T, Ohwada T (1995) Diagnostic significance of serum neuron-specific enolase and myelin basic protein assay in patients with acute head injury. *Surg Neurol* 43:267-270; discussion 270-271.

133. Yang K, Taft WC, Dixon CE, Yu RK, Hayes RL (1994) Endogenous phosphorylation of a 61,000 dalton hippocampal protein increases following traumatic brain injury. *J Neurotrauma* 11:523-532.

134. Ytrebo LM, Nedredal GI, Korvald C, Holm Nielsen OJ, Ingebrigtsen T, Romner B, Aarbakke J, Revhaug A (2001) Renal elimination of protein S-100beta in pigs with acute encephalopathy. *Scand J Clin Lab Invest* 61:217-225.

135. Zauner A, Bullock R (1995) The role of excitatory amino acids in severe brain trauma: opportunities for therapy: a review. *J Neurotrauma* 12:547-554.

136. Zemlan FP, Jauch EC, Mulchahey JJ, Gabbita SP, Rosenberg WS, Speciale SG, Zuccarello M (2002) C-tau biomarker of neuronal damage in severe brain injured patients: association with elevated intracranial pressure and clinical outcome. *Brain Res* 947:131-139.

Cell-Specific Upregulation of Survivin after Experimental Traumatic Brain Injury in Rats

ERIK A. JOHNSON,[1,2] STANISLAV I. SVETLOV,[1,2] BRIAN R. PIKE,[1,2]
PAUL J. TOLENTINO,[1,4] GERALD SHAW,[1,2,5] KEVIN K.W. WANG,[1,2,6]
RONALD L. HAYES,[1,2,4,6] and JOSE A. PINEDA[1,3]

ABSTRACT

In this study, we examined the expression and cellular localization of survivin and proliferating cell nuclear antigen (PCNA) after controlled cortical impact traumatic brain injury (TBI) in rats. There was a remarkable and sustained induction of survivin mRNA and protein in the ipsilateral cortex and hippocampus of rats after TBI, peaking at five days post injury. In contrast, both survivin mRNA and protein were virtually undetectable in craniotomy control animals. Concomitantly, expression of PCNA was also significantly enhanced in the ipsilateral cortex and hippocampus of these rats with similar temporal and spatial patterns. Immunohistochemistry revealed that survivin and PCNA were co-expressed in the same cells and had a focal distribution within the injured brain. Further analysis revealed a frequent co-localization of survivin and GFAP, an astrocytic marker, in both the ipsilateral cortex and hippocampus, while a much smaller subset of cells showed co-localization of survivin and NeuN, a mature neuronal marker. Neuronal localization of survivin was observed predominantly in the ipsilateral cortex and contralateral hippocampus after TBI. PCNA protein expression was detected in both astrocytes and neurons of the ipsilateral cortex and hippocampus after TBI. Collectively these data demonstrate that the anti-apoptotic protein survivin, previously characterized in cancer cells, is abundantly expressed in brain tissues of adult rats subjected to TBI. We found survivin expression in both astrocytes and a sub-set of neurons. In addition, the expression of survivin was co-incident with PCNA, a cell cycle protein. This suggests that survivin may be involved in regulation of neural cell proliferative responses after traumatic brain injury.

Key words: astrocyte; neuron; PCNA; survivin; traumatic brain injury

INTRODUCTION

TRAUMATIC BRAIN INJURY (TBI) is a major health care issue that can lead to permanent motor, cognitive and behavioral deficits. These deficits are the result of neural tissue injury and cell death, most of which occurs within the first days after injury (Raghupathi et al., 2000). The ability of this tissue to resist injury and recover depends

[1]Center for Traumatic Brain Injury Studies, E.F and W.L. McKnight Brain Institute of the University of Florida, Gainesville, Florida.

Departments of [2]Neuroscience, [3]Pediatrics, [4]Neurosurgery, [5]Anatomy and Cell Biology, and [6]Psychiatry, University of Florida, Gainesville, Florida.

largely on two factors, the survival potential of the cells and the proliferative ability of the cells in the affected area. Therefore, proliferation of cells in response to injury is important in the compensatory/reparative process. Astrocytes multiply possibly to support surviving neurons and prevent further tissue damage through formation of the glial scar (Ridet et al., 1997; Bush et al., 1999; Smith et al., 2001). Microglia increase to remove cellular debris and promote recovery (Giulian, 1991). Neurons may be replenished by neural stem cells in the dentate gyrus and subventricular zones (Doetsch et al., 1999; Cameron and McKay, 2001; Kernie et al., 2001; Yagita et al., 2001; Peterson, 2002). Consistent with these findings, cell cycle protein expression has been shown after TBI (Kaya et al., 1999a). However, studies have not investigated the role of survivin, a pro-mitotic and anti-apoptotic protein, in the adult brain after TBI.

Survivin is a novel member of the inhibitor of apoptosis protein (IAP) family that can inhibit activated caspases (Ambrosini et al., 1997; LaCasse et al., 1998; Takahashi et al., 1998; Tamm et al., 1998; Deveraux and Reed, 1999; Li and Altieri, 1999; Muchmore et al., 2000; Jiang et al., 2001). Survivin is also an evolutionarily conserved chromosomal passenger protein that is required for proper completion of mitosis. Survivin is present during normal tissue development (Adida et al., 1998; Kobayashi et al., 1999) but is absent in most adult tissues including the brain (Ambrosini et al., 1997; Kobayashi et al., 1999). Many cancer cell lines and cancer tumors, such as neural derived neuroblastoma and glioblastoma, which proliferate at high rates, exhibit survivin over-expression (Altieri et al., 1999; Sasaki et al., 2002). In addition, blocking survivin expression with anti-sense oligonucleotides in these cell lines leads to cell death (Shankar et al., 2001).

In this paper, we demonstrate the induction of survivin expression at the levels of mRNA and protein in the cortex and hippocampus of rats after traumatic brain injury. Survivin protein was primarily localized to astrocytes and in a small subset of neurons as indicated by its co-localization with GFAP and NeuN. In addition, a remarkable induction of proliferating cell nuclear antigen (PCNA) was observed after TBI and also localized to astrocytes and neurons. Finally, survivin and PCNA were co-expressed in single cells suggesting a possible role for survivin in regulation of cellular proliferative responses following TBI.

MATERIALS AND METHODS

Induction of Controlled Cortical Impact Brain Injury

The surgical and cortical impact injury procedures were conducted as previously described (Dixon et al., 1991; Pike et al., 1998). Briefly, adult male Sprague-

Dawley rats (250–300 g) were anesthetized with 4% isoflurane (Halocarbon Laboratories; River Edge, NJ) in 1:1 O_2/N_2O for 4 min and maintained during surgery with 2.5% isoflurane. Core body temperature was continuously monitored using a rectal thermistor probe and maintained at 36.5–37.5°C using an adjustable heating pad. A unilateral craniotomy (ipsilateral to injury) was performed over the right cortex between the sagittal suture, bregma, and lambda while leaving the dura intact. Traumatic insult was generated by impacting the exposed cortex with a 5-mm-diameter aluminum tip at a velocity of 4 m/sec, a 150-msec dwell time, and a 1.6-mm compression. Craniotomy control animals received the cra-niotomy but not the impact injury. All procedures were performed according to guidelines established by the University of Florida Institutional Animal Care and Use Committee (IACUC) and the National Institutes of Health (NIH).

Quantitative Real-Time Polymerase Chain Reaction (Q-PCR)

Survivin primers were generated using GeneBank locus AF 276775: forward primer 5' TAAGC CACTT GTCCC AGCTT 3', and reverse primer 5' AGGAT GGTAC CCCAT TACCT 3'. GAPDH: forward primer 5' GGCTG CCTTC TCTTG TGAC 3' and the reverse primer 5' CACCA CTTCG TCCGC CGG 3'. Cortical and hippocampal tissues from the ipsilateral and contralateral hemispheres were rapidly excised at either 1, 2, 3, 5, 7, or 14 days and "snap-frozen" with liquid nitro-
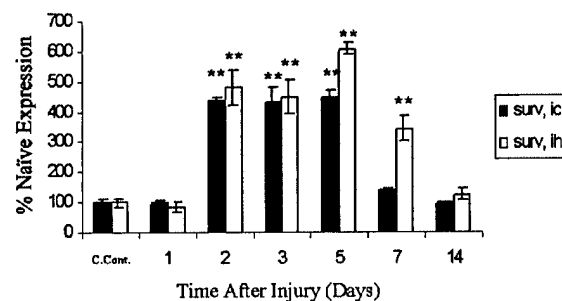
FIG. 1. Survivin mRNA induction in rat brain after traumatic brain injury. Rats were subjected to craniotomy followed by controlled cortical impact brain injury. Total RNA was isolated from injured (ipsilateral) cortex (ic) and hippocampus (ih) at indicated post-injury times. cDNA was synthesized, and quantitative PCR using survivin primers was performed. Data are given as percent of survivin expression over craniotomy controls (C. Cont.); each time point represents mean ± SEM of four independent measurements in craniotomy control or TBI group. $**p < 0.01$ versus craniotomy control (one-way ANOVA test with *post hoc* Bonferroni analysis).
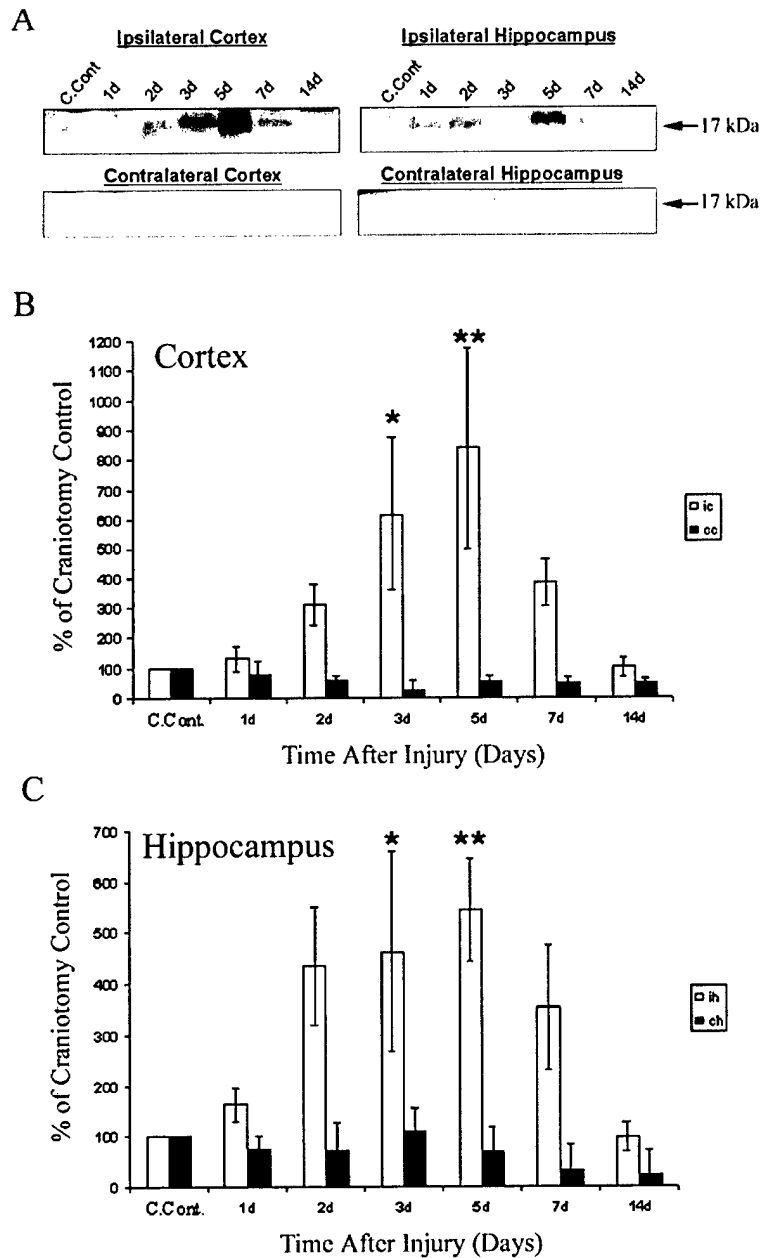
1184

FIG. 2. Expression of survivin protein after TBI in rats. Brain tissue homogenate proteins (40 μg) were separated using SDS-PAGE, immunoblotted with survivin antibody, and visualized. **(A)** Representative Western blot of survivin (17-kDa protein) in ipsilateral cortex (ic) and hippocampus (ih), contralateral cortex (cc) and hippocampus (ch) obtained from injured rats, and from craniotomy control rats without cortical impact (C. Cont.). Densitometry analysis representation of survivin-positive bands in ipsilateral (ic) and contralateral (cc) cortex **(B)** and ipsilateral (ih) and contralateral (ch) hippocampus **(C)** after TBI is shown as percent of craniotomy control values. Each data point represents the mean ± SEM of four to six independent experiments. *$p <$ 0.05, **$p <$ 0.001 versus craniotomy control (one-way ANOVA test with *post hoc* Bonferroni analysis).
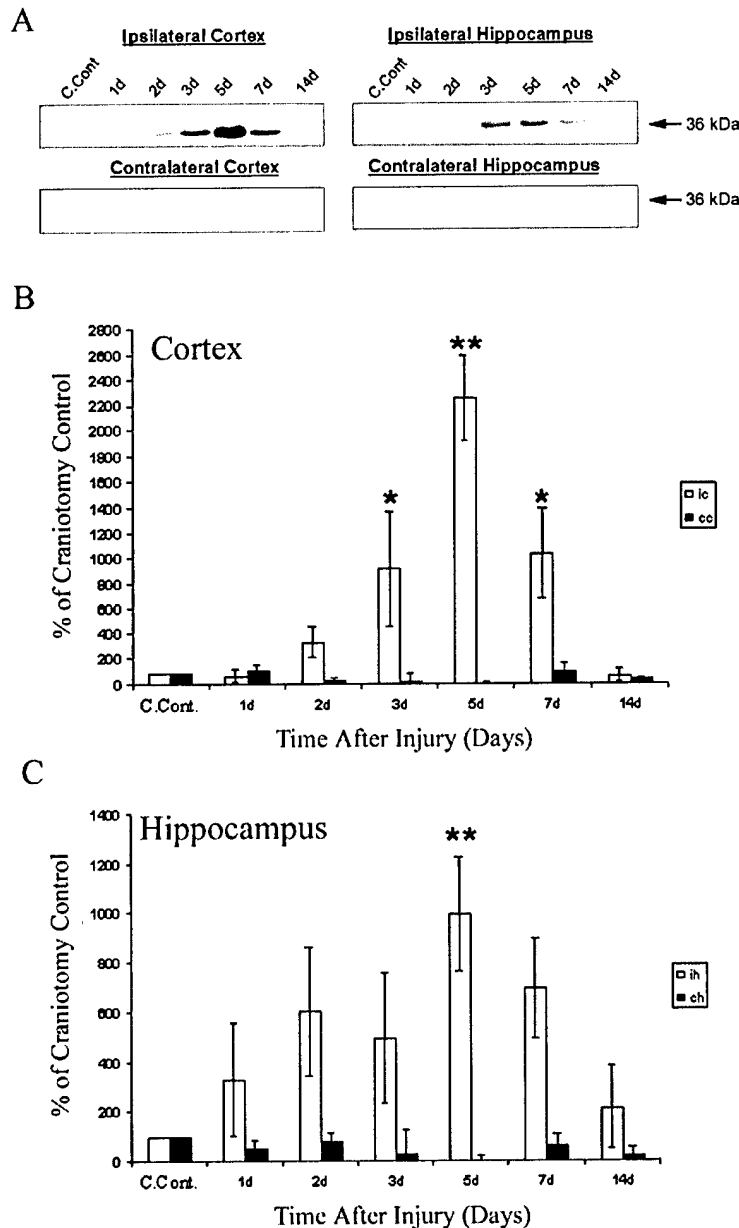
FIG. 3. Expression of PCNA after TBI in rats. PVDF membranes visualized for survivin were stripped and re-probed with PCNA antibody. Representative western blots showing PCNA (36 kDa) **(A)** and densitometry analysis of PCNA-positive bands **(B,C)** are presented. Experimental conditions, sample size and abbreviations are identical to those in Figure 2. *$p < 0.05$, **$p < 0.01$ versus craniotomy control (one-way ANOVA test with *post hoc* Bonferroni analysis).

gen. Total RNA was isolated from the samples using TRI-zol reagent (Invitrogen, Carlsbad, CA) according to the manufacturer's instructions. cDNA synthesis was performed using 1 μg of total RNA with the SuperScript™ First-Strand Synthesis System for RT-PCR kit (Invitrogen/Life Technologies, Carlsbad, CA) according to the manufacturer's instructions. Q-PCR was performed as previously described (Tolentino et al., 2002) using the LightCycler-FastStart DNA Master SYBR Green I reaction mix (Roche Diagnostics, Indianapolis, IN) in combination with 0.5 μM primers, 2.5 mM $MgCl_2$ in the Light Cycler rapid thermal cycler system (Roche Diag-
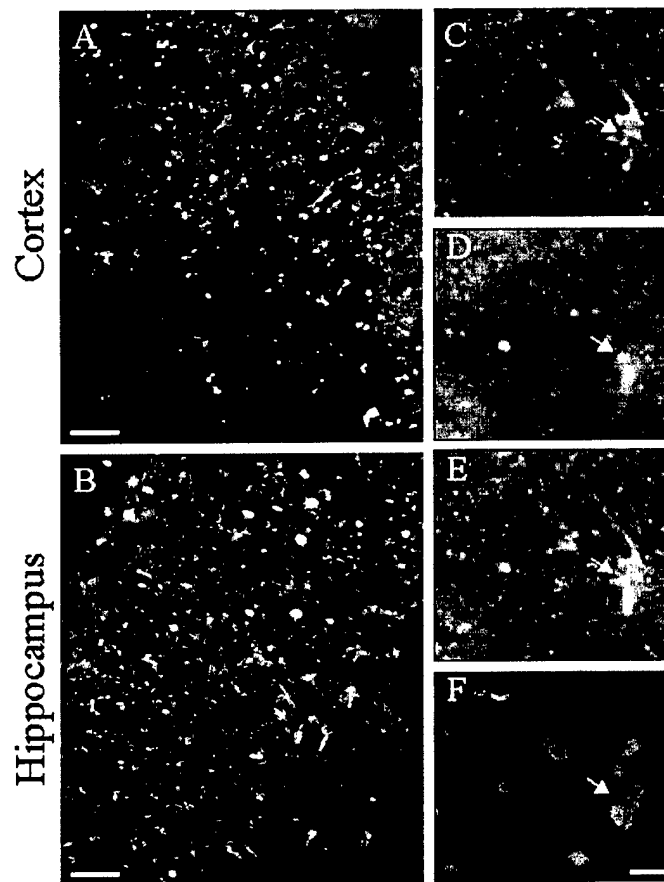
FIG. 4. Immunohistochemistry of survivin and PCNA. Double fluorescent immunostaining for survivin (red) and PCNA (green) was performed in the ipsilateral cortex **(A)** and hippocampus **(B)** at 5 day post-injury. Survivin is expressed in the cytoplasm **(C,** red), while PCNA is expressed in the nucleus **(D,** green). The white arrow indicates the typical focal co-expression of survivin and PCNA as shown in merged survivin and PCNA images **(E)**. PCNA expression was co-incident with DAPI staining **(F,** blue, white arrow). Original magnification, ×200; bar = 50 μm (A,B); original magnification ×400, bar = 20 μm (C–F).

nostics, Indianapolis, IN). Briefly, the primers were amplified then quantified by online monitoring and identification of the crossing point value (CPV) which is the exact time point at which the logarithmic linear phase could be distinguished from the background. The survivin primer sets were subjected to serial dilution and linear regression analysis of the logarithm of the dilution factor versus the CPV generated a standard curve for each transcript-speci-fic template. Results are presented as percentage of cranio-tomy control. Data were analyzed by ANOVA with a post-hoc Bonferroni-test and are given as mean ± SEM. Differences were considered significant at the level of $p \leq 0.05$.

Western Blot Analyses

Brain tissue was removed as described above, rinsed with cold PBS, snap frozen in liquid nitrogen and ho-

mogenized in ice-cold triple detergent lysis buffer containing a Complete™ protease inhibitor cocktail (Roche Biochemicals, Indianapolis, IN). Protein concentration was determined by bicinchoninic acid (BCA) micro protein assays (Pierce, Inc., Rockford, IL). Forty micrograms of protein per well was loaded and separated by SDS-PAGE, transferred to PVDF membranes and probed with goat-anti-rabbit survivin antibody (Novus Biologicals; Littleton, CO; 1:1000). After incubation with goat anti-rabbit HRP-labeled secondary antibody (Biorad, Hercules, CA), the membranes were developed using Enhanced Chemiluminescence Plus reagents (ECL Plus; Amersham, Arlington Heights, IL). For further PCNA analysis, developed PVDF membranes were incubated in stripping buffer, rinsed twice in TBST and incubated with PCNA antibody (Santa Cruz Biotech; Santa Cruz, CA;

1187

JOHNSON ET AL.

1:1000) as described above. Semi-quantitative, densito-metric analysis was performed using the AlphaImager™ 2000 Digital Imaging System (San Leandro, CA). Transformed data (experimental densitometry value/ craniotomy control densitometry value × 100) was evaluated by ANOVA and a post-hoc Bonferroni-test. Values are expressed as percentage of craniotomy controls and are given as mean ± SEM. Differences were considered significant at the level of $p \leq 0.05$.

Characterization of Survivin Antibody (R51)

First, we compared the specificity of the survivin antibody developed within our group (R51; Dr. G. Shaw) and a commercially available survivin antibody (Chemicon; Temecula, CA). Our antibody showed characteristic staining of the cleavage furrow between dividing HeLa cells consistent with other reports (Li et al., 1998, 1999; Uren et al., 2000). In addition, double labeling with both survivin antibodies showed co-localization at the cleavage furrow. The peptides used to develop our survivin antibody are specific to survivin and do not recognize other IAP family proteins according to SDSC Biology Workbench BLASTP (2.2.2) (Altschul et al., 1997) and CLUSTAL W (1.81) analysis (Higgins et al., 1992; Thompson et al., 1994), resulting in the survivin antibody's specificity.

Immunohistochemistry (IHC)

Animals were transcardially perfused with 2% Heparin (Elkins-Sinn, Inc.; Cherry Hill, NJ) in 0.9% saline solution (pH 7.4) followed by 4% paraformaldehyde in 0.1 M phosphate buffer (pH 7.4). The brains were post-fixed in 4% paraformaldehyde and stored in 0.1M PBS or cryobuffer. Forty micron sections were fluorescent immunolabeled with two primary antibodies in the following experiments: survivin (1:500)/GFAP for astrocytes (Sternberger; Lutherville, MD; 1:1000), survivin/NeuN for mature neurons (Chemicon; Temecula, CA; 1:1000), survivin/PCNA (Santa Cruz Biotech; Santa Cruz, CA; 1:200), PCNA/GFAP and PCNA/NeuN. The nuclear dye DAPI (in Vectashield; H-1200; Vector Laboratories; Burlingame, CA) was used to label the nuclei. The first primary antibody was incubated at 4°C for 24–48 h in a 2% goat serum/2% horse serum/0.2% Triton-X 100 in 0.1 M PBS (block) solution followed by the second primary antibody at 4°C for 1 h in block solution. Fluorescent-tagged secondary antibody (Molecular Probes; Eugene, OR) was used for visualization. For double-labeling using same species antibodies, we used the tyramide signal amplification (TSA) kit (PerkinElmer Life Sciences, Boston, MA) according to the manufacturer's instructions and as previously described (Stone et al., 2002). The

sections were viewed and digitally captured with a Zeiss Axioplan 2 microscope (Zeiss, Thornwood, NY) equipped with a SPOT Real Time Slider high-resolution color CCD digital camera (Diagnostic Instruments, Inc., Sterling Heights, MI). The number of animals used for dual-labeling IHC is as follows: survivin × PCNA = 4, survivin × GFAP = 6, survivin × NeuN = 4, PCNA × GFAP = 4, and PCNA × NeuN = 4. Cell counts were obtained by comparing the number of double-labeled cells to total single-labeled cells in the following groups: survivin/NeuN positive cells to total NeuN positive cells, survivin/PCNA positive cells to total PCNA positive cells, PCNA/NeuN positive cells to total NeuN positive cells, and survivin/GFAP positive cells to total GFAP positive cells. Percentages were calculated by dividing the number of double-labeled cells with the total number of single-labeled cells. For each group, representative photomicrographs were selected and counted. Cells were counted in a total area of at least 188,000 μm^2 for each group, with no distinction made between cortical and hippocampal regions.

RESULTS

Induction of Survivin Expression after TBI

Q-PCR analysis revealed an initial increase in survivin mRNA at 2 days post injury in the ipsilateral cortex and hippocampus. These transcripts remained elevated in both regions, reached maximum levels at day 5 post-injury and declined at 7 days in the cortex and at 14 days in the hippocampus. All experimental animals remained alive and exhibited slightly impaired motor and cognitive impairments (data not shown). Cortical mRNA levels reached a maximum of 448 ± 10.0%, whereas hippocampal mRNAs attained 606 ± 10.0% compared to craniotomy control values (Fig. 1). To determine if the induction of survivin mRNA resulted in corresponding increases in survivin protein, western blot analysis was performed. Survivin (17-kDa protein) was readily detectable in the ipsilateral cortex and hippocampus of TBI rats, while it was negligible in contralateral cortex and hippocampus (Fig. 2A). Survivin was expressed in a time-dependent manner with a maximum increase at 5 days after injury followed by a gradual decline by 14 days. Specifically, the levels of survivin in cortical tissue were 616 ± 257% at 3 days and 839 ± 339% at 5 days compared to craniotomy controls (Fig. 2B). Similar increases of survivin protein in the ipsilateral hippocampus were detected at 3 d and 5 days post injury: 464 ± 196% and 545 ± 102% compared to craniotomy control, respectively (Fig. 2C).

1188

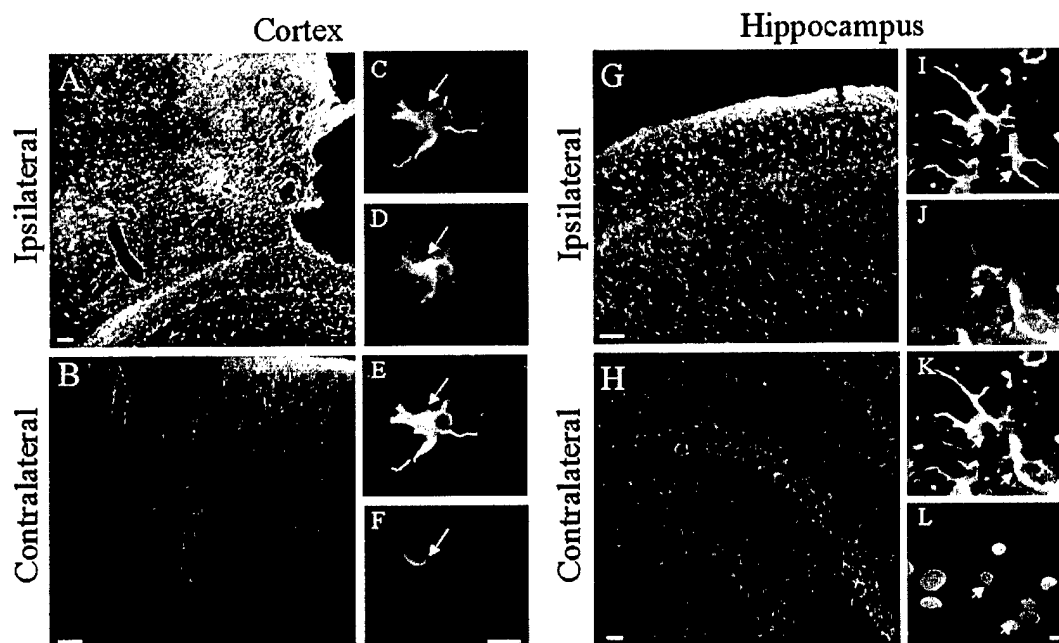**Cortex**

Hippocampus

FIG. 5. Co-localization of survivin and GFAP in brain tissue after TBI. Fluorescent immunohistochemistry for survivin (green) and GFAP (red) was performed in the ipsilateral and contralateral cortex **(A,B)** and in the CA1 and dentate gyrus regions of the hippocampus **(G,H)** at 5 day post-injury. The injury has completely destroyed the cortex in G leaving only the hippocampus in this picture. Survivin was expressed in the cytoplasm **(D,J,** green) of GFAP-positive astrocytes **(C,I,** red) of the ipsilateral cortex and hippocampus and was found to co-localize to these cells as shown in merged C/D and I/J images **(E,K,** respectively, yellow). White arrows indicate typical survivin-positive astrocytes. Nuclei are shown using DAPI **(F,L,** blue). Original magnification, ×100, bar = 50 μm (A,B,G,H); ×400, bar = 20 μm (C–F and I–L).

Cortex
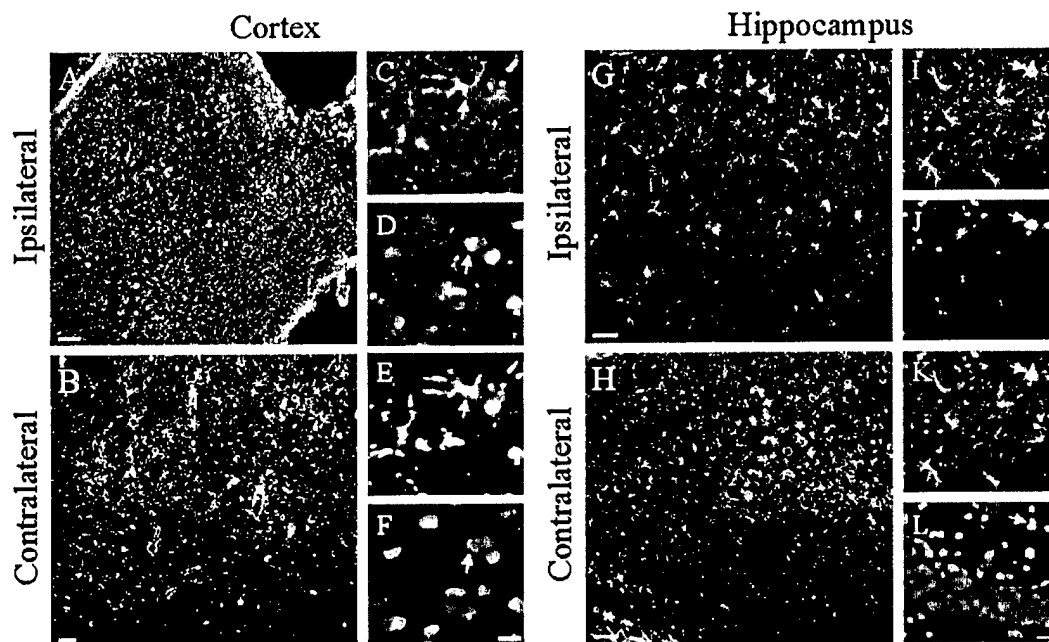
Hippocampus

FIG. 6. Co-localization of PCNA and GFAP in brain tissue after TBI. Double immunostaining for PCNA (green) and GFAP (red) was performed in the ipsilateral and contralateral cortex **(A,B)** and the CA1 and dentate gyrus regions of the hippocampus **(G,H)** at 5 day post-injury. PCNA is present in GFAP-positive cells of ipsilateral cortex **(C,D)** and, to a lesser extent hippocampus **(I,J)**. **(E,K)** Merged C/D and I/J, respectively. White arrows indicate typical PCNA-positive astrocytes. PCNA expression was co-incident with DAPI staining **(F,L,** blue). Original magnification, ×100; bar = 50 μm (A,B,G,H); ×400, bar = 20 μm (C–F, and I–L).

PCNA Expression after TBI

For detection of proliferating cell nuclear antigen (PCNA), PVDF membranes immunostained for survivin were stripped and re-probed using a PCNA-specific antibody. PCNA (36-kDa protein) was significantly detectable in the ipsilateral cortex and hippocampus of TBI rats, but only negligible amounts were observed in the contralateral cortex and hippocampus (Fig. 3A). The temporal patterns exhibited by PCNA protein were similar to that of survivin protein. Namely, PCNA expressed in a time-dependant fashion with a maximum increase at 5 days after injury followed by a gradual decline by 14 days. The levels of PCNA in ipsilateral cortical tissue were raised over craniotomy control by $919 \pm 459\%$ at 3 days, $2263 \pm 333\%$ at 5 days, and $1035 \pm 356\%$ at 7 days post injury (Fig. 3B). Similar increases of PCNA protein in ipsilateral hippocampus were detected at 5 days post injury with a maximum of $1006 \pm 229\%$ compared to craniotomy controls (Fig. 3C). No significant increase was found in the contralateral regions when compared to craniotomy controls (Fig. 3A).

Co-Expression of Survivin and PCNA following TBI

To examine spatial co-localization of survivin and PCNA, double-label immunohistochemistry of brain tissue sections was performed on day 5 post injury, when peak expression of these proteins was observed.

At this time point, a remarkable survivin and PCNA immunoreactivity was found in the ipsilateral cortex (Fig. 4A) and ipsilateral hippocampus (Fig. 4B) consistent with data obtained using Western blot analyses. Within both regions, focal co-expression patterns of survivin and PCNA in single cells were detected, which was demonstrated by both separate fluorescent visualization of individual proteins and by merging the images of double-stained slides (Fig. 4C–E). However, the dual expression of survivin and PCNA occurred infrequently as survivin and PCNA immunoreactivity could readily be found separately (Fig. 4C–E). Approximately 12% of the total number of PCNA-positive cells also labeled with survivin. The nuclear morphology of dual survivin and PCNA-positive cells was ambiguous as indicated by DAPI staining (Fig. 4F). Therefore, DAPI staining was simply used for cell identification in all subsequent experiments.

Survivin and PCNA Are Expressed in Astrocytes after TBI

To determine the cell types expressing survivin and PCNA, double-label immunohistochemistry for these proteins and GFAP, a marker of astrocytes, was performed on day 5 post injury.

In accordance with Western blot data, remarkable survivin-positive immunoreactivity was observed in the ipsilateral cortex and hippocampus proximal to the injury cavity (Fig. 5A,G, green) but not in the contralateral areas (Fig. 5B,H). Survivin was co-localized with GFAP in the cells of injured cortex and hippocampus, which strongly suggested primary accumulation of survivin in cells of astrocytic lineage (Fig. 5C–E,I–L). Survivin was uniformly distributed in the cytoplasm and processes of astrocytes in both cortex and hippocampus (Fig. 5D,J). DAPI staining is shown in Figure 5F,L3. Approximately 88% of the total number of GFAP-positive cells also labeled with survivin.

PCNA-positive immunoreactivity staining was observed in the ipsilateral cortex (Fig. 6A, green) and hippocampus (Fig. 6G, green) of injured brain, while contralateral cortex and hippocampus exhibited negligible PCNA immunoreactivity (Fig. 6B,H). PCNA (Fig. 6C,I) was partially co-localized with GFAP (Fig. 6D,J, red) in both regions, and was characteristically distributed in the nucleus of the cells in both cortex and hippocampus (Fig. 6E,K). DAPI staining is shown in Figure 6F,L.

Taken together, double-label immunohistochemistry data provides evidence that both survivin and PCNA can be detected in GFAP-positive astrocytes following traumatic insult. Since survivin and PCNA immunoreactivity was not exclusively localized in GFAP-positive cells, we next addressed a question what other cell type might express survivin after TBI. We suggested that a certain population of mature neurons might express survivin in response to injury.

Survivin and PCNA Are Expressed in a Sub-Set of Neurons after TBI

As can be seen in Figure 7, survivin and PCNA were each co-expressed with NeuN, a marker of mature neurons. NeuN-positive cells were found to express survivin in the ipsilateral cortex distal to the injury cavity (Fig. 7A–D) and in the contralateral hippocampus (Fig. 7E–H). It should be noted, however, that NeuN-positive cells that also expressed survivin occurred infrequently. For example, we estimated the number of dual survivin/NeuN positive cells as 0.1–1.5% of the total number of NeuN-positive cells in these regions. Survivin immunoreactivity was negligible in either hemisphere of craniotomy control brains (Fig. 7Q,R). No co-localization of survivin and NeuN was observed in ipsilateral hippocampus (data not shown). As can be seen in Figure 7B,F, survivin was predominantly localized to the cytoplasm and axons of NeuN-positive neurons. DAPI staining is shown in Figure 7D,H.

PCNA-positive neurons were found in the ipsilateral cortex (Fig. 7I–L) and hippocampus after TBI (Fig.
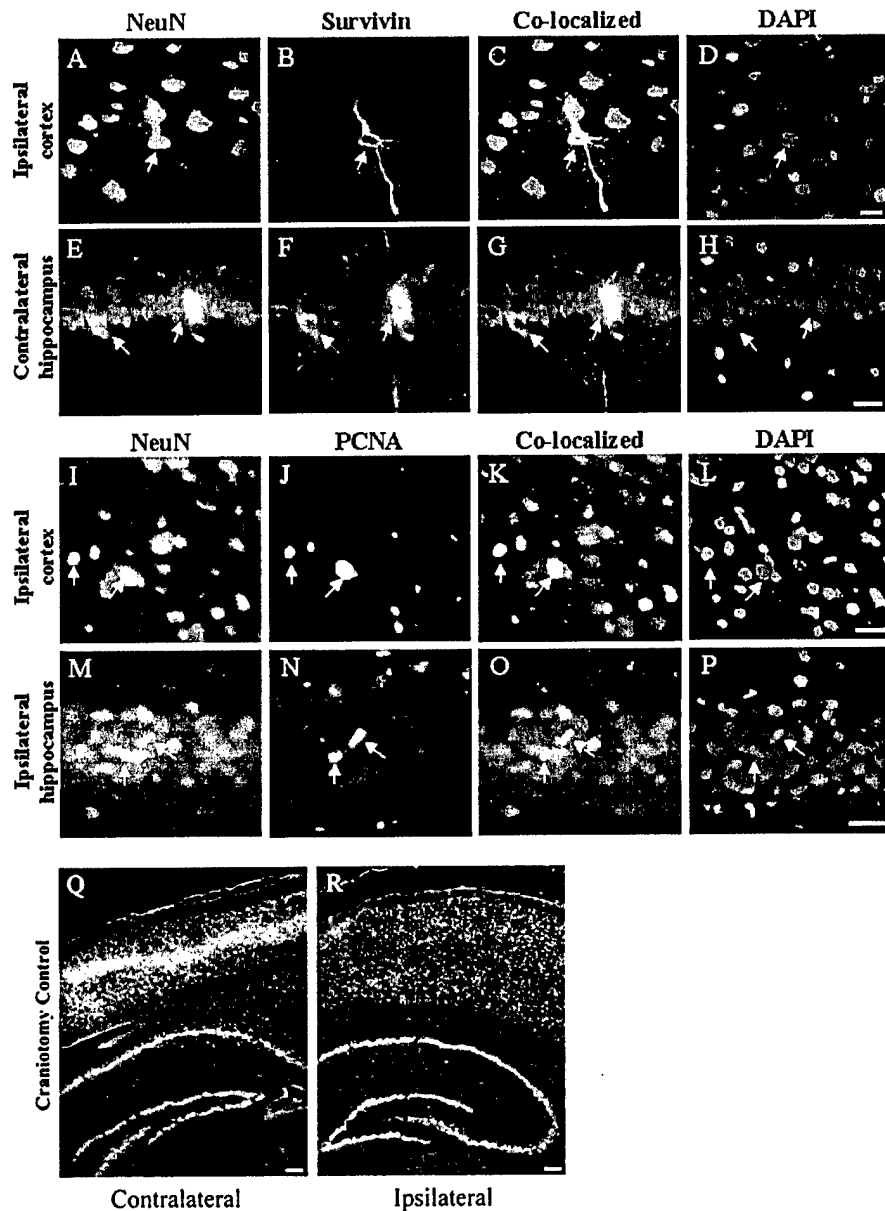
FIG. 7. A sub-set of NeuN-positive neurons express survivin and PCNA after TBI. Double fluorescent immunohistochemistry for survivin (green) and NeuN (red) in the ipsilateral cortex **(A,B)** and the CA1 pyramidal layer of the contralateral hippocampus **(E,F)** was performed. Survivin is expressed in the cytoplasm and, to a limited extent, in the processes of NeuN-positive neurons (merged images **C/G**). Dual staining for PCNA (green) and NeuN (red) is shown in the ipsilateral cortex **(I,J)** and the CA1 pyramidal layer of the ipsilateral hippocampus **(M,N)**. The nuclei are shown using DAPI staining **(D,H,** blue). PCNA is expressed in the nucleus of NeuN-positive neurons (merged images **K/O**). PCNA expression was co-incident with DAPI staining in these examples **(L,P,** blue). White arrows indicate focal co-localization of survivin/NeuN and PCNA/NeuN. Survivin/NeuN co-localization of survivin (green) and NeuN (red) was seen only in TBI rats as opposed to either hemisphere of craniotomy control **(Q,R)**. Original magnification, ×400, bar = 20 μm (A–P); original magnification, ×50, bar = 100,000 μm (Q,R).

7M–P), whereas craniotomy control tissue exhibited only trace amounts of PCNA (data not shown). Similar to the survivin/NeuN co-localization data, dual PCNA/NeuN immunostaining was a rare event accounting for approximately 4% of the total number of NeuN positive cells. PCNA was distributed in the nuclei of these neurons (Fig. 7K,O) although the nuclear morphology of these cells was not clearly resolved by DAPI staining (Fig. 7L,P).

DISCUSSION

Traumatic brain injury (TBI) sets into motion various biochemical cascades that induce neural tissue injury and cell death. Conversely, several proteins expressed in neural cells after TBI are directed to resist cell death and promote recovery in the injured CNS (Ridet et al., 1997; Chen and Swanson, 2003). Survivin is a multi-functional protein that inhibits apoptosis and is also required for the proper completion of mitosis. Anti-apoptotic and pro-mitogenic roles for survivin have been documented in proliferating cells of neural origin *in vitro*, such as in neuroblastoma and glioma cells (LaCasse et al., 1998; Tamm et al., 1998; Deveraux and Reed, 1999; Conway et al., 2000; Shin et al., 2001; Sasaki et al., 2002). However, no studies have investigated the potential role of survivin in the adult brain after TBI, when a sub-population of CNS cells may initiate a cell cycle-related process in response to injury.

In the present paper, we demonstrate the induction of survivin expression in rat brain subjected to TBI. The expression of survivin was time-dependent and cell-specific, and was present in astrocytes and, to a much lesser extent, in neurons in brain cortex and hippocampus. Induction of survivin in these cells was accompanied by occasional expression of PCNA, a cell cycle protein involved in mitotic G1/S progression. Our present data are the first to show that survivin mRNA and protein are significantly up-regulated after traumatic brain injury in rats. PCNA expression after TBI has been described previously (Miyake et al., 1992; Chen et al., 2003), suggesting its role in mechanisms of brain recovery after injury. The concurrent up-regulation of survivin with a similar temporal profile as PCNA shown herein further suggests that survivin may play a role in cellular proliferation after TBI.

Brain injury evoked the expression of survivin and PCNA in a time-dependent manner (Figs. 2 and 3). Western blot analysis revealed maximal co-expression of both survivin and PCNA at five days post injury. Immunohistochemistry at this time point, demonstrated co-localization of these proteins (Fig. 4), although most cells were labeled separately with PCNA and survivin. In fact, only 12% of the total number of PCNA-positive cells were

also survivin positive. It has been reported that PCNA is expressed predominantly in G1/S (Bravo et al., 1987), while survivin is found at the G2/M phase of the cell cycle (Bravo et al., 1987; Otaki et al., 2000). Hence, a lack of strict co-localization of survivin and PCNA in our study may be explained by their expression at different points in the cell cycle.

In our experimental model, we observed survivin- as well as PCNA-positive astrocytes in the proximal area of the injury and in the ipsilateral hippocampus. Proliferation of astrocytes is well documented after TBI as shown by cell labeling with BrdU as well as expression of PCNA (Latov et al., 1979; Dunn-Meynell and Levin, 1997; Carbonell and Grady, 1999; Norton, 1999; Csuka et al., 2000; Kernie et al., 2001; Chen et al., 2003). Because survivin and PCNA were expressed in astrocytes following TBI (Figs. 5 and 6), it is possible that survivin plays an important role linking astrocyte survival and proliferation after traumatic insult. Astrocyte proliferation has been implicated in the formation of the glial scar observed after injury (Latov et al., 1979) and creates a non-permissive environment for repair (Sykova et al., 1999). However, glial proliferation may also enhance neuronal survival (Smith et al., 2001; Wei et al., 2001).

Of particular interest is a sub-set of NeuN-positive neurons found to express survivin only after TBI (Fig. 7). These cells were much less abundant than survivin-positive astrocytes, and their functional significance is currently unknown. However, both neurons and astrocytes have been documented previously to express cell cycle proteins after various insults such as exposure to β-amyloid–activated microglia (Wu et al., 2000), TBI (Kaya et al., 1999a,b), chlorine toxicity (Magavi et al., 2000), or as a consequence of Alzheimer's disease (Yang et al., 2001). These papers underscore the significant controversy that exists regarding the function of cell cycle proteins such as PCNA in neurons after different types of injury. We are currently conducting further studies which will elucidate the roles for PCNA and survivin in neurons after TBI.

It should be noted that dual staining of survivin and PCNA could not be directly attributed to a specific cell type due to the technical difficulties of triple labeling antibody-based IHC. Therefore, we cannot rule out the possibility that other cell types, such as endothelial (Conway et al., 2003) or inflammatory cells (Hill-Felberg et al., 1999), may also contribute to survivin and PCNA expression after TBI. The appearance of survivin and PCNA separately in neurons (NeuN-positive) and astrocytes (GFAP-positive) along with co-localization of survivin with PCNA in the same cells provide correlative data to suggest an activation of cell cycle-like program in astrocytes and possibly in a small subtype of neurons after

1192

TBI. In our experiments, survivin co-localization with PCNA does suggest that survivin may be associated with a pro-mitotic process. In an attempt to clarify these protein's roles after TBI, we analyzed the nuclear morphology of survivin-positive cells to define the apoptotic or mitotic architecture of nuclei. DAPI staining proved too ambiguous in identifying apoptotic versus mitotic phenotypes likely due to the thickness of the brain sections (40 μm). Further studies using direct markers of mitosis such as BrdU incorporation as well as simultaneous labeling with cell death related proteins is required to delineate anti-apoptotic and pro-mitotic activities of survivin and PCNA in these cells.

In conclusion, our data demonstrate the induction of survivin in the rat brain following TBI. Expression of survivin occurred predominantly in astrocytes as compared to neurons in a time-dependant fashion and was accompanied by expression of PCNA. Taken together, these results suggest that survivin plays a role in neural cell responses following traumatic brain injury in rats. Future studies will investigate the implications of these findings to the pathophysiology of TBI.

ACKNOWLEDGMENTS

REFERENCES

ADIDA, C., CROTTY, P.L., McGRATH, J., BERREBI, D., DIEBOLD, J., and ALTIERI, D.C. (1998). Developmentally regulated expression of the novel cancer anti-apoptosis gene survivin in human and mouse differentiation. Am. J. Pathol. 152, 43–49.

ALTIERI, D.C., MARCHISIO, P.C., and MARCHISIO, C. (1999). Survivin apoptosis: an interloper between cell death and cell proliferation in cancer. Lab. Invest. 79, 1327–1333.

ALTSCHUL, S.F., MADDEN, T.L., SCHAFFER, A.A., et al. (1997). Gapped BLAST and PSI-BLAST: a new generation of protein database search programs. Nucleic Acids Res. 25, 3389–3402.

AMBROSINI, G., ADIDA, C., and ALTIERI, D.C. (1997). A novel anti-apoptosis gene, survivin, expressed in cancer and lymphoma. Nat. Med. 3, 917–921.

BRAVO, R., FRANK, R., BLUNDELL, P.A., and MAC-DONALD-BRAVO, H. (1987). Cyclin/PCNA is the auxiliary protein of DNA polymerase-delta. Nature 326, 515–517.

BUSH, T.G., PUVANACHANDRA, N., HORNER, C.H., et al. (1999). Leukocyte infiltration, neuronal degeneration, and neurite outgrowth after ablation of scar-forming, reactive astrocytes in adult transgenic mice. Neuron 23, 297–308.

CAMERON, H.A., and McKAY, R.D. (2001). Adult neurogenesis produces a large pool of new granule cells in the dentate gyrus. J. Comp. Neurol. 435, 406–417.

CARBONELL, W.S., and GRADY, M.S. (1999). Regional and temporal characterization of neuronal, glial, and axonal response after traumatic brain injury in the mouse. Acta Neuropathol. (Berl.) 98, 396–406.

CHEN, X.H., IWATA, A., NONAKA, M., BROWNE, K.D., and SMITH, D.H. (2003). Neurogenesis and glial proliferation persist for at least one year in the subventricular zone following brain trauma in rats. J. Neurotrauma 20, 623–631.

CHEN, Y., and SWANSON, R.A. (2003). Astrocytes and brain injury. J. Cereb. Blood Flow Metab. 23, 137–149.

CONWAY, E.M., POLLEFEYT, S., CORNELISSEN, J., et al. (2000). Three differentially expressed survivin cDNA variants encode proteins with distinct antiapoptotic functions. Blood 95, 1435–1442.

CSUKA, E., HANS, V.H., AMMANN, E., TRENTZ, O., KOSSMANN, T., and MORGANTI-KOSSMANN, M.C. (2000). Cell activation and inflammatory response following traumatic axonal injury in the rat. Neuroreport 11, 2587–2590.

DEVERAUX, Q.L., and REED, J.C. (1999). IAP family proteins—suppressors of apoptosis. Genes Dev. 13, 239–252.

DIXON, C.E., CLIFTON, G.L., LIGHTHALL, J.W., YAGHMAI, A.A., and HAYES, R.L. (1991). A controlled cortical impact model of traumatic brain injury in the rat. J. Neurosci. Methods 39, 253–262.

DOETSCH, F., CAILLE, I., LIM, D.A., GARCIA-VERDUGO, J.M., and ALVAREZ-BUYLLA, A. (1999). Subventricular zone astrocytes are neural stem cells in the adult mammalian brain. Cell 97, 703–716.

DUNN-MEYNELL, A.A., and LEVIN, B.E. (1997). Histological markers of neuronal, axonal and astrocytic changes after lateral rigid impact traumatic brain injury. Brain Res. 761, 25–41.

GIULIAN, D. (1991). Microglia—neuron interactions after injury to the central nervous system, in: Peripheral Signaling of the Brain: Role in Neural-Immune Interactions, Learning and Memory. R. Frederickson, J. McGaugh, and D. Felton (eds.) Lewiston, NY: Hogrefe and Huber, pps. 73–82.

HIGGINS, D.G., BLEASBY, A.J., and FUCHS, R. (1992). CLUSTAL V: improved software for multiple sequence alignment. Comput. Appl. Biosci. 8, 189–191.

HILL-FELBERG, S.J., McINTOSH, T.K., OLIVER, D.L., RAGHUPATHI, R., and BARBARESE, E. (1999). Concurrent loss and proliferation of astrocytes following lateral fluid percussion brain injury in the adult rat. J. Neurosci. Res. 57, 271–279.

JIANG, X., WILFORD, C., DUENSING, S., MUNGER, K,, JONES, G., and JONES, D. (2001). Participation of Survivin in mitotic and apoptotic activities of normal and tumor-derived cells. J. Cell. Biochem. **83,** 342–354.

KAYA, S.S., MAHMOOD, A., LI, Y., YAVUZ, E., and CHOPP, M. (1999a). Expression of cell cycle proteins (cyclin D1 and cdk4) after controlled cortical impact in rat brain. J. Neurotrauma **16,** 1187–1196.

KAYA, S.S., MAHMOOD, A., LI, Y., YAVUZ, E., GOKSEL, M., and CHOPP, M. (1999b). Apoptosis and expression of p53 response proteins and cyclin D1 after cortical impact in rat brain. Brain Res. **818,** 23–33.

KERNIE, S.G., ERWIN, T.M., and PARADA, L.F. (2001). Brain remodeling due to neuronal and astrocytic proliferation after controlled cortical injury in mice. J. Neurosci. Res. **66,** 317–326.

KOBAYASHI, K., HATANO, M., OTAKI, M., OGASAWARA, T., and TOKUHISA, T. (1999). Expression of a murine homologue of the inhibitor of apoptosis protein is related to cell proliferation. Proc. Natl. Acad. Sci. USA **96,** 1457–1462.

LaCASSE, E.C., BAIRD, S., KORNELUK, R.G., and MacKENZIE, A.E. (1998). The inhibitors of apoptosis (IAPs) and their emerging role in cancer. Oncogene **17,** 3247–3259.

LATOV, N., NILAVER, G., ZIMMERMAN, E.A., et al. (1979). Fibrillary astrocytes proliferate in response to brain injury: a study combining immunoperoxidase technique for glial fibrillary acidic protein and radioautography of tritiated thymidine. Dev. Biol. **72,** 381–384.

LI, F., and ALTIERI, D.C. (1999). The cancer antiapoptosis mouse survivin gene: characterization of locus and transcriptional requirements of basal and cell cycle-dependent expression. Cancer Res. **59,** 3143–3151.

LI, F., AMBROSINI, G., CHU, E.Y., et al. (1998). Control of apoptosis and mitotic spindle checkpoint by survivin. Nature **396,** 580–584.

LI, F., ACKERMANN, E.J., BENNETT, C.F., et al. (1999). Pleiotropic cell-division defects and apoptosis induced by interference with survivin function. Nat. Cell. Biol. **1,** 461–466.

MAGAVI, S.S., LEAVITT, B.R., and MACKLIS, J.D. (2000). Induction of neurogenesis in the neocortex of adult mice. Nature **405,** 951–955.

MIYAKE, T., OKADA, M., and KITAMURA, T. (1992). Reactive proliferation of astrocytes studied by immunohistochemistry for proliferating cell nuclear antigen. Brain Res. **590,** 300–302.

MUCHMORE, S.W., CHEN, J., JAKOB, C., et al. (2000). Crystal structure and mutagenic analysis of the inhibitor-of-apoptosis protein survivin. Mol. Cell. **6,** 173–182.

NORTON, W.T. (1999). Cell reactions following acute brain injury: a review. Neurochem. Res. **24,** 213–218.

OTAKI, M., HATANO, M., KOBAYASHI, K., et al. (2000). Cell cycle–dependent regulation of TIAP/m-survivin expression. Biochim. Biophys. Acta **1493,** 188–194.

PETERSON, D.A. (2002). Stem cells in brain plasticity and repair. Curr. Opin. Pharmacol. **2,** 34–42.

PIKE, B.R., ZHAO, X., NEWCOMB, J.K., POSMANTUR, R.M., WANG, K.K., and HAYES, R.L. (1998). Regional calpain and caspase-3 proteolysis of alpha-spectrin after traumatic brain injury. Neuroreport **9,** 2437–2442.

RAGHUPATHI, R., GRAHAM, D.I., McINTOSH, T.K. (2000). Apoptosis after traumatic brain injury. J. Neurotrauma **17,** 927–938.

RIDET, J.L., MALHOTRA, S.K., PRIVAT, A., and GAGE, F.H. (1997). Reactive astrocytes: cellular and molecular cues to biological function. Trends Neurosci. **20,** 570–577.

SASAKI, T., LOPES, M.B., HANKINS, G.R., and HELM, G.A. (2002). Expression of survivin, an inhibitor of apoptosis protein, in tumors of the nervous system. Acta Neuropathol. (Berl.) **104,** 105–109.

SHANKAR, S.L., MANI, S., O'GUIN, K.N., KANDIMALLA, E.R., AGRAWAL, S., and SHAFIT-ZAGARDO, B. (2001). Survivin inhibition induces human neural tumor cell death through caspase-independent and -dependent pathways. J. Neurochem. **79,** 426–436.

SHIN, S., SUNG, B.J., CHO, Y.S., et al. (2001). An anti-apoptotic protein human survivin is a direct inhibitor of caspase-3 and -7. Biochemistry **40,** 1117–1123.

SMITH, C., BERRY, M., CLARKE, W.E., and LOGAN, A. (2001). Differential expression of fibroblast growth factor–2 and fibroblast growth factor receptor 1 in a scarring and non-scarring model of CNS injury in the rat. Eur. J. Neurosci. **13,** 443–456.

STONE, J.R., OKONKWO, D.O., SINGLETON R.H., MUTLU, L.K., HELM, G.A., and POVLISHOCK, J.T. (2002). Caspase-3–mediated cleavage of amyloid precursor protein and formation of amyloid Beta peptide in traumatic axonal injury. J. Neurotrauma **19,** 601–614.

SYKOVA, E., VARGOVA, L., PROKOPOVA, S., and SIMONOVA, Z. (1999). Glial swelling and astrogliosis produce diffusion barriers in the rat spinal cord. Glia **25,** 56–70.

TAKAHASHI R., DEVERAUX, Q., TAMM, I., et al. (1998). A single BIR domain of XIAP sufficient for inhibiting caspases. J. Biol. Chem. **273,** 7787–7790.

TAMM, I., WANG, Y., SAUSVILLE, E., et al. (1998). IAP-family protein survivin inhibits caspase activity and apoptosis induced by Fas (CD95), Bax, caspases, and anticancer drugs. Cancer Res. **58,** 5315–5320.

THOMPSON, J.D., HIGGINS, D.G., and GIBSON, T.J. (1994). CLUSTAL W: improving the sensitivity of progressive multiple sequence alignment through sequence weighting, position-specific gap penalties and weight matrix choice. Nucleic Acids Res. **22,** 4673–4680.

TOLENTINO, P.J., DeFORD, S.M., NOTTERPEK, L., et al. (2002). Up-regulation of tissue-type transglutaminase after traumatic brain injury. J. Neurochem. **80**, 579–588.

UREN, A.G., WONG, L., PAKUSCH, M., et al. (2000). Survivin and the inner centromere protein INCENP show similar cell-cycle localization and gene knockout phenotype. Curr. Biol. **10**, 1319–1328.

WEI, L.H., HUANG, C.Y., CHENG, S.P., CHEN, C.A., and HSIEH, C.Y. (2001). Carcinosarcoma of ovary associated with previous radiotherapy. Int. J. Gynecol. Cancer **11**, 81–84.

WU, Q., COMBS, C., CANNADY, S.B., GELDMACHER, D.S., and HERRUP, K. (2000). Beta-amyloid activated microglia induce cell cycling and cell death in cultured cortical neurons. Neurobiol. Aging **21**, 797–806.

YAGITA, Y., KITAGAWA, K., OHTSUKI, T., et al. (2001). Neurogenesis by progenitor cells in the ischemic adult rat hippocampus. Stroke **32**, 1890–1896.

YANG, Y., GELDMACHER, D.S., and HERRUP, K. (2001). DNA replication precedes neuronal cell death in Alzheimer's disease. J. Neurosci. **21**, 2661–2668.

Address reprint requests to:
Jose A. Pineda, Ph.D.
E.F and W.L. McKnight Brain Institute
University of Florida
100 S Newell Dr., Bldg. 59
L1-118 Dept. of Pediatrics
Gainesville, FL 32610

E-mail: pinedja@peds.ufl.edu

Concurrent Assessment of Calpain and Caspase-3 Activation After Oxygen–Glucose Deprivation in Primary Septo-Hippocampal Cultures

Jennifer K. Newcomb-Fernandez, Xiurong Zhao, *Brian R. Pike, †Kevin K. W. Wang, ‡Andreas Kampfl, ‡Ronald Beer, *S. Michelle DeFord, and *Ronald L. Hayes

*University of Texas Health Science Center-Houston, Department of Neurosurgery, The Vivian L. Smith Center for Neurologic Research, Houston, Texas, *Evelyn F. and William L. McKnight Brain Institute of the University of Florida, Department of Neuroscience, Gainesville, Florida, and †Park-Davis Pharmaceutical Research, Warner-Lambert Company, Ann Arbor, Michigan, U.S.A.; and ‡University Hospital Innsbruck, Department of Neurology, Innsbruck, Austria*

Summary: The contributions of calpain and caspase-3 to apoptosis and necrosis after central nervous system (CNS) trauma are relatively unexplored. No study has examined concurrent activation of calpain and caspase-3 in necrotic or apoptotic cell death after any CNS insult. Experiments used a model of oxygen–glucose deprivation (OGD) in primary septo-hippocampal cultures and assessed cell viability, occurrence of apoptotic and necrotic cell death phenotypes, and protease activation. Immunoblots using an antibody detecting calpain and caspase-3 proteolysis of α-spectrin showed greater accumulation of calpain-mediated breakdown products (BDPs) compared with caspase-3–mediated BDPs. Administration of calpain and caspase-3 inhibitors confirmed that activation of these proteases contributed to cell death, as inferred by lactate dehydrogenase release. Oxygen–glucose deprivation resulted in expression of apoptotic and necrotic cell death phenotypes, especially in neurons. Immunocytochemical studies of calpain and caspase-3 activation in apoptotic cells indicated that these proteases are almost always concurrently activated during apoptosis. These data demonstrate that calpain and caspase-3 activation is associated with expression of apoptotic cell death phenotypes after OGD, and that calpain activation, in combination with caspase-3 activation, could contribute to the expression of apoptotic cell death by assisting in the degradation of important cellular proteins. **Key Words:** Apoptosis—Calpain—Caspases—Necrosis—Stroke—TBI.

Increased activation of calpain and caspase-3 occurs in many central nervous system (CNS) injuries and diseases. Caspase-3 is considered a key executioner in the apoptotic cell death cascade and shares numerous substrates with the Ca^{2+}-dependent protease calpain, including the cytoskeletal protein α-spectrin (Wang, 2000). Studies examining animal models of ischemia have reported increased calpain (Bartus et al., 1995; Roberts-

Lewis et al., 1994; Yokota et al., 1995; Rami et al., 2000) or caspase-3 (Chen et al., 1998; Namura et al., 1998) activation after injury. Furthermore, inhibition of calpain (Hong et al., 1994; Markgraf et al., 1998) or caspase-3 (Fink et al., 1998; Himi et al., 1998) reduced infarct volume, substrate proteolysis, DNA fragmentation, and hippocampal cell death after focal and global ischemia. Activation of these proteases also has been observed in animal models of traumatic brain injury (TBI) (Newcomb et al., 1997; Pike et al., 1998a; Saatman et al., 1996; Yakovlev et al., 1997; Clark et al., 2000; Beer et al., 2000; Buki et al., 2000). Inhibition of calpain (Postmantur et al., 1997) or caspase-3 (Yakovlev et al., 1997) is protective in these models, although conflicting data has been reported (Clark et al., 2000; Saatman et al., 2000). However, few investigations have examined concurrent activation of calpain and caspase-3 after CNS injury or disease (Buki et al., 2000; Nath et al., 1998; Pike et al., 1998a).

Although apoptosis and necrosis occur after ischemia (Linnik et al., 1993) and TBI (Colicos and Dash, 1996; Newcomb et al., 1999; Rink et al., 1995), the relation between protease activation and the expression of apoptotic and necrotic cell death phenotypes is relatively unexplored. Traditionally, calpain activation has been associated with necrosis, and caspase-3 activation with apoptosis. Although caspase-3 activation has not been detected in models of necrosis (Wang et al., 1996; Zhao et al., 1999), calpain activation has been implicated in various models of apoptosis (Nath et al., 1996; Pike et al., 1998*b*; Squier et al., 1994; Vanags et al., 1996). However, inconsistencies in criteria associated with cell death phenotypes have complicated data interpretation (Charriaut-Marlangue and Ben-Ari, 1995).

Oxygen–glucose deprivation (OGD) is a widely used *in vitro* model of ischemia, which produces apoptotic (Kalda et al., 1998) and necrotic (Gwag et al., 1995; Goldberg and Choi, 1993) cell death phenotypes and increased calpain and caspase-3 activity (Nath et al., 1998). Currently, no study has investigated the concurrent activation of calpain and caspase-3 in archetypal necrotic and apoptotic cell death phenotypes after any CNS insult. The current study sought to determine the contributions of these proteases to apoptotic and necrotic cell death after OGD. The current findings demonstrate that coactivation of calpain and caspase-3 is usually associated with the expression of apoptotic cell death phenotypes after OGD.

MATERIALS AND METHODS

Primary septo-hippocampal cultures

Septi and hippocampi were dissected from 18-day-old rat fetuses, dissociated by trituration, and the dissociated cells were plated on poly-L-lysine coated 24-well culture plates, 6-well culture plates or 12-mm German Glass (Erie Scientific, Portsmouth, NH, U.S.A.) at a density of 4.36×10^5 cells/mL. Cultures were maintained in Delbecco's modified Eagle's medium (DMEM) with 10% fetal bovine serum in a humidified incubator in an atmosphere of 5% CO_2 at 37°C. After 5 days in culture, the media was changed to DMEM with 5% horse serum. Subsequent media changes were performed three times a week. Experiments were performed on days 10 to 11 *in vitro* when astroglia had formed a confluent monolayer beneath morphologically mature neurons. All animal studies conformed to the guidelines outlined in *Guide for the Care and Use of Laboratory Animals* from the National Institutes of Health and were approved by the University of Florida and the University of Texas-Houston Health Science Center Animal Welfare Committee.

Oxygen–glucose deprivation

To achieve oxygen–glucose deprivation (OGD), a technique similar to that described by Copin et al. (1998) was used. Normal media was replaced with low glucose media (Hank's balanced salt solution containing 1.8 mmol/L Ca^{2+}, 0.8 mmol/L Mg^{2+}, and 0.2 g/L d-glucose) and culture plates were placed in an airtight chamber (Billups-Rothenberg, Del Mar, CA, U.S.A.). The chamber was flushed with 95% N_2/5% CO_2 for 3 minutes, sealed, and placed in a 37°C incubator for the appro-

priate duration. Initial experiments that manipulated the amount of time (1 to 10 minutes) the chamber was flushed with 95% N_2/5% CO_2 confirmed that 3 minutes of flushing combined with the low glucose media produced an environment severe enough to result in a consistent model of cell injury. After the insult, low glucose media was replaced with DMEM (serum-free) and cultures were returned to a normoxic environment. Initial experiments deprived cells of oxygen and glucose for various durations (1 to 12 hours) and samples were collected 24 hours after the cultures had returned to a normal environment. These data suggested that 10 hours of OGD resulted in substantial cell death and protease activation. To examine the effects of altering the length of reperfusion (that is, duration of normoxia after OGD) samples were collected at various times (immediately through 48 hours) after 10 hours of OGD. Subsequent experiments focused on 10 hours of OGD combined with 24 hours of reperfusion, unless stated otherwise.

Chemical inducers of apoptotic or necrotic cell death phenotypes

To provide comparisons of OGD with classic apoptotic and necrotic profiles, cultures were treated with staurosporine, a general protein kinase inhibitor, or maitotoxin, a potent marine toxin that activates both voltage-sensitive and receptor-operated calcium channels (Wang et al., 1996). Cultures were challenged with 0.5 μmol/L staurosporine for 24 hours, a dose and duration that produces apoptotic but not necrotic neuronal cell death in this *in vitro* system (Pike et al., 1998*b*). Separate cultures were treated with maitotoxin (0.1 nmol/L) for 1 hour, a dose and duration that produces an exclusively necrotic cell death profile in neurons and glia and is associated with calpain, but not caspase-3 activation (Zhao et al., 1999).

Pharmacologic inhibition of calpain and caspase activation

Cultures were pretreated 1 hour before and were cotreated during OGD, with various doses of calpain inhibitor-3 (CI-3, [MDL28170], 1 to 300 μmol/L; CalBiochem, San Diego, CA, U.S.A.), the pan-caspase inhibitor (Z-D-DCB, 50 to 200 μmol/L; Bachem, Philadelphia, PA, U.S.A.) or the specific caspase-3 inhibitor (z-DEVD-fmk, 50 to 200 μmol/L; CalBiochem). Stock solutions (50 mmol/L) of CI-3 (in dimethyl sulfoxide), Z-D-DCB (in EtOH), and z-DEVD-fmk (in dimethyl sulfoxide) were added directly to the low glucose media for the 1-hour pretreatment, and then cells were deprived of oxygen. Initial experiments confirmed that incubating cells with low glucose media for 1 hour had no effect on control cells or injury magnitude in cells later exposed to OGD (data not shown). After OGD, low glucose media was replaced with DMEM (serum-free) containing fresh inhibitor. Samples were collected 12 or 24 hours after OGD for lactate dehydrogenase (LDH) release and immunoblot analyses. Western blot analyses confirmed whether the drugs and doses used inhibited activation of calpain and caspase-3–like proteases inferred by α-spectrin proteolysis.

Determination of lactate dehydrogenase activity

Lactate dehydrogenase activity assessed cell viability (Koh and Choi, 1987) in experiments examining the effects of OGD and protease inhibition. Lactate dehydrogenase released from damaged cells was measured by standard kinetic assay for pyruvate (Hoffmann-LaRoche Ltd., Basel, Switzerland). Briefly, culture medium was removed from each well and centrifuged at 5,000 *g* for 5 minutes. One hundred microliters of supernatant was transferred to each well of 96-well flat bottom plate and 100 μL of detection reagent was added. After incubation, the

absorbance of samples was measured at 490 nm using Bio-Rad model 450 microplate reader (Hercules, CA, U.S.A.).

Annexin V and propidium iodide staining

Control cells and cells exposed to OGD, staurosporine, or maitotoxin were simultaneously stained with Annexin V and propidium iodide (PI) to differentiate apoptotic and necrotic cell death phenotypes. Cells were rinsed with phosphate-buffered saline (PBS) and incubated in staining solution consisting of HEPES buffer, Annexin V fluorescein labeling reagent (Molecular Probes; Eugene, OR, U.S.A.), and PI (Molecular Probes) for 15 minutes in the dark. Stained cells were examined with a Zeiss Axiovert 135 fluorescence microscope (Oberkochen, Germany) fitted with a filter combination that allowed green and red fluorescing cells to be seen simultaneously. The number of apoptotic and necrotic cells was calculated (10 sequential 320× fields were counted and averaged per well) for n = 3 wells per condition.

DNA gel electrophoresis

DNA gel electrophoresis was performed as previously described (Zhao et al., 2000; Gong et al., 1994). At the appropriate time after injury, cells were collected by centrifugation, fixed in 70% cold ethanol, and stored in fixative at −20°C for 24 to 72 hours. After subsequent centrifugation and removal of ethanol, cell pellets were resuspended in phosphate-citrate buffer at room temperature for 1 hour, centrifuged, and the supernatant was concentrated by vacuum in a SpeedVac concentrator (ThermoSavant, Holbrook, NY, U.S.A.). The pellet was incubated in Nonidet NP-40 and DNase-free RNase followed by proteinase K. After the incubation, 6× loading buffer was added and the contents of the tube were transferred to a 1.5% agarose gel. Electrophoresis was performed in 1× 0.1 mol/L Tris, 0.09 mol/L boric acid, 1 mmol/L EDTA, pH 8.4 at 40 V for 2 hours. DNA was visualized and photographed under UV light after staining with 5 μg/mL ethidium bromide.

DNA fragmentation ELISA

Apoptotic cell death also was examined with an assay that allowed specific determination of mono- and oligonucleosomes in the cytoplasmic fraction of cell lysates (Cell Death Detection ELISA Plus; Hoffman-LaRoche Ltd., Basel, Switzerland). At the appropriate time after injury, cells were collected by centrifugation and 2 mL lysis buffer was mixed with the pellet. The solution was incubated for 30 minutes at room temperature and stored at −20°C for 24 to 72 hours. After thawing, diluted samples (5 μL sample + 15 μL lysis buffer) were added to each well of a streptavidin-coated, 96-well microtiter plate (separate studies confirmed that this dilution resulted in a suitable cell concentration, data not shown). Eighty microliters of reagent solution containing incubation buffer, anti–histone-biotin, and anti–DNA-POD was added to each well and incubated with the sample on a shaker for 2 hours. The solution was removed and wells were rinsed with incubation buffer to remove unbound antibody. The amount of POD retained in the immunocomplex—and thus the amount of DNA fragments—was determined colorimetrically with the substrate ABTS using a microplate reader (Bio-Rad Model 450) at 405 nm with a reference filter of 490 nm. Absorbance values were calculated and reported as percent of control.

Assessment of caspase-3 and calpain activity

The cytoskeletal protein α-spectrin contains sequence motifs preferred by calpain and caspase-3 proteases; thus, activation of these proteases can be assessed concurrently by immunoblot identification of calpain and/or caspase-3 signature cleavage products. Although calpains and caspases produce initial frag-

ments of nearly identical size (150 kDa), calpains further process α-spectrin into a distinctive breakdown product (BDP) of 145 kDa (Harris et al., 1988; Nath et al., 1996), whereas caspase-3 produces a unique 120-kDa BDP (Wang et al., 1998*b*). Notably, the initial 150-kDa fragment produced by calpain differs from that produced by the caspases. Immunocytochemistry using antibodies specific for this calpain-mediated fragment (SBDP 150) or the 120-kDa fragment produced by caspase-3 (SBDP 120) allows detection of calpain- and/or caspase-3–mediated proteolysis of α-spectrin in individual cells. Caspase-3 activation also can be inferred by the appearance of BDPs to the proenzyme, because activation occurs when caspase-3 is proteolyzed into smaller subunits.

Sodium dodecyl sulfate-polyacrylamide gel electrophoresis and immunoblotting. Gel electrophoresis and immunoblotting were performed as described previously (Pike et al., 2000). At the appropriate time after injury, media was removed and cells were collected from each well with lysis buffer and sheared with a 25-gauge needle. Protein content was assayed by the Micro BCA method (Pierce, Rockford, IL, U.S.A.). For protein electrophoresis, equal amounts of total protein (25 μg) were prepared in 4× loading buffer and heated at 95°C for 10 minutes. For analysis of α-spectrin proteolysis, samples were resolved in a vertical electrophoresis chamber using a 4% stacking gel over a 6.5% acrylamide resolving gel. Separated proteins were laterally transferred to a nitrocellulose membrane (0.45 μm). For analysis of caspase-3 proteolysis, samples were resolved using a 4% to 20% gradient acrylamide gel or a Tris-Tricine gel (16.5% + 4% stacking). Separated proteins were laterally transferred to a nitrocellulose membrane (0.2 μm). Nitrocellulose membranes were stained with Panceau red (Sigma, St. Louis, MO, U.S.A.) to ensure even transfer of all samples to the membranes and to confirm that equal amounts of protein were loaded in each lane. Blots were blocked overnight in 5% nonfat milk in 20 mmol/L Tris, 0.15 mol/L NaCl, and 0.005% Tween-20 at 4°C.

Immunoblots were probed with an anti–α-spectrin monoclonal antibody (Affiniti Research Products, U.K.) that detects intact α-spectrin (MW$_r$ = 240 kDa) and 150-, 145-, and 120-kDa BDP, as described previously (Pike et al., 2000). Separate blots were probed with a caspase-3 polyclonal antibody (1:500; Santa Cruz Biotechnology, Santa Cruz, CA, U.S.A.) that detects the caspase-3 proenzyme (32 kDa) and proteolytic fragments. After incubation in primary antibody for 2 hours at room temperature, blots were incubated in peroxidase-conjugated goat anti-rabbit IgG (1:3000) for 1 hour. Enhanced chemiluminescence reagents (ECL; Amersham, Buckinghamshire, U.K.) were used to visualize immunolabeling on Hyperfilm (Hyperfilm ECL; Amersham).

Semiquantitative evaluation of protein levels detected by immunoblotting was performed through computer-assisted, one-dimensional densitometric scanning (AlphaImager 2000 Digital Imaging System; San Leandro, CA, U.S.A.). Data were acquired as integrated densitometric values and transformed to percentages of the densitometric values obtained from control samples. Data from multiple Western blots (n = 4) were combined and analyzed statistically.

Calpain- and caspase-3–mediated α-spectrin BDPs in individual cells. Cells were cultured on German Glass for immunocytochemistry protocols. Control cultures or cells exposed to OGD, staurosporine, or maitotoxin were fixed in 4% paraformaldehyde for 5 minutes and rinsed in PBS. Cells were blocked in 10% normal goat serum in PBS for 30 minutes at 37°C and incubated simultaneously in primary antibodies specific for SBDP 150 (1:100, polyclonal, made in rabbit; gift

from T.C. Saido, Japan, (Saido et al., 1993)) and SBDP 120 (1:100, polyclonal, made in chicken; gift from Kevin Wang, Parke-Davis, Ann Arbor, MI (Buki et al., 2000)) for 30 minutes at 37°C. After rinsing in PBS/0.05% Tween 20, cells were incubated in secondary antibodies linked to Alexa Fluor 488 (1:50, goat α-chicken; Molecular Probes, Eugene, OR, U.S.A.) or Alexa Fluor 568 (1:50, goat α-rabbit; Molecular Probes) for 30 minutes at 37°C. To assess nuclear morphology (that is, characteristics of necrotic or apoptotic alterations) cells were counterstained with the DNA dye, 4′ 6-diamidino-2-phenylindole, dihydrochloride (DAPI, 1:500; Molecular Probes). German Glass were mounted onto glass slides with Fluoromount-G (Southern Biotechnology Associates; Birmingham, AL, U.S.A.).

Cells were examined under oil immersion at 1000× magnification with a Zeiss Axiovert 135 fluorescence microscope equipped as described above. DAPI staining was viewed with a UV2A filter (Zeiss). Nuclear morphology was assessed in cells immunoreactive for SBDP 150, or SBDP 120, or both, and cells were categorized (blind to treatment condition) as healthy, apoptotic, or necrotic. Nuclei of healthy cells can be identified by a homogenous and diffuse fluorescent chromatin, whereas cells classified as apoptotic fluoresce intensely and are characterized by highly condensed chromatin, visibly shrunken and often irregular shaped nuclei, margination of chromatin along the periphery of the nuclear envelope, or by the separation of the nucleus into discrete nuclear fragments (apoptotic bodies). In contrast, necrotic cells fluoresce brightly with pyknotic chromatin where nuclei have maintained their basic morphology or have become rounded or swollen in appearance. These cells also fail to exhibit apoptotic morphology (Schmechel, 1999; Purnanam and Boustany, 1999). Using these criteria, the number of healthy, apoptotic, and necrotic SBDP 150 and SBDP 120 immunoreactive cells were quantified in control and OGD cultures.

Analysis of cell types

Control cells or cells exposed to OGD were prepared for immunocytochemistry as described above. Cells were labeled with both neuronal nuclear marker (NeuN) and microtubule-associated protein (MAP)2 or GFAP (glial fibrillary acidic protein) to evaluate neuronal and astroglial morphology, respectively. Using both NeuN and MAP2 allowed clear visualization of the neuronal cell body and processes. All cells were blocked in 10% normal goat serum in PBS and were incubated in primary antibodies specific for NeuN (1:1000, monoclonal; Chemicon, Temecula, CA, U.S.A.) and MAP2 (1:1000, monoclonal; Sternberger Monoclonals, Lutherville, MD, U.S.A.) or GFAP (1:1000, monoclonal; Sigma). After rinsing in PBS/0.05% Tween 20, cells were incubated in secondary antibody linked to Alexa Fluor 488 (1:50, goat α-mouse; Molecular Probes). Cells were counterstained with DAPI and mounted onto glass slides with Fluoromount-G.

Samples immunolabeled with NeuN and MAP2 were examined under low magnification to assess neuronal loss after OGD (10 sequential 320× fields were counted and added per sample, n = 6). Samples immunolabeled with GFAP also were examined under low magnification, however quantitative data on loss of GFAP-positive cells could not be obtained because of the high density of these cells and the inability to differentiate individual glia. Under high magnification (1000×), DAPI staining was examined in NeuN- and/or MAP2-positive cells and GFAP-positive cells (50 random immunoreactive cells per sample) to assess the nuclear morphology of neurons and astroglia, respectively. Values for healthy, apoptotic, and necrotic

neurons and astroglia were calculated for control and OGD cells using the criteria described above.

Statistical analysis

Data were evaluated by one-way analysis of variance and *post hoc* least significant difference *t* test. Values are given as mean ± SD. Differences were considered significant at $P \leq 0.05$.

RESULTS

Effects of oxygen–glucose deprivation on primary mixed septo-hippocampal cultures

Effects of oxygen–glucose deprivation duration and reperfusion. An initial set of experiments (data not shown) was conducted to evaluate duration of OGD on cell viability. Primary mixed septo-hippocampal cultures were deprived of oxygen and glucose for 1, 6, 8, 10, or 12 hours and media was collected 24 hours after cultures were returned to normal conditions for analysis of LDH release. Reported as percent of control, significant increases in LDH release ($P < 0.01$) occurred after 6 (204% ± 18.1%), 8 (233% ± 30.1%), 10 (895% ± 43.1%), and 12 (725% ± 70.5%) hours of OGD. Subsequent experiments (data not shown) investigated the effect of reperfusion length on cell viability. Samples were subjected to OGD for 10 hours and media were collected immediately or after 3, 12, 24, or 48 hours of reperfusion for analysis of LDH release. Significant increases in LDH release were evident immediately after injury (172% ± 15.2%, $P < 0.05$) compared with control cultures. Moreover, increasing the length of reperfusion resulted in a time-dependent and significant increase in LDH release ($P < 0.001$) at all later times tested—3 (367% ± 51.7%), 12 (561% ± 5.6%), 24 (674% ± 14.7%), and 48 (784% ± 5.6%) hours after injury, compared with control samples.

Characterization of cell death phenotypes after oxygen-glucose deprivation. To distinguish apoptotic and necrotic cell death, control cells and cells subjected to OGD (10 hours + 24 hours of reperfusion) were stained with Annexin V and PI (data not shown). Staurosporine- (0.5 mmol/L for 24 hours) and maitotoxin- (0.1 nmol/L for 1 hour) treated cells were used as positive controls of apoptosis and necrosis, respectively. Values are reported as total apoptotic or necrotic cells per well (10, 320× fields). Uninjured control cultures contained few apoptotic (78.0 ± 40.0) or necrotic (8.3 ± 2.1) cells. Cultures subjected to OGD contained significantly ($P < 0.001$) more apoptotic (356.3 ± 32.0) and necrotic (180.7 ± 37.4) cells compared with control cultures. In comparison, staurosporine treatment produced a significant increase ($P < 0.001$) in apoptotic cells (389.3 ± 37.5) with fewer necrotic cells (38.3 ± 14.4), whereas maitotoxin treatment resulted in a significant increase ($P < 0.001$) in necrotic cells (597.0 ± 73.4) with fewer apoptotic cells (13.7 ± 3.8) compared with control cultures.

Examination of DAPI staining (10, 1000× fields) revealed morphologic changes in chromatin staining that

were clearly distinguishable from the classic necrotic phenotype (Fig. 1A and 1B). These nonnecrotic changes showed different evolutionary stages of chromatin margination, condensation, and formation of apoptotic bodies. Thus, these nuclear profiles were termed apoptotic-like. Most stained nuclei in control cultures were healthy; however, some apoptoticlike nuclei were observed and were probably because of spontaneous apoptosis (Fig. 1A). Compared with control cultures, OGD cultures contained significantly less healthy nuclei ($P < 0.001$) and significantly more apoptoticlike nuclei ($P < 0.001$). Necrotic nuclei were rarely observed in either control or
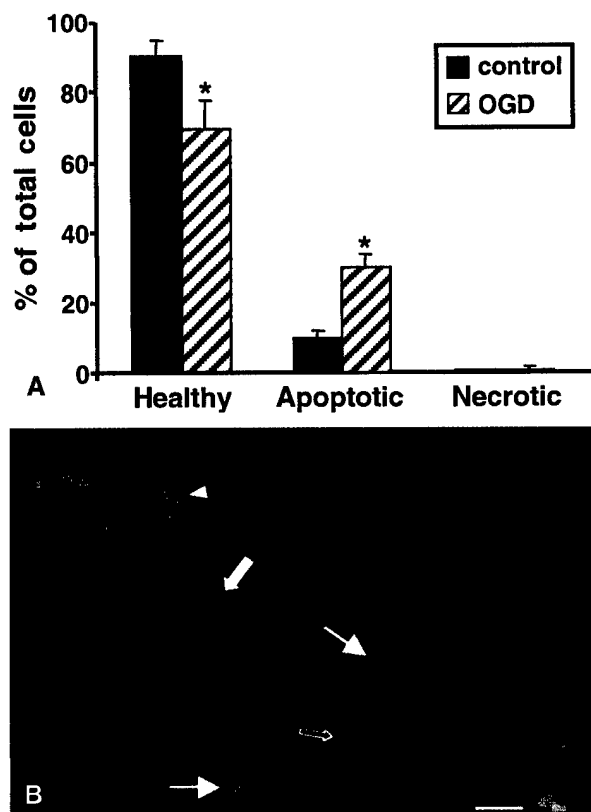
FIG. 1. Analysis of nuclear morphology after oxygen–glucose deprivation (OGD). **(A)** Control cultures and cultures deprived of oxygen and glucose (10 hours + 24 hours of reperfusion) were stained with DAPI, and cells were characterized as healthy, apoptoticlike, or necrotic based on nuclear morphology. Control cultures contained mostly healthy nuclei (90.1% ± 6.1%), although apoptoticlike nuclei (9.6% ± 2.9%) were detected. Compared with control cultures, OGD contained significantly fewer healthy nuclei (69.3% ± 10.5%) and significantly more apoptoticlike nuclei (30.0% ± 5.4%). No significant differences were observed in the percentage of necrotic cells between control (0.3% ± 0.2%) and OGD (0.7% ± 1.0%) cultures. *$P < 0.001$. **(B)** DAPI staining of septo-hippocampal cultures after OGD. Representative image illustrating the typical distribution of cell death phenotypes after OGD (10 hours + 24 hours of reperfusion). Nuclei exhibiting apoptoticlike morphology such as chromatin condensation (arrowhead), irregular-shaped nuclei (open arrow), and the formation of apoptotic bodies (thin arrows) were frequently detected after OGD. Healthy nuclei (wide arrow) also were observed after injury. Scale bar = 1 µm.

OGD cultures. Figure 1B shows a representation of the typical distribution of cell death phenotypes after OGD in this culture system. Nuclei exhibiting apoptoticlike morphology were frequently detected after OGD, as well as cells with healthy nuclei. Surprisingly, examination of DAPI staining in OGD cultures failed to reveal a substantial number of necrotic cells, in contrast with data collected with Annexin V and PI staining. This reduction in necrotic cells may be caused by the frequent rinses and incubations performed during the immunocytochemistry and DAPI staining protocol that may have caused many necrotic cells to detach and go undetected by DAPI in the culture system. However, quite similar data were obtained using these separate techniques to calculate the number of apoptoticlike cells per sample. If values are adjusted to reflect the different field magnifications (320× for Annexin and 1000× for DAPI), the average number of apoptoticlike cells per sample is similar for Annexin (356.3 cells per sample) and DAPI (332.8 cells per sample, data not shown). These data stress the reliability of the authors' assessments of the contribution of apoptosis to cell death in the culture system.

Condensation and aggregation of chromatin, as shown with DAPI staining (Fig. 1B), may occur independently of endonuclease activation (Oberhammer et al., 1993). Therefore, two separate techniques were used to qualitatively (Fig. 2A) and quantitatively (Fig. 2B) assess internucleosomal DNA fragmentation, and thus endonuclease activation, after OGD. DNA electrophoresis (Fig. 2A) revealed a robust ladder pattern, characteristic of internucleosomal DNA fragmentation, after 10 hours of OGD with 12, 24, and 48 hours of reperfusion. Faint bands also were detected after 3 hours of reperfusion. Staurosporine treatment produced a characteristic DNA ladder pattern, whereas control samples and cells subjected to maitotoxin failed to show any internucleosomal fragments.

As an additional indicator of internucleosomal fragmentation, the amount of mono- and oligonucleosomes in the cytoplasmic fraction of cell lysates was quantitatively assessed (Fig. 2B). Control cultures showed little DNA fragmentation, whereas cells deprived of oxygen and glucose for 10 hours contained significantly more mono- and oligonucleosomes after 24 ($P < 0.001$) and 48 ($P < 0.001$) hours of reperfusion, but not after 3 or 12 hours of reperfusion. In comparison, staurosporine treatment resulted in a significant increase ($P < 0.001$) in mono- and oligonucleosomes, whereas samples exposed to maitotoxin were not statistically different from control samples.

Induction of cell death by oxygen–glucose deprivation in neurons and glia. To identify the type of cell (that is, neuron vs. astroglia) affected by OGD, primary mixed septo-hippocampal cultures were stained with NeuN and MAP2 (for neurons) or GFAP (for astroglial)
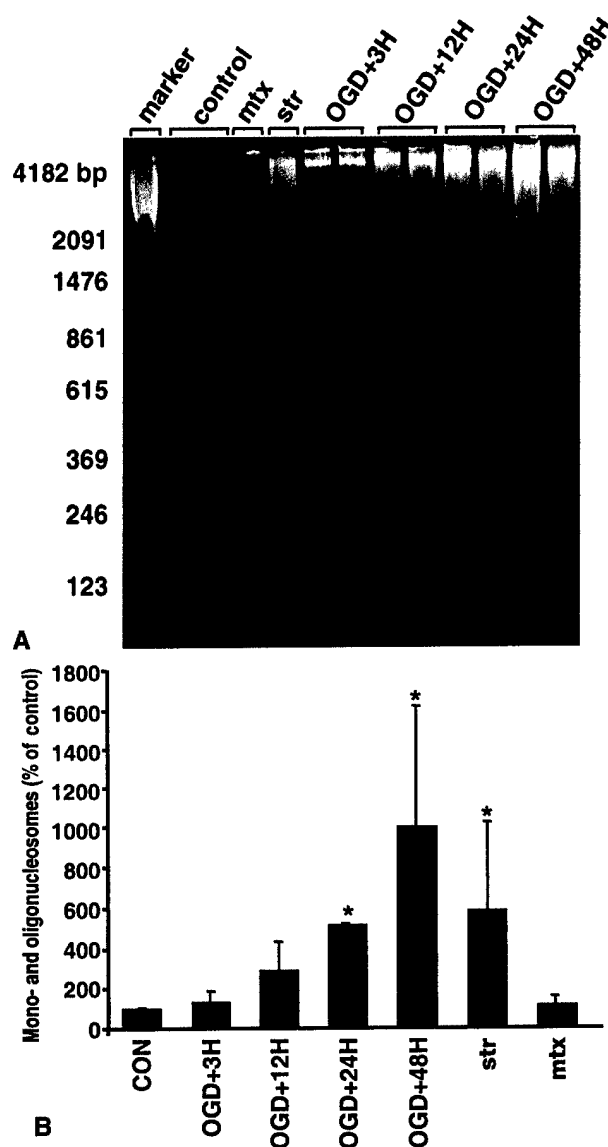
FIG. 2. Assessment of internucleosomal DNA fragmentation after oxygen–glucose deprivation (OGD). **(A)** DNA electrophoresis. Samples collected from control and maitotoxin (mtx)-treated cultures showed no internucleosomal DNA fragmentation, whereas staurosporine (str) treatment produced a characteristic DNA ladder pattern. Cultures subjected to OGD for 10 hours and collected 3 hours after injury exhibited a faint ladder. Prominent DNA laddering was observed 12, 24, and 48 hours after injury. **(B)** DNA fragmentation assay. DNA fragmentation was quantitatively assessed by detection of mono- and oligonucleosomes in the cytoplasmic fraction of cell lysates. Analysis of control cultures demonstrated little DNA fragmentation, similar to cells deprived of oxygen and glucose for 10 hours after 3 (129% ± 46.8%) or 12 (287% ± 163.0%) hours of reperfusion. However, a significant increase in mono- and oligonucleosomes was detected in cells deprived of oxygen and glucose for 10 hours after 24 (513% ± 5.6%) and 48 (998% ± 606.9%) hours of reperfusion. Staurosporine (str) treatment resulted in a significant increase (582% ± 441.7%) in mono- and oligonucleosomes, whereas samples exposed to maitotoxin (mtx) were not statistically different from control samples (111% ± 58.1%). *$P < 0.001$.

and counterstained with DAPI (Fig. 3). Low magnification examination of NeuN and MAP2 staining in OGD cultures revealed a significant loss (68% ± 9.3% of control values, $P < 0.001$) of immunoreactive (IR) neurons (data not shown). Examination of GFAP staining in cells subjected to OGD showed that OGD had a modest effect on astroglia that was not readily apparent under low magnification.

High magnification (1000×) examination of NeuN, or MAP2 IR cells, or both (Fig. 3), showed that the majority of positive cells in control cultures possessed large cell bodies and several intact processes that were intensely labeled for both neuronal markers (Fig. 3A). These cells contained healthy, oval-shaped nuclei with diffuse chromatin distribution (Fig. 3B). In contrast, NeuN and MAP2 staining of OGD cultures showed a substantial number of neurons with shrunken cell bodies and fragmented processes (Fig. 3C). Nuclei of these neurons were shrunken, irregularly shaped, and possessed highly condensed chromatin (Fig. 3D). Apoptoticlike nuclei that were not IR for NeuN or MAP2 also were observed (Fig. 3D). These cells may have been apoptotic astroglia, or more likely, neurons in an advanced stage of apoptosis in which the phenotype is most apparent and degeneration of cellular proteins may compromise the retention of epitopes necessary for cell type identification. Quantitative analysis of DAPI staining in NeuN, or MAP2 IR cells, or both (50 random IR cells per sample), demonstrated that the majority of positive cells in control cultures exhibited healthy nuclear morphology (83.3% ± 4.4%). Although cells with apoptoticlike nuclei (16.7% ± 1.8%) were occasionally observed, neurons with necrotic nuclei were not detected in this set of control cultures. Analysis of DAPI staining in OGD cultures revealed a significantly lower percentage of healthy nuclei (57.3% ± 9.3%, $P < 0.001$) and significantly higher percentage of apoptoticlike nuclei (40.3% ± 8.6%, $P < 0.001$), compared with control cultures. Although OGD cultures also contained more necrotic nuclei (2.3% ± 1.5%) than control cultures, necrotic cells were rarely observed.

Examination of GFAP staining in control and OGD cultures showed that most GFAP-positive cells were healthy astroglia with large cell bodies, extensive processes, and diffuse and even immunoreactivity (Fig. 3E and 3G, respectively). Astroglial nuclei were large and oval-shaped with even chromatin distribution (Fig. 3F and 3H). Although most IR cells in OGD cultures appeared healthy, cells with shrunken cell bodies, broken processes, and aggregated GFAP immunoreactivity also were observed (Fig. 3G).

These cells possessed shrunken nuclei with highly condensed chromatin and apoptotic bodies (Fig. 3H). Quantitative assessment of DAPI staining in GFAP IR cells (50 random IR cells per sample) showed that most GFAP-positive cells in control (98.3% ± 12.7%) and
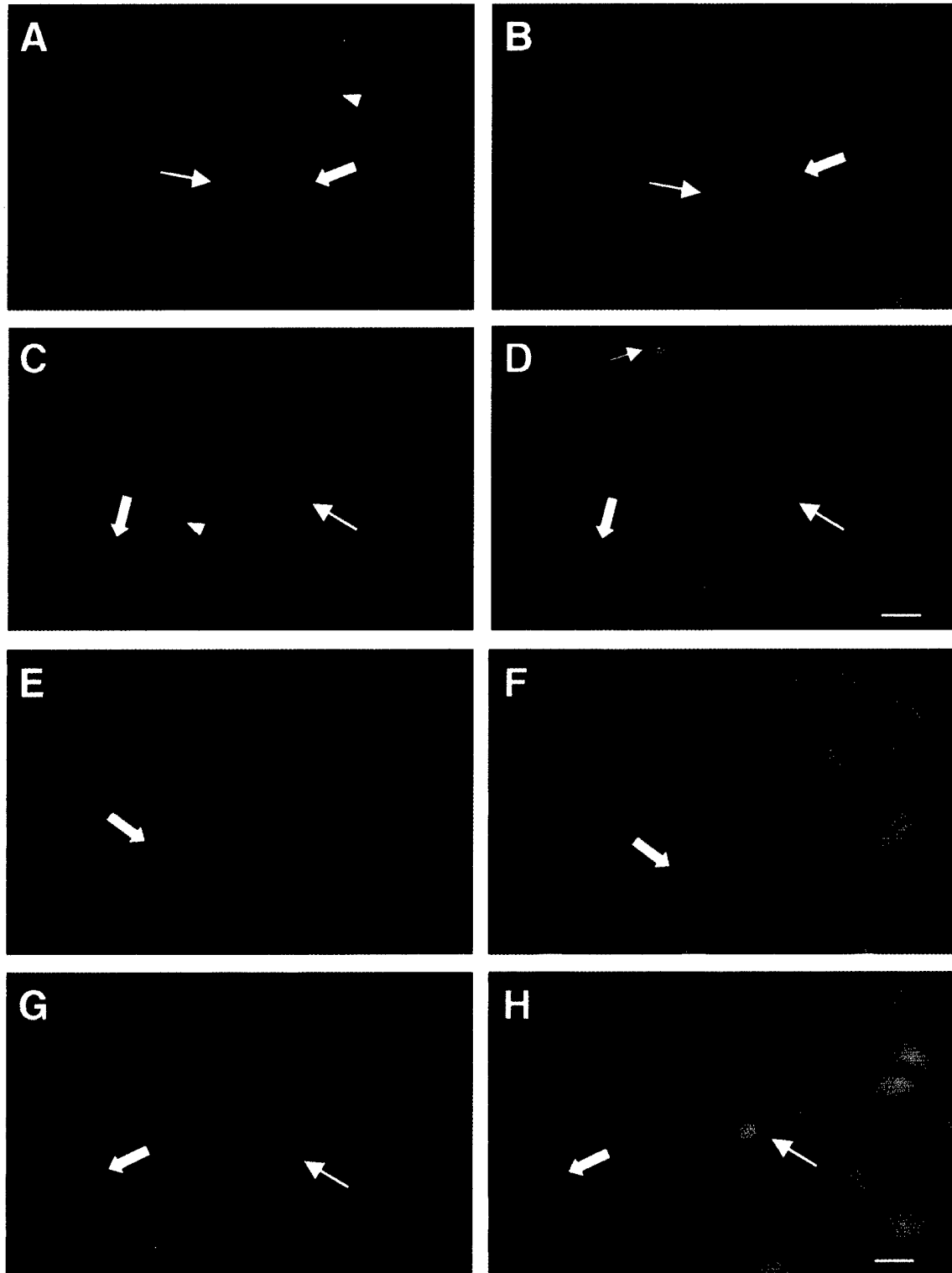
FIG. 3. Neuronal and glial morphology after oxygen–glucose deprivation (OGD). Cultures were immunolabeled with NeuN and MAP2 or GFAP (glial fibrillary acidic protein) and were counterstained with DAPI to assess morphologic and nuclear changes after OGD (10 hours + 24 hours of reperfusion). Cells were examined under high magnification (1000x). **(A)** NeuN/MAP2 immunoreactive (IR) cells in control cultures possessed large cell bodies (thin arrow, wide arrow) and several intact processes (arrowhead) that were intensely labeled for both neuronal markers. **(B)** These cells contained healthy, oval-shaped nuclei with diffuse chromatin distribution (thin arrow, wide arrow). **(C)** Cultures deprived of oxygen and glucose showed a substantial number of neurons with shrunken cell bodies (thin arrow, wide arrow) and fragmented processes (arrowhead). **(D)** Neuronal nuclei were shrunken, irregularly shaped and possessed highly condensed chromatin (thin arrow, wide arrow). Apoptotic nuclei not IR for NeuN or MAP2 also were observed (small arrow). **(E)** Control cultures contained healthy astroglia with large cell bodies, extensive processes, and diffuse and even immunoreactivity (arrow). **(F)** Nuclei were large and oval-shaped with even chromatin distribution (arrow). **(G)** OGD cultures contained a majority of healthy GFAP-positive cells (wide arrow), but cells with shrunken cell bodies, broken processes, and aggregated GFAP immunoreactivity also were observed (thin arrow) and characterized as apoptoticlike. **(H)** Nuclei in healthy astroglia resembled those detected in control cultures (wide arrow). Apoptotic astroglia contained shrunken nuclei with highly condensed chromatin and apoptotic bodies (thin arrow). Scale bars = 1 μm.

OGD (91.4% ± 27.2%) cultures possessed healthy nuclei. DAPI staining revealed some effects of OGD, including a decreased percentage of healthy nuclei and an increased percentage of apoptoticlike nuclei (8.4% ± 2.0%), compared with control cells (1.6% ± 1.5%), but these differences were not statistically significant. Necrotic nuclei were rarely observed in either control (0.2% ± 0.5%) or OGD (0.2% ± 0.5%) cultures.

Calpain and caspase-3 proteolysis of α-spectrin after oxygen–glucose deprivation

Western blots. Activation of calpain and caspase-3 after OGD was assessed with Western blots examining proteolysis of α-spectrin (Fig. 4A and 4B). After 10 hours of OGD, samples were collected immediately (0 hour), 3, 12, 24, or 48 hours after cultures were returned to a normal environment. Control samples and samples

deprived of oxygen and glucose for 10 hours and collected immediately after injury showed no evidence of calpain-mediated proteolysis of α-spectrin. However, 3 hours after reperfusion, proteolysis of α-spectrin into 150-kDa and calpain-mediated 145-kDa BDPs was significantly increased over control values ($P < 0.001$). Degradation of α-spectrin continued and proteolysis into the 145-kDa BDP also was increased after 12, 24, and 48 hours of reperfusion ($P < 0.001$). Modest degradation of native α-spectrin was observed after 48 hours of reperfusion ($P < 0.01$). Slight increases in caspase-3–mediated proteolysis were detected after injury, but formation of the 120-kDa BDP was variable and did not differ significantly from control. However, immunoblots detected proteolysis of the caspase-3 proenzyme to the activated isoform (Fig. 4C), suggesting that analyses of autolytic
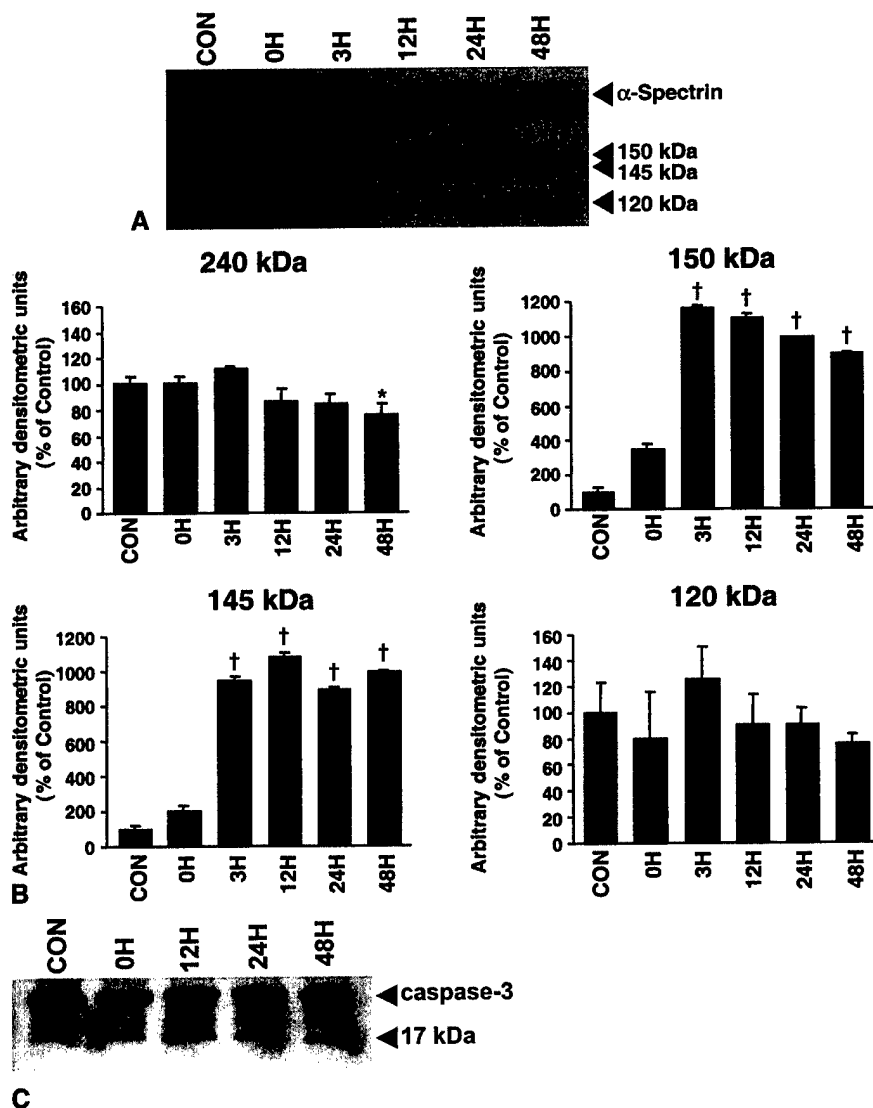
FIG. 4. Calpain- and caspase-3–mediated proteolysis of α-spectrin after oxygen–glucose deprivation (OGD). **(A)** Representative Western blot showing calpain- and caspase-3–mediated proteolysis of α-spectrin after OGD. Control samples and samples collected immediately (0 hour) after injury showed no evidence of calpain-mediated proteolysis of α-spectrin. Accumulation of the 150- and 145-kDa BDPs was detected 3, 12, 24, and 48 hours after OGD. Moderate increases in the caspase-3–mediated BDP were detected after injury, but formation of the 120-kDa BDP was variable. **(B)** Calpain- and caspase-3–mediated proteolysis of α-spectrin semiquantitative analysis. Data from multiple Western blots analyzing α-spectrin proteolysis were acquired as integrated densitometric values and transformed to percentages of the densitometric values obtained from control samples. Formation of the 150- and 145-kDa BDPs was increased after OGD with 3, 12, 24, and 48 hours of reperfusion, whereas modest degradation of native α-spectrin (240 kDa) was detected after 48 hours of reperfusion. Accumulation of the caspase-3–mediated 120-kDa BDP was variable. $*P < 0.01$. $†P < 0.001$. **(C)** Activation of caspase-3 after OGD. Proteolysis of caspase-3 (32 kDa) to the activated isoform (17 kDa) was examined after 10 hours of OGD and 0, 12, 24, or 48 hours of reperfusion. Degradation of the proenzyme (32 kDa) was evident 12, 24, and 48 hours after injury. Proteolysis of caspase-3 into the 17-kDa subunit was detected with all lengths of reperfusion examined.

activation of the caspase-3 proenzyme may be more sensitive than analyses of processing of cytoskeletal protein substrates.

Immunocytochemistry. Primary mixed septo-hippocampal cultures were double-labeled with antibodies specific for calpain (SBDP 150) and caspase-3 (SBDP 120) mediated α-spectrin proteolytic fragments and were counterstained with DAPI (Fig. 5). Across all treatment conditions, cells with evidence of nuclear damage exhibited strong immunoreactivity, whereas most healthy cells showed faint or no immunoreactivity. Cultures deprived of oxygen and glucose had significantly increased cellular colocalization of SBDP 150 and SBDP 120 (93.5 ± 16.7 cells per sample, $P < 0.001$), compared with control cultures (23 ± 8.6 cells per sample). Although OGD cultures contained substantially more IR cells than control cultures, examination of immunocytochemistry showed a similar distribution of protease activation, regardless of treatment condition (Fig. 5A and 5C). Virtually all IR cells in control and OGD cultures showed concurrent calpain and caspase-3 proteolysis in varying magnitudes (Fig. 5A and 5C). Immunolabeling in control (Fig. 5A) and OGD (Fig. 5C) cultures resulted in subcellular localization of BDPs unique from staurosporine (Fig. 5E) or maitotoxin cultures (Fig. 5G). In control and OGD cells, SBDP 150 was localized exclusively within the cell body, that is, near the nuclear membrane. Conversely, SBDP 120 immunoreactivity was detected throughout the entire cell body, specifically along the outer boundary of the cell membrane, and in the proximal processes (Fig. 5A and 5C). The nuclei of IR cells were shrunken, irregularly shaped, possessed condensed chromatin, and were considered apoptoticlike (Fig. 5B and 5D). Staurosporine injured cells were immunoreactive for both SBDP 120 and SBDP 150 in cells exhibiting apoptotic-like nuclear morphology (Fig. 5E and 5F). Notably, different relative magnitudes of caspase-3 and calpain activation were evident in individual cells, but distinct localization of BDPs was not as apparent as the immunoreactivity in control and OGD cells. Maitotoxin-injured cells showed predominantly calpain-mediated BDPs in cells exhibiting the classic necrotic nuclear morphology of rounded, brightly fluoresced nuclei with pyknotic chromatin (Fig. 5G and 5H).

Quantitative analysis of DAPI staining in cells immunoreactive for SBDP 150 or SBDP 120 (data not shown) revealed that the majority of IR cells possessed apoptoticlike nuclei in control (95.7% ± 38.7%) and OGD (97.9% ± 17.2%) cultures. Few IR cells exhibiting a necrotic cell death phenotype were observed in control (1.4% ± 3.7%) or OGD (1.4% ± 1.5%) cultures. Occasionally, IR cells with healthy nuclei were present in control (2.9% ± 3.2%) and OGD (0.7% ± 1.0%) cultures. However, these cells may have been in the initial stages of cell death in which nuclear changes were not yet apparent.

Effects of calpain and caspase inhibitors

Preliminary experiments using protease inhibitors in cultures subjected to 10 hours of OGD and 24 hours of reperfusion data failed to show protection against cell death when LDH release was assayed (data not shown). These data suggested that 24 hours of reperfusion was too long a period to allow the inhibitors to be effective, or that the inhibitors became toxic after such long periods. Moreover, the current data demonstrated robust cell death, DNA fragmentation (Fig. 2), and protease activation (Fig. 4) with 10 hours of OGD and 12 hours of reperfusion. In an attempt to show protection and therefore involvement of calpain and caspase-3, cells were subjected to 10 hours of OGD with 12 hours of reperfusion in the presence of protease inhibitors. Lactate dehydrogenase analysis (Fig. 6A) showed significant decreases in release with CI-3 (100 μmol/L; $P < 0.001$) compared with vehicle-treated cultures. The specific caspase-3 inhibitor, DEVD-fmk (100 μmol/L, $P < 0.05$), also inhibited LDH release; however, decreases were not statistically significant compared with vehicle-treated cultures. The pan-caspase inhibitor, Z-D-DCB (100 μmol/L), had no effect on LDH release. Dimethyl sulfoxide also decreased LDH release, but this effect was not significantly different from the OGD and media cultures.

Consistent with the LDH data, Western blot analyses of these samples (Fig. 6B) showed that CI-3 decreased proteolysis of native 240 kDa α-spectrin and almost completely blocked the formation of the 150/145 kDa doublet. Z-D-DCB also inhibited formation of the 145 kDa BDP to a small extent, but had only a minor effect on the caspase-3–mediated BDP (120 kDa). Surprisingly, DEVD-fmk dramatically reduced the calpain-mediated BDP, but only had a modest effect on the 120 kDa band. Subsequent experiments investigating combined inhibition using CI-3 and DEVD-fmk failed to show a synergistic mechanism. Future experiments should examine more extensive dosing protocols.

DISCUSSION

Although numerous studies have investigated calpain and caspase-3 activation after acute CNS trauma, no study has examined the relation between protease activation and expression of cell death phenotypes. In the current study, the authors detected prominent expression of apoptoticlike cell death phenotypes following a model of OGD, especially in neurons. Moreover, coactivation of calpain and caspase-3 was almost always detected in cells exhibiting apoptoticlike cell death phenotypes.

Oxygen–glucose deprivation resulted in both apoptosis and necrosis in this culture system. Although apop-
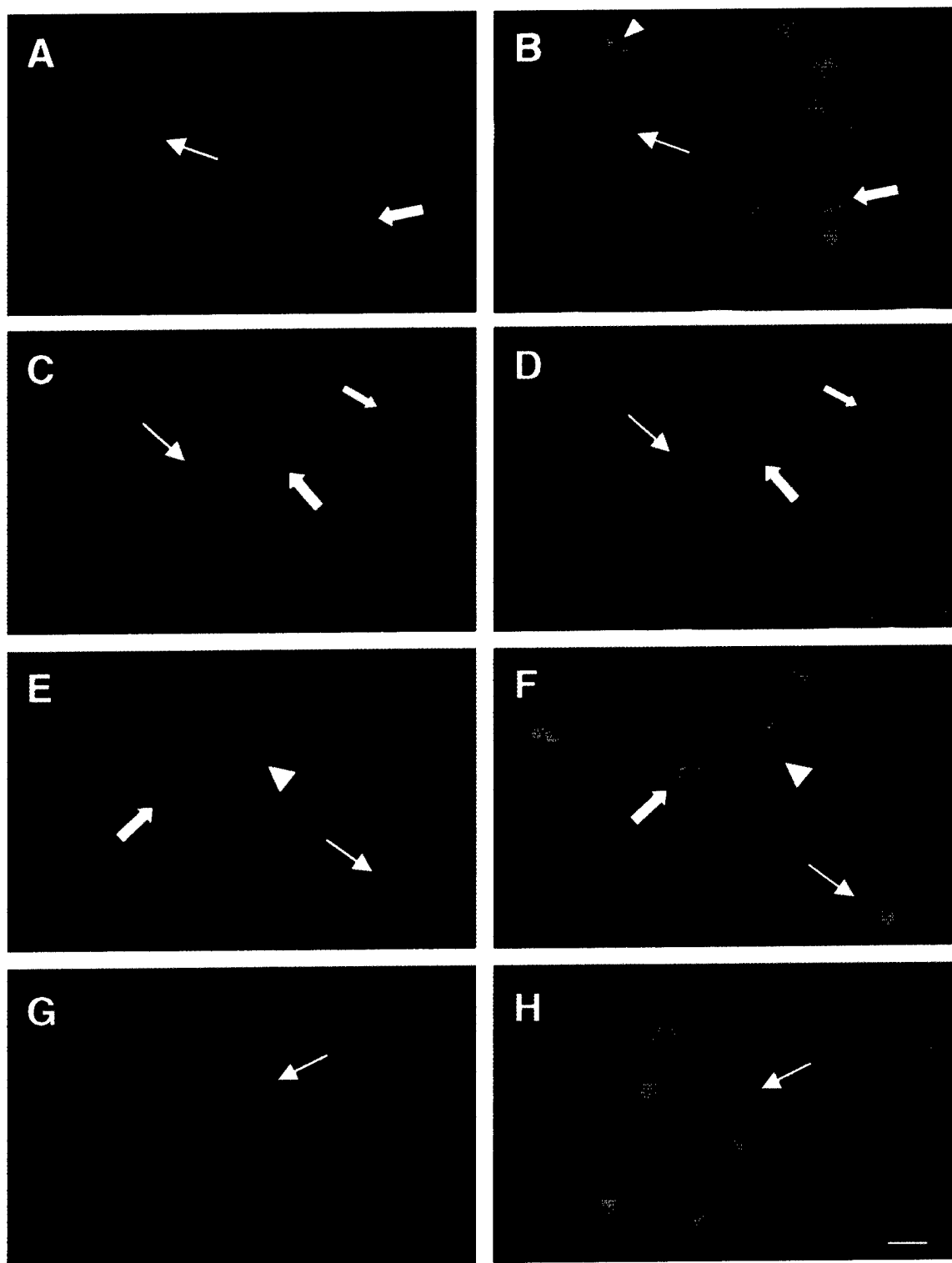
FIG. 5. Calpain and caspase-3 proteolysis of α-spectrin in individual cells following oxygen–glucose deprivation (OGD). Primary mixed septo-hippocampal cultures were immunolabeled with antibodies specific for calpain- (SBDP 150, red fluorescence) and caspase-3 (SBDP 120, green fluorescence)–mediated α-spectrin fragments, and counterstained with DAPI. **(A)** The majority of cells in control cultures were not immunoreactive (IR) for α-spectrin BDPs; however, cells that were IR exhibited both calpain- and caspase-3–mediated BDPs (thin arrow, wide arrow). **(B)** Nuclei of IR cells were shrunken and exhibited chromatin condensation (thin arrow, wide arrow) and apoptotic bodies were also evident (arrowhead). **(C)** OGD cultures also showed concurrent calpain and caspase-3 proteolysis (thin arrow, wide arrows). In addition, IR cells from control (A) and OGD (C) cultures showed subcellular localization of BDPs; SBDP 150 was detected exclusively within the cell body, while SBDP 120 was observed throughout the entire cell body and the proximal processes (A, C, all arrows). **(D)** Nuclei of IR cells in OGD cultures were shrunken, irregularly shaped, and possessed highly condensed chromatin (wide arrows). Nuclei with chromatin margination along the periphery of the nuclear membrane were also detected (thin arrow). **(E)** Staurosporine-injured cells were IR for SBDP 120 and SBDP 150 and different relative magnitudes of protease activation were evident in individual cells (thin arrow, wide arrow, arrowhead). **(F)** IR cells exhibited nuclear morphology consistent with apoptosis (thin arrow, wide arrow, arrowhead). **(G)** Maitotoxin-injured cells exhibited calpain-mediated BDPs (arrow). **(H)** Nuclei of IR cells were rounded, brightly fluoresced, exhibited pyknotic chromatin, and were considered necrotic (arrow). Scale bar = 1 μm.
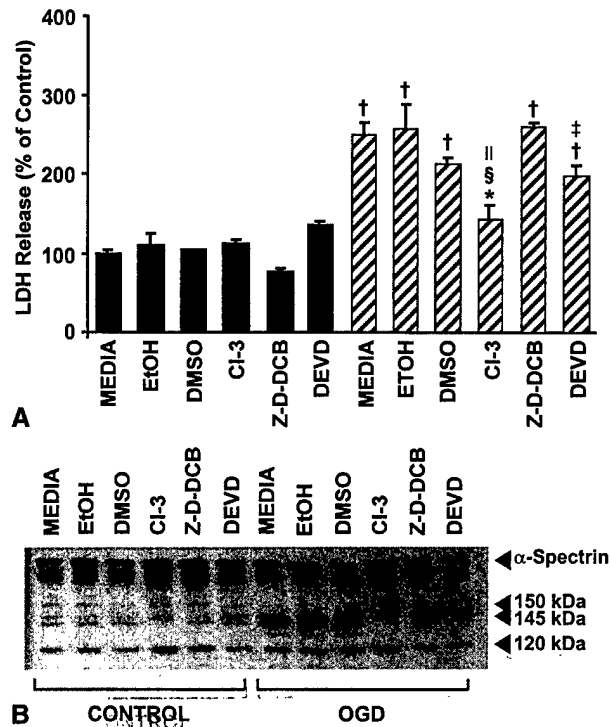
FIG. 6. (A) Effect of protease inhibition on lactate dehydrogenase (LDH) release following oxygen–glucose deprivation (OGD). Cultures were subjected to OGD (10 hours + 12 hours of reperfusion) alone, or combined with varying doses of protease inhibitors. Cell viability was assessed by measuring LDH release and expressed as percent of control. Significant decreases in LDH release were detected with administration of CI-3 (100 µmol/L) compared to vehicle-treated cultures. DEVD-fmk (100 µmol/L) also inhibited LDH release; however, decreases were not statistically significant compared to vehicle-treated cultures. Z-D-DCB (100 µmol/L) had no effect on cell viability. DMSO (2 µL/mL) also decreased LDH release, but its effect was not significantly different from the OGD/media cultures. $*P < 0.05$ and $\dagger P < 0.001$ compared to control; $\ddagger P < 0.05$ and $\S P < 0.001$ compared to OGD/media; $\| P < 0.01$ compared to vehicle-treated OGD. **(B)** Effect of protease inhibition on α-spectrin proteolysis. Western blot analyses of α-spectrin proteolysis assessed inhibition of appropriate proteases. CI-3 (100 µmol/L) decreased proteolysis of native 240 kDa α-spectrin and the formation of the 150/145 kDa doublet. Z-D-DCB (100 µmol/L) had a small effect on the accumulation of the 145 kDa and 120 kDa BDPs. DEVD-fmk (100 µmol/L) substantially reduced the formation of the 145 kDa BDP, but had only a modest effect on the formation of the 120 kDa BDP.

totic and necrotic cell death have been observed in some models of in vitro ischemia (Kalda et al., 1998), other models do not observe apoptosis unless glutamate receptor antagonists are used (Gottron et al., 1997; Gwag et al., 1995; Lobner and Choi, 1996). Variations in cell culture methodology, including culture age at time of injury and glial density, may be responsible for these discrepancies. Consistent with the prominent role of apoptosis in development, younger cultures, such as those used in this study, are more susceptible to apoptosis after cyclosporine or staurosporine treatment (McDonald et

al., 1997), whereas older neurons are more vulnerable to N-methyl-d-aspartate toxicity (McDonald et al., 1997) and hypoxia (Di Loreto and Balestrino, 1997). In contrast to this article, studies that detected only necrosis after OGD used neuronally enhanced cell cultures (Goldberg and Choi, 1993; Gottron et al., 1997; Lobner and Choi, 1996). Increased sensitivity to glutamate toxicity and OGD has been observed in neuronally enhanced cultures (Zhao et al., 2000; Dugan et al., 1995), suggesting that the absence of glia may intensify a neuron's response to injury. It is conceivable that higher glial concentrations in the current model of OGD blunted the effects of deprivation and resulted in a slower and milder injury. Notably, in vitro studies have shown that the same insult can produce apoptosis or necrosis depending on its severity (Bonfoco et al., 1995).

Cell death after OGD was associated with concurrent activation of calpain and caspase-3. Although immunocytochemical experiments revealed robust caspase-3–mediated proteolysis of α-spectrin (120 kDa), Western blots failed to detect consistent increases in this proteolytic fragment. Use of different primary antibodies (monoclonal versus polyclonal) and methods of detection (enhanced chemiluminescence reagents versus fluorescence) may be responsible for these inconsistencies. Western blots using an antibody to the activated caspase-3 17-kDa subunit did provide evidence of caspase-3 activation, confirming immunohistochemical observations of caspase-3 activation and suggesting that Western blot assessments of proenzyme processing may be more sensitive than measures of substrate degradation in some model systems.

Cells phenotypically showing apoptoticlike nuclear profiles exhibited prominent expression of calpain and caspase-3, suggesting that there may be as yet undefined interactions between these two proteases in the expression of the apoptotic phenotype. Calpain and caspase-3 share a variety of substrates that are proteolyzed during apoptosis (Wang, 2000). In addition, these proteases cleave proteins important to each other's regulation—that is, caspase-3–mediated proteolysis of calpastatin, calpain-mediated proteolysis of pro-caspase-3 and pro-caspase-9 (Wang et al., 1998a; McGinnis et al., 1999; Wolf et al., 1999). Furthermore, calpains, but not caspases, promote apoptoticlike events during platelet activation (Wolf et al., 1999). Additional evidence for calpain's involvement in apoptotic cell death in CNS injury is provided by recent studies examining in vivo TBI and ischemia. Calpain-mediated breakdown products have been detected in the injured cortex after TBI (Beer et al., 2000; Pike et al., 1998a), a site associated with prominent apoptotic cell death (Beer et al., 2000; Newcomb et al., 1999), although evidence of caspase-3 activation in this region has yielded conflicting data

(Beer et al., 2000; Pike et al., 1998*a*). These discrepancies may be attributable to differences in injury magnitude, animal age, or species; these issues currently are being addressed in both laboratories. After *in vivo* ischemia, approximately 50% of TUNEL-positive cells failed to show caspase-3 activation (Namura et al., 1998), suggesting that other proteases, such as calpain, are involved in the apoptotic changes observed after injury.

Inhibition of calpain substantially decreased LDH release after OGD with 12 hours of reperfusion, suggesting that calpain activation contributes to cell death in this model. Inhibition of caspase-3 with DEVD-fmk also reduced LDH release, although this drug also showed marked inhibition against calpain activation. Thus, the current study did not allow for comparisons of the relative contribution of these two proteases to cell death in this model. It is unclear why DEVD-fmk showed substantial calpain inhibition and only modest caspase-3 inhibition, but these data suggest that this agent is not a specific inhibitor of caspase-3 activation, at least in this model system. Although not directly addressed in this study, future experiments must more rigorously investigate the relative contribution of calpain and caspase-3 to the expression of apoptotic cell death phenotypes.

Although the current study relied in part on morphologic characteristics of cell death phenotypes, a number of observations suggest that biochemical markers ultimately may be more useful indicators of cell death, especially in acute neurologic insults characterized by heterogeneous or ambiguous cell death phenotypes. In this study, appearance of necrotic cell death depended on method of detection. Using chromatin dyes to distinguish necrotic and apoptotic nuclear morphology is problematic because nuclei may exhibit characteristics either of both types (Colicos and Dash, 1996) or neither type (Zhao et al., 2000) of cell death. In fact, most techniques used to differentiate apoptosis also have been reported to label necrosis, perhaps because late events are similar in both types of cell death (Choi, 1996). Some investigators have argued that necrosis and apoptosis may not be phenotypically distinct events, but rather represent a morphologic continuum (Bonfoco et al., 1995; Portera-Cailliau et al., 1997). This issue is further complicated by evidence showing that the same insult can cause apoptosis and necrosis in different cell populations (Sloviter et al., 1996) or can result in an acute necrotic death with a delayed apoptotic death (Ankarcrona et al., 1995; Pang and Geddes, 1997).

In summary, the current data demonstrate that coactivation of calpain and caspase-3 is a reliable characteristic of apoptotic cell death in the current model system. These observations strongly suggest that calpain activation, in combination with caspase-3 activation, could contribute to the expression of apoptotic cell death by

assisting in the proteolytic degradation of important cellular proteins (Wang, 2000). Finally, interactions between these two cysteine proteases could be important determinants of cell death.

REFERENCES

Ankarcrona M, Dypbukt JM, Bonfoco E, Zhivotovsky B, Orrenius S, Lipton SA, Nicotera P (1995) Glutamate-induced neuronal death: a succession of necrosis or apoptosis depending on mitochondrial function. *Neuron* 15:961–973

Bartus RT, Dean RL, Cavanaugh K, Eveleth D, Carriero DL, Lynch G (1995) Time-related neuronal changes following middle cerebral artery occlusion: implications for therapeutic intervention and the role of calpain. *J Cereb Blood Flow Metab* 15:969–979

Beer R, Franz G, Srinivasan A, Hayes RL, Pike BR, Newcomb JK, Zhao X, Schmutzhard E, Poewe W, Kampfl A (2000) Temporal profile and cell subtype distribution of activated caspase-3 following experimental traumatic brain injury. *J Neurochem* 75:1264–1273

Bonfoco E, Krainc D, Ankarcrona M, Nicotera P, Lipton S (1995) Apoptosis and necrosis: two distinct events induced, respectively, by mild and intense insults with N-methyl-D-aspartate or nitric oxide/superoxide in cortical cell cultures. *Proc Natl Acad Sci U S A* 92:7162–7166

Buki A, Okonkwo DO, Wang KKW, Povlishock JT (2000) Cytochrome c release and caspase activation in traumatic axonal injury. *J Neurosci* 20:2825–2834

Charriaut-Marlangue C, Ben-Ari Y (1995) A cautionary note on the use of TUNEL stain to determine apoptosis. *Neuroreport* 7:61–64

Chen J, Nagayama T, Jin K, Stetler A, Zhu RL, Graham SH, Simon RP (1998) Induction of caspase-3 like protease may mediate delayed neuronal death in the hippocampus after transient cerebral ischemia. *J Neurosci* 18:4914–4928

Choi DW (1996) Ischemia-induced neuronal apoptosis. *Curr Opin Neurobiol* 6:667

Clark RSB, Kochanek PM, Watkins SC, Chen M, Dixon CE, Seidberg NA, Melick J, Loeffert JE, Nathaniel PD, Jin KL, Graham SH (2000) Caspase-3 mediated neuronal death after traumatic brain injury in rats. *J Neurochem* 74:740–753

Colicos MA, Dash PK (1996) Apoptotic morphology of dentate gyrus granule cells following experimental cortical impact injury in rats: possible role in spatial memory deficits. *Brain Res* 739:120–131

Copin JC, Li Y, Reola LF, Chan PH (1998) Trolox and 6, 7-dinitro-quinoxaline-2-3dione prevent necrosis but not apoptosis in cultured neurons subjected to oxygen deprivation. *Brain Res* 784:25–36

Di Loreto S, Balestrino M (1997) Development of vulnerability to hypoxic damage in *in vitro* hippocampal neurons. *Int J Dev Neurosci* 15:225–230

Dugan LL, Bruno VMG, Amagasu SM, Giffard RG (1995) Glia modulate the response of murine cortical neurons to excitotoxicity: glia exacerbate AMPA toxicity. *J Neurosci* 15:4545–4555

Fink K, Namura S, Shimizu-Sasamata M, Endres M, Ma J, Dalkara T, Yuan J, Moskowitz MA (1998) Prolonged therapeutic window for ischemic brain damage caused by delayed caspase activation. *J Cereb Blood Flow Metab* 18:1071–1076

Goldberg MP, Choi DW (1993) Combined oxygen and glucose deprivation in cortical cell culture: calcium-dependent and calcium-independent mechanisms of neuronal injury. *J Neurosci* 13:3510–3524

Gong J, Traganos F, Darzynkiewicz Z (1994) A selective procedure for DNA extraction from apoptotic cells applicable for gel electrophoresis and flow cytometry. *Anal Biochem* 218:314–319

Gottron FJ, Ying HS, Choi DW (1997) Caspase inhibition selectively reduces the apoptotic component of oxygen-glucose deprivation-induced cortical neuronal death. *Mol Cell Neurosci* 9:159–169

Gwag BJ, Lobner D, Koh JY, Wie MB, Choi DW (1995) Blockade of glutamate receptors unmasks neuronal apoptosis after oxygen-glucose deprivation *in vitro. Neuroscience* 68:615–619

Harris AS, Croall DE, Morrow JS (1988) The calmodulin-binding site in alpha-fodrin is near the calcium-dependent protease-1 cleavage site. *J Biol Chem* 263:15754–15761

Himi T, Ishizaki Y, Murota S (1998) A caspase inhibitor blocks ischemia-induced delayed neuronal death in the gerbil. *Eur J Neurosci* 10:777–781

Hong SC, Goto Y, Lanzino G, Soleau S, Kassell NF, Lee KS (1994) Neuroprotection with a calpain inhibitor in a model of focal cerebral ischemia. *Stroke* 25:663–669

Kalda A, Eriste E, Vassiljev V, Zharkovsky A (1998) Medium transitory oxygen-glucose deprivation induced both apoptosis and necrosis in cerebellar granule cells. *Neurosci Lett* 240:21–24

Koh JY, Choi DW (1987) Quantitative determination of glutamate mediated cortical neuronal injury in cell culture by lactate dehydronase efflux assay. *J Neurosci Meth* 20:83–90

Linnik MD, Zobrist RH, Hatfield MD (1993) Evidence supporting a role for programmed cell death in focal cerebral ischemia in rats. *Stroke* 24:2002–2009

Lobner D, Choi DW (1996) Preincubation with protein synthesis inhibitors protects cortical neurons against oxygen-glucose deprivation-induced death. *Neuroscience* 72:335–341

Markgraf CG, Velayo NL, Johnson MP, McCarty DR, Medhi S, Koehl JR, Chmielewski PA, Linnik MD (1998) Six-hour window of opportunity for calpain inhibition in focal cerebral ischemia in rats. *Stroke* 29:152–158

McDonald JW, Behrens MI, Chung C, Bhattacharyya T, Choi DW (1997) Susceptibility to apoptosis is enhanced in immature cortical neurons. *Brain Res* 759:228–232

McGinnis KM, Gnegy ME, Park YH, Mukerjee N, Wang KKW (1999) Procaspase-3 and poly(ADP)ribose polymerase (PARP) are calpain substrates. *Biochem Biophys Res Comm* 263:94–99

Namura S, Zhu J, Fink K, Endres M, Srinivasan A, Tomaselli KJ, Yuan J, Moskowitz MA (1998) Activation and cleavage of caspase-3 in apoptosis induced by experimental cerebral ischemia. *J Neurosci* 18:3659–3668

Nath R, Raser KJ, Stafford D, Hajimohammadreza I, Posner A, Allen H, Talanian RV, Yuen P, Gilbertsen RB, Wang KKW (1996) Non-erythroid alpha-spectrin breakdown by calpain and interleukin 1 beta-converting-enzyme-like protease(s) in apoptotic cells: contributory roles of both protease families in neuronal apoptosis. *Biochem J* 319:683–690

Nath R, Probert A, McGinnis KM, Wang KKW (1998) Evidence for activation of caspase-3-like protease in excitotoxin- and hypoxia/hypoglycemia-injured neurons. *J Neurochem* 71:186–195

Newcomb JK, Kampfl A, Posmantur RM, Zhao X, Pike BR, Liu SJ, Clifton GL, Hayes RL (1997) Immunohistochemical study of calpain-mediated breakdown products to α-spectrin following controlled cortical impact injury in the rat. *J Neurotrauma* 14:369–383

Newcomb JK, Zhao X, Pike BR, Hayes RL (1999) Temporal profile of apoptotic-like changes in neurons and astrocytes following controlled cortical impact injury in the rat. *Exp Neurol* 158:76–88

Oberhammer F, Fritsch G, Schmied M, Pavelka M, Printz D, Purchio R, Lassman H, Schulte-Hermann R (1993) Condensation of chromatin at the membrane of an apoptotic nuclease is not associated with activation of an endonuclease. *J Cell Sci* 104:317–326

Pang Z, Geddes JW (1997) Mechanisms of cell death induced by the mitochondrial toxin 3-nitropropionic acid: acute excitotoxic necrosis and delayed apoptosis. *J Neurosci* 17:3064–3073

Pike BR, Zhao X, Newcomb JK, Posmantur RM, Wang KKW, Hayes RL (1998a) Regional calpain and caspase-3 proteolysis of α-spectrin after traumatic brain injury. *Neuroreport* 9:2437–2442

Pike BR, Zhao X, Newcomb JK, Wang KKW, Posmantur RM, Hayes RL (1998b) Temporal relationship between *de novo* protein synthesis, calpain and caspase-3 like protease activation, and DNA fragmentation during apoptosis in septo-hippocampal cultures. *J Neurosci Res* 52:505–520

Pike BR, Zhao X, Newcomb JK, Glenn CC, Anderson DK, Hayes RL (2000) Stretch injury causes calpain and caspase-3 activation and necrotic and apoptotic cell death in septo-hippocampal cell cultures. *J Neurotrauma* 17:283–298

Portera-Cailliau C, Price DL, Martin LJ (1997) Excitotoxic neuronal death in the immature brain is an apoptosis-necrosis morphological continuum. *J Comp Neurol* 378:70–87

Posmantur RM, Kampfl A, Simon R, Liu SJ, Zhao X, Clifton GL, Hayes RL (1997) A calpain inhibitor attenuates cortical cytoskeletal protein loss after experimental brain injury in the rat. *Neuroscience* 77:875–888

Purnanam KL, Boustany R-M (1999) Assessment of cell viability and histochemical methods in apoptosis. In: *Apoptosis in neurobiology* (Hannun YA, Boustany R-M, eds), Boca Raton, FL: CRC Press, pp 129–152

Rami A, Agarwal R, Botez G, Winckler J (2000) α-Calpain activation, DNA fragmentation, and synergistic effects of caspase and calpain inhibitors in protecting hippocampal neurons from ischemic damage. *Brain Res* 866:299–312

Rink A, Fung KM, Trojanowski JQ, Lee VMY, Neugebauer E, McIntosh TK (1995) Evidence of apoptotic cell death after experimental traumatic brain injury in the rat. *Am J Path* 147:1575–1583

Roberts-Lewis JM, Savage MJ, Marcy V, Pinsker LR, Simon R (1994) Immunolocalization of μ-calpain mediated spectrin degradation to vulnerable neurons in ischemic gerbil brain. *J Neurosci* 14:3934–3944

Saatman KE, Bozyczko-Coyne D, Marcy V, Simon R, McIntosh TK (1996) Prolonged calpain-mediated spectrin breakdown occurs regionally following experimental brain injury in the rat. *J Neuropathol Exp Neurol* 55:850–860

Saatman KE, Zhang C, Bartus RT, McIntosh TK (2000) Behavioral efficacy of posttraumatic calpain inhibition is not accompanied by reduced spectrin proteolysis, cortical lesion, or apoptosis. *J Cereb Blood Flow Metab* 20:66–73

Saido TC, Yokota M, Nagao S, Yamaura I, Tani E, Tsuchiya T, Suzuki K, Kawashima S (1993) Spatial resolution of fodrin proteolysis in postischemic brain. *J Biol Chem* 268:25239–25243

Schmechel DE (1999) Assessment of ultrastructural changes associated with apoptosis. In: *Apoptosis in neurobiology* (Hannun YA, Boustany R-M, eds), Boca Raton, FL: CRC Press, pp 153–181

Sloviter RS, Dean E, Sollas AL, Goodman JH (1996) Apoptosis and necrosis induced in different hippocampal neuron populations by repetitive perforant path stimulation in the rat. *J Comp Neurol* 366:516–533

Squier MK, Miller AC, Malkinson AM, Cohen JJ (1994) Calpain activation in apoptosis. *J Cell Physiol* 159:229–237

Vanags DM, Porn-Ares MI, Coppola S, Burgess DH, Orrenius S (1996) Protease involvement in fodrin cleavage and phosphatidylserine exposure in apoptosis. *J Biol Chem* 271:31075–31081

Wang KKW, Nath R, Raser KJ, Hajimohammadreza I (1996) Maitotoxin induces calpain activation in SH-SY5Y neuroblastoma cells and cerebrocortical cultures. *Arch Biochem Biophys* 331:208–214

Wang KKW, Posmantur RM, Nadimpalli R, Nath R, Nixon R, Talanian RV, Allen H (1998a) Caspase-mediated fragmentation of calpain inhibitor protein calpastatin during apoptosis. *Arch Biochem Biophys* 356:187–196

Wang KKW, Posmantur RM, Nath R, McGinnis KM, Whitton M, Talanian RV, Glartz SB, Morrow JS (1998b) Simultaneous degradation of αII- and βII-spectrin by caspase 3 (CPP32) apoptotic cells. *J Biol Chem* 273:22490–22497

Wang KKW (2000) Calpain and caspase: can you tell the difference? *Trends Neurosci* 23:20–26

Wolf BB, Goldstein JC, Stennicke HR, Beere H, Amarante-Mendes GP, Salvesen GS, Green DR (1999) Calpain functions in a caspase-independent manner to promote apoptotic-like events during platelet activation. *Blood* 94:1683–1692

Yakovlev AG, Knoblach SM, Fan L, Fox GB, Goodnight R, Faden AI (1997) Activation of CPP32-like caspases contributes to neuronal apoptosis and neurological dysfunction after traumatic brain injury. *J Neurosci* 17:7415–7424

Yokota M, Saido TC, Tani E, Kawashima S, Suzuki K (1995) Three distinct phases of fodrin proteolysis induced in postischemic hippocampus. Involvement of calpain and unidentified protease. *Stroke* 26:1901–1907

Zhao X, Pike BR, Newcomb JK, Wang KKW, Postmantur RM, Hayes RL (1999) Maitotoxin induces calpain but not caspase-3 activation

and necrotic cell death in primary septo-hippocampal cultures. *Neurochem Res* 24:371–382

Zhao X, Newcomb JK, Pike BR, Posmantur RM, Wang KKW, Hayes RL (2000) Novel characteristics of glutamate-induced cell death in primary septo-hippocampal cultures: relationship to calpain and caspase-3 protease activation. *J Cereb Blood Flow Metab* 20:550–562

Systemic Administration of a Calpain Inhibitor Reduces Behavioral Deficits and Blood–Brain Barrier Permeability Changes after Experimental Subarachnoid Hemorrhage in the Rat

A. GERMANÒ,[1] C. COSTA,[2] S.M. DeFORD,[3] F.F. ANGILERI,[1] F. ARCADI,[4] B.R. PIKE,[3] P. BRAMANTI,[4] B. BAUSANO,[5] X. ZHAO,[5] A.L. DAY,[6] D.K. ANDERSON,[3] and R.L. HAYES[3]

ABSTRACT

Increases in intracellular calcium and subsequent activation of calcium-activated proteases (e.g., calpains) may play a critical role in central nervous system injury. Several studies have implicated calpain activation following subarachnoid hemorrhage (SAH). This study evaluated the effect of a calpain inhibitor administration following SAH in the rat on behavioral deficits (postinjury days 1–5, employing a battery of well-characterized assessment tasks), and blood–brain barrier permeability changes (48 h post-SAH, quantifying the microvascular alterations according to the extravasation of protein-bound Evans Blue using a spectrophotofluorimetric technique). Rats were injected with 400 μl of autologous blood into the cisterna magna to induce SAH. Within 5 min after the surgical procedure, Calpain Inhibitor II or vehicle was continuously administered intravenously for 2 days. Results indicated that Calpain Inhibitor II treatment after SAH significantly improved (a) beam balance time (day 1, $p < 0.05$), but not beam balance score, (b) latency to traverse the beam on days 1–4 (day 1–3, $p < 0.001$; day 4, $p < 0.01$), and (c) loss in body weight on days 4–5 ($p < 0.05$). Evans Blue dye extravasation was significantly less in SAH Calpain Inhibitor II–treated rats compared to SAH vehicle-treated rats in seven out of the eight brain regions studied ($p < 0.001$, 0.01, and 0.05). These results suggest that pharmacological inhibition of a relatively selective, membrane-permeant calpain inhibitor can significantly reduce some pathophysiological SAH consequences, and indicate that the inhibition of calpain may be a beneficial therapeutic approach to reduce post-SAH global brain dysfunction.

Key words: behavioral deficits; blood–brain barrier; calpain; rats; subarachnoid hemorrhage

[1]Neurosurgical Clinic, University of Messina, Messina, Italy.

[2]C.I.T.S.A.L., University of Messina, Messina, Italy.

[3]Evelyn F. and William L. McKnight Brain Institute of the University of Florida, Center for Traumatic Brain Injury Studies, Gainesville, Florida.

[4]Centro per lo Studio ed il Trattamento dei Neurolesi Lungodegenti and Department of Neurophysiopathology, University of Messina, Messina, Italy.

[5]University of Texas Medical Center, Houston, Texas.

[6]Evelyn F. and William L. McKnight Brain Institute of the University of Florida, Department of Neurosurgery, Gainesville, Florida.

INTRODUCTION

THERE IS considerable clinical and experimental evidence that, since its acute stage, subarachnoid hemorrhage (SAH) induces focal and generalized disturbances of several brain functions, including brain edema and cerebral swelling, increased intracranial pressure, reduced cerebral blood flow and perfusion pressure, disrupted brain metabolism, free-radical generation associated with peroxidation phenomena, macro and blood–brain barrier (BBB) microvascular changes, together with cognitive consequences (Doczi, 1985; Zuccarello et al., 1989; d'Avella et al., 1990; Jackowski et al., 1990; Joshita et al., 1990; Kassell et al., 1990; Mayberg et al., 1990; Germanò et al., 1992, 1998b, 2000; d'Avella et al., 1996; Hutter et al., 1996; Imperatore et al., 2000). Relatively little is known, however, about the cellular mechanisms contributing to the global brain dysfunction that follows SAH.

Increase in intracellular calcium and subsequent activation of the calcium-activated neutral proteases (e.g., calpains) may play a major role in a variety of central nervous system injuries including traumatic brain injury, cerebral ischemia, spinal cord injury and SAH (Kampfl et al., 1997; Yokota et al., 1999; Vanderklish and Bahr). Observations include increased autolysis of calpain reduction in in native calpain, reduction in calpastatin activity, and proteolysis of calpain substrates (Minami et al., 1992; Yamaura et al., 1993; Lee et al., 1997). Other studies have shown that topical application or systemic administration of calpain inhibitors can attenuate cerebral vasospasm after SAH (Kawamata et al., 1990, Minami et al., 1992, 1993; Yamaura et al., 1993; Wang and Yuen, 1994; Lee et al., 1997; Sato et al. 1997, Fujikawa et al., 1999). However, no studies to date have addressed the effects of calpain inhibitors on behavioral deficits or BBB opening following experimental SAH.

Our laboratory has developed a rodent model of SAH that has produced extensive information about changes on macro- and microvascular, biochemical, hemodynamic, acute, and chronic behavioral parameters (d'Avella et al., 1990, 1993, 1994, 1996; Germanò et al., 1992, 1994, 1998b, 2000; Imperatore et al., 2000), paralleling those seen in humans after SAH (Germanò et al., 1997, 1998a).

The aim of the present study was to evaluate the protective effects of systemic administration of a calpain inhibitor on behavioral and microvascular changes in this rodent model of SAH. In the first experiment, we evaluated the effect of Calpain Inhibitor II upon the behavioral consequences of SAH, employing a battery of well-characterized tests over a 5-day observation period. In the

second experiment, we assessed the effect of Calpain Inhibitor II on microvascular BBB permeability changes 2 days after SAH, quantifying the extravasation of protein-bound Evans Blue using a spectrophotofluorimetric technique.

MATERIALS AND METHODS

Experimental Design and Induction of SAH

Studies were conducted using 48 male Albino Sprague-Dawley rats (Charles River Italia SpA Calco [Lecco], Italy; Crl: CD [SD] BR), each weighing approximately 200 g. Animals were housed (four per cage) at a constant temperature of 22°C, under a 12-h light/dark cycle (light switched on at 6 a.m.) with free access to food and water. The procedures used in this study were based on the guidelines of the ethical committee on the care and use of laboratory animals at our institution.

All surgical procedures were performed after induction of ketalar anesthesia (ketamine, Parke-Davis, 150 mg/kg i.p. in a volume of 3 mL/kg). The jugular vein was exposed through a midline linear 2 cm ventral neck incision, and a PE50 catheter (Clay Admas, Parsippany, NJ) filled with saline was inserted and exteriorized at the nape of the neck. The wounds were infiltrated with bupivacaine (Marcaina 0.5%; Pierrel SpA, SS Appia, Capua [CE], Italy; 0.25 mg/kg/500μL). The catheter, exiting from the neck, was connected with a Tether steel spring, secured to a custom-designed jacket, connected to a single channel swivel, and to an infusion pump set at a rate of 0.15 mL/h for vehicle or Calpain Inhibitor II administration in order to maintain continuous intravenous infusion.

The rats were divided into four experimental groups (n = 12): groups I and II (sham operated + vehicle continuous infusion, sham operated + Calpain Inhibitor II continuous infusion, respectively) were used to evaluate the possible effects on investigational parameters of vehicle infusion and Calpain Inhibitor II administration in sham-operated rats. Groups III and IV (SAH + vehicle continuous infusion, SAH + Calpain Inhibitor II continuous infusion, respectively) were used to compare the effect of Calpain Inhibitor II administration on SAH-induced changes in investigational parameters.

The experiments were conducted as follows. On day −1, baseline preassessment for behavioral tasks were performed. On day 0, SAH or sham operation procedures were performed. Behavioral parameters were assessed on days 1–5, since in previous studies performed in our laboratory using this rodent model, SAH rats evidenced the occurrence of enduring behavioral deficits over a 5-day observation period (Germanò et al., 1994, 1998b; Im-

peratore et al., 2000). BBB permeability changes were assessed 48 h after SAH, since previous studies of this rodent model of SAH demonstrated that BBB alterations begin 36 h after SAH, reach a maximum at 48 h, and return to normal values within 60 h after SAH (Germanò et al., 2000).

SAH was induced in 24 rats by injection of autologous blood into the subarachnoid space via the cisterna magna. Details of the procedure have been previously published (d'Avella et al., 1990, 1993, 1996; Germanò et al., 1992, 1994, 1998b, 2000; Imperatore et al., 2000). Briefly, the atlanto-occipital membrane was exposed through a midline occipital incision. For the simulated SAH, 0.4 mL of autologous arterial nonheparinized blood was injected into the cisterna magna over a period of approximately 30 sec via a 30-gauge needle fitted to a 500-μL Hamilton syringe. The sham-operated groups consisted of 24 rats in which the atlanto-occipital membrane was exposed through a midline occipital incision and punctured as described above. No intracisternal injection was made, since previous studies performed in our laboratory using this rodent model, mock CSF-injected rats did not display any enduring behavioral deficits (Germanò et al., 1994, 1998b; Imperatore et al., 2000) or change in BBB quantitative assessment (Germanò et al., 1992) as compared with uninjected control rats.

Calpain Inhibitor II Administration

Within 5 min of SAH or sham-operation, N-acetyl-leu-leu-methioninal (Calpain Inhibitor II, lot no. 83929820-18; Boehringer Mannheim, Milano, Italy) and vehicle (ethanol) were continuously administered intravenously to each of the 48 rats for two days through the cannulated jugular vein. Calpain Inhibitor II was dissolved in ethanol and diluted in saline to a final concentration of 150 μmol/L (final concentration of ethanol: 0.03%). The dose of vehicle (ethanol diluted in saline)/kg/day was 0.486 g, for a total volume/day of 5.76 mL (final concentration of ethanol: 0.03%). The selection of this dose

regimen for Calpain Inhibitor II was based on previous experimental studies characterizing the neuroprotective effects of Calpain Inhibitor II both in in vivo (Posmantur et al., 1997) and in vitro (Kampfl et al., 1995; Kampfl et al., 1996) experiments.

Behavioral Assessment Protocol

Three assessment tasks were used to characterize behavioral deficits over a 5-day period after treatment. These tasks have already been employed in our laboratory in order to assess the occurrence of behavioral changes in this rodent SAH model (Germanò et al., 1994) and to evaluate the effects of pharmacological agents to treat SAH consequences (Germanò et al., 1998; Imperatore et al., 2000). Six animals per group were preassessed the day before the procedure (day −1), and tests were conducted daily from the day after the procedure through the following 5 days (days 1–5) in a blind fashion.

Beam balance. The beam balance test is a task that is used to assess both motor and vestibular function by quantifying an animal's ability to balance on a narrow wooden beam (1.0 cm wide) for up to 60 sec. Beam balance was assessed by two measures: (1) duration (time) and (2) balance score. The duration the rat remained on the balance beam was recorded, with a maximum duration of 60 sec. The balance rating scale was used to determine balance score. Briefly, a rat's ability to balance was evaluated on a five-point scale (Levin et al., 1982; Table 1).

Beam walking. The beam walking test is a learned avoidance test similar to that used by Feeney et al. (1982). This task is used to evaluate the somatomotor, motivational and attentional functions together with memory and locomotor activities. The rats were trained with a negative reinforcement paradigm, in which termination of the adverse stimuli (nose + light) served as reward. Each animal had to traverse the top of an elevated (1.0

TABLE 1. BEAM BALANCE RATING SCALE

Score	Behavior
1	Balances with steady posture
2	Grasps top edges of beam (paws do not extend below upper half of beam) and/or has shaky movements (but all four paws maintain contact with beam)
3	Hugs the beam (paws extend below upper half of beam) or slips (one or more paws lose contact with beam) or spins (rat assumes an inverted position for any length of time) on beam
4	Attempts to balance on the beam but falls off
5	Falls off—no attempt to balance or hang on the beam

m) narrow wooden beam (120 × 5 cm) with the reward consisting of the cessation of loud white noise and bright light by entering a darkened goal box (30 × 15 × 18 cm). Task difficulty was increased by placing four equally spaced pegs (5 cm height) along the top of the beam. The noise and light were turned off immediately after the animal had traversed the beam and had entered the darkened goal box with its two forelegs. Latency to traverse the beam and reach the goal box was recorded. Data for each daily session represented the mean ± SD of three consecutive trials.

Body weight. Body weight, a gross measure of food and water intake, is a parameter that is used to asses the appetite drive and the occurrence of motivational deficits. Rats were preweighed on day −1 and their weight was recorded daily for the following 5 days.

BBB Evaluation Protocol

The BBB assessment protocol was conducted in six animals per group, 48 h after the SAH or sham procedures. The method employed was the quantitative evaluation of the vascular permeation of Evans Blue dye by means of a fluorescence spectrophotometer technique, according to the measurement protocol of Uyama et al. (1988), the extraction technique of Rossner and Tempel (1966), and modified in our laboratory (Germanò et al., 1998b). Briefly, 2% Evans Blue in saline, in a volume of 5 mL/kg, was administered intravenously through the cannulated jugular vein as a BBB permeability tracer and was allowed to circulate for 60 min. To remove the intravascularly localized dye, rats were pericardially perfused with saline through the left ventricle at pressure of 110 mm Hg until colorless perfusion fluid was obtained from the right atrium. In addition, in order to maximize the loss of residual intravascular tracer, animals were killed by decapitation producing cranial exsanguinations. The whole brain was removed and vascular permeability measured by comparing its weight with preweighed bilateral loci in cerebral cortices (frontal, temporal, parietal, occipital regions), as defined by the Paxinos and Watson atlas (1982-Paxinos et al., 1982). Each brain area was homogenized in 1.0 mL of 50% trichloroacetic acid (w/v) and centrifuged (10,000 rpm, 20 min). One mL of the supernatant was added to 1.5 mL of the solvent (50% trichloroacetic acid/ethanol, 1:3). A FP-920 fluorescence detector (Jasco Corp., Tokyo, Japan) was used at an excitation wavelength of 620 nm (bandwidth 10 nm) and an emission wavelength of 680 nm (bandwidth 10 nm). Calculations were based on external standards in the solvent (10–500 ng/mL). Data are expressed as mean ± SD g of extravasated Evans Blue/g of tissue.

Statistical Analyses

Data were analyzed using parametric or nonparametric methods. And ANOVA or Kruskall-Wallis one-way analysis was carried out. Post-hoc Steel-Dwass and Tukey multiple comparison tests were employed. Differences were significant at the $p < 0.05$ level after Bonferroni's adjustments.

RESULTS

General observations and systemic physiological evaluations concerning this model (including mean arterial blood pressure, arterial blood gas levels, blood pH, plasma glucose levels, and body temperature as monitored throughout the experimental procedure) have been described in detail elsewhere (d'Avella et al., 1990, 1993, 1996; Germanò et al., 1992, 1994, 1998, 2000; Imperatore et al., 2000). Briefly, rats tolerated the procedure well, and no signs of acute neurological dysfunction were noted. In rats sacrificed on the second day after SAH, a blood clot was still clearly identifiable in the cisterna magna and in the basal cisterns: no extradural hemorrhages were found, while the presence of blood in the ventricles was detected in approximately 25% of cases. In rats sacrificed on day 5 post-SAH, no blood clot was visible in the cisterna magna or in other brain loci. Vehicle infusion and Calpain inhibitor II administration per se did not induce any significant alteration of the rodent physiologic parameters, neither in control animals nor in SAH rats.

Behavioral Assessment

None of the experimental groups differed significantly from others in baseline preinjection assessments (day -1) (Figs. 1–3).

Beam balance. Vehicle infusion and Calpain Inhibitor II administration in sham-operated animals did not induce any significant beam balance alteration (Fig. 1). The blood-injected vehicle-treated rats exhibited significant deficits in balance time (day 1, $p < 0.05$), as compared with sham-operated vehicle-treated animals. SAH Calpain Inhibitor II–treated animals exhibited significantly improved beam balance time (day 1, $p < 0.05$; Fig. 1), but not beam balance score, as compared with SAH vehicle-treated rats.

Beam walking. Vehicle infusion and Calpain Inhibitor II administration in sham-operated animals did not induce any significant beam walking alteration. The blood-injected vehicle-treated rats exhibited significantly in-
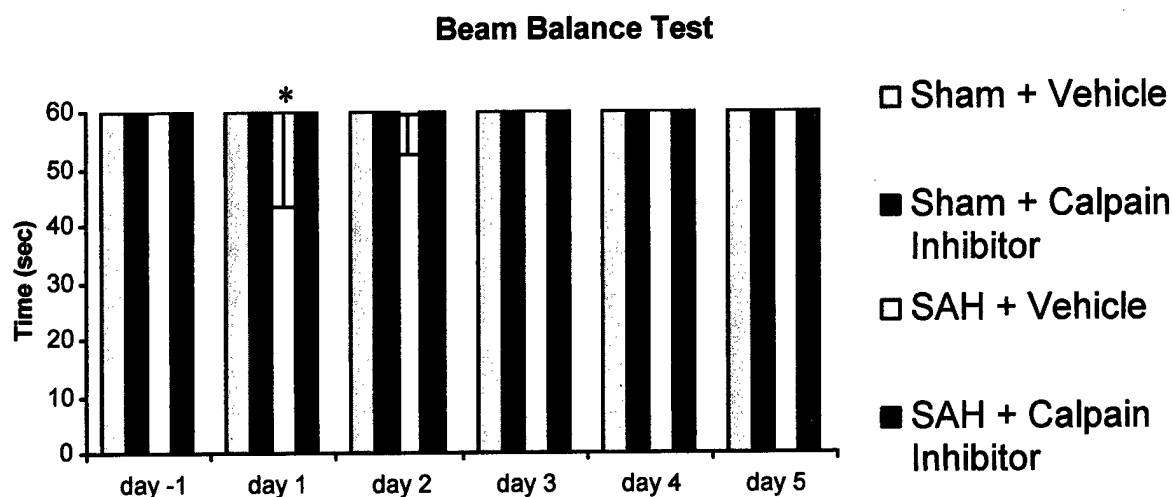
Beam Balance Test

FIG. 1. Beam balance test. Bar graph comparing the time (sec) that animals remained on the beam at daily time points (days −1 to 5). The values shown are means of three consecutive trials ± SE for six animals in each group. *$p < 0.05$, SAH + saline versus SAH + Calpain Inhibitor II groups.

creased latency to traverse the beam on days 1–4 (days 1–3, $p < 0.001$; day 4, $p < 0.01$), as compared with sham-operated animals. In SAH Calpain Inhibitor II–treated rats, latency to traverse the beam was significantly reduced on days 1–4 (days 1–3, $p < 0.001$; day 4, $p < 0.01$), as compared with SAH vehicle-treated rats (Fig. 2).

Body weight. Vehicle infusion and Calpain Inhibitor II administration in sham-operated animals did not induce any significant body weight alteration. SAH rats exhib-

ited significantly decreased body weight on days 1–5 ($p < 0.05$), as compared to vehicle-treated sham-operated rats. Administration of Calpain Inhibitor II significantly reduced the SAH-related loss in body weight on days 4–5 ($p < 0.05$), as compared to SAH vehicle-treated animals (Fig. 3).

BBB Evaluations

Table 2 summarizes the mean concentration ± SD of extravasated Evans Blue dye expressed as micrograms per gram of brain tissue for all loci examined in the eight
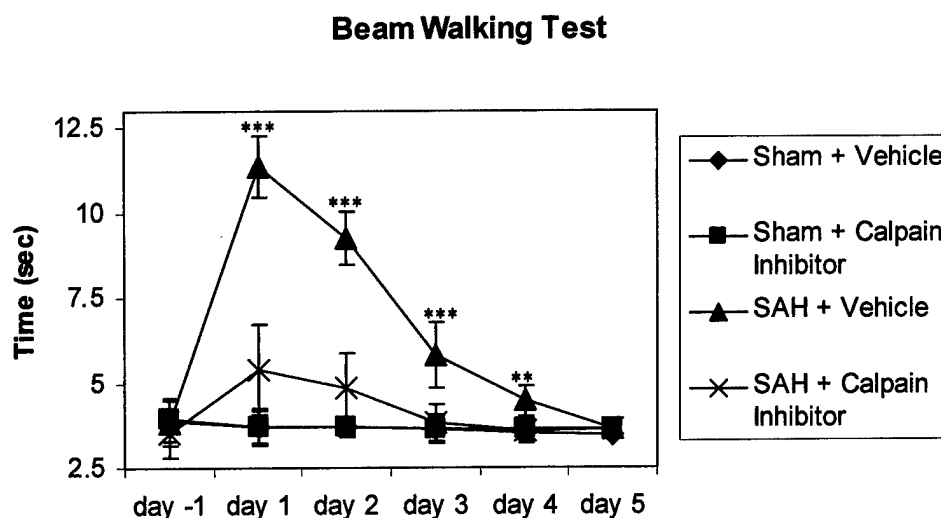
Beam Walking Test

FIG. 2. Beam walking test. Line graph showing latency (sec) to traverse the beam at daily time points (days −1 to 5). The values shown are means of three consecutive trials ± SE for six animals in each group. **$p < 0.01$, ***$p < 0.001$, SAH + vehicle versus SAH + Calpain Inhibitor II groups.

Body Weight
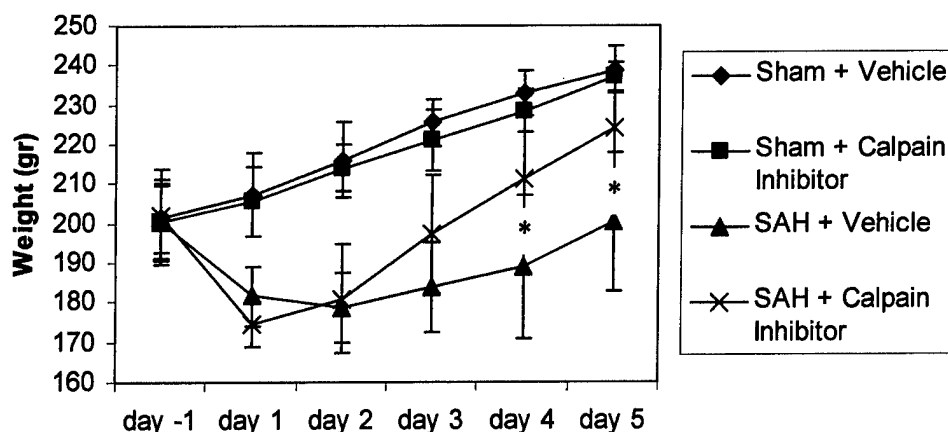
FIG. 3. Body weight. Line graph showing changes in body weight (g) of body weight at daily time points (days −1 to 5). The values shown are means ± SE for six animals in each group. *$p < 0.05$, SAH + vehicle versus SAH + Calpain Inhibitor II groups.

experimental groups. In sham-operated vehicle-treated rats baseline levels of Evans Blue ranged from 0.214 ± 0.027 to 1.938 ± 0.154. Values obtained in sham-operated and SAH vehicle-treated animals were consistent with those described in previous experiments performed in our laboratory (Germanò et al., 1992, 1998, 2000; d'Avella et al., 1994; Imperatore et al., 2000). As compared with sham-operated vehicle-treated animals, in SAH vehicle-treated rats, Evans Blue dye extravasation was significantly increased ($p < 0.001$) in the frontal, temporal, parietal, occipital, and cerebellar cortices, in subcortical gray matter, cerebellar nuclei and brain stem. Administration of Calpain Inhibitor II significantly reduced the post-SAH Evans Blue dye extrava-

sation in the frontal and parietal cortices, in cerebellar and brain stem nuclei ($p < 0.001$), in the occipital and cerebellar cortices ($p < 0.01$), and in the temporal cortex ($p < 0.05$), but did not significantly differ in the subcortical GM (CPT), as compared to SAH vehicle-treated animals.

DISCUSSION

This research represents the first experimental assessment in rats of the effect of administration of a calpain inhibitor on behavioral deficits and BBB opening after SAH *in vivo*. Post-SAH Calpain Inhibitor II administra-

TABLE 2. RESULTS OF BBB PERMEABILITY CHANGE ASSESSMENTS IN ALL GROUPS OF RATS

Area	Evans Blue dye (μg/g tissue)			
	Sham + vehicle	Sham + Calpain Inhibitor II	Sham + vehicle	SAH + Calpain Inhibitor II
Frontal cortex	2.424 ± 0.139	2.346 ± 0.361	8.546 ± 1.584***	3.920 ± 1.317
Temporal cortex	0.599 ± 0.019	0.625 ± 0.087	3.273 ± 1.083*	2.022 ± 0.541
Parietal cortex	0.231 ± 0.026	0.226 ± 0.016	0.771 ± 0.207***	0.368 ± 0.047
Occipital cortex	1.791 ± 0.185	1.816 ± 0.147	5.234 ± 0.620**	4.114 ± 0.540
Subcortical GM (CPT)	0.214 ± 0.027	0.225 ± 0.047	0.998 ± 0.246	0.833 ± 0.130
Cerebellar cortex	0.793 ± 0.060	0.795 ± 0.087	2.957 ± 0.631**	2.085 ± 0.238
Cerebellar nuclei	4.938 ± 0.154	2.199 ± 0.159	5.045 ± 0.980***	3.114 ± 0.493
Brainstem	0.353 ± 0.055	0.356 ± 0.033	2.538 ± 0.178***	1.136 ± 0.159

BBB alterations were measured as μg of extravased Evans Blue per gram of tissue 48 h after sham operations or SAH procedures. The values shown are means ± SD for animals in each group. *$p < 0.05$; **$p < 0.01$; ***$p < 0.001$ in SAH + vehicle versus SAH + Calpain Inhibitor II groups.

tion significantly improved performance in a well-described battery of behavioral and cognitive tests and reduced BBB opening in seven out of eight brain areas. In sham-operated animals, Calpain Inhibitor II administration did not demonstrate any significant effect per se on the chosen investigational parameters.

This study used a simple experimental rodent model of SAH, which has already been extensively investigated in our laboratory, and has confirmed that the pathophysiological changes seen in this and in similar models may parallel those seen in humans after SAH (Doczi, 1985; Kassell et al., 1985, 1990). Observations include time course of changes of intracisternal TXB_2, PGE_2 and $PGF_2\alpha$, the occurrence of angiographical arterial spasm, the induction of quantitative and qualitative marked regional alterations in BBB permeability, the occurrence of a widespread depression of brain metabolism together with the induction of enduring behavioral deficits (Germano et al., 1994). The specificity of extravasated blood for causing the observed pathophysiological changes has been demonstrated, together with the usefulness of pharmacological treatments (d'Avella et al., 1990, 1993, 1994, 1996; Germanò et al., 1992, 1994, 1998, 2000; Imperatore et al., 2000).

The experimental parameters investigated in the present study may reflect the effect of SAH on global brain performance as well as on microvascular systems.

Neuropsychological outcome after SAH is receiving increased attention by the neurosurgical community (Hutter et al., 1999; Mavaddat et al., 1999; Hillis et al., 2000). In previous investigations our laboratory has provided normative values depicting the spectrum and time course of SAH-induced behavioral alterations in the rat peaking on days 1–4 and normalizing by day 5 after SAH (Germanò et al., 1994) and the effects of pharmacological treatment (Imperatore et al, 2000). These behavioral changes were similar to those observed in other brain injury models (Levin et al., 1982; Feeney et al., 1992; Saatman et al., 1996) and may represent a rodent analogue of deficits seen in humans after SAH.

Early changes in BBB function have been described as an important causative factor for post-SAH cerebral dysfunction (Doczi, 1985; Zuccarello et al., 1989; Joshita et al., 1990-Jackowski et al., 1990) An impairment of BBB following SAH has been reported in nearly two-fifths of patients within 5 days of SAH (Doczi, 1985). In the present study, we chose a 2-day post-SAH time interval on the basis of previous observations made by ourselves (Germanò et al., 2000 al., 1992) and others (Doczi, 1985, 1986; Zuccarello et al., 1989) that the BBB dysfunction peaks in the rat on the second day post-SAH.

SAH-related global brain dysfunction results in rapid loss of high-energy phosphate compounds and generalized depolarization, which induces release of glutamate, opening of both voltage-dependent and glutamate-regulated calcium channels (Schulz et al., 2000). This allows a large increase in cytosolic Ca^{2+} associated with activation of mu-calpain, calcineurin, and phospholipases with consequent proteolysis of calpain substrates (including spectrin and eIF4G), activation of NOS. This process engages multiple independently fatal terminal pathways involving loss of membrane integrity in partitioning ions, progressive proteolysis, and inability to check these processes because of loss of general translation competence and reduced survival signal transduction (White et al., 2000).

A number of observations have implicated calpain activation after SAH. Data include increased calpain autolysis reduction in native calpain, reduction in calpastatin activity and proteolysis of calpain substrates (Minami et al., 1992; Yamaura et al., 1993; Lee et al., 1997). Topical application and systemic administration of calpain inhibitors can reduce cerebral vasospasm in different animal species (Kawamata et al., 1990; Minami et al., 1992, 1993; Yamaura et al., 1993; Wang and Yuen, 1994; Lee et al., 1997; Sato et al., 1997; Fujikawa et al., 1999). Mechanisms for calpain mediation of vasospasm are currently unknown. Minami et al. (1992) have speculated that limited proteolysis of protein kinase C (PKC) by calpain could increase kinase activity in vascular smooth muscle cells reducing the calcium requirement for kinase activation and resulting in sustained vasoconstriction. This hypothesis has been supported by other observations implicating PKC in the initiation and maintenance of cerebral vasospasm (Matsui et al., 1991; Nishizawa et al., 1992; Sako et al., 1993; Takuwa et al., 1993; Fujikawa et al., 1999). Calpain-mediated processing of cytoskeletal substrates can contribute to structural changes in the vasculature occurring during later stages of cerebral vasospasm (Bevan and Bevan, 1988).

There are a variety of calpain inhibitors currently available, each has its own advantages and disadvantages (for reviews, see Yuen and Wang, 1998; Hayes et al., 1998). In the present study, we choose calpain inhibitor II as it is a potent calpain inhibitor, is cell permeable, and administration of calpain inhibitor II over 24 h after TBI attenuates cytoskeleton loss (Posmantur et al., 1997). Although our own and other laboratories have shown that systemic administration of Calpain Inhibitor II reliably inhibits calpain activation (Posmantur et al., 1997), these studies by themselves do not allow us to conclude that Calpain Inhibitor II attenuated the pathophysiological effects of SAH solely through inhibition of calpain, as this inhibitor is known to inhibit cathepsins and, to a lesser degree, chymotrypsin (Posmantur et al., 1997). However,

it has to be emphasized that the mechanism of action of Calpain Inhibitor II after SAH in this rodent model can be multifactorial, is not completely understood in details, and is well beyond the scope of this study.

Results of the present study are consistent with the hypothesis that SAH-induced activation of the calcium-dependent protease calpain contributes to post-SAH brain dysfunction (Wang and Yuen, 1994; Lee et al., 1997; Vanderklish et al., 2000). In this view, timely administration of a relatively selective, membrane-permeant Calpain Inhibitor II, can significantly reduce some pathophysiological aspect of the global brain dysfunction that follow SAH. This information is important because it provides additional insights on the pharmacological profile of Calpain Inhibitor II in an experimental setting reproducing some aspects of post-SAH cerebral dysfunctions in humans.

ACKNOWLEDGMENTS

REFERENCES

BEVAN, J.A., and BEVAN, R.D. (1988). Arterial wall changes in chronic cerebrovasospasm *in vitro* and *in vivo* pharmacological evidence. Annu. Rev. Pharmacol. Toxicol. **28**, 311–329.

D'AVELLA, D., GERMANÓ, A., SANTORO, G., et al. (1990). Effects of experimental subarachnoid hemorrhage on CSF eicosanoids in the rat. J. Neurotrauma **7**, 121–129.

D'AVELLA, D., ZUCCARELLO, M., and TOMASELLO, F. (1993). Protective effect of U-78157G on local cerebral glucose utilization in the acute stage following subarachnoid hemorrhage (SAH), in: *Cerebral Vasospasm*. J.M. Findlay (ed), Elsevier Science Publishers B.V.: Amsterdam, pps. 427–430.

D'AVELLA, D., GERMANÒ, A., and TOMASELLO, F. (1994). Early blood–brain barrier changes after experimental subarachnoid haemorrhage: a quantitative and electron microscopy study, in: *New Trends in Management of Cerebro-Vascular Malformations*. A. Pasqualin and R. Da Pian (eds), Springer-Verlag: New York, pps. 48–51.

D'AVELLA, D., CICCIARELLO, R., ZUCCARELLO, M. et al. (1996). Brain energy metabolism in the acute stage of experimental subarachnoid haemorrhage: local changes in cerebral glucose utilization. Acta Neurochir. (Wien) **138**, 737–744.

DOCZI, T. (1985). The pathogenetic and prognostic significance of blood–brain barrier damage at the acute stage of aneurysmal subarachnoid hemorrhage. Clinical and experimental studies. Acta Neurochir. (Wien) **77**, 110–132.

DOCZI, T., JOO, F., ADAM, G., et al. (1986). Blood-brain barrier damage during the acute stage of subarachnoid hemorrhage, as exemplified by a new animal model. Neurosurgery **18**, 733–739.

FEENEY, D.M., GONZALEZ, A., and LAW, W.A. (1982). Amphetamine, haloperidol and experience interact to affect rate of recovery after motor cortex injury. Science **271**, 855–877.

FUJIKAWA, H., TANI, E., YAMAURA, I., et al. (1999). Activation of protein kinases in canine basilar artery in vasospasm. J. Cereb. Blood Flow Metab. **19**, 44–52.

GERMANÒ, A., D'AVELLA, D., CICCIARELLO, R., et al. (1992). Blood–brain barrier permeability changes after experimental subarachnoid hemorrhage. Neurosurgery **30**, 882–886.

GERMANÒ, A., DIXON, E., D'AVELLA, D., et al. (1994). Behavioural deficits following experimental subarachnoid hemorrhage in the rat. J. Neurotrauma **11**, 345–353.

GERMANÒ, A., TISANO, A., RAFFAELE, M. et al. (1997). Is there a group of early surgery aneurysm SAH patients who can expect to achieve a complete long-term neuropsychological recover? Acta Neurochir. (Wien) **139**, 507–514.

GERMANÒ, A., CARUSO, G., CAFFO, M., et al. (1998). Does subarachnoid hemorrhage per se induce long-term neuropsychological and cognitive alterations? Acta Neurochir. (Wien) **140**, 805–812.

GERMANÒ, A., IMPERATORE, C., D'AVELLA, D., et al. (1998). Antivasospastic and brain-protective effects of a hydroxyl radical scavenger (AVS) after experimental subarachnoid hemorrhage. J. Neurosurg. **88**, 1075–1081.

GERMANÒ, A., D'AVELLA, D., IMPERATORE, C., et al. (2000). The time-course of BBB permeability changes after experimental subarachnoid hemorrhage in the rat. Acta Neurochir. (Wien) **142**, 575–581.

HAYES, R.L., WANG, K.K.W., KAMPFL, A., et al. (1998). Potential contribution of proteases to neuronal damage. Drug News Perspect. **11**, 215–222.

HILLS, A.E., ANDERSON, N., SAMPATH, P., et al. (2000). Cognitive impairment after surgical repair of ruptured and unruptured aneurysms. J. Neurol. Neurosurg. Psychiatry **69**, 608–615.

HUTTER, B.O., and GILSBACH, J.M. (1996). Early neuropsychological sequelae of aneurysm surgery and subarachnoid hemorrhage. Acta Neurochir. (Wien) **138**, 1370–1378.

HUTTER, B.O., KREITSCHMANN-ANDERMAHR, I., MAYFRANK, L., et al. (1999). Functional outcome after aneurismal subarachnoid hemorrhage. Acta Neurochir. Suppl. (Wien) **72**, 157–174.

IMPERATORE, C., GERMANÒ, A., D'AVELLA, D., et al. (2000). Effects of the radical scavanger AVS on behavioral

and BBB changes after experimental subarachnoid hemorrhage. Life Sci. **66,** 779–790.

JACKOWSKI, A., CROCKARD, A., BURNSTOCK, G., et al. (1990). The time course of intracranial pathophysiological changes following experimental subarachnoid hemorrhage in the rat. J. Cereb. Blood Flow Metab. **10,** 835–849.

JOHSHITA, H., KASSELL, N.F., and SASAKI, T. (1990). Blood–brain barrier disturbance following subarachnoid hemorrhage in rabbits. Stroke **21,** 1051–1058.

KAMPFL, A., WHITSON, S., ZHAO, X., et al. (1995). Calpain inhibitors reduce depolarization induced loss of tau protein in primary septo-hippocampal cultures. Neurosci. Lett. **194,** 149–152.

KAMPFL, A., ZHAO, X., WHITSON, S.J., et al. (1996). Calpain inhibitor protects against depolarization induced neurofilament protein loss of septo-hippocampal neurons in culture. Eur. J. Neurosci. **8,** 344–352.

KAMPFL, A., POSMANTUR, R.M., ZHAO, X., et al. (1997). Mechanisms of calpain proteolysis following traumatic brain injury: implications for pathology and therapy: implications for pathology and therapy: a review and update. J. Neurotrauma **14,** 121–134.

KASSELL, N.F., SASAKI, T., and COLOHAN ART (1985). Cerebral vasospasm following aneurysmal subarachnoid hemorrhage. Stroke **16,** 562–572.

KASSELL, N.F., TORNER, J.C., HALEY, E.C., Jr., et al. (1990). The international cooperative study on the timing of aneurysm surgery. Part I: Overall management results. J. Neurosurg. **73,** 18–36.

KAWAMATA, T., PETERSON, J.W., BUN, T., et al. (1990). Augmentation of both hemolysate-induced contraction and activation of protein kinase C by submaximum activation in canine cerebral arteries *in vitro.* J. Neurosurg. **87,** 908–915.

LEE, K.S., YANAMOTO, H., FERGUS, A., et al. (1997). Calcium-activated proteolysis as a therapeutic target in cerebrovascular disease. Ann. N.Y. Acad. Sci. **825,** 95–103.

LEVIN, H.S., BENTON, A.L., and GROSSMAN, R.G. (1982). *Neurobehavioral consequences of severe head injury.* Oxford University Press: New York.

MATSUI, T., TAKUWA, Y., JOHSHITA, H., et al. (1991). Possible role of protein kinase C–dependent smooth muscle contraction in the pathogenesis of chronic cerebral vasospasm. J. Cereb. Blood Flow Metab. **11,** 143–149.

MAYBERG, M.R., OKADA, T., and BARK, D.K. (1990). The role of hemoglobin in arterial narrowing after subarachnoid hemorrhage. J. Neurosurg. **72,** 634–640.

MAVADDAT, N., SAHAKIAN, B.J., HUTCHINSON, P.J., et al. (1999). Cognition following subarachnoid hemorrhage from anterior communicating artery aneurysm: relation to timing of surgery. J. Neurosurg. **91,** 402–407.

MINAMI, N., TANI, E., and MAEDA, Y. (1992). Effects of inhibitors of protein kinase C and calpain in experimental delayed cerebral vasospasm. J. Neurosurg. **76,** 111–118.

MINAMI, N., TANI, E., MAEDA, Y., et al. (1993). Immunoblotting of contractile and cytoskeletal proteins of canine basilar artery in vasospasm. Neurosurgery **33,** 698–705.

NISHIZAWA, S., NEZU, N., and UEMURA, K. (1992). Direct evidence for a key role of protein kinase C in the development of vasospasm after subarachnoid hemorrhage. J. Neurosurg. **79,** 635–639.

PAXINOS, G., WATSON, C. (1982). *The rat brain in stereotaxic coordinates.* Academic Press: New York.

POSMANTUR, R., KAMPL, A., SIMAN, R., et al. (1997). A calpain inhibitor attenuates cortical cytoskeletal protein loss after experimental traumatic brain injury in the rat. Neuroscience **77,** 875–888.

RÖSSNER, W., TEMPEL, K. (1966). Quantitative bestimmung der permeabilit‰t der sogenannten blut-hirnschranke für Evans-Blau (T 1824). Med. Pharmacol. Exp. **14,** 169–182.

SAATMAN, K.E., MURAI, H., BARTUS, R., et al. (1996). Calpain Inhibitor AK295 attenuates motor and cognitive deficits following experimental brain injuty in the rat. Proc. Natl. Acad. Sci. USA **93,** 3428–3433.

SAKO, M., NISHIHARA, J., and OHTA, S. (1993). Role of protein kinase C in the pathogenesis of cerebral vasospasm after subarachnoid hemorrhage. J. Cereb. Blood Flow Metab. **13,** 247–254.

SATO, M., TANI, E., MATSUMOTO, T., et al. (1997). Generation of the catalytic frament of protein kinase C alpha in spastic canine basilar artery. J. Neurosurg. **87,** 752–756.

SCHULZ, M.K., WANG, L.P., TANGE, M., et al. (2000). Cerebral microdialysis monitoring: determination of normal and ischemic cerebral metabolisms in patients with aneurysmal subarachnoid hemorrhage. J. Neurosurg. **93,** 808–814.

TAKUWA, Y., MATSUI, T., ABE, Y., et al. (1993). Alterations in protein kinase C activity and membrane lipid metabolism in cerebral vasospasm after subarachnoid hemorrhage. J. Cereb. Blood Flow Metab. **13,** 409–415.

UYAMA, O., OKAMURA, N., YANASE, M., et al. (1988). Quantitative evaluation of vascular permeability in the gerbil brain after transient ischemia using Evans blue fluorescence. J. Cereb. Blood Flow Metab. **8,** 282–284.

VANDERKLISH, P.W., and BAHR, B.A. (2000). The pathogenic activation of calpain: a marker and mediator of cellular toxicity and disease states. Int. J. Exp. Pathol. **81,** 323–339.

WANG, K.K.W., and YUEN, P.W. (1994). Calpain inhibition: an overview of its therapeutic potential. Trends. Pharmacol. Sci. **15,** 412–419.

WHITE, B.C., SULLIVAN, J.M., DeGRACIA, D.J., et al. (2000). Brain ischemia and reperfusion: molecular mechanisms of neuronal injury. J. Neurol. Sci. **179,** 1–33.

YAMAURA, I., TANI, E., SAIDO, T.C., et al. (1993). Calpain-calpastatin system of canine basilar artery in vasospasm. J. Neurosurg. **79,** 537–543.

YOKOTA, M., TANI, E., and TSUBUKI, S. (1999). Calpain inhibitor entrapped in liposome rescues ischemic neuronal damage. Brain Res. **819,** 8–14.

YUEN, P., and WANG, K.K.W. (1998). Calpain inhibitors: novel neuroprotectants and potential anticataract agents. Drugs Future **23,** 741–749.

ZUCCARELLO, M., and ANDERSON, D.K. (1989). Protective effect of a 21–aminosteroid on the blood–brain barrier following subarachnoid hemorrhage in rats. Stroke **20,** 367–371.

Address reprint requests to:
F.F. Angileri, M.D.
Neurosurgical Clinic
Policlinico Universitario
98125 Messina, Italy

E-mail: fangileri@infinito.it

Up-regulation of tissue-type transglutaminase after traumatic brain injury

Paul J. Tolentino,* S. Michelle DeFord,* Lucia Notterpek,* Christopher C. Glenn,* Brian R. Pike,* Kevin K. W. Wang† and Ronald L. Hayes*

*Department of Neuroscience Evelyn F. and William L. McKnight Brain Institute of the University of Florida Center for Traumatic Brain Injury Studies, Gainesville, Florida, USA

†Department of Neuroscience Therapeutics, Pfizer Inc., Ann Arbor, Michigan, USA

Abstract

Tissue-type transglutaminase (tTG, EC 2.3.2.13) has been implicated in various disease paradigms including neurodegenerative disease. In these studies, tTG induction after traumatic brain injury was studied using a rat cortical impact model. Using western blots, two forms of tTG protein expression were identified – a ~79-kDa primary form (tTG-L) and a less abundant ~70-kDa form (tTG-S). Both forms of tTG protein were elevated after injury. In ipsilateral cortex, peak induction of tTG-L protein [561% ± 80% of control ($n = 5$)] was observed five days after injury, with expression remaining elevated after two weeks. Peak induction of tTG-S protein [302% ± 81% of control ($n = 5$)] was observed three days after injury. Lesser tTG protein induction was observed in hippocampus. Northern blot analysis demonstrated two tTG transcripts in the ipsilateral cortex with peak induction of tTG-L mRNA three days after injury. However, tTG-S mRNA was not identified in control samples and only faintly detected in injured tissue. To facilitate analysis of low abundance transcripts in smaller tissue samples, a semiquantitative real-time PCR strategy was used. Semi-quantitative PCR analysis of tTG-L mRNA induction in ipsilateral cortex (peak after three days; 414% ± 21% of control, $n = 3$) confirmed tTG-L mRNA induction determined by northern blot (410% of control).

Keywords: quantitative PCR, transglutaminase, traumatic brain injury.

J. Neurochem. (2002) **80**, 579–588.

Tissue-type transglutaminase (type II transglutaminase, transglutaminase C, tTG) has been implicated and may play a role in apoptotic cell death, neurodegenerative disease and in protein aggregation associated with neurodegenerative disease. Although apoptosis is a prominent feature of cell death following TBI and TBI, it is a risk factor for a number of neurodegenerative diseases, such as Alzheimer's disease, no studies have examined the alteration in tTG following CNS injury (CNS).

tTG is a Ca^{2+} dependent enzymeand is a member of a family of transglutaminases (TG) that catalyzes the transamidation of glutamine residues. tTG can catalyze the incorporation of a polyamine into a polypeptide-bound glutamine leading to the formation of a (γ-glutamyl) polyamine bond. Alternatively, when this reaction occurs between the γ-carboxamide group of a peptide-bound glutamine residue and the ε-amino group of a peptide-bound lysine residue, ε-(γ-glutamyl) lysine isopeptide bond is formed (Greenberg *et al.* 1991). This isopeptide bond is resistant to proteolytic cleavage, and may serve not only to stabilize proteins against degradation, but also to alter their function. There are numerous substrates for tTG, including structural proteins, enzymes, and elements of signal transduction pathways (Chen and Mehta 1999).

Though there are currently seven known TGs, only TG 1 (106 kDa), tTG (80 kDa) and TG 3 (77 kDa) have been identified within the brain (Selkoe *et al.* 1982). Importantly, Kim *et al.* (1999) revealed that only TG 1 and tTG were expressed within the cerebral cortex, with tTG most abundantly expressed.

Additionally, tTG functions as a G-protein, designated $G\alpha_h$, that interacts with phospholipase C-δ1 (Nakaoka *et al.* 1994; Feng *et al.* 1996; Park *et al.* 1998). $G\alpha_h$ was originally identified as the signal transducer between epinephrine binding to α_1-adrenoreceptor and phospholipase C (PLC) activation (Im *et al.* 1990; Im and Graham 1990; Das *et al.* 1993), specifically PLC-δ1 (Feng *et al.* 1996). The identity of $G\alpha_h$ as tTG was clarified by peptide foot-print analysis between tTG and $G\alpha_h$ and cross-reactivity between antibodies for rat liver $G\alpha_h$ and antibodies for guinea pig liver tTG (Nakaoka *et al.* 1994). The C-terminal region of tTG is important for its ability to interact with PLC (Hwang *et al.* 1995; Feng *et al.* 1996) and with receptor molecules (Feng *et al.* 1999).

Previous reports have described changes in over all TG activity during the development of mouse brain (Maccioni and Seeds 1986) and rat brain (Gilad and Varon 1985; Perry and Haynes 1993). Other proposed functions include involvement in cell–matrix interactions, wound healing, regeneration and neurodegenerative disease (for a review see Lesort *et al.* 2000). Among its many possible functions, tTG has been implicated as a mediator of apoptosis. In the neuroblastoma cell line SK-N-BE(2), tTG overexpression stimulated apoptosis while inhibition of tTG expression with an antisense construct decreased both spontaneous and retinoic acid-induced apoptosis (Melino *et al.* 1994). tTG-mediated apoptosis may involve multiple target substrates. During apoptosis tTG modifies several proteins including histone protein (Ballestar *et al.* 1996), actin (Nemes *et al.* 1997), troponin (Gorza *et al.* 1997), and retinoblastoma protein (Oliverio *et al.* 1997). Given the complexity with which tTG interacts with numerous proteins, the role of tTG in apoptosis is not yet understood (for a review see Melino and Piacentini 1998).

tTG mRNA and protein expression have been demonstrated in cultured astrocytes from two-day postnatal rats (Monsonego *et al.* 1997). In astrocyte cultures treated with IL-1β, two transcripts encoding tTG were identified – a full-length long form (encoding a ~77-kDa protein), and a less abundant short form (encoding a ~73-kDa protein) that lacked a portion of the C-terminus coding region and had a truncated 3′ untranslated region. Interestingly, the enzymatic activity of the tTG short form lacked the GTP-dependence observed in the tTG long form (Monsonego *et al.* 1997). The functional significance of the two types of tTG expressed in cultured astrocytes is not yet clear.

Induction of tTG expression by IL-1β and TNF-α *in vitro* may prove relevant to the *in vivo* response to traumatic injury. Traumatic brain injury (TBI) induces the expression of both IL-1β and TNF-α (Woodroofe *et al.* 1991; Taupin *et al.* 1993; Rostworowski *et al.* 1997; Herx *et al.* 2000). Using a microdialysis probe to induce mechanical trauma as well as measure cytokine levels, Woodroofe *et al.* (1991) showed a 15-fold induction of IL-1 within a two-day period.

Using a fluid percussion model of traumatic brain injury, Taupin *et al.* (1993) demonstrated IL-1 induction in cortex and hippocampus up to 18 h after injury and TNF-α induction 3–8 h after injury. After stab injury, IL-1β mRNA is induced 3–12 h after injury, while TNF-α mRNA is induced from 3 to 96 h after injury (Rostworowski *et al.* 1997). After corticectomy, both IL-1β and TNF-α transcripts were increased three hours after injury (Herx *et al.* 2000). If injury-induced IL-1β and TNF-α elevate tTG expression *in vivo* as has been shown for *in vitro* astrocytes, then tTG may play a role in the subsequent CNS response to trauma. In particular, the pro-apoptotic effects of tTG expression may contribute to the post-traumatic apoptotic phenotype seen in CNS injury. The apoptotic components of cell death after experimental TBI have been examined in models of fluid compression (Rink *et al.* 1995; Yakovlev *et al.* 1997; Conti *et al.* 1998) and cortical impact (Colicos and Dash 1996; Newcomb *et al.* 1999).

The aim of this study was to determine whether tTG is up-regulated as a result of TBI, and if so, to determine the time course of induction. Using western blot analyses, we found that both forms of tTG [tTG-L (~79 kDa) and tTG-S (~70 kDa)] were strongly induced in ipsilateral cortex after traumatic injury with predominant expression of tTG-L. These two forms are similar to the long and short forms seen in cytokine-induced astrocytes (Monsonego *et al.* 1997). To further analyze this phenomenon, induction of specific tTG transcripts was verified by northern blot and semiquantitative PCR analysis.

Materials and methods

Surgical preparation and controlled cortical impact traumatic brain injury

A previously described cortical impact injury device was used to produce TBI in adult rats (Dixon *et al.* 1991; Pike *et al.* 1998). Cortical impact TBI results in cortical deformation within the vicinity of the impactor tip associated with contusion, and neuronal and axonal damage that is constrained in the hemisphere ipsilateral to the site of injury (Gennarelli 1994; Meaney *et al.* 1994). Adult male (280–300 g) Sprague–Dawley rats (Harlan, Indianapolis, IN, USA) were anesthetized with 4% isoflurane in a carrier gas of 1 : 1 O_2/N_2O (4 min) followed by maintenance anesthesia of 2.5% isoflurane in the same carrier gas. Core body temperature was monitored continuously by a rectal thermistor probe and maintained at 37° ± 1°C by placing an adjustable temperature controlled heating pad beneath the rats. Animals were mounted in a stereotactic frame in a prone position and secured by ear and incisor bars. A midline cranial incision was made, the soft tissues were reflected, and a unilateral (ipsilateral to site of impact) craniotomy (7 mm diameter) was performed adjacent to the central suture, midway between bregma and lambda. The dura mater was kept intact over the cortex. Brain trauma was produced by impacting the right cortex (ipsilateral cortex) with a 5-mm diameter aluminum impactor tip (housed in a pneumatic cylinder) at a velocity of 3.5 m/s with a

1.6-mm compression and 150 ms dwell time (compression duration). Velocity was controlled by adjusting the pressure (compressed N_2) supplied to the pneumatic cylinder. Velocity and dwell time were measured by a linear velocity displacement transducer (Lucas Shaevitz™ model 500 HR, Detroit, MI, USA) that produces an analogue signal that was recorded by a storage-trace oscilloscope (BK Precision, model 2522B, Placentia, CA, USA). Sham-injured animals underwent identical surgical procedures but did not receive an impact injury. Appropriate pre- and post-injury management was maintained and these measures complied with all guidelines set forth by the University of Florida Institutional Animal Care and Use Committee and the National Institutes of Health guidelines detailed in the *Guide for the Care and Use of Laboratory Animals*.

Tissue lysis and protein purification

Cortical and hippocampal tissues were collected from animals at 1–14 days after sham-injury or TBI. At the appropriate time-points, TBI or sham-injured animals were killed with CO_2 and subsequent decapitation. Ipsilateral and contralateral (to the impact site) cortices and hippocampi were rapidly dissected and snap-frozen in liquid nitrogen. Tissue samples were stored at $-80°C$. Cortices were homogenized in a glass tube with a Teflon dounce pestle in 15 volumes of ice-cold triple detergent lysis buffer (20 mM HEPES, 1 mM EDTA, 2 mM EGTA, 150 mM NaCl, 0.1% SDS, 1.0% IGEPAL 40, 0.5% deoxycholic acid, pH 7.5) containing a broad range protease inhibitor cocktail (cat. no. 1-836-14; Roche Molecular Biochemicals, Indianapolis, IN, USA). Samples were sonicated and centrifuged at 800 g for 5 min at 4°C. The supernatant was then collected for western blot analysis.

Western blot analysis

Protein concentrations of tissue homogenates were determined by bicinchoninic acid microprotein assays (Pierce Inc., Rockford, IL, USA) with albumin standards. 20 μg aliquots of each sample were prepared for sodium dodecyl sulfate–polyacrylamide gel electrophoresis (SDS–PAGE) by addition of 2× loading buffer (1× loading buffer contains 125 mM Tris-HCl (pH 6.8), 100 mM DTT, 4% SDS, 0.01% bromophenol blue, and 10% glycerol). Samples with loading buffer were heated for 10 min at 100°C, centrifuged for 1 minute at 10 000 g, and were resolved by SDS–PAGE on 7.5% Tris/glycine gels at 200 V for 1 h at 4°C. Following electrophoresis, fractionated proteins were transferred to Immobilon-*p* polyvinylidene fluoride (PVDF) membrane (Millipore, Bedford, MA, USA) in a transfer buffer containing 192 mM glycine, 25 mM Tris-HCl (pH 8.3), and 10% methanol at 100 V for 1 h at 4°C. Ponceau Red (Sigma, St Louis, MO, USA) was used to stain membranes to confirm successful transfer of protein and to insure that an equal amount of protein was loaded in each lane. Blots were blocked for 1 h at room temperature in 5% non-fat milk in TBST (20 mM Tris-HCl, 150 mM NaCl, and 0.005% Tween-20, pH 7.5).

Immunoblots were probed with one of two monoclonal anti-tTG antibodies, designated CUB 7402 or TG100 (LabVision, Fremont, CA, USA). Following overnight incubation at 4°C with the primary antibody (1 : 3000), blots were incubated for 1 h at room temperature (22°C) in 3% non-fat milk/TBST containing a horseradish peroxidase-conjugated goat anti-mouse IgG (1 : 3000; Bio-Rad, Hercules, CA, USA). Bound antibodies were visualized with enhanced chemiluminescence (ECL; Amersham, Piscataway, NJ, USA) on Kodak Biomax ML chemiluminescent film.

RNA purification

Total RNA was isolated from control and injured samples of cortical or hippocampal tissue using TRIzol reagent (Gibco BRL, Rockville, MD, USA), isopropanol precipitation, and ethanol washes according to the manufacturer's instructions. Samples were resuspended in 50–100 μL DEPC-treated water.

Reverse transcription

Total RNA (3 μg) was incubated with 1 μL oligo(dT) (0.5 mg/mL, Gibco BRL) at 70°C for 10 min, then at 4°C for five minutes. A reverse transcription reaction mixture was then added to the RNA-oligo(dT) sample for a final volume of 20 μL, containing 20 mM Tris-HCl (pH 8.4), 50 mM KCl, 5 mM $MgCl_2$, 500 μM dNTP's, 10 mM DTT, 50 units SuperScript II reverse transcriptase (Gibco BRL) and 40 units RNaseOUT recombinant ribonuclease inhibitor (Gibco BRL). The sample was incubated at 42°C for 55 min, 70°C for 15 min for enzyme denaturation, and then transferred to 4°C. Each sample was diluted to a final volume of 100 μL with DEPC-treated water.

Primer selection

tTG-specific primers

All base pair designations refer to GeneBank locus AF106325, rat tissue-type transglutaminase (TGaseII). *5'TG* (actttgacgtgtttgcccac; bp 1470–1489) recognizes an upstream homologous sequence in tTG-L and tTG-S transcripts. *3'tTG-L* (caatatcagtcgggaacaggtc; bp 1961–82) recognizes a downstream tTG-L mRNA-specific sequence. *3'tTG-S* (gctgagtctgggtgaagacacag; bp 1861–1872 and 2083–93) recognizes a downstream tTG-S mRNA-specific sequence. *3'tTG-S* primer bridges the junction created absence of bp 1873–2082 (a sequence present exclusively in tTG-L). The underlined 3' half of the 3'tTG-S sequence will hybridize to both tTG-L- and tTG-S-specific sequence, while the full length primer will hybridize only to tTG-S mRNA sequence.

GAPDH-specific primers

All base pair designations for GAPDH-specific primers refer to GeneBank locus AF106860. The upstream primer is designated *5'GPD* (ggctgccttctcttgtgac; bp 903–921) and the downstream primer is designated *3'GPD* (ggccgcctgcttcaccac; bp 1624–1641).

Standard PCR

A PCR reaction buffer was added to 2 μL of reverse transcription product for a final volume of 25 μL containing 20 mM Tris-HCl (pH 8.4), 50 mM KCl, 2.5 mM $MgCl_2$, 200 μM dNTP's, 0.5 μM dNTP's, 6% DMSO, 1.25 units Taq DNA polymerase (Gibco BRL). The mixture was then transferred to a PCR apparatus for amplification: each denaturation, annealing, and extension step was held for 30 s (two cycles of 95°, 65°C, and 72°C; then two cycles of 95°C, 62.5°C, and 72°C; then 32 cycles of 95°C, 60°C, and 72°C). Aliquots of PCR products were loaded onto 1.5% agarose gels and separated by electrophoresis in TAE buffer (40 mM Tris-acetate, 1 mM EDTA, pH 7.5) containing 5 μg/mL ethidium bromide. To assay for genomic DNA contamination, RNA samples

underwent PCR amplification without prior reverse transcription. Any samples showing genomic contamination underwent repurification and repeat assay for genomic contamination prior to PCR analysis for transcript expression.

Northern blot analysis

Total RNA (10 μg) was size-fractionated by electrophoresis in 1.5% agarose gels containing 6% formaldehyde, then transferred onto Hybond N + nylon membrane (Amersham), and fixed by baking at 80°C for 1 h under vacuum. Membranes were hybridized in a solution containing 5× SSPE (1× SSPE contains 180 mM NaCl, 10 mM sodium phosphate, and 1 mM EDTA, pH 7.7), 5× Denhardt's solution (1× Denhardt's solution contains 0.02% bovine serum albumin, 0.02% Ficoll, and 0.02% polyvinylpyrrolidone), 0.5% SDS, 20 μg/mL sheared denatured salmon sperm DNA, and random primer-generated probe at 65°C overnight. DNA probes were radiolabeled to a specific activity of 1×10^9 dpm/μg by random-primed labeling (Gibco BRL) with [α-^{32}P]dCTP (3000 Ci/mmol; DuPont NEN, Boston, MA, USA). After hybridization, membranes were washed sequentially with 2× SSPE/0.1% SDS at room temperature, then 1× SSPE/0.1% SDS at 65°C, and then 0.1× SSPE/0.1% SDS at 65°C. Membranes were exposed to film with one intensifying screen at −80°C.

TTG and GAPDH cDNA

For northern blot analysis of tTG expression, a 414-bp tTG-cDNA was generated via PCR. This fragment corresponds to 403 bp of tTG-L coding sequence and to 414 bp of tTG-S coding sequence. To monitor GAPDH expression, a 1.2-kb EcoRI fragment from HHCMC32 (American Type Culture Collection, Manassas, VA, USA) was used.

Semi-quantitative/light cycler PCR

Real time PCR was performed using a Light Cycler rapid thermal cycler system (Roche Diagnostics, Indianapolis, IN, USA) according to the manufacturer's instructions. Reactions were performed in a 10 μL volume with 0.5 μM primers, 2.5 mM MgCl₂. Other reagents including nucleotides, FastStart Taq DNA polymerase, and buffer were used as provided in the LightCycler-FastStart DNA Master SYBR Green I reaction mix (Roche Diagnostics). Amplification protocol included a 5 minute 95°C denaturation; one cycle with 95°C denaturation for 5 s, 65°C annealing for 10 s, and 72°C extension for 35 s; one cycle with 95°C denaturation for 5 s, 62.5°C annealing for 10 s, and 72°C extension for 35 s; then 30–40 cycles of 95°C denaturation for 5 s, 60°C annealing for 10 s, and 72°C extension for 35 s. Detection of the fluorescent product occurred at the end of the 72°C extension periods. Specificity of the amplification product from each primer pair was confirmed by melting curve analysis of the PCR product and subsequent gel electrophoresis.

Quantification was performed by online monitoring for identification of the exact time point at which the logarithmic linear phase could be distinguished from the background (crossing point). The crossing point is expressed as a cycle number.

Standard curve preparation and semiquantitative PCR analysis

From the northern blot analysis, maximal tTG-L and tTG-S mRNA expression was identified three days after injury. The reverse

transcription product from ipsilateral cortical RNA collected three days after injury underwent serial dilution, creating a standard curve of 100%, 33%, 11% and 3.7% of original RT product. Each dilution from the standard curve was analyzed with the LightCycler PCR using primer sets for tTG-L, tTG-S, or GAPDH mRNA. For each primer set, a crossing point cycle number was determined for each dilution of the standard curve. Linear regression analysis of the logarithm of the dilution factor vs. the crossing point cycle number generated a standard curve for each transcript-specific primer set. From each primer set's standard curve, a crossing point cycle number could be converted to a relative amount of RNA.

For individual samples, the crossing point cycle number was identified with the LightCycler PCR. Then, using the standard curve for each primer set, the amount of tTG-L, tTG-S, or GAPDH mRNA was determined. The amount of each transcript in sham animals was set at 100%, and the level of expression in an experimental sample was calculated as a percentage of sham expression.

Statistical analyses

For the western and northern blots, semiquantitative analysis was performed by computer-assisted densitometric scanning (AlphaImager 2000 Digital Imaging System, San Leandro, CA, USA). Data were acquired as integrated densitometric values and transformed to percentages of the densitometric levels obtained from sham-injured animals visualized on the same blot. PCR data was evaluated by least squares linear regression followed by ANOVA and Dunnett's multiple comparison test. All values are given as mean ± SEM. Differences were considered significant if $p < 0.05$.

Results

Western blot analysis of tTG expression in cortex after traumatic injury

Total protein was prepared from rat ipsilateral cortex after cortical impact injury. Expression of tTG was examined using two monoclonal anti-tTG antibodies, TG-100 and CUB-7402. Figure 1(a) shows western blot analyses for tTG expression in rat ipsilateral cortex one to 14 days after injury. Using the TG-100 antibody, two distinct tTG protein bands were identified: a ~79-kDa band corresponding to the tTG long form (tTG-L) and a ~70-kDa band that may represent the tTG short form (tTG-S). The presence of tTG-S was not detected with the CUB-7402 antibody; however, with prolonged film exposure of the TG-100 blots, tTG-S was more clearly identified (Fig. 1b).

Western blot analyses of ipsilateral cortex samples using TG-100 were quantified by densitometric analysis (Fig. 1c). Levels of tTG-L and tTG-S were expressed as percentage of sham levels. Sham-operated animals showed no change in tTG-L or tTG-S expression one day and five days after craniotomy (Fig. 1a). tTG-L induction was observed 1–14 days after cortical injury. tTG-L expression peaked at 561% ± 16% ($n = 5$) five days after injury, with statistically significant elevated expression at 3–14 days. tTG-S induc-
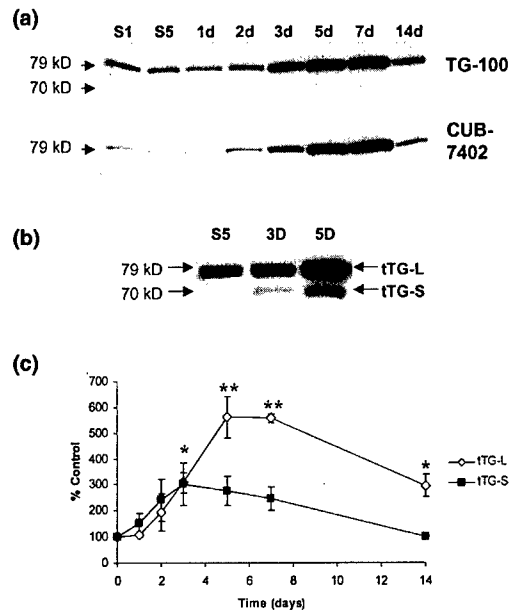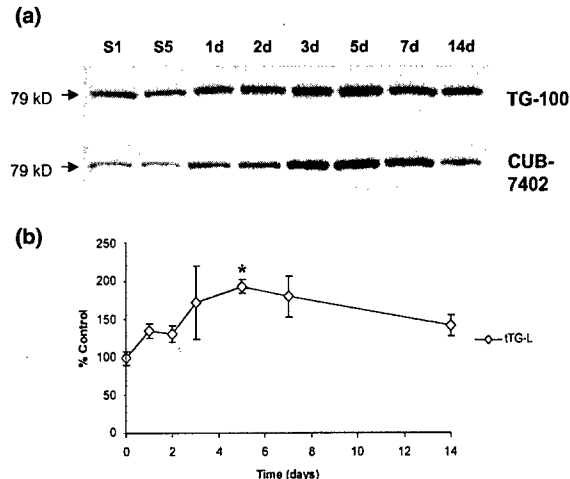
(a)

(b)

(c)

Fig. 1 Western blot analysis for tTG expression in ipsilateral cortical protein samples using the anti-TG-II antibodies TG-100 and CUB-7402. (a) Samples were collected from sham-operated animals one and five days after surgery (S1, S5) as well as from injured animals from one day to 14 days after injury (1d–14d). (b) Longer exposure of the western blot using TG-100 antibody suggests co-expression of tTG-L (~79 kDa, full length tTG) and tTG-S (~70 kDa, a short form of tTG). (c) Quantitative analysis: western blot analyses using TG-100 antibody were quantified by densitometry, and the level of tTG (tTG-L and tTG-S) expression in the ipsilateral cortex of injured animals was calculated as a percentage of sham (control) tTG expression. For each condition, $n = 5$ animals. One-way ANOVA was performed, followed by Dunnett's multiple comparison test to evaluate statistical significance. Comparing tTG-L expression from injured animals to control/sham animals, increased levels of expression were statistically significant at three, five, seven, and 14 days ($^*p < 0.05$, $^{**}p < 0.01$). Comparing tTG-S expression from injured animals to control/sham animals, increased levels of expression were not statistically significant.

tion was observed 1–7 days after cortical injury, with peak expression (302% ± 81%, $n = 5$) at three days. However, levels of tTG-S induction did not reach statistical significance (Fig. 1c). No changes in tTG-L or tTG-S expression were observed in the contralateral cortex (not shown).

Western blot analysis of tTG expression in hippocampus after traumatic injury

Total protein was prepared from rat ipsilateral hippocampus after cortical impact injury. Expression of tTG was examined using TG-100 and CUB-7402 antibodies. Figure 2(a) shows western blot analyses for tTG expression in rat ipsilateral hippocampus one to 14 days after injury. Compared to ipsilateral cortex, lower levels of tTG induction were identified in the hippocampus, and tTG-S was not detected with either antibody. Quantitative densitometric analysis of

(a)

(b)

Fig. 2 Western blot analysis for tTG expression in ipsilateral hippocampal protein samples using the anti-tTG antibodies TG-100 and CUB-7402. Samples were collected from sham-operated animals one day and five days after surgery (S1, S5) as well as from injured animals one day to 14 days after injury (1d-14d). tTG-S, the shorter form of tTG (70 kDa), was not identified in these samples even at longer exposures. (b) Quantitative analysis: western blot analyses using TG-100 were quantified by densitometry, and the level of tTG expression in the ipsilateral hippocampus of injured animals was calculated as a percentage of sham (control) tTG expression. Only tTG-L was quantified, as tTG-S expression was not identified in every sample. For each condition, $n = 5$ animals. One-way ANOVA was performed, followed by Dunnett's multiple comparison test to evaluate statistical significance. Comparing tTG-L expression from injured animals to control/sham animals, increased levels of expression were statistically significant at five days ($^*p < 0.05$).

tTG-L expression revealed peak levels (194% ± 9%, $n = 5$) five days after injury. Increased tTG-L expression was observed 1–14 days after injury, but statistically significant increases were only detected five days after injury (Fig. 2b).

tTG transcript PCR analysis

Given the previous report of two types of tTG expressed in rat brain astrocytes (Monsonego *et al.* 1997), and the current findings suggesting long (tTG-L) and short (tTG-S) forms of tTG in ipsilateral rat cortex after injury, the molecular analysis of tTG transcripts was performed. Figure 3(a) provides a schematic diagram of the two tTG transcripts previously described (Monsonego *et al.* 1997). The tTG-L transcript contains an additional 209 bp sequence (bp 1873–2082) absent in tTG-S mRNA. To investigate which tTG transcripts were expressed after injury, total RNA was purified from rat ipsilateral cortex five days after injury. The sample was then reverse transcribed and underwent standard PCR to detect tTG-L, tTG-S and GAPDH transcripts. Figure 3(b) shows the results of the PCR analysis, indicating the presence of both tTG-L and tTG-S mRNA in rat ipsilateral cortex five days after injury. The identity of the
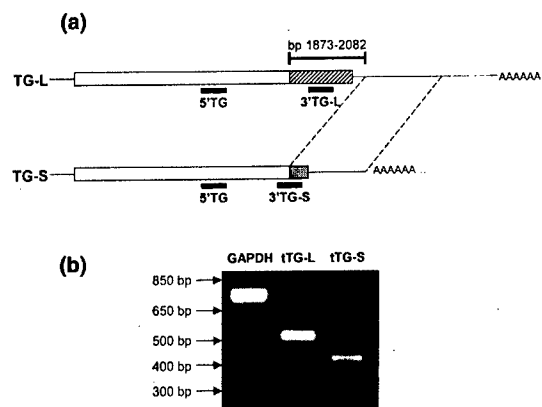
Fig. 3 (a) Schematic diagram of tTG transcripts. tTG-L mRNA contains an additional sequence (bp 1873–2082) not present in tTG-S mRNA. This sequence encodes additional coding region and 3′ untranslated region. PCR primer sites are designated: 5′TG (bp 1470–1489) recognizes homologous sequence in tTG-L and tTG-S transcripts. 3′TG-L (bp 1961–82) recognizes tTG-L mRNA-specific sequence. 3′TG-S recognizes the junctional sequence created by the absence of the tTG-L-specific sequence (bp 1861–1872 and 2083–93). All base pair designations refer to GeneBank locus AF106325, rat tissue-type transglutaminase (TGaseII). (b) PCR analysis of ipsilateral cortex RNA. GPD, 739 bp PCR product generated with rat GAPDH-specific primers. (5′GAPDH primer includes bp 903–921; 3′GAPDH primer includes bp 1624–1641, as designated in GeneBank locus AF106860). tTG-L, 513 bp PCR product generated with tTG-L-specific primers. tTG-S, 414 bp PCR product generated with tTG-S-specific primers.

Fig. 4 Northern blot analysis of ipsilateral cortex RNA after injury. (a) Above: northern blot using tTG-S PCR product as template for random hexamer-generated probe. Positions of tTG-L mRNA (3.7 kb) and tTG-S mRNA (2.4 kb) are noted. Below: northern blot using GAPDH cDNA as template for random hexamer-generated probe. Position of GAPDH (2 kb) mRNA is noted. (b) Northern blot analysis for tTG-L mRNA expression (◇) were quantified by densitometry and corrected for loading by the level of GAPDH expression. tTG-L mRNA expression is represented as a percentage of sham expression. For each condition, tissue from three replicate animals was combined prior to northern analysis.

PCR products was verified by restriction endonuclease analysis (not shown).

Northern blot analysis of ipsilateral cortex RNA postinjury

Given the observation of both tTG-L and tTG-S transcripts in ipsilateral cortex after injury by PCR, northern blot analysis was performed to assess the temporal profile of tTG induction (Fig. 4a). Under sham conditions tTG-L mRNA was barely detectable. tTG-L mRNA expression was elevated 1–5 days after injury, with maximal tTG-L transcript expression (410% of sham expression) observed three days after injury. The northern blot analysis of tTG-L expression in ipsilateral cortex samples was quantified by densitometry and total RNA loading was corrected using GAPDH expression (Fig. 4b). Although maximal tTG-S transcript expression was also observed three days after injury, the degree of induction cannot be calculated, as tTG-S mRNA was undetectable under sham conditions.

Northern blot analysis was able to demonstrate the temporal profile of tTG-L transcript induction in response to cortical injury. However, clear identification and analysis of tTG-S transcript was not possible due to background signal on the northern blots, as well as the low levels of

tTG-S transcript expression. To address these limitations, a semiquantitative PCR strategy was developed to independently measure tTG-L and tTG-S transcript levels. This approach has two major advantages: (1) PCR amplification allows for detection of much lower levels of transcript expression and (2) a PCR-based approach decreases the amount of total RNA required for analysis, thereby facilitating analysis of smaller tissue samples and obviating the need to pool RNA samples prior to analysis.

Standard curve generation for semiquantitative PCR using serially diluted cDNA

As the highest level of tTG-L and tTG-S transcript expression was observed in ipsilateral cortex three days after injury, ipsilateral cortex total RNA was collected three days after injury, reverse transcribed, and serially diluted to generate a standard curve of relative amounts of RNA. These samples underwent analysis using the LightCycler PCR with primer sets for tTG-L, tTG-S, or GAPDH mRNA. For each dilution sample (100%, 33.3%, 11.1% and 3.7%), the PCR analysis yielded a crossing point cycle number for each primer pair (tTG-L, tTG-S or GAPDH-specific). Figure 5 shows the linear regression analysis of each primer set's crossing point cycle number vs. the logarithm of the dilution factor. For
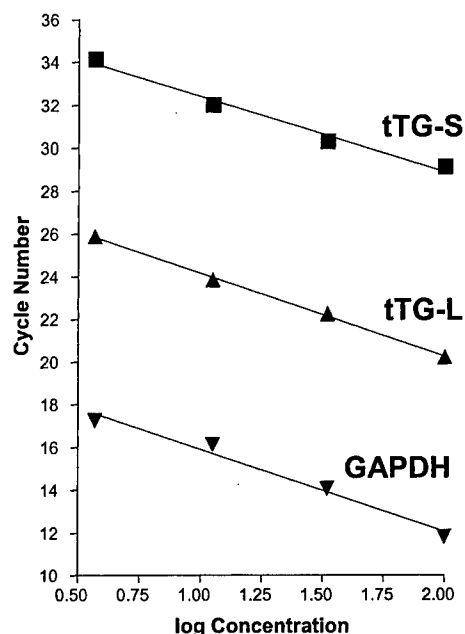
Fig. 5 Standard curve generation for tTG-L-, tTG-S-, and GAPDH-specific quantitative PCR. Total RNA was extracted from rat ipsilateral cortical tissue three days after injury. RNA samples were reverse transcribed, and then the cDNA's were serially diluted. Aliquots of the cDNA dilution curve underwent real-time PCR using primer pairs for tTG-L mRNA, tTG-S mRNA, or GAPDH mRNA. For each dilution and each primer set, the cycle number at which the PCR amplification entered the log-linear region was identified (crossing point cycle number). Standard curves were generated by plotting the log concentration of total RNA versus the crossing point cycle number, and a linear regression analysis was performed (r^2 ranged from 0.980 to 0.998). For quantitation, individual sham and experimental RNA samples underwent real time PCR, generating a crossing point cycle number for each primer set. Using the standard curves, the cycle number was converted to an amount of RNA. These amounts were then expressed as percentage of control/sham RNA.

each primer set, the range of crossing point cycle numbers required to cover the serially diluted standard curve varied: 11–18 cycles for GAPDH, 20–26 cycles for tTG-L, 29–35 cycles for tTG-S. These differences reflect primarily the abundance of the transcripts. GAPDH mRNA is the most abundant transcript and requires the fewest cycles, whereas tTG-S mRNA is the least abundant transcript and requires the most cycles. Furthermore, each primer set amplified its target transcript with different efficiencies (GAPDH 79%, tTG-L 80%, and tTG-S 90%).

Semi-quantitative PCR analysis of experimental samples

Experimental RNA samples were analyzed with the Light-Cycler PCR system, generating crossing point cycle numbers for tTG-L-, tTG-S- and GAPDH-specific primers. Using the standard curves, the crossing point cycle numbers were
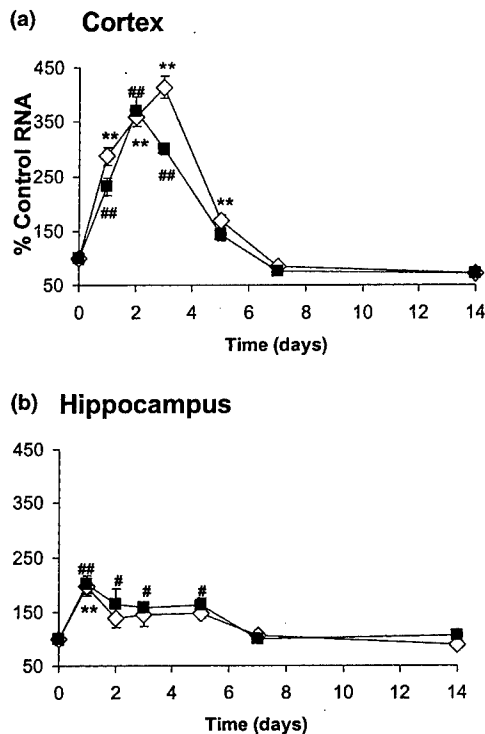
Fig. 6 Semi-quantitative PCR analysis of tTG-L and tTG-S mRNA expression in cortex (a) and hippocampus (b). tTG-L (◇) and tTG-S (■) mRNA levels are expressed as a percentage of control/sham animal expression. One-way anova was performed, followed by Dunnett's multiple comparison test, to evaluate statistical significance. Comparing tTG-L mRNA expression from injured animals to control/sham animals. $*p < 0.05$; $**p < 0.01$. Comparing tTG-S mRNA expression from injured animals to control/sham animals. $\#p < 0.05$; $\#\#p < 0.01$.

converted to relative amounts of RNA. These relative amounts were then expressed as percentage of control/sham levels. Figure 6 shows the time course of tTG-L and tTG-S RNA expression in ipsilateral cortex and hippocampus after cortical injury. In cortex, maximal tTG-L mRNA expression was observed (414% ± 21% ($n = 3$) of control) three days after injury, while maximal tTG-S mRNA expression was observed [369% ± 28% ($n = 3$) of control] two days after injury. In hippocampus, maximal tTG-L and tTG-S mRNA levels were observed one day after injury, 196% ± 14% ($n = 3$) of control, and 201% ± 16% ($n = 3$) of control, respectively.

Linear regression analysis of tTG-L mRNA quantification by PCR versus northern blot

To verify that semiquantitative PCR methods would yield results similar to northern blot analysis, a linear regression analysis was performed to compare tTG-L mRNA expression determined by PCR and northern blot (Fig. 7). Results from northern blot and PCR analyses fit a linear correlation with a slope = 1.01, $r^2 = 0.95$. This comparison is unavailable for
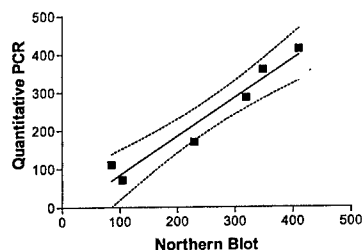
Fig. 7 Linear regression analysis of tTG-L mRNA expression in ipsilateral cortex, comparing quantification by PCR and by northern blot analysis. The linear relation with 95% confidence interval lines are shown. Regression analysis revealed a slope of 1.01 and $r^2 = 0.95$.

tTG-S mRNA since the transcript was not clearly quantified on the northern blot.

Discussion

This study describes the increased expression of tTG in cortex and hippocampus after traumatic brain injury. Two forms of tTG were expressed, tTG-L and tTG-S, that differ in their C-terminal regions. Western blot analysis with two separate antibodies for tTG identified tTG-L as the predominant form. In cortex, tTG-L protein expression peaked five days after injury and remained elevated at least two weeks after injury. tTG-L protein expression in the hippocampus also peaked five days after injury, but the degree of induction was more modest. tTG-L protein induction was supported by northern blot and semiquantitative PCR transcript analysis. The relatively delayed response of tTG to TBI suggests that it is not a major contributor to the more acute pathophysiological events such as those mediated by activation of calcium-dependent proteases. The contribution of these more delayed changes in tTG to more prolonged mechanisms of TBI recovery remained to be examined.

tTG-S expression was more difficult to analyze, since tTG-S protein was identified with only one of the two antitTG antibodies and tTG-S protein was less abundant than tTG-L protein. Although northern blot analysis detected tTG-S transcript three days after injury, tTG-S mRNA was undetectable in sham animals and at later time points after injury. Semi-quantitative PCR presents the most compelling evidence that tTG-S mRNA induction occurs. These studies provide the first evidence of tTG induction in response to traumatic CNS injury.

In a spinal cord ischemia model, over all TG activity underwent a transient increase that declined to control levels after one week (Fujita *et al.* 1995). In the superior cervical ganglion, TG activity was increased within one hour after axotomy and returned to baseline after 24 h (Gilad *et al.* 1985; Ando *et al.* 1993). TG activity also increased in the vagus nerve after crush injury (Tetzlaff *et al.* 1988). These previous studies measured over all TG activity and did not

measure expression of tTG protein or transcript. While the current studies did not address tTG activity, TBI induction of tTG activity may have been further potentiated by the increased intracellular calcium flux consistent with traumatic injury (Hubschmann and Nathanson 1985; Katayama *et al.* 1995), as tTG is a Ca^{++} dependent enzyme.

The role of tTG induction in the neural response to injury is not known; however, based on other experimental injury models, both damaging and protective functions can be proposed. For example, application of TG to injured optic nerve promoted axonal regeneration and recovery of visual evoked responses (Eitan *et al.* 1994). It was proposed that the supportive effects of TG treatment were due to stabilization of matrix proteins or protection of growing axons from oligodendrocyte-mediated growth inhibition. It had been previously shown that TG dimerizes interleukin-2 and that IL-2 dimers were cytotoxic to cultured oligodendrocytes (Eitan and Schwartz 1993).

Future studies of TBI-induced tTG expression will need to examine the cell type localization of tTG induction as it relates to the postinjury time course. This question is best answered by immunohistochemical analysis or *in situ* hybridization experiments. Also, the pathophysiology of tTG induction bears further examination. tTG may not only be important for subsequent cell death after traumatic injury, but also for compensatory mechanisms of other brain systems as they respond to the injury.

TG expression has been implicated in the cellular pathogenesis of Alzheimer's disease (for a review see Lesort *et al.* 2000). Increased over all TG activity and tTG-specific immunoreactivity have been observed in prefrontal areas of Alzheimer's disease brains compared to controls, with no differences observed in cerebellar expression (Johnson *et al.* 1997). Tau, the microtubule-associated-protein present in neurofibrillary tangles of Alzheimer's disease, is readily cross-linked by tTG (Dudek and Johnson 1993; Miller and Johnson 1995; Appelt *et al.* 1996; Appelt and Balin 1997; Murthy *et al.* 1998). TG also cross-links amyloid α-protein *in vitro*, producing amyloid protein oligomers similar to those seen in the neuritic plaques of Alzheimer's disease (Ikura *et al.* 1993; Dudek and Johnson 1994; Ho *et al.* 1994). tTG-specific immunoreactivity has been observed in neuritic plaques and amyloid cores from Alzheimer's disease brain (Zhang *et al.* 1998).

If TG activity is pathophysiologically relevant to the development of Alzheimer's disease, then TG induction after traumatic brain injury may contribute to the epidemiological observation that a subset of individuals who experience a traumatic brain injury are at a greater risk for developing Alzheimer's disease. Individuals with the apolipoprotein-α4 allele are at higher risk for developing Alzheimer's disease than other genotypes (Saunders *et al.* 1993). When the risks of Alzheimer's disease were examined in an elderly population, it was found that the apolipoprotein-α4 allele

conferred a two-fold increase in risk while the apolipoprotein-å4 allele combined with a history of traumatic head injury was associated with a 10-fold increase in risk (Mayeux *et al.* 1995). Subsequent studies have shown that the frequency of apolipoprotein-α4 expression is higher in individuals with amyloid α-protein deposition after head injury than in head-injured individuals without amyloid α-protein deposition (Nicoll *et al.* 1995). Although the pathophysiological mechanism linking head trauma and Alzheimer's disease is not known, it has been shown that traumatic head injury increased levels of amyloid precursor protein (APP) and this correlated with the presence of activated microglia expressing IL-1 (Griffin *et al.* 1994; Griffin *et al.* 1994; McKenzie *et al.* 1994; McKenzie *et al.* 1994). The induction of both APP and tTG by traumatic brain injury provides a potential mechanism by which head injury may contribute to Alzheimer's pathology. This hypothesis awaits further *in vivo* and *in vitro* experiments.

Acknowledgements

References

Ando M., Kunii S., Tatematsu T. and Nagata Y. (1993) Selective alterations in transglutaminase activity of rat superior cervical ganglia in response to neurotransmitters, high potassium and sialic acid-containing compounds. *Brain Res.* **604**, 64–68.

Appelt D. M. and Balin B. J. (1997) The association of tissue transglutaminase with human recombinant tau results in the formation of insoluble filamentous structures. *Brain Res.* **745**, 21–31.

Appelt D. M., Kopen G. C., Boyne L. J. and Balin B. J. (1996) Localization of transglutaminase in hippocampal neurons: implications for Alzheimer's disease. *J. Histochem. Cytochem.* **44**, 1421–1427.

Ballestar E., Abad C. and Franco L. (1996) Core histones are glutaminyl substrates for tissue transglutaminase. *J. Biol. Chem* **271**, 18817–18824.

Chen J. S. and Mehta K. (1999) Tissue transglutaminase: an enzyme with a split personality. *Int. J. Biochem. Cell Biol.* **31**, 817–836.

Colicos M. A. and Dash P. K. (1996) Apoptotic morphology of dentate gyrus granule cells following experimental cortical impact injury in rats: possible role in spatial memory deficits. *Brain Res.* **739**, 120–131.

Conti A. C., Raghupathi R., Trojanowski J. Q. and McIntosh T. K. (1998) Experimental brain injury induces regionally distinct apoptosis during the acute and delayed post-traumatic period. *J. Neurosci.* **18**, 5663–5672.

Das T., Baek K. J., Gray C. and Im M. J. (1993) Evidence that the Gh protein is a signal mediator from alpha 1- adrenoceptor to a phospholipase C. II. Purification and characterization of a Gh-coupled 69-kDa phospholipase C and reconstitution of alpha 1-adrenoceptor, Gh family, and phospholipase C. *J. Biol. Chem* **268**, 27398–27405.

Dixon C. E., Clifton G. L., Lighthall J. W., Yaghmai A. A. and Hayes R. L. (1991) A controlled cortical impact model of traumatic brain injury in the rat. *J. Neurosci. Meth* **39**, 253–262.

Dudek S. M. and Johnson G. V. (1993) Transglutaminase catalyzes the formation of sodium dodecyl sulfate- insoluble, Alz-50-reactive polymers of tau. *J. Neurochem.* **61**, 1159–1162.

Dudek S. M. and Johnson G. V. (1994) Transglutaminase facilitates the formation of polymers of the beta- amyloid peptide. *Brain Res.* **651**, 129–133.

Eitan S. and Schwartz M. (1993) A transglutaminase that converts interleukin-2 into a factor cytotoxic to oligodendrocytes. *Science* **261**, 106–108.

Eitan S., Solomon A., Lavie V., Yoles E., Hirschberg D. L., Belkin M. and Schwartz M. (1994) Recovery of visual response of injured adult rat optic nerves treated with transglutaminase. *Science* **264**, 1764–1768.

Feng J. F., Rhee S. G. and Im M. J. (1996) Evidence that phospholipase delta1 is the effector in the Gh (transglutaminase II)-mediated signaling. *J. Biol. Chem* **271**, 16451–16454.

Feng J. F., Gray C. D. and Im M. J. (1999) Alpha 1B-adrenoceptor interacts with multiple sites of transglutaminase II: characteristics of the interaction in binding and activation. *Biochemistry* **38**, 2224–2232.

Fujita K., Ando M., Yamauchi M., Nagata Y. and Honda M. (1995) Alteration of transglutaminase activity in rat and human spinal cord after neuronal degeneration. *Neurochem. Res.* **20**, 1195–1201.

Gennarelli T. A. (1994) Animate models of human head injury. *J. Neurotrauma* **11**, 357–368.

Gilad G. M. and Varon L. E. (1985) Transglutaminase activity in rat brain: characterization, distribution, and changes with age. *J. Neurochem.* **45**, 1522–1526.

Gilad G. M., Varon L. E. and Gilad V. H. (1985) Calcium-dependent transglutaminase of rat sympathetic ganglion in development and after nerve injury. *J. Neurochem.* **44**, 1385–1390.

Gorza L., Menabo R., Di Lisa F. and Vitadello M. (1997) Troponin T cross-linking in human apoptotic cardiomyocytes. *Am. J. Pathol* **150**, 2087–2097.

Greenberg C. S., Birckbichler P. J. and Rice R. H. (1991) Transglutaminases: multifunctional cross-linking enzymes that stabilize tissues. *FASEB J.* **5**, 3071–3077.

Griffin W. S., Sheng J. G., Gentleman S. M., Graham D. I., Mrak R. E. and Roberts G. W. (1994) Microglial interleukin-1 alpha expression in human head injury: correlations with neuronal and neuritic beta-amyloid precursor protein expression. *Neurosci. Lett.* **176**, 133–136.

Herx L. M., Rivest S. and Yong V. W. (2000) Central nervous system-initiated inflammation and neurotrophism in trauma: IL-1 beta is required for the production of ciliary neurotrophic factor. *J. Immunol.* **165**, 2232–2239.

Ho G. J., Gregory E. J., Smirnova I. V., Zoubine M. N. and Festoff B. W. (1994) Cross-linking of beta-amyloid protein precursor catalyzed by tissue transglutaminase. *FEBS Lett.* **349**, 151–154.

Hubschmann O. R. and Nathanson D. C. (1985) The role of calcium and cellular membrane dysfunction in experimental trauma and subarachnoid hemorrhage. *J. Neurosurg* **62**, 698–703.

Hwang K. C., Gray C. D., Sivasubramanian N. and Im M. J. (1995) Interaction site of GTP binding Gh (transglutaminase II) with phospholipase C. *J. Biol. Chem* **270**, 27058–27062.

Ikura K., Takahata K. and Sasaki R. (1993) Cross-linking of a synthetic partial-length (1–28) peptide of the Alzheimer beta/A4 amyloid protein by transglutaminase. *FEBS Lett.* **326**, 109–111.

Im M. J. and Graham R. M. (1990) A novel guanine nucleotide-binding protein coupled to the alpha 1- adrenergic receptor. I. Identification by photolabeling or membrane and ternary complex preparation. *J. Biol. Chem* **265**, 18944–18951.

Im M. J., Riek R. P. and Graham R. M. (1990) A novel guanine nucleotide-binding protein coupled to the alpha 1- adrenergic receptor. II. Purification, characterization, and reconstitution. *J. Biol. Chem* **265**, 18952–18960.

Johnson G. V., Cox T. M., Lockhart J. P., Zinnerman M. D., Miller M. L. and Powers R. E. (1997) Transglutaminase activity is increased in Alzheimer's disease brain. *Brain Res.* **751**, 323–329.

Katayama Y., Maeda T., Koshinaga M., Kawamata T. and Tsubokawa T. (1995) Role of excitatory amino acid-mediated ionic fluxes in traumatic brain injury. *Brain Pathol* **5**, 427–435.

Kim S. Y., Grant P., Lee J. H., Pant H. C. and Steinert P. M. (1999) Differential expression of multiple transglutaminases in human brain. Increased expression and cross-linking by transglutaminases 1 and 2 in Alzheimer's disease. *Biol. Chem.* **274**, 30715–30721.

Lesort M., Tucholski J., Miller M. L. and Johnson G. V. (2000) Tissue transglutaminase: a possible role in neurodegenerative diseases. *Prog. Neurobiol.* **61**, 439–463.

Maccioni R. B. and Seeds N. W. (1986) Transglutaminase and neuronal differentiation. *Mol Cell Biochem.* **69**, 161–168.

Mayeux R., Ottman R., Maestre G., Ngai C., Tang M. X., Ginsberg H., Chun M., Tycko B. and Shelanski M. (1995) Synergistic effects of traumatic head injury and apolipoprotein-epsilon 4 in patients with Alzheimer's disease. *Neurology* **45**, 555–557.

McKenzie J. E., Gentleman S. M., Roberts G. W., Graham D. I. and Royston M. C. (1994) Increased numbers of beta APP-immunoreactive neurones in the entorhinal cortex after head injury. *Neuroreport* **6**, 161–164.

Meaney D. F., Ross D. T., Winkelstein B. A., Brasko J., Goldstein D., Bilston L. B., Thibault L. E. and Gennarelli T. A. (1994) Modification of the cortical impact model to produce axonal injury in the rat cerebral cortex. *J. Neurotrauma* **11**, 599–612.

Melino G. and Piacentini M. (1998) 'Tissue' transglutaminase in cell death: a downstream or a multifunctional upstream effector? *FEBS Lett.* **430**, 59–63.

Melino G., Annicchiarico-Petruzzelli M., Piredda L., Candi E., Gentile V., Davies P. J. and Piacentini M. (1994) Tissue transglutaminase and apoptosis: sense and antisense transfection studies with human neuroblastoma cells. *Mol Cell Biol.* **14**, 6584–6596.

Miller M. L. and Johnson G. V. (1995) Transglutaminase cross-linking of the tau protein. *J. Neurochem.* **65**, 1760–1770.

Monsonego A., Shani Y., Friedmann I., Paas Y., Eizenberg O. and Schwartz M. (1997) Expression of GTP-dependent and GTP-independent tissue-type transglutaminase in cytokine-treated rat brain astrocytes. *J. Biol. Chem* **272**, 3724–3732.

Murthy S. N., Wilson J. H., Lukas T. J., Kuret J. and Lorand L. (1998) Cross-linking sites of the human tau protein, probed by reactions with human transglutaminase. *J. Neurochem.* **71**, 2607–2614.

Nakaoka H., Perez D. M., Baek K. J., Das T., Husain A., Misono K., Im M. J. and Graham R. M. (1994) Gh: a GTP-binding protein with transglutaminase activity and receptor signaling function. *Science* **264**, 1593–1596.

Nemes Z. Jr, Adany R., Balazs M., Boross P. and Fesus L. (1997) Identification of cytoplasmic actin as an abundant glutaminyl substrate for tissue transglutaminase in HL-60 and U937 cells undergoing apoptosis. *J. Biol. Chem* **272**, 20577–20583.

Newcomb J. K., Zhao X., Pike B. R. and Hayes R. L. (1999) Temporal profile of apoptotic-like changes in neurons and astrocytes following controlled cortical impact injury in the rat. *Exp Neurol.* **158**, 76–88.

Nicoll J. A., Roberts G. W. and Graham D. I. (1995) Apolipoprotein E epsilon 4 allele is associated with deposition of amyloid beta-protein following head injury. *Nat Med.* **1**, 135–137.

Oliverio S., Amendola A., Di Sano F., Farrace M. G., Fesus L., Nemes Z., Piredda L., Spinedi A. and Piacentini M. (1997) Tissue transglutaminase-dependent posttranslational modification of the retinoblastoma gene product in promonocytic cells undergoing apoptosis. *Mol Cell Biol.* **17**, 6040–6048.

Park E. S., Won J. H., Han K. J., Suh P. G., Ryu S. H., Lee H. S., Yun H. Y., Kwon N. S. and Baek K. J. (1998) Phospholipase C-delta1 and oxytocin receptor signalling: evidence of its role as an effector. *Biochem. J.* **331**, 283–289.

Perry M. J. and Haynes L. W. (1993) Localization and activity of transglutaminase, a retinoid-inducible protein, in developing rat spinal cord. *Int. J. Dev Neurosci.* **11**, 325–337.

Pike B. R., Zhao X., Newcomb J. K., Posmantur R. M., Wang K. K. and Hayes R. L. (1998) Regional calpain and caspase-3 proteolysis of alpha-spectrin after traumatic brain injury. *Neuroreport* **9**, 2437–2442.

Rink A., Fung K. M., Trojanowski J. Q., Lee V. M., Neugebauer E. and McIntosh T. K. (1995) Evidence of apoptotic cell death after experimental traumatic brain injury in the rat. *Am. J. Pathol* **147**, 1575–1583.

Rostworowski M., Balasingam V., Chabot S., Owens T. and Yong V. W. (1997) Astrogliosis in the neonatal and adult murine brain post-trauma: elevation of inflammatory cytokines and the lack of requirement for endogenous interferon-gamma. *J. Neurosci.* **17**, 3664–3674.

Saunders A. M., Strittmatter W. J., Schmechel D., George-Hyslop P. H., Pericak-Vance M. A., Joo S. H., Rosi B. L., Gusella J. F., Crapper-MacLachlan D. R. and Alberts M. J. (1993) Association of apolipoprotein E allele epsilon 4 with late-onset familial and sporadic Alzheimer's disease. *Neurology* **43**, 1467–1472.

Selkoe D. J., Abraham C. and Ihara Y. (1982) Brain transglutaminase: in vitro crosslinking of human neurofilament proteins into insoluble polymers. *Proc. Natl Acad. Sci. USA* **79**, 6070–6074.

Taupin V., Toulmond S., Serrano A., Benavides J. and Zavala F. (1993) Increase in IL-6, IL-1 and TNF levels in rat brain following traumatic lesion. Influence of pre- and post-traumatic treatment with Ro5, 4864, a peripheral-type (, p. site) benzodiazepine ligand. *J. Neuroimmunol.* **42**, 177–185.

Tetzlaff W., Gilad V. H., Leonard C., Bisby M. A. and Gilad G. M. (1988) Retrograde changes in transglutaminase activity after peripheral nerve injuries. *Brain Res.* **445**, 142–146.

Woodroofe M. N., Sarna G. S., Wadhwa M., Hayes G. M., Loughlin A. J., Tinker A. and Cuzner M. L. (1991) Detection of interleukin-1 and interleukin-6 in adult rat brain, following mechanical injury, by in vivo microdialysis: evidence of a role for microglia in cytokine production. *J. Neuroimmunol.* **33**, 227–236.

Yakovlev A. G., Knoblach S. M., Fan L., Fox G. B., Goodnight R. and Faden A. I. (1997) Activation of CPP32-like caspases contributes to neuronal apoptosis and neurological dysfunction after traumatic brain injury. *J. Neurosci.* **17**, 7415–7424.

Zhang W., Johnson B. R., Suri D. E., Martinez J. and Bjornsson T. D. (1998) Immunohistochemical demonstration of tissue transglutaminase in amyloid plaques. *Acta Neuropathol. Berl.* **96**, 395–400.

Increased expression of tissue-type transglutaminase following middle cerebral artery occlusion in rats

Paul J. Tolentino, Anuradha Waghray,* Kevin K. W. Wang*'† and Ronald L. Hayes*

*Department of Neuroscience and †Department of Psychiatry, Evelyn F. and William L. McKnight Brain Institute of the University of Florida, Center for Traumatic Brain Injury Studies, Gainesville, Florida, USA

Abstract

Tissue-type transglutaminase (TG-2) has been implicated in neurodegenerative diseases. In this study, induction of TG-2 was studied in rats following transient middle cerebral artery occlusion. Alterations in 2,3,5-triphenylterazolium chloride staining revealed maximum infarction 3 days after injury. Measurement of mRNA transcript levels by real-time PCR analysis showed both forms of TG-2 mRNA peaking on day 5 after injury in ipsilateral cortex, with greater induction of the full-length TG-2 (TG-L) transcript than the truncated form of the TG-2 (TG-S) transcript. However, in the ipsilateral hippocampus, peak induction of both forms of TG-2 mRNA peaked 1 day after injury and to a lesser extent than observed in the ipsilateral cortex. Western blot analysis demonstrated that TG-L protein expression progressively increased from 1 to 7 days after ischemia, with greater expression in cortex than hippocampus (525 ± 10% vs. 196 ± 8% of control, respectively). However, expression of TG-S was not detected. These results demonstrate that increased TG-2 mRNA and protein expression occurs in a delayed fashion following ischemic injury. The temporal profile of TG-2 induction after ischemia was similar to that observed after traumatic brain injury (previously described), suggesting a similar role of TG-2 in both pathological conditions.

Keywords: brain injury, cross-linking, ischemia, transglutaminase.

J. Neurochem. (2004) 10.1111/j.1471-4159.2004.02436.x

Stroke, the permanent or prolonged occlusion of an artery in the brain, is a major cause of death and the primary cause of adult disability in many countries. Arterial occlusion results in tissue infarction and neuronal death (Elkind and Sacco 1998). Thus, it is critical to develop therapeutic interventions to ameliorate this damage. However, the mechanisms underlying cell loss due to cerebral ischemia remain incompletely understood. Recent findings suggest that much of the neuronal death following stroke occurs as a result of apoptosis (Mattson 2000; Graham and Chen 2001). Cerebral ischemia leads to increased Ca^{2+} influx due to membrane depolarization (Kristian and Siesjo 1998), resulting in the activation of proteases (Buki *et al.* 2000; Beer *et al.* 2001) and tissue-type transglutaminase (TG-2) (Lai *et al.* 2001). These are pivotal events in apoptotic neuronal death (Facchiano *et al.* 2001; Hayes *et al.* 2001), in conjunction with mitochondrial dysfunction, release of cytochrome *c* and increased cytokine production (Bratton *et al.* 2000; Zipfel *et al.* 2000; Chu *et al.* 2002).

Tissue-type transglutaminase belongs to a family of Ca^{2+}-dependent transglutaminases (TGs) that catalyses the incorporation of a polyamine into a polypeptide-bound glutamine, leading to the formation of an (γ-glutamyl) isopeptide bond (Greenberg *et al.* 1991). This isopeptide bond is resistant to proteolytic cleavage and may serve to not only stabilize proteins against degradation but also to alter their function. The most ubiquitously expressed member of the TG family is TG-2. It is abundantly expressed in the brain (Kim *et al.* 1999) and is induced in cultured cells by various agents including cytokines (Ikura *et al.* 1994) and cAMP (Maddox and Haddox 1988). The most potent inducers of

2 P. J. Tolentino *et al.*

TG-2 are retinoids, which promote apoptosis in various cells including neurons (Ferrari *et al.* 1998; Lefebvre *et al.* 1999). Tissue-type transglutaminase has been implicated in numerous processes, including axonal regeneration, cellular differentiation, neurite outgrowth, apoptosis and neurodegeneration (Suedhoff *et al.* 1990; Eitan and Schwartz 1993; Piredda *et al.* 1999; Citron *et al.* 2001; Tucholski *et al.* 2001).

In addition to isopeptide bond formation, TG-2 has GTPase activity (Nakaoka *et al.* 1994). GTP binds at the COOH-terminal of full-length protein (Casadio *et al.* 1999) and inhibits its cross-linking activity. Recently, an alternatively spliced, short form (encoding $\sim$70 kDa protein) of TG-2 induced by cytokine treatment was produced in cultured rat astrocytes and had greater activity at much lower Ca^{2+} concentrations (Monsonego *et al.* 1997). The short form lacks a GTP-binding region and loss of GTPase activity correlates with increased cross-linking activity. This loss of function might have an impact on apoptotic neuronal death after brain injury. For the current study, we used a model of middle cerebral arterial occlusion (MCAO) to assess mRNA and protein levels of these two forms of TG-2 and examined how these changes correlated with the extent of ischemic injury.

Materials and methods

Middle cerebral artery occlusion
Transient occlusion of the right middle cerebral artery was achieved via intraluminal occlusion with a nylon suture (He *et al.* 2000). Adult male (250–300 g) Sprague-Dawley rats were anesthetized with an abdominal injection of ketamine (60 mg/kg) and xylazine (10 mg/kg). Core body temperature was monitored continuously by a rectal thermistor probe and maintained at 37 ± 1°C by placing an adjustable heating pad beneath the rats. The right common carotid artery and right external carotid artery were exposed through a midline neck incision. A 3-0 monofilament nylon suture (25 mm long) was inserted through an arteriotomy of the right common carotid artery and gently advanced into the internal carotid artery to a point approximately 17 mm distal to the carotid bifurcation. Mild resistance to further advancement indicated that the suture had entered the anterior cerebral artery, thereby occluding the origin of the middle cerebral artery. After 1 h of occlusion, the nylon suture was withdrawn and the common carotid artery was ligated. The neck incision was closed with nylon suture. Sham-injured animals underwent an identical surgical procedure but did not experience occlusion. Appropriate pre- and post-injury management was maintained and these measures complied with all guidelines set forth by the University of Florida Institutional Animal Care and Use Committee and the National Institutes of Health guidelines detailed in the Guide for the Care and Use of Laboratory Animals.

Histological assessment
Staining with 2,3,5-triphenylterazolium chloride was used to assess the extent of ischemic injury after MCAO. Following a 1-h occlusion, animals were killed immediately (0 days) or 1, 3, 5 or 7 days after injury with CO_2 and subsequently decapitated. Each brain was removed and placed in a metallic brain matrix (Harvard Instruments, South Natick, MA, USA) for tissue slicing. A coronal section (2 mm thick) at the level of the optic chiasm was incubated for 30 min at room temperature in a solution of 2% 2,3,5-triphenylterazolium chloride in saline and then fixed in 10% formalin.

RNA purification
Ipsilateral (side of injury) cortices and hippocampi were rapidly dissected from animals at 1–7 days after occlusion and from sham-injured animals on day 5. At the appropriate time-points, animals were killed with CO_2 and subsequently decapitated. Total RNA was isolated using TRIzol reagent (Gibco BRL, Rockville, MD, USA). Isopropanol precipitation and ethanol washes were performed according to the manufacturer's instructions and samples were resuspended in 50–100 μL DEPC-treated water.

Reverse transcription
Total RNA (3 μg) was incubated with 1 μL oligo(dT) (0.5 mg/mL; GibcoBRL) at 70°C for 10 min and then at 4°C for 5 min. A RT reaction mixture was added to the RNA-oligo(dT) sample for a final volume of 20 μL, containing 20 mM Tris-HCl (pH 8.4), 50 mM KCl, 5 mM $MgCl_2$, 500 μM dNTPs, 10 mM dithiothreitol, 50 units SuperScript II reverse transcriptase (GibcoBRL) and 40 units RNaseOUT recombinant ribonuclease inhibitor (GibcoBRL). The sample was incubated at 42°C for 55 min, 70°C for 15 min for enzyme denaturation and then transferred to 4°C. Each sample was diluted to a final volume of 100 μL with DEPC-treated water.

Primer selection

Tissue-type transglutaminase-specific primers
All base pair designations refer to GeneBank locus AF106325, rat TG-2. 5′TG (ACTTTGACGTGTTTGCCCAC, bp 1470–1489) recognizes an upstream homologous sequence in full-length TG-2 (TG-L) and truncated TG-2 (TG-S) transcripts. 3′TG-L (CAAT-ATCAGTCGGGAACAGGTC, bp 1961–1982) recognizes a downstream TG-L mRNA-specific sequence. 3′TG-S (GCTGAGTCTGG, GTGAAGACACAG, bp 1861–1872 and 2083–2093) recognizes a downstream TG-S mRNA-specific sequence. 3′TG-S primer bridges the junction created by the absence of bp 1873–2082 (a sequence present exclusively in TG-L). The underlined 3′ half of the 3′TG-S sequence will hybridize to both the TG-L- and TG-S-specific sequences while the full-length primer will hybridize only to the TG-S mRNA sequence.

GAPDH-specific primers
All base pair designations for GAPDH-specific primers refer to GeneBank locus AF106860. The upstream primer is designated 5′GPD (GGCTGCCTTCTCTTGTGAC, bp 903–921) and the downstream primer is designated 3′GPD (GGCCGCCTGCTTCAC-CAC, bp 1624–1641).

Semi-quantitative/light cycler PCR
Real-time PCR was performed using a Light Cycler rapid thermal cycler system (Roche Diagnostics, Indianapolis, IN, USA), as previously described (Tolentino *et al.* 2002). Reactions were performed in a 10-μL volume with 0.5 μM primers and 2.5 mM $MgCl_2$. Other reagents, including nucleotides, Fast Start Taq DNA

polymerase and buffer, were used as provided in the Light-Cycler-FastStart DNA Master SYBR Green I reaction mix (Roche Diagnostics). The amplification protocol included a 5-min 95°C denaturation; one cycle with 95°C denaturation for 5 s, 65°C annealing for 10 s and 72°C extension for 35 s; one cycle with 95°C denaturation for 5 s, 62.5°C annealing for 10 s and 72°C extension for 35 s and then 30–40 cycles of 95°C denaturation for 5 s, 60°C annealing for 10 s and 72°C extension for 35 s. Detection of the fluorescent product occurred at the end of the 72°C extension periods. Specificity of the amplification product from each primer pair was confirmed by melting curve analysis of the PCR product and subsequent gel electrophoresis.

Quantification was performed by online monitoring for identification of the exact time-point at which the logarithmic linear phase could be distinguished from the background (crossing point). The crossing point is expressed as a cycle number.

Standard curve preparation and semiquantitative PCR analysis
The RT product from ipsilateral cortical RNA collected 3 days (when the initial mRNA induction was observed) after ischemic injury underwent serial dilution creating a standard curve of 100, 33, 11 and 3.7% of original real-time product. Each dilution from the standard curve was analyzed with the Light Cycler PCR using primer sets for TG-L, TG-S or GAPDH mRNA. For each primer set, a crossing point cycle number was determined for each dilution of the standard curve. Linear regression analysis of the logarithm of the dilution factor versus the crossing point cycle number generated a standard curve for each transcript-specific primer set. From the standard curve of each primer set, a crossing point cycle number could be converted to a relative amount of RNA. For individual samples, the crossing point cycle number was identified with the Light Cycler PCR. Using the standard curve for each primer set, the amount of TG-L, TG-S or GAPDH mRNA was determined. The amount of each transcript in sham animals was set at 100% and the level of expression in an occluded sample was calculated as a percent of sham expression.

Tissue lysis and protein purification
Cortical and hippocampal tissues were collected from animals 1–7 days after ischemic injury and from sham-injured animals 5 days after injury. At the appropriate time-points, animals were killed by CO_2 and subsequent decapitation. Ipsilateral and contralateral cortices and hippocampi were rapidly dissected and snap-frozen in liquid nitrogen. Tissue samples were stored at −80°C. Tissues were homogenized in a glass tube with a Teflon dounce pestle in 15 volumes of ice-cold triple detergent lysis buffer [20 mM Hepes, 1 mM EDTA, 2 mM EGTA, 150 mM NaCl, 0.1% sodium dodeyl sulfate, 1.0% IGEPAL 40 and 0.5% deoxycholic acid, pH 7.5] containing a broad-range protease inhibitor cocktail (Roche Molecular Biochemicals, Indianapolis, IN, USA). Samples were sonicated and centrifuged at 800 g for 5 min at 4°C. The supernatant fluid was then collected for western blot analysis.

Western blot analysis
Protein concentrations of tissue homogenates were determined by bicinchoninic acid microprotein assays (Pierce, Rockford, IL, USA) cwith albumin standards. Aliquots (20 μg) of each sample

were prepared for sodium dodeyl sulfate–polyacrylamide gel electrophoresis by the addition of 2× loading buffer [1× loading buffer contains 125 mM Tris-HCl (pH 6.8), 100 mM dithiothreitol, 4% sodium dodeyl sulfate, 0.01% bromophenol blue and 10% glycerol]. Samples with loading buffer were heated for 10 min at 100°C, centrifuged for 1 min at 10 000 g and resolved by sodium dodeyl sulfate–polyacrylamide gel electrophoresis on 7.5% Tris/glycine gels at 200 V for 1 h at 4°C. Following electrophoresis, fractionated proteins were transferred to Immobilon-P polyvinylidene fluoride membrane (Millipore Corporation, Bedford, MA, USA) in a transfer buffer containing 192 mM glycine, 25 mM Tris-HCl (pH 8.3) and 10% methanol at 100 V for 1 h at 4°C. Blots were blocked for 1 h at room temperature in 5% non-fat milk in TBST (20 mM Tris-HCl, 150 mM NaCl and 0.005% Tween-20, pH 7.5).

Immunoblots were probed with TG-100, a monoclonal anti-TG-2 antibody (LabVision, Fremont, CA, USA). Following overnight incubation at 4°C with the primary antibody (1 : 3000), blots were incubated for 1 h at room temperature in 3% non-fat milk/TBST containing a horseradish peroxidase-conjugated goat anti-mouse IgG (1 : 3000; Bio-Rad Laboratories, Hercules, CA, USA). Bound antibodies were visualized with enhanced chemiluminescence (Amersham Pharmacia Biotech, Piscataway, NJ, USA) on Biomax ML chemiluminescent film (Kodak).

Statistical analyses
For the western blots, semiquantitative analysis was performed by computer-assisted densitometric scanning (Alpha Imager 2000 Digital Imaging System, San Leandro, CA, USA). For each time-point studied, $n = 4$ per group. Data were acquired as integrated densitometric values and transformed to percentages of the densitometric levels obtained from sham-injured animals visualized on the same blot. Data were evaluated by two-tailed Student's t-test. All values are given as mean ±SEM. Differences were considered significant if $p < 0.05$.

Results

Histological assessment of ischemic injury
Coronal sections of rat brain (2 mm thick) were collected immediately to 7 days after transient MCAO and stained with 2,3,5-triphenylterazolium chloride (Fig. 1). Decreased 2,3,5-triphenylterazolium chloride staining was noted in areas of infarction. The maximal effect of occlusion was noted 3 days after ischemic injury, with a smaller infarct revealed at later time-points.

PCR analysis of tissue-type transglutaminase transcripts
A previous report described the use of a semiquantitative PCR analysis to measure the expression of TG-L and TG-S mRNA in rat cortex and hippocampus after traumatic brain injury (Tolentino *et al.* 2002). The same technique was used to measure the expression of these transcripts in rat cortex and hippocampus after ischemic injury. Figure 2 shows the time-course of TG-L and TG-S mRNA expression in

Fig. 1 2,3,5 -Triphenylterazolium chloride staining of rat brain coronal sections after ischemic injury. 1–7 days after transient right middle cerebral arterial occlusion, rat brains were dissected and sectioned in the coronal plane. Areas of infarcted tissue were revealed by decreased staining. Maximal effect of occlusion was noted 3 days after injury with a smaller infarct revealed at later time-points.
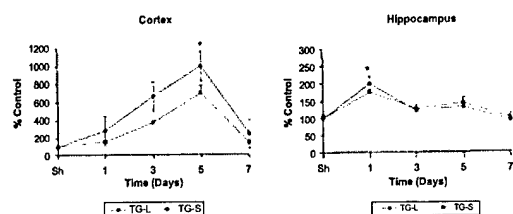

Fig. 2 Semi-quantitative PCR analysis of full-length tissue-type transglutaminase (TG-L) and truncated form of tissue-type transglut-aminase (TG-S) mRNA expression in (a) ipsilateral cortex and (b) hippocampus. TG-L (◆) and TG-S (■) mRNA levels were calculated as a percent of sham control. In cortex, maximal TG-L and TG-S mRNA expression was noted 5 days after ischemia while, in hippo-campus, maximal expression was noted 1 day after ischemia.
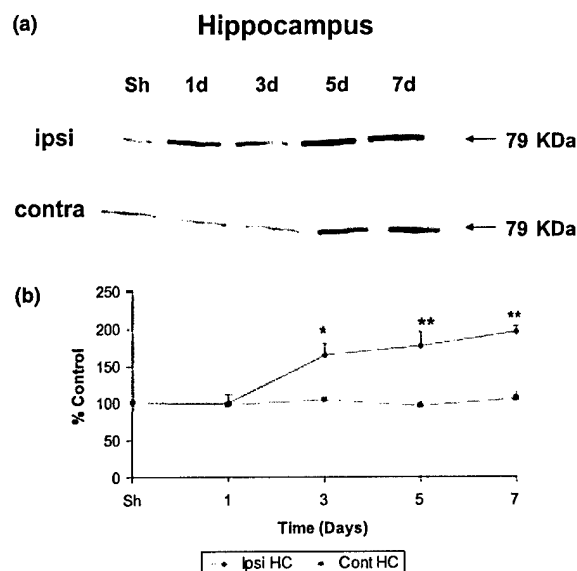

Fig. 3 (a) A representative western blot showing tissue-type transgl-utaminase (TG-2) expression in cortical protein samples using the anti-TG-2 antibody (TG-100). Samples were collected from injured animals 1, 3, 5 and 7 days after ischemic injury and from sham-injured animals. Full-length tissue-type transglutaminase (TG-L) (79 kDa) expression was increased in a time-dependent manner while the truncated form of tissue-type transglutaminase (70 kDa) was not identified in these samples, even at longer exposures. The TG-L protein expression in contralateral (Contra) samples remained the same. (b) Data from multiple ($n = 3$) western blots were acquired as densitometric values and transformed to percentages of the densito-metric values obtained from control samples (sham-injured animals). Quantitative analysis of western blots showed increases in protein level following injury in a time-dependent manner on days 3, 5 and 7 compared with control animals. Comparing TG-L expression from ipsilateral (Ipsi) and contralateral cortex (ctx) at each time-point, increased levels of expression were statistically significant at 3–7 days in the ipsilateral cortex ($^*p < 0.05$, $^{**}p < 0.005$).

ipsilateral cortex and hippocampus after ischemia. In ipsilateral cortex, maximal and significantly elevated expres-sion of TG-L and TG-S mRNA was observed 5 days after injury ($990 \pm 130\%$ and $690 \pm 90\%$ of control, respect-ively). In the hippocampus, maximal and significantly elevated TG-L and TG-S mRNA levels were observed 1 day after injury ($200 \pm 20\%$ and $175 \pm 11\%$ of control, respectively).

Western blot analysis of cortical tissue-type transglutaminase expression after ischemic injury

Total protein was prepared from ipsilateral and contralateral rat cortex after sham and ischemic injury. Figure 3(a) shows TG-2 protein expression in rat cortex 1–7 days after ischemic injury. Using the TG-100 (monoclonal anti-TG-2) antibody, a distinct TG-2 protein band at $\sim$79 kDa was identified, corresponding to TG-L. However, TG-S ($\sim$70 kDa) was not identified using this antibody. The expression of TG-L was increased in a time-dependent manner compared with the sham-injured control. Western blot data were quantified by densitometric analysis (Fig. 3b). Levels of TG-L expression were calculated as a percent of the sham control. The induction of TG-L was observed 3–7 days after cortical occlusion with maximum induction on day 7 ($525 \pm 10\%$ of control). Comparing expression between matched ipsilateral

and contralateral cortical tissues, statistically significant elevated expression was observed at 3, 5 and 7 days. Contralateral samples that showed no change in TG-2 expression were used as equal loading controls.

Western blot analysis of hippocampal tissue-type transglutaminase expression after ischemic injury

Total protein was prepared from ipsilateral and contralateral rat hippocampus after ischemic and sham injury and the expression of TG-2 was examined using TG-100. Figure 4(a) shows TG-2 protein expression in rat hippocampus 1–7 days after ischemic injury. Similar to western blot analyses of cortical samples, only TG-L (~79 kDa) was identified. The expression of TG-L protein was increased in a time-dependent manner from days 3 to 7 compared with the sham control. However, the induction level was lower than in ipsilateral cortex. Quantitative densitometric analysis (Fig. 4b) revealed maximum expression at 7 days after injury (196 ± 8%). Comparing expression between matched ipsilateral and contralateral hippocampal tissues, statistically significant elevated expression was observed at 3, 5 and 7 days after injury. Contralateral samples that showed no change in TG-2 expression were used as equal loading controls.

Discussion

The TG family has been studied in a variety of injury models. The current study provides the first evidence of TG-2 induction in response to cerebral ischemia in a trend similar to that observed after traumatic brain injury (Tolentino et al. 2002), suggesting that TG-2 may be a good predictor for the pathophysiology accompanying traumatic and ischemic brain injury. Moreover, in a model of spinal cord ischemia, TG activity underwent a transient increase that declined to control levels after 1 week (Fujita et al. 1995). The TG-2 protein and transcript expression were observed after spinal cord injury and both the short- and long-form transcripts were identified after injury (Festoff et al. 2002). In the superior cervical ganglion, TG activity was increased within 1 h of axotomy and returned to baseline after 24 h (Gilad et al. 1985; Ando et al. 1993). The TG activity also increased in the vagus nerve after crush injury (Tetzlaff et al. 1988).

The role of TG-2 induction in the neural response to injury is not well understood; however, based on other experimental injury models, both damaging and protective functions can be proposed. For example, exogenous application of TG to injured optic nerve promoted axonal regeneration and recovery of visual-evoked responses (Eitan et al. 1994). In SH-SY5Y neuroblastoma cells, TG-2 stimulated neuronal differentiation (Tucholski et al. 2001). It was proposed that the supportive effects of TG treatment were due to stabilization of matrix proteins or protection of growing axons from oligodendrocyte-mediated growth inhibition. It had been previously shown that TG dimerizes interleukin-2 and that interleukin-2 dimers were cytotoxic to cultured oligodendrocytes (Eitan and Schwartz 1993).

Several studies have demonstrated the dual role of TG-2 in neuronal life and death processes (Im et al. 1997; Gill et al. 1998; Casadio et al. 1999). Increase in the TG-S transcript predicts production of a more active enzyme. As GTP is inhibitory to the cross-linking activity of TG-2, loss of this region presumably results in a switch of TG-2 function to programmed cell death with increases in cross-linking and production of aggregated proteins (Norlund et al. 1999; Citron et al. 2001, 2002). Our studies have demonstrated an increased message level of TG-S after MCAO; however, its protein expression was not detected, suggesting that TG-S protein may be expressed at an undetectable level. However, TG-S protein expression was recently detected in the spinal cord injury model by using a different set of antibodies (Festoff et al. 2002). Apoptotic neuronal death has been widely documented after ischemic brain injury (Mattson 2000; Graham and Chen 2001) and induction of TG-S mRNA expression may increase apoptotic neuronal death and cross-

(a) **Hippocampus**

Sh 1d 3d 5d 7d

ipsi ← 79 KDa

contra ← 79 KDa

(b)

Fig. 4 (a) A representative western blot showing tissue-type transglutaminase (TG-2) expression in hippocampal protein samples using the anti-TG-2 antibody (TG-100). Samples were collected from injured animals 1, 3, 5 and 7 days after ischemic injury and from sham-injured animals. Full-length tissue-type transglutaminase (TG-L) (79 kDa) protein expression increased in a time-dependent manner compared with sham-injured controls while the truncated form of tissue-type transglutaminase (70 kDa) was not identified, even with longer exposure time. (b) Data from multiple (n = 3) western blots were acquired as densitometric values and transformed to percentages of the densitometric values obtained from control samples (sham-injured animals). Quantitative analysis of western blots showed increases in protein level following injury in a time-dependent manner on days 3, 5 and 7 compared with control animals. Comparing TG-L expression from ipsilateral (Ipsi) and contralateral (Contra) hippocampus at each time-point, increased levels of expression were statistically significant at 3–7 days in ipsilateral hippocampus (*p < 0.05, **p < 0.005).

linking activity. Further understanding of the regulation of TG-2 transcription may provide additional opportunities to control TG-2 expression as a potential therapy against inappropriate apoptosis and cross-linking activity that may lead to neurodegenerative diseases. In addition, the cell type localization and pathophysiology of TG-2 induction bear further examination. Tissue-type transglutaminase may be important not only for subsequent cell death after brain injury but also for compensatory mechanisms of other brain systems as they respond to the injury.

Tissue-type transglutaminase expression has been implicated in the cellular pathogenesis of Alzheimer's disease (AD) (Lesort *et al.* 2000; Citron *et al.* 2001) and increased TG-2 mRNA, protein expression and TGase activity have been observed in brains of AD and Parkinson's disease patients compared with controls (Citron *et al.* 2001, 2002). The TG-S isoform message was absent in normal brains but present in AD patients and accompanied by an increase in cross-linking of disease-specific proteins, such as tau and α-synuclein (Citron *et al.* 2002). If TG activity is physiologically relevant to the development of AD, then TG induction after MCAO may contribute to the epidemiological observation that a subset of individuals who experience ischemia are at a greater risk of developing AD. Recent advances suggest that cerebral ischemia may promote AD (Kalaria 2000). The underlying pathophysiological mechanisms of AD and stroke are similar (Blass and Ratan 2003). Cerebral ischemia may promote AD by triggering the development of senile plaques and neurofibrillary tangles (Vermeer *et al.* 2003). Further, MCAO increases the expression of presenilin, APP and APE (Pennypacker *et al.* 1999; Pluta 2000). These studies suggest that cerebral ischemia may cause cellular and molecular events that have neurodegenerative consequences and subsequently lead to the development of AD (Pennypacker *et al.* 1999; Kalaria 2000; Pluta 2000; Blass and Ratan 2003; Vermeer *et al.* 2003). The induction of both AD-related proteins and TG-2 following brain injury provides a potential mechanism by which cerebral ischemia may contribute to AD pathology. This hypothesis awaits further *in vivo* and *in vitro* experiment.

References

Ando M., Kunii S., Tatematsu T. and Nagata Y. (1993) Selective alterations in transglutaminase activity of rat superior cervical ganglia in response to neurotransmitters, high potassium and sialic acid-containing compounds. *Brain Res.* **604**, 64–68.

Beer R., Franz G., Krajewski S. *et al.* (2001) Temporal and spatial profile of caspase 8 expression and proteolysis after experimental traumatic brain injury. *J. Neurochem.* **78**, 862–873.

Blass J. P. and Ratan R. R. (2003) 'Silent' strokes and dementia. *N. Engl. J. Med.* **348**, 1277–1278.

Bratton S. B., MacFarlane M., Cain K. and Cohen G. M. (2000) Protein complexes activate distinct caspase cascades in death receptor and stress-induced apoptosis. *Exp. Cell Res.* **256**, 27–33.

Buki A., Okonkwo D. O., Wang K. K. and Povlishock J. T. (2000) Cytochrome c release and caspase activation in traumatic axonal injury. *J. Neurosci.* **20**, 2825–2834.

Casadio R., Polverini E., Mariani P., Spinozzi F., Carsughi F., Fontana A., Polverino de Laureto P., Matteucci G. and Bergamini C. M. (1999) The structural basis for the regulation of tissue transglutaminase by calcium ions. *Eur. J. Biochem.* **262**, 672–679.

Chu D., Qiu J., Grafe M., Fabian R., Kent T. A., Rassin D., Nesic O., Werrbach-Perez K. and Perez-Polo R. (2002) Delayed cell death signaling in traumatized central nervous system: hypoxia. *Neurochem. Res.* **27**, 97–106.

Citron B. A., SantaCruz K. S., Davies P. J. and Festoff B. W. (2001) Intron-exon swapping of transglutaminase mRNA and neuronal Tau aggregation in Alzheimer's disease. *J. Biol. Chem.* **276**, 3295–3301.

Citron B. A., Suo Z., SantaCruz K., Davies P. J., Qin F. and Festoff B. W. (2002) Protein crosslinking, tissue transglutaminase, alternative splicing and neurodegeneration. *Neurochem. Int.* **40**, 69–78.

Eitan S. and Schwartz M. (1993) A transglutaminase that converts interleukin-2 into a factor cytotoxic to oligodendrocytes. *Science* **261**, 106–108.

Eitan S., Solomon A., Lavie V., Yoles E., Hirschberg D. L., Belkin M. and Schwartz M. (1994) Recovery of visual response of injured adult rat optic nerves treated with transglutaminase. *Science* **264**, 1764–1768.

Elkind M. S. and Sacco R. L. (1998) Stroke risk factors and stroke prevention. *Semin. Neurol.* **18**, 429–440.

Facchiano F., D'Arcangelo D., Riccomi A., Lentini A., Beninati S. and Capogrossi M. C. (2001) Transglutaminase activity is involved in polyamine-induced programmed cell death. *Exp. Cell Res.* **271**, 118–129.

Ferrari N., Pfahl M. and Levi G. (1998) Retinoic acid receptor gamma1 (RARgamma1) levels control RARbeta2 expression in SK-N-BE2(c) neuroblastoma cells and regulate a differentiation-apoptosis switch. *Mol. Cell Biol.* **18**, 6482–6492.

Festoff B. W., SantaCruz K., Arnold P. M., Sebastian C. T., Davies P. J. and Citron B. A. (2002) Injury-induced 'switch' from GTP-regulated to novel GTP-independent isoform of tissue transglutaminase in the rat spinal cord. *J. Neurochem.* **81**, 708–718.

Fujita K., Ando M., Yamauchi M., Nagata Y. and Honda M. (1995) Alteration of transglutaminase activity in rat and human spinal cord after neuronal degeneration. *Neurochem. Res.* **20**, 1195–1201.

Gilad G. M., Varon L. E. and Gilad V. H. (1985) Calcium-dependent transglutaminase of rat sympathetic ganglion in development and after nerve injury. *J. Neurochem.* **44**, 1385–1390.

Gill L. S., Pabbathi V. K., Vignes M. and Haynes L. W. (1998) Altered distribution of Galphah/type 2 transglutaminase following catecholamine deprivation is associated with depression of adrenoreceptor signal transduction in cultured ventricular zone germinal cells. *Brain Res.* **788**, 95–103.

Graham S. H. and Chen J. (2001) Programmed cell death in cerebral ischemia. *J. Cereb. Blood Flow Metab.* **21**, 99–109.

Greenberg C. S., Birckbichler P. J. and Rice R. H. (1991) Transglutaminases: multifunctional cross-linking enzymes that stabilize tissues. *Faseb J.* **5**, 3071–3077.

Hayes R. L., Pike B. R. and DeFord S. M. (2001) Contributions of calpains and caspases to cell death following brain injury. In: *Head Trauma, Preclinical and Clinical Directions* (Miller P. L. a. H. R. L., ed.), Chap. 10, pp. 219–237. John Wiley.

He Z., Yang S. H., Naritomi H., Yamawaki T., Liu Q., King M. A., Day A. L. and Simpkins J. W. (2000) Definition of the anterior choroidal artery territory in rats using intraluminal occluding technique. *J. Neurol. Sci.* **182**, 16–28.

Ikura K., Shinagawa R., Suto N. and Sasaki R. (1994) Increase caused by interleukin-6 in promoter activity of guinea pig liver transglutaminase gene. *Biosci. Biotechnol. Biochem.* **58**, 1540–1541.

Im M. J., Russell M. A. and Feng J. F. (1997) Transglutaminase II: a new class of GTP-binding protein with new biological functions. *Cell Sign.* **9**, 477–482.

Kalaria R. N. (2000) The role of cerebral ischemia in Alzheimer's disease. *Neurobiol. Aging* **21**, 321–330.

Kim S. Y., Grant P., Lee J. H., Pant H. C. and Steinert P. M. (1999) Differential expression of multiple transglutaminases in human brain. Increased expression and cross-linking by transglutaminases 1 and 2 in Alzheimer's disease. *J. Biol. Chem.* **274**, 30715–30721.

Kristian T. and Siesjo B. K. (1998) Calcium in ischemic cell death. *Stroke* **29**, 705–718.

Lai T. S., Hausladen A., Slaughter T. F., Eu J. P., Stamler J. S. and Greenberg C. S. (2001) Calcium regulates S-nitrosylation, denitrosylation, and activity of tissue transglutaminase. *Biochemistry* **40**, 4904–4910.

Lefebvre O., Wouters D., Mereau-Richard C., Facon T., Zandecki M., Formstecher P. and Belin M. T. (1999) Induction of apoptosis by all-trans retinoic acid in the human myeloma cell line RPMI 8226 and negative regulation of some of its typical morphological features by dexamethasone. *Cell Death Differ.* **6**, 433–444.

Lesort M., Tucholski J., Miller M. L. and Johnson G. V. (2000) Tissue transglutaminase: a possible role in neurodegenerative diseases. *Prog. Neurobiol.* **61**, 439–463.

Maddox A. M. and Haddox M. K. (1988) Characteristics of cyclic AMP enhancement of retinoic acid induction of increased transglutaminase activity in HL60 cells. *Exp. Cell Biol.* **56**, 49–59.

Mattson M. P. (2000) Apoptotic and anti-apoptotic synaptic signaling mechanisms. *Brain Pathol.* **10**, 300–312.

Monsonego A., Shani Y., Friedmann I., Paas Y., Eizenberg O. and Schwartz M. (1997) Expression of GTP-dependent and GTP-independent tissue-type transglutaminase in cytokine-treated rat brain astrocytes. *J. Biol. Chem.* **272**, 3724–3732.

Nakaoka H., Perez D. M., Baek K. J., Das T., Husain A., Misono K., Im M. J. and Graham R. M. (1994) Gh: a GTP-binding protein with transglutaminase activity and receptor signaling function. *Science* **264**, 1593–1596.

Norlund M. A., Lee J. M., Zainelli G. M. and Muma N. A. (1999) Elevated transglutaminase-induced bonds in PHF tau in Alzheimer's disease. *Brain Res.* **851**, 154–163.

Pennypacker K. R., Hernandez H., Benkovic S., Morgan D. G., Willing A. E. and Sanberg P. R. (1999) Induction of presenilins in the rat brain after middle cerebral arterial occlusion. *Brain Res. Bull.* **48**, 539–543.

Piredda L., Farrace M. G., Lo Bello M., Malorni W., Melino G., Petruzzelli R. and Piacentini M. (1999) Identification of 'tissue' transglutaminase binding proteins in neural cells committed to apoptosis. *Faseb J.* **13**, 355–364.

Pluta R. (2000) The role of apolipoprotein E in the deposition of beta-amyloid peptide during ischemia-reperfusion brain injury. A model of early Alzheimer's disease. *Ann. NY Acad. Sci.* **903**, 324–334.

Suedhoff T., Birckbichler P. J., Lee K. N., Conway E. and Patterson M. K. Jr (1990) Differential expression of transglutaminase in human erythroleukemia cells in response to retinoic acid. *Cancer Res.* **50**, 7830–7834.

Tetzlaff W., Gilad V. H., Leonard C., Bisby M. A. and Gilad G. M. (1988) Retrograde changes in transglutaminase activity after peripheral nerve injuries. *Brain Res.* **445**, 142–146.

Tolentino P. J., DeFord S. M., Notterpek L., Glenn C. C., Pike B. R., Wang K. K. and Hayes R. L. (2002) Up-regulation of tissue-type transglutaminase after traumatic brain injury. *J. Neurochem.* **80**, 579–588.

Tucholski J., Lesort M. and Johnson G. V. (2001) Tissue transglutaminase is essential for neurite outgrowth in human neuroblastoma SH-SY5Y cells. *Neuroscience* **102**, 481–491.

Vermeer S. E., Prins N. D., den Heijer T., Hofman A., Koudstaal P. J. and Breteler M. M. (2003) Silent brain infarcts and the risk of dementia and cognitive decline. *N. Engl. J. Med.* **348**, 1215–1222.

Zipfel G. J., Babcock D. J., Lee J. M. and Choi D. W. (2000) Neuronal apoptosis after CNS injury: the roles of glutamate and calcium. *J. Neurotrauma* **17**, 857–869.

Cathepsin B mRNA and protein expression following contusion spinal cord injury in rats

Rebecca C. Ellis,* J. Nicole Earnhardt,* Ronald L. Hayes,*·†·§ Kevin K.W. Wang*·‡·§ and Douglas K. Anderson*·¶·**

*Department of Neuroscience, †Department of Neurosurgery, ‡Department of Psychiatry, §Center for Traumatic Brain Injury Studies, and ¶Evelyn F and William L. McKnight Brain Institute of the University of Florida, University of Florida, Gainesville, Florida, USA
**Malcom Randall VAMC, Gainesville, Florida, USA

Abstract

We provide the first data that cathepsin B (Cath B), a lysosomal cysteine protease, is up-regulated following contusion-spinal cord injury (SCI). Following T12 laminectomy and moderate contusion, Cath B mRNA and protein expression profiles were examined from 2 to 168 h post-injury in rats using real-time PCR and immunoblots, respectively. Contusion injury significantly increased [mRNA]$_{\text{Cath B}}$ in the injury site and adjacent segments over sham injury levels. While the largest [mRNA]$_{\text{Cath B}}$ induction (20-fold over naive) was seen in the injury site, the caudal segment routinely yielded [mRNA]$_{\text{Cath B}}$ levels greater than 10-fold over naive. Interestingly, sham injury animals also experienced mRNA induction at several time points at the injury site and in segments rostral and caudal to the injury site. Contusion injury also significantly elevated levels of Cath B proenzyme protein (37 kDa) over sham injury in the injury site (48, 72 and 168 h post-injury). Furthermore, significant protein increases of single and double chain Cath B (both active forms) occurred at the injury site at 72 and 168 h post-injury. Similar significant increases in Cath B protein levels were seen in areas adjacent to the injury site. The induction of Cath B mRNA and protein expression following contusion injury is previously undescribed and suggests that Cath B may potentially be involved in the secondary injury cascade, perhaps for as long as 1 week post-injury.

Keywords: cathepsin B, trauma, spinal cord, induction.
J. Neurochem. (2004) **88**, 689–697.

Injury to the spinal cord is typically the result of some type of mechanical insult. This primary injury can be contusive, shearing, stretching or concussive in nature. Primary injury deforms neuronal cell bodies, axons and oligodendrocytes. Disruption of vascular elements and structures within injured tissue leads to petechial hemorrhage, the release of vasoactive molecules and loss of autoregulation by the vascular system (Anderson and Hall 1993; Amar and Levy 1999; Mautes *et al.* 2000). The primary injury also initiates a cascade of pathochemical and pathophysiological events, collectively known as the secondary injury. These events include but are not limited to lipid hydrolysis, eicosanoid production, lipid peroxidation, loss of mitchondrial function and ionic homeostasis, invasion of neutrophils and macrophages, cytokine production, loss of the blood–spinal cord barrier integrity and excitotoxicity (Velardo *et al.* 1999; Demediuk *et al.* 1985, 1987; Anderson and Hall 1993; Amar and Levy 1999; McGrath 1999; Lu *et al.* 2000). Ultimately there is significant loss of neural tissue via apoptotic and

necrotic cell death, which frequently results in cavitation around the injury site. As a result, there is a loss of function and sensation distal to the injury site and the prognosis for substantial functional recovery is usually poor.

There has been significant interest in understanding the activation and involvement of enzymatic cascades in the secondary injury response associated with trauma to the spinal cord. Several phospholipases, kinases, endonucleases and proteases are activated by injury-induced increases in intracellular Ca^{2+} levels. Of these proteases, calpain and

caspase, and now to some extent cathepsin B (Cath B), have been linked to neurodegeneration and cell death in multiple models of central nervous system (CNS) injury. The literature on calpain and caspase involvement in neurodegeneration is quite extensive. Calpain has been associated with tissue destruction and cell death in traumatic brain injury (Kampfl *et al.* 1996, 1997; Saatman *et al.* 1996), ischemia (Rami and Krieglstein 1993; Bartus *et al.* 1994) and spinal cord injury (SCI) (Li *et al.* 1996; Ray *et al.* 1999, 2000; Schumacher *et al.* 1999; Shields *et al.* 2000). In these cases, the increases in calpain activity and immunoreactivity associated with injury are accompanied by increased breakdown of cytoskeletal and myelin proteins (Banik *et al.* 1997; Posmantur *et al.* 1998; Buki *et al.* 1999; Ray *et al.* 1999; Banik and Shields 2000). With more than 40 reported substrates (Stroh and Schulze-Osthoff 1998), caspases (predominantly caspase-3, 9 and -12) have also been linked to tissue loss and cell death in models of traumatic (Crowe *et al.* 1997; Liu *et al.* 1997; Keane *et al.* 2001; Larner *et al.* 2003) brain and spinal cord injury and in ischemic SCI (Sakurai *et al.* 1998; Mackey *et al.* 1997; Hayashi *et al.* 1998; Matsushita *et al.* 2000). Caspases were activated in models of global and focal brain ischemia (Chen *et al.* 1998; Fink *et al.* 1998; Namura *et al.* 1998; Ni *et al.* 1998; Didenko *et al.* 2002). Furthermore, the inhibition of some caspase pathways reduced tissue damage and improved neurological functions (Cheng *et al.* 1998; Mouw *et al.* 2002) in rodent models of focal ischemia (reviewed by Robertson *et al.* 2000).

To date, the role of Cath B in traumatic CNS insults has not been the focus of investigation. Under normal conditions, Cath B is synthesized as an inactive preproenzyme (39 kDa) in the *trans*-golgi, which is processed to the still inactive proenzyme (37 kDa) in the lysosomal compartment (Fig. 1) (Mort and Buttle 1997). Removal of the 63-residue propeptide from its N-terminal converts the inactive proenzyme to a single chain active form (30 kDa) (Fig. 1). This single chain Cath B is further processed within the lysosome into a double chain form consisting of heavy (25 kDa) and light (5 kDa) components held together by a disulfide bond (Fig. 1) (Mort and Buttle 1997). Cath B is involved in protein turnover and digestion of cellular debris (Mort and Buttle 1997; Turk *et al.* 2000) and is capable of hydrolyzing carbohydrates, nucleic acids and lipids. Increased levels of Cath B expression and activity have been reported in several pathologies (Rempel *et al.* 1994; Berquin and Sloane 1996; Bever *et al.* 1997; Mackay *et al.* 1997; Kikuchi *et al.* 2003) including ischemia and oxidative stress (Kohda *et al.* 1996; Seyfried *et al.* 1997; Tsuchiya *et al.* 1999). These changes in Cath B expression and activity are frequently accompanied by its redistribution from the lysosome to the cytosol, and in some cases to the nucleus (Roberts *et al.* 1997) in the injured tissues.

While Cath B has not been characterized following traumatic CNS injury, it has been well studied in a model of cerebral ischemic injury. Yamashima *et al.* (1996) found
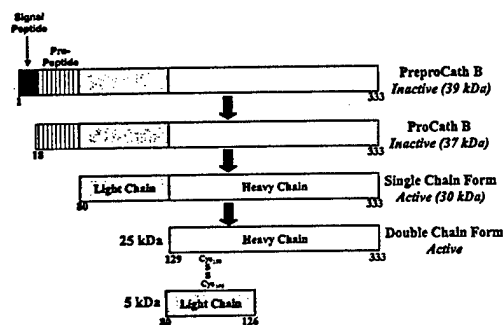
Fig. 1 Schematic of Cath B protein. Preprocathepsin B (333 amino acids) is synthesized on the rough ER where the signal peptide is cleaved cotranslationally. Following transport to the Golgi apparatus, the enzyme is glycosylated and the mannose-6-phosphate signal is assembled. This receptor allows for transport to the *trans*-Golgi network and then onto an acidic compartment where the pro-peptide is removed and enzyme is activated. Within the lysosome, the active single chain form of Cath B (30 kDa) is further modified (loss of a dipeptide) to produce the active double chain form (25 and 5 kDa) held together via disulfide bond.

that the CA1 neuronal population in the hippocampus was completely obliterated five days following transient ischemia. In addition to increased levels of Cath B activity, the protein itself was also redistributed. The administration of two different Cath B inhibitors, CA-074 and E-64c, immediately following ischemia reduced enzyme activity, diminished Cath B immunoreactivity to near negligible levels and spared approximately 67 and 84%, respectively, of CA1 neurons from delayed neuronal death (Tsuchiya *et al.* 1999; Yamashima *et al.* 1998, 1999). These findings suggest that Cath B plays a role in the development of neuropathology following cerebral ischemia and that the inhibition of Cath B may represent a possible avenue for therapeutic intervention.

We propose that Cath B alone, and/or in conjunction with other proteases such as calpain and caspase, could be destructive in spinal cord tissue after injury. However, to date, the effects of contusion injury on Cath B expression levels have not been examined. Thus, the purpose of this study was to examine the effects of sham and contusion injury on expression of Cath B in the spinal cord. Our results demonstrate that contusion injury increased expression of both Cath B mRNA and protein in the injury site and in segments immediately rostral and caudal to the injury site.

Experimental procedures

All experimental procedures were conducted in accordance with the guidelines set forth by the University of Florida's Institute Animal Care and Use Committee (IACUC).

Laminectomy and injury

Female Long–Evans rats weighing approximately 230–300 g (Harlan, Indianapolis, IN, USA) were used in this study. All

surgical procedures were conducted under sterile conditions with supplemental heat. Intraperitoneal administration of nembutal (sodium pentobarbital, 50–60 mg/kg) was used to induce anesthesia. Following a T12, partial T11 laminectomy (intact dura mater), injury to the spinal cord was produced with an NYU impactor device (10 g, 25 mm). The sham injury animals received a laminectomy and were placed in the injury apparatus, but were not injured. The incisions were closed in layers. Animals were recovered in a heated incubator with food and water available *ad libitum*. Bladders were expressed and fluids were administered when required. In the immunoblot analysis ($n = 60$), four animals were used for each treatment group (sham and contusion injury) at each time point (2, 6, 12, 24, 48, 72, and 168 h post-injury). Four naive animals were also utilized. For the real-time PCR experiments (total $n = 44$), both sham and contusion injury ($n = 3$–6 each) were sacrificed at 2, 6, 24, 48, and 168 h post-injury in addition to a group ($n = 5$) of naive animals. Spinal cord tissue was collected after extending the laminectomy to allow three segments of tissue to be removed: (i) rostral to injury site, (ii) injury site, and (iii) caudal to injury site. Each segment was approximately 6–7 mm in length. The fresh tissue was rinsed with cold 1 × phosphate-buffered saline (PBS) and either (i) homogenized with a guanidinum thiocyanate salt solution (500 μL) or (ii) flash frozen with liquid nitrogen. All samples were stored at − 70°C until either (i) RNA isolation or (ii) protein homogenization.

RNA isolation and cDNA synthesis

Total RNA isolation from the spinal cord tissue was achieved using a modified protocol, described by Earnhardt *et al.* (2002), based on the guanidinium thiocyanate/phenol/chloroform extraction developed by Chomczynski and Sacchi (1987). Final RNA concentrations were determined via spectrophotometry and samples were stored at −20°C in diethyl pyrocarbonate water for future cDNA preparation.

For cDNA synthesis, 1 μg of total RNA from all samples was used for enzymatic conversion of mRNA to first strand cDNA using an oligo-dT primer (Invitrogen/Life Technologies, Carlsbad, CA, USA; SuperScript™ First-Strand Synthesis System for RT-PCR). DNA contamination was monitored in our RNA samples by 'no reverse transcriptase' reactions which were performed in conjunction with cDNA synthesis reaction.

Primer design

Base pairs designations for rat GAPDH refer to GeneBank locus AF106860. The primers used for all GAPDH PCR reactions were: sense 5′-ggtga aggtc ggtgt gaac-3′ corresponding to base pairs 852–870 and antisense 5′-ggcat cctgg gctac actg-3′ corresponding to base pairs 1657–1675. Cath B primers were designed using GeneBank locus NM022597. The sense Cath B primer recognized an upstream rat Cath B specific mRNA sequence 5′-tgagg acctg cttac ctgct-3′ corresponding to base pairs 466–485. The antisense Cath B primer recognized a downstream rat Cath B specific mRNA sequence 5′-gcagg gagtg aggca gatag-3′ corresponding to base pairs 1141–1160.

Real-time PCR

The Roche LightCycler and the double-stranded DNA binding dye, SYBR Green I, were used to continuously monitor all PCR reactions. The LightCycler (Roche Biochemicals) is an advanced instrument that conducts rapid thermal cycling of the polymerase

chain reaction. SYBR Green I dye™ preferentially binds to double stranded DNA and emits a fluorescent signal proportional to the DNA concentration. The reaction kinetics of this PCR reaction are represented by an amplification curve. Each amplification curve (fluorescence versus cycle number) is assigned a crossing point value (CPV), which is defined as the point of intersection between the amplification curve and the noise band. A lower CPV indicates a more rapid increase in the level of fluorescence and, thus a larger initial concentration of message. When comparing templates, those with lower CPVs contain more amplified message for the gene of interest than those with higher CPVs.

For each PCR reaction the LightCycler FastStart DNA Master[PLUS] SYBR Green I (Roche) reagent was used according to manufacturer's instructions in combination with primers, cDNA template, dimethyl sulfoxide and $MgCl_2$ at final concentrations of 0.5 μM, 10 ng, 6%, and 2 mM, respectively. After an initial 300 s, 95°C denaturation step, 40 cycles of amplification were performed (95°C for 5 s; denaturation, 65°C for 10 s; annealing, 72°C for 40 s; extension). SYBR Green I fluorescent detection of double stranded PCR products occurred at the end of each 72°C extension within each of the 40 amplification cycles. The specificity of the amplified product was confirmed by (i) the melting curve analysis and (ii) gel electrophoresis. To generate standard curves for the Cath B primer set, contusion injury templates were subjected to serial dilution. Linear regression analysis of the logarithm of the dilution factor versus the CPV generated a standard curve for each specific template. All standard curves were run concomitant with segment- and time-matched unknowns (naive, sham). The relative amount of RNA in the unknown sample was extrapolated from its CPV in relation to the standard curve. Results are reported as relative concentrations.

Northern blot analysis

Northern blot analysis was used to confirm the validity of the real-time PCR technique that we employed to examine mRNA expression. A northern blot prepared as described by Earnhardt *et al.* (2002) was probed with ^{32}P-labeled rat Cath B cDNA (gift from S. Chan, University of Chicago, IL, USA). Autoradiographic films were analyzed using Scion image analysis software. Any differences resulting from loading variability were controlled by normalizing the intensity of the Cath B mRNA signal in each sample to its mRNA signal for cyclophilin.

Tissue lysis and protein purification

Lysis buffer (1 mM EDTA, 2 mM EGTA, 1 small Protease Cocktail Pill™ (Roche Molecular Biochemicals), 0.1% SDS, 1.0% IGEPAL, 0.5% deoxycholic acid, 150 mM NaCl, 20 mM Hepes, ddH₂O, pH = 7.5) was added to each sample based on the mass of the tissue (15 μL/1 mg). The tissue was homogenized on ice with a rotary pestle, returned to Eppendorf tubes and placed at 4°C for at least 30 min Samples were sonicated and spun at 800 g for 5 min at 4°C before the supernatant was collected and stored at −70°C.

Immunoblotting

Protein concentrations of the tissue homogenates were determined by bichinchoninic acid (BCA) assay (Pierce Inc., Rockford, IL, USA). Unless otherwise noted, all procedures were performed at room temperature. Eighteen micrograms of total protein were mixed

with 2 × loading buffer (1 × = 125 mM Tris-HCl, 100 mM dithio-threitol, 4.0% sodium dodecyl sulfate (SDS), 0.01% bromophenol blue and 10.0% glycerol) and were resolved by SDS–polyacrylamide gel electrophoresis (PAGE) on 10% Tris/HCl gels (Bio-Rad, Hercules, CA). The fractionated proteins were subsequently transferred to a 0.20-μM nylon membrane (Bio-Rad) in transfer buffer (192 mM glycine, 25 mM Tris/HCl, 10.0% methanol). Staining with ponceau red (Sigma, St. Louis, MO, USA) confirmed transfer of the proteins. Blots were blocked in 5.0% non-fat milk/Tris-buffered saline-Tween (TBS-T) 20 mM Tris/HCl, 150 mM NaCl, 0.005% Tween 20, pH 7.5. Membranes were washed with TBS-T and incubated overnight with a polyclonal anti-Cath B antibody (1 : 1000) (Upstate Biotechnology Inc.). Membranes were washed and then incubated in 3.0% non-fat milk/TBS-T with an anti-rabbit IgG horseradish peroxidase conjugated antibody (1 : 3000) (Bio-Rad). After additional washing, bound antibodies were visualized using the chemiluminescent developing reagent ECL⁺ (Amersham Pharmacia Biotech, UK). The Cath B antibody recognized three bands: the inactive proenzyme (37 kDa), the active single chain form (30 kDa) and the heavy component of the double chain form (25 kDa). Representative blots were stripped and reprobed with a monoclonal anti-GAPDH antibody (gift of Dr Gerry Shaw, University of Florida, FL, USA) for loading control purposes. Data were acquired as integrated densitometry values (IDVs) by computer-assisted densitometric scanning (Alpha Imager 2000 Digital Imaging System, San Leandro, CA, USA).

Statistical analyses
In these experiments, the levels of Cath B mRNA and protein in the sham and contusion injury animals were normalized to naive levels (or control, in the case of the northern blot analysis) to generate fold induction values (± SEM) referred to as 'fold over naive' (FON). Within each segment (rostral, injury site and caudal), FON values from both the sham and contusion injury groups were analyzed via a two-way ANOVA. Each of the three different protein species (37, 30 and 25 kDa) in the immunoblot experiments required its own ANOVA. Statistically significant differences between the treatment groups were identified with post hoc tests (Tukey's for real-time PCR, immunoblots; independent *t*-test for northern blot analysis).

Results

Contusion-spinal cord injury increased Cath B mRNA levels
Before examining the gene of interest, Cath B, the samples were tested for template integrity using the housekeeping gene GAPDH. Within each set of reactions, the CPVs for the three groups (naive, and sham and contusion injury) were not significantly different at any of the experimental time points (data not shown). Having confirmed template integrity, standard curves were used to ascertain the [mRNA]$_{Cath B}$ of the templates within each group. The increase in Cath B mRNA expression in both the sham and contusion injury groups was normalized against the naive levels and represented as the relative induction of (fold over naive). In all segments and at almost all time points

examined, [mRNA]$_{Cath B}$ was increased following both sham and contusion injury (Fig. 2a).

Sham injury increased [mRNA]$_{Cath B}$ although to a lesser degree than the contusion injury. In both the rostral segment (FON = 4.1) and injury site (FON = 5.6), the sham injury induced increase peaked at 48 h post-injury and returned to near basal levels by the last time point examined (168 h). While the pattern of mRNA induction was similar in the rostral and injury segments, the caudal segment responded differently. Here, sham injury induction of Cath B mRNA expression appeared to be more robust than in the other two segments, i.e. at four of the five time points, the mRNA levels exceeded five FON.

Within the injury site, the expression of Cath B mRNA following contusion injury was significantly elevated over the sham injury values at 168 h post-injury. FON increases of 4.2, 10.7 and 19.2 were seen at 24, 48 and 168 h post-injury, respectively, with the largest recorded increase occurring at 168 h post-injury. An injury-induced elevation of Cath B mRNA expression in the injury site 24 h post-injury was demonstrated by northern analysis (Fig. 2b,c). Northern analysis also confirmed a sham injury induced increase in mRNA expression albeit to a lesser degree than the contusion injury (Fig. 2c).

Contusion injury also induced Cath B mRNA expression in areas beyond the injury site. Within the rostral segment, contusion injury significantly increased [mRNA]$_{Cath B}$ over sham injury values at 48 and 168 h post-injury. The maximum contusion injury induced increase occurred at 48 h post-injury (6.4 FON) and remained at this level (6.0 FON) until the last time point examined (168 h post-injury). Caudal to the injury site, contusion injury appeared to induce an expression of Cath B mRNA that, like the sham injury animals, was more robust than that seen in the other two segments. [mRNA]$_{Cath}$ was increased at 24, 48 and 168 h post-injury (10 + FON), although a significant increase over sham injury levels occurred solely at the 48 h time point.

Cath B protein expression is elevated following spinal cord injury
Figure 3 displays representative immunoblots (probed with anti-Cath B antibody) for the rostral (Fig. 3a), injury site (Fig. 3b) and caudal (Fig. 3c) segments at 168 h post-injury. Also shown are the GAPDH loading controls. Naive samples produced faint bands while sham and contusion injury yielded broader and more intense bands for the proenzyme and active forms of Cath B. Although the most robust FON increases occurred in the injury site, increased expression of all Cath B protein species was observed in the three segments examined after both sham and contusion injury (Fig. 4). Sham injury did increase Cath B protein levels, but the increases rarely exceeded two FON. In fact, sham injury
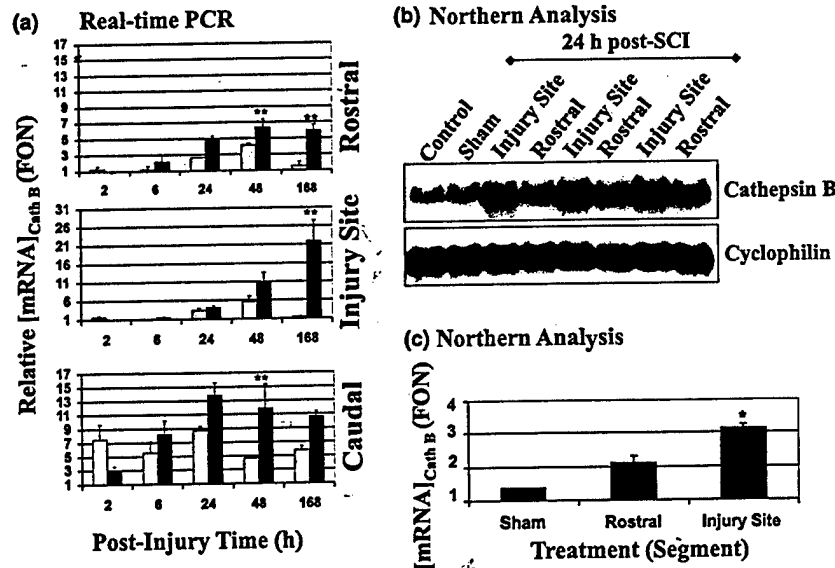
Fig. 2 Sham- and contusion-spinal cord injury (SCI) induced increases in Cath B mRNA. (a) The increases in $[mRNA]_{Cath\ B}$ induced by sham (gray bars) and contusion injury (black bars) are presented here as relative induction of $[mRNA]_{Cath\ B}$ (fold over naive). Cath B mRNA expression was induced following both sham and contusion injury. The post-injury data are presented for the rostral (top panel), injury site (middle panel) and caudal (bottom panel) segments of the spinal cord (Note the different scales for FON values in injury site segment versus the rostral and caudal segments). Following contusion injury, the expression of Cath B mRNA was significantly greater than that of the sham injury in the rostral segment. Similarly, in the injury site, significant differences between the two groups occurred only at 168 h post-injury, where the highest level observed in this study was recorded. In the caudal segment, the $[mRNA]_{Cath\ B}$ peaked at 24 h post-injury but remained elevated at 48 and 168 h post-injury. For this graph and the others, asterisks indicate significant increases (*$p < 0.05$, **$p < 0.01$) between the sham and contusion injury groups. (b) Northern blot analysis of $[mRNA]_{Cath\ B}$ in both the injury site (vertebral level T13) and rostral (vertebral level T12) segment 24 h following contusion injury. The increases in $[mRNA]$Cath B in three experimental animals were compared to those observed in control and sham injury animals. Each lane was loaded with 12 µg of total RNA. The signal obtained for the 2.3 kb Cath B message was normalized to the signal previously obtained for cyclophilin (Earnhardt et al. 2002). (c) Densitometric analyses of the northern blot shown in (b). Again, contusion injury produced a significant increase in Cath B mRNA. The data represent the mean ± SEM induction (FON) of the three rostral and three injury site samples.

elicited an induction with a two FON or greater at only three of 63 time points (maximum FON value was 2.3).

Contusion injury results in significant increase over sham injury in the 37 kDa proenzyme form of Cath B at 48, 72 and 168 h post-injury at the injury site and at 24, 48, 72 and 168 h post-injury in the caudal segment (Fig. 4). No significant change in the level of proenzyme was seen in the rostral segment. The single chain 30 kDa active form of Cath B was significantly higher following the contusion injury than in sham injury at 168 h post-injury in the rostral segment, and at 72 and 168 h post-injury in both the injury site and in the caudal segment (Fig. 4). The double chain (25 kDa) form of Cath B in contusion injured spinal cord was significantly elevated over sham injury at 168 h post-injury in the injury site and in the rostral (but not caudal) segment (Fig. 4).

In order to examine the relationship between the increases in Cath B[mRNA] and Cath B[protein] following sham and contusion injury, a linear regression analysis was performed for each segment. The FON$_{mRNA}$ (generated in the real-time experiments) was used as the independent factor and the FON$_{protein}$ for the Cath B proenzyme (37 kDa) was the dependent factor. There was a near linear correlation between the increases in FON$_{mRNA}$ and FON$_{protein}$ following contusion injury in the rostral ($r^2 = 0.941$, $p < 0.006$), injury site ($r^2 = 0.971$, $p < 0.002$) and caudal ($r^2 = 0.844$, $p < 0.028$) segments, suggesting that the level of Cath B proenzyme increases linearly relative to the increases in Cath B mRNA levels after contusion injury. The same analysis of sham injury samples yielded low r^2 values, suggesting that in the case of sham injury, modest increases of Cath B[mRNA] did not translate into increases in Cath B[protein].

Discussion

Mechanical trauma to the spinal cord initiates a complex cascade of biochemical processes that collectively contribute to neuronal and glial cell death, tissue cavitation, functional deficits and, to date, limited opportunity for restoration and/ or functional improvement. Despite the suggestion that

(a)

Rostral

—37 kDa — ProCath B
—30 kDa — Single Chain
—25 kDa — Heavy Chain

N   N   S   S   I   I

—GAPDH (Loading Control)

(b)

Injury Site

—37 kDa — ProCath B
—30 kDa — Single Chain
—25 kDa — Heavy Chain

N   N   S   S   I   I

—GAPDH (Loading Control)

(c)

Caudal

—37 kDa — ProCath B
—30 kDa — Single Chain
—25 kDa — Heavy Chain

N   N   S   S   I   I

—GAPDH (Loading Control)
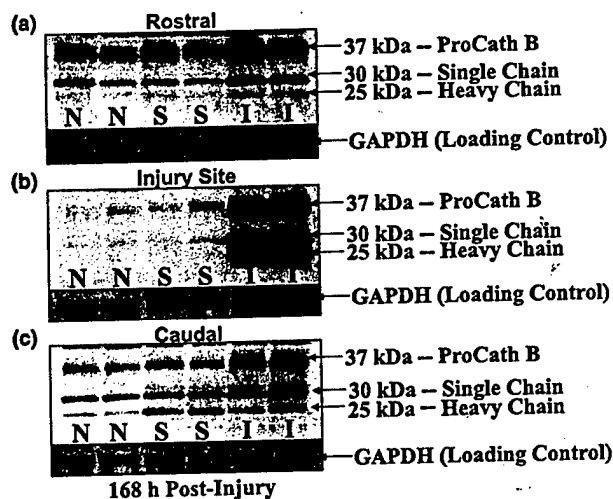
168 h Post-Injury

Fig. 3 Sham and contusion injury increase levels of Cath B proenzyme and its two active forms. Naive, sham and contusion injury samples are shown from the 168 h post-injury time point. Three bands were detected: the inactive proenzyme at 37 kDa and two active mature forms, 30 kDa (single chain) and 25 kDa (double chain). Naive samples produced very faint bands in all blots examined. In the injury site (b), the sham injury animals yielded only slightly more dense bands. The contusion injury animals, however, had noticeably more intense and broad bands. These increases also extended to areas rostral (a) and caudal (c) to the injury site. The GAPDH loading control blots are also shown for each panel.

Cath B mRNA induction 3 days after hemisection and sciatic nerve crush (Fan *et al.* 2001) or dorsal root avulsion (Hu *et al.* 2002) using microarray analysis. However, these early studies give a highly circumscribed view of the injury process as they provided the differential expression data for several hundred genes at only one post-injury time point. Our study represents the first in depth analysis of contusion injury induced changes on Cath B expression, as it examines the mRNA and protein levels at several post-injury time points and in areas in and surrounding the injury site.

An examination of the expression profiles revealed significant induction following contusion injury in both the levels of Cath B mRNA (Fig. 2) and protein (Figs 3 and 4). Importantly, the increased presence of the single chain and double chain active forms of Cath B protein illustrate that Cath B proenzyme is being processed after contusion injury (Fig. 1). In addition, following sham injury (i.e. laminectomy and placement in the injury device), elevations in $[mRNA]_{Cath B}$ were observed in each segment (Fig. 2). Cath B protein levels were also affected, but to a much smaller extent across the experimental time line (Fig. 4). Laminectomy has been reported to decrease spinal cord blood flow, alter energy metabolism and initiate changes in membrane lipid composition (Anderson *et al.* 1978; Anderson and Means 1985; Demediuk *et al.* 1985, 1987). We previously reported that laminectomy alone induced MnSOD mRNA and protein expression (Earnhardt *et al.* 2002). While great care was taken not to perturb the dura mater or the spinal cord during the sham injury, the increases in Cath B mRNA and protein expression confirm that laminectomy itself is an intrusive procedure. The exact mechanism(s) behind laminectomy-induced increases in Cath B mRNA and protein expression is still unknown.

As a powerful hydrolytic enzyme, Cath B likely contributes to necrotic tissue destruction via degradation of several important cellular proteins. Although little is known about

lysosomal rupture and/or leakage may possess the greatest mechanistic potential to directly kill cells (Nixon and Cataldo 1993), the reported increases in calpain and caspase expression and activity levels have overshadowed the characterization of lysosomal hydrolyses following contusion-SCI. While the investigation of SCI-induced changes in Cath B expression has lagged, two separate groups have reported

(a) Rostral   (b) Injury Site   (c) Caudal

[Protein]$_{Cath B}$ (FON)

Inactive (37 kDa)

Active (30 kDa)

Active (25 kDa)

Post-Injury Time Points (h)

Fig. 4 Increases in levels of the three forms of Cath B following sham and contusion spinal cord injury. The 'fold over naive' (FON) values for the sham injury group (gray bars) were compared to those of the contusion injury (black bars) at seven post-injury time points. The time course of these changes in the proenzyme (37 kDa) and two active forms of Cath B (30 and 25 kDa) are presented for the rostral (a), injury site (b) and caudal (c) segments (Note the different scales for FON values in injury site segment versus the rostral and caudal segments.).

the response of Cath B to traumatic CNS injuries, there is evidence from other models of CNS insults to suggest how sensitive cellular substrates are to Cath B. For example, in one model of transient ischemia, Ca^{2+} influx was accompanied by increased calpain expression and activity (Yamashima et al. 1996). These workers characterized the delayed neuronal death that followed the insult in the context of the 'calpain–cathepsin' hypothesis. They noted that activated calpain was localized to vacuolated and disrupted lysosomal membranes, where it acted to degrade the lysosomal membrane. This lysosomal membrane breakdown allowed activated Cath B to escape as showed by a shift of Cath B immunoreactivity from a lysosomal to a cytosolic distribution. Cath B subsequently degraded cellular substrates such as cytoskeletal and myelin proteins contributing to the self-digestion and delayed neuronal death seen in this injury model. The events described by the 'calpain-cathepsin' hypothesis may be applicable to SCI as it has been reported that calpain expression and activity were increased following SCI (Banik et al. 1997; Ray et al. 1999; Shields et al. 2000). However, the specific interaction between these protease systems following SCI is currently unresolved. The concomitant increase in Cath B protein levels we now report may in part reflect this postulated role of calpain, and also contribute to the general degree of protein breakdown, cellular damage and tissue loss seen following SCI.

There is also increasing evidence for Cath B involvement in apoptosis (Leist and Jaattela 2001). While the executioner caspases-3 and -7 are relatively poor substrates for direct Cath B cleavage, the proinflammatory caspases-1 and -11 are readily processed (Schotte et al. 1998; Vancompernolle et al. 1998). Furthermore, Cath B reportedly participates in several models of apoptosis including nuclear apoptosis (Vancompernolle et al. 1998), neuronal apoptosis (Kingham and Pocock 2001), serum deprivation induced apoptosis (Shibata et al. 1998), cytokine induced apoptosis (Deiss et al. 1996), and tumor necrosis factor-α induced apoptosis (Guicciardi et al. 2000; Foghsgaard et al. 2001). There is speculation that Cath B acts to induce cytochrome c release and caspase-9 activation (Guicciardi et al. 2000). Most likely, a universal mechanism underlying the participation of Cath B in apoptosis does not exist. Rather, several apoptotic pathways may utilize Cath B alone or in conjunction with some other factor (lysosomal, cytosolic, mitchondrial). Whether Cath B is acting upstream or downstream (or perhaps both) of cyto c release and activation of caspases-3 and -9 remains unclear. With time, these questions will be elucidated and help to further explain any role of Cath B may have in apoptotic cell death following SCI.

The impetus driving the induction of Cath B mRNA expression following contusion injury is unknown. Both the human and mouse Cath B genes have been characterized and contain putative promoter regions that exhibit characteristics of housekeeping genes (i.e. absence of TATA or CAAT boxes). However these regions also have high GC content and binding sites for the Sp1 transcription factor (Ferrara et al. 1990; Qian et al. 1991; Gong et al. 1993). Furthermore, Yan et al. 2000 reported that the transcription factors Sp1, Sp3 and Ets1 are important factors in the regulation of Cath B transcription. While the presence of a housekeeping-like promoter suggests the constitutive expression of Cath B, the presence of these other regulatory elements coupled with the variations in Cath B mRNA levels in normal and diseased tissues (San Segundo et al. 1986) suggest that additional regulators of Cath B transcription may exist. Berquin and Sloane (1996) summarize the results of several studies reporting transcriptional regulation by agents such as phorbol ester, cytokines, interleukins and dexamethasone. At this time, the gene structure of the rat has yet to be resolved. Therefore, the transcriptional regulation of Cath B following contusion injury is outside the scope of this study.

It should be noted that Cath B mRNA expression and levels of the 37 kDa proenzyme form appeared to be greater in the caudal segment than in the rostral segment. However, the increase in the active 30 kDa form was similar in these two segments and the active 25 kDa form was higher in the rostral segment than in the caudal segment. The cause of these differences is unknown but likely reflects a variable spread of the secondary autodestructive cascade over time.

In summary, we report that expression of Cath B, a powerful and ubiquitous protease, is significantly induced by contusion injury and to a lesser extent by laminectomy only. Furthermore, this induction is seen on both the mRNA and protein level and extends beyond the confines of the original injury site. Third, active forms (30 and 25 kDa) of Cath B are also significantly elevated after contusion injury and this elevation is sustained for at least 7 days within the injury site. While its potential substrates and its exact role following contusion injury require further elucidation, by inference of the contributory role of Cath B in the pathobiology of ischemic brain injury and peripheral pathologies, we propose that Cath B is a potentially important mediator of secondary spinal cord injury.

Acknowledgements

References

Amar A. P. and Levy M. L. (1999) Pathogenesis and pharmacological strategies for mitigating secondary damage in acute spinal cord injury. Neurosurgery 44, 1027–1039.

Anderson D. K. and Hall E. D. (1993) Pathophysiology of spinal cord trauma. *Ann. Emerg. Med.* **22**, 987–992.

Anderson D. K. and Means E. D. (1985) The effect of laminectomy on spinal cord blood flow, energy metabolism and ATPase activity. *Paraplegia* **23**, 55.

Anderson D. K., Nicolosi G. R., Means E. D. and Hartley L. E. (1978) Effects of laminectomy on spinal cord blood flow. *J. Neurosurg.* **48**, 232–238.

Banik N. L. and Shields D. C. (2000) The role of calpain in neurofilament protein degradation associated with spinal cord injury. *Methods Mol. Biol.* **144**, 195–201.

Banik N. L., Matzelle D. C., Gantt-Wilford G. and Osborne Hogan E. L. (1997) Increased calpain content and progressive degradation of neurofilament protein in spinal cord injury. *Brain Res.* **752**, 301–306.

Bartus R. T., Baker K. L., Heiser A. D., Sawyer S. D., Dean R. L., Elliott P. J. and Straub J. A. (1994) Postischemic administration of AK275, a calpain inhibitor, provides substantial protection against focal ischemic brain damage. *J. Cereb. Blood Flow Metab.* **14**, 537–544.

Berquin I. M. and Sloane B. F. (1996) Cathepsin-B expression in human tumors, in *Intracellular Protein Catabolism* (Suzuki, K., Bond, J., eds), pp. 281–294. Plenum Press, New York.

Bever C. T. Jr, Panitch H. S. and Johnson K. P. (1994) Increased cathepsin B activity in peripheral blood mononuclear cells of MS patients. *Neurology* **44**, 745–748.

Buki A., Siman R., Trojanowski J. Q. and Povlishock J. T. (1999) The role of calpain-mediated spectrin proteolysis in traumatically induced axon injury. *J. Neuropath. Exp. Neurol.* **58**, 365–375.

Chen J., Nagayama T., Jin K., Stetler R. A., Zhu R. L., Graham S. H. and Simon R. P. (1998) Induction of caspase-3-like protease may mediate delayed neuronal death in hippocampus after transient cerebral ischemia. *J. Neurosci.* **18**, 4914–4928.

Cheng Y., Deshmukh M., D'Costa A., Demaro J. A., Gidday J. M., Shah A., Sun Y., Jacquin M. F., Johnson E. M. and Holtzman D. M. (1998) Caspase inhibitor affords neuroprotection with delayed administration in a rat model of neonatal hypoxic-ischemic brain injury. *J. Clin. Invest.* **101**, 1992–1999.

Chomczynski P. and Sacchi N. (1987) Single-step method of RNA isolation by acid guanidinium thiocyanate–phenol–chloroform extraction. *Anal. Biochem.* **162**, 156–159.

Crowe M. J., Bresnahan J. C., Shuman S. L., Masters J. N., Beattie M. S. (1997) Apoptosis and delayed degeneration after spinal cord injury in rats and monkeys. *Nat. Med.* **3**, 73–76.

Deiss L. P., Galinka H., Berissi H., Cohen O. and Kimchi A. (1996) Cathepsin D protease mediates programmed cell death induced by interferon-gamma, Fas/APO-1 and TNF-alpha. *EMBO J.* **15**, 3861–3870.

Demediuk P., Saunders R. D., Anderson D. K., Means E. D. and Horrocks L. A. (1985) Membrane lipid changes in laminectomized and traumatized cat spinal cord. *Proc. Natl Acad. Sci. USA* **82**, 7071–7075.

Demediuk P., Saunders R. D., Anderson D. K., Means E. D. and Horrocks L. A. (1987) Early membrane lipid changes in laminectomized and traumatized cat spinal cord. *Neurochem. Pathol.* **7**, 79–89.

Didenko W., Ngo H., Minchew C. L., Boudreaux D. J., Widmayer M. A. and Baskin D. S. (2002) Caspase-3-dependent and -independent apoptosis in focal brain ischemia. *Mol. Med.* **8**, 347–352.

Earnhardt J. N., Streit W. J., Anderson D. K., O'Steen W. A. and Nick H. S. (2002) Induction of manganese superoxide dismutase in acute spinal cord injury. *J. Neurotrauma* **19**, 1065–1079.

Fan M., Mi R., Yew D. T. and Chan W. Y. (2001) Analysis of gene expression following sciatic nerve crush and spinal cord hemisection in the mouse by microarray expression profiling. *Cell. Mol. Neurobiol.* **21**, 497–508.

Ferrara M., Wojcik F., Rhaissi H., Mordier S., Roux M. P. and Bechet D. (1990) Gene structure of mouse cathepsin B. *FEBS Lett.* **273**, 195–199.

Fink K., Zhu J., Namura S., Shimizu-Sasamata M., Endres M., Ma J., Dalkara T., Yuan J. and Moskowitz M. A. (1998) Prolonged therapeutic window for ischemic brain damage caused by delayed caspase activation. *J. Cereb. Blood Flow Metab.* **18**, 1071–1076.

Foghsgaard L., Wissing D., Mauch D., Lademann U., Bastholm L., Boes M., Elling F., Leist M. and Jaattela M. (2001) Cathepsin B acts as a dominant execution protease in tumor cell apoptosis induced by tumor necrosis factor. *J. Cell Biol.* **153**, 999–1010.

Gong Q., Chan S. J., Bajkowski A. S., Steiner D. F. and Frankfater A. (1993) Characterization of the cathepsin B gene and multiple mRNAs in human tissues: evidence for alternative splicing of cathepsin B pre-mRNA. *DNA Cell Biol.* **12**, 299–309.

Guicciardi M. E., Deussing J., Miyoshi H., Bronk S. F., Svingen P. A., Peters C., Kaufmann S. H. and Gores G. J. (2000) Cathepsin B contributes to TNF-α-mediated hepatocyte apoptosis by promoting mitochondrial release of cytochrome c. *J. Clin. Invest.* **106**, 1127–1137.

Hayashi T., Sakurai M., Abe K., Sadahiro M., Tabayashi K. and Itoyama Y. (1998) Apoptosis of motor neurons with induction of caspases in the spinal cord after ischemia. *Stroke* **29**, 1007–1012.

Hu J., Fink D. and Mata M. (2002) Microarray analysis suggests the involvement of proteasomes, lysosomes, and matrix metalloproteinases in the response of motor neurons to root avulsion. *Eur. J. Neurosci.* **16**, 1409–1416.

Kampfl A., Posmantur R., Nixon R., Grynspan F., Zhao X., Liu S. J., Newcomb J. K., Clifton G. L. and Hayes R. L. (1996) mu-calpain activation and calpain-mediated cytoskeletal proteolysis following traumatic brain injury. *J. Neurochem.* **67**, 1575–1583.

Kampfl A., Posmantur R. M., Zhao X., Schmutzhard E., Clifton G. L. and Hayes R. L. (1997) Mechanisms of calpain proteolysis following traumatic brain injury: implications for pathology and therapy: a review and update. *J. Neurotrauma* **14**, 121–134.

Keane R. W., Kraydieh S., Lotocki G., Bethea J. R., Krajewski S., Reeds J. C. and Dietrich W. D. (2001) Apoptotic and anti-apoptotic mechanisms following spinal cord injury. *J. Neuropathol. Exp. Neurol.* **60**, 422–429.

Kikuchi H., Yamada T., Furuya H., Doh-ura K., Ohyagi Y., Iwaki T. and Kira J. (2003) Involvement of cathepsin B in the motor neuron degeneration of amyotrophic lateral sclerosis. *Acta Neuropathol. (Berl.)* **105**, 462–468.

Kingham P. J. and Pocock J. M. (2001) Microglial secreted cathepsin B induces neuronal apoptosis. *J. Neurochem.* **76**, 1475–1784.

Kohda Y., Yamashima T., Sakuda K., Yamashita J., Ueno T., Kominami E. and Yoshioka T. (1996) Dynamic changes of cathepsins B and L expression in monkey hippocampus after transient ischemia. *Biochem. Biophys. Res. Commun.* **228**, 616–622.

Larner S. F., Hayes R. L., McKinsey D. M., Pike B. R. and Wang K. K. W. (2003) Increased expression and processing of caspase-12 after traumatic brain injury in rats. *J. Neurochem.* in press.

Leist M. and Jaattela M. (2001) Triggering of apoptosis by cathepsins. *Cell Death Differ.* **8**, 324–326.

Li Z., Hogan E. L. and Banik N. L. (1996) Role of calpain in spinal cord injury: increased calpain immunoreactivity in rat spinal cord after impact trauma. *Neurochem. Res.* **21**, 441–448.

Liu X. Z., Xu X. M., Du Hu R. C., Zhang S. X., McDonald J. W., Dong H. X., Wu Y. J., Fan G. S., Jacquin M. F., Hsu C. Y. *et al.* (1997) Neuronal and glial apoptosis after traumatic spinal cord injury. *J. Neurosci.* **17**, 5395–5406.

Lu J., Ashwell K. W. and Waite P. (2000) Advances in secondary spinal cord injury: role of apoptosis. *Spine* **25**, 1859–1866.

Mackay E. A., Ehrhard A., Moniatte M., Guenet C., Tardif C., Tarnus C., Sorokine O., Heintzelmann B., Nay C., Remy J. M. *et al.* (1997) A possible role for cathepsins D, E, and B in the processing of beta-amyloid precursor protein in Alzheimer's disease. *Eur. J. Biochem.* 244, 414–425.

Mackey M. E., Wu Y., Hu R., DeMaro J. A., Jacquin M. F., Kanello-poulos G. K., Hsu C. Y. and Kouchoukos N. T. (1997) Cell death suggestive of apoptosis after spinal cord ischemia in rabbits. *Stroke* 28, 2012–2017.

Matsushita K., Wu Y., Qiu J., Lang-Lzdunski L., Hirt L., Waeber C., Hyman B. T., Yuan J. and Moskowitz M. A. (2000) Fas receptor and neuronal cell death after ischemia. *J. Neurosci.* 20, 6879–6887.

Mautes A. E., Weinzierl M. R., Donovan F. and Noble L. J. (2000) Vascular events after spinal cord injury: contribution to secondary pathogenesis. *Phys. Ther.* 80, 673–687.

McGrath M. E. (1999) The lysosomal cysteine proteases. *Annu. Rev. Biophys. Biomol. Struct.* 28, 181–204.

Mort J. S. and Buttle D. J. (1997) Cathepsin B. *Int. J. Biochem. Cell Biol.* 29, 715–720.

Mouw G., Zechel J. L., Zhou Y., Lust W. D., Selman W. R. and Ratcheson R. A. (2002) Caspase-9 inhibition after focal cerebral ischemia improves outcome following reversible focal ischemia. *Metab. Brain Dis.* 17, 143–151.

Namura S., Zhu J., Fink K., Endres M., Srinivasan A., Tomaselli K. J., Yuan J. and Moskowitz M. A. (1998) Activation and cleavage of caspase-3 in apoptosis induced by experimental cerebral ischemia. *J. Neurosci.* 18, 3659–3668.

Ni B., Wu X., Su Y., Stephenson D., Smalstig E. B., Clemens J. and Paul S. M. (1998) Transient global forebrain ischemia induces pro-longed expression of caspase-3 mRNA in rat hippocampal CA1 pyramidal neurons. *J. Cereb. Blow Flow Metab.* 18, 248–256.

Nixon P. A. and Cataldo A. M. (1993) The lysosomal system in neuronal cell death: a review. *Ann. NY Acad. Sci.* 679, 87–109.

Posmantur R. M., Zhao X., Kampfl A., Clifton G. L. and Hayes R. L. (1998) Immunoblot analyses of the relative contributions of cys-teine and aspartic proteases to neurofilament breakdown products following experimental brain injury in rats. *Neurochem. Res.* 23, 1265–1276.

Qian F., Frankfater A., Chan S. J. and Steiner D. F. (1991) The structure of the mouse cathepsin B gene and its putative promoter. *DNA Cell Biol.* 10, 159–168.

Rami A. and Krieglstein J. (1993) Protective effects of calpain inhibitors against neuronal damage caused by cytotoxic hypoxia in vitro and ischemia in vivo. *Brain Res.* 609, 67–70.

Ray S. K., Matzelle D. D., Wilford G. G., Hogan E. L. and Banik N. L. (2000) Increased calpain expression is associated with apoptosis in rat spinal cord injury: calpain inhibitor provides neuroprotection. *Neurochem. Res.* 25, 1191–1198.

Ray S. K., Shields D. C., Saido T. C., Matzelle D. C., Wilford G. G., Hogan E. L. and Banik N. L. (1999) Calpain activity and translational expression increased in spinal cord injury. *Brain Res.* 816, 375–380.

Rempel S. A., Rosenblum M. L., Mikkelsen T., Yan P. S., Ellis K. D., Golembieski W. A., Sameni M., Rozhin J., Ziegler G. and Sloane B. F. (1994) Cathepsin B expression and localization in glioma progression and invasion. *Cancer Res.* 54, 6027–6031.

Roberts L. R., Kurosawa H., Bronk S. F., Fesmier P. J., Agellon L. B., Leung W. Y., Mao F. and Gores G. J. (1997) Cathepsin B contri-butes to bile salt-induced apoptosis of rat hepatocytes. *Gastroen-terology* 113, 1714–1726.

Robertson G. S., Crocker S. J., Nicholson D. W. and Schulz J. B. (2000) Neuroprotection by inhibition of apoptosis. *Brain Pathol.* 10, 283–292.

Saatman K. E., Murai H., Bartus R. T., Smith D. H., Hayward N. J., Perri B. R. and McIntosh T. K. (1996) Calpain inhibitor AK295 attenuates motor and cognitive deficits following experimental brain injury in the rat. *Proc. Natl Acad. Sci. USA* 93, 3428–3433.

Sakurai M., Hayashi T., Abe K., Sadahiro M. and Tabayashi K. (1998) Delayed selective motor neuron death after transient spinal cord ischemia: a role of apoptosis? *J. Thorac. Cardiovasc. Surg.* 115, 1310–1315.

San Segundo B., Chan S. J. and Steiner D. F. (1986) Differences in cathepsin B mRNA levels in rat tissues suggest specialized func-tions. *FEBS Lett.* 201, 251–256.

Schotte P., Van Criekinge W., Van de Craen M., Van Loo G., Desmedt M., Grooten J., Cornelissen M., De Ridder L., Vandekerckhove J., Fiers W. *et al.* (1998) Cathepsin B-mediated activation of the proinflammatory caspase-11. *Biochem. Biophys. Res. Commun.* 251, 379–387.

Schumacher P. A., Eubanks J. H. and Fehlings M. G. (1999) Increased calpain I-mediated proteolysis, and preferential loss of dephos-phorylated NF200, following traumatic spinal cord injury. *Neuro-science* 91, 733–744.

Seyfried D., Han Y., Zheng Z., Day N., Moin K., Rempel S., Sloane B. and Chopp M. (1997) Cathepsin B and middle cerebral artery occlusion in the rat. *J. Neurosurg.* 87, 716–723.

Shields D. C., Schaecher K. E., Hogan E. L. and Banik N. L. (2000) Calpain activity and expression increased in activated glial and inflammatory cells in penumbra of spinal cord injury lesion. *J. Neurosci. Res.* 61, 146–150.

Shibata M., Kanamori S., Isahara K., Ohsawa Y., Konishi A., Kametaka S., Watanabe T., Ebisu S., Ishido K., Kominami E. and Uchiyama Y. (1998) Participation of cathepsins B and D in apoptosis of PC12 cells following serum deprivation. *Biochem. Biophys. Res. Com-mun.* 251, 199–203.

Stroh C. and Schulze-Osthoff K. (1998) Death by a thousand cuts: an ever increasing list of caspase substrates. *Cell Death Differ.* 5, 997–1000.

Tsuchiya K., Kohda Y., Yoshida M., Zhao L., Ueno T., Yamashita J., Yoshioka T., Kominami E. and Yamashima T. (1999) Postictal blockade of ischemic hippocampal neuronal death in primates using selective cathepsin inhibitors. *Exp. Neurol.* 155, 187–194.

Turk B., Turk D. and Turk V. (2000) Lysosomal cysteine proteases: more than scavengers. *Biochim. Biophys. Acta.* 1477, 98–111.

Vancompernolle K., Van Herreweghe F., Pynaert G., Van de Craen M., De Vos K., Totty N., Sterling A., Fiers W., Vandenabeele P. and Grooten J. (1998) Atractyloside-induced release of cathepsin B, a protease with caspase-processing activity. *FEBS Lett.* 438, 150–158.

Velardo M. J., Reier P. J. and Anderson D. K. (1999) Spinal Cord Injury, in *Neurosurgery: Principles of Basic and Clinical Science* (Hoff, J., Crockard, A., Hayward, R., eds), pp. 499–515. Blackwell Sci-ence Publications, Oxford.

Yamashima T. (1999) Postictal blockade of ischemic hippocampal neuronal death in primates using selective cathepsin inhibitors. *Exp. Neurol.* 155, 187–194.

Yamashima T., Kohda Y., Tsuchiyak K., Ueno T., Yamashita J., Yoshioka T. and Kominami E. (1998) Inhibition of ischaemic hippocamal neuronad death in primates with cathepsin B inhibitor CA-074: a novel strategy for neuroprotection based on 'calpain-cathepsin hypothesis.' *Eur. J. Neuro Sci.* 10, 1723–1733.

Yamashima T., Saido T. C., Takita M., Miyazawa A., Yamano J., Miyakawa A., Nishijyo H., Yamashita J., Kawashima S., Ono T. *et al.* (1996) Transient brain ischaemia provokes Ca^{+2}, PIP_2 and calpain responses prior to delayed neuronal death in monkeys. *Eur. J. Neurosci.* 9, 1932–1944.

Yan S., Berquin I. M., Troen B. R. and Sloane B. F. (2000) Transcription of human cathepsin B is mediated by Sp1 and Ets family factors in glioma. *DNA Cell Biol.* 19, 79–91.

Diffusion Magnetic Resonance Imaging Study of a Rat Hippocampal Slice Model for Acute Brain Injury

*Timothy M. Shepherd, *Peter E. Thelwall, *†Stephen J. Blackband, *Brian R. Pike,
§Ronald L. Hayes, and *Edward D. Wirth, III

*Department of Neuroscience, Evelyn F. & William McKnight Brain Institute, University of Florida, Gainesville, Florida,
U.S.A.; †National High Magnetic Field Laboratory, Tallahassee, Florida, U.S.A.; and §Center for Traumatic Brain Injury
Studies, Department of Neuroscience, Evelyn F. & William McKnight Brain Institute, University of Florida,
Gainesville, Florida, U.S.A.

Summary: Diffusion magnetic resonance imaging (MRI) provides a surrogate marker of acute brain pathology, yet few studies have resolved the evolution of water diffusion changes during the first 8 hours after acute injury, a critical period for therapeutic intervention. To characterize this early period, this study used a 17.6-T wide-bore magnet to measure multicomponent water diffusion at high b-values (7 to 8,080 s/mm^2) for rat hippocampal slices at baseline and serially for 8 hours after treatment with the calcium ionophore A23187. The mean fast diffusing water fraction (F_{fast}) progressively decreased for slices treated with 10-μmol/L A23187 (−20.9 ± 6.3% at 8 hours). Slices treated with 50-μmol/L A23187 had significantly reduced F_{fast} 80 minutes earlier than slices treated with 10-μmol/L A23187 ($P < 0.05$), but otherwise, the two doses had equivalent effects on the diffusion properties of tissue water. Correlative histologic analysis showed dose-related selective vulnerability of hippocampal pyramidal neurons (CA1 > CA3) to pathologic swelling induced by A23187, confirming that particular intravoxel cell populations may contribute disproportionately to water diffusion changes observed by MRI after acute brain injury. These data suggest diffusion-weighted images at high b-values and the diffusion parameter F_{fast} may be highly sensitive correlates of cell swelling in nervous issue after acute injury. **Key Words:** Calcium—Neurotoxicity—Cell death—A23187—Multicomponent diffusion.

Many neuroprotective strategies have proven successful for treating animal models of ischemic stroke and traumatic brain injury, yet have failed to improve clinical outcome in human patients during clinical trials (Faden, 2001). The frequent disappointments in these studies have often been attributed, in part, to defects in clinical trial design wherein studies fail to rapidly assess and stratify potential subjects based on the severity, location, and complexity of their acute brain injuries (Faden,

2001). Appropriate subject selection is particularly important because brain injury patients represent a far more heterogeneous population compared to their corresponding animal models of disease (Statler et al., 2001). To address this problem, it has recently proven beneficial to incorporate diffusion-weighted magnetic resonance imaging (MRI) into clinical trials (Warach, 2001) because of its sensitivity to changes in nervous-tissue water diffusion that occur immediately after injury (Moseley et al., 1990). Diffusion-weighted MRI of stroke patients, for example, aids recognition of the "perfusion-diffusion mismatch," which identifies penumbral volumes of nervous tissue that may be rescued from subsequent injury by prompt infusion of tissue plasminogen activator (Warach, 2002).

An improved understanding of water diffusion in nervous tissue and the acute water-diffusion changes that follow injury may further increase the sensitivity and specificity of diffusion-weighted MRI as a surrogate marker of acute brain injury. Unfortunately, previous clinical diffusion MRI studies have provided limited data from the first 24 hours after ischemic or traumatic brain

injury (for example, Beaulieu et al., 1999). Although this information has proven useful for understanding the chronic progression of diffusion changes after brain injury, it is well beyond the optimal therapeutic windows when experimental interventions are most likely to succeed (Marler et al., 2000). Thus, studies that better resolve the acute temporal progression of diffusion changes after brain injury are needed to provide improved patient stratification based on injury severity and to monitor the effects of therapeutic interventions early after brain injury.

Unlike previous clinical studies of acute brain injury, recent studies have demonstrated that diffusion-weighted signal attenuation is nonmonoexponential in rat (Niendorf et al., 1996) and human brains (Mulkern et al., 1999) when measured with very strong diffusion-sensitizing gradients (high b-values). As a first approximation, a biexponential function may be used to describe water diffusion in nervous tissue by separating the MRI signal into contributions from fast and slow diffusing components. Shifts between these two components may correlate with changes in the relative size of the intracellular compartment (Niendorf et al., 1996; Thelwall et al., 2002). Although the biexponential model is an incomplete description of tissue water diffusion, it is more appropriate than the monoexponential fits currently employed clinically.

Continuous acquisition of water diffusion data for multicomponent analysis throughout the first 8 hours after an acute brain injury would prove extremely difficult in human or animal subjects because of their limited tolerance for long imaging times, and because high b-value diffusion weighting is difficult to obtain on relatively large subjects owing to current hardware limitations. Thus, to further investigate the value of diffusion MRI as a surrogate marker of acute brain injury, we measured water diffusion in perfused rat hippocampal slices using a 17.6-T magnet with strong diffusion-sensitizing gradients (1,000 mT/m). Unlike human and animal subjects, rat hippocampal slices tolerate long periods of investigation yet maintain the heterogeneous neuronal and glial cell populations (Aitken et al., 1995) that determine in vivo MRI contrast. Furthermore, studies of hippocampal slices are not confounded by anesthesia or movement and perfusion artifacts (Aitken et al., 1995). Previous studies have used diffusion-weighted MRI of rat hippocampal slices (Blackband et al., 1997) and have shown that slices perturbed by ouabain and N-methyl-D-aspartate respond similarly (Buckley et al., 1999; Bui et al., 1999) to the same perturbations of in vivo rat brain (Benveniste et al., 1992). Also, human brain slices have water diffusion properties comparable to those reported for human patients and rat brain slices, improving the confidence that the rat hippocampal

slices are a valid model of human brain tissue (Shepherd et al., 2003).

In the present study, water diffusion was monitored in rat hippocampal slices before and after treatment with different doses of the neurotoxin A23187. This carboxylic acid calcium ionophore rapidly diminishes calcium gradients across cell membranes (Pressman, 1976) as is known to occur in vivo after ischemic or traumatic injury (Choi 1988). Previous studies have shown that neuronal cultures treated with high doses of calcium ionophores, such as A23187, experienced rapid loss of calcium homeostasis and pathologic cell swelling (Chan et al., 1998; Gwag et al., 1999; Takadera and Ohyashiki, 1997). We hypothesized that this cellular response would be detectable in rat hippocampal slices using diffusion-weighted MRI and correlative histology. Unlike previous diffusion studies of nervous tissue injury, using A23187 allows this study to uniquely evaluate water-diffusion changes after calcium overload (Petersen et al., 2000), a downstream integrating event in many forms of acute brain injury (e.g., ischemic stroke or traumatic brain injury) (Choi, 1988; McIntosh et al., 1998). Results of this investigation indicated that the biexponential diffusion parameter F_{fast} and diffusion-weighted MRI at high b-values provide rapid and sensitive measures of A23187-induced tissue injury that are correlated with neuronal cell swelling and overt histopathology in selectively vulnerable regions of the rat hippocampal slice.

MATERIALS AND METHODS

Brain slice procurement

The University of Florida Institutional Animal Care and Use Committee approved the use of laboratory animals for this study. Rat hippocampal slice procurement has been described previously (Aitken et al., 1995). Briefly, male Long-Evans rats (250 to 350 g) were anesthetized with isoflurane and decapitated. The brain was removed and placed into ice-cold artificial cerebrospinal fluid (aCSF) (120-mmol/L NaCl, 3-mmol/L KCl, 10-mmol/L glucose, 26-mmol/L NaHCO₃, 2-mmol/L CaCl₂, 1.5-mmol/L KH₂PO₄, and 1.4-mmol/L MgSO₄) gassed with 95% O₂ and 5% CO₂ to maintain a pH of 7.4. The aCSF osmolality was 300 ± 1 mOsm/kg as determined by Osmette A freezing point depression osmometer (Precision System, Natick, MA,, U.S.A.). Both hippocampi were dissected and cut orthogonal to the septohippocampal axis into 500-μm-thick sections with a McIlwain tissue chopper within 10 minutes of decapitation. Hippocampal slices remained immersed in ice-cold aCSF for 1 hour after decapitation to minimize procurement-induced ischemic damage (Newman et al., 1992). Slices then were warmed gradually to room temperature (20°C) for the MRI experiment and placed into a multislice perfusion chamber (Shepherd et al., 2002).

Slices were perfused continuously with aCSF (2 mL/min) while the perfusion chamber was lowered into the magnet and during pilot image acquisition. Although perfusion was discontinued during all diffusion measurements (described below), calculations based on the published metabolic rates of nervous tissue (Magistretti, 1999) indicate that the typical 6-mg hippocampal slice consumes less than 0.2% of the glucose available

in the perfusion chamber (containing 3.0 mL aCSF) during a 35-minute MRI acquisition. Further, it has been shown previously that intermittent cessation of aCSF flow does not affect slice viability for at least 8 hours after slice procurement (Shepherd et al., 2002).

Diffusion MRI of rat hippocampal slices

All MRI data were obtained at room temperature using a 15-mm birdcage coil interfaced to a Bruker 17.6-T vertical wide-bore magnet and console. Pilot multislice axial, sagittal, and coronal T_1 and diffusion-weighted imaging sequences were used to locate the perfusion chamber, then to optimize the positions of axial magnetic resonance-defined slices through the center of the 500-μm-thick rat hippocampal slices. Diffusion-weighted images were acquired using a pulsed gradient spin-echo multislice sequence with a diffusion time of 14 milliseconds and an echo time of 30 milliseconds. This diffusion measurement consisted of a series of 8 diffusion-weighted images (128 × 64 matrix, 1.5-cm field of view, 2-second repetition, 30-millisecond echo time, 2 averages, δ = 3 milliseconds, Δ = 15 milliseconds) using diffusion gradients aligned perpendicular to the plane of the MRI images in linear strength increments from 0 to 940 mT/m. This resulted in 8 diffusion-weighted images with b-values between 7 and 8080 s/mm^2 (including imaging terms). Image slice thickness was 300 μm with 117 × 234-μm in-plane resolution and the protocol required 34 minutes for completion. Additional pilot images were acquired between diffusion measurements to monitor for slice movement due to aCSF perfusion; data from hippocampal slices that moved during the experiment were rejected (n = 1).

Slice perturbation with A23187

Before slice procurement, rat hippocampal slices were randomly assigned to treatment by control aCSF, or aCSF containing 10–μmol/L A23187 or 50–μmol/L A23187. Hippocampal slices were exposed to higher doses of A23187 than previous studies in neuronal cultures (Mattson et al., 1991; Petersen et al., 2000) because the slice model was composed of high-density, heterogeneous cell populations studied at lower temperatures. Dimethyl sulfoxide (DMSO) was required to solubilize A23187 in aCSF, so control aCSF contained 0.1% DMSO. The additions of 0.1% DMSO with or without A23187 did not affect the pH or osmolality of the aCSF solution. Previous studies in our laboratories suggest that 0.1% DMSO does not affect calcium movement in slices as indicated by the absence of calcium-mediated calpain activation (Zhao et al., 1999). Each of the aCSF treatment solutions were gassed with 95% O_2 and 5% CO_2 throughout the experiment. All slices were perfused with standard aCSF during pilot scans and before initial baseline diffusion measurements were acquired. Slices then were perfused with the assigned treatment aCSF for 20 minutes, then perfusion was stopped and a post-treatment diffusion protocol obtained. Preliminary studies demonstrated that an initial perfusion duration of 20 minutes with treatment aCSF was sufficient for perfusate exchange. A cycle consisting of 6 minutes of perfusion with the assigned treatment aCSF followed by an additional diffusion measurement (34 minutes) was repeated serially until 12 hours after initial brain slice procurement (each complete cycle required 40 minutes).

The initial treatment period for slices occurred at slightly different times after brain slice procurement because of variations in the time required for hippocampal slice placement and pilot MRI scans (mean time delay from procurement to baseline diffusion measurement was 3.1 ± 0.4 hours). Therefore diffusion data from rat brain slices required assignment to time-bins for statistical comparisons. The baseline diffusion mea-

surement for each slice was assigned to 0 minutes and subsequent data were assigned to time points increasing in 40-minute increments. Although data were reassigned to time points relative to the initial MRI measurement, diffusion data acquired more than 12 hours after slice procurement were excluded from the analysis.

Analysis of diffusion data

To analyze changes in the diffusion-weighted signal intensity in rat hippocampal slices after treatment with the various aCSF solutions, a region of interest (ROI) was drawn on the images to enclose the entire hippocampal slice. Previous studies demonstrated that diffusion-weighted water signal attenuation in rat hippocampal slices is nonmonoexponential at high b-values (Buckley et al., 1999). A biexponential equation (Eq. 1) was fitted to the diffusion-weighted signal attenuation in the rat hippocampal slice ROIs using the Levenberg-Marquandt nonlinear least-squares fitting routine:

$$S(b) = S_0 \cdot [F_{fast} \cdot \exp(-bD_{fast}) + (1 - F_{fast}) \cdot \exp(-bD_{slow})]$$

where S_0 is signal intensity without diffusion weighting, F_{fast} is the fraction of water with fast apparent diffusion coefficient (ADC), and D_{fast} and D_{slow} represent the ADCs of the fast and slow diffusing water components, respectively. Observed changes over time from baseline in the biexponential parameters of the three treatment groups (control, 10-μmol/L A23187, and 50-μmol/L A23187) were compared statistically using a two-way repeated-measures analysis of variance (ANOVA) with one factor repeated (Sigma Stat 2.03). If the ANOVA test detected a statistically significant difference among treatment groups at a particular time point, a Tukey multiple comparisons test was used to isolate treatments that differed significantly from one another. Statistical significance for all tests was defined as $P < 0.05$.

Histology of rat hippocampal slices

Because it proved difficult to consistently recover rat hippocampal slices used in the diffusion MRI experiments for subsequent study, three additional rats were required to provide slices for histologic correlation. These slices experienced the same experimental procedure as slices used in the diffusion MRI measurements and at 12 hours after procurement, the slices were gently removed from the perfusion chambers and immersion-fixed with 4% paraformaldehyde in phosphate-buffered saline. Some slices were fixed either immediately after procurement or before perfusion with treatment aCSF (4 hours after procurement) to serve as additional controls. In addition, a few slices that were recovered after the MRI experiments were fixed for histologic analyses to assess whether differences existed for slices treated in the magnet versus slices treated in the correlative protocol.

The fixed slices were embedded in paraffin wax, cut into 8-μm-thick sections, mounted onto slides and stained with hematoxylin and eosin (H&E). Most slices were sectioned parallel to the plane of the slice (orthogonal to the septotemporal axis of the rat hippocampus), but in some slices, sections were cut perpendicular to the plane of the tissue (cross section). These sections were used to determine whether cells at different depths from the tissue surface were affected differently by the various aCSF treatment solutions. Superficial and central planar sections, stained with H&E, also were compared to assess the potential variable effects of tissue depth on tissue response to A23187 treatment.

In all H&E-stained sections, morphologic characteristics of granule and pyramidal neurons from the dentate gyrus, CA1,

CA2, and CA3 fields were noted. Nuclear changes such as pyknotic and eosinophilic nuclei, karyorrhexis, or karyolysis were noted. The cytoplasm of cells was observed for evidence of eosinophilia, microvacuolation, and loss of structure or fragmentation. The surrounding neuropil, in such regions as the stratum radiatum, were also inspected for vacuolization and other pathologic changes. These features were compared between the slices treated with control, 10-μmol/L A23187, or 50-μmol/L A23187 aCSF solutions for differences in injury-induced cellular morphology and pathology.

RESULTS

Diffusion-weighted MRI of rat hippocampal slices

Twenty-nine of the 35 rat hippocampal slices procured from 17 rats were included for the diffusion MRI aspects of this investigation. The other six slices were rejected because of perfusion chamber flooding (n = 3), susceptibility artifacts due to air bubbles in the perfusion chamber (n = 2), and slice movement (n = 1). In comparing the three treatment groups, there were no significant differences for the post-procurement time when the first baseline diffusion measurements were obtained (ANOVA, P = 0.265) or for the time when slices were subsequently treated (ANOVA, P = 0.393). Mean time to treatment for all slices (3.8 ± 0.5 hours) closely matched the time when correlative rat hippocampal slices were treated outside the magnet for histology studies (4 hours). Diffusion measurements were obtained on all 29 slices up to 6 hours after treatment, on 28 of 29 slices up to 7.3 hours after treatment, and on 20 of 29 slices 8 hours after treatment.

Preliminary high-resolution diffusion-weighted images were obtained of rat hippocampal slices to determine achievable signal-to-noise ratio (SNR) and spatial resolution per unit time. Such images (Fig. 1) exhibited the detailed laminar anatomy of the hippocampus, but required long acquisition times (4.5 hours per *b*-value measurement) without sufficient perfusion to maintain slice viability (Shepherd et al., 2002). For this study, such high spatial resolution was sacrificed for better temporal resolution of the water-diffusion changes that accompany slice perturbation with A23187 (4.2 minutes per *b*-value measurement). In Fig. 2, the lower-resolution images show the signal intensity changes that occur after treatment with 10-μmol/L A23187. Plotting the signal intensity of the hippocampal slice ROI versus *b*-value gave nonmonoexponential diffusion-weighted signal attenuation curves. Figure 3 shows that treatment with 10-μmol/L A23187 caused a progressive decrease in the rate of diffusion-weighted signal attenuation over the 8 hours. This change was most evident at *b*-values above 4000 s/mm² (see box B). Similar results to those shown in Figs. 2 and 3 were also observed for slices treated with 50-μmol/L A23187.
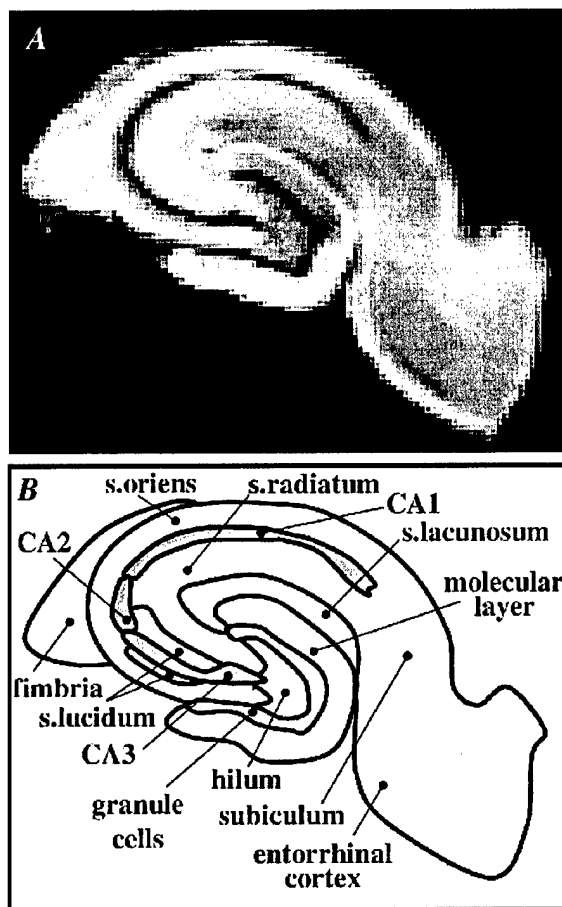
FIG. 1. A diffusion-weighted magnetic resonance image with 59-μm in-plane resolution (**A**) reveals the detailed lamellar anatomy of a 500-μm-thick rat hippocampal slice cut perpendicular to the septotemporal axis (MRI scan parameters: repetition time/echo time = 2,000/34 milliseconds, *b* = 3,630 s/mm², matrix = 256 × 256, field of view = 15 × 15 mm, slice thickness = 300 μm, averages = 32, time = 4.5 hours). As illustrated in panel **B**, many anatomical regions of the hippocampus and dentate gyrus can be distinguished in this sample based on differences in diffusion-weighted signal intensity (s, stratum).

Biexponential analysis of diffusion in hippocampal slices treated with A23187

The diffusion-weighted signal attenuation curves of rat hippocampal slices (Fig. 3) were well described by the biexponential function (Eq. 1) (R^2 > 0.99). The biexponential-derived diffusion parameters for all 29 rat hippocampal slices before treatment (mean ± SD) were 0.601 ± 0.057 for F_{fast}, 1.14 ± 0.14 × 10⁻³ mm²/s for D_{fast} and 0.067 ± 0.010 × 10⁻³ mm²/s for D_{slow}. These values were comparable to previous reports of water diffusion in rat hippocampal slices (Buckley et al., 1999; Bui et al., 1999; Shepherd et al., 2002) and were qualitatively similar to biexponential diffusion parameters reported for *in vivo* human brain (Mulkern et al., 1999). There were small yet statistically significant differences in the baseline biexponential parameters F_{fast} and D_{slow} for slices
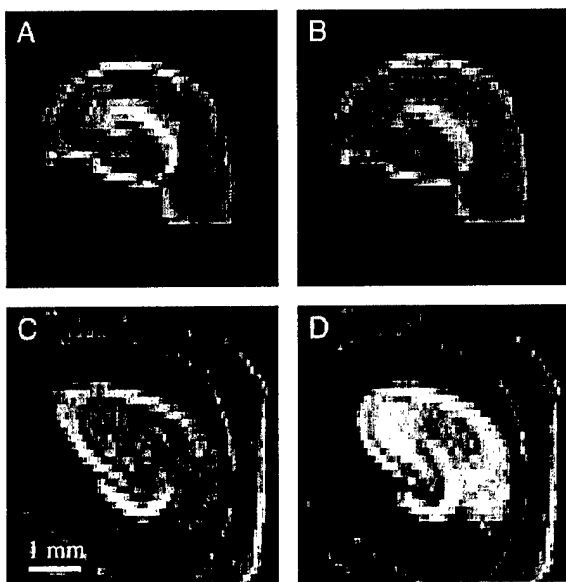
FIG. 2. Typical diffusion-weighted images (b = 7,977 s/mm^2) of rat hippocampal slices. Panels **A** and **B** show a control rat hippocampal slice before and after 8 hours of treatment with 0.1% DMSO vehicle, respectively. Panels **C** and **D** show a different slice before and 8 hours after treatment with 10-μmol/L A23187, respectively (the latex spacer of the perfusion chamber is visible in these two images). At this b-value, signal intensity in the A23187-treated slice increased 42% whereas the vehicle-treated slice signal intensity increased 6% over 8 hours.

assigned to the three different aCSF treatment groups (Table 1). Possible explanations for these differences are addressed in the Discussion.

The biexponential water diffusion parameters for control slices before and immediately after treatment with aCSF containing 0.1% DMSO were not statistically dif-

ferent (ANOVA, $P > 0.05$). The mean F_{fast} of DMSO-treated slices decreased stepwise by approximately 5% only 9 hours after procurement. This change, although not statistically significant, represented a trend present in the data from most individual slices. For the three treatment groups, there were statistically significant interactions between time and treatment in the change from baseline for the diffusion parameter F_{fast} (ANOVA, $P < 0.001$), but not for D_{fast} ($P = 0.945$) or D_{slow} ($P = 0.870$). Figure 4 depicts the mean percentage change from baseline in the biexponential parameters F_{fast} for slices treated with aCSF containing 0.1% DMSO, 10–μmol/L A23187, and 50-μmol/L A23187. Compared to vehicle-treated slices, the percentage change in the fraction of fast diffusing water (F_{fast}) for slices treated with 50-μmol/L A23187 was significantly different for all time points after baseline (Tukey, $P < 0.05$). Changes from baseline for slices treated with 10-μmol/L A23187 were significantly different than vehicle-treated slices for all time points after 80 minutes (Tukey, $P < 0.05$). Although the dose of A23187 (10 or 50 μmol/L) predicted when the F_{fast} diffusion parameter of A23187-treated slices would first differ statistically from vehicle-treated slices, at no time point were data from the 10-μmol/L or 50-μmol/L A23187-treated slices statistically distinct from each other.

Histology of A23187-induced pathologic cell swelling

Correlative H&E histology of the rat hippocampal slices exhibited clear dose-related differences in particular hippocampal regions (Fig. 5). In rat hippocampal slices treated with A23187, susceptible neurons typically manifested pathologic change by intense microvacuolation of the neuronal perikaryon and stranded, slightly

FIG. 3. Typical semilog plot showing temporal changes in the diffusion-weighted signal attenuation curves for a rat hippocampal slice treated with 10-μmol/L A23187. Each point represents the log signal intensity for the slice ROI in a diffusion-weighted image normalized to the signal intensity of the first image (b = 7 s/mm^2). Although diffusion data were collected every 40 minutes, only alternating data from baseline (0 minutes), 80, 160, 240, 320, and 400 minutes are shown for clarity. Comparison of boxes labeled A and B illustrates that the signal intensity changes after A23187 treatment are better resolved at higher b-values given sufficient signal-to-noise. The arrow indicates approximately where data from Fig. 2 (b = 7,977 s/mm^2) would be plotted in the signal-attenuation curve.
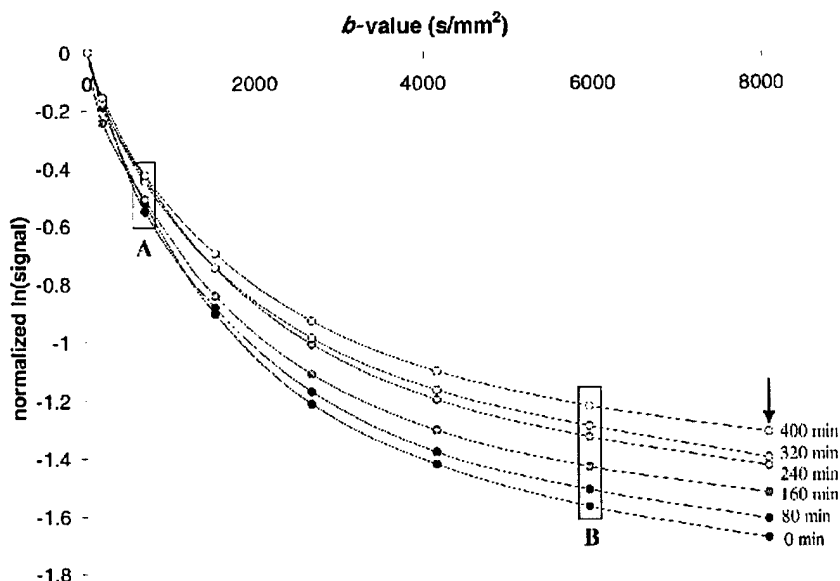
TABLE 1. *Baseline diffusion characteristics for rat hippocampal slices in each of the three treatment groups*

Group	0.1% DMSO	10-μmol/L A23187	50-μmol/L A23187	P (ANOVA)	Total/mean
F_{fast}	0.560 ± 0.040*	0.617 ± 0.070	0.623 ± 0.037*	0.025	0.601 ± 0.057
D_{fast} (× 10^{-3} mm^2/s)	1.08 ± 0.11	1.19 ± 0.17	1.16 ± 0.12	0.216	1.14 ± 0.14
D_{slow} (× 10^{-3} mm^2/s)	0.060 ± 0.006*	0.071 ± 0.012*	0.067 ± 0.008	0.045	0.067 ± 0.010

Data are mean ± SD.
* Groups that were statistically different from one another as determined post-ANOVA by a Tukey multiple comparisons test ($P < 0.05$).
DMSO, dimethyl sulfoxide, ANOVA, analysis of variance, F_{fast}, fast diffusing water fraction, D_{fast}, fast apparent diffusion coefficient, D_{slow}, slow apparent diffusion coefficient.

pyknotic nuclei. These features are typical oncotic changes that frequently lead to the appearance of necrotic cells at later time points than observable for this study (Majno and Joris, 1995). The described cellular changes were most prominent in aspects of the CA1 cell band (CA1a), but also present in the ends of the CA3 cell band (CA3a and CA3c) and the granule cell layer in the internal blade of the dentate gyrus. The changes were more severe in slices treated with aCSF containing 50-μmol/L A23187 than slices treated with 10-μmol/L A23187. Other regions of the hippocampus, such as CA2, appeared relatively unaffected by A23187, although the neuropil surrounding the affected pyramidal and granule cells did exhibit some staining pallor and vacuolation as well (Fig. 5).

Similar to previous studies (Newman et al., 1992), comparison of H&E-stained cross sections and planar sections from different depths in the hippocampal slices did not suggest different reactions to A23187-treatment based on tissue depth. Additional control slices taken shortly after slice procurement (at 30 minutes after rat decapitation) and before perfusion with aCSF treatment solutions (at 4 hours after procurement) did not show differences from hippocampal specimens obtained by intracardiac perfusion of normal rats with 4% paraformaldehyde except for some minor pathology of the internal

FIG. 4. Mean percentage change from baseline over time for the fraction of fast diffusing water in rat hippocampal slices treated with aCSF containing 0.1% DMSO vehicle (▲; n = 9), 10-μmol/L A23187 (□; n = 10) or 50-μmol/L A23187 (●; n = 10) (mean ± SEM). At early time points, slices treated with 50-μmol/L A23187 statistically differed from vehicle-treated slices (#) whereas at later time points slices treated with either 10-μmol/L or 50-μmol/L A23187 differed from vehicle-treated slices (*) (P < 0.05).

blade of the dentate gyrus (see Discussion). The histologic appearance of the few slices recovered from the diffusion MRI studies also did not differ from correlative slices with the same aCSF treatment assignment (data not shown).

DISCUSSION

Pyramidal neurons and granule cells in rat hippocampal slices treated with A23187 showed substantial cytoplasmic microvacuolation indicative of pathologic cell swelling. The neuropil apposed to such damaged neurons also appeared vacuolated. The neuronal pathology after A23187 treatment resembles early ischemic cell changes (Brierley et al., 1973) and electron microscopy studies have correlated such microvacuolation with mitochondrial swelling (Auer and Benveniste, 1997). Although pathologic oncotic swelling is clearly evident, it is difficult to determine whether some neurons ruptured during the experiment because cellular membranes rendered unstable by A23187 treatment might also rupture on fixation (Auer et al., 1985). These findings concur with previous descriptions of pathologic swelling in cultured neurons treated with the calcium ionophores ionomycin or A23187 (Takadera and Ohyashiki, 1997; Chan et al., 1998; Gwag et al., 1999) and are appropriate to the mechanisms of A23187 toxicity. A23187 initiates a rapid intracellular calcium overload in the neuropil that spreads to the neuronal perikaryon at higher doses (Gwag et al., 1999). This calcium overload then provokes mitochondrial permeability transition pore formation and pathologic cell swelling (Petersen et al., 2000).

Unlike previous neuronal cell culture studies (Chan et al., 1998; Petersen et al., 2000), A23187 treatment did not affect all neurons in the hippocampal slices equally. This anatomically selective pattern of pathology in slices after A23187 treatment reproduces the selective vulnerability of the CA1 and CA3 hippocampal regions to ischemic and traumatic injuries (Kotapka et al., 1994). Selective vulnerability of the hippocampus has been attributed to differences in *N*-methyl-D-aspartate receptor distributions (Monaghan and Cotman, 1985), yet A23187 initially bypasses neurotransmitter–receptor interactions by increasing calcium concentrations inside the cell. This
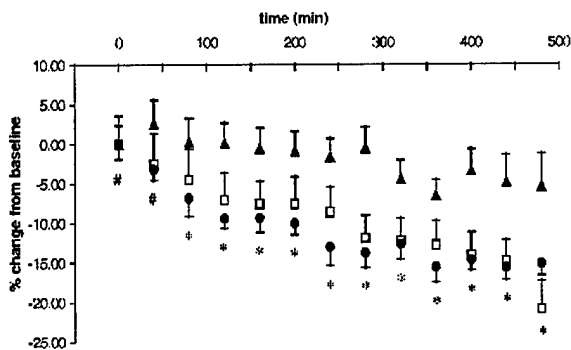
FIG. 5. Correlative histology of rat hippocampal slices 8 hours after treatment with DMSO vehicle (A–D), 10-µmol/L A23187 (E– H). and 50-µmol/L A23187 (I–L) A23187 had dose-related effects on the CA1 subfield, CA3 subfield, stratum radiatum, and internal blade of the dentate gyrus. Arrows illustrate cells ruptured from pathologic swelling and arrowheads denote artifact from paraffin wax embedding. Sections (8-µm thick) were stained with hematoxylin and eosin and are shown at 630x magnification with oil immersion.
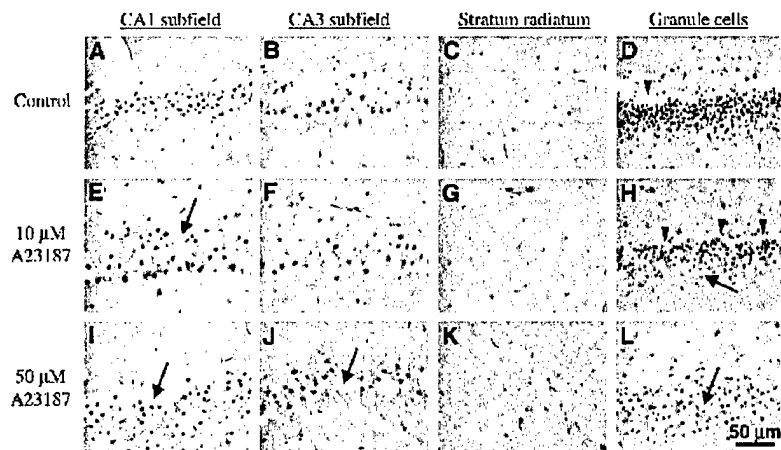
suggests there may be differences in intracellular calcium-dependent enzyme cascades that contribute to selective vulnerability in the rat hippocampal slice. Pathology in the granule cell layer differed from previous reports of perturbation-induced granule cell injury (Auer et al., 1985) and suggests metabolic injury occurring during procurement may increase the vulnerability of this particular hippocampal region to A23187 (Newman et al., 1992).

Vulnerable regions of the rat hippocampal slices also showed dose-related differences in the magnitude of pathological cell swelling induced by A23187 (see Fig. 5). These dose-related histopathologic differences were difficult to distinguish with the diffusion MRI measurements using the whole-slice ROI method because regions affected by A23187 in a dose-related fashion were volume-averaged with relatively unaffected regions. However, dose-related differences were noted after A23187 treatment when the F_{fast} of slices became statistically distinct from control slices. With either A23187 dose, the F_{fast} for slices was reduced 7% to 10% from baseline during the first 2 hours after treatment, but it then took an additional 6 hours of A23187 treatment to double this reduction.

The biophysical interpretation of F_{fast} reductions observed in rat hippocampal slices treated with A23187 is not trivial because the biexponential model of water diffusion in nervous tissue is too simplistic. Although the fast and slow diffusing components of water diffusion can not be directly attributed to the extracellular and intracellular compartments respectively, studies have shown that changes in the F_{fast} do correlate with perturbation-induced changes in the relative size of the intracellular compartment (Niendorf et al., 1996; Thelwall et al., 2002). There are several additional biophysical properties of nervous tissue that affect water diffusion and are unaccounted for by the biexponential model; for example, transmembrane water exchange rates, intracellu-

lar restriction, and extracellular tortuosity also influence the biexponential diffusion parameters obtained (including F_{fast}) (Thelwall et al., 2002). When neurons are pathologically injured by A23187 treatment, these additional biophysical features are also likely to be altered and influence the biexponential parameters obtained. Given sufficient time and SNR, future studies could use more complex analytical models, such as the one developed by Stanisz et al. (1998), to better describe the biophysical tissue properties of hippocampal slices altered by A23187-induced pathologic cell swelling.

Despite these limitations, the biexponential model does provide a more complete description of nervous-tissue water diffusion than the monoexponential ADC fits currently in clinical use, and it is reasonable to cautiously interpret changes in F_{fast} to correlate with changes in the relative size of the intracellular compartment. Previous clinical studies have shown decreased ADC in acute ischemic brain followed by an increase in ADC beyond normal values several days later (Beaulieu et al., 1999). These diffusion changes, noted in animal models of both ischemic and traumatic injury, may be due to cellular swelling followed by lysis (Assaf et al., 1997; Knight et al., 1994;). Because high doses of A23187 caused a similar yet accelerated pattern of cell swelling and lysis in neuronal cultures (Chan et al., 1998; Takadera and Ohyashiki, 1997), a biphasic pattern of F_{fast} changes was hypothesized to be observable for F_{fast} within the time span of this experiment on rat hippocampal slices treated with A23187. Thus, as cells swell, F_{fast} would decrease, but then as cells rupture, F_{fast} would be predicted to increase.

Because potential dose-related differences in F_{fast} were only observable during the first 80 minutes after A23187 treatment, the results of this study might suggest that there were a limited number of A23187-sensitive cell populations within the rat hippocampal slices. At high doses of A23187, these cells swell more quickly

Despite the neuroprotective effects of hypothermia, some histopathology was notable in control slices 12 hours after slice procurement (e.g., CA1 and the internal blade of the granule cell layer). Although not statistically significant, there also was a 5% decrease in mean F_{fast} for control slices at the conclusion of the experiment. Further, the conditions under which brain slice experiments occur (e.g., slice procurement and intermittent aCSF perfusion) might enhance A23187-induced tissue injury (Newman et al., 1992). These findings indicate that brain slices can not perfectly model healthy and pathologic *in vivo* nervous tissue, yet over the duration of the present experiment, changes to control slices were of limited magnitude compared to the histopathology and water diffusion changes due to pathologic swelling induced by A23187 treatment. Thus, hippocampal slices provided a workable tissue model for comparing water diffusion in injured and viable nervous tissue. Brain slices tolerate long imaging periods in very-high-field magnets that enable data collection not possible in current clinical scanners. Thus, brain slice methodology will remain highly relevant in the future to developing a better understanding of the biophysical basis for water diffusion changes after acute brain injury.

CONCLUSION

This study successfully used diffusion-weighted MRI of rat hippocampal slices to study the acute temporal evolution of multicomponent water-diffusion changes after A23187 treatment. Brain slices provided a stable and highly controllable nervous tissue model. Data obtained from this model of acute brain injury suggest that the biexponential diffusion parameter F_{fast} may be a sensitive correlate of cellular swelling in nervous tissue and that diffusion changes after acute brain injury may be intravoxel volume-averaged summations of responses from anatomically or temporally distinct healthy and pathologically injured cell populations. These results suggest that regional analysis of A23187-treated hippocampal slices may improve our understanding of the unique and heterogeneous morphologic processes that follow acute cellular injury and contribute to improved clinical measurements of diffusion in human stroke and traumatic brain injury patients. In addition, data from this study concur with findings of previous clinical studies that diffusion-weighted images at high *b*-values may offer improved characterization of normal and pathologic nervous tissue. Future perturbation studies of rat hippocampal slices may be capable of reconciling complex, data-intensive mathematical models of nervous-tissue water diffusion with diffusion MRI data obtained from human patients with acute brain injuries.

REFERENCES

Aitken PG, Breese GR, Dudek FF, Edwards F, Espanol MT, Larkman PM, Lipton P, Newman GC, Nowak TS Jr, Panizzon KL, Raley-susman KM, Reid KH, Rice ME, Sarvey JM, Schoepp DD, Segal M, Taylor CP, Teyler TJ, Voulalas PJ (1995) Preparative methods for brain slices: a discussion. *J Neurosci Methods* 59:139–149

Assaf Y, Beit-Yannai E, Shohami E, Berman E, Cohen Y (1997) Diffusion- and T2-weighted MRI of closed-head injury in rats: a time course study and correlation with histology. *Magn Reson Imaging* 15:77–85

Auer R, Kalimo H, Olsson Y, Wieloch T (1985) The dentate gyrus in hypoglycemia: pathology implicating excitotoxin- mediated neuronal necrosis. *Acta Neuro Pathol (Berl)* 67:279–288

Auer RN, Benveniste H (1997) Hypoxia and related conditions. In: *Greenfield's neuropathology, Vol. 1* (Graham DI, Lantos PL, eds), London: Oxford University Press, pp 315–396

Beaulieu C, de Crespigny A, Tong DC, Moseley ME, Albers GW, Marks MP (1999) Longitudinal magnetic resonance imaging study of perfusion and diffusion in stroke: evolution of lesion volume and correlation with clinical outcome. *Ann Neurol* 46:568–578

Benveniste H, Hedlund LW, Johnson GA (1992) Mechanism of detection of acute cerebral ischemia in rats by diffusion-weighted magnetic resonance microscopy. *Stroke* 23:746–754

Blackband SJ, Bui JD, Buckley DL, Zelles T, Plant HD, Inglis BA, Phillips MI (1997) MR microscopy of perfused brain slices. *Magn Reson Med* 38:1012–1015

Brierley JB, Meldrum BS, Brown AW (1973) The threshold and neuropathology of cerebral "anoxic-ischemic" cell change. *Arch Neurol* 29:367–374

Buckley DL, Bui JD, Phillips MI, Zelles T, Inglis BA, Plant HD, Blackband SJ (1999) The effect of ouabain on water diffusion in the rat hippocampal slice measured by high resolution NMR imaging. *Magn Reson Med* 41:137–142

Bui JD, Buckley DL, Phillips MI, Blackband SJ (1999) Nuclear magnetic resonance imaging measurements of water diffusion in the perfused hippocampal slice during N-methyl-D-aspartate-induced excitotoxicity. *J Neurosci* 93:487–490

Chan SO, Runko E, Anyane-Yeboa K, Ko L, Chiu FC (1998) Calcium ionophore-induced degradation of neurofilament and cell death in MSN neuroblastoma cells. *Neurochem Res* 23:393–400

Choi DW (1988) Calcium-mediated neurotoxicity: relationship to specific channel types and role in ischemic damage. *Trends Neurosci* 11:465–469

Faden AI (2001) Neuroprotection and traumatic brain injury: the search continues. *Arch Neurol* 58:1553–1555

Gwag BJ, Canzoniero LM, Sensi SL, Demaro JA, Koh JY, Goldberg MP, Jacquin M, Choi DW (1999) Calcium ionophores can induce either apoptosis or necrosis in cultured cortical neurons. *Neuroscience* 90:1339–1348

Harris, KR, Woolf, LA (1980) Pressure and temperature-dependence of the self-diffusion coefficient of water and O-18 water. *J Chem Soc Faraday Trans 1* 76:377–385

Knight RA, Dereski MO, Helpern JA, Ordidge RJ, Chopp M (1994) Magnetic resonance imaging assessment of evolving focal cerebral ischemia. Comparison with histopathology in rats. *Stroke* 25:1252–1261

Kotapka MJ, Graham DI, Adams JH, Gennarelli TA (1994) Hippocampal pathology in fatal human head injury without high intracranial pressure. *J Neurotrauma* 11:317–324

Magistretti P (1999) Brain energy metabolism. In: *Fundamental neuroscience* (Zigmond, Bloom, Landis, Roberts, Squire, eds), London: Academic Press, p 389

Majino G, Joris I (1995) Apoptosis, oncosis, and necrosis. An overview of cell death [see comments]. *Am J Pathol* 146:3–15

Marler JR, Tilley BC, Lu M, Brott TG, Lyden PC, Grotta JC, Broderick

JP, Levine SR, Frankel MP, Horowitz SH, Haley EC Jr, Lewandowski CA, Kwiatkowski TP (2000) Early stroke treatment associated with better outcome: the NINDS rt-PA stroke study. *Neurology* 55:1649–1655

Mattson MP, Rychlik B, Chu C, Christakos S (1991) Evidence for calcium-reducing and excito-protective roles for the calcium-binding protein calbindin-D28k in cultured hippocampal neurons. *Neuron* 6:41–51

McIntosh TK, Saatman KE, Raghupathi R, Graham DI, Smith DH, Lee VM, Trojanowski JQ (1998) The Dorothy Russell Memorial Lecture. The molecular and cellular sequelae of experimental traumatic brain injury: pathogenetic mechanisms. *Neuropathol Appl Neurobiol* 24:251–267

Meyer JR, Gutierrez A, Mock B, Hebron D, Prager JM, Gorey MT, Homer D (2000) High-b-value diffusion-weighted MR imaging of suspected brain infarction. *AJNR Am J Neuroradiol* 21:1821–1829

Monaghan DT, Cotman CW (1985) Distribution of N-methyl-D-aspartate-sensitive L-[3H]glutamate-binding sites in rat brain. *J Neurosci* 5:2909–2919

Moseley ME, Cohen Y, Mintorovitch J, Chileuitt L, Shimizu H, Kucharczyk J, Wendland MF, Weinstein PR (1990) Early detection of regional cerebral ischemia in cats: comparison of diffusion- and T2-Weighted MRI and Spectroscopy. *Magn Reson Med* 14:330–346

Mulkern RV, Gudbjartsson H, Westin CF, Zengingonul HP, Gartner W, Guttmann CR, Robertson RL, Kyriakos W, Schwartz R, Holtzman D, Jolesz FA, Maier SE (1999) Multi-component apparent diffusion coefficients in human brain. *NMR Biomed* 12:51–6

Nagesh V, Welch KM, Windham JP, Patel S, Levine SR, Hearshen D, Peck D, Robbins K, D'Olhaberriague L, Soltanian-Zadeh H, Boska MD (1998) Time course of ADCw changes in ischemic stroke: beyond the human eye! *Stroke* 29:1778–1782

Newman GC, Qi H, Hospod FE, Grundmann K (1992) Preservation of hippocampal brain slices with in vivo or in vitro hypothermia. *Brain Res* 575:159–163

Niendorf T, Dijkhuizen RM, Norris DG, van Lookeren CM, Nicolay K (1996) Biexponential diffusion attenuation in various states of brain tissue: implications for diffusion-weighted imaging. *Magn Reson Med* 36:847–857

Petersen A, Castilho RF, Hansson O, Wieloch T, Brundin P (2000)

Oxidative stress, mitochondrial permeability transition and activation of caspases in calcium ionophore A23187-induced death of cultured striatal neurons. *Brain Res* 857:20–29

Pressman BC (1976) Biological applications of ionophores. *Annu Rev Biochem* 45:501–530

Shepherd TM, Blackband SJ, Wirth ED III (2002) Simultaneous diffusion MRI measurements from multiple perfused rat hippocampal slices. *Magn Reson Med* 48:565–569

Shepherd TM, Wirth ED III, Thelwall PE, Chen HX, Roper SN, Blackband SJ (2003) Water diffusion measurements in perfused human hippocampal slices undergoing tonicity changes. *Magn Reson Med* 49:856–863

Stanisz GJ, Li JG, Wright GA, Henkelman RM (1998) Water dynamics in human blood via combined measurements of T2 relaxation and diffusion in the presence of gadolinium. *Magn Reson Med* 39:223–233

Statler KD, Jenkins LW, Dixon CE, Clark RS, Marion DW, Kochanek PM (2001) The simple model versus the super model: translating experimental traumatic brain injury research to the bedside. *J Neurotrauma* 18:1195–1206

Sze G, Anderson A (2000) Diffusing into the future. *AJNR Am J Neuroradiol* 21:1780–1782

Takadera T, Ohyashiki T (1997) Apoptotic cell death and caspase 3 (CPP32) activation induced by calcium ionophore at low concentrations and their prevention by nerve growth factor in PC12 cells. *Eur J Biochem* 249:8–12

Thelwall PE, Grant SC, Stanisz GJ, Blackband SJ (2002) Human erythrocyte ghosts: exploring the origins of multiexponential water diffusion in a model biological tissue with magnetic resonance. *Magn Reson Med* 48:649–657

Warach S (2001) New imaging strategies for patient selection for thrombolytic and neuroprotective therapies. *Neurology* 57:S48–S52

Warach S (2002) Thrombolysis in stroke beyond three hours: Targeting patients with diffusion and perfusion MRI. *Ann Neurol* 51:11–13

Zhao X, Pike BR, Newcomb JK, Wang KKW, Posmantur RM, Hayes RL (1999) Maitotoxin induces calpain but not caspase-3 activation and necrotic cell death in primary septo-hippocampal cultures. *Neurochem Res* 24(3):371–382

PROTEOMICS STUDIES OF TRAUMATIC BRAIN INJURY

Kevin K. W. Wang,*, †, ‡, § Andrew Ottens,*, †, § William Haskins,*, †, §
Ming Cheng Liu,*, †, § Firas Kobeissy,*, †, ‡, § Nancy Denslow,*, ‖
SuShing Chen,*, ¶ and Ronald L. Hayes†, ‡, §

*Center of Neuroproteomics and Biomarkers Research, University of Florida
Gainesville, Florida 32610
†Center for Traumatic Brain Injury Studies, University of Florida, Gainesville, Florida 32610
‡Department of Psychiatry, University of Florida, Gainesville, Florida 32610
§Department of Neuroscience, University of Florida, Gainesville, Florida 32610
‖Interdisciplinary Center of Biomedical Research, University of Florida
Gainesville, Florida 32610
¶Computing and Information Science Engineering, University of Florida
Gainesville, Florida 32610

I. Introduction

With the completion of human and rat genomes, the next major technological challenge facing the biomedical community is the deciphering of the human proteome. Study of the proteome has been aided by recent advances in protein

separation, protein identification/quantification, and bioinformatics. Although the application of proteomics technologies in brain injury research is still in its infancy, enormous insights can be achieved from such endeavors. There are approximately 30,000–40,000 hypothetical protein products transcribable from the human genome (Aebersold and Watts, 2002; Grant and Blackstock, 2001; Grant and Husi, 2001; Hanash, 2003; Hochstrasser *et al.*, 2002; Service, 2001; Smith, 2000). Yet, the proteome is extremely complex. Even in a single cell type the set of proteins that are expressed, as well as their steady state levels, depend on time and the specific state of the cells in response to environmental stimuli or challenges. In addition, cellular proteins are almost constantly subjected to various forms of post-translational modifications (PTMs), including phosphorylation/dephosphorylation by different kinases and phosphatases, proteolysis, or processing by different protease families, acetylation, glycosylation, and cross-linking by transglutaminases or conjugation to small protein tags such as ubiquitin or SUMO (similar to ubiquitin modifier) (Janssen, 2003; Schäfer *et al.*, 2003; Schwartz and Hochstrasser, 2003). Because of these challenges, one often has to focus on a specific subproteome. The case in point is neuroproteomics, or the study of nervous system proteomes. The importance of neuroproteomics studies is that they will help elucidate the poorly understood biochemical mechanisms or pathways that currently underlie various psychiatric, neurological, and neurode-generative diseases. The example we will focus on here is traumatic brain injury (TBI), a neurological disorder currently with no Food and Drug Administration (FDA) approved therapeutic treatment.

II. Traumatic Brain Injury

Traumatic brain injury or traumatic head injury is characterized as a direct, physical impact or trauma to the head, causing brain injury (Denslow *et al.*, 2003; Hayes *et al.*, 2001). Annually there are 2 million TBI cases in the United States alone. They result in 500,000 hospitalizations, 100,000 deaths, 70,000–90,000 people with long-term disabilities, and 2000 people who survive but live in a permanent, vegetative state. Medical costs of TBI are estimated to be more than $48 billion annually in the United States. The cause of TBI can be broken down into the following catalogories: Motor vehicle accidents (50%), falls (21%), assault and violence (12%), sports and recreation (10%), and all others (7%) (Fig. 1). Importantly, 30–40% of all battlefield injuries also have a head injury component.

Because of intensive research both in clinical settings and in employing experimental animal models of TBI, there is now a general understanding of the pathology of TBI. Typically there is mechanical, compression-induced direct tissue injury often associated with hemorrhage and contusion at the site of
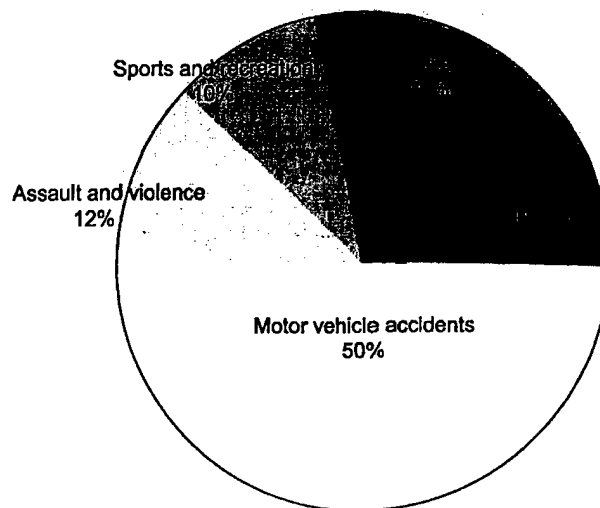
FIG. 1. Different causes of traumatic brain injury in humans.

impact. A significant amount of cell death will occur very rapidly in this zone. More distal to the injury zone, due to the impact of the force, long fiber tracts (axons) are especially at risk to this type of injury. Usually after the first phase of cell injury/death occurs, there is also the secondary injury, which is believed to be mediated by secondary biochemical events such as neurotoxic glutamate release (neurotoxicity) or oxidative damage. Other significant alterations include inflammation responses by microglia cells, astroglia activation, and proliferation. Over time, if the TBI patient survives, these events lead to long-lasting brain tissue remodeling, possibly including stem cells differentiation. Therefore the spatial and temporal levels of biochemical and proteomic changes of TBI can be investigated.

A. ANIMAL MODELS OF TBI

Over the past decades, basic science researchers have developed several animal models of TBI (Finnie, 2001; Raghupathi *et al.*, 2000). There are several well-characterized models of TBI, including controlled cortical impact (CCI), which is controlled by compressed gas; a fluid percussion model that transduces a contusion force by the movement of fluid in the chamber, and vertical weight drop models in which a weight is dropped from a certain height within a hollow chamber for guidance. The weight drop model creates an acceleration force that
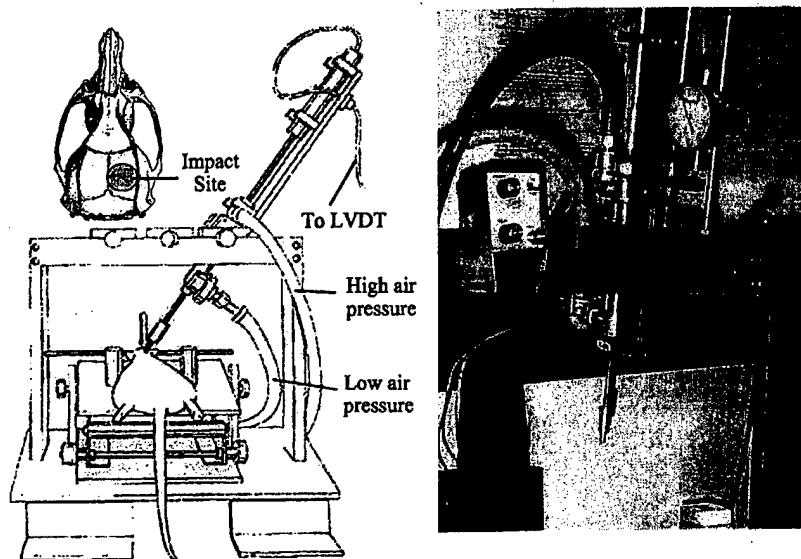
Fig. 2. Rat model of TBI: Controlled cortical impact (CCI). Left panel shows a schematic drawing of the CCI setup. Right panel is a photograph of the CCI device.

is directed to the top of the skull either unilaterally or bilaterally (reviewed by Finnie in 2001). In our work, we employ the rat CCI model of TBI (Dixon *et al.*, 1991; Fig. 2). We have argued that use of proteomics will greatly facilitate the biochemical mechanisms underlying the various phases of TBI pathology (Denslow *et al.*, 2003).

B. Source of Biological Materials

Proteomics studies for TBI generally can be categorized into human studies, animal studies, and cell culture-based studies. For the purposes of this review, cell culture-based studies will not be discussed further. When comparing human versus. animal studies, there are pros and cons in each scenario (Table I). Regarding the sample types that can be exploited for proteomics analysis, they will include brain tissues, cerebrospinal fluid (CSF), and blood (serum and plasma). For human TBI studies, blood samples (which are further fractionated into plasma or serum) are the easiest to obtain. Interestingly, there is increasing interest now focused on using CSF because its status will reflect that status of the central nervous system itself. After severe traumatic brain injury, spinal shunt or spinal tap are routinely performed, thus obtaining CSF is not an issue. One of the major challenges of

Table I
COMPARING HUMAN VERSUS ANIMAL TBI PROTEOMIC STUDIES

	Human studies	Animal studies
Sample heterogeneity	High	Low
Environmental variables	High	Low
Brain tissue samples	Difficult to obtain (postmortem only)	Routine
CSF samples	Routine (large volume available)	Routine (small volume only)
Blood samples	Routine (large volume available)	Routine (sufficient volume available)
Results relevance to human disease	Yes	Likely (confirmation needed)

using clinical, samples-based proteomic studies is that it is extremely difficult to control individual (biological) and environmental variables (see Table I).

1. *Brain Samples*

Brain tissue from human TBI studies would inevitably come from deceased TBI patients. These brain samples could be subjected to postmortem artifacts, compounded by various and significant time delay before samples can be obtained. The biggest advantage of animal neuroproteomics studies over human counterparts is the ability to obtain brain tissues in a controlled laboratory environment. Furthermore, it is possible to harvest samples from defined anatomical regions. For example, for our TBI studies we often focus on cortical and hippocampal samples. This is important because different brain regions might be selectively more vulnerable to traumatic or ischemic insults.

2. *CSF*

CSF can be collected from the cisterna magna from lab animals such as rats and mice. CSF may contain rich brain proteome information that is relevant to disease diagnosis (Davidsson *et al.*, 2002). However, only approximate 50–100 μl can be withdrawn from rats and 25–30 μl from mice. Care must also be taken not to contaminate samples with blood as a result of puncture. Although more than one CSF draw might be possible, in our laboratory we generally withdraw only one CSF sample, followed by sacrifice. In the case of human TBI, CSF can also be collected routinely from ventriculotomy or from spinal tap. Importantly, a relatively large amount (2–5 ml) of CSF can be routinely obtained from human TBI patients from each CSF sampling time point, and repeating samples can often be achieved.

3. *Blood Samples (Serum and Plasma)*

In both human and animal TBI studies, blood can be routinely collected and usually further processed into either serum or plasma fractions before subjecting to proteomics analysis. Like CSF, most proteomics researchers believe there is significant proteomic information in the blood that would reflect the status of the brain, particularly after TBI caused by possible blood-brain barrier compromise (Raabe *et al.*, 1999; Romner, 2000).

C. SAMPLE COLLECTION AND PROCESSING CONSISTENCY

It needs to be emphasized that for proteomics results to be consistent and reproducible, one needs to use extra caution to ensure the variables can be kept to a minimum. All sample collection procedures should be discussed and finalized and the operators made familiar with the procedures. Some practice runs are highly desirable. For human studies, detailed record keeping is extremely important for future analysis or trouble-shooting purposes. For example, for human studies, CSF or blood samples should be taken at consistent intervals and before food consumption, because it might significantly affect the blood proteomics profile. For animal studies that are conducted in controlled environments, it should be possible to keep brains and biofluid sample collection time and routine as standardized as possible. Also, the animal subjects should be tagged and observed carefully and regularly, with any out-of-the-norm observations recorded. They might become very helpful in enhancing proteomics analysis. Tissue and biofluid samples, once obtained and processed, should be snap frozen and stored at $-85\ ^{\circ}C$ until use.

D. SAMPLE POOLING CONSIDERATIONS

There is also an important decision to be made before the proteomics analysis (i.e., whether to pool samples for analysis or to analyze individual samples). Pooling samples significantly reduces minor individual variability and the amount of workload. Yet, at the same time its disadvantage is that it might miss certain proteomics changes that are present in only a subset of samples. On the other hand, analysis of individual samples has the advantage of being an exhaustive analysis of individual proteomics profiles but can be highly time consuming and cost-prohibitive. Another consideration is that it would be useful to pool samples when protein amount is a limiting factor.

A known biochemical marker that correlates with TBI, such as alphaII-spectrin breakdown products, can be used as positive control for quality assurance, and might even be used to guide inclusion criteria for sample pooling (Pike
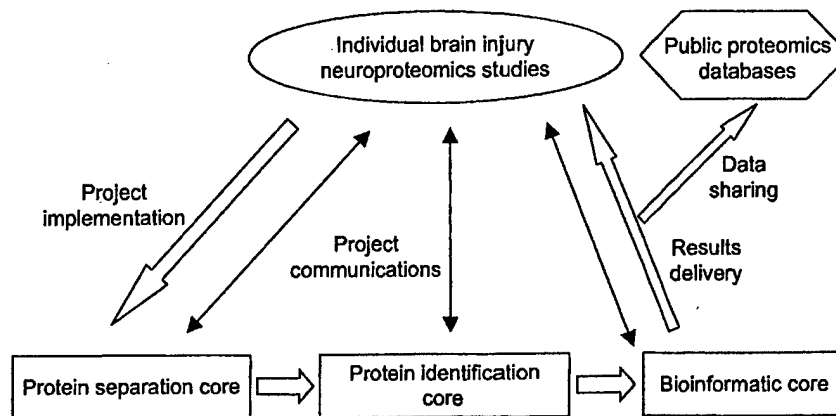
FIG. 3. Flowchart and organization of traumatic brain injury neuroproteomics studies. See text for details.

et al., 2001, 2004). It is also possible to incorporate both pooling and individual proteomics analysis in the same studies. For example, pilot studies or initial proteomics profiling of TBI can be performed with pooled samples while final detailed analysis can be done with individual samples.

III. Proteomics Analysis Overview

Regardless of whether we are dealing with human or animal samples, or whether they are tissue lysate or biofluid (CSF, serum, or plasma), the strategy we developed can be organized into three interacting, scientific disciplines or phases: protein separation, protein identification followed by quantification, and bioinformatics analysis (Fig. 3). By design, any proteomics center should spend two-thirds of its scientific and financial resources to establish a robust and readily usable proteomics platform. However, it is equally important for the center to develop new and improved neuroproteomics technologies on all fronts.

IV. Protein Separation Methods

In TBI neuroproteomics studies, we are less interested in descriptive and exhaustive characterization of the whole neuroproteome; rather we will focus on protein level or post-translational changes that occur in TBI. With this in mind, it

is important to devise methods in comparing and contrasting the two proteomics data sets: control versus TBI. To productively identify all the proteins in a specific system of interest (subproteome) or a subset of proteins that are differentially expressed in TBI, it is essential that complex protein mixtures (e.g., brain samples or biofluids) be first subjected to multidimensional protein separation. Because proteins differ in size, hydrophobicity, surface charges, abundance, and other properties, there is no single protein separation method that can satisfactorily resolve all proteins in a proteome.

To date there are two mainstream protein separation methods used for proteomic analysis: (1) two-dimensional gel isoelectrofocusing/electrophoresis and (2) multidimensional liquid chromatography.

A. Two-Dimensional Gel Electrophoresis Approach

Two-dimensional gel electrophoresis (2DE) is the most established protein separation method for the analysis of a proteome or subproteome (Boguslavsky, 2003). It is achieved by subjecting protein mixtures to two protein separation methods under denaturing condition (in the presence of 6–8 M urea and cationic detergent such as sodium dodecylsulfate [SDS]). Traditionally proteins are first separated based on their isoelectric point (pI) value with a tube gel (polyacrylamide), by isoelectric focusing (IEF) with the aid of mobile ampholytes with different (pI) values. After IEF, the tube gel is placed atop a polyacrylamide gradient gel within which the SDS-bound proteins are separated by size. Because of poor gel consistency, the IEF step (the first dimension) is most variable. However, a recent breakthrough in IEF technology using immobilized pH gradient (IPG) strips, provides improved reproducibility (Bjellqvist *et al.*, 1982; Gorg *et al.*, 1988; Hanash, 2003; Jungblut *et al.*, 1996). Another disadvantage with 2D gels is the inevitable gel-to-gel variability in exact location and patterns of protein spots. This proves problematic when comparing two samples directly (e.g., control versus TBI brain samples).

The recent advance of 2D-differential in-gel electrophoresis (2D-DIGE) has resolved this problem (Patton, 2002; Unlu *et al.*, 1997). The fluorescent cyanine dyes Cy3 and Cy5 are a match in molecular weight and charge but have distinct excitation and emission wavelengths (Yan, 2002). One dye is used to label control samples, and the other to label treated samples, which are then mixed and differentially compared in the same gel (Fig. 4). These advantages are incorporated into our approach, as outlined in Table I. They include in particular the high resolving power for complex mixtures of proteins and the capability of resolving post-translationally modified proteins, including acetylation, phosphorylation, glycosylation, and protein cross-linking (Janssen, 2003; Schäfer *et al.*, 2003). It is possible to annotate each protein of a proteome by pI and molecular
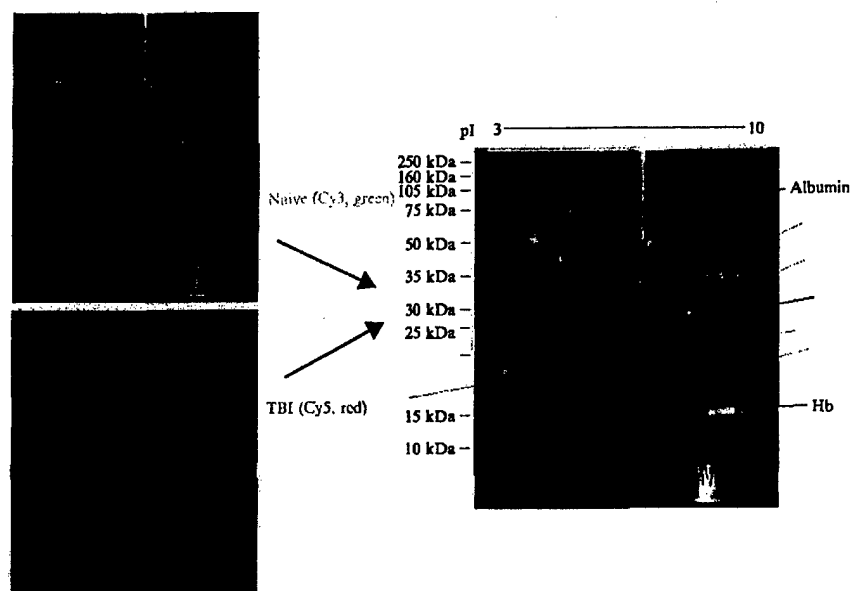
FIG. 4. Rat TBI protein separation by 2D differential in-gel electrophoresis *(DIGE)*. Pooled naïve and TBI rat cortex samples were labeled with Cy3 and Cy5 dyes, respectively (left panels) and co-run and resolved by 2DE. The fluorescence signals were merged, allowing the identification of differentially expressed proteins (right panel). Yellow spots represent proteins common to both samples. Green and orange-red spots are differentially expressed proteins in pooled naive and TBI sample, respectively. Blue arrows point to blood-borne protein contaminants found in TBI sample (e.g., albumin and hemoglobins [Hb]).

weight values in X-Y coordinates to form a 2D protein map, of which publicly accessible and searchable databases already exist (Appel *et al.*, 1999; Fountoulakis *et al.*, 1999, 2000; Lemkin, 1997; Lubec *et al.*, 2003). There are, however, several persistent weaknesses of 2D gels (See Table II). Proteins of extreme pl or minute quantity and proteins that are either very small or very large may be missed. Also, integral membrane proteins, of which many are central nervous system (CNS) disorder drug targets (membrane-bound receptors or neurotransmitter transporters), are lost because of their extreme hydrophobicity.

Regarding protein separation, there is also research in the direction of microfluidic 2D protein separation with miniaturized IEF and electrophoresis. This approach has the advantage of reducing sample usage with less waste and without compromising detection sensitivity (Derra, 2003; Reyes *et al.*, 2002).

B. Two-Dimensional Liquid Chromatography Approach

Alternative protein separation methods are needed to overcome some of the shortcoming of 2D gels. Recently there has been significant movement toward multidimensional liquid chromatography methods to resolve complex protein mixtures (Peng and Gygi, 2001). The general idea draws on classic chromatographic principles including size chromatography (gel filtration), ionic interaction (strong cation exchange [SCX] and strong anion exchange [SAX]), hydrophobic interaction (C4- or phenyl-agarose chromatography), and IEF chromatography. One can envision combining multiple chromatographic approaches in a series to achieve multidimensional separations. In our own work we have also combined the use of a size exclusion column (SEC) and a SAX column (Fig. 5) in series with some success. Challenging this method are: (1) incompatibilities of buffer components (e.g., salt concentration, organic components) and (2) the logistics of configuring fraction elution from one column with loading of a second column. Often, individual fractions are manually loaded onto the second column, but this is extremely labor intensive and may introduce run-to-run variability.

When selecting chromatographic separation methods, considerations must be given to take advantage of the size, pI, and hydrophobicity differences of the proteins of interest. In addition, when dealing with membrane-bound proteins, the chromatographic method must be compatible with the use of the proper
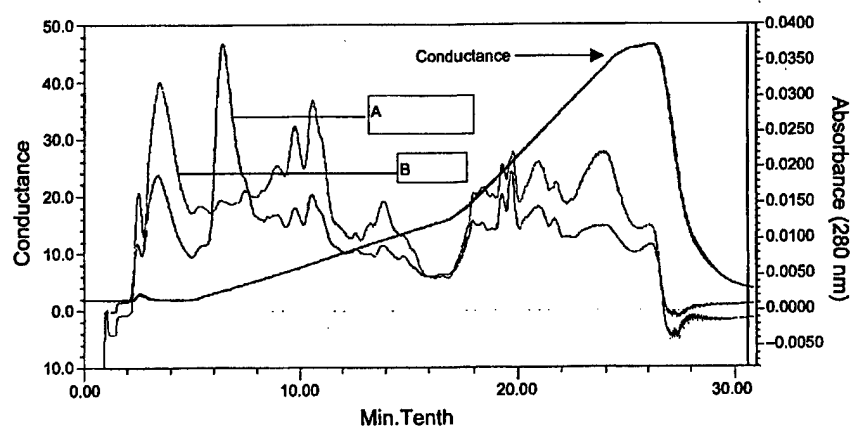
Fig. 5. Example of rat brain protein separation by strong ion exchange chromatography. Protein elution (30 min, 30 fractions) chromatograms (proteins are measured as absorbance at 280 nm). A = pooled rat cerebellum lysate and B = pooled rat cerebrum lysate. Chromatographic differences between A and B are detected readily throughout the elution. The third line is relative conductance measured over the NaCl gradient elution of the column.

neutral detergent (e.g., Triton X-100 or CHAPS). Importantly, minute proteins can be concentrated to enhance their detection. One weakness of this approach is that even with 2D liquid chromatographic (LC) separation, it is often not possible to separate all proteins individually. This problem will be addressed in the next section. In summary, when compared to 2DE, tandem LC is more compatible with membrane-bound proteins and can enrich proteins in minute quantity.

V. Protein Identification and Quantification Methods

The approach we are taking represents an effort to apply systematically the most contemporary proteomics approaches to identify and develop clinically useful biomarkers for brain injury from trauma, disease, or drugs. Classical methods of protein identification involving protein separation by gels or LC (see previous section), coupled with mass spectrometry, provide a potent and novel methodological array never before applied systematically to the detection of biomarkers of CNS injury, either alone or in combination. This integrated strategy makes possible both "targeted" analyses of known potential biomarker candidates as well as "untargeted" searches for novel proteins and protein fragments that could prove even more useful. Each of these technologies has advantages and disadvantages that together complement each other. Thus combining multiple proteomics strategies optimizes the opportunity for successful brain injury proteomics studies. Lastly, protein identification research also benefits from improved bioinformatics tools for protein database searching (Chakravarti *et al.*, 2003). Thus, importantly, research designs must incorporate appropriate bioinformatics support (see next Section).

A. Mass Spectrometry Approach

1. *MALDI-TOF MS*

The most classical method for protein identification in a given protein mixture is to perform 2DE, followed by in-gel digestion of the gel band(s) of interest with protein identification by mass spectrometry. The 2D-gel method has been improved by the use of IPG strips for the first dimension and the ability to label protein samples from control and experimental tissues with cyanine dyes (e.g., Cy3 and Cy5) that form co-migrating labeled samples that are compared in the same gel. Differentially expressed proteins are easily found, cut from the gel, digested in the gel spot with trypsin, and then identified by MALDI-TOF MS (matrix-assisted laser desorption ionization time-of-flight mass spectrometry) approach (Bienvenut *et al.*, 2002). It is important to understand that

MALDI-TOF MS identifies peptides based on the accurate determination of peptide masses. Because each amino acid has a unique mass, any given peptide composed of a unique amino acid sequence will have a unique mass. However, this method of protein identification is not infallible. Peptides can have identical amino acid composition but with a different order, or more often peptides of similar length will have mass-to-charge values that are slightly, but indistinguishably, different from one another within the mass accuracy and resolution limits of the instrumentation. Thus it is common practice to use at least four to nine peptide fragments to positively identify a protein, which can be difficult with complex mixtures. In addition, any significant post-translational modifications that will change the mass-to-charge (m/z) value of multiple peptides will make protein identification extremely difficult (Table II).

By using 2D-gel separation, this method is useful for distinguishing proteins that are either up-regulated or down-regulated because of to injury, but it is suboptimal for finding very basic, very acidic, or hydrophobic proteins, and the identification of smaller peptides can be difficult because of chemical noise from matrix ions. Complementary to this method are direct MS procedures that capture the entire range of proteins and peptides but may not distinguish proteins that are post-translationally modified, and the maximal protein size is limited to approximately 25–30 kDa (kilodaltons). A modified MALDI approach, called surface-enhanced laser desorption ionization (SELDI) (invented by Ciphergen, Fremont, CA), combines an affinity matrix-based protein separation phase with the TOF MS-based protein mass determination (also called Protein Chips) (Wiesner, 2004).

2. *LC-MS/MS Approach*

Protein separations strategies including 1D- and 2D-LC techniques (Adkins *et al.*, 2002) and gel separations are commonly used to resolve complex protein mixtures. Subsequent LC fractions or gel bands are processed by in-solution or in-gel digestion (most often with trypsin) to form peptides small enough to be effectively measured by MS. Complex peptide mixtures of protein digests are typically separated by reverse-phase chromatography placed on-line with electro-spray ionization mass spectrometry (ESI MS), which not only resolves peptides from one another but also concentrates them, providing greater sensitivity. LC-MS is most often performed on high-powered tandem mass spectrometers, including the quadrupole ion-traps (QIT), quadrupole time-of-flight (QTOF), and Fourier transform ion cyclotron resonance (FT-ICR) mass spectrometers. Tandem mass spectrometry (MS/MS) allows the advantage of providing peptide sequence information in addition to the parent peptide mass (Gygi *et al.*, 2000). (Figs. 6 and 7). In brief, ions of the peptide of interest are isolated (first stage of mass spectrometry) then fragment along the peptide backbone by colliding with neutrals. Pairs of b- and y-daughter ions, formed by fragmentation from the n- or c-terminal side of each residue, respectively, will predominantly be generated.

Table II

ATTRIBUTES OF VARIOUS PROTEIN IDENTIFICATION APPROACHES

Protein identification method	Strengths	Weaknesses
MALDI-TOF MS	-Can analyze both proteins and peptides	-Ion suppression with complex samples (no peptide separations)
	-High mass accuracy ± 0.01%	
	-Resolution 50 ppm	-Does not provide sequence information
	-Protein ID by mass mapping of peptides from tryptic digests	-Requires detection of multiple peptides for protein identification
	-Sensitive to 50 fmol routine	
	-Rapid analysis for high throughput	
	-Preserves sample for later analysis	
LC-MS/MS	-Provides peptide sequence for protein ID—less reliant on mass accuracy	-Slow sample analysis due to long chromatograms
	-Can reliably identify protein with 1 to 2 peptides	-Consumes entire sample loaded
	-Sensitive in the amol range	-Greater complexity of nano-LC requires dedicated operator
	-Provides precise/reproducible quantitation	
	-Routine analysis of multiprotein digests	
Antibody panels/arrays	-Easy protein ID decoding	-Non exhaustive
	-Easy confirmation	-Uneven sensitivity
	-Can potentially detect PTM	
	-Sensitive to high fmol range	

The b- and y-daughter ions are then mass analyzed to form a daughter ion spectrum (second stage of mass spectrometry). Using MS/MS information, the peptide sequence can be reconstructed, which can be performed rapidly with available bioinformatics software (see Table II). LC-MS/MS systems work extremely well for protein identification by coupling the generated mass and sequence information with database searches, and the technique is sensitive enough to identify pM levels of proteins present in complex mixtures such as tissue lysates.

B. Protein and Peptide Quantification by MS

There are currently no less than half a dozen MS-based protein/peptide quantification methods, which were reviewed recently (Denslow, 2003). We will focus on two prominent quantification methods that are applicable to TBI proteomics.

1. *ICAT*

Isotope-coded affinity tags (ICAT) are a direct chromatographic approach to evaluate differential expression (Gygi *et al.*, 1999). ICAT reagent pairs are cysteine-binding tags that differ in molecular weight by use of hydrogen or carbon isotopes. These reagents are used to differentially label two protein samples, which are then mixed together and digested into peptides. Cysteine-containing fragments labeled with the tags can then be selectively isolated and analyzed by LC-MS/MS with differential expression determined from the peak height ratio of the tagged peptides. MS/MS data on the peptides is then searched against a protein database, providing the identity of the differentially expressed proteins (Peng *et al.*, 2003; Yates *et al.*, 1999).

2. *AQUA*

Another innovative method to quantify differential expression is through the use of *A*bsolute *qua*ntitation (AQUA) probes (Gerber *et al.*, 2003). Unlike ICAT, which can be used to tag any cysteine-containing protein, AQUA is applicable

Naïve and TBI rat cortex samples

DIGE

Trypsin digestion

Capillary liquid chromatography (LC)

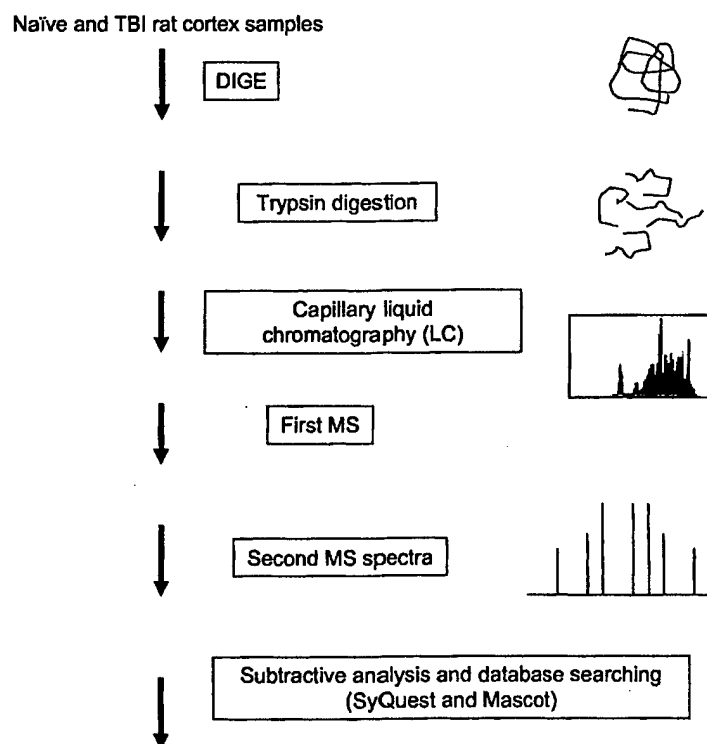First MS

Second MS spectra

Subtractive analysis and database searching (SyQuest and Mascot)

FIG. 6. Schematic sample flow of protein separation/protein identification by LC-MS/MS. See text for details.

Seq	#	b	y	(+1)
T	1	102.1	1950.0	20
P	2	199.1	1848.9	19
G	3	256.1	1751.9	18
P	4	353.2	1694.9	17
L	5	466.3	1597.8	16
S	6	553.3	1484.7	15
S	7	640.3	1397.7	14
Q	8	768.4	1310.7	13
G	9	825.4	1182.6	12
A	10	896.4	1125.6	11
P	11	993.5	1054.6	10
V	12	1092.6	957.5	9
D	13	1207.6	858.4	8
T	14	1308.6	743.4	7
Q	15	1436.7	642.4	6
P	16	1533.8	514.3	5
A	17	1604.8	417.2	4
A	18	1675.8	346.2	3
Q	19	1803.9	275.2	2
K	20	1932.0	147.1	1

MAFSKGFRIY HKLDPPPFSL IVETRHKEEC LMFESGAVAV LSSAEKEAIK GTYAKVLDAY GLLGVLRLNL GDTMLHVLVL
VTGCMSVGKI QESEVFRVTS TEFISLRVDA SDEDRISEVR KVLNSGNFYF AWSASGVSLD LSLNAHRSMQ EHTTDNRFFW
NQSLHLHLKH YOVNCDDWLL RLMCGOVEIR TIYAAHKQAK ACLISRLSCE RAGTRFNVRG TNDDOHVANF VETEQVIYLD
DCVSSFIQIR GSVPLFWEQP GLQVGSHRVR MSRGFEANAP AFDRHFRTLK DLYGKQIVVN LLGSKEGEHM LSKAFQSHLK
ASEHASDIHM VSFDYHQMVK GGKAEKLHSV LKPQVQKFLD YGFFYFDGSA VQRCQSGTVR TNCLDCLDRT NSYQAFLGLE
MLAKQLEALG LAEKPQLVTR FQEVPRSMWS VNGDSISKIY AGTGALEGKA KLKDGARSVT RTIQHNPFDS SKQEAIDVLL
LGNTLNSDLA DKARALLTTG SLRVSEQTLQ SASSKVLKNM CENFYKYSKP KKIRVCVGTW NVNGGKQFRS IAFKNQTLTD
WLLDAPKLAG IQEFQDKRSK PTDIFAIDFE EMVELNAGNI VNASTTNQKL WAVELQKTIS RDNKYVLLAS EQLVGVCLFV
FIRPQHAPFI RDVAVDTVKT GMGGATGNKG AVAIRMLFHT TSLCFVCSHF AAGQSQVKER NEDFVEIARK LSFPMGRMLF
SHDYVFWCGD FNYRIDLPNE EVKELIRQQN WDSLIAGDQL INQKNAGQIF RGFLEGKVTF APTYKYDLFS EDYDTSEKCR
TPAWTDRVLW RRRKWPFDRS AEDLDLLNAS FQDESKILYT WTP GTLLHYG RAELKTSDHR PVVALIDIDI FEVEAEERQK
IYKEVIAVQG PPDGTVLVSI KSSAQENTFF DDALIDELLQ QFAHFGEVIL IRFVEDKMWV TFLEGSSALN VLSLNGKELL
NRTITITLKS PDWIKTLEEE MSLEKISVTL PSS~~FSSTLLO EDAEVSADFD MEGDTP~~DYSA EVEELLPQHL QPSSSSGLGT
SPSSSPRTSP CQSPTAPEY3 APSLPIRPSR APSHTPGPLS SQGAPVDTQP AAQKJSSQTI EPKRFPPPRP VAPPARPAPP
QRPPPPSGAR SPAPARKEFG APKSPGTARK DNIGRNQPSP QAGLAGPGPS GYGAARPTIP ARAGVISAPQ SQARVSAGRL
TPESQSKPLE TSKGPAVLPE PLKPQAAFPP QPSLPTPAQK LQDPLVPIAA PMPPSIPQSN LETPPLPPPR SRSSQSLPSD
SSPQLQQEQP TG

Mass (mono): 142869.8   Identifier: gi|166575   Database: C:/Xcalibur/database/rat.fasta
Protein Coverage: 262/1292 = 20.3% by amino acid count, 28224.7/142869.8 = 19.8% by mass
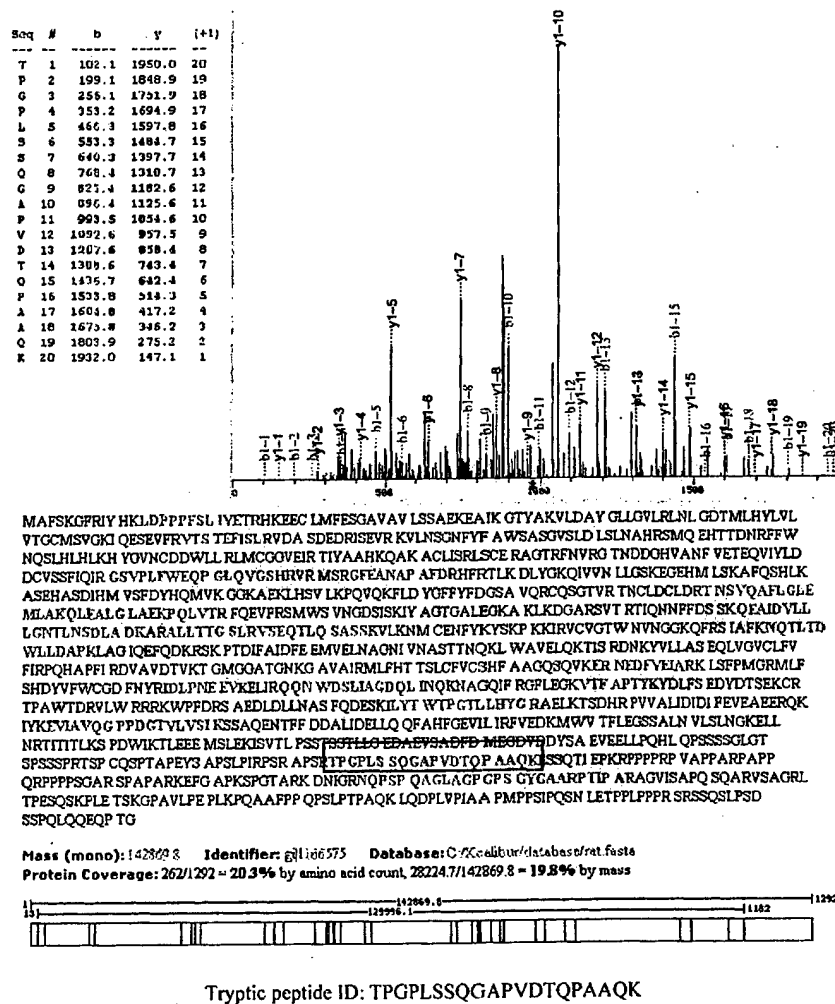
Tryptic peptide ID: TPGPLSSQGAPVDTQPAAQK

FIG. 7. Example of LC-coupled MS-MS identification of a protein differentially expressed in rat brain hippocampus after TBI. A protein band (in an SDS-PAGE gel) that is uniquely expressed in TBI-48 hr was cut out and digested with trypsin, and a distinct tryptic peptide was sequenced based on MS-MS data (top panel) and identified to be originated from a brain protein synaptojanin, based on proteomics database searching results (lower panel).

only to target proteins. A peptide of the selected protein is synthesized with an isotopically labeled amino acid. A known amount of the probe is then added to the digested sample, which is analyzed by LC-MS/MS. Because the probe exactly matches the endogenous peptide of interest except for a modest mass difference,

thc two will coelute with reverse-phase chromatography and have identical ionization properties, which minimizes variation in ion signal intensities. The tandem mass spectrometer then resolves the two peptidcs by the small m/z diffcrence, allowing the ion signal of the two to be compared across the chromatographic peak. This method is very precise and can be applied to nearly any protein (with or without cysteine). By accurately measuring the amount of probe added, the absolute amount of a protein can also be determined, though relative protcin amounts can also be determined without having to know the exact amount of probe added. In practice this method would follow a nontargeted diffcrential method such as 2D-DIGE or ICAT, which produces a list of potential differentially expressed proteins. This method can then be used to quickly and precisely validate the differential expression of the targeted proteins across many samples. In comparison to thc more traditional targeted quantitation of western analysis, AQUA is a much quicker way of validating differential expression than waiting for a specific antibody to be developed.

C. ANTIBODY PANEL/ARRAY APPROACH

Protein identification is also assisted by the availability of various platforms of antibody arrays or panels (e.g., Zyomyx protein biochips, BD Powerblot, and BD antibody arrays) (Graslund *et al.*, 2002; James 2002; Kusnezow and Hoheisel, 2002; Moody, 2001). These methods all rely on antibody-based capturing of the protein of interest. The quantitation of the captured protein can be performed by prelabeling (including differential labeling) of the protein with fluorescent dye(s) (dye-labeling detection) such as BD antibody arrays, which is similar to the gene chip mRNA quantification method. Alternatively, quantitative detection can be accomplished with a second primary antibody specific to the same protein antigen (sandwich detection), which is similar to the sandwich enzyme-linked immunoabsorbant assay (sandwich ELISA) method (e.g., Zyomyx protein Biochips). A third option is the BD Powerblot, which is a high-throughput Western blotting (immunoblotting) system with two distinct protein samples that are differentially subjected to a set of five blots. Each blot has 39 usable lanes with the use of a manifold system. Each lanc is developed with five to six different fluorophore-linked monoclonal antibodies (toward antigen with nonoverlapping molecular weight). With this method samples are probed with a total of 1000 monoclonal antibodies. We have actually conducted several Powerblot experiments with animal TBI studies. Figure 8 gives examples of differential protein changes observed in the rat hippocampus after TBI.

The major advantage of the antibody panel or array approach is that proteins of interest can be readily identified, because all antibodies used have known antigens and their positional assignment on the antibody chip or panel is
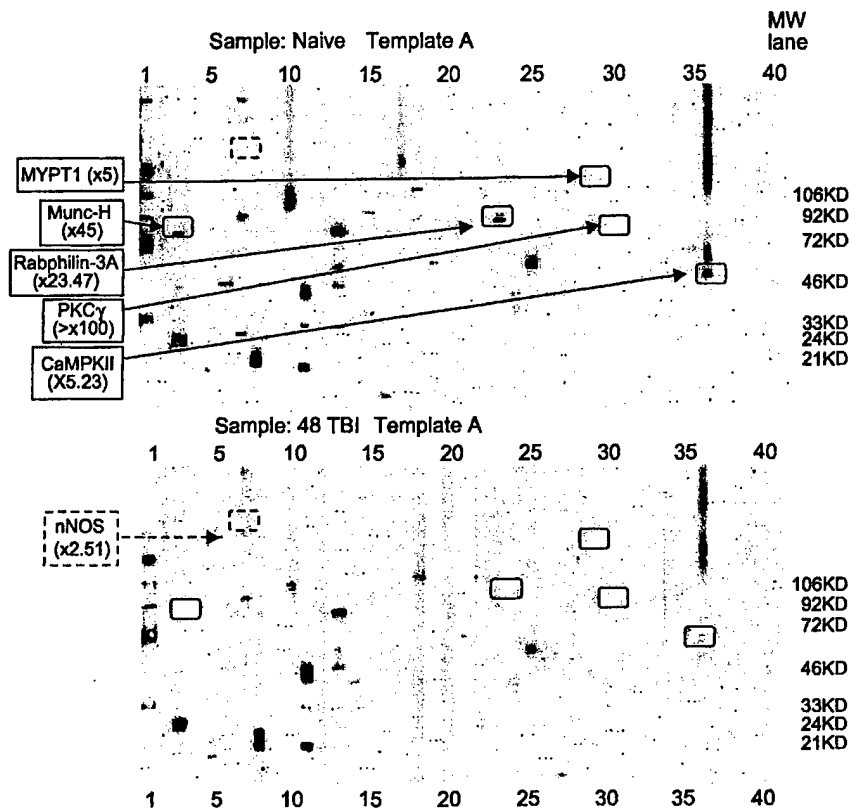
FIG. 8. Example of antibody panel approach-based by indentification of several protein differentially expressed in rat brain hippocampus after TBI. When comparing pooled naïve (top panel) and TBI-48 hr (bottom panel) hippocampal samples, five proteins (MYPT1, Munc-H, Rabphilin-3A, PKCdelta and CaMpKII; solid line) with reduced levels and one protein (nNOS; dotted line) with increased levels after TBI (average fold changes are shown in brackets) were identified.

known (See Table II). Also, quantification is already built into this antibody-based approach without any additional effort. On the other hand, the major disadvantage of this approach is that it is practically impossible to be exhaustive, because one would only have high fidelity antibodies to a subset of proteins. Furthermore, using antibodies collected from many different sources will likely result in uneven sensitivity. As in other immunoassay methods (e.g., Western blotting, immunostaining, or ELISA), it is a given that antibody array methods will likely detect nonspecifically bound proteins or other substances, affecting quantitation with high chemical noise and leading to false positive reactions. Despite its shortcoming,

the antibody array-based protein identification approach is a useful complement to the MS-based approach discussed previously.

VI. TBI Proteomics Bioinformatics

The current advance in databases and web portals has a natural convergence for knowledge and data sharing among local and remote scientists in any National Institutes of Health (NIH) domain. Large databases will be networked, whereas web portals will "federate and access" large databases. Such efforts need to be developed for the neuroproteomics domain. Neuroscience has one of the most complex information structures—concepts, data types, and algorithms—among scientific disciplines. Its richness in organisms, species, cells, genes, and proteins and their signal-transduction pathways provides many challenging issues for biological sciences, computational sciences, and information technology. The advances in neuroscience urgently need developing portal services to access databases for analyzing and managing the following information: sequences, structures, and functions arising from genes, proteins, and peptides (e.g., protein segments and biomarkers) (Chakravarti *et al.*, 2003).

In the bioinformatic phase, two interlinked mandates are: (1) to build a local user-friendly proteomics database, and (2), to develop interoperable proteomics tools and architecture for multiple data integration and to integrate user and public domain-based databases (Fig. 9). Data analysis applications should interoperable with database operations and portal access. The TBI proteomics core technologies will provide an integrative approach to genomic and proteomics information by developing a common portal architecture—the TBI proteomics portal—at the University of Florida for data archiving and retrieval among core researchers and end users, and data linking and sharing to national and international neuroproteomics websites (e.g., Human Proteome Organization [HUPO, United States]) (Hanash, 2004) and Human Brain Proteome Project (HBPP, Germany) (Meyer *et al.*, 2003). Lastly, bioinformatic tools and software are also needed to enhance our ability to data mine as well as to study protein-protein interaction, protein pathways and networks, and complex post-translational modification such as protein phosphorylation, processing, cross-linking, and conjugation. This will help us develop knowledge bases about neuroproteomics functions and signal-transduction pathways in terms of dynamic objects and processes (Cattell, 1996; Mendes, 1993, 1997; Reddy, 1993; Somogyi, 1996). In addition, clinical information should be integrated with genomics and proteomics databases. The three major functions of the bioinformatic component of TBI proteomics studies can be further explained in the following section.
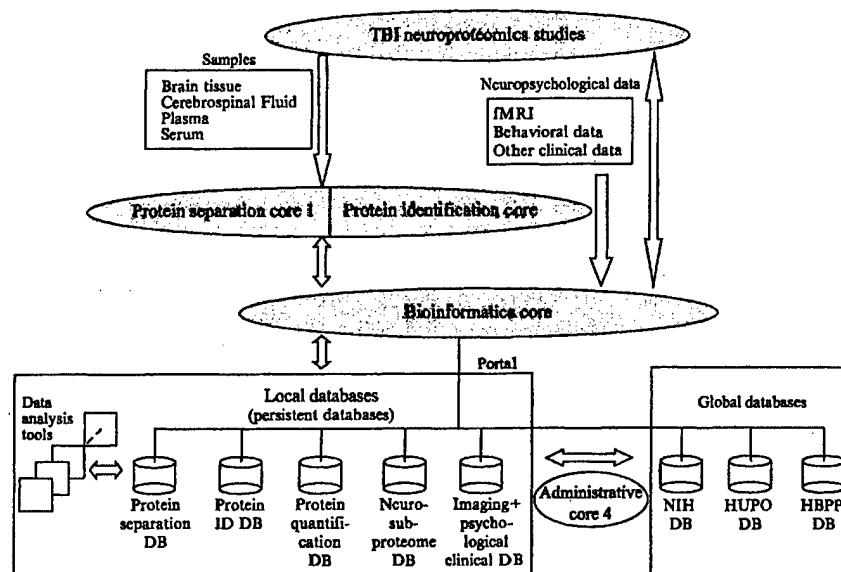
Fig. 9. Schematics of the central role of the bioinformatic core of TBI neuroproteomics studies. The bioinformatics core not only plays a key role in analyzing and archiving protein separation and identification data, but also plays a key role in integrating local TBI databases to global neuroproteome databases. See text for details.

A. PERMANENCE

Permanence is defined here as developing local databases for proteomics separation and identification and linking with national and international data sources. Local databases will include chromatograms, mass spectra, gel images, peptide and protein sequences, and functional magnetic resonance imaging (fMRI) images for control and TBI samples. Data modeling and semantics will be developed by proteomics and computer scientists together, so that semantic equivalence of search attributes and semantic associations can be established.

Our bioinformatics core is in the process of combining different data semantics and knowledge trees in separate genomics, proteomics, and clinical databases. A key requirement is the development of semantics (or ontology) of biological information, which is then captured in two components—semantic indexing and metainformation (i.e., "information about information")—of the intelligent search engines. A book by Chen (1998) has described these two important methods. Furthermore, semantic indexing and metainformation complement each other, reduce the complexity of neural taxonomy and classification, and correlate semantically the proteomics types and phenotypes (e.g., behavior in

drug abuse) at various (e.g., subcellular, cellular, and tissue or fluid) levels of neural activities. Dissemination to national and international data sources (e.g., HUPO and HBPP) will be consistently maintained through our intelligent search engines.

B. INTEROPERABILITY

Interoperability is defined here as integrating existing data analysis tools with local databases. A proteomics problem-solving environment will be established to provide users with rapid access to TBI neuroproteome center databases and analysis tools. This will include existing tools for proteomics research and drug abuse research. The range of these tools is very broad, from peptide sequencing and protein identification to image processing for fMRI images and data analysis for neuropsychological tests and diagnosis.

A critical component of our bioinformatics core is to conduct research at widely distributed resources of data analysis and multiple levels of proteomic clinical and behavior information. The distributed collections of heterogeneous information resources will be large-scale. The intelligent search engines are beyond the capability of current web search engines and protocols. The TBI neuroproteome center distributed information retrieval component is a set of search engines that extend Emerge. Such an intelligent search engine should allow nomenclature, syntactic, and semantic differences in queries, data, and meta information. It should permit type, format, representation, and model differences as well in databases. In our TBI neuroproteome research, we have to compare information among proteomics and clinical data, such as chromatograms, mass spectra, gel images, peptide and protein sequences, and fMRI images. We will need a set of interoperable search engines to guide users finding information of various domains, formats, types, and levels of granularity (e.g., peptide, protein, cell, and system levels).

In addition, the interoperability of databases and analysis tools will establish a proteomics problem-solving environment. Thus users of the problem-solving environment will also be factored into the interoperability. Whatever users need—small versus large data sets, interactive versus batch computation—will require design and implementation of data and event services. For the current studies we intend to develop a neuroproteomics workbench to gather a collection of data analysis tools for neuroproteomics, as well as TBI neuroproteomics datasets:

1. Peptide sequencing and protein identification by MALDI-TOF MS and LC-MS/MS (Lu and Chen, 2003; Tabb *et al.*, 2002).
2. Protein peak patterns and single protein retention time from 1D or 2D liquid chromatograms.

3. Protein database searching algorithms such as SEQUEST (Yates, 1998).

The integration of databases with proteomic computational algorithms will be based on the object-oriented data modeling and data semantics discussed earlier. The Object Data Management Group (ODMG)-compliant data analysis and databases are highly relevant to the Common Component Architecture. In high-throughput computing, in terms of parallel or multithreaded objects, components (data and algorithms alike) may be distributed over a wide area grid of resources and distributed services.

C. Data Mining

Our neuroproteomics initiative has placed significant effort in new data mining and analysis tools for differential protein expression, protein network and modification analysis, and validation. A unique data-mining workbench will be created to explore protein network and pathways underlying the pathobiology of TBI from a neuroproteomics perspective. Novel data-mining tools will include a differential analysis tool for research on proteins and protein fragments involved in TBI and construction of cognitive maps. Furthermore, the cognitive maps will be used for TBI-induced differential neuroproteome validation and possible brain injury diagnosis.

1. Creating Cognitive Maps for TBI-Induced Differential Proteome

New data mining tools for TBI-induced differential proteome analysis and validation are being developed at our center. There are three major zones of neuroproteomics information: (1) pathophysiological stasis (including TBI, other CNS injuries such as ischemic stroke, aging, environmental toxin or substance-abuse–induced brain injury, and neurodegenerative diseases such as Alzheimer's or Parkinson's), (2) neuroproteome stasis (pathology-mediated differential protein expression, protein synthesis and metabolism, alternative mRNA splicing and RNA editing, protein-protein interaction, enzymatic activity, or protein functions), post-translational modifications (e.g., protein cross-linking, acetylation, glycosylation protein proteolysis and processing, phosphorylation), and protein-protein interaction and networks and signal-transduction pathways, and (3) sources of neuroproteomics data (Fig. 10). These sources include brain tissue (from different areas or anatomical regions of the brain, such as hippocampus and cerebral cortex), biological fluids such as CSF, and blood samples (including plasma and serum) in which brain proteins stasis might be reflected upon via diffusion-based equilibrium or blood-brain barrier compromise (e.g., from brain to CSF to blood).

Collection of data from these three components will enable the construction of multiple cognitive maps (Axelrod, 1976; Kohn and Letzkus, 1983; Kosko,
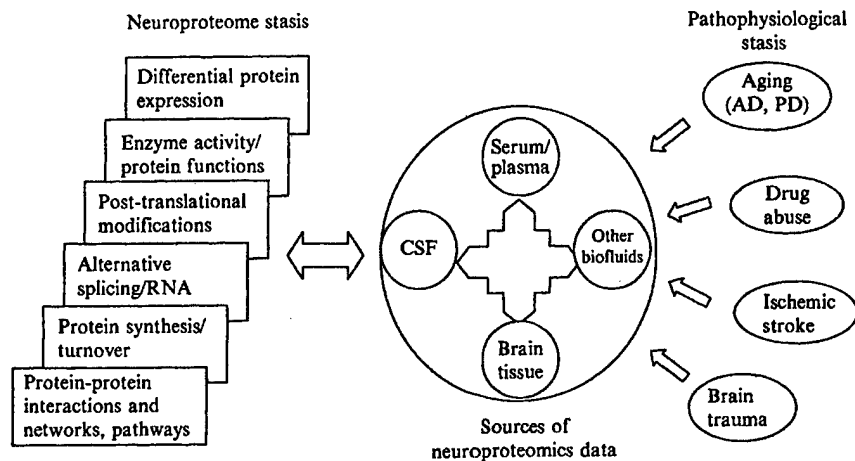
FIG. 10. Putative cognitive maps for the brain injury neuroproteome. The brain injury cognitive maps encompass three major areas (pathophysiological stasis, neuroproteome stasis, and sources of neuroproteomic data).

1986; Shi et al., 2002; Zhang et al., 1989). For instance, cognitive maps will be constructed for the TBI-induced differential proteome, such as the one shown in Fig. 9 for the brain injury neuroproteome. Automated reasoning and knowledge discovery algorithms (Chen, 1986, 1987; Chen and Markowitz, 1995, 1988, 2000a; Kitano, 2000) will distill the information and present the knowledge gained from a systems biology perspective. Thus cognitive maps will enable the brain trauma researchers to gain a greater understanding of the entire TBI-induced differential neuroproteome and hopefully the mechanistic protein-pathways of TBI.

2. Using Cognitive Maps for TBI-induced Differential Neuroproteome Validation

A statistical analysis tool is also being developed for TBI-induced differential neuroproteome validation and possible TBI protein-pathways elucidation. For example, up- or down-regulation of multiple proteins and protein fragments in control and injured samples will be quantified by ICAT, AQUA, or ELISA to validate differential TBI neuroproteome. Linear discriminant analysis (LDA) will be used to calculate the probability of a correct diagnosis given the number of injury-specific biomarkers measured the number of samples, etc. Thus statistical analysis tools are expected to provide an important component for all the TBI neuroproteomics research conducted at our neuroproteomics center.

VII. Prospective Utilities of TBI Proteomics Data

In summary, proteomics study of both human and rat traumatic brain injury, if approached systemically, is a very fruitful and powerful analytical technology. To obtain a comprehensive TBI neuroproteome dataset, it is important to integrate multiple protein separation and protein identification technologies. Equally important is the optimization of individual protein separation and identification methods. The bioinformatic platform then becomes the critical adhesive component by serving two purposes: (1) integrating all proteomics datasets and other relevant biological or clinical information, and (2) inferring and elucidating the protein-based pathways and biochemical mechanisms underlying the pathobiology of TBI and identifying and validating biomarkers for the diagnosis and monitoring of TBI (Goldknopf *et al.*, 2003). Ultimately, if we are to be successful, the TBI proteomics approach outlined here must be further integrated with genomics, cytomics, as well as systems biology approaches (Kitano, 2002a,b).

References

Adkins, J. N., Varnum, S. M., Auberry, K. J., Moore, R. J., Angell, N. H., Smith, R. D., Springer, D. L., and Pounds, J. G. (2002). Toward a human blood serum proteome: Analysis by multidimensional separation coupled with mass spectrometry. *Mol. Cell Proteomics* **1**, 947–955.

Aebersold, R., and Watts, J. D. (2002). The need for national centers for proteomics. *Nature Biotech.* **20**(7), 651.

Appel, R. D., Bairoch, A., and Hochstrasser, D. F. (1999). 2-D databases on the World Wide Web in methods in molecular biology. *In* "2-D Proteome Analysis Protocols" (A. J. Link, Ed.), vol. 112, pp. 383–391. Humana Press, Totowa, NJ.

Axelrod, R. (1976). "Structure of Decision." Princeton University Press, Princeton, NJ.

Bienvenut, W. V., Deon, C., Pasquarello, C., Campbell, J. M., Sanchez, J. C., Vestal, M. L., and Hochstrasser, D. F. (2002). Matrix-assisted laser desorption/ionization-tandem mass spectrometry with high resolution and sensitivity for identification and characterization of proteins. *Proteomics* **2**, 868–876.

Bjellqvist, B., Ek, K., Righetti, P. G., Gianazza, E., Gorg, A., and Westermeier, R. (1982). Isoelectric focusing in immobilized pH gradients: Principle, methodology and some applications. *J. Biochem. Biophys. Methods* **6**, 317–339.

Boguslavsky, J. (2003). Resolving the proteome by relying on 2DE methods. *Drug Discovery Develop.* **6**(7), 57–60.

Cattell, R. G. G. (Ed.) (1996). "The Object Database Standard: ODMG-93." Morgan Kaufmann, San Mateo, CA.

Chakravarti, D. N., Chakrarti, B., and Moutsatsos, I. (2003). Informatic tools for proteome profiling. High throughput proteomics; protein arrays. *BioTechnoques* **3**(Suppl.), 4–15.

Chen, S. (1988). Knowledge acquisition on neural networks, uncertainty and intelligent systems. In "Lecture Notes in Computer Science" (B. Bouchon, L. Saitta, and R. R. Yager, Eds.), vol. 313, pp. 281–289. Springer-Verlag.

Chen, I. A., and Markowitz, V. M. (1995). An overview of the object protocol model (OPM) and the OPM data management tools. Information Systems 20, 393–418.

Chen, S., (1986). Some extensions of probabilistic logic, Proc. AAAI Workshop on Uncertainty in Artificial Intelligence, Philadelphia, August 8–10, 1986, pp. 43–48, an extended version appeared in "Uncertainty in Artificial Intelligence," vol. 2, (L. N. Kanal, and J. F. Lemmer Eds.), North-Holland, Amsterdam, Holland.

Chen, S. (1987). Automated reasoning on neural networks: A probabilistic approach. IEEE First International Conference on Neural Networks, San Diego, June 21–24, 1987.

Chen, S. (2000a). Knowledge discovery of gene functions and metabolic pathways. IEEE BioInformatic and Biomedical Engineering Conference, Washington, November 2000.

Chen, S. (1998). "Digital Libraries: The Life Cycle of Information." BE Publisher, Columbus, OH.

Davidsson, P., Westman-Brinkmalm, A., Nilsson, C. L., Lindbjer, M., Paulson, L., Andreasen, N., Sjogren, M., and Blennow, K. (2002). Proteome analysis of cerebrospinal fluid proteins in Alzheimer patients. Neuroreport 13(5), 611–615.

Denslow, N. D., Michel, M. E., Temple, M. D., Hsu, C., Saatman, K., and Hayes, R. L. (2003). Application of proteomics technology to the field of neurotrauma. J. Neurotrauma 20, 401–407.

Derra, S. (2003). Lab-on-a-chip technologies emerging from infancy. Drug Disc. Develop. 6(5), 40–45.

Dixon, C. E., Clifton, G. L., Lighthall, J. W., Yaghmai, A. A., and Hayes, R. L. (1991). A controlled cortical impact model of traumatic brain injury in the rat. J. Neurosci. Methods 39(3), 253–262.

Fang, Z., Polacco, M., Chen, S., Schroeder, S., Hancock, D., Sanchez, H., and Coe, E. (2003). cMap: The comparative genetic map viewer. Bioinformatics 19, 416–417.

Finnie, J. (2001). Animal models of traumatic brain injury: A review. Aust. Vet. J. 79(9), 628–633.

Fountoulakis, M., Hardmaier, R., Schuller, E., and Lubec, G. (2000). Differences in protein level between neonatal and adult brain. Electrophoresis 21(3), 673–678.

Fountoulakis, M., Schuller, E., Hardmeier, R., Berndt, P., and Lubec, G. (1999). Rat brain proteins: Two-dimensional protein database and variations in the expression level. Electrophoresis 20(18), 3572–3579.

Gerber, S. A., Rush, J., Stemman, O., Kirschner, M. W., and Gygi, S. P. (2003). Absolute quantification of proteins and phosphoproteins from cell lysates by tandem MS. Proc. Natl. Acad. Sci. USA 100, 6940–6945.

Goldknopf, I., Park, H. R., and Kuerer, H. M. (2003). Merging diagnostics with therapeutic proteomics. IVD Technology 9(1), 1–6.

Gorg, A., Postel, W., and Gunther, S. (1988). The current state of two-dimensional electrophoresis with immobilized pH gradients. Electrophoresis 9, 531–546.

Grant, S. G., and Blackstock, W. P. (2001). Proteomics in neuroscience: From protein to network. J. Neurosci. 21(21), 8315–8318.

Grant, S. G. N., and Husi, H. (2001). Proteomics of multiprotein complexes: Answering fundamental questions in neuroscience. Trends Biotechnol. (Suppl. 10), S49–S54.

Graslund, S., Falk, R., Brundell, E., Hoog, C., and Stahl, S. (2002). A high-stringency proteomics concept aimed for generation of antibodies specific for cDNA-encoded proteins. Biotechnol. Appl. Biochem. 35(Pt 2), 75–82.

Gygi, S. P., Rist, B., Gerber, S. A., Turecek, F., Gelb, M. H., and Aebersold, R. (1999). Quantitative analysis of complex protein mixtures using isotope-coded affinity tags. Nat. Biotechnol. 17, 994–999.

Gygi, S. P., et al. (2000). Mass spectrometry and proteomics. Analytical Techniques 4, 489–494.

Hanash, S. (2004). HUPO initiatives relevant to clinical proteomics. Mol. Cell Proteomics. 298–301.

Hanash, S. M. (2003). Disease proteomics. Nature 422(6928), 226–232.

Hayes, R. L., Newcomb, J. K., Pike, B. R., and DeFord, S. M. (2001). Contributions of calpains and caspases to cell death following traumatic brain injury. *In* "Head Trauma: Basic, Preclinical and Clinical Aspects" (L. P. Miller and R. L. Hayes, Eds.), vol. 10, pp. 219–237. Wiley & Sohs, New York, NY.

Hochstrasser, D. F., Sanchez, J. C., and Appel, R. D. (2002). Proteomics and its trends facing nature's complexity. *Proteomics* **2**(7), 807–812.

James, P. (2002). Chips for proteomics; a new tool or just hype? High throughput proteomics; protein arrays *BioTechniques* **12**(Suppl.), 14–23.

Janssen, D. (2003). Major approaches to identifying key PTMs. *Genomics and Proteomics* **3**(1), 38–41.

Jungblut, P., Thiede, B., Zimny-Arndt, U., Muller, E. C., Scheler, C., and Wittmann-Liebold, B. (1996). Resolution power of two-dimensional electrophoresis and identification of proteins from gels. *Electrophoresis* **17**, 839–847.

Kitano, H. (2000). Perspectives on systems biology, "New Generation Computing," Vol. 18, No. 3. Ohm-sha, Springer-Verlag, New York Inc.

Kitano, H. (2002a). Systems biology: A brief overview. *Science* **295**(5560), 1662–1664.

Kitano, H. (2002b). Computational systems biology. *Nature* **420**(6912), 206–210 (review).

Kohn, M. C., and Letzkus, W. J. (1983). A graph theoretical analysis of metabolic regulation. *J. Theoretical Biology* **100**, 293–304.

Kosko, B. (1986). Fuzzy cognitive maps. *Int. J. Man-Machine Studies* **24**, 65–75.

Kusnezow, W., and Hoheisel, J. D. (2002). Antibody microarrays: Promises and problems. High throughput proteomics; protein arrays. *Bio Tech.* **12**(Suppl.), 14–23.

Lemkin, P. F. (1997). Comparing two-dimensional electrophoretic gel images across the Internet. *Electrophoresis* **18**, 2759–2773.

Lu, B., and Chen, T. (2003). A suffix tree approach to the interpretation of tandem mass spectra: Applications to peptides of non-specific digestion and post-translational modifications. *Bioinformatics* **19**(Suppl. 2), II113–II121.

Lubec, G., Krapfenbauer, K., and Fountoulakis, M. (2003). Proteomics in brain research: Potentials and limitations. *Prog. Neurobiol.* **69**(3), 193–211.

Mendes, P. (1993). GEPASI: A software package for modelling the dynamics, steady, states and control of biochemical and other systems. *Comput. Appli. Biosci.* **9**, 563–571.

Mendes, P. (1997). Biochemistry by numbers: Simulation of biochemical pathways with Gepasi 3. *Trends Biochem. Sci.* **22**, 361–363.

Meyer, H. E., Klose, J., and Hamacher, M. (2003). HBPP and the pursuit of standardisation. *Lancet Neurol.* **2**(11), 657–658.

Moody, M. D. (2001). Array-based ELISAs for high-throughput analysis of human cytokines. *Bio Tech.* **31**, 186–194.

Patton, W. F. (2002). Detection technologies in proteome analysis. *J. Chromatogr. B. Analyt. Technol. Biomed. Life Sci.* **771**(1–2), 3–31.

Peng, J., Elias, J. E., Thoreen, C. C., Licklider, L. J., and Gygi, S. P. (2003). Evaluation of multidimensional chromatography coupled with tandem mass spectrometry (LC/LC-MS/MS) for large scale protein analysis: The yeast proteome. *J. Proteome Res.* **2**, 43–50.

Peng, J., and Gygi, S. P. (2001). Proteomics: The move to mixtures. *J. Mass. Spectrom.* **36**(10), 1083–1091.

Pike, B. R., Flint, J., Dave, J. R., Lu, X.-C. M., Wang, K. K. W., Tortella, F. C., and Hayes, R. L. (2004). Accumulation of calpain and caspase-3 proteolytic fragments of brain-derived all-spectrin in CSF after middle cerebral artery occlusion in rats. *J. Cereb. Blood Flow Metab.* **24**(1), 98–106.

Pike, B. R., Flint, J., Dutta, S., Johnson, E., Wang, K. K. W., and Hayes, R. L. (2001). Accumulation of non-erythroid all-spectrin and calpain-cleaved all-spectrin breakdown products in cerebrospinal fluid after traumatic brain injury in rats. *J. Neurochem.* **78**, 1297–1306.

Raabe, A., Grolms, C., and Seifert, V. (1999). Serum markers of brain damage and outcome prediction in patients after severe head injury. *Br. J. Neurosurg.* **13**, 56–59.

Raghupathi, R., Graham, D. I., and McIntosh, T. K. (2000). Apoptosis after traumatic brain injury. *J. Neurotrauma* **17**(10), 927–938.

Reddy, V. N., Mavrovouniotis, M. L., and Liebman, M. N. (1993). Petri net representations in metabolic pathways. *Proc. ISMB* **1**, 328–336.

Reyes, D. R., Iossifidis, D., Auroux, P. A., and Manz, A. (2002). Micro total analysis systems. I. Introduction, theory, and technology. *Anal. Chem.* **74**(12), 2623–2636.

Romner, B., Ingebrigtsen, T., Kongstad, P., and Borgesen, S. E. (2000). Traumatic brain damage: Serum S-100 protein measurements related to neuroradiological findings. *J. Neurotrauma* **17**(8), 641–647.

Schäfer, H., Marcus, K., Sickmann, A., Herrmann, M., Klose, J., and Meyer, H. E. (2003). Identification of phosphorylation and acetylation sites in alphaA-crystallin of the eye lens (mus musculus) after two-dimensional gel electrophoresis. *Anal. Bioanal. Chem.* **376**(7), 966–972.

Schwartz, D. C., and Hochstrasser, M. (2003). A superfamily of protein tags: Ubiquitin, SUMO and related modifiers. *Trends Biochem. Sci.* **28**(6), 321–328.

Service, R. F. (2001). Gold rush—High-speed biologists search for gold in proteins. *Science* **294**(5549), 2074–2077.

Shi, H., Rodriguez, O., Shang, Y., and Chen, S. (2002). Integrating adaptive and intelligent techniques into a web-based environment for active learning. *In* "Intelligent Systems: Technology and Applications" (C. T. Leondes, Ed.), vol. 4, pp. 229–260. CRC Press, Boca Raton, Fla.

Smith, R. D. (2000). Probing proteomes—seeing the whole picture? *Nat. BioTech.* **18**, 1041–1042.

Somogyi, R., and Sniegoski, C. A. (1996). Modeling the complexity of genetic networks: Understanding multigenic and pleiotropic regulation. *Complexity* **1**, 45–63.

Tabb, D. L., McDonald, W. H., and Yates, J. R. (2002). DTASelect and contrast: Tools for assembling and comparing protein identifications from shotgun proteomics. *J. Proteome Res.* **1**, 21–26.

Unlu, M., Morgan, M. E., and Minden, J. S. (1997). Difference gel electrophoresis: A single gel method for detecting changes in protein extracts. *Electrophoresis* **18**(11), 2071–2077.

Wiesner, A. (2004). Detection of tumor markers with ProteinChip technology. *Curr. Pharm. Biotechnol.* **5**(1), 45–67.

Yan, J. X., Devenish, A. T., Wait, R., Stone, T., Lewis, S., and Fowler, S. (2002). Fluorescence two-dimensional difference gel electrophoresis and mass spectrometry based proteomic analysis of *Escherichia coli. Proteomics* **2**(12), 1682–1698.

Yates, J. R., III, Carmack, E., Hays, L., Link, A. J., and Eng, J. K. (1999). Automated protein identification using microcolumn liquid chromatography-tandem mass spectrometry. *In* "Methods in Molecular Biology" (A. J. Link, Ed.), vol. 112, pp. 553–569. Human Press, Totowa, N. J.

Yates, J. R., Morgan, S. F., Gatlin, C. L., Griffin, P. R., and Eng, J. K. (1998). Method to compare collision-induced dissociation spectra of peptides: Potential for library searching and subtractive analysis. *Anal. Chem.* **70**, 3557–3565.

Zhang, W. R., Chen, S., and Bezdek, J. C. (1989). Pool2: A generic system for cognitive map development and decision analysis. *IEEE Trans. SMC* **19**, 31–39.

Application of Proteomics Technology to the Field of Neurotrauma

NANCY DENSLOW,[1] MARY ELLEN MICHEL,[2] MEREDITH D. TEMPLE,[3]
CHUNG Y. HSU,[4] KATHRYN SAATMAN,[5] and RONALD L. HAYES[6]

ABSTRACT

Near-completion of the Human Genome Project has stimulated scientists to begin looking for the next step in unraveling normal and abnormal functions within biological systems. Consequently, there is new focus on the role of proteins in these processes. Proteomics is a burgeoning field that may provide a valuable approach to evaluate the post-traumatic central nervous system (CNS). Although we cannot provide a comprehensive assessment of all methods for protein analysis, this report summarizes some of the newer proteomic technologies that have propelled this field into the limelight and that are available to most researchers in neurotrauma. Three technical approaches (two-dimensional gel electrophoresis, direct analysis by mass spectrometry, including two-dimensional chromatography coupled to mass spectrometry and isotope coded affinity tags, and antibody technologies) are reviewed, and their advantages and disadvantages presented. A discussion of proteomic technology in the context of brain and spinal cord trauma follows, addressing current and future challenges. Proteomics will likely be very useful for developing diagnostic predictors after CNS injury and for mapping changes in proteins after injury in order to identify new therapeutic targets. Neurotrauma results in complex alterations to the biological systems within the nervous system, and these changes evolve over time. Exploration of the "new nervous system" that follows injury will require methods that can both fully assess and simplify this complexity.

Key words: brain trauma; mass spectroscopy; proteomics; spinal cord trauma

INTRODUCTION

THE MAPPING OF THE HUMAN GENOME has provided new technologies and theories necessary to tackle evaluation of very complex biological systems. Assessment of genetic information and the interactions of genes with environmental influences will advance understanding of basic neurobiology, pathophysiology of disease states, and potential therapies. However, genetics cannot completely answer the questions that arise in studying injury in the nervous system. Indeed in a variety of fields, scientists criticize the use of genomics as a tool, because DNA sequencing provides only a snapshot of the different ways a cell may use its genes. Any cell constantly reacts to its

[1]Biotechnology Program, University of Florida, Gainesville, Florida.
[2]Repair and Plasticity Program, National Institute for Neurological Disorders and Stroke, Bethesda, Maryland.
[3]National Institute of Biomedical Imaging and Bioengineering, Bethesda, Maryland.
[4]Department of Neurology, Washington University School of Medicine, St. Louis, Missouri.
[5]Department of Neurosurgery, University of Pennsylvania School of Medicine, Philadelphia, Pennsylvania.
[6]McKnight Brain Institute, University of Florida College of Medicine, Gainesville, Florida.

changing environment, creating a dynamic system (Persidis, 2000), and there seems to be a low correspondence ($R^2 = 0.61$) between changes at the transcription level and changes at the proteomic level (Ideker et al., 2001). Although proteomics is in some ways a "catch-all" term, it conceptualizes the many complex interactions that occur in the cellular repertoire for proteins. These events include genome-coded processes and posttranslational modifications, as well as interactions among proteins, nucleic acids, lipids, and carbohydrates (Persidis, 2000).

As of 2001, the Human Genome Project estimated that there are only about 30,000 genes (Claviere, 2001; Venter et al., 2001). Although the final figure is currently under debate (Shouse, 2002), this relatively low number of genes suggests greater roles for regulation of RNA translation and posttranslational modifications of resulting proteins in the cellular response to normal and pathological stimuli. Researchers have been investigating individual proteins or protein families in basic biology and disease for decades, but the field of proteomics offers a more global perspective. Because such analysis embraces the study of large numbers of inter-related proteins and their involvement in selected physiological or pathological states, a more robust appreciation of the injured nervous system may emerge.

This report serves as a beginning for the broad appreciation of the burgeoning field of proteomics. Here, we discuss the advantages and disadvantages of selected methodologies, and how they can be applied to study cellular events that occur after trauma to the brain or spinal cord. We will concentrate on the "gold standard" two-dimensional gel electrophoresis (2D GE) and a representation of emerging technologies for the field of neurotrauma that can be used in laboratories that do not have proteomics per se as a focus. The usefulness of proteomic investigation in neuroscience in general is currently under intense discussion (Grant, 2001; Grant and Blackstock, 2001), and the field of neurotrauma can position itself to embrace or reject findings as they emerge.

CURRENT AND FUTURE TECHNIQUES FOR PROTEOMIC ANALYSIS

Acknowledged challenges for proteomics research surround the analysis of complex mixtures of proteins to identify expression profiles after a physical or chemical stress, and these issues certainly apply in neurotrauma. It has been estimated that there are around 300,000 proteins in the human proteome and likely similar numbers in animal models. The large number of proteins relative to genes can result from alternative splicing of transcripts, direct protein modifications due to specific cleavages, or

other post-translational events. Because so many potential proteins and multiple time points will be involved in any analysis of neural injury, approaches must be based on established biochemical principles and amenable to high throughput technologies. Techniques should allow sorting out of protein complexity, as well as analyzing and identifying proteins in low abundance or with atypical characteristics, such as basic or glycosylated proteins. Methods still need to be refined for studying protein–protein interactions, protein structure, and metabolic pathways. It is unlikely that one method of analysis can yield full information; most likely, a combination of different methods, each with its own specific advantages, will need to be employed. In addition, a major challenge will come in data storage and analysis, and biocomputing must be given extensive consideration whenever proteome-directed research is undertaken.

Two-Dimensional Gel Electrophoresis followed by Mass Spectrometric Identification of Proteins

This approach is the classic method for analyzing multiple proteins. Proteins are separated in the first dimension by isoelectric focusing (a property that depends on the relative amounts of acidic and basic amino acids in each protein) and in the second dimension by size. It is possible to see over 1,000 well-resolved proteins on a single gel. While the application of 2D GE is not new to neuroscience research (Amess and Tolkovsky, 1995; Buonocore et al., 1999; Charriaut-Marlangue et al., 1996), the new interest in this method is the ability to directly identify proteins that are differentially expressed by mass spectrometry (MS).

To identify proteins, each spot of interest is cut from the gel and digested with trypsin. The masses of the tryptic peptides are then obtained by MS (either MALDI TOF [Matrix-Assisted Laser Desorption Ionization Time-of-Flight] or LC-MS [Liquid Chromatography coupled to a Mass Spectrometer] and MS/MS) and are used to search databases for proteins that best match the experimental fragments obtained. With LC-MS/MS, it is possible to further subdivide the fragments and obtain amino acid sequence information which, when added to the database search, increases the chance of matching the protein.

Several improvements have made this method more robust and reproducible, including the discovery of better detergents and buffer combinations, new pH gradient strips, pre-cast SDS slab gels, more sensitive gel stains, and the development of difference gel electrophoresis (DIGE) (Unlu et al., 1997), which is now marketed freely as a kit by Amersham). The DIGE system involves a modification of the normal 2D gel method such that one is able to resolve both control and experimental samples in one gel. The two protein samples that are to be com-

pared, for example a control tissue and an injury tissue, are each pre-labeled with one of two cyanine dyes, Cy3 or Cy5. The labeled samples are mixed and co-migrated on the same gel in both dimensions, removing imperfections in the separation due to differences in the gel matrix, pH field, and other procedural effects. Because the samples are co-migrated, it is easy to quantify changes in protein expression and pick proteins that are altered by the treatment. The co-migration also reduces the number of gels that need to be performed for statistical purposes. The coupling of this method with mass spectrometry to identify proteins that are differentially expressed has recently been validated by Tonga et al. (2001) and is reviewed by Patton (2002).

These advances result in better resolution and visualization. Despite the improvements, 2D GE/MS remains technically complicated, and requires at least triplicate samples to be processed for statistical purposes. In addition, some classes of proteins are not detectable. including those that are rare (i.e., low abundance), small (i.e., under 2 kDa), glycosylated, of basic pH, or are integral membrane proteins. Table 1 lists the advantages and disadvantages to this method.

Overall Assessment of 2D GE

In general, 2D GE, especially DIGE, works well for protein discovery and is currently the most widely used technique for detecting proteins that have changed upon treatment. It is the only high-resolution method currently available to detect changes in post-translational modifications, including phosphorylation, which is critical to many proteins of significance to neuroscience. But 2D GE is still not able to detect the entire proteome, missing proteins that are present in low abundance and that

have isoelectric points outside the normal range of pH 4–9. A substantial advancement would be the development of high-throughput affinity purification methods for low abundance proteins. Kits to affinity purify specific groups of proteins, for example phosphoproteins, are now available through some commercial vendors, and these have catapulted the study of differential protein expression. New techniques and improvements continually arise in this area; however, the need for specialized training of personnel is critical for 2D GE and MS.

Non–Gel-Based Separations of Proteins Coupled to Mass Spectrometry

This technical category is very broad and constantly evolving (Washburn et al., 2001). Methodologies include, but are not limited to, separations of protein digests by various chromatography procedures. Table 2 summarizes advantages and disadvantages of these methods. Several two-dimensional chromatography methods have been developed that separate proteins by orthogonal chromatography steps, for example, ion exchange followed by reverse phase high-performance liquid chromatography (HPLC) (Washburn et al., 2001). Complex fractions can be further resolved by mass spectrometry (MS and MS/MS). For instance, advances with this technology enabled the identification of as many as 1,484 yeast proteins in a single experiment. This technology is particularly useful for comprehensive proteome projects, and specifically can be applied to identify proteins, for example, integral membrane proteins, that are normally missed by 2D GE.

Another innovative technology in this general area has been the development of isotope coded affinity tags (ICAT) (Gygi et al., 1999; Patton, 2002). A new, im-

TABLE 1. TWO-DIMENSIONAL GEL ELECTROPHORESIS WITH MASS SPECTROMETRY

Advantages	Disadvantages
Simultaneous high resolution of multiple proteins	Technical expertise required
Rapid comparison of multiple gels	Sample-to-sample variability
Ability to fluorescently label proteins and co-migrate them in the same gel	Multiple controls/experiimental samples necessary
Improved reagents available	Many rare proteins not visible
Compatible with pre-fractionation of samples (enriches rarer proteins)	Some classes of proteins not detectable (e.g., <2 kDa, basic, glycosylated)
Mass spectrometry identifies lower amounts of protein	Integral membrane proteins are under-represented in gels
Identify some post-translational modifications	
High-throughput capability	
Discovery of new, differentially expressed proteins	

TABLE 2. NON–GEL-BASED MASS SPECTROMETRY METHODS

Advantages	Disadvantages
No two-dimensional gel electrophoresis for initial separation	Requires high-resolution separation methods
Direct comparison of complex protein samples	For ICAT method, proteins without cysteine residues missed (10–15%)
High-throughput capability	Unlikely to identify post-translational modifications
Analyze wider range of protein concentrations	Requires sophisticated mass spectrometers and skill in running them
Discover novel/differentially expressed proteins and peptides	Commercially available reagents are very expensive
Analyses of proteins that are missed by two-dimensional gel electrophoresis (basic, acidic, small, integral membrane proteins)	

proved version of these tags, named cleavable ICAT, is now available in kit form from Applied Biosystems. Briefly, ICAT refers to a pair of affinity directed reagents, which differ from each other by nine mass units (a difference of nine ^{13}C-groups in the linker portion of the tag), and that target cysteine residues in proteins. A pair of reagents is used to tag the full proteome from control and treated cells (or tissue) with one or the other ICAT reagent, respectively. Every protein containing a cysteine residue would then be tagged appropriately. The reaction is highly specific and occurs with high efficiency. After tagging, the two protein groups are mixed and digested with trypsin. Fragments tagged by the reagents are separated on an avidin column, and the mixture is then further separated and analyzed by LC-MS/MS. Fragments generated from proteins in equal abundance in the two tissues will be only nine mass units apart (or multiples of nine, if the fragment contains more than one Cys), and of equal height in the mass spectrometer. Fragments from proteins that are differentially expressed will appear to be higher (or lower) than their corresponding partners. These fragments can then be targeted for MS sequencing. Identities of the parent compounds can be obtained by comparing the sequences to databases. While this method is outstanding for determining the amount of protein in relation to a treatment or injury, it is not useful for the detection of changes due to post-translational modifications. Because the protein is identified solely on the basis of MS/MS fragmentation of a single peptide, ICAT analysis works best with mass spectrometers that have high resolution and mass accuracy.

Overall Assessment of Direct Mass Spectrometry Methods

Non–gel-based mass spectrometry methods for identifying differentially expressed proteins have great po-

tential. These methods depend on high-resolution chromatography to separate complex mixtures of proteins prior to mass spectrometry, requiring capillary chromatography for sensitivity and high-resolution mass spectrometry for identification of proteins. In addition, new advances in bioinformatics are required for complex analyses of very large data files that are generated by these procedures. New developments in all these areas appear frequently in the literature, and as these methods become more robust and routine they may enable direct proteome analyses.

ICAT has the potential to provide excellent data in a short time frame and is worth considering, if the proper mass spectrometer is available. Even though post-translational modifications may not be amenable to this analysis, it can yield information for proteins that are newly synthesized in response to a stressor. This method may be the technique of choice for analyzing "pull downs" or "immunoprecipitates" without having to analyze the samples first by gel electrophoresis. Importantly, ICAT and other direct methods of global protein analysis complement the 2D GE/MS method.

Protein and Antibody Chips

The concept of evaluating thousands of proteins at once by a chip-based method is very appealing; however, this technology is still in early stages of development and will require considerable work to arrive at a point where it can be widely used to assess global differential protein expression. There are, however, several commercial companies that are currently offering protein arrays (Table 3) and others that have them under development (ProteoMonitor, 2002). Many approaches are used, but two main types of chips are being investigated: antibody-based and protein-based. In the case of antibody-based chips, antibodies to proteins of interest are fixed on an

404

TABLE 3. COMPANIES CURRENTLY OFFERING PROTEIN MICROARRAYS

Company name and website	Chip description
Adaptive screening www.adaptive-screening.com	Recombinant protein array
BD Biosciences Clontech www.clontech.com	Antibody array; fluorescent technology
Discerna www.discerna.co.uk	*In situ* array; cell-free synthesis
Hypromatrix www.hypromatrix.com	Four array products and custom antibody array services
Jenni Array Technologies www.jenni.com	Peptide, small molecule, kinase substrate arrays
Luminex www.luminexcorp.com	Microsphere/bead; cell signaling and kinase activity
Molecular Staging www.molecularstaging.com	Antibody arrays; rolling circle amplification technology
Pepscan www.pepscan.nl	Peptide arrays anchored to glass slides
Zeptosens www.zeptosens.com	Six pre-spotted microarrays with recognition elements

Adapted from ProteoMonitor (www.proteomonitor.com). Total listing was 30 companies, many of which are still developing their products.

inert surface (i.e., glass slide, membrane, beads) and probed with the full complement of proteins from the tissue of interest. Antibody-based chips will be used primarily to measure differential expression. Protein-based chips rely on placing proteins directly on the surface, and would be used primarily to test for protein–protein or protein–drug interactions. There are advantages and disadvantages to chip technology. For antibody-based chips, advantages include the use of single-chain, Fv antibody phage libraries to rapidly find appropriate antibodies for a large number of antigens. For protein-based chips, a critical need will be the use of recombinant vectors (e.g., full length expression; LaBaer personal communication)

for producing a full complement of proteins, including rare ones, for placement on a chip. Additional technical advantages are outlined in Table 4. However, disadvantages (Table 4) may likely include the need for prior knowledge of the protein (i.e., not ideal for protein discovery) as well as availability of high-affinity antibodies for the proteins to be examined.

Overall Assessment of the Chip and Antibody Method

This technology holds considerable promise for identifying differentially expressed proteins. Thus, it will be

TABLE 4. CHIP TECHNOLOGY

Advantages	Disadvantages
Measurement of hundreds of proteins in parallel	Prior knowledge of protein required
Antibodies of differing affinities can be on one chip	Necessary to have the antibodies
Possible use of very small samples (microdissection)	Antibody specificity is critical
Potential to distinguish post-translational modifications	Limited use with post-translational modifications (antibody must distinguish modified site)
Methods for amplifying signals under development	Dependent on antibody affinity and protein concentration

important to begin to consider how to build chips that may be of specific interest to CNS trauma. One starting point is the application of antibodies to proteins that are already known to be involved in CNS injury and/or repair. In the last two decades, an extensive body of literature has developed with respect to biochemical and cellular changes following traumatic injury to the brain and spinal cord. This knowledge could be a valuable starting point for developing "injury chips." In addition, studies using DNA microarrays could provide valuable information about changes at the mRNA level that may suggest additional proteins to evaluate. Although the technology is not standardized, starting to work in the area now could ensure that chips are developed that will be useful to the neurotrauma field in the future.

Bioinformatics

In order to achieve the best value of any method, full and meaningful analysis will be critical, and any proteomics approach will generate extensive data. It will be important to develop methods, or to apply methods developed by others, to interpret and categorize information in a useful manner. Approaches to analyzing proteomic data are already being addressed in a variety of fields. The use of large-scale proteomics technologies yielding proteome-wide maps to study expression or interaction will depend heavily on information storage, representation, and analysis. It is possible to access proteomics databases and software through the World Wide Web; however, the evolution of resources is very rapid. Trends and probable changes are discussed in a paper by Wojcik and Schachter (2000). Other investigators have also recognized the need for fast, accurate computational analysis of protein function, and have begun development of large-scale computational systems for the analysis of sequence and structure of proteins (Weir et al., 2001). In addition, researchers have employed searching algorithms to study proteomics spectra generated by mass spectroscopy (Petricoin et al., 2002). Investigators in CNS injury can usefully appropriate existing bioinformatics strategies and sculpt them to meet their specific needs.

DISCUSSION

The gold standard for protein determination is still two-dimensional gel electrophoresis (2D GE) followed by mass spectrometry (MS). This two-stage method allows for both hypothesis-driven and discovery-driven research strategies. New methods on the horizon include separations of proteins by non–gel-based methods followed by MS, methods that rely exclusively on molecular biology,

and protein/antibody chips. Although both antibody-based and protein-based chips are now available commercially, development is at a very early stage and interpretations of any studies will be cautious. All of these methods permit parallel processing of several proteins at once and have the potential for increasing the sensitivity of detection to allow the use of small amounts of material. With improvements in such methods, rare proteins and cell type–specific proteins may be evaluated.

Although the study of proteins is not new, the field of "proteomics" is. In the past, several studies of CNS injury have used the high-resolution power of 2D gel electrophoresis (Amess and Tolkovsky, 1995; Buonocore et al., 1999; Charriaut-Marlangue et al., 1996; Jenkins et al. 2002; Leski and Steward, 1996). The work of Kirschenbaum and Pulsinelli (1990) performed over a decade ago to analyze differences in phosphorylation patterns in ischemic rat hippocampus, striatum, and neocortex tissues was extremely interesting and forward thinking for its time. Now with the coupling of MS to aid in the identification of proteins that are regulated, this 2D GE approach becomes even more powerful. Many of the newer mass spectrometric techniques can identify proteins down in the attomole (10^{-18} moles) to low femtomole (10^{-15} moles) levels.

The study of CNS trauma is a dynamic and exciting area of neuroscience, and because there is a readily defined event, dissection of complex neurobiological consequences can be attempted in this context. Information gained will provide insight into processes of cell death, regeneration, and plasticity that will have relevance to many other developmental or degenerative neurological disorders. There are limitations to current proteomic technologies, including minimal rapid high-throughput screening and detection of post-translational modifications, as well as issues regarding appropriate and meaningful bioinformatics/data analysis and interpretation. In neurotrauma, protein modifications will be important: injury initiates a complicated sequence of cellular events that affects many aspects of cell signaling, genome-coded events, protein–protein interactions, and post-translational processes. It is clear that proteomic technologies could have a large impact on the study of CNS injury. Information obtained may be extremely valuable for several reasons: (1) use of high-throughput screening for proteins after injury may provide a timecourse of how large numbers of critical events are simultaneously altered after CNS injury; (2) use of proteomic techniques could help to develop reliable biomarkers for CNS trauma and post-injury outcome; and (3) proteomic techniques could be useful for screening potential therapeutic targets.

Both the field of proteomics and the application of proteomic technologies to CNS trauma are in early stages.

Proteomics as a field is growing and changing almost daily. At this point, there does not appear to be a "magic bullet" proteomic technology that will be applicable for every research question. Each investigator will need to carefully consider the goals of the proposed experiments in determining the appropriate proteomic approach to utilize. There will be many technical challenges that CNS trauma investigators will face as the field advances. As they begin to utilize proteomics more regularly, the potential "payoff" to be attained with this type of data far outweighs the current difficulties and limitations.

REFERENCES

AMES, B., and TOLKOVSKY, A.M. (1995). Programmed cell death in sympathetic neurons: a study by two-dimensional polyacrylamide gel electrophoresis using computer image analysis. Electrophoresis 16, 1255–1267.

BUONOCORE, G., LIBERATORI, S., BINI, L., et al. (1999). Hypoxic response of synaptosomal proteins in term guinea pig fetuses. J. Neurochem. 73, 2139–2148.

CHARRIAUT-MARLANGUE, C., DESSI, F., and BEN-ARI, Y. (1996). Use of two-dimensional gel electrophoresis to characterize protein synthesis during neuronal death in cerebellar culture. Electrophoresis 17, 1781–1786.

CLAVIERE, J.-M. (2001). What if there are only 30,000 human genes? Science 291, 1255–1258.

GRANT, S.G.N., and BLACKSTOCK, W.P. (2001). Proteomics and neuroscience: from protein to network. J. Neurosci. 21, 8315–8318.

GRANT, S.G.N., and HUSI, H. (2001). Proteomics of multiprotein complexes: answering fundamental questions in neuroscience. Trends Biotechnol. 19, S49–S54.

IDEKER, T., THORSSON, V., RANISH, J.A., et al. (2001). Integrated genomic and proteomic analyses of a systematically perturbed metabolic network. Science 292, 929–934.

JENKINS, L.W., PETERS, G.W., DIXON, C.E., et al. (2002). Conventional and functional proteomics using large format 2D gel electrophoresis 24 hours after controlled cortical impact (CCI) in postnatal day 17 rats. J. Neurotrauma 19, 715–740.

KIRSCHENBAUM, B., and PULSINELLI, W.A. (1990). Posthoc phosphorylation of proteins derived from ischemic rat hippocampus, striatum and neocortex. Brain Res. 12, 21–29.

LESKI, M.L., and STEWARD, O. (1996). Protein synthesis within dendrites: ionic and neurotransmitter modulation of synthesis of particular polypeptides characterized by gel electrophoresis. Neurochem. Res. 6, 681–690.

PATTON, W.F. (2002). Review: detection technologies in proteome analysis. J. Chromatogr. B 771, 3–31.

PERSIDIS, A. (2001). Proteomics. Nat. Biotechnol, 18, Suppl, IT45–IT46.

PETRICOIN, E.F., ARDEKANI, A.M., HITT, B.A., et al. (2002). Use of proteomic patterns in serum to identify ovarian cancer. Lancet 359, 572–577.

PROTEOMONITOR. (2002). On-line. Available: www.proteomonitor.com.

SHOUSE, B. (2002). Revisiting the numbers: human genes and whales. Science 295, 1457.

TONGE, R. SHAW, J., MIDDLETON, B., et al. (2001). Validation and development of fluorescence two-dimensional differential gel electrophoresis proteomics technology. Proteomics 1, 377–396.

UNLU, M., MORGAN, M.E., MINDEN, J.S. (1997). Difference gel electrophoresis: a single gel method for detecting changes in protein extracts. Electrophoresis 18, 2071–2077.

VENTER, J.C., ADAMS, M.D., MYERS, E.W., et al. (2001). The sequence of the human genome. Science 291, 1304–1351.

WASHBURN, M.P., WOLTERS, D., YATES III, J.R. (2001). Large-scale analysis of the yeast proteome by multidimensional protein identification technology. Nat. Biotechnol. 19, 242–247.

WEIR, M., SWINDELLS, M., and OVERINGTON, J. (2001). Insights into protein function through large-scale computational analysis of sequence and structure. Trends Biotechnol. 19, S61–S66.

WOJCIK, J., and SCHACHTER, V. (2000). Proteomic databases and software on the web. Brief Bioinform. 1, 250–259.

Address reprint requests to:
Mary Ellen Michel, Ph.D.
National Institute of Neurological
Disorders and Stroke
6001 Executive Blvd., Rm. 2227, MSC 9525
Bethesda, MD 20982-9525

E-mail: mm108w@nih.gov

Increased expression and processing of caspase-12 after traumatic brain injury in rats

Stephen F. Larner,* Ronald L. Hayes,*,† Deborah M. McKinsey,* Brian R. Pike*,[1] and Kevin K. W. Wang*,†

*Department of Neuroscience, Evelyn F. and William L. McKnight Brain Institute of the University of Florida, Center for Traumatic Brain Injury Studies, Gainesville, Florida, USA

†Department of Psychiatry, Evelyn F. and William L. McKnight Brain Institute of the University of Florida, Gainesville, Florida, USA

Abstract
Traumatic brain injury (TBI) disrupts tissue homeostasis resulting in pathological apoptotic activation. Recently, caspase-12 was reported to be induced and activated by the unfolded protein response following excess endoplasmic reticulum (ER) stress. This study examined rat caspase-12 expression using the controlled cortical impact TBI model. Immunoblots of fractionalized cell lysates found elevated caspase-12 proform (~60 kDa) and processed form (~12 kDa), with peak induction observed within 24 h post-injury in the cortex (418% and 503%, respectively). Hippocampus caspase-12 proform induction peaked at 24 h post-injury (641%), while processed form induction peaked at 6 h (620%). Semi-quantitative reverse transcriptase-polymerase chain reaction (RT-PCR) analysis confirmed elevated caspase-12 mRNA levels after TBI. Injury severity (1.0, 1.2 or 1.6 mm compression) was associated with increased caspase-12 mRNA expression, peaking at 5 days in the cortex (657%, 651% and 1259%, respectively) and 6 h in the hippocampus (435%, 451% and 460%, respectively). Immunohistochemical analysis revealed caspase-12 induction in neurons in both the cortex and hippocampus as well as in astrocytes at the contusion site. This is the first report of increased expression of caspase-12 following TBI. Our results suggest that the caspase-12-mediated ER apoptotic pathway may play a role in rat TBI pathology independent of the receptor- or mitochondria-mediated apoptotic pathways.
Keywords: apoptosis, calpain, caspase, traumatic brain injury, unfolded protein response.
J. Neurochem. (2004) **88**, 78–90.

Traumatic brain injury (TBI) causes progressive neuronal degeneration resulting from acute and delayed cell death that is mediated in part by caspases (Yakovlev *et al.* 1997; Clark *et al.* 1999, 2000). Previously, necrosis was thought to be the primary mode of cell death after TBI, but current reports have implicated apoptosis in the neuropathology of TBI (Rink *et al.* 1995; Colicos *et al.* 1996; Yakovlev *et al.* 1997; Conti *et al.* 1998; Newcomb *et al.* 1999; Clark *et al.* 2000). Apoptosis is critical to the sculpting and pruning of the CNS during development (Oppenheim 1991; Raff *et al.* 1993; Vaux and Korsmeyer 1999) and for homeostasis of tissues that require the elimination of aged and abnormal cells (Johnson *et al.* 1999). However, while apoptosis is normally under strict control, during acute and chronic pathological conditions such as after stroke or TBI, apoptosis can contribute to neuronal death. To date, studies of apoptosis in TBI have concentrated on two caspase-mediated apoptotic pathways termed the extrinsic and intrinsic pathways (Daniel 2000; Yakovlev and Faden 2001). The extrinsic pathway is initiated by the binding of specialized ligands to a family of plasma membrane receptors termed death receptors that results in the activation of caspases-8/10. In contrast, the intrinsic pathway involves the release of cytochrome c from the mitochondria which, in turn, activates caspase-9. Both pathways ultimately

lead to the activation of caspase-3. Recently, a novel caspase-12-mediated apoptotic pathway has been described that involves endoplasmic reticulum (ER) stress and the unfolded protein response (UPR) (Nakagawa et al. 2000).

The protease family of caspases plays a key role in the implementation of apoptosis in vertebrates (Jacobson et al. 1997). They are constitutively expressed as precursor proteins (pro-caspases) and are believed to have little or no enzymatic activity. Once activated, they are processed into large subdomains of approximately 20 kDa (p20) and small subdomains of approximately 10 kDa (p10) (Cohen 1997) that form heterotetramers, which possess enzymatic activity. The caspase family has been divided into two broad functional categories: initiator caspases (caspase-8, -9, -10 and -12) and effector caspases (caspase-3, -6 and -7). The initiator caspases are upstream in the apoptotic pathway and respond to apoptotic stimuli by undergoing autoproteolytic activation. The downstream effector caspases are processed by the active initiator caspases and are responsible for dismantling cellular structure. Recent studies have shown that caspase-12 functions as an initiator caspase and has been implicated in ER stress-induced apoptosis (Nakagawa et al. 2000; Rao et al. 2001, 2002; Yoneda et al. 2001).

The ER plays a critical role in a variety of processes, including protein synthesis and folding, and the maintenance of Ca^{2+} homeostasis. A number of recent studies demonstrate that ER stress causes the disruption of these and other normal functions and thus, the ER has garnered increased interest for its putative role in cellular pathology. In addition, the disruption of ER homeostasis is considered a causal factor in pathologically-relevant apoptosis and has been implicated in several neurodegenerative disorders (Aridor and Balch 1999; Soto 2003). For example, disruption of Ca^{2+} homeostasis leads to increased levels of cytosolic Ca^{2+}, which induce pathological activation of calpains after TBI (Pike et al. 1998), and the translocation of calpains to the ER surface where they can activate caspase-12 (Nakagawa and Yuan 2000). Recent attention has centered on the role of caspase-12 and its unique functional characteristic of being specifically activated by ER stress. For example, Nakagawa et al. (2000) have shown that caspase-12-deficient cells are resistant to inducers of ER stress-induced apoptosis. The molecular mechanisms by which caspase-12 mediates apoptosis are still under investigation, but recent work suggests that it functions by cleaving pro-caspase-9 without the involvement of cytochrome c and the apoptosome (Rao et al. 2001, 2002; Morishima et al. 2002). The hypothesized pathway of caspase activation in response to ER stress is active caspase-12 activates caspase-9 which, in turn, activates caspase-3 (Rao et al. 2001, 2002; Morishima et al. 2002). Importantly, this hypothesis suggests a putative therapeutic target that is temporally upstream of those focused on attenuating the mitochondrial-mediated (intrinsic) or extrinsic pathway.

This study tests the hypothesis that TBI induces increased expression of caspase-12 mRNA and protein levels that are related to injury severity in the cortex and hippocampus of rats, and that this expression is found primarily in neurons. Using a rodent model of lateral controlled cortical impact injury, this investigation characterized the time course for induction of caspase-12 mRNA, up-regulation of the zymogen and cleavage of caspase-12 into its processed and alleged active form. Induction of caspase-12 mRNA was observed with semi-quantitative real-time polymerase chain reaction (PCR) analysis within 6 h of TBI in the hippocampus and within 3 days in the cortex. Immunoblot analyses of the caspase-12 proform (~60 kDa) and processed form (~12 kDa) showed increased protein expression within 6 h as well. Immunochemical analyses revealed that caspase-12 was induced in neurons in both the ipsilateral cortex and hippocampus. There was also evidence that caspase-12 was up-regulated in astrocytes at the contusion site. Our findings demonstrate that caspase-12 is rapidly induced and processed after TBI, suggesting that caspase-12 may be an important upstream mediator and part of a newly discovered pathway leading to apoptosis following TBI.

Materials and methods

Surgical preparation and controlled cortical impact traumatic brain injury

A previously described cortical impact injury device was used to produce TBI in adult rats (Dixon et al. 1991; Pike et al. 1998). Cortical impact TBI results in cortical deformation within the vicinity of the impactor tip associated with contusion, and neuronal and axonal damage that is confined to the hemisphere ipsilateral to the site of injury. Adult male (280–300 g) Sprague–Dawley rats (Harlan, Indianapolis, IN, USA) were anesthetized with 4% isoflurane in a carrier gas of 1 : 1 O_2/N_2O (4 min), followed by maintenance anesthesia of 2.5% isoflurane in the same carrier gas. Core body temperature was monitored continuously by a rectal thermistor probe and maintained at 37 ± 1°C by placing an adjustable temperature controlled heating pad beneath the rats. Animals were mounted in a stereotactic frame in a prone position and secured by ear and incisor bars. A mid-line cranial incision was made, the soft tissues were reflected, and a unilateral (ipsilateral to site of impact) craniotomy (7 mm diameter) was performed adjacent to the central suture, midway between bregma and lambda. The dura mater was kept intact over the cortex. Brain trauma was produced by impacting the right cortex (ipsilateral cortex) with a 5 mm diameter aluminum impactor tip (housed in a pneumatic cylinder) at a velocity of 3.5 m/s with a 1.0 mm, 1.2 mm or 1.6 mm compression and 150 ms dwell time (compression duration). Velocity was controlled by adjusting the pressure (compressed N_2) supplied to the pneumatic cylinder. Velocity and dwell time were measured by a linear velocity displacement transducer (Lucas Shaevitz model 500 HR, Detroit, MI, USA) that produces an analog signal recorded by a storage-trace oscilloscope (BK Precision, model 2522B, Placentia, CA, USA). Sham-injured animals underwent identical surgical procedures but

did not receive an impact injury. Naïve animals received no surgery or injury. Appropriate pre- and post-injury management was maintained, and these measures complied with all guidelines set forth by the University of Florida Institutional Animal Care and Use Committee and the National Institutes of Health guidelines detailed in the Guide for the Care and Use of Laboratory Animals.

Tissue lysis and protein purification

Cortical and hippocampal tissues were collected from naïve animals or at 6 h to 14 days after sham injury or TBI. At the appropriate post-injury time-points, the animals were anesthetized with 4% isoflurane in a carrier gas of 1 : 1 O_2/N_2O (4 min) and subsequently killed by decapitation. Ipsilateral and contralateral (to the impact site) cortices and hippocampi were rapidly dissected and snap-frozen in liquid nitrogen. Tissue samples were stored at $-20°C$. The samples were homogenized in a glass tube with a Teflon dounce pestle in 15 volumes of ice-cold detergent-free buffer [50 mM Tris-HCl, pH 7.4, 1 mM EDTA, 2 mM EGTA, 0.33 M sucrose, 1 mM dithiothreitol (DTT)] containing a broad-range protease inhibitor cocktail (Roche Molecular Biochemicals, Indianapolis, IN, USA). Samples were centrifuged at 8000 *g* for 5 min at 4°C to remove the nuclei and mitochondria in order to increase the ER and cytosolic protein concentration. The subcellular supernatant fluids containing the lysosomal/ER and cytosolic proteins were then collected and sonicated for immunoblot analysis.

Immunoblot analysis

Protein concentrations of the subcellular tissue homogenate fractions were determined by the Detergent Compatible (DC) Assay for Protein (Bio-Rad Laboratories, Hercules, CA, USA) with albumin standards. Aliquots (40 µg) of each sample were prepared for sodium dodecyl sulfate–polyacrylamide gel electrophoresis (SDS–PAGE) by addition of 8× loading buffer [1× loading buffer contains 125 mM Tris-HCl (pH 6.8), 100 mM 2-mercapto-ethanol, 4% SDS, 0.01% bromophenol blue and 10% glycerol]. Samples with loading buffer were heated for 10 min at 96°C, centrifuged for 1 min at 10 000 *g*, and then resolved by SDS–PAGE on 4–20% Tris/glycine gels (Invitrogen Life Technologies, Carlsbad, CA, USA) at 150 V for 90 min at room temperature. Following electrophoresis, fractionated proteins were transferred to Immobilon-P polyvinylidene fluoride (PVDF) membrane (Millipore, Bedford, MA, USA) by the semi-dry method in a transfer buffer containing 39 mM glycine, 48 mM Tris and 5% methanol at 20 V for 2 h at room temperature. Ponceau Red (Sigma, St. Louis, MO, USA) was used to stain membranes to confirm successful transfer of protein and to insure that an equal amount of protein was loaded in each lane. Blots were blocked for 1 h at room temperature in 5% non-fat milk in TBST (20 mM Tris-HCl, 150 mM NaCl and 0.003% Tween-20, pH 7.5).

Immunoblots were probed with either the anti-β-actin monoclonal antibody to confirm equal amounts of protein loading (Sigma-Aldrich Co., St Louis, MO, USA) or anti-caspase-12 generated by Drs Michael Kalai and Peter Vandenabeele at the Flanders Interuniversity Institute for Biotechnology, University of Ghent, Ghent, Belgium. Following overnight incubation at 4°C (at 1 : 3000 for both primary antibodies) in 3% blocking solution plus 1% bovine serum albumin, blots were incubated for 1 h at room temperature in 3% non-fat milk/TBST containing a biotinylated-conjugated goat-anti-rabbit IgG (1 : 5000, Amersham Life Science,

Inc., Arlington Heights, IL, USA). Blots were then incubated for 30 min at room temperature in TBST containing a streptavidin alkaline phosphatase conjugate (1 : 5000, Amersham Life Science, Inc.). Bound antibodies were visualized at room temperature by color development with BCIP/NBT Phosphatase Substrate (Kirkegaard & Perry Laboratories, Gaithersburg, MD, USA).

Immunochemistry analysis

Brain tissues were collected from animals with naïve or with 1 day TBI. At the appropriate time-point, the animals were anesthetized using 4% isoflurane in a carrier gas of 1 : 1 O_2/N_2O (4 min) and subsequently killed by decapitation after transcardial perfusion. The animals were perfused with 200 mL 2% heparin (Elkins-Sinn, Inc., Cherry Hill, NJ, USA) in 0.9% saline (pH 7.4) followed by 400 mL 4% paraformaldehyde in 0.1 M phosphate buffer (pH 7.4). A total of 2 h in fix was followed by storage in either phosphate-buffered saline (PBS) or cryoprotection buffer.

Vibratome-cut 40 µm sections were fluorescent immunolabeled with cell type-specific monoclonal antibodies, the anti-caspase-12 polyclonal antibody and a nuclear counterstain. Briefly, tissue sections were rinsed in PBS then incubated for 1 h at room temperature in 2% goat serum/2% horse serum/0.2% Triton-X 100 in Tris-buffered saline (TBS; block) to decrease non-specific labeling. The sections were then incubated with two primary antibodies: the anti-caspase-12 (IN) antibody (Cell Signaling, Technologies, Beverly, MA, USA) at a concentration of 1 : 500, and either the mouse anti-neuron-specific nuclear protein antibody (neuronal nuclei–anti-NeuN) at a concentration of 1 : 1000 (Chemicon, Temecula, CA, USA), or the mouse astrocyte-specific anti-glial fibrillary acidic protein antibody (anti-GFAP) at a concentration of 1 : 1000 (Roche Molecular Biochemicals, Mannheim, Germany), for 4 days in block at 4°C. After being rinsed in TBST, the tissue sections were incubated with species-specific Alexa Fluor (Molecular Probes, Inc., Eugene, OR, USA) secondary antibodies at a concentration of 1 : 3000 in block for 1 h at room temperature. The sections were then washed in PBS, cover–slipped in Vectashield with DAPI (Vector Laboratories), viewed and digitally-captured with a Zeiss Axioplan 2 microscope equipped with a Spot Real Time (RT) Slider high resolution color CCD digital camera (Diagnostic Instruments, Inc., Sterling Heights, MI, USA). Sections without primary antibodies were similarly processed to control for binding of the secondary antibodies. On control sections, no specific immunoreactivity was detected.

RNA purification

Total RNA was isolated from control and injured samples of cortical or hippocampal tissue using TRIzol reagent (Gibco BRL, Rockville, MD, USA). Isopropanol precipitation and ethanol washes were performed according to the manufacturer's instructions. Samples were resuspended in 50–100 µL DEPC-treated water.

Reverse transcription

Total RNA (3 µg) was incubated with 1 µL oligo(dT) (0.5 mg/mL, Gibco BRL) at 70°C for 10 min, then at 4°C for 5 min. A reverse transcription reaction mixture was added to the RNA-oligo(dT) sample for a final volume of 20 µL, containing 20 mM Tris-HCl (pH 8.4), 50 mM KCl, 5 mM $MgCl_2$, 500 µM dNTPs, 10 mM DTT, 50 U SuperScript II reverse transcriptase (Gibco BRL) and 40 U

RNaseOUT recombinant ribonuclease inhibitor (Gibco BRL). The sample was incubated at 42°C for 55 min, 70°C for 15 min for enzyme denaturation, and then transferred to 4°C. Each sample was diluted to a final volume of 100 µL with DEPC-treated water.

Primer selection

Caspase-12-specific primers

For all base pair designations, refer to GeneBank locus AF317633, *Rattus norvegicus* caspase-12. 5′C12 (gcacattcctggtctttatgtccc, bp 743–766) recognizes an upstream mRNA-specific sequence in caspase-12 transcripts. 3′C12 (gccactgctgatacagatgaggaa, bp 961–984) recognizes a downstream caspase-12 mRNA-specific sequence.

GAPDH-specific primers

For all base pair designations for GAPDH-specific primers, refer to GeneBank locus AF106860. The upstream primer is designated 5′GPD (ggctgccttctcttgtgac, bp 903–921) and the downstream primer is designated 3′GPD (ggccgcctgcttcaccac, bp 1624–1641).

Standard PCR

A PCR reaction buffer was added to 2 µL of reverse transcription product for a final volume of 25 µL containing 20 mM Tris-HCl (pH 8.4), 50 mM KCl, 2.5 mM $MgCl_2$, 200 µM dNTPs, 0.5 µM dNTPs, 6% DMSO and 1.25 U *Taq* DNA polymerase (Gibco BRL). The mixture was then transferred to a PCR apparatus for amplification. Each denaturation, annealing and extension step was held for 30 s (two cycles of 95°C, 65°C and 72°C; then two cycles of 95°C, 62.5°C and 72°C; then 32 cycles of 95°C, 60°C and 72°C). Aliquots of PCR products were loaded onto 1.5% agarose gels and separated by electrophoresis in TAE buffer (40 mM Tris-acetate, 1 mM EDTA, pH 7.5) containing 5 µg/mL ethidium bromide. To assay for genomic DNA contamination, RNA samples underwent PCR amplification without prior reverse transcription. Any samples showing genomic contamination underwent repurification and repeat assay for genomic contamination prior to PCR analysis for transcript expression.

Semi-quantitative/LightCycler PCR

Real-time PCR was performed using a LightCycler rapid thermal cycler system (Roche Diagnostics) according to the manufacturer's instructions. Reactions were performed in a 10 µL volume with 0.5 µM primers and 2.5 mM $MgCl_2$. Other reagents including nucleotides, FastStart *Taq* DNA polymerase and buffer were used as provided in the LightCycler-FastStart DNA Master SYBR Green I reaction mix (Roche Diagnostics). The amplification protocol included: 5 min 95°C denaturation; one cycle with 95°C denaturation for 5 s, 65°C annealing for 10 s and 72°C extension for 35 s; one cycle with 95°C denaturation for 5 s, 62.5°C annealing for 10 s and 72°C extension for 35 s; then 30–40 cycles of 95°C denaturation for 5 s, 60°C annealing for 10 s and 72°C extension for 35 s. Detection of the fluorescent product occurred at the end of the 72°C extension periods. Specificity of the amplification product from each primer pair was confirmed by melting curve analysis of the PCR product and subsequent gel electrophoresis.

Quantification was performed by online monitoring for identification of the exact time-point at which the logarithmic linear phase could be distinguished from the background (crossing point). The crossing point is expressed as a cycle number.

Standard curve preparation and semi-quantitative PCR analysis

Maximal caspase-12 mRNA expression was identified between 6 h (cortex) and 1 day (hippocampus) after injury. The reverse transcription (RT) product from ipsilateral cortical and hippocampal RNA collected 6 h (cortex) and 1 day (hippocampus) after injury underwent serial dilution, creating a standard curve of 100%, 33%, 11% and 3.7% of original RT product. Each dilution from the standard curve was analyzed with the LightCycler PCR using primer sets for caspase-12 or GAPDH mRNA. For each primer set, a crossing point cycle number was determined for each dilution of the standard curve. Linear regression analysis of the logarithm of the dilution factor versus the crossing point cycle number generated a standard curve for each transcript-specific primer set. From each primer set's standard curve, a crossing point cycle number could be converted to a relative amount of RNA. For individual samples, the crossing point cycle number was identified with the LightCycler PCR. Using the standard curve for each primer set, the amount of caspase-12 or GAPDH mRNA was determined. The amount of each transcript in sham-injured animals was set at 100%, and the level of expression in an impact-injured sample was calculated as a percentage of sham-injured expression.

Statistical analyses

For the immunoblots ($n = 4$), semi-quantitative analysis was performed by computer-assisted densitometric scanning (ImageJ, version 1.29x, NIH, USA). Data were acquired as integrated densitometric values and transformed to percentages of the densitometric levels obtained from naïve animals visualized on the same blot. One-way ANOVA with Dunnett's multiple comparison tests was performed on the data using GraphPad Prism Version 3.03 for Windows (GraphPad Software, San Diego, CA, USA, http://www.graphpad.com). The 1 day and 7 day densitometric values for sham-injured animals were pooled after analysis by one-way ANOVA with Dunnett's multiple comparison tests for each specific day revealed no statistical differences. All values are given as mean ± SEM. Differences were considered significant if $p < 0.05$.

Verification that the semi-quantitative PCR method yielded results similar to northern blot analysis was shown in a previous paper by our laboratory (Tolentino *et al.* 2002). In summary, the northern blot analysis demonstrated a temporal profile of transcript induction in response to cortical injury. A linear regression analysis was performed comparing mRNA expression determined by PCR and northern blot, and the results from northern blot and PCR analyses fit a linear correlation with a slope = 1.01, $r^2 = 0.95$. A semi-quantitative PCR strategy that independently measures mRNA transcript levels has two major advantages over northern blot analyzes: (i) PCR amplification allows for detection of much lower levels of transcript expression, which is important for the analysis of caspase-12 mRNA expression in the brain; and (ii) a PCR-based approach decreases the amount of total RNA required for analysis, thereby facilitating analysis of smaller tissue samples and obviating the need to pool RNA samples prior to analysis. One-way ANOVA with Dunnett's multiple comparison tests was performed on the semi-quantitative PCR data using GraphPad Prism Version 3.03 for Windows. The data were normalized using logarithmic transformation. All values are given as mean ± SEM. Differences were considered significant if $p < 0.05$.

Results

Immunoblot analysis of caspase-12 expression after traumatic injury

Total cellular fractions, less nuclear and mitochondrial components as described above for the 1.6 mm cortical impact injury, were prepared from rat ipsilateral cortex and hippocampus to test the results of one of the three injury levels examined in the mRNA expression experiments. Caspase-12 expression was examined using the anti-caspase-12-specific antibody (Belgium), quantified by densitometric analysis and expressed as percentage of naïve control

levels adjusted for the sham effect (Figs 1 and 2). Figures 1(a) and 2(a) show immunoblot analyses for caspase-12 expression in rat ipsilateral cortex and hippocampus, respectively, for naïve and sham-injured control animals, and for TBI animals from 6 h to 14 days post-injury. Using the anti-caspase-12 antibody (Belgium), two distinct protein bands were identified: an approximately 60 kDa band corresponding to the zymogen (pro-casp12) and an approximately 12 kDa band that represents the small subunit of the active form of caspase-12 (Rao *et al.* 2001). Immunoblots were also run with equivalent amounts of protein and probed with the anti-β-actin antibody, which served as an internal control for
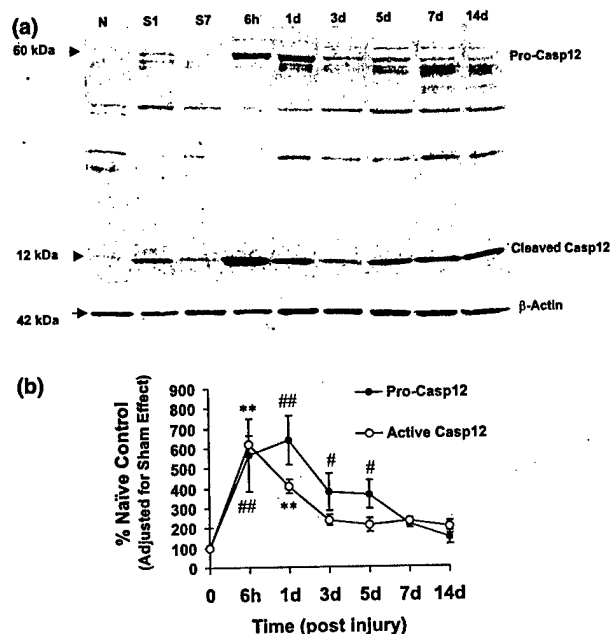

Fig. 1 Immunoblot analysis of pro- and active caspase-12 expression in ipsilateral cortical protein samples ($n = 4$ animals) using the anti-caspase-12-specific antibody (Belgium). (a) Samples were collected from naïve (N) rats, sham-operated rats 1 and 7 days after surgery (S1, S7), and from injured rats (1.6 mm impact) 6 h to 14 days after injury (6 h, 1d, 3d, 5d, 7d and 14d). The full-length caspase-12 protein and cleaved product (sizes in kDa) are indicated. Naïve rats served as injury controls. β-actin was directly assessed as an internal methods control. Since β-actin may itself be cleaved by caspases, blots were examined for cleaved fragments, but no fragments were detected. (b) Quantitative analysis: immunoblot analyses using the anti-caspase-12 antibody (Belgium) were quantified by densitometry and the levels of caspase-12 (pro- and active) expression in the ipsilateral cortex of injured animals after adjustment for the sham effect were calculated as a percentage of naïve control caspase-12 expression. One-way ANOVA with Dunnett's multiple comparison tests was performed to evaluate statistical significance. Comparison of caspase-12 expression in injured animals with naïve control animals adjusted for sham effect showed increased levels of expression that were statistically significant at 6 h, 1 day and 3 days post-injury for pro-caspase-12 ($^{\#\#}p < 0.01$) and cleaved caspase-12 ($^{**}p < 0.01$).

Fig. 2 Immunoblot analysis of pro- and active caspase-12 expression in ipsilateral hippocampal protein samples ($n = 4$ animals) using the anti-caspase-12-specific antibody (Belgium). (a) Samples were collected from naïve (N) rats, sham-operated rats 1 and 7 days after surgery (S1, S7), and from injured rats (1.6 mm impact) 6 h to 14 days after injury (6 h, 1d, 3d, 5d, 7d and 14d). The full-length caspase-12 protein and cleaved product (sizes in kDa) are indicated. Naïve rats served as injury controls. β-actin was directly assessed as an internal methods control. Since β-actin may itself be cleaved by caspases, blots were examined for cleaved fragments, but no fragments were detected. (b) Quantitative analysis: immunoblot analyses using the anti-caspase-12 antibody (Belgium) were quantified by densitometry and the levels of caspase-12 (pro- and active) expression in the ipsilateral hippocampus of injured animals were calculated after adjustment for the sham effect as a percentage of naïve control caspase-12 expression. One-way ANOVA with Dunnett's multiple comparison tests was performed to evaluate statistical significance. Comparison of caspase-12 expression in injured animals with naïve control animals adjusted for sham effect showed increased levels of expression that were statistically significant at 6 h and 1, 3 and 5 days post-injury for pro-caspase-12 ($^{\#}p < 0.05$, $^{\#\#}p < 0.01$) and 6 h and 1 day following injury for cleaved caspase-12 ($^{**}p < 0.01$).

protein loading and transfer. Loading and transfer were essentially equivalent in all wells, as shown by comparable 42 kDa signal intensities.

Immunoblot analysis of caspase-12 expression in cortex after traumatic injury

Tissue from sham-operated animals showed a modest increase in caspase-12 proform expression 1 day after craniotomy that was not statistically significant and declined to naïve levels by 7 days (Fig. 1a). After adjustment for sham effect, significant induction of the caspase-12 proform was observed within 6 h of cortical injury ($p < 0.01$) and peaked on day 1 (418% ± 30%, $p < 0.01$). Elevated expression was also detected 3 days post-injury before declining to naïve levels by 7 days (Fig. 1b, $p < 0.01$). Increased levels of processed caspase-12 were also observed within 6 h after cortical injury, with peak expression 1 day after injury (503% ± 40%, $p < 0.01$). Elevated expression levels continued to be statistically significant up to 3 days following injury before declining to near naïve levels (Fig. 1b).

Immunoblot analysis of caspase-12 expression in hippocampus after traumatic injury

Hippocampi from sham-injured animals showed a slight increase in proform and processed caspase-12 expression 1 day after craniotomy that was not statistically significant and declined to naïve levels by 7 days (Fig. 2a). After adjustment for the sham effect, elevated levels of caspase-12 induction for both the proform ($p < 0.01$) and processed form ($p < 0.01$) were observed within 6 h of TBI. In fact, levels of processed caspase-12 expression peaked at this early time-point (620% ± 46%) and remained significantly elevated 1 day post-injury (Fig. 2b). Pro-caspase-12 induction peaked later at 1 day after injury (641% ± 124%) and expression remained significantly elevated at 3 and 5 days following injury (Fig. 2b). Compared to the ipsilateral cortex, the ipsilateral hippocampus possessed greater caspase-12 protein induction over naïve controls for both the proform and the processed form. In addition, peak induction of the processed form occurred earlier in the hippocampus compared to the cortex (6 h vs. 1 day).

Standard curve generation for semi-quantitative PCR using serially-diluted cDNA

The highest levels of caspase-12 transcript expression were observed in ipsilateral cortex and hippocampus from 6 h to 1 day after injury (Fig. 3). Therefore, total RNA was collected 6 h and 1 day after injury from the ipsilateral cortex and hippocampus, respectively. Total RNA was then reverse transcribed and serially diluted to generate a standard curve of relative amounts of RNA. Samples underwent analysis using the LightCycler PCR with primer sets for caspase-12 or GAPDH mRNA. For each dilution sample (100%, 33.3%, 11.1% and 3.7%), the PCR analysis yielded a
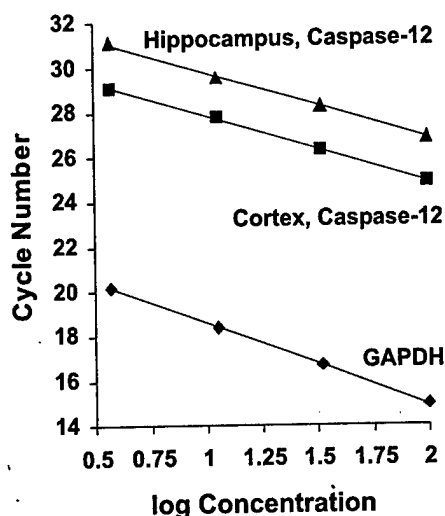

Fig. 3 Standard curve generation for caspase-12 and GAPDH specific quantitative real-time PCR. Total RNA was extracted from rat ipsilateral hippocampal (6 h post-injury) and cortical (1 day post-injury) tissue for caspase-12 expression and from ipsilateral cortical tissue (3 days post-injury) for GAPDH expression. RNA samples were reverse transcribed and cDNAs were serially diluted. Aliquots of the cDNA dilution curve underwent real-time PCR using primer pairs for caspase-12 mRNA or GAPDH mRNA. For each dilution and each primer set, the cycle number at which the PCR amplification entered the log-linear region was identified (crossing point cycle number). Standard curves were generated by plotting the log concentration of total RNA versus the crossing point cycle number. A linear regression analysis was performed; the r^2 ranged from 0.9895 to 1.000. For quantitation, RNA samples from naïve, sham and injured rats underwent real-time PCR, generating a crossing point cycle number for each primer set. Using the standard curves, the cycle number was converted to an amount of RNA. These amounts are expressed as a percentage of sham control RNA (= 100%).

crossing point cycle number for each primer pair (caspase-12 or GAPDH-specific). Figure 3 shows the linear regression analysis of each primer set's crossing point cycle number for each brain region versus the logarithm of the dilution factor. For each primer set, the range of crossing point cycle numbers required to cover the serially-diluted standard curve varied: 14–21 cycles for GAPDH, 25–29 cycles for caspase-12 (cortex) and 27–31 cycles for caspase-12 (hippocampus). These differences primarily reflect the abundance of the transcripts. GAPDH mRNA was the most abundant transcript requiring the fewest cycles, whereas caspase-12 hippocampal mRNA was the least abundant transcript and therefore required the most cycles.

Semi-quantitative PCR analysis of experimental samples

Using the standard curves generated as described above, the crossing point cycle numbers were converted to relative amounts of mRNA. These relative amounts were then expressed as percentage of naïve control adjusted for the
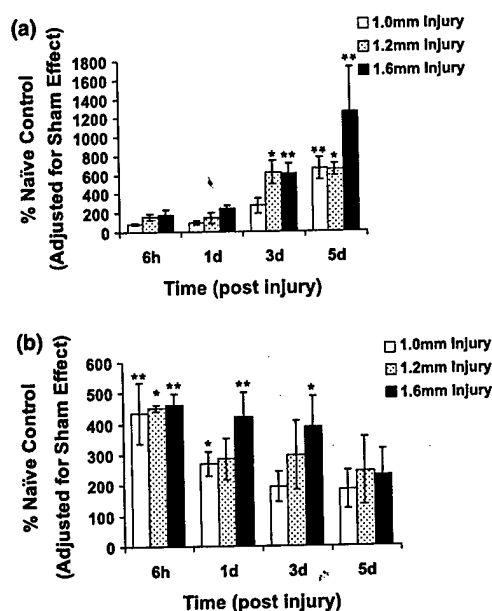
Fig. 4 Semi-quantitative real-time PCR analysis of caspase-12 mRNA expression in (a) cortex and (b) hippocampus. mRNA levels after adjustment for sham effect are expressed as a percentage of naïve control. One-way ANOVA with Dunnet's multiple comparison test was performed to evaluate statistical significance. Comparison of caspase-12 mRNA expression in the ipsilateral cortex (a) from injured animals with naïve control adjusted for sham effect, increased levels of expression were statistically significant at 3 days (1.2 and 1.6 mm injury) and 5 days (1.0, 1.2, and 1.6 mm injury) ($*p < 0.05$, $**p < 0.01$). Comparison of caspase-12 mRNA expression in the ipsilateral hippocampus (b) from injured animals with naïve control adjusted for sham effect, increased levels of expression were statistically significant at 6 h (1.0, 1.2 and 1.6 mm injury), 1 day (1.0 and 1.6 mm injury) and 3 days (1.6 mm injury) after injury ($*p < 0.05$, $**p < 0.01$).

sham effect. Figure 4 shows the time course of caspase-12 mRNA expression in ipsilateral cortex and hippocampus after cortical injury for three magnitudes of injury. The data noticeably convey the similarities in the up-regulation of mRNA levels following injury and illustrate the effect of injury severity on caspase-12 mRNA expression.

In the cortex, maximal and statistically significant caspase-12 mRNA expression was observed for all three injury magnitudes 5 days after injury: 1.0 mm, 657% ± 119% ($n = 3$, $p < 0.01$); 1.2 mm, 651% ± 65% ($n = 3$, $p < 0.05$); and 1.6 mm, 1259% ± 465% ($n = 3$, $p < 0.01$). Three days after injury, the 1.2 mm and 1.6 mm injury magnitudes produced significant increases in mRNA expression ($p < 0.05$ and $p < 0.01$, respectively), while mild impact (1.0 mm) failed to produce significant increases. However, in the hippocampus, maximal and significant caspase-12 mRNA levels were observed at 6 h for all three injury magnitudes: 1.0 mm, 435% ± 98% ($n = 3$, $p < 0.01$); 1.2 mm, 451% ± 10% ($n = 3$, $p < 0.05$); and 1.6 mm, 460% ± 36% ($n = 3$, $p < 0.01$). Significantly elevated

expression was detected at the 1 day (1.0 and 1.6 mm injury, $p < 0.05$ and $p < 0.01$, respectively) and 3 day (1.6 mm injury, $p < 0.05$) time-points.

Immunohistochemical analysis of caspase-12 expression after traumatic injury

Ipsilateral and contralateral cortical and hippocampal tissues were examined for caspase-12 induction following TBI. High magnification photomicrographs of the Alexa Fluor stains of uninjured animals revealed healthy cell bodies and little detectable caspase-12 expression (Fig. 5a, panel 1 and Fig. 6a, panel 1). In contrast, 1 day following injury caspase-12 expression was readily observed in both the ipsilateral cortex and hippocampus, with significant levels in the former immediately below the impact site (Fig. 5, panels 2 and 6; Fig. 6, panels 2 and 6).

Immunohistochemical analysis of caspase-12 expression in cortex after traumatic injury

The ipsilateral cortex at the site of the contusion revealed a considerable increase in caspase-12 expression with decreasing levels distal to the site of impact. The morphology of the injury site where the highest levels of caspase-12 induction were located had a decidedly disorganized, almost chaotic appearance when compared to the contralateral and naïve tissue. Caspase-12-immunopositive neurons (Fig. 5a, panel 5) included those cells with apoptotic bodies. It was also clear that caspase-12 was induced in astrocytes at the site of the contusion (Fig. 5b, panel 9) but could not be specifically identified in astrocytes distal to this location.

Immunohistochemical analysis of caspase-12 expression in hippocampus after traumatic injury

The ipsilateral hippocampus revealed induction of caspase-12 with caspase-12-immunopositive cells co-localizing with neuronal cell-specific marker NeuN (Fig. 6a, panel 5) but not with the astrocytic marker GFAP (Fig. 6b, panel 9).

Discussion

This is the first study to show increased expression of caspase-12 mRNA in injured cortex and hippocampus after mild to severe traumatic brain injury in rats, and increased caspase-12 protein expression and processing after severe injury. The study also shows evidence that the increased caspase-12 expression after TBI is found, predominantly, in neurons in the ipsilateral cortex and hippocampus, but also in cortical astrocytes located at the site of the contusion. In the ipsilateral cortex, immunoblot analysis revealed that levels of both the zymogen and the processed form of caspase-12 protein rapidly increased within 6 h of injury, peaking by about 1 day after injury when compared to naïve control. This was followed by a slow decline over the next 2 weeks, with protein levels returning to naïve levels by day 14. In the ipsilateral
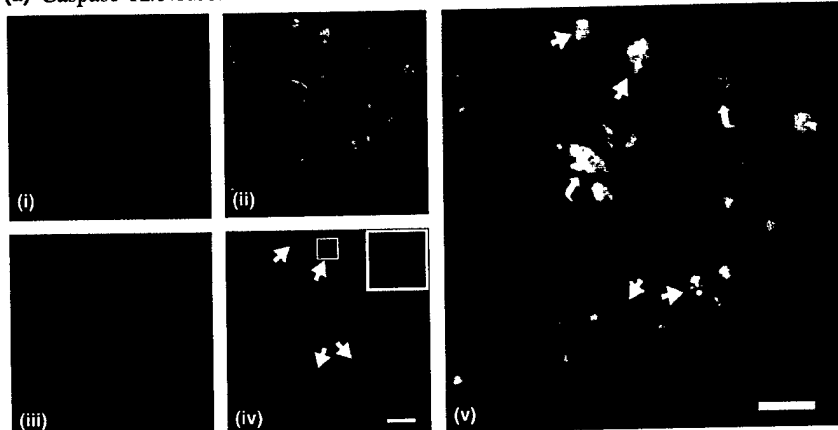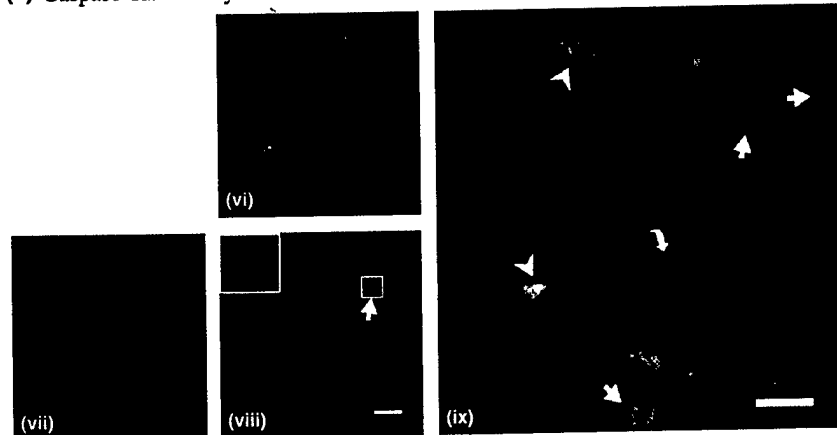
(a) Caspase-12/Neurons

(b) Caspase-12/Astrocytes

Fig. 5 Immunohistochemical analysis of the ipsilateral cortex in naïve rats and 1 day post-injury rats following controlled cortical impact injury (1.6 mm). (a) Injured brain tissue revealed that caspase-12 is induced in neurons and can be found co-localized in cells showing apoptotic bodies. Naïve brain tissue shows no caspase-12-immunoreactivity (i). In contrast, 1 day, 1.6 mm injured brain tissue revealed immunopositive caspase-12 expression (ii). NeuN stained neuronal cells (iii) show evidence of morphopathology. Apoptotic bodies are clearly present as illustrated by DAPI staining (arrows, iv, see insert for example) and co-localize with caspase-12 and the neuronal cell marker NeuN (arrows, v). Caspase-12 is also seen to co-localize in neurons with NeuN, which do not show apoptotic bodies (curved arrows, v). (b) There is evidence of caspase-12 expression co-localizing in astrocytes at the site of the contusion (arrowheads, ix). Caspase-12 was found primarily in cells that were not labeled with the astrocytic marker GFAP (arrows, ix) including cells showing apoptotic bodies (arrow, viii, see insert), but not in most of the astrocytes examined (curved arrow, ix). Photomicrographs are at 400×; scale bar 20 μm; caspase-12, panels i, ii and vi; NeuN, panel iii; GFAP, panel vii; DAPI, panels iv and viii; co-localized images, panels v and ix.

hippocampus, caspase-12 protein expression increased rapidly within the first 6 h where expression peaked for the processed form. Levels of the proform peaked later, at 1 day post-injury, when compared with naïve control. The increase in protein expression was more robust in the hippocampus than in the cortex, comparatively speaking.

Immunohistochemical analysis demonstrated that caspase-12 immunoreactivity was considerably increased 24 h following injury when compared with naïve animals, and was found primarily in neurons at the site of the contusion and, to a lesser extent, in areas distal to the site of impact, including the hippocampus (Figs 5 and 6). In addition, astrocytes expressing caspase-12 could also be found at the

contusion site (Fig. 5b). However, no astrocytes located distal to this area showed evidence of caspase-12 immunoreactivity. Examination of the NeuN stained tissue at the contusion location, in cells displaying caspase-12 immunoreactivity, showed evidence of pronounced morphological changes when compared with the contralateral side or in naïve animal brain tissue (results not shown). These observations further confirm the previous findings by our laboratory that morphopathological changes occur within 24 h following TBI (Newcomb et al. 1997, 1999).

Previous studies of TBI have concentrated on the well characterized extrinsic and intrinsic pathways that were found to be involved in neuronal cell death after TBI (Keane
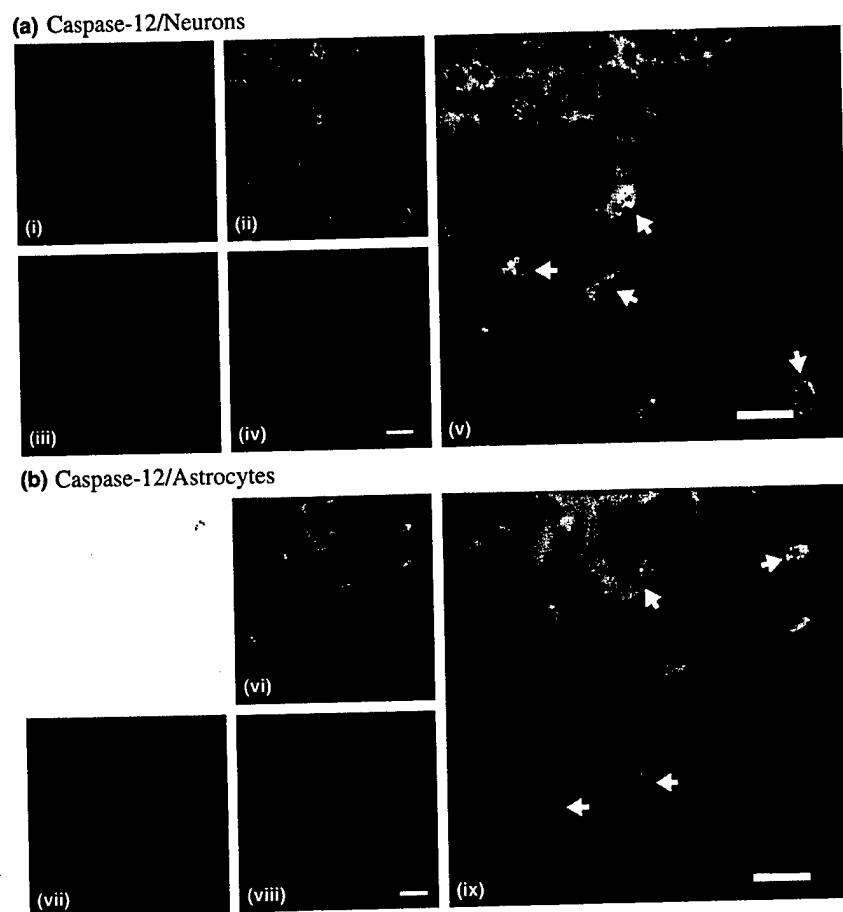
(a) Caspase-12/Neurons

(b) Caspase-12/Astrocytes

Fig. 6 Immunohistochemical analysis of the ipsilateral hippocampus in naïve rats and 1 day post-injury rats following controlled cortical impact injury (1.6 mm). (a) Injured brain tissue revealed that caspase-12 is up-regulated in neurons. Naïve brain tissue shows no specific caspase-12 immunoreactivity (i). In contrast, 1 day, 1.6 mm injured brain tissue revealed immunopositive caspase-12 expression (ii). NeuN stained neuronal cells (iii) shows no evidence of morphopa-thology in the hippocampus as compared to the cortex. Caspase-12 co-localizes with the neuronal cell marker NeuN (arrows, v). (b) Caspase-12 does not co-localize with the astrocytic marker GFAP (arrows, ix). Photomicrographs are at 400×; scale bar 20 μm; caspase-12, panels i, ii and vi; NeuN, panel iii; GFAP, panel 7; DAPI, panels iv and viii; co-localized images, panels v and ix.

et al. 2001). The extrinsic apoptotic pathway is triggered by binding of specialized ligands to death domain-containing members of the tumor necrosis factor receptor (TNFR) superfamily, such as Fas and tumor necrosis factor receptor-1 (TNFR-1), allowing for the formation of a death-inducing signaling complex (DISC). Increased expression and inter-action of the Fas receptors with FasL ligands (Beer *et al.* 2000; Qui *et al.* 2002) and TNFR-1 with TNF (Taupin *et al.* 1993; Beer *et al.* 2000) have been demonstrated in TBI. The Fas DISC containing the adaptor protein Fas-associated death domain protein (FADD), and the TNFR-1 DISC containing the TNF-associated receptor with death domain (TRADD), and their respective procaspases-8 and -10, leads to the autoproteolytic processing of these zymogens, initi-ating the subsequent activation of procaspase-3. The intrinsic pathway involves alterations in mitochondria homeostasis and plays a key role in TBI-associated cell death (Yang *et al.*

1985; Xiong *et al.* 1997; Raghupathi *et al.* 2000). These disruptions generally involve the release of cytochrome c and the formation of the apoptosome consisting of Apaf-1, dATP, cytochrome c, and the recruitment and activation of caspase-9. Procaspase-9, generally believed to reside in and be released from the mitochondria, is activated during apoptosis and then activates the executioner procaspase-3.

Recent studies have challenged the exclusivity of these two pathways with the discovery that apoptosis is independ-ently induced by an ER stress pathway (Nakagawa *et al.* 2000; Rao *et al.* 2001, 2002; Yoneda *et al.* 2001). The ER is the site for a number of critical processes, including lipid synthesis, maintenance of intracellular Ca^{2+} homeostasis, and the synthesis, initial post-translation modification and proper Ca^{2+}-dependent folding of most secretory and transmem-brane proteins. This includes their sorting and export for delivery to appropriate cellular destinations (Aridor and

Balch 1999; Kaufman 1999; Paschen and Doutheil 1999). ER functions are disturbed in many acute and chronic diseases of the brain (Yuan and Yankner 2000) such as global and focal ischemia, ischemia-reperfusion injury that occurs during stroke and cardiac arrest (DeGracia et al. 2002), epileptic seizures (Pelletier et al. 1999; Henshall et al. 2000), Alzheimer's disease (Imaizumi et al. 2001) and TBI (Weber et al. 2001). A variety of stimuli including changes in the luminal environment (Nakamura et al. 2000), glucose deprivation, oxidative stress, and the disruption of homeostasis and release of Ca^{2+} from the ER, may induce ER stress and subsequently induce apoptosis (Yu et al. 1999; Mattson et al. 2000; Nakagawa et al. 2000; Weber et al. 2001). Any one of these conditions will result in an increase of unfolded or malfolded proteins and the induction of the ER molecular chaperone BiP/GRP78 (Yu et al. 1999; Bertolotti et al. 2000). The induction of BiP/GRP78 triggers the unfolded protein response. Once activated, the UPR pathway is responsible for communicating changes required to modulate the behavior of the cell, allowing it to adapt and survive or to commit apoptosis. The three stressor proteins found in the ER membrane that generate the response include PERK (also known as PEK), ATF6 and IRE1α. Caspase-12 appears to act within the UPR pathway as a key component of the reaction of IRE1α to trauma and the increase of unfolded or malfolded proteins.

The functions of activated IRE1α, which oligomerizes and transautophosphorylates when released from BiP/GRP78, is complex. Activated IRE1α recruits, via its cytoplasmic domain, JIK (Jun inhibitor kinase) (Yoneda et al. 2001) into a protein complex with cytosolic adaptor protein TRAF2 (tumor necrosis factor receptor-associated factor-2). TRAF2 is involved in a pro-survival pathway that is dependent on protein synthesis, mediated by activation of NF-κB (Natoli et al. 1997) through the interaction with NF-κB-inducing kinase (NIK) (Bradley and Pober 2001; Tada et al. 2001). The activation of IRE1α stimulates the release of TRAF2 from its stable complex with procaspase-12 (Yoneda et al. 2001).

Caspase zymogens require a minimum of two cleavages to be converted to a mature enzyme, one separating the prodomain from the large subunit and small subunit and a second to separate the two subunits. Once released from TRAF2, procaspase-12, which is found on the cytoplasmic side of the ER, dimerizes in preparation for the initial cleavage by the proteases calpain (Nakagawa and Yuan 2000) and/or caspase-7 (Rao et al. 2001). Calpain has been shown to be activated early in TBI (Pike et al. 1998). When activated, both proteases are attracted to the ER membrane by some yet unknown mechanism. The processed form of caspase-12 then autoprocesses into the p20 and p10 subdomains, and the resulting two subunits associate to form an (alpha)2(beta)2-tetramer which is the active enzyme. The activation of caspase-12 appears to lead to cellular apoptosis

mediated by caspase-9 (Rao et al. 2001, 2002; Morishima et al. 2002) and caspase-3.

In contrast to rodent studies, a recent report suggests that the human caspase-12 sequence has acquired deleterious mutations, rendering it non-functional (Fischer et al. 2002). The study revealed that all splice variants examined had a frame shift mutation and a premature stop codon which would preclude expression of a full length protein. The evidence also points to a loss-of-function mutation within the SHG box, a critical catalytic site in caspases. On the other hand, the authors mentioned a caspase-12 allele residing in the SNP database (dbSNP Acc rs#648264) that restores the open reading frame, suggesting that a full length human caspase-12 allele may exist, but did not choose to pursue this information further. The study was limited to genetic expression and, as a result, no protein expression analysis was done to confirm their conclusions. This analysis is important because currently there are at least five human cell lines with evidence for the presence of caspase-12 protein. These cell lines include HeLa cells (Nakagawa et al. 2000), HEK293T human embryonic kidney cells (Rao et al. 2001; Yoneda et al. 2001), A549 human lung epithelial cells (Bitko and Barik 2001), T-ALL CCRF-CEM (subclone CEM-C7H2 vector control cell line, C7H2-VC) human T-cell acute lymphoblastic leukemia cells (Tinhofer et al. 2002) and Huh7 human liver-derived cells (Xie et al. 2002). These differences will need to be clarified by additional research before human TBI can be interpreted from rodent TBI.

Two recent studies of focal cerebral ischemia in mouse and rat, produced by middle cerebral artery occlusion and the resultant reperfusion injury, offered new evidence that stress to the ER leads to the increase in protein expression of caspase-12, and that it is an important component in neuronal death following ischemia/reperfusion (Mouw et al. 2003; Shibata et al. 2003). The elements involved in the tissue damage induced by reperfusion include excess free radical production and perturbation of intracellular calcium homeostasis (Paschen and Doutheil 1999), the factors known to trigger ER stress and UPR. The finding by Shibata et al. (2003) that there is increased expression of BiP/GRP78 with the same temporal profile as the increased protein expression of the activated caspase-12 strongly suggests that the ER has been stressed. In addition, they detected DNA fragmentation by TUNEL, a characteristic indication of the occurrence of apoptosis, in many of the caspase-12-positive cells. By using semi-quantitative RT-PCR, Mouw and colleagues (Mouw et al. 2003) observed a significant increase in caspase-12 mRNA in the ipsilateral side of the striatum following ischemia. Both studies found that the increase in caspase-12 protein expression was localized mainly in the ipsilateral striatal neurons. These findings complement our study, suggesting that there is a mechanistic link between the ischemic-like conditions that occur following TBI, the increase in caspase-12 expression, and neuronal death in the cortex and hippocampus.

Caspase-12 protein induction, in our study, was further supported by semi-quantitative PCR transcript analysis. In both the cortex and the hippocampus, mRNA transcripts showed statistically significant elevation within 3 days of injury and remained elevated for at least 5 days. The delayed and sustained induction of caspase-12 mRNA, in particular in the cortex, suggests the impairment of cellular mechanisms. The cortex may be most vulnerable to this disruption due to its proximity to the injury site. There are several possibilities that are not mutually exclusive. First, it suggests that caspase-12 is involved in protracted apoptosis as well as acute cell death. This is in keeping with the proposal by Rao *et al.* (2001) that prolonged ER stress may induce further caspase-12 activation via caspase-7, contributing to a delayed but continuing apoptosis through its interaction with caspase-9 (Rao *et al.* 2001, 2002; Morishima *et al.* 2002). Second, the normal cellular protein metabolism is most likely impaired. One of the responses of UPR, in response to ER stress, is for there to be a general global inhibition of protein synthesis following the activation of PERK (Harding *et al.* 2000; Harding *et al.* 1999; DeGracia *et al.* 2002) with exceptions for proteins that will either return the cell to normal activity or commit the cell to apoptosis (Mori *et al.* 1992; Kohno *et al.* 1993; Natoli *et al.* 1997; Yoshida *et al.* 1998). There is no evidence to suggest that UPR interferes with mRNA transcription. In addition, there may also be either a decrease in the normal degradation of proteins, including transcription factors, due to the lack of the protein ubiquitin because of the inhibition of protein synthesis, or the process may be overloaded by the UPR as the cell attempts to reduce its backlog of unfolded and malfolded proteins engendered by the ER stress initiated by TBI. A third possibility is that while the transcription of the mRNA continues in response to UPR, the proform is not being transcribed, nor is it being processed to its active form, as the cells regain control over their cellular metabolism. Our study shows the proform returning to normal levels within 7 days; caspase-12 mRNA may follow later. This remains to be determined by future investigations.

The early responses provide compelling evidence that caspase-12 mRNA induction and increased protein expression occur in response to TBI and that caspase-12 may be a major contributor to the more acute pathophysiological events of TBI. In previous studies, caspase-12 has been characterized as an initiator, or upstream, caspase (Rao *et al.* 2001, 2002). The actual mechanisms and consequences of caspase-12 induction and activation in TBI remain to be examined.

In summary, this study provides the first characterization of caspase-12 mRNA and protein expression and processing in a model of TBI. These findings provide insight into a novel mechanism of cell death following injury. These data also provide clues into the potential ways TBI might contribute to the pathogenesis of a number of neuropathologies through the caspase-12 apoptotic pathway.

References

Aridor M. and Balch W. E. (1999) Integration of endoplasmic reticulum signaling in health and disease. *Nature Med.* **5**, 745–751.

Beer R., Franz G., Schöpf M., Reindl M., Zelger B., Schmutzhard E., Poewe W. and Kampfl A. (2000) Expression of Fas and Fas ligand after experimental traumatic brain injury in the rat. *J. Cereb. Blood Flow Metab.* **20**, 669–677.

Bertolotti A., Zhang Y., Hendershot L. M., Harding H. P. and Ron D. (2000) Dynamic interaction of BiP and ER stress transducers in the unfolded-protein response. *Nat. Cell Biol.* **2**, 326–332.

Bitko V. and Barik S. (2001) An endoplasmic reticulum-specific stress-activated caspase (caspase-12) is implicated in the apoptosis of A549 epithelial cells by respiratory syncytial virus. *J. Cell Biochem.* **80**, 441–454.

Bradley J. R. and Pober J. S. (2001) Tumor necrosis factor receptor-associated factors (TRAFs). *Oncogene* **20**, 6482–6491.

Clark R. S., Kochanek P. M., Chen M., Watkins S. C., Marion D. W., Chen J., Hamilton R. L., Loeffert J. E. and Graham S. H. (1999) Increases in Bcl-2 and cleavage of caspase-1 and caspase-3 in human brain after head injury. *FASEB J.* **13**, 813–821.

Clark R. S., Kochanek P. M., Watkins S. C. *et al.* (2000) Caspase-3 mediated neuronal death after traumatic brain injury in rats. *J. Neurochem.* **74**, 740–753.

Cohen G. M. (1997) Caspases: the executioners of apoptosis. *Biochem. J.* **326**, 1–16.

Colicos M. A., Dixon C. E. and Dash P. K. (1996) Delayed, selective neuronal death following experimental cortical impact injury in rats: possible role in memory defects. *Brain Res.* **739**, 111–119.

Conti A. C., Raghupathi R., Trojanowski J. Q. and McIntosh T. K. (1998) Experimental brain injury induces regionally distinct apoptosis during the acute and delayed post-traumatic period. *J. Neurosci.* **18**, 5663–5672.

Daniel P. T. (2000) Dissecting the pathways to death. *Leukemia* **14**, 2035–2044.

DeGracia D. J., Kumar R., Owen C. R., Krause G. S. and White B. C. (2002) Review: Molecular pathways of protein synthesis inhibition during brain reperfusion: implications for neuronal survival or death. *J. Cereb. Blood Flow Metab.* **22**, 127–141.

Dixon C. E., Clifton G. L., Lighthall J. W., Yaghmai A. A. and Hayes R. L. (1991) A controlled cortical impact model of traumatic brain injury in the rat. *J. Neurosci. Methods* **39**, 252–262.

Fischer H., Koenig U., Eckhart L. and Tschachler E. (2002) Human caspase-12 has acquired deleterious mutations. *Biochem. Biophys. Res. Commun.* **293**, 722–726.

Harding H. P., Zhang Y. and Ron D. (1977) Protein translation and folding are coupled by an endoplasmic-reticulum-resident kinase. *Nature* **397**, 271–274.

Harding H. P., Zhang Y., Bertolotti A., Zeng H. and Ron D. (2000) Perk is essential for translational regulation and cell survival during the unfolded protein response. *Mol. Cell* **5**, 897–904.

Henshall D. C., Chen J. and Simon R. P. (2000) Involvement of caspase-3-like protease in the mechanism of cell death following focally evoked limbic seizures. *J. Neurochem.* **74**, 1215–1223.

Imaizumi K., Miyoshi K., Katayama T., Yoneda T., Taniguchi M., Kudo T. and Tohyama M. (2001) Review: The unfolded protein response and Alzheimer's disease. *Biochim. Biophys. Acta* **1536**, 85–96.

Jacobson M. D., Weil M. and Raff M. C. (1997) Programmed cell death in animal development. *Cell* **88**, 347–354.

Johnson F. B., Sinclair D. A. and Guarente L. (1999) Molecular biology of aging. *Cell* **96**, 291–302.

Kaufman R. J. (1999) Stress signaling from the lumen of the endoplasmic reticulum: coordination of gene transcriptional and translational controls. *Genes Dev.* **13**, 1211–1233.

Keane R. W., Kraydieh S., Lotocki G., Ofelia F. A., Aldana P. and Dietrich W. D. (2001) Apoptotic and antiapoptotic mechanisms after traumatic brain injury. *J. Cereb. Blood Flow Metab.* **21**, 1189–1198.

Kohno K., Normington K., Sambrook J., Gething M. J. and Mori K. (1993) The promoter region of the yeast KAR2 (BiP) gene contains a regulatory domain that responds to the presence of unfolded proteins in the endoplasmic reticulum. *Mol. Cell Biol.* **13**, 877–890.

Mattson M. P., LaFerla F. M., Chan S. L., Leissring M. A., Shepel P. N. and Geiger J. D. (2000) Calcium signaling in the ER: its role in neuronal plasticity and neurodegenerative disorders. *Trends Neurosci.* **23**, 222–229.

Mori K., Sant A., Kohno K., Normington K., Gething M. J. and Sambrook J. F. (1992) A 22 bp *cis*-acting element is necessary and sufficient for the induction of the yeast KAR2 (BiP) gene by unfolded proteins. *EMBO J.* **11**, 2583–2593.

Morishima N., Nakanishi K., Takenouchi H., Shibata G. and Yasuhiko Y. (2002) An endoplasmic reticulum stress-specific caspase cascade in apoptosis: cytochrome c-independent activation of caspase-9 by caspase-12. *J. Biol. Chem.* **277**, 34287–34294.

Mouw G., Zechel J. L., Gamboa J., Lust W. D., Selman W. R. and Ratcheson R. A. (2003) Activation of caspase-12, an endoplasmic reticulum resident caspase, after permanent focal ischemia in rat. *Neuroreport* **14**, 183–186.

Nakagawa T. and Yuan J. (2000) Cross-talk between two cysteine protease families: activation of caspase-12 by calpain in apoptosis. *J. Biol. Chem.* **150**, 887–894.

Nakagawa T., Zhu H., Morishima N., Li E., Xu J., Yankner B. A. and Yuan J. (2000) Caspase-12 mediates endoplasmic-reticulum-specific apoptosis and cytotoxicity by amyloid-β. *Nature* **403**, 98–103.

Nakamura K., Bossy-Wetzel E., Burns K., Fadel M. P., Lozyk M., Goping I. S., Opas M., Bleackley R. C., Green D. R. and Michalak M. (2000) Changes in endoplasmic reticulum luminal environment affect cell sensitivity to apoptosis. *J. Biol. Chem.* **150**, 731–740.

Natoli G., Costanzo A., Ianni A., Templeton D. J., Woodgett J. R., Balsano C. and Levrero M. (1997) Activation of SAPK/JNK by TNF receptor 1 through a noncytotoxic TRAF2-dependent pathway. *Science* **275**, 200–203.

Newcomb J. K., Kampfl A., Posmantur R. M., Zhao X., Pike B. R., Liu S., Clifton G. L. and Hayes R. L. (1997) Immunohistochemical study of calpain-mediated breakdown products to alpha-spectrin following controlled cortical impact injury in the rat. *J. Neurotrauma* **14**, 369–383.

Newcomb J. K., Zhao X., Pike B. R. and Hayes R. L. (1999) Temporal profile of apoptotic-like changes in neurons and astrocytes following controlled cortical impact injury in the rat. *Exp. Neurol.* **158**, 76–88.

Oppenheim R. W. (1991) Cell death during development of the nervous system. *Annu. Rev. Neurosci.* **14**, 453–501.

Paschen W. and Doutheil J. (1999) Disturbances of the functioning of endoplasmic reticulum: a key mechanism underlying neuronal cell injury. *J. Cereb. Blood Flow Metab.* **19**, 1–18.

Pelletier M. R., Wadia J. S., Mills L. R. and Carlen P. L. (1999) Seizure-induced cell death produced by repeated tetanic stimulation in vitro: possible role of endoplasmic reticulum calcium stores. *J. Neurophysiol.* **81**, 3054–3064.

Pike B. R., Zhao X., Newcomb J. K., Posmantur R. M., Wang K. K. and Hayes R. L. (1998) Regional calpain and caspase-3 proteolysis of alpha-spectrin after traumatic brain injury. *Neuroreport* **9**, 2437–2442.

Qui J., Whalen M. J., Lowenstein P., Fiskum G., Fahy B., Darwish R., Aarabi B., Yuan J. and Moskowitz M. A. (2002) Upregulation of the Fas receptor death inducing-signaling complex in traumatic brain injury in mice and humans. *J. Neurosci.* **22**, 3504–3511.

Raff M. C., Barres B. A., Burne J. F., Coles H. S., Ishizaki Y. and Jacobson M. D. (1993) Programmed cell death and the control of cell survival: lessons from the nervous system. *Science* **262**, 695–700.

Raghupathi R., Graham D. I. and McIntosh T. K. (2000) Apoptosis after traumatic brain injury. *J. Neurotrauma* **17**, 927–938.

Rao R. V., Hermel E., Castro-Obregon S., del Rio G., Ellerby L. M., Ellerby H. M. and Bredesen D. E. (2001) Coupling endoplasmic reticulum stress to the cell death program. *J. Biol. Chem.* **276**, 33869–33874.

Rao R. V., Castro-Obregon S., Frankowski H., Schuler M., Stoka V., del Rio G., Bredesen D. E. and Ellerby H. M. (2002) Coupling endoplasmic reticulum stress to the cell death program. *J. Biol. Chem.* **277**, 21836–21842.

Rink A., Fung K. M., Trojanowski J. Q., Lee B. M., Neugebauer E. and McIntosh T. K. (1995) Evidence of apoptotic cell death after experimental traumatic brain injury in the rat. *Am. J. Pathol.* **147**, 1575–1583.

Shibata M., Hattori H., Sasaki T., Gotoh J., Hamada J. and Fukuuchi Y. (2003) Activation of caspase-12 by endoplasmic reticulum stress induced by transient middle cerebral artery occlusion in mice. *Neuroscience* **118**, 491–499.

Soto C. (2003) Unfolding the role of protein misfolding in neurodegenerative diseases. *Nat. Rev. Neurosci.* **4**, 49–60.

Tada K., Okazaki T., Sakon S. *et al.* (2001) Critical roles of TRAF2 and TRAF5 in tumor necrosis factor-induced NF-kappaB activation and protection from cell death. *J. Biol. Chem.* **276**, 36530–36534.

Taupin V., Toulmond S., Serrano A., Benavides J. and Zavala F. (1993) Increase in IL-6, IL-1 and TNF levels in rat brain following traumatic lesion. Influence of pre- and post-traumatic treatment with Ro5, 4864, a peripheral-type (p site) benzodiazepine ligand. *J. Neuroimmunol.* **42**, 177–185.

Tinhofer I., Anether G., Senfter M., Pfaller K., Bernhard D., Hara M. and Greil R. (2002) Stressful death of T-ALL tumor cells after treatment with the anti-tumor agent Tetrocarcin-A. *FASEB J.* **16**, 1295–1297.

Tolentino P. J., DeFord S. M., Notterpek L., Glenn C. C., Pike B. R., Wang K. K. W. and Hayes R. L. (2002) Up-regulation of tissue-type transglutaminase after traumatic brain injury. *J. Neurochem.* **80**, 579–588.

Vaux D. L. and Korsmeyer S. J. (1999) Cell death in development. *Cell* **96**, 245–254.

Weber J. T., Rzigalinski B. A. and Ellis E. F. (2001) Traumatic injury of cortical neurons causes changes in intracellular calcium stores and capacitative calcium influx. *J. Biol. Chem.* **276**, 1800–1807.

Xie Q., Khaoustov V. I., Chung C. C., Sohn J., Krishnan B., Lewis D. E. and Yoffe B. (2002) Effect of tauroursodeoxycholic acid on endoplasmic reticulum stress-induced caspase-12 activation. *Hepatology* **36**, 592–601.

Xiong Y., Gu Q., Peterson P. L., Muizelaar J. P. and Lee C. P. (1997) Mitochondrial dysfunction and calcium perturbation induced by traumatic brain injury. *J. Neurotrauma* **14**, 23–34.

Yakovlev A. G. and Faden A. L. (2001) Caspase-dependent apoptotic pathways in CNS injury. *Mol. Neurobiol.* **24**, 131–144.

Yakovlev A. G., Knoblach S. M., Fan L., Fox G. B., Goodnight R. and Faden A. I. (1997) Activation of CPP32-like caspases contributes to neuronal apoptosis and neurological dysfunction after traumatic brain injury. *J. Neurosci.* **17**, 7415–7424.

Yang M. S., DeWitt D. S., Becker D. P. and Hayes R. L. (1985) Regional brain metabolite levels following mild experimental head injury in the cat. *J. Neurosurg.* **63**, 617–621.

Yoneda T., Imaizumi K., Oono K., Yui D., Gomi F., Katayama T. and Tohyama M. (2001) Activation of caspase-12, an endoplasmic reticulum (ER) resident caspase, through tumor necrosis factor receptor-associated factor 2-dependent mechanism in response to the ER stress. *J. Biol. Chem.* **276**, 13935–13940.

Yoshida H., Haze K., Yanagi H., Yura T. and Mori K. (1998) Identification of the *cis*-acting endoplasmic reticulum stress response element responsible for transcriptional induction of mammalian glucose-regulated proteins; involvement of basic-leucine zipper transcription factors. *J. Biol. Chem.* **273**, 33741–33749.

Yu Z., Luo H., Fu W. and Mattson M. P. (1999) The endoplasmic reticulum stress-responsive protein GRP78 protects neurons against excitotoxicity and apoptosis: suppression of oxidative stress and stabilization of calcium homeostasis. *Exp. Neurol.* **155**, 302–314.

Yuan J. and Yankner B. A. (2000) Apoptosis in the nervous system. *Nature* **407**, 802–809.